BOSTON ARCHITECTURAL CENTER

LIBRARY

Digitized by the Internet Archive
in 2022 with funding from
Boston Public Library

https://archive.org/details/passivesolarjour00inte

Passive Solar Journal

Heating, Cooling, Hybrid Technologies and Strategies for Sustainable Design.

Official Journal of the Passive Systems Division

EDITED BY
Jeffrey Cook, Arizona State University, Tempe AZ and Michael J. Holtz, Solar Energy Research Institute, Golden CO
PUBLISHED BY
The American Section of the INTERNATIONAL SOLAR ENERGY SOCIETY®

Vol. 1, NO 1/January 1982

Published with the cooperation of the American Section of the International Solar Energy Society, the U.S. Department of Energy, and the Solar Energy Research Institute.

PASJDF 1(1) 1-64(1982) ISSN: 0277-6456

Cover: The interrelationship of climate/nature, the built environment, and the human element forms the basis for the study and practice of passive/hybrid solar research and design.

Photo Credits: 1 Boulder Energy Conservation Center, 2 3 6 7 Bruce Flynn, 4 Henry Mueller, 5 Sharyn Towle

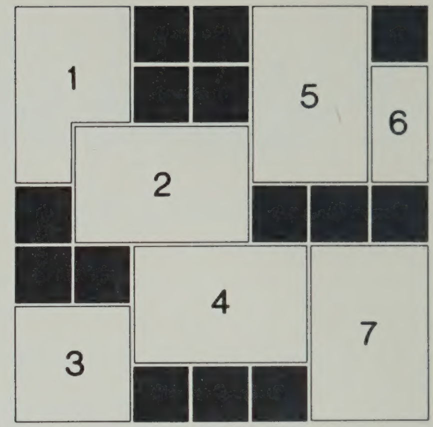

This publication contains accounts of work sponsored by the United States Government. Neither the United States nor the United States Department of Energy, nor the American Section of the International Solar Energy Society, nor any of their employees, nor any of their contractors, subcontractors, or their employees, makes any warranty, express or implied, or assumes any legal liability or responsibility for the accuracy, completeness, or usefulness of any information, apparatus, product, or process disclosed, or represents that its use would not infringe privately owned rights.
Material may be reprinted with credit to **Passive Solar Journal** Pilot Edition.

LIBRARY
BOSTON ARCHITECTURAL CENTER

A Message from the Publishers and the Editors ...

Passive Solar Journal is the first journal published by the American Section of the International Solar Energy Society. It is being launched in response to the important developments in passive solar and related technology. The quickly approaching realities of mass marketability and widespread acceptance require an authoritative source of information about tested designs, credible performance results, accurate design and measurement methods, and thorough understanding of the use and control of thermal processes.

The journal will include full length position papers and definitive articles, as well as technical notes, book reviews, letters, essays, and exchanges.

A publication of high quality standards guided by an outstanding editorial advisory board can draw together the work of diverse scientists, researchers, architects, engineers and provide an important focal point for the literature of passive and hybrid systems. This authoritative journal authored by the leaders of a rapidly developing field is intended to become the archival record as well as the immediate reference for state of the art practice.

The excellence of the recent passive research and professional applications together with the Society's stake in the effective dissemination of technical information mean that subscribers to **Passive Solar Journal** will have access to the finest contributions in the field at a reasonable subscription price.

ORDER FORM:

To: American Section of the
INTERNATIONAL SOLAR ENERGY SOCIETY®
110 West 34th Street New York 10001

Please enter my subscription to the new quarterly journal, **The Passive Solar Journal** beginning with volume 1, 1982.

	U.S.	Foreign (surface mail)
AS of ISES Members	☐ $20.00	☐ $28.00
Nonmembers/Institutions	☐ $80.00	☐ $88.00

Member rates are for personal use only, paid with personal funds.

☐ I am an AS of ISES member ID no: ____________________
☐ I am not an AS of ISES member.

Institution ____________________
Attention ____________________
Address ____________________ ☐ **home** ☐ **business**
City/State/Zip ____________________
Country ____________________
Authorized by____________________**Title** _____**P.O. No.** ________**Date**_____

Completing the following information is required:
Nature of Business
- ☐ Architectural, engineering firms, consulting engineers
- ☐ Government agency, university, testing and research
- ☐ Manufacturing product(s)
- ☐ Other____________________

Foreign payment must be made in U.S. currency, by international money order,UNESCO coupons, or U.S. bank draft. Orders will be accepted through recognized subscription agencies.

— —

FOR YOUR LIBRARIAN

To:____________________, Librarian

I recommend that a subscription to the new PASSIVE SOLAR JOURNAL (quarterly) published by the American Section of the International Solar Energy Society, be purchased for our library.

From: ____________________
(Name)
____
(Department)

Thank you.

Volume 1, Number 1
January 1982

The Passive Solar Journal is published by the American Section of the International Solar Energy Society, 110 West 34th Street, New York 10001. Quarterly: January, April, July, October.
The Official publication of the Passive Systems Division of the American Section of the International Solar Energy Society.

The Passive Solar Journal is covered by *Engineering Index* (monthly and annual), *Energy Abstracts*, and is indexed and abstracted by *Energy Information Abstracts*.

Second class postage paid at
Norwich, Connecticut
POSTMASTER: Send address changes to
AS of ISES, 110 West 34th St.,
New York NY 10001.
Member rates are for personal use only, paid with personal funds.

Subscription Rates:
AS of ISES Members for one year: U.S. $20.00 Foreign $28.00. Nonmembers/Institutions for one year: U.S. $80.00, Foreign $88.00. Member rates are for personal use only, paid with personal funds.

Changes of address:
Allow six weeks for all changes of address to become effective. All communications should include both old and new addresses and zip codes and should be accompanied by a recent mailing label. Members and subscribers should send changes of address to Passive Solar Journal, AS of ISES, RIAT, US Hwy 190 West, Killeen TX 76541.

Claims for missing issues will not be allowed if received more than 90 days from date of mailing plus the time normally required for postal delivery of the issue and the claim. No claims will be allowed because of failure to notify a change of address or because a copy is "missing from files."

AS of ISES assumes no responsibility for the statements and opinions advanced by contributors to the Society's publications. Editorial views do not necessarily represent the official position of AS of ISES. Acceptance of an advertisement does not confer endorsement of the product by AS of ISES.

Membership:

	AS of ISES only	Combined ISES and AS of ISES
Full member	$35	$60
Student	15	30
Joint-Chapter	30	55
Household	40	65

Corporate and Contributing memberships are also available. Please apply for information to the Executive Director, AS of ISES, 110 West 34th St., New York 10001

Contents

2 **Editor's Note**
Rachel Snyder

3 **Statements of Intent**
Michael Maybaum, Michael J. Holtz, Jeffrey Cook

ARTICLES

4 **A Comparison of Ground and Above-Ground Climates for Identifying Appropriate Cooling Strategies**
Kenneth Labs, Keith Harrington

12 **Transparent and Opaque Louvers for Thermal Control in Passive Solar Buildings**
Joseph K.E. Ortega, J. Michael Connolly, Carl E. Bingham, Mark McDade, Michael J. Holtz

21 **New Mexico Solar Greenhouse Study**
W. Scott Morris, Claire Reiniger

28 **Natural Convection in Passive Solar Buildings: Experiments, Analysis, and Results**
Ashok Gadgil, Fred Bauman, Ronald Kammerud

41 **Market Potential Indexing: A New Technique for Analyzing Solar Markets**
Scott A. Noll, William M. Robson, Marilyn K. Yeamans

TECHNICAL NOTES

52 **Heat Exchangers Effective in Radon Control**
Condensed from *Atmospheric Environment* (William W. Nazaroff, Mary L. Boegel, Craig D. Hollowell, Gary D. Roseme)

54 **Overview: Procedures for Validating BEAS**
David Wortman, Bob O'Doherty, Ron Judkoff

UPDATES

56 **Trinity Develops Efficient AC Unit**
57 **SERI to Publish Monitoring Results**
57 **Double-Envelope Evaluation Begun**
58 **New Prototype of Transwall Tested**

REVIEW

59 **Passive Solar Design Handbook (Volumes 1 & 2)**
Jeffrey Cook, Bill Wright, William A. Shurcliff

Staff

Rachel Snyder
Infinite Energy
Managing Editor

Susan Sczepanski
Solar Energy Research Institute
Art Director

Suzanne Gripman
The Write One
Contributing Editor

Special thanks to Barbara Glenn, Joyce Barrett, and Evan Evans of the Solar Energy Research Institute for their help in the early development of **Passive Solar Journal.**

Editorial Advisory/Review Board

Dennis A. Andrejko
SEAgroup
Nevada City, California

Jeffrey Cook
Arizona State University
Tempe, Arizona

Don Elmer
Lawrence Berkeley Laboratory
Berkeley, California

Keith Haggard
Solar Energy Research Institute
Golden, Colorado

Michael J. Holtz
Solar Energy Research Institute
Golden, Colorado

Ron Judkoff
Solar Energy Research Institute
Golden, Colorado

Edward Mazria
Edward Mazria & Associates
Albuquerque, New Mexico

Lynn Nelson
The Habitat Center
Pacheco, California

Joseph K.E. Ortega
Solar Energy Research Institute
Golden, Colorado

Editor's Note

In the Foreword to the *Proceedings of the Fifth National Passive Solar Conference,* John Hayes and I characterized that event as symbolic of passive solar's "coming of age." We spoke of the field ripening, maturing, and throwing off the trappings of awkward adolescence. Conference organizers conveyed with a high degree of success their two-pronged message: "Passive solar works and passive solar sells."

The quickly approaching reality of mass marketability and widespread consumer acceptance represents a significant advancement for passive/hybrid technology — an advancement built on the foundation created in the laboratory; on the test site; and during hours spent with calculator, computer, and the creative senses. Passive/hybrid buildings that *work* evolve from tested designs, credible performance results, accurate design methods, and a thorough understanding of the use and control of thermal processes. Passive/hybrid buildings that *sell* do so only as a result of an intimate understanding of the marketplace; a keen perspective on the consumer/client decisionmaking process; and a judicious mix of aesthetics, economics, and concern for human comfort.

Passive Solar Journal emerges to enrich and support the continuing development of the research base on which well-built, well-operating, beautiful passive buildings must rely. It is a welcome component to the arena that provides design professionals with proven concepts and accurate performance data, builders with reliable facts on materials capabilities and use, and developers and marketers with an awareness of passive/hybrid consumer attitudes and motivations.

Passive Solar Journal carries with it three messages: One, that passive/hybrid research has developed a distinct identity and need no longer be tucked under the arm of a related discipline. Thus, it should boast a distinct vehicle for communications among its own. Second, that the quality of passive research and development today falls nowhere short of the quality of scientific effort in other fields, and a journal of corresponding rigor and thoroughness is deserved. Third, that the passive/hybrid discipline melds understandings of science as well as aesthetics, and the journal representing it must be pleasing to both sides of the brain.

As is often the case, the paper you hold in your hand far from adequately represents the human effort that preceded it. **Passive Solar Journal** arose to fill a need identified by private and public sectors individually and then met by those same players cooperatively. Nevertheless, while testimony to volunteer authors, advisors, reviewers, and the private or public organizations they represent, this Pilot Edition is but a first attempt. The continued development and honing of **Passive Solar Journal** rely on a prolific field, a supportive yet demanding readership, and an atmosphere in which research progress and results — regardless of their origins — are under constant scrutiny and pointed review.

This publication was initiated by those in a position to do so, but it is designed to serve as *your* tool and as a representation of *your* efforts. Be generous with your feedback — it alone will shape the direction of **Passive Solar Journal.**

Rachel Snyder
Managing Editor/Pilot Edition

Statements of Intent

I am delighted to welcome this first issue of **Passive Solar Journal,** since it has been with a good deal of personal and professional satisfaction that I have watched this periodical take shape and then become a reality. My pleasure in this enterprise is twofold; first, that at last there is a vehicle for communicating valued findings to the entire research community; and second, that the journal, sponsored as it is by SERI, AS of ISES, and DOE, may well serve as a model for similar collaborative efforts between the public and Federal sectors.

The Department's Passive and Hybrid Solar Program has come a long way in the 4 years since its establishment. Dramatic increases in program funding since 1977, industry involvement, and public interest have combined with rising costs to strengthen the Program's commitment to accelerate the development and widespread use of passive and hybrid technology over the next 5 years. I look to the **Passive Solar Journal** to highlight some of the important research coming out of that program.

Indeed, the Passive and Hybrid Solar Program's successes are the successes of the Regional Solar Energy Centers, SERI, the national laboratories, and hundreds of individuals. I look forward to counting the **Passive Solar Journal** as one of these successes.

Michael Maybaum,
Acting Director,
Passive and Hybrid Solar
Buildings Division,
U.S. Department of Energy

Passive research, development, and design is no longer an oddity undertaken by backyard inventors or innovative architects. Today, passive R&D is serious business, performed by dedicated researchers and designers using all the scientific rigor that existing analysis and experimental methods will allow. Where only a few years ago passive systems were not considered a worthy design or research problem, we are now in the midst of a revival of interest in building climatology and building physics. We have come to realize how little we actually know about how buildings process energy and about how we can reduce their energy consumption.

The resurgence of research and development into passive design has necessitated establishing a means of communicating results among the building energy research community and between researchers and design practitioners. For this reason, **Passive Solar Journal** exists. It is a publication dedicated to the rigorous and thoughtful presentation of significant results from completed and ongoing passive research and development. Although its audience is primarily those conducting research into passive systems, we hope that designers will be able to see the practical application of these research results to their building solutions.

We encourage an open and frank discussion of the research presented within the journal and ask for your comments, recommendations, and contributions.

Michael J. Holtz, Chief,
Building Systems
Development Branch,
Solar Energy Research Institute

We have argued almost endlessly about the name of this new periodical, but we all understand its purposes. There have been growing needs for a referenced periodical since the emergence of an identifiable passive solar field in 1974-75 and its culmination with the First National Passive Conference in Albuquerque in May 1976.

As it has developed, "passive" has been an integrative subject, providing an energy ethic, a resource attitude, and a cultural goal that goes beyond good design. The persuasive idea has not been a changed lifestyle, but rather a comprehensive man-nature-life-work schema within which all human activity fits. All of us live in buildings, and all buildings are to some degree passive. Thus we all have experiential as well as experimental knowledge to bring to the passive table.

The success of the Passive Systems Division of AS of ISES in fielding successive intensive national passive conferences has provided the discipline with a series of proceedings, of instant literary cross-sections of the field. The shifting balances of passive interests and developing maturity of the field as revealed in those proceedings underline the important dialogues between research and applications and between programs funded by public agencies and the productive activities of private enthusiasm. It is refreshing that this journal is a product of federal programs, national laboratories, a voluntary association, and some continuously independent performers. All share common goals. May we all thrive.

Jeffrey Cook, Chairman,
Passive Systems Division,
American Section of the
International Solar Energy
Society, Inc.

A Comparison of Ground and Above-Ground Climates for Identifying Appropriate Cooling Strategies*

Kenneth Labs
147 Livingston Street, New Haven, CT 06511
and
Keith Harrington
P.O. Box 216, Fort Defiance, AZ 86504

Abstract *A mathematical model of undisturbed ground temperature is applied to the problem of assessing the value of earth tempering techniques in five regions of the contiguous United States. Synthesized ground temperature tables and comparative normal and design air temperatures are presented and briefly discussed with regard to the suitability of subgrade construction and earth-air heat exchangers. Emphasis is placed on evaluating earth tempering within the context of other passive cooling strategies, which are identified as to the percentage of annual hours that each is effective within the five study regions. It is concluded that ground cooling techniques are of greatest value in temperate and arid areas, and of limited benefit in warm, humid zones, where they may even be counterproductive by compromising natural ventilating capability.*

Introduction

Interest in the cooling potential of the ground has expanded rapidly in the past two years. Unfortunately, there exists at this time little in the way of a ground temperature data base or methodology for making design decisions about earth tempering practices. Although theory of ground climate is well documented in the literature of such fields as geophysics and agronomy, little of this information has found its way into the hands of building designers and researchers. As a result, old myths continue to be promulgated in the professional and popular press. For instance, a recent government-sponsored report on climate design guidelines for energy conserving homes refers to "taking advantage of the stable temperature conditions of approximately 56°F (13°C), below the frost line"—conditions which certainly do not exist anywhere near central Florida, to which this recommendation was directed.

This paper presents ground temperatures synthesized by an often validated theoretical model for five regions in the United States identified by the following major cities: Atlanta, Ga.; Dallas, Tex.; Houston, Tex.; Kansas City, Kans.; and Phoenix, Ariz. Although these represent undisturbed temperatures which would be elevated by the presence of some ground "coolth"-exploiting device, they offer a first attempt at identifying the locations of at least initially useful ground cooling potentials.

With the belief that no climate control strategy should be considered in isolation from alternative or complementary practices, ground temperature data are presented here together with corresponding simultaneous air temperature normals, ASHRAE design temperatures, and a bioclimatic analysis of appropriate above-surface design strategies.

Temperature Model

In 1965, T. Kusuda and P.R. Achenbach [1] posited that periodic heat-conduction theory can be used to model annual ground temperature variation with accuracy sufficient for most building engineering purposes. An extensive review of earth temperature literature in geophysics, agronomy, and other disciplines generally confirms this position and has provided insights into the limitations of the Kusuda model as well [2]. Although data synthesized by the theoretical method have been widely published, they appear as seasonal average temperatures of a soil profile extending from the surface to a depth of 10 ft (3m). This profile has been used for estimating the temperature of the earth surrounding fallout shelters [3], heat losses from buried steam lines [4], and as input for building load simulation models [5].

Heat-conduction theory is employed here for estimating instantaneous temperatures for a range of depths and for computing the average temperature of various subgrade profiles. The theory itself is developed in numerous textbooks on heat conduction and environmental physics [6,7]. In a form in which time is represented in days, the model may be written,

---

* This paper is based in part upon material from a forthcoming report, "A Regional Analysis of Ground and Above-Ground Climate for Evaluating the Suitability of Earth Tempering Practices in Architectural Design," which is being prepared through sponsorship of the Oak Ridge National Laboratory for the U.S. Department of Energy. The report will be available from the Underground Space Center of the University of Minnesota, Minneapolis, MN 55455.

$$T_{(x,t)} = T_m - A_s\, e^{-x\sqrt{\frac{\pi}{365\alpha}}} \cos\left[\frac{360}{365}\left(t - t_o - \frac{x}{2}\sqrt{\frac{365}{\pi\alpha}}\right)\right], \quad (1)$$

where

$T_{(x,t)}$ = temperature of soil at depth x and time t;
T_m = mean annual earth temperature (steady state temperature);
A_s = amplitude of surface temperature wave;
e = Euler's number, approximately 2.71828
x = depth below surface;
α = thermal diffusivity of soil (area/day);
t = time of year (days); and
t_o = phase constant (days).

An expression for the average temperature of any selected profile ranging from depth a to depth b is obtained by integrating Eq. 1 with respect to depth x and dividing the result by the height of the profile $(b - a)$,

$$T_{(a-b,t)} = T_m + \frac{A_s}{(b-a)r\sqrt{2}} e^{-xr} \cos\left[\frac{360}{365}\left(t - t_o - 46 - \frac{x}{2}\sqrt{\frac{365}{\pi\alpha}}\right)\right]\Bigg|_b^a, \quad (2)$$

where

a = upper bounds of soil profile;
b = lower bounds of soil profile; and
$r = \sqrt{\frac{\pi}{365\alpha}}$.

Selection of Variables

The theoretical model applies to a semi-infinite homogenous solid, the properties of which are constant over time, with a perfectly sinusoidal temperature variation at the surface. None of these conditions are strictly met in soils, yet most observed ground temperature measurements agree remarkably well with theory. The major problem, therefore, is accurate estimation of the variables of the model, most of which will be unknown to the investigator at any given location.

Criteria for selecting values for the variables and their ranges are discussed in detail in Ref. 2 and will not be treated at length here. The values chosen to generate the tables presented in this paper are given below, accompanied by brief explanations.

Ground temperature mean, T_m

A recently prepared isothermal map of wellwater temperatures has been obtained from the National Water Well Association (Fig. 1). It was constructed from records of observed groundwater temperatures in wells 50 to 150 ft (15 to 46 m) deep. This is believed to be the best available regional index of steady-state ground temperatures and is considered accurate enough for selecting T_m for use in the mathematical model. For locations for which actual ground temperature records have been kept, the records have been considered in verifying or adjusting values obtained from the map.

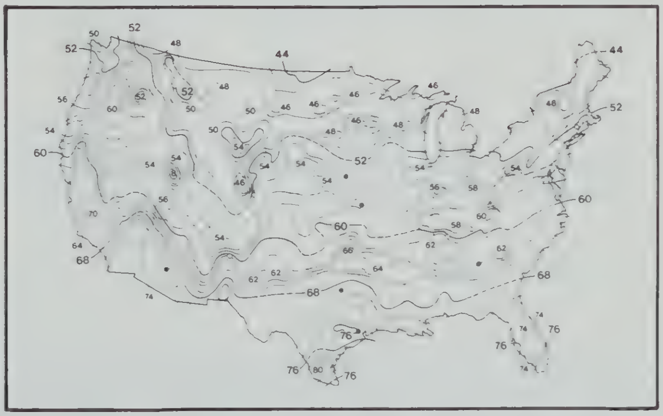

Fig. 1. Assumed T_m values, redrawn from a map of observed wellwater temperatures prepared by Doug Bacon, National Water Well Association. (Temperature given in °F; °C = (°F − 32)/1.8).

The form of Eqs. 1 and 2 shows that every degree by which T_m is misjudged results in a one-degree error in ground temperature estimate, regardless of depth. Assumed T_m for each of the five cities discussed here is indicated on the tables for those cities.

Surface temperature amplitude, A_s

All other things being equal, surface temperature amplitude* increases with latitude; many other factors complicate the relationship, however, so that no simple regional generalizations can be made. The values selected here have been estimated from records of nearby stations, as reported by Kusuda [8] and others. For soils of average thermal diffusivity, a difference of two degrees in amplitude at the surface creates a difference of one degree amplitude at a depth of 6 ft (1.8 m); therefore, a reasonable approximation of A_s is considered adequate.

---

* Maximum temperature minus mean temperature

Thermal diffusivity, α

Thermal diffusivity (thermal conductivity/heat capacity) is the most difficult parameter to determine in the ground temperature model because it varies with soil type, depth, moisture content, and, consequently, with time. Use of a carefully chosen constant α does, however, produce good agreement between predicted temperatures and field observations.

Analysis of observed ground temperature records by applying a least squares technique to Eq. 1 yielded thermal diffusivity values ranging from approximately 0.25 to 0.85 ft²/day (0.023 - 0.079 m²/day) [8]. The arithmetic average of 71 of these computed values is 0.508 ft²/day (0.047 m²/day). The authors performed cluster analysis to select average values from three groupings intended to represent soils of low, medium, and high thermal diffusivity. The results obtained were 0.33, 0.53, and 0.75 ft²/day (0.031, 0.049, and 0.070 m²/day). According to ASHRAE's characterizations [3], 0.26 ft²/day corresponds to a light, dry soil; 0.6 ft²/day to a heavy, damp soil; and 0.79 ft²/day to dense concrete.

Givoni [9] has used a graphic technique to analyze the attenuation of measured temperature amplitudes with depth. He reports that an envelope bounding the observed data is described by the expression

$$\frac{A_s}{A_x} = e^{-0.32x} \qquad (3)$$

for "humid" locations (Minnesota; Washington, D.C.; Kentucky), and by

$$\frac{A_s}{A_x} = e^{-0.48x} \qquad (4)$$

for "dry" locations (Texas, Israel, Egypt), where x here is given in meters. In the English system, Eqs. 3 and 4 correspond to thermal diffusivity values of 0.4 and 0.9 ft²/day, respectively. One would expect lower α in arid regions and higher α in soils of higher moisture content; however, since α can also be expected to vary locally with soil type, topography, and other factors, such a simple generalization cannot be used to predict regional distribution of thermal diffusivity. A constant α of 0.52 ft²/day (0.048 m²/day) has, therefore, been applied to all regions except Phoenix. Since Dallas and Phoenix share the same T_m and A_s values, a lower α of 0.33 ft²/day (0.031 m²/day) was assigned to Phoenix to allow comparison between the two locations.

Phase constant, t_o

The delay in phase of the ground temperature wave with respect to air temperature is largely responsible for the usefulness of the ground for cooling. Theory indicates that the minimum surface temperature should occur 1/8 cycle after minimum surface heat flux, on December 21 (in the absence of snow cover and latent heat exchanges). That is, December 21 + 45 days equals the 35th day of the calendar year. Although a sampling of stations analyzed by Kusuda exhibits an average phase constant of almost 35 days, individual stations may vary by 10 days or more to either side of the average. Moreover, plotting the predicted temperatures against observations sometimes shows a discrepancy of several weeks, with the observed ground temperature wave usually preceding the predicted wave (i.e., $t_o < 35$).

Large departures in t_o from the assumed norm of 35 days used in the tables are likely to be responsible for the greatest errors that can occur in using the theoretical model. Such fluctuations are especially important in comparing temperature events in the ground to long-term air temperature normals as an indication of relative benefit of above- and below-grade climatic conditions at any fixed time. It is recommended that users of the tables graphically plot the predicted temperatures and shift the $t = 35$ curve forward and backward in time so as to examine the possible range of ground temperatures resulting from conditions other than $t_o = 35$ (see Fig. 2).

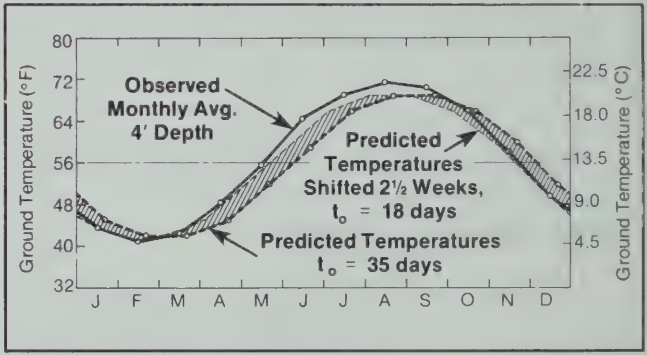

Fig. 2. Monthly averages of observed ground temperatures at the 4-ft (1.2-m) depth in Manhattan, Kans., are compared to predicted temperatures (Table 4) in the Kansas City vicinity, using $t_o = 35$. The relatively large difference between the curves is corrected by shifting the phase of the predicted temperatures by 2½ weeks, so that $t_o = 18$ days. Agreement is then within 3°F (1.726°C) for the entire year.

Earth Tempering as a Cooling Strategy

Earth cooling is one of 16 hypothetical climate control strategies, of which eight are identified for overheated conditions (Fig.3). Not all of these strategies are practicable, so the total list reduces to eight, seven of which are applicable to overheated conditions. Of the seven, three are strategies to minimize heat gain, and only four can be regarded as "cooling" in the sense of disposing of heat already present.

Givoni [10,11] has proposed a procedure whereby weather data can be analyzed to assess the relative appropriateness of ventilation, thermal mass, and evaporative cooling and the number of comfort hours when only shading is necessary (Fig. 4). Although soil temperatures cannot be analyzed directly by the Givoni method, the percentage of annual hours that

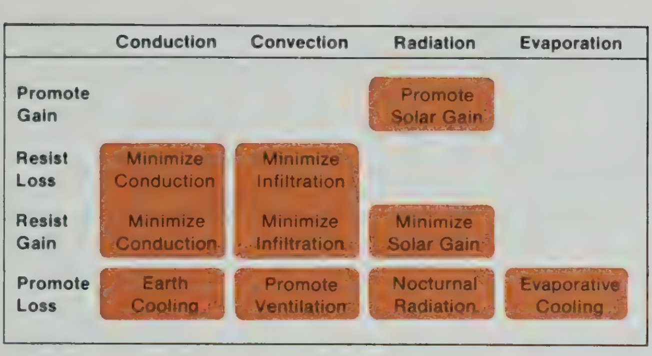

	Conduction	Convection	Radiation	Evaporation
Promote Gain			Promote Solar Gain	
Resist Loss	Minimize Conduction	Minimize Infiltration		
Resist Gain	Minimize Conduction	Minimize Infiltration	Minimize Solar Gain	
Promote Loss	Earth Cooling	Promote Ventilation	Nocturnal Radiation	Evaporative Cooling

Fig. 3. Earth cooling is one of 16 hypothetical climate control strategies, or one of 7 usable strategies for overheated periods. Some combinations of strategies are mutually beneficial while other combinations may act against one another.

synthesized ground temperatures or profile temperatures fall below, within, or above comfort limits can easily be counted and evaluated in parallel with the hours of effectiveness of other strategies. The simultaneous conditions presented in the tables then offer a way to assess whether ground cooling potential occurs at a useful time.

In using undisturbed ground temperatures for evaluation, it must be recognized that the soil surrounding a building or a device that exchanges heat with the ground will increase in temperature above predicted undisturbed levels. The temperatures given here, therefore, represent initial conditions and, as such, the lower limits of temperatures in the ground. Thus, if ground temperatures appear to be of marginal value for heat absorption in their undisturbed state, they are certain to be of no value for building cooling.

Earth tempering may be understood to include recessed placement and berming ("earth sheltering"), the use of earth-air heat exchangers ("earth pipes"), and sod roofs. The desirability of sod roofs is indicated in part through the appropriateness of thermal mass as a control strategy in the Givoni scheme. Not accounted for here is the evaporative cooling effect of a well-watered ground cover, which alone typically dissipates 75 percent or more of net solar radiation during summer months.

In application, earth sheltering practices usually complement or conflict with other climate control strategies. Past and present uses of cooling tunnels and shafts in the ground with evaporative sprays are well documented, as are fountains and water walls in courtyards, which may be recessed to serve as catch basins to collect cool, downward-draining nighttime

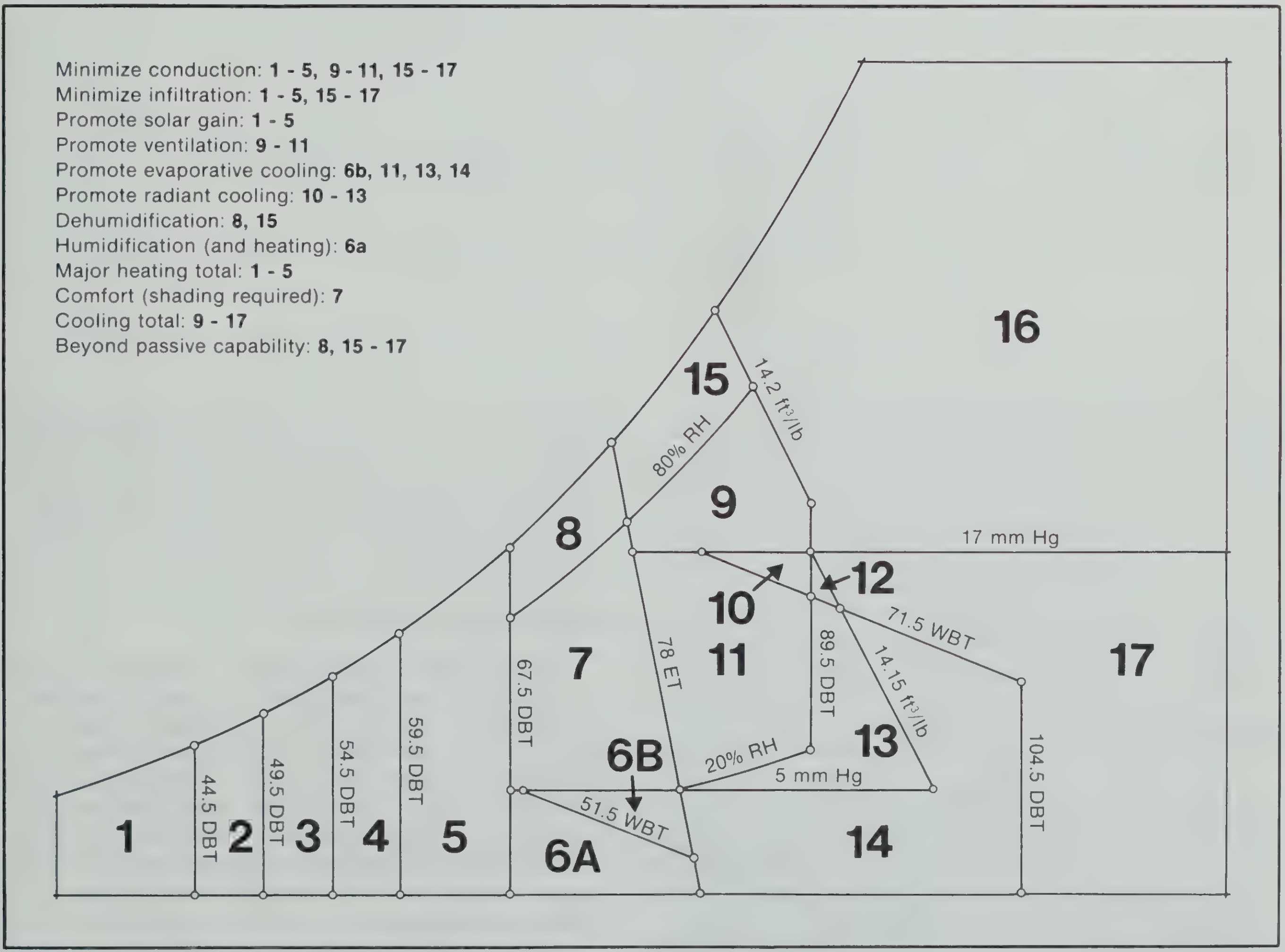

Fig. 4. The appropriateness of cooling strategies has been evaluated by plotting weather data on a modified version of Givoni's Building Bioclimatic Chart. Note that the cooling strategies overlap, so that the total hours of applicability of all of these exceed 100 percent (temperature given in °F; °C = (°F–32)/1.8).

City: Atlanta

T_m 62		Temperature on 21st Day of											
A_s 18		J	F	M	A	M	J	J	A	S	O	N	D
Air	Daily Max.	52	55	62	73	80	85	87	86	80	71	60	51
	Daily Avg.	43	46	52	63	70	77	78	77	71	61	49	43
	Daily Min.	34	36	42	53	61	68	70	68	62	50	39	34
Ground	2	49	48	50	55	61	68	73	75	74	69	62	55
	4	54	51	51	54	59	64	69	72	72	69	65	59
	6	57	54	53	54	57	61	66	69	70	69	66	62
	8	60	57	55	55	57	60	63	66	68	68	66	63
	10	61	59	57	57	57	59	62	64	66	66	66	64
	12	62	60	59	58	58	59	61	62	64	65	65	64
	15	63	62	60	59	59	59	60	61	62	64	64	64
Profile Avg. 0-6		51	49	50	55	60	67	71	74	73	69	63	57
Profile Avg. 2-12		58	55	54	55	58	62	65	68	69	68	65	62

Bioclimatic Analysis of Cooling Effectiveness, % Annual Hours

Heating Total		59.3
Comfort (Shading)		12.5
Cooling Total		17.2
Ventilation	14.2	
Thermal Mass	9.2	
Evaporative Cooling	7.1	
Beyond Passive Capability	12.7	

Ground Temperature Profile Ranges, % Annual Hours

	0-6 Profile	2-12 Profile
T<68	66	81
68<T<78	34	19
T>78	0	0

Summer Design Temperature (DBT), Air (With Coincident WBT)		
	5%	90/73
	2½%	92/74
	1%	94/74

Summer Design Temperatures (WBT), Air		
	5%	75
	2½%	76
	1%	77

City: Dallas

T_m 70		Temperature on 21st Day of											
A_s 20		J	F	M	A	M	J	J	A	S	O	N	D
Air	Daily Max.	55	61	68	78	84	92	96	95	86	77	64	57
	Daily Avg.	45	51	57	68	75	83	86	85	76	66	54	47
	Daily Min.	36	41	46	58	66	74	77	76	67	56	43	38
Ground	2	56	54	56	62	69	77	83	85	83	78	70	62
	4	61	58	58	61	66	73	78	81	81	78	73	67
	6	65	61	60	62	65	69	74	77	79	78	74	70
	8	67	64	63	63	64	68	71	74	76	76	75	72
	10	69	67	65	64	65	67	70	72	74	75	74	72
	12	70	68	66	65	65	67	68	71	72	74	74	73
	15	71	70	68	67	67	67	68	69	71	72	72	72
Profile Avg. 0-6		58	56	57	62	68	75	81	83	82	78	71	64
Profile Avg. 2-12		65	62	61	63	65	70	74	77	78	77	74	70

Bioclimatic Analysis of Cooling Effectiveness, % Annual Hours

Heating Total		48.8
Comfort (Shading)		12.7
Cooling Total		31.9
Ventilation	21.5	
Thermal Mass	15.6	
Evaporative Cooling	9.2	
Beyond Passive Capability	11.1	

Ground Temperature Profile Ranges, % Annual Hours

	0-6 Profile	2-12 Profile
T<68	45	42
68<T<78	28	58
T>78	27	0

Summer Design Temperature (DBT), Air (With Coincident WBT)		
	5%	97/75
	2½%	100/75
	1%	102/75

Summer Design Temperatures (WBT), Air		
	5%	77
	2½%	78
	1%	78

City: Houston

T_m 76		Temperature on 21st Day of											
A_s 18		J	F	M	A	M	J	J	A	S	O	N	D
Air	Daily Max.	62	67	73	81	87	92	94	94	89	82	71	65
	Daily Avg.	52	56	62	71	77	82	83	83	78	69	59	54
	Daily Min.	42	46	51	61	67	72	73	72	67	56	48	43
Ground	2	63	62	64	69	75	82	87	89	88	83	76	69
	4	68	65	65	68	73	78	83	86	86	83	79	73
	6	71	68	67	68	71	75	80	83	84	83	80	76
	8	74	71	69	69	71	74	77	80	82	82	80	77
	10	75	73	71	71	71	73	76	78	80	80	80	78
	12	76	74	73	72	72	73	75	76	78	79	79	78
	15	77	76	74	73	73	73	74	75	76	78	78	78
Profile Avg. 0-6		65	63	64	69	74	81	85	88	87	83	77	71
Profile Avg. 2-12		72	69	68	69	72	76	79	82	83	82	79	16

Bioclimatic Analysis of Cooling Effectiveness, % Annual Hours

Heating Total		39.0
Comfort (Shading)		6.6
Cooling Total		40.4
Ventilation	22.9	
Thermal Mass	1.4	
Evaporative Cooling	1.2	
Beyond Passive Capability	31.5	

Ground Temperature Profile Ranges, % Annual Hours

	0-6 Profile	2-12 Profile
T<68	27	0
68<T<78	31	64
T>78	42	36

Summer Design Temperature (DBT), Air (With Coincident WBT)		
	5%	92/77
	2½%	94/77
	1%	96/77

Summer Design Temperatures (WBT), Air		
	5%	79
	2½%	79
	1%	80

air [12]. Unfortunately, the earth-sheltered houses constructed in the past two years appear to have been designed with little regard for ventilation. Eager builders seem to have been willingly seduced by a belief that we have but to snuggle into Mother Earth to avert the often bewildering complexities of climate-responsive design. Like all design, earth tempering requires an integrated approach, one which is able to exploit the best of both surface and subsurface climates. This can be achieved only through study of simultaneous above- and below-ground conditions.

Presentation and Discussion of Data

Synthesized ground temperatures for five regions are presented in Tables 1–5, together with simultaneous surface temperature normals and ASHRAE design temperatures [13]. Also presented by region are the results of the building bioclimatic analysis of appropriate cooling strategies, in terms of the percentage of hours of the year that each is effective. The percentage of hours of the year in which undisturbed soil profile temperatures fall in the ranges of less than 68° F (20° C), between 68° and 78° F (20° and 26° C), and in excess of 78° F (26° C) are included here to relate earth sheltering to the other cooling strategies.

Each reader will interpret the data presented here in different ways, depending upon individual areas of interest and working needs. A detailed discussion of the results is not, therefore, considered necessary,* although some remarks are warranted.

Southern coastal zones

The Gulf Coastal Region is characterized by such high ground temperatures that even a fully subgrade wall is expected to experience profile temperatures in the 80s (° F) from the end of July through November. During October and November, profile temperatures exceed not only comfort limits but normal daily air temperature maxima as well. In Houston, ventilation is the only important passive cooling strategy; it is

---

* Discussion of the comparative data given here is contained in a larger report, "A Regional Analysis of Ground and Above-Ground Climate for Evaluating the Suitability of Earth Tempering Practices in Architectural Design," upon which this paper is based.

City: Kansas City

T_m 56 / A_s 24		J	F	M	A	M	J	J	A	S	O	N	D
Air	Daily Max.	36	44	52	67	76	84	89	86	77	67	50	39
	Daily Avg.	28	35	43	58	66	75	79	77	67	57	41	31
	Daily Min.	19	26	33	48	57	67	70	67	57	46	32	23
Ground	2	39	37	40	46	55	65	71	74	72	65	56	47
	4	45	42	42	45	52	59	66	69	69	66	60	52
	6	50	46	44	46	50	55	61	65	67	65	61	56
	8	53	49	47	47	49	53	58	61	64	64	62	58
	10	55	52	50	49	50	52	56	59	61	62	61	59
	12	57	54	52	51	51	52	54	57	59	60	60	59
	15	57	56	54	53	52	52	53	55	57	58	59	59
Profile Avg. 0-6		42	39	41	46	54	62	69	72	70	65	58	49
Profile Avg. 2-12		50	47	46	47	51	56	60	64	65	64	61	56

Temperature on 21st Day of

Bioclimatic Analysis of Cooling Effectiveness, % Annual Hours

Heating Total		64.2
Comfort (Shading)		13.6
Cooling Total		17.9
Ventilation	14.1	
Thermal Mass	10.4	
Evaporative Cooling	8.3	
Beyond Passive Capability	5.8	

Ground Temperature Profile Ranges, % Annual Hours

	0-6 Profile	2-12 Profile
T < 68	76	100
68 < T < 78	24	0
T > 78	0	0

Summer Design Temperature (DBT), Air (With Coincident WBT)	
5%	93/74
2½ %	96/74
1%	99/75

Summer Design Temperatures (WBT), Air	
5%	76
2½ %	77
1%	78

City: Phoenix

T_m 70 / A_s 20		J	F	M	A	M	J	J	A	S	O	N	D
Air	Daily Max.	65	70	75	85	94	103	105	102	97	86	72	65
	Daily Avg.	51	56	61	69	78	86	92	88	83	70	58	52
	Daily Min.	38	42	46	53	61	69	79	75	68	55	43	38
Ground	2	57	55	57	61	69	76	81	84	83	78	71	64
	4	63	60	59	61	65	71	76	79	80	78	74	69
	6	67	64	62	62	65	68	72	75	77	77	75	71
	8	69	67	65	64	65	67	69	72	74	75	74	72
	10	71	69	67	66	66	67	68	70	72	73	73	73
	12	71	70	68	67	67	67	68	69	71	72	72	72
	15	71	70	70	69	68	68	68	68	69	70	71	71
Profile Avg. 0-6		60	57	58	62	68	74	79	82	81	78	72	66
Profile Avg. 2-12		67	64	63	63	65	69	72	75	76	76	74	71

Temperature on 21st Day of

Bioclimatic Analysis of Cooling Effectiveness, % Annual Hours

Heating Total		44.7
Comfort (Shading)		12.9
Cooling Total		34.7
Ventilation	13.6	
Thermal Mass	27.6	
Evaporative Cooling	29.6	
Beyond Passive Capability	2.8	

Ground Temperature Profile Ranges, % Annual Hours

	0-6 Profile	2-12 Profile
T < 68	45	42
68 < T < 78	28	58
T > 78	27	0

Summer Design Temperature (DBT), Air (With Coincident WBT)	
5%	105/71
2½ %	107/71
1%	109/71

Summer Design Temperatures (WBT), Air	
5%	75
2½ %	75
1%	76

Tables 1-5. Synthesized ground temperatures for five regions are presented, together with simultaneous surface temperature normals and ASHRAE design temperatures. Also presented are the results of the building bioclimatic analysis of appropriate cooling strategies, in terms of the percentage of hours of the year that each is effective. Each reader will interpret the data presented in different ways, depending upon individual area of interest and working needs. (Temperature given in °F; °C = (°F – 32)/1.8)

required for more than 95 percent of the entire overheated period, or 54.4 percent of annual hours. Considering that the temperature of a 2- to 12-ft (0.6- to 3.6-m) profile exceeds 78° F (26° C) for 36 percent of the year and never falls below 68° F, (20° C), there seems to be little to recommend earth sheltering in Southern coastal zones. Design emphasis should be placed on optimizing ventilation effectiveness.

Humid and arid southern inland zones

Although isolated from the coast by 260 miles, (418 km), Dallas experiences humidity levels high enough to make ventilation its single most important cooling strategy. Ventilation is normally effective for 67.4 percent of the total overheated period, and it is the only means of comfort control for 11 percent of total overheated hours. While evaporation is effective for 9.2 percent of the cooling period, most of these hours overlap with ventilation hours; thus, given adequate ventilation, evaporative cooling is not a significant control strategy. Only thermal mass offers significant additional value, being effective for 15.6 percent of the overheated period and uniquely effective for 4.2 percent of the cooling period.

A shallow bermed or basement space [0- to 6-ft (0- to 1.8-m) profile] will experience ground temperatures exceeding comfort limits for 27 percent of the year, including the most overheated months of the year, July and August. The average undisturbed temperature of a deep profile [2 to 12 ft (0.6 - 3.6 m)] escapes temperatures above 78° F (26° C), although this limit is reached in September. For this same profile, 58 percent of annual hours are spent between 68° to 78° F (20° - 26° C). While undisturbed temperatures do not constitute a source of heat gain, neither do they offer a useful sink for an overheated interior space. Given the low cooling ability of the earth in such warm, mildly humid climates, it can be concluded that ventilating ability should be optimized. Moreover, if earth sheltered design compromises free ventilation, its overall effect can be counterproductive. Because fan-forced and passive-induced forms of ventilation and ground temperature modification techniques could override this conclusion, earth sheltering here seems to be of marginal value.

As in Dallas, ventilation is the most important cooling strategy in Atlanta. Proper ventilation can provide adequate cooling for 82 percent of overheated hours, and it is uniquely capable (among surface strategies) of attaining comfort conditions for 35 percent of overheated hours. Although neither deep nor shallow ground profiles exceed 78° F (26° C), their temperatures are not low enough to absorb significant amounts of heat from the interior. Given relatively high humidity levels, condensation could be a problem with subgrade walls and earth pipes.

The overwhelming effectiveness of ventilation clearly makes it the optimal design strategy in Atlanta. Earth tempering may be viewed as marginal in its applicability and, if achieved at the expense of reducing ventilating capability, it may be counterproductive.

Ground temperatures in the Phoenix area are very similar to those of Dallas. Although, for the sake of argument, a thermal diffusivity value of 0.33 ft^2/day (0.03 m^2/day) has been used in generating the Phoenix temperature table, the results are not markedly different from those when α equals 0.52 ft^2/day (0.048 m^2/day). Accordingly, the comments on the Dallas ground climate apply in Phoenix as well. The priorities of above-surface cooling strategies are quite different, however, so the usefulness of the ground can be viewed in a different light. Thermal mass and evaporative cooling, for instance, are favored for 77 percent and 83 percent of the overheated period. Ventilation is relatively unimportant; comfort conditions are attainable for 38 percent of overheated hours, only 5 percent of which are uniquely met by ventilation. Since earth tempering techniques are not incompatible with thermal mass and evaporative cooling strategies, the milder climate of the ground can be exploited without compromising other desirable design devices. Given this fact and the extreme temperature conditions prevalent throughout the Southwest, earth tempering should be a useful climate control agent here, especially if it is used to enhance other control strategies.

Midwestern region

Kansas City has an overheated period of 17.9 percent of annual hours. Its most important traditional cooling strategies are ventilation and thermal mass, which are normally able to meet comfort requirements for 78.7 and 58.1 percent of the overheated hours of the year, respectively. Since ventilation is an exclusive climate control strategy for 30 percent of the overheated period, its role is significant.

The earth remains relatively cool throughout the summer; deep profile temperatures range 15° to 20° F (8° - 11° C) below the daily air temperature average during July and August, and not until October does the 2- to 12-ft (0.6- to 3.6-m) profile average rise above the air temperature average. During these months also, undisturbed temperatures at the relatively shallow depth of 4 ft (1.2 m) fall about 20° F (11° C) below daily maxima. The deep profile average temperature never exceeds 65° F (18° C) and the shallow [0- to 6-ft. (0- to 18-m)] profile average rises above 68° F (20° C) for only 24 percent of the year.

Earth tempering offers valuable cooling potential in the Kansas City region, even though ventilation, mass, and evaporative cooling are theoretically able to meet normal comfort needs. Detailed analyses of individual buildings would be of interest to determine the self-sufficiency of earth cooling practices in this area.

Conclusion

The data presented here offer a way to assess the usefulness of earth tempering practices for cooling in a variety of regions. Although subgrade construction and the use of earth pipes and other devices show some merit in almost all regions, their value is frequently eclipsed in warm, humid areas by the need for maximum ventilation and by the likelihood of condensation. The value of earth cooling seems to be greatest in the more temperate parts of the country, where the carryover of winter cold is proportionately better able to satisfy less demanding summer cooling requirements.

The discussion presented here is not intended to be conclusive, in that numerous methods can lower and alter the phase of ground temperatures. The desirability of temperature modification techniques can be deduced from the ambient conditions predicted by the tables. An excellent review of several ground temperature depression practices is contained in Ref. 9. Insulation practices to enhance summer cooling in northern zones are discussed in Ref. 14, and fundamentals of ground climate and some control opportunities are described in Ref. 2.

A complete set of bioclimatic and ground temperature data for 29 locations in the United States appears in the project report, and summary data for 28 locations are published in Ref. 15. Design implications of the data are described in Ref. 16.

The final realization of cooling benefits from the ground will always be a matter of effective design. It is hoped that the data presented here contribute toward that end.

Acknowledgments

The regional bioclimatic analysis program from which data have been drawn for this paper was begun by the Office of Donald Watson, FAIA, under a contract with the National Association of Home Builders Research Foundation, with the cooperation of the U.S. Department of Housing and Urban Development. Expansion of the climatic analysis program to include development of a national ground temperature data base has been made possible through the sponsorship of Oak Ridge National Laboratory for the Innovative Structures Program of the U.S. Department of Energy. Computational support services of Bob Frew and Carl Williams of ARGA Associates of New Haven are greatly appreciated.

References

1. Kusuda, T. and Achenbach, P.R. "Earth Temperature and Thermal Diffusivity at Selected Stations in the United States. " *ASHRAE Transactions* 71, Part I: 1965.
2. Labs, K. "The Underground Advantage: Climate of Soils." *Passive Solar: Subdivisions, Windows and Underground,* 1981, Mid-American Solar Energy Complex, Minneapolis, Minn.

3. "Environmental Control for Survival." Chapter 12 in *ASHRAE 1978 Applications Handbook.* New York: 1978.
4. Standing Committee on Mechanical Engineering, Federal Construction Council. *Criteria for Underground Heat Distribution Systems.* Technical Report No. 66. Building Research Advisory Board, NCR/NAS. Washington, D.C.: 1975.
5. Kusuda, T. *NBSLD, The Computer Program for Heating and Cooling Loads in Buildings.* Building Science Series No. 69. Washington, D.C.: National Bureau of Standards, 1969.
6. Carslaw, H.S. and Jaeger, J.C. *Conduction of Heat in Solids.* Oxford: Clarendon Press, 1959.
7. van Wijk, W.R. and de Vries, D.A. "Periodic Temperature Variations in a Homogeneous Soil." In *Physics of Plant Environment.* Edited by W.R. van Wijk. Amsterdam: North-Holland Publishing Company, 1966.
8. Kusuda, T. *Least Squares Analysis of Annual Earth Temperature Cycles for Selected Stations in the Contiguous United States.* NBS Report 9493. Washington, D.C.: National Bureau of Standards, 1968.
9. Givoni, B. "Earth Integrated Buildings — An Overview." *International Expert Group Meeting on Passive and Low Energy Cooling, Heating, and Dehumidification.* Edited by A. Bowen. Miami: 1980.
10. Givoni, B. *Man, Climate and Architecture.* London: Applied Science Publishers, Ltd., 1976.
11. Milne, M. and Givoni, B. "Architectural Design Based on Climate." *Energy Conservation through Building Design.* Edited by D. Watson. New York: Architectural Record Books/McGraw-Hill Book Co., 1979.
12. Labs, K. "Terratypes: Underground Housing for Arid Zones." *Housing in Arid Lands: Design and Planning.* Edited by G. Golany. London: The Architectural Press, Ltd., 1980.
13. ASHRAE 1977 Fundamentals Handbook. New York: 1977.
14. Meixel, G.D., Shipp, P.H., and Bligh, T.P. "The Impact of Insulation Placement on the Seasonal Heat Loss through Basement and Earth Sheltered Walls." *Passive Solar: Subdivisions, Windows and Underground,* 1981, Mid-American Solar Energy Complex, Minneapolis, Minn.
15. Labs, K. and Watson, D. "Analysis of Weather Data for Determining Appropriate Climate Control Strategies in Architectural Design." *Proceedings of the 1981 Annual Meeting of the American Section of the International Solar Energy Society.* Philadelphia: 1981.
16. Watson, D. and Labs, K. *Climatic Design for Home Building.* Distributed by Donald Watson, FAIA, Box 401, Guilford, CT 06437: 1980.

Transparent and Opaque Louvers for Thermal Control in Passive Solar Buildings

Joseph K. E. Ortega, J. Michael Connolly, Carl E. Bingham,
Mark McDade, and Michael J. Holtz
Building Systems Development Branch
Solar Energy Research Institute
1617 Cole Boulevard, Golden, CO 80401

Abstract *The use of transparent and opaque louvers with thermal storage is described and investigated for passive thermal control and improved storage wall performance. The results of both experimental and analytical investigations provide information pertaining to the quality and quantity of thermal control and improved storage wall performance.*

Introduction

Once a passive building is constructed, its thermal behavior is controlled by its environment. In general, passive buildings are designed and sized to perform optimally for average design days. Weather conditions different from the average value result in larger or smaller loads and lower or higher room temperatures. Depending on the building design and the magnitude of the weather fluctuations, the room temperature variations can be larger than 10°C. The problem of temperature fluctuation is aggravated by the fact that in many passive designs (direct gain/single-zone, direct gain/two-zone, and attached greenhouse), the high temperatures occur during the day, when solar radiation is present in the room. Since human comfort is a function of air temperature, mean radiant temperature, and solar radiation, the presence of solar and thermal radiation requires a decrease in air temperature to maintain the same comfort level.

Thermal control is essential in passive solar buildings. There are few suitable and convenient methods available to control the temperature in passive buildings on an hourly or daily basis that do not use auxiliary heat from conventional sources (e.g., electric heaters, gas furnaces). One approach to thermal control in a passive solar building is to regulate the release of thermal energy from mass walls used for thermal storage. The use of a radiation and free convection shield (RFS) with any mass wall used mainly for thermal storage is one means of thermal control [1]. An RFS decreases heat flow into the room by reducing both thermal radiation and free convection from the storage wall surface to the room. When more heat is needed to maintain the desired room temperature, the RFS is removed or opened, partially or totally, depending on the amount of heat needed.

In addition to providing thermal control, an RFS can improve the thermal performance of masonry and water storage walls by increasing the impedance of heat transfer from the storage wall to the room during charging (periods of incoming solar radiation). Furthermore, the use of an RFS can improve the thermal performance of multizone passive designs. Although free convection can passively transfer energy from the south to north zone [2], this method is inadequate in many situations because of the small heat capacitance of air together with general difficulties in controlling and ensuring free convection patterns. An RFS used with a transfer wall [3] or water wall can significantly increase interzonal heat transfer by conduction through the storage wall separating the two zones.

Description

Louvers or sliding panels, parallel and adjacent to a storage wall but not in contact with it, are two forms of an RFS. Only louvers have been studied in this investigation. In a passive design, transparent louvers (transparent to solar radiation but opaque to thermal radiation) would be positioned adjacent to the south surface of the storage wall for direct gain/single-zone and direct gain/two-zone systems (Figs. 1a and 1b). Opaque (opaque to both solar and thermal radiation) or transparent louvers might be used on the north side of the storage wall for direct gain/two-zone and indirect gain/single-zone systems (Figs. 1b and 1c). Transparent (glass) louvers adjacent to the south surface, in the opened or closed position, would transmit solar radiation to the storage wall. The solar radiation would be absorbed by the storage wall and converted into thermal energy. When closed during charging (periods of incident solar radiation), transparent or opaque louvers would impede heat transfer (thermal radiation and free convection) from the storage wall to the room, allowing more energy to be stored for all systems shown in Fig. 1. A graduated increase in heat transfer could be achieved by partly opening the louvers. For the direct gain/two-zone design with a water or transfer wall [3], increased interzonal heat transfer could be obtained during charging by closing the transparent louvers on the south surface and opening the opaque

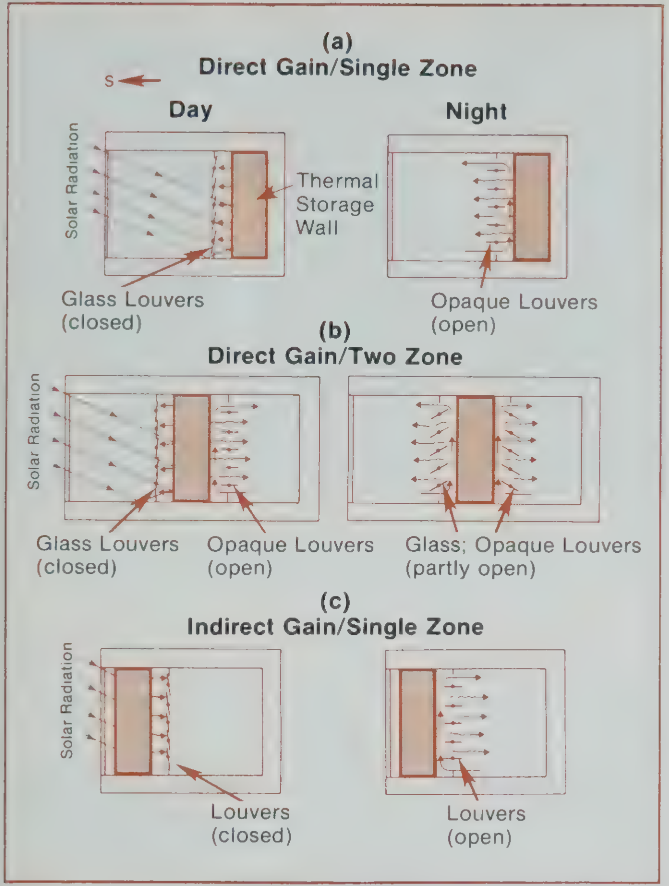

Fig. 1. Schematic illustration demonstrating the use of a radiation and free convection shield (louvers) to provide thermal control and improved storage wall performance for various passive building systems.

louvers on the north surface. Selective heating for the north or south rooms could be achieved simply by opening the louvers in the respective rooms.

In principle, the use of transparent and opaque louvers could provide temporal control of thermal energy discharged to the room, directional control of thermal energy discharged, graduated control over the rate of thermal energy discharged from the storage wall, improved interzonal heat transfer, and increased stored energy (in storage wall) per unit of incident energy.

In this investigation, we tested glass louvers in the indirect gain/single-zone system and demonstrated that glass louvers do impede heat transfer to the air space (room) when they are closed. A reduction in room temperature fluctuation caused by opening and closing glass louvers was demonstrated. Furthermore, we showed that during charging, closed louvers increase the amount of energy stored in the storage wall (per unit of incident energy). Various combinations of opening and closing louvers demonstrate the versatility provided by this method for temporal control of the room air temperature in periods of large and small thermal loads.

Materials and Methods

To test the use of louvers for thermal control, we constructed two identical test boxes, one experimental and one control. The inner dimensions of the test boxes are 0.91 m x 0.91 m x 0.91 m (3 ft x 3 ft x 3 ft) and they have hinged panels on the front (south) and back (north) sides (Figs. 2 and 3). During the day, the panels are lowered to allow solar radiation into the boxes from the south side and heat loss from an aluminum plate on the north side. The panels are closed at night. Polyurethane insulation (R-16) covers the outside of the boxes. A 9.2-cm (3.6-in.) thick concrete brick wall is located inside the boxes in one of three positions, depending on which system is being tested (direct gain/single-zone, direct gain/two-zone, indirect gain/single-zone). For the present study, the wall was positioned for an indirect gain/single-zone system (Figs. 1c and 3a).

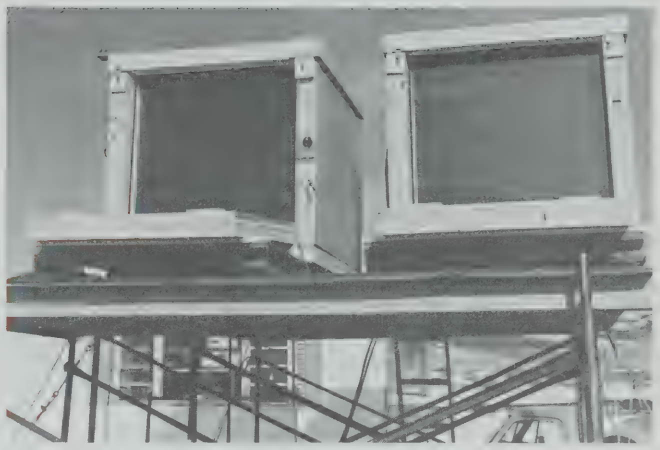

Fig. 2. Test boxes with south-facing panels open.

Glass louvers are positioned adjacent to the north surface of the storage wall in both test boxes (Fig. 3b). The louvers were opened and closed in one test box only. Each test box is instrumented with 16 type-T thermocouples, the location of which depends on the test being conducted.

Four types of tests were conducted: (1) tests to determine and compare the thermal behavior of the test boxes without louvers and with open louvers; (2) tests to determine the total load of the test boxes; (3) comprehensive tests and numerical analyses to determine the added thermal control and improved thermal performance provided by the use of glass louvers; and (4) tests of various louver opening and closing combinations to demonstrate the versatility of the louvers for temporal control of room air temperature. The temperatures were averaged and recorded on a Kaye digistrip II datalogger every 15 min during the day and every hour during the night. Although the thermocouple locations varied somewhat in the different tests, some measurements were common: room air temperature, ambient air temperature, storage wall temperatures, and wall temperatures of the test box. The room air temperature and ambient air temperature measurements were made with a thermocouple embedded in a radiation shield constructed so that the thermocouple is exposed to the air but not to the radiation environment. The thermocouples measuring ambient temperature were located behind the boxes so that they were shaded from direct solar radiation. The storage wall temperatures were measured by thermocouples on the surface of the wall and embedded in the wall. To calculate the average storage wall temperature, a poly-

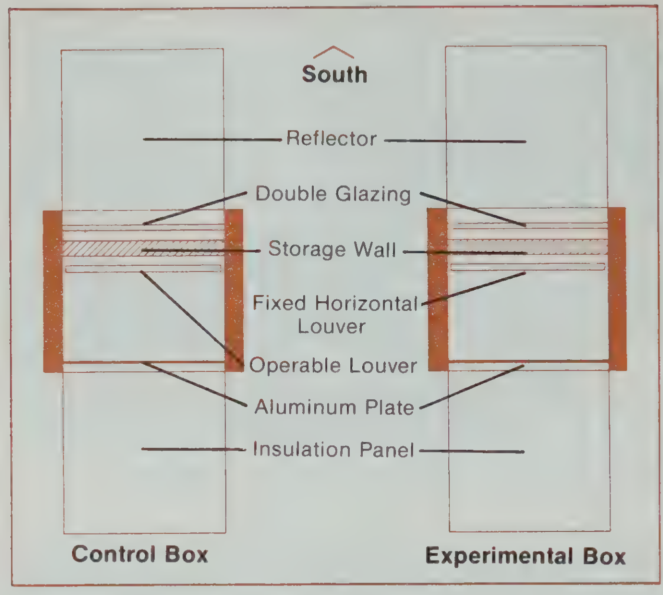

Fig. 3a. A plan-view of the test boxes.

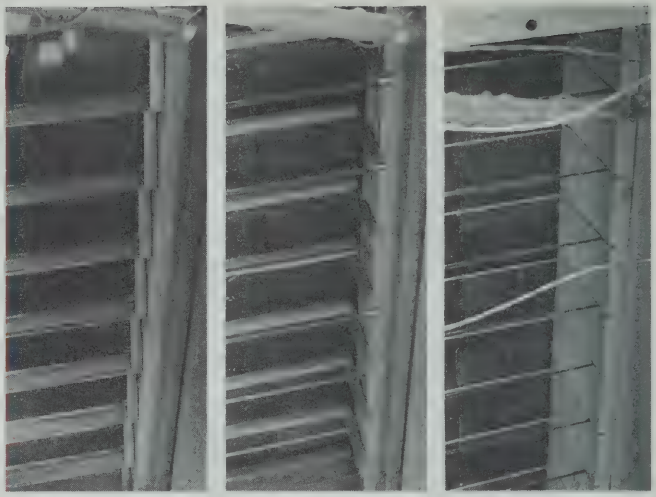

Fig. 3b. Louvers in the open and closed positions in the experimental box; stationary louvers in the control box.

nomial curve was fit to the temperature distribution through the storage wall; the temperature was then numerically integrated from surface to surface and divided by the thickness of the wall.

The added thermal control and the improved thermal performance provided by the glass louvers was determined by conducting comprehensive tests and numerical thermal analyses to define the detailed thermal behavior of the test boxes and the heat transfer paths within the test boxes. Three additional measurements were made for these tests: horizontal and vertical incident solar radiation and ambient wind speed. The thermophysical properties of materials used to construct the test boxes were also measured and used in the numerical thermal analysis; these values are presented in Table 1.

Infiltration was determined by an additional set of experiments, for which the storage wall and louvers were removed from the boxes. An electric heater with thermostat control placed inside the empty test box maintained a constant room temperature. The amount of energy consumed, the room air temperature, inside and outside wall surface temperatures, and the ambient air temperature were monitored. The experiments were conducted at night so that no solar radiation was incident on the test boxes. By selecting a reasonably long period (approximately two hours) when the ambient temperature is nearly constant we were able to calculate the total load (total UA) of the test box. This value reflects the sum of the conductance (UA) of each of the walls, the floor, and the ceiling plus infiltration. From the measured thermophysical properties presented in Table 1, the UA for the walls, floor, and ceiling can be calculated and summed. The difference between the total UA obtained from the tests and the summed UA (from Table 1) is the infiltration. A value for the infiltration was obtained by this method for the test boxes with front and back panels opened and closed.

The infiltration values together with the thermophysical data presented in Table 1, the horizontal and vertical solar radiation, and wind speed were used to generate the input for a detailed numerical thermal nodal model of the test boxes with glass louvers. The model has 24 nodes: 11 diffusion nodes (nodes with thermal capacitance), 11 arithmetic nodes (nodes without thermal capacitance), and 2 boundary nodes (nodes with infinite thermal capacitance). There are 52 conductors in the model that account for solid conduction through the storage wall and test box walls, and for internal and external convection and radiation.

The generalized, three-dimensional heat transfer computer program, MITAS, was used to obtain a transient solution for node temperatures and heat flows between nodes [4]. The MITAS program uses

	Solar Absorptivity		Infrared Emissivity		Thermal Conductivity (W/m°C)		Specific Heat (kJ/kg°C)		Density (kg/m³)	
Material	Measured	Model	Measured	Model	Measured	Model	Measured	Model	Measured	Model
Concrete brick	0.895-0.931	0.91	0.905-0.913	0.90	1.13	1.13	—	0.88	—	1470
Polyurethane	0.316-0.409	0.35	0.746-0.818	0.78	0.032*	0.032*	—	1.21	—	28.8
Plywood with white paint	0.282-0.300	0.28	0.884-0.886	0.90	—	—	—	1.21	—	545
Aluminum with black paint	0.918-0.956	0.91	0.753-0.851	0.85	—	202	—	0.88	—	2750
Glass	—	0.07	—	0.90	—	—	—	—	—	—

*Conductance for composite of 7.6-cm-thick polyurethane and 0.9-cm-thick plywood (W/°C).

Table 1. Thermophysical Properties

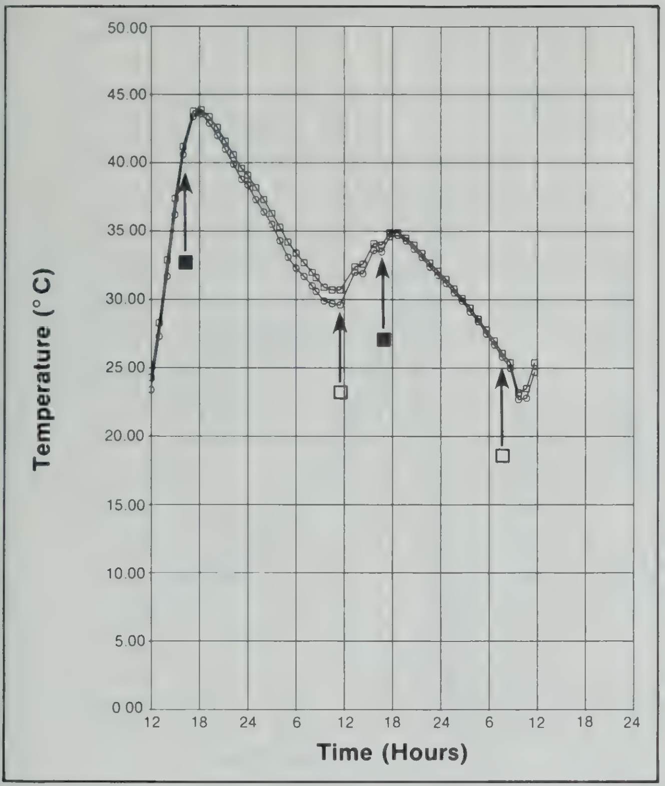

Fig. 4. Room air temperature of the test boxes without louvers as a function of time for two days. Front and back panels (south and north, respectively) are opened at 10:00 a.m. (not shown) and closed at 4:00 p.m. the first day, and opened at 11:35 a.m. and closed at 4:00 p.m. the second day. The arrow indicates when the panels are opened and closed. The symbol (☐) indicates opening the test boxes and the symbol (■) indicates closing the boxes.

finite differencing techniques (forward, backward, and forward-backward) to obtain the transient solution. The solution technique obtains a closed-form solution to a quartic equation for radiation conductors, thus eliminating the need to linearize radiation conductors. The surface properties used for external and internal radiation exchange are given in Table 1. Radiation exchange is calculated from each external surface to the ground and to the sky. The effective sky radiation temperature is calculated each time step with a subroutine whose algorithm is taken from Duffie and Beckman [5]. Radiation exchange inside the box is determined by means of the ERN technique [6]. The ERN technique was validated with a full graybody analysis, and the resulting temperatures correlated within 1°C.

Subroutines were used to calculate the free convection conductors as a function of temperature from vertical and horizontal surfaces within enclosures [7]. Forced convection from external surfaces was also calculated with a subroutine that uses an empirical relationship for the conductance as a function of the Reynolds number [7].

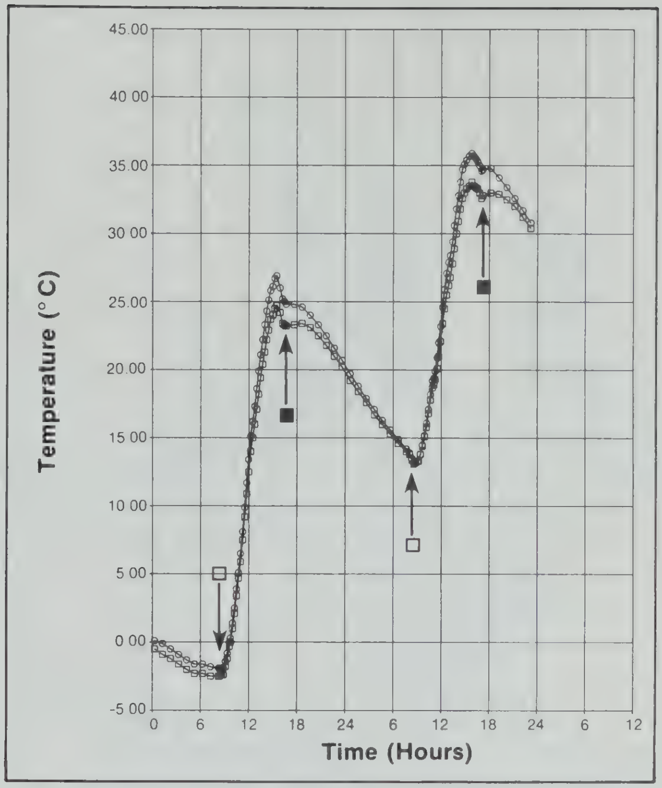

Fig. 5. Room air temperature of the test boxes with open louvers as a function of time.

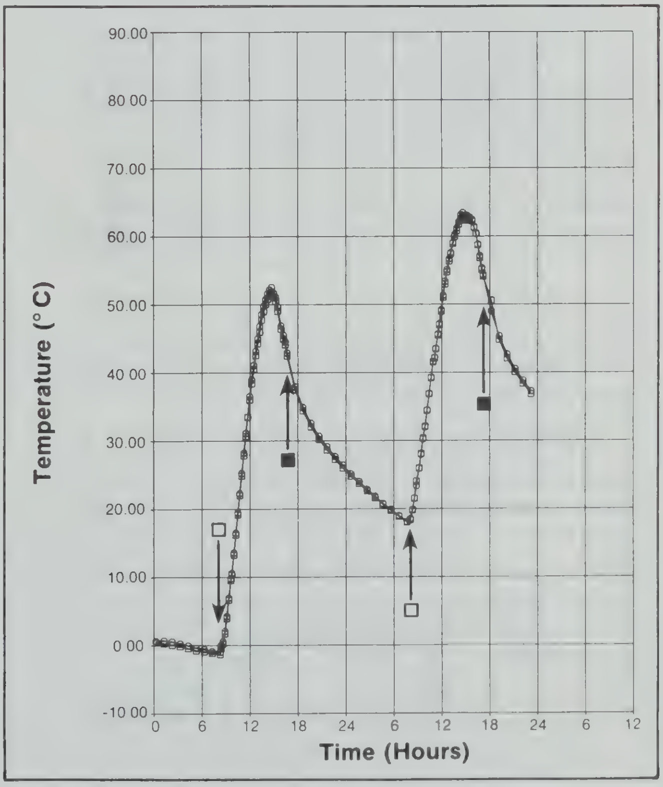

Fig. 6. Average storage wall temperature of the test boxes as a function of time for the same test and time period presented in Fig. 5.

Results

Figure 4 is a plot of the room air temperature of the test boxes without louvers as a function of time. The room air temperature behaviors of both boxes are nearly identical. Figure 5 demonstrates similar room air temperature behavior when louvers are added to the boxes but remain open. Figure 6 demonstrates

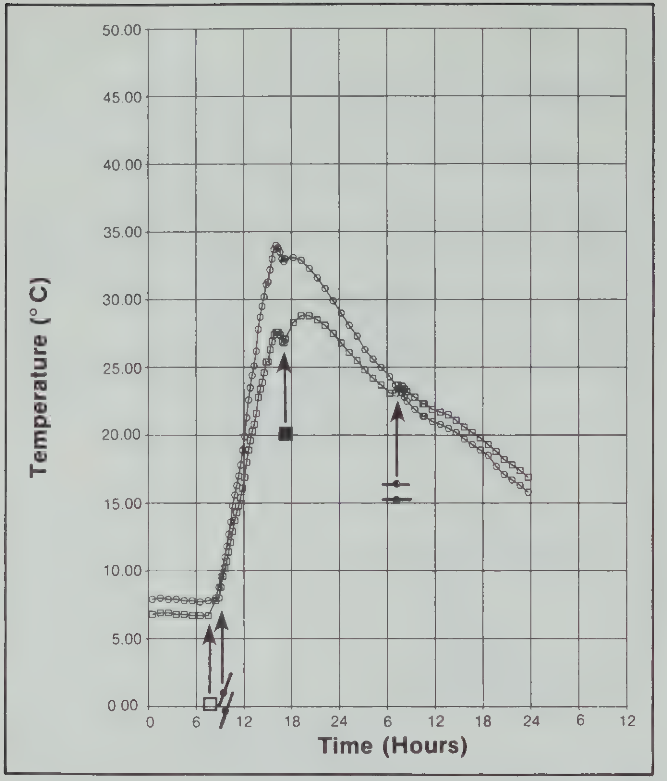

Fig. 7. Effect of opening and closing glass louvers on the room air temperature. Front and back panels of both boxes were opened at 8:20 a.m., and the glass louvers in the experimental test box were closed at 9:30 a.m. The front and back panels were closed at 5:00 p.m. The glass louvers in the experimental box were opened again at 7:00 a.m. the following day. The symbol (//) indicates closed louvers and the symbol (≑) indicates open louvers.

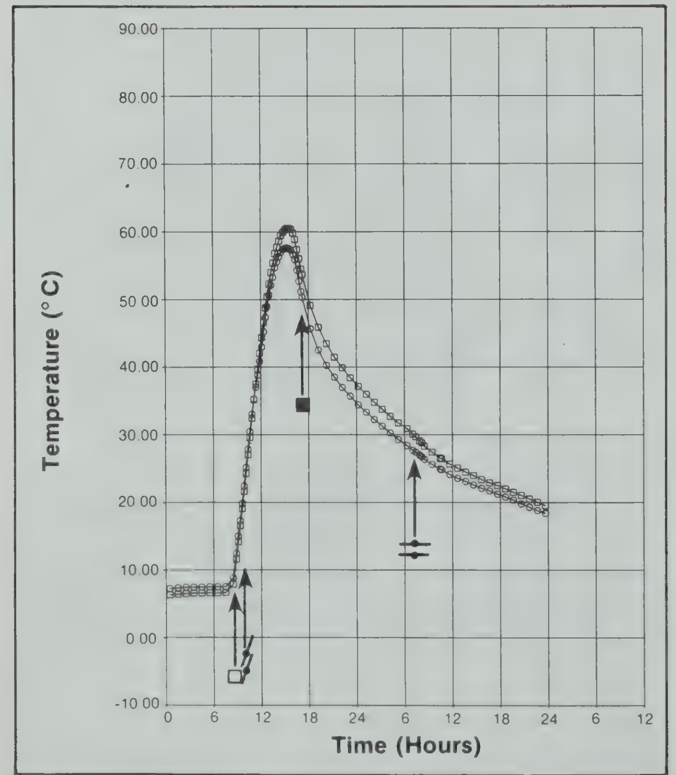

Fig. 8. Average storage wall temperature of the test boxes for the test and time period presented in Fig. 7.

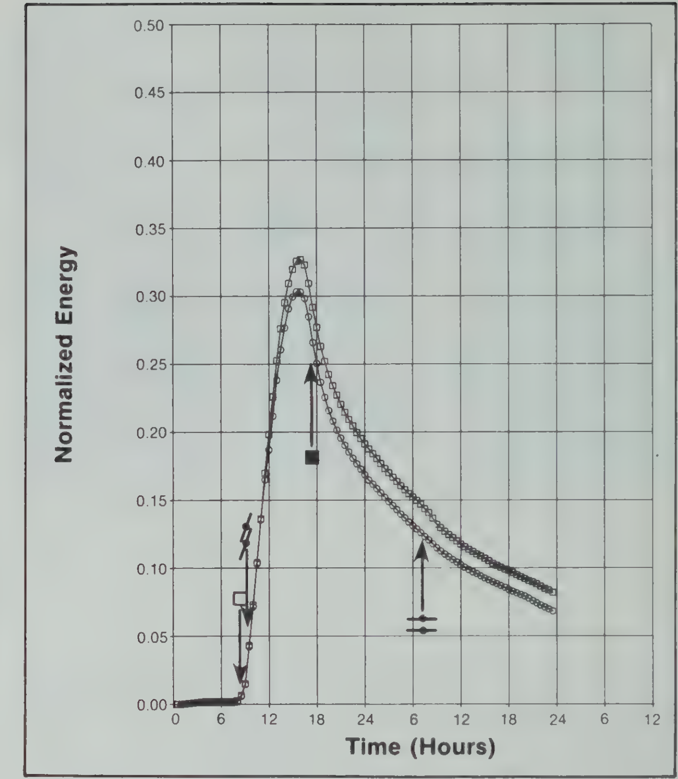

Fig. 9. The energy stored in the storage wall, minus the energy previously stored, normalized by the total incident solar energy. The data were obtained from the tests used in Figs. 7 and 8.

that the average storage wall temperatures of both boxes are also nearly identical when they are plotted as a function of time. Other plots, not presented here, show that the temperature behavior of the front and back storage wall surfaces and other test box components are also nearly identical. The temperatures for respective test box components and surfaces never differed by more than 2° C and on the average differed by less than 1° C.

Because of the similar temperature behavior of the test boxes, the altered temperature behavior caused by opening and closing the louvers can be evaluated by comparing the results of the experimental test box (with louvers that open and close) to those of the control test box whose louvers remain open. Figures 7 and 8 demonstrate the effect of closing the louvers during charging and opening the louvers during discharging. Figure 7 plots room air temperature as a function of time for both the experimental and control test boxes. The glass louvers were closed at the beginning of the first charging cycle (9:30 a.m.). The results show that at peak temperatures, the room air temperature for the experimental test box was lower than that of the control test box by more than 5° C. Thus, the closed louvers help to prevent overheating during charging. At 7 a.m. the next morning the glass louvers were opened and the room air temperature increased. The thermal energy not released to the room during charging is stored in the storage wall for future discharge (Fig. 8). Plots of the average temperature of the respective storage wall versus time for both the experimental and control test boxes demonstrate that the average temperature of the storage wall in the experimental test box was higher than that

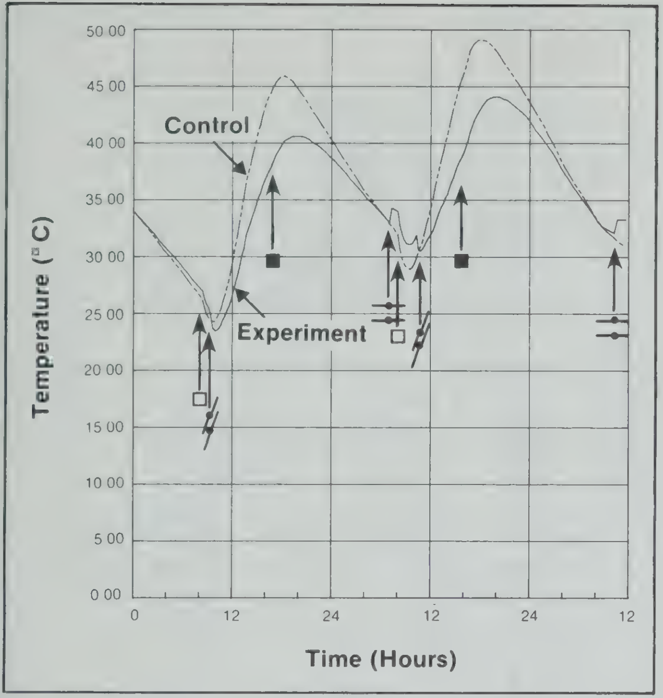

Fig. 10a. The effect of opening and closing glass louvers over a 2-day period. Front and back panels were opened at 8:15 a.m. the first day; the glass louvers were closed in the experimental box at 9:15 a.m. The panels were closed at 4:45 p.m. that same day and remained closed until 7:00 a.m. the second day. The louvers were opened between 7:00 a.m. and 10:30 a.m. the second day, then closed for the remainder of the day and night. The front and back panels were opened at 8:00 a.m. and closed at 4:20 p.m. the second day.

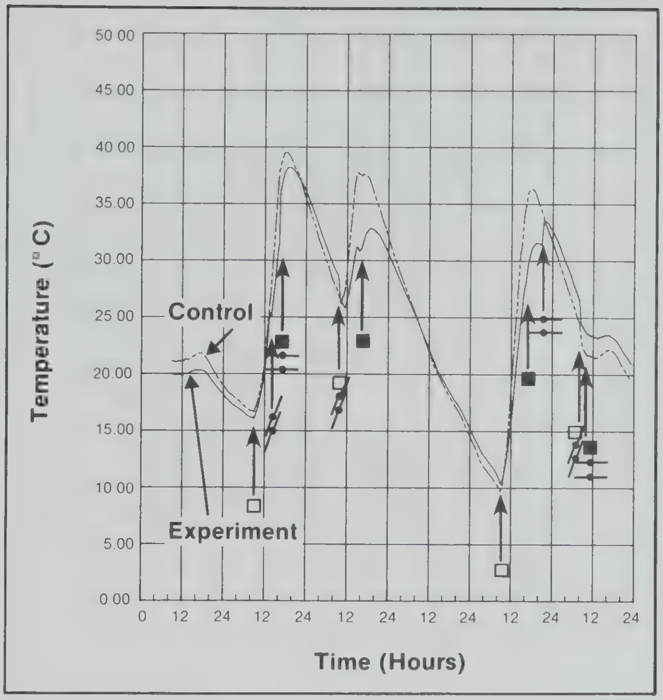

Fig. 10b. The effect of opening and closing glass louvers on the room air temperature over a 6-day period. The front and back panels were opened at 8:45 a.m. and closed at 4:15 p.m. the second day. The glass louvers in the experimental box were closed at 1:30 p.m. and opened again at 4:15 p.m. the same day. The glass louvers were closed and the front and back panels were opened at 9:30 a.m. the third day. The panels were closed at 4:00 p.m. that day. The glass louvers in the experimental box remained closed through the third, fourth, and fifth days. The glass louvers were opened again at 9:00 p.m. the fifth day. The front and back panels were opened and closed at 8:15 a.m. and 6:15 p.m., respectively, the fifth day. The glass louvers were closed and opened and the panels were opened and closed for one hour (between 8 and 9 a.m.) on the sixth day.

in the control test box, both during and after charging. Since the capacitance of both storage walls is the same, the higher temperature indicates more stored energy.

The energy stored in the storage wall, normalized by the integrated total incident solar energy (during charging), is plotted against time in Fig. 9. The results show that a larger percentage of the incident solar energy was stored during and after charging when the louvers were closed. Thus the performance of the storage wall improves with the use of louvers.

Various opening/closing louver scenarios were tested to demonstrate the temporal control provided by the use of louvers. Figure 10 (a & b) plot room air temperature as a function of time and demonstrates the effect of a variety of opening/closing louver scenarios. In general, opening and closing the glass louvers reduces the magnitude of room air temperature fluctuations, in some cases by as much as 44 percent. Thus, the glass louver provides a significant amount of thermal control.

A later investigation, which studied the effect of the thermophysical properties of the construction material on the impedance provided by an RFS [1], demonstrated that glass provides a smaller impedance than almost any other louver construction material.

Materials such as polished aluminum can provide two-and-one-half times the thermal impedance of glass. Certain combinations of materials can provide over four times the impedance of glass. To assess the control and improved storage wall performance provided by more effective louvers, a detailed numerical thermal nodal model was constructed for the test boxes. All inputs used in the simulation were obtained from measured data. Figures 11 and 12 present the room air temperature, T_r, and the average storage wall temperature, T_{sw}, calculated by the numerical simulation program (solid line) for the time period for which results are presented in Figs. 7 and 8. Also plotted on the figures are the test results; comparison shows that the simulation results correlate very well with the test results. The energy stored in the storage wall, normalized by the integrated total incident solar energy versus time (calculated from the simulation), is presented in Fig. 13 together with the test results. Again, the correlation is good.

With this validated numerical thermal model of the test box, we determined the effect of using louvers

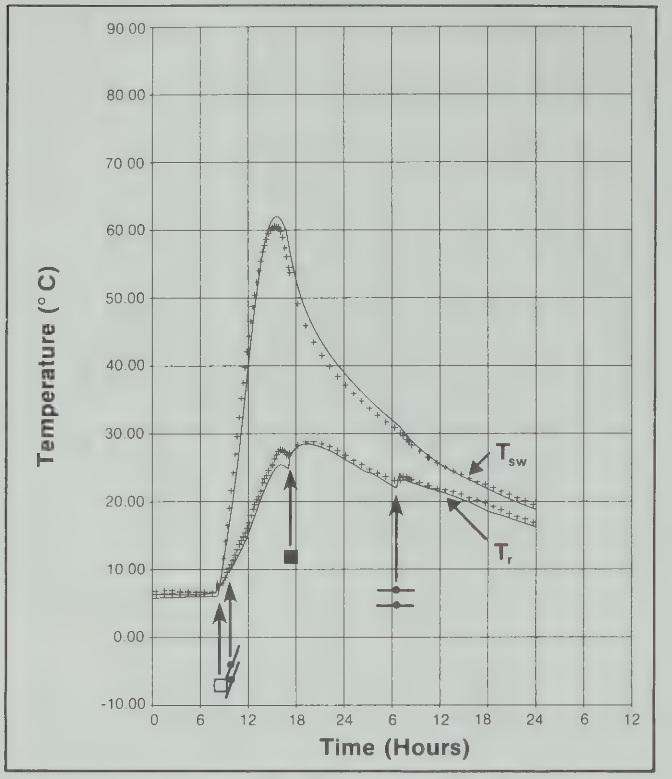

Fig. 11. Correlation between numerical simulation (solid line) and experimental results (data points, ++) for the room air temperature, T_r, and the average storage wall temperature, T_{sw}. The results presented are for the experimental test box with opening and closing glass louvers.

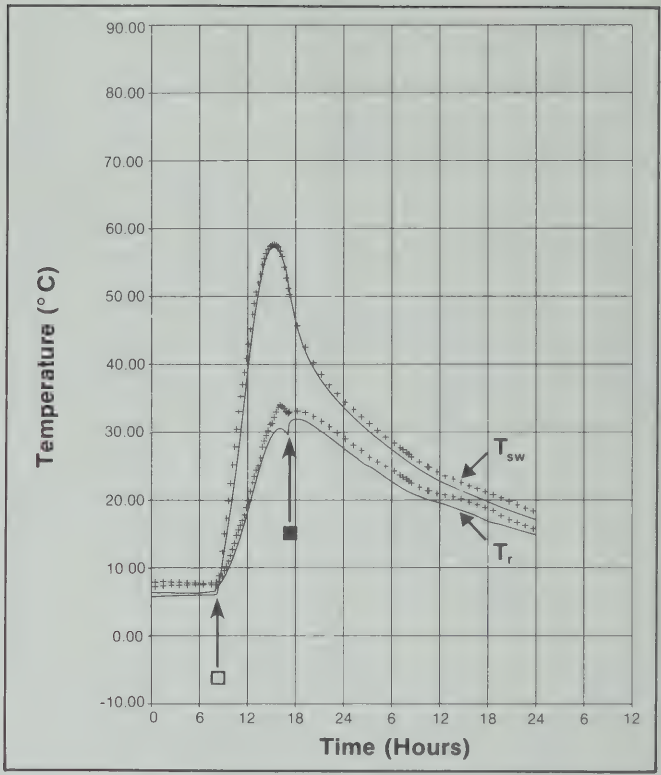

Fig. 12. Correlation between numerical simulation (solid line) and experimental results (data points, ++) for the room air temperature, T_r, and the average storage wall temperature, T_{sw}. The results presented are for the control test box with permanently opened louvers.

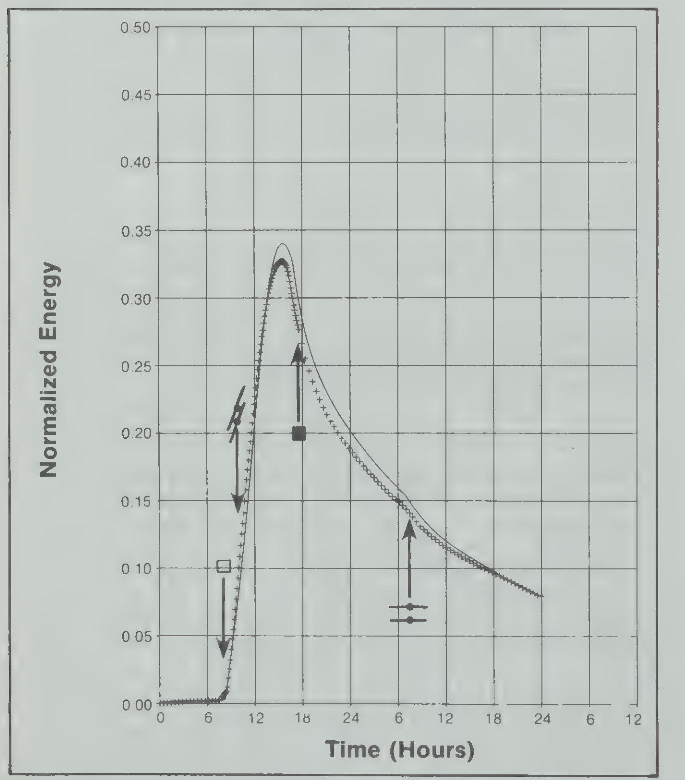

Fig. 13a. Correlation between numerical simulation (solid line) and experimental results (data points, ++) for the energy stored normalized by the total incident solar energy for the experimental test box.

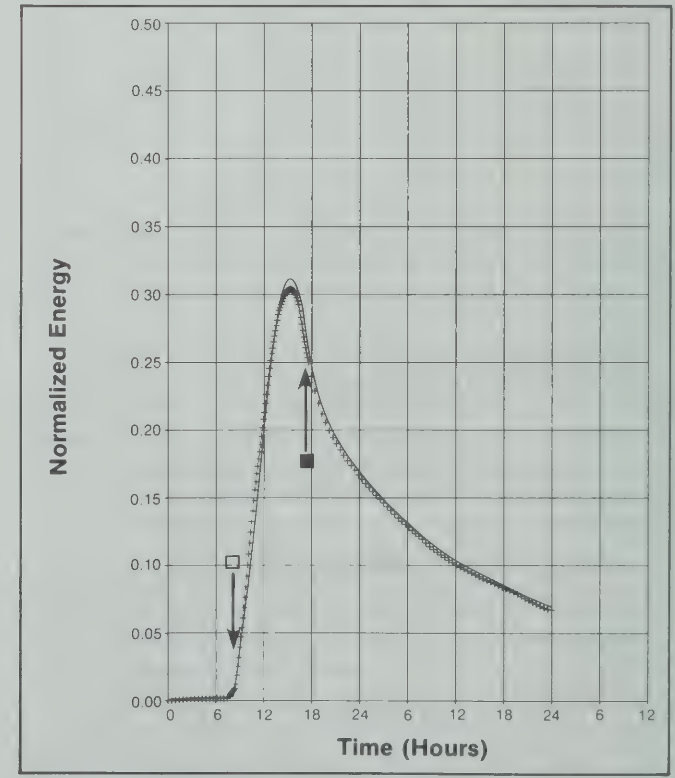

Fig. 13b. Correlation between numerical simulation (solid line) and experimental results (data points, ++) for the energy stored normalized by the total incident solar energy for the control test box.

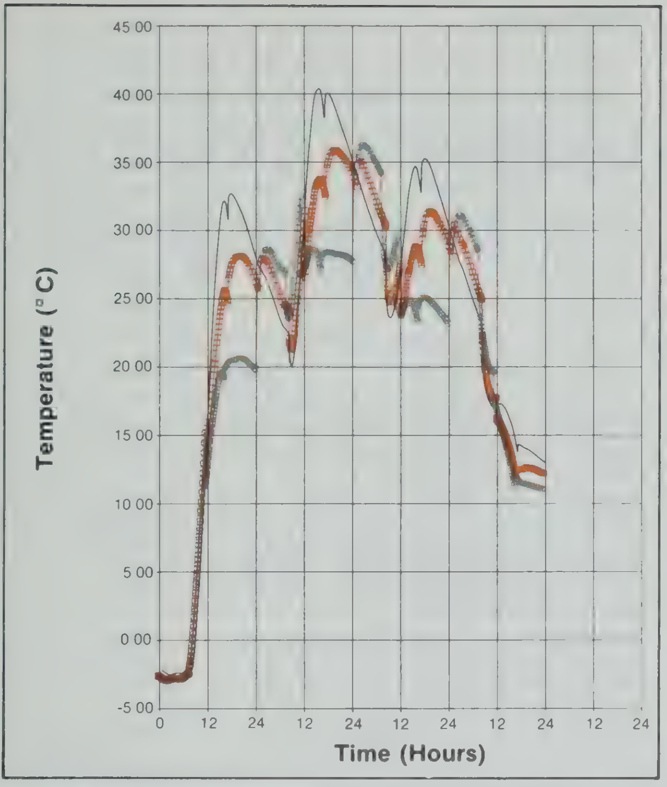

Fig. 14. The effect of opening and closing louvers on the room air temperature over a 4-day period, calculated by the validated numerical simulation model: control (solid line), glass louvers (□), and aluminum louvers (O). The louvers are closed at 12:00 noon every day and opened at 1:00 a.m. every morning. The front and back panels are opened at 8:00 a.m. and closed at 5:00 p.m. every day.

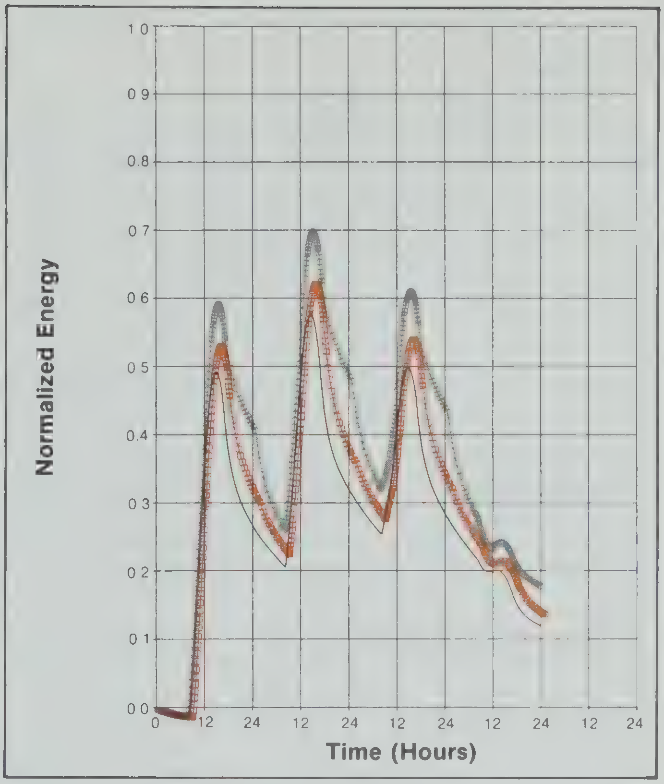

Fig. 15. The effect of opening and closing louvers on the normalized stored energy (of the storage wall), calculated by the validated numerical simulation model: control (solid line), glass louvers (□), and aluminum louvers (O). The results are for the same test and time period whose results are presented in Fig. 14.

that provide larger impedance. Figure 14 presents the room air temperature versus time for two louver designs. Also plotted for comparison is the room air temperature of the control (louvers remain open). The results show that the opening and closing of glass louvers significantly reduces the temperature fluctuation, however even more control is obtained with thin, polished aluminum. Figure 15, which presents the normalized storage wall energy versus time for the same two cases, demonstrates that more energy is stored during charging using louvers, and that using aluminum louvers can improve the normalized stored energy by more than 12 percent. Other louver designs are shown to provide almost twice the impedance of polished aluminum [1], but these louver designs could not be easily simulated in the numerical thermal model.

Conclusions

The ability to control room air temperature is essential to building design. Obviously, hybrid systems offer a completely solar alternative, but often the active component of the total solar system is expensive. The use of an RFS with massive walls used for thermal storage can provide a cheaper and totally passive (unless the operation of the panels or louvers is automated) solar alternative to thermal control.

This study investigated the use of a radiation and free convection shield (RFS), in the form of louvers, both experimentally and analytically, for both passive thermal control and improved storage wall performance. The experimental results show glass louvers can produce a considerable amount of temporal control over room air temperatures and that opening and closing the glass louvers can reduce the room air temperature fluctuation by as much as 44 percent. When the glass louvers are closed during charging, more energy is stored in the storage wall for future use, typically about 5 percent of the incident energy. Thus, the use of louvers also improves the efficiency of the storage wall. Numerical simulations using a thermal nodal model, validated with test results, demonstrate that aluminum louvers can provide even more thermal control (aluminum louvers provide more than twice the thermal impedance of glass louvers) and further improve the efficiency of the storage wall (13 percent more of the incident energy is stored).

The improved thermal storage performance when the RFS is closed during charging provides the basis for ongoing investigations related to cost and thermal tradeoffs. Examples of these tradeoffs are (1) possible reductions in the mass and volume of the storage wall allowed by use of the RFS and (2) possible reductions of the area of south glazing allowed by use of the RFS, thus reducing the building load and perhaps eliminating the need for movable insulation in some cases.

The investigation described here indicates that the use of an RFS with mass walls can add two attractive features to passive solar buildings: temporal control of room air temperature without the use of auxiliary heat from conventional sources and improved storage wall efficiency. Other potential benefits have not been demonstrated and are the subject of ongoing and future investigations: directional control of thermal energy discharge, graduated control over the rate of thermal energy discharge, and improved interzonal heat transfer. Present investigations are concerned with full-scale assessments and cost benefits that can result from using an RFS with mass walls. Both the demonstrated temporal control and improved storage wall efficiency may provide real cost benefits to the user, in addition to the many comfort benefits that are more difficult to assess in terms of cost.

The results of these investigations will contribute to the complete thermal characterization and detailed understanding of the RFS system. The final results will be reported in a format that will provide guidance for integrating an RFS system into building systems and optimizing cost and thermal tradeoffs. In addition, a simplified algorithm for the thermal behavior of the RFS system will be developed for incorporation into a variety of simulation codes.

References

1. Ortega, Joseph K. E. *Radiation and Free Convection Shield for Passive Thermal Control.* SERI/TP-721-682, 1980, Solar Energy Research Institute, Golden, Colo.
2. Wray, William O. and Weber, Dennis D. "Hot Zone/Cold Zone: A Quantitative Study of Natural Heat Distribution Mechanisms in Passive Solar Buildings." *Proceedings of the 4th National Passive Solar Conference.* 1979, pp. 226-230.
3. Ortega, Joseph K. E., Bingham, Carl E., and Connolly, J. Michael. "Performance of Storage Walls with Highly Conductive Covering Plates and Connecting Fins." *Proceedings of the ASME 19th National Heat Transfer Conference,* Orlando, Fla. 1980. SERI/TP-721-574, 1980.
4. Conner, R. J. et al. *Martin Interactive Thermal Analysis System (MITAS).* MDS-SPLPD-71-FD238. Denver, Colo.: Martin Marietta Corporation, June 1971.
5. Duffie, J. A. and Beckman, W. A. *Solar Energy Thermal Processes.* New York: John Wiley and Sons, 1974.
6. Chapter, J. J. and Connolly, J. M. "Simplified Radiation Analysis Using Modularized Enclosures." *Journal of Spacecraft and Rockets* 8 (No. 9), Sept. 1971.
7. McAdams, William H. *Heat Transmission.* 3rd ed. New York: McGraw-Hill Book Company, 1954.

New Mexico Solar Greenhouse Study

W. Scott Morris and Clair Reiniger
P.O. Box 4815, Santa Fe, NM 87502

Abstract *Throughout New Mexico, attached solar greenhouses have proliferated since innovators in passive solar applications perfected the technology in the late 1960s and early 1970s. Current popularity has been accelerated by escalating fuel costs and increasing interest in self-help and self-sufficiency movements. A community study team of New Mexico residents interviewed 150 solar greenhouse owners from March to October 1979 to obtain information on the social/community, technological, legal/political, and economic/financial aspects and impacts of solar greenhouses. This report presents a user experience and attitude profile as well as an economic analysis of questionnaire data. Most solar greenhouses surveyed produce heat at a cost that compares favorably with present conventional fuel costs and have simple payback periods of four to eight years. The study indicates that there are no serious barriers to solar greenhouse technology, although increased education, greater tax incentives, and low-interest loans would stimulate greater use of solar greenhouses by low-income residents.*

Introduction

New Mexico, a land of long, cold winters but plentiful sunshine, has witnessed a blossoming of the solar greenhouse. Escalating costs for heating fuels and a growing self-help and self-sufficiency movement within the state have contributed to the proliferation of solar greenhouses, particularly in the colder mountainous sections of the state.

Some of the first intentional solar greenhouses were built in the early 1970s in the Taos, New Mexico, area by Tom Watson, a local inventor. However, the solar greenhouse became most popular through the work of Bill and Susan Yanda. The idea of a food-and-heat-producing attached solar greenhouse occurred to the Yandas when they observed the thermal performance of their pit greenhouse during one of the coldest winters in northern New Mexico. "Why not help heat your home with that excess heat instead of venting it to the outside?" To date, the Yandas have built more than 30 greenhouses in New Mexico, mainly through workshops carried out in the "barn raising" style.

Solar enthusiasts in New Mexico have found a focal point in the New Mexico Solar Energy Association (NMSEA) since the early 1970s. Since the spring of 1977, NMSEA, with the Yandas' encouragement, has been introducing and building solar greenhouses in the state. NMSEA has organized over 40 solar greenhouse construction workshops with homeowners, community groups, and local institutions. Because of the perseverance of a handful of solar advocates, the New Mexico solar tax rebate was passed in 1975. It was the first legislation of its kind in the United States; both active and passive solar systems are covered in the regulations.

As a result of the efforts of NMSEA and a growing interest in solar energy, solar associations have sprung up all over New Mexico. Local solar associations (Alamogordo, Roswell, Silver City, Albuquerque, Santa Fe, Taos, Las Vegas, El Rito, Shiprock), together with many other individuals (see Acknowledgments), cooperated in gathering data for the *New Mexico Solar Greenhouse Study*, conducted from March to October 1979.

The major portion of the study was funded by a government agency seeking information on the social, technological, and economic aspects and impacts of solar greenhouses. Early in the project, a community study team of 18 members was organized to (1) develop study objectives; (2) develop a questionnaire for solar greenhouse owners; (3) conduct personal interviews with greenhouse owners; (4) draft reports on the historical, legal, political, economic/financial, and social factors of the study; and (5) act as reviewers for the draft and final reports. Each team member developed a list of greenhouse owners in his or her region, seeking a representative sample of interviewees.

The team then compiled information on over 150 solar greenhouses, conducting detailed interviews to obtain direct information from the technology end-users. The 100-question interview explored, documented, and assessed who builds solar greenhouses and why; what financial, social, legal, and technical barriers greenhouse owners and operators face; and how solar greenhouses perform in terms of producing heat and food. In addition, recommendations for the evaluation of greenhouses on local, state, and national levels were made. The following paper sum-

According to the *New Mexico Solar Greenhouse Study*, rising fuel costs and a growing self-reliance trend have accelerated the proliferation of attached solar greenhouses in the state.

marizes the findings of the *New Mexico Solar Greenhouse Study*.

A wealth of information was uncovered during the course of this project. Aside from the detailed analyses of many facets of solar greenhouses, the *New Mexico Solar Greenhouse Study* is a portrait of an appropriate technology that, born of local needs, has already decided to run away from home.

Questionnaire Respondents*

Although a great variety of people were interviewed during the survey, most solar greenhouse owners were Anglo white-collar workers. Equal numbers of males and females were interviewed. On the whole, respondents were not solar advocates; 59 percent of the interviewees were not involved with solar energy groups or programs, and 79 percent did not participate in a greenhouse workshop before building their greenhouses. The interviewees were "do-it-yourself" types; most had designed and built their own greenhouses.

With solar greenhouses, the process is an integral part of the experience. Both the NMSEA and Yanda workshops have strongly emphasized the "do-it-yourself" concept, which has given people the confidence to "give it a try." Owners avoided institutional support; most respondents paid for their greenhouses with out-of-pocket cash and did not file for a state tax rebate. Most interviewees appeared to enjoy "just doing it on my own," as one interviewee said. When asked what factors inspired them to build their greenhouses, 81 percent checked "saving on heat," 59 percent checked "horticultural interests," 55 percent marked "saving on food," and 53 percent said "having a nice sunspace."

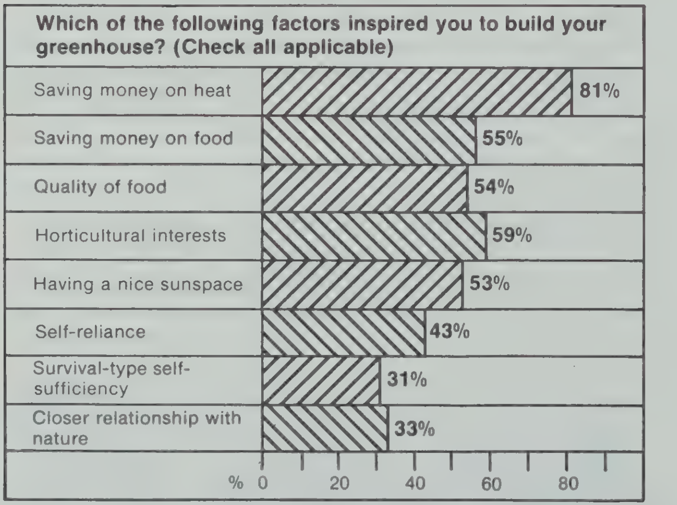

Increased self-reliance and a closer relationship with nature were also important to the interviewees. Many people who become involved with solar energy do so because they want to be more self-sufficient; it's only natural that such people would avoid institutional involvement. As one interviewee said, "It is very important for the American people to take personal responsibility for their fuel needs . . . solar greenhouses are an excellent step toward a sane community."

Low-income people and cultural groups, such as the Hispanics and Native Americans, have been reached through the Yanda and NMSEA workshops, where building costs are reduced by the provision of materials or labor. Eleven percent of the interviewees built their greenhouses through a workshop.

The Hispanic and Native American cultures are very traditional; process and time are very important when new technologies are introduced to these groups. For example, a solar greenhouse was built over several months in a small Navajo community. Since the sun is very important in the Navajo religion, a medicine man was asked to bless the structure. A great deal of time was spent with the Navajos in working out the planting design for the greenhouse. Vegetables were planted in raised container beds, and planting schedules were outlined. However, the appropriate technologist working with the group returned a few months later to find that all the containers had disappeared, and the ground had been dug up and planted. The Navajo women working in the greenhouse explained that they did not think it was natural to plant in boxes; seeds belonged in the ground. They had also decided to let all the plants die during the winter because "growing things in the winter was not right. Everything has a certain time and season." This greenhouse is, however, extremely productive in spring, summer, and fall.

Solar greenhouses have proliferated on the Navajo reservation during the last two years; people waited to see if the greenhouses really worked before accepting them.

Greenhouse Design and Construction

Only greenhouses (or sunspaces) that attempted to make some use of basic solar heating principles were surveyed. The survey revealed that a great variety of solar greenhouse designs had evolved to meet individual needs. Of the 150 greenhouses studied, 58 percent were retrofitted onto existing homes (some by enclosing porches) and 33 percent were integrated into the house design. Only 7 percent were freestanding.

Although most literature shows sloping south walls on these structures, nearly 50 percent of those surveyed used vertical south glazing. Forty-five percent employed some slope to the south wall, and a few used lean-to or curved wall designs. A very large range of sizes was found [48 to 1400 ft^2 (4.5 to 130 m^2)], but 65 percent fell into the 100- to 300-ft^2 (9- to 28-m^2) range. The most popular size (26 percent) was 150 to 200 ft^2 (14 to 19 m^2).

In answer to the question of who designed the greenhouse, most respondents gave design credit to themselves (69 percent), but some greenhouses were designed by builders (21 percent) and architects (17 percent). Solar organizations were credited for the design by 6 percent of the respondents, and published plans or manufactured kits were mentioned by a very few. There were obviously some joint design efforts. Problems in finding good design information

---

* Since most questions elicited multiple responses from interviewees, figures will not always total 100 percent.

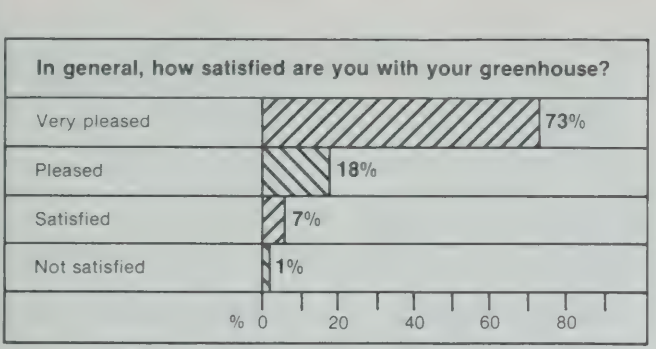

were reported by 19 percent of the respondents. Most noted that they were "pleased" (24 percent) or "very pleased" (63 percent) with the design. The 5 percent that checked "not satisfied" were nearly all owners of greenhouses they had designed themselves and built before 1977.

Aside from being predominantly owner-designed, most greenhouses surveyed were also owner-built (66 percent). Builders were credited by 33 percent of the respondents, and workshops were credited by 11 percent. An average of 60 percent of the labor that went into the construction of all greenhouses surveyed was "free" or donated by friends or in workshops. (An impressive figure!) Only 6 percent of those surveyed indicated they were not satisfied with the construction.

The large number of greenhouses designed and built by homeowners is a clear reflection of the "grassroots" approach stressed by early solar greenhouse advocates (Yanda) and workshop programs (NMSEA and others), as well as self-help interests of owners.

Building codes and zoning regulations are sometimes cited as serious deterrents to solar greenhouse construction. Although the survey covered only greenhouses actually built, only 5 percent of the owners noted problems with building codes, and 7 percent indicated difficulties with zoning regulations.

A majority of the owners (75 percent) believed that their greenhouses were tight and well sealed against air leaks. Fiberglass sheets were the most popular glazing; glass was used as the primary glazing in about one-third of the structures. Acrylics were used occasionally, and plastic films like polyethylene served as the primary glazing in some of the least expensive greenhouses. Although these plastic films may last only one or two years as an exterior glazing, their very low initial cost makes them attractive for simple, temporary structures. About 70 percent of the designs used some glazing in the roof.

Perhaps because of the favorable New Mexico sunshine, only 14 percent of those surveyed used any kind of night insulation on the greenhouse glazing. Such movable insulation, however, might be essential in more difficult climates if plants are to grow through the winter months. Perimeter insulation was installed during construction in only 60 percent of the greenhouses studied.

The construction of the common wall between house and greenhouse was most often adobe (43

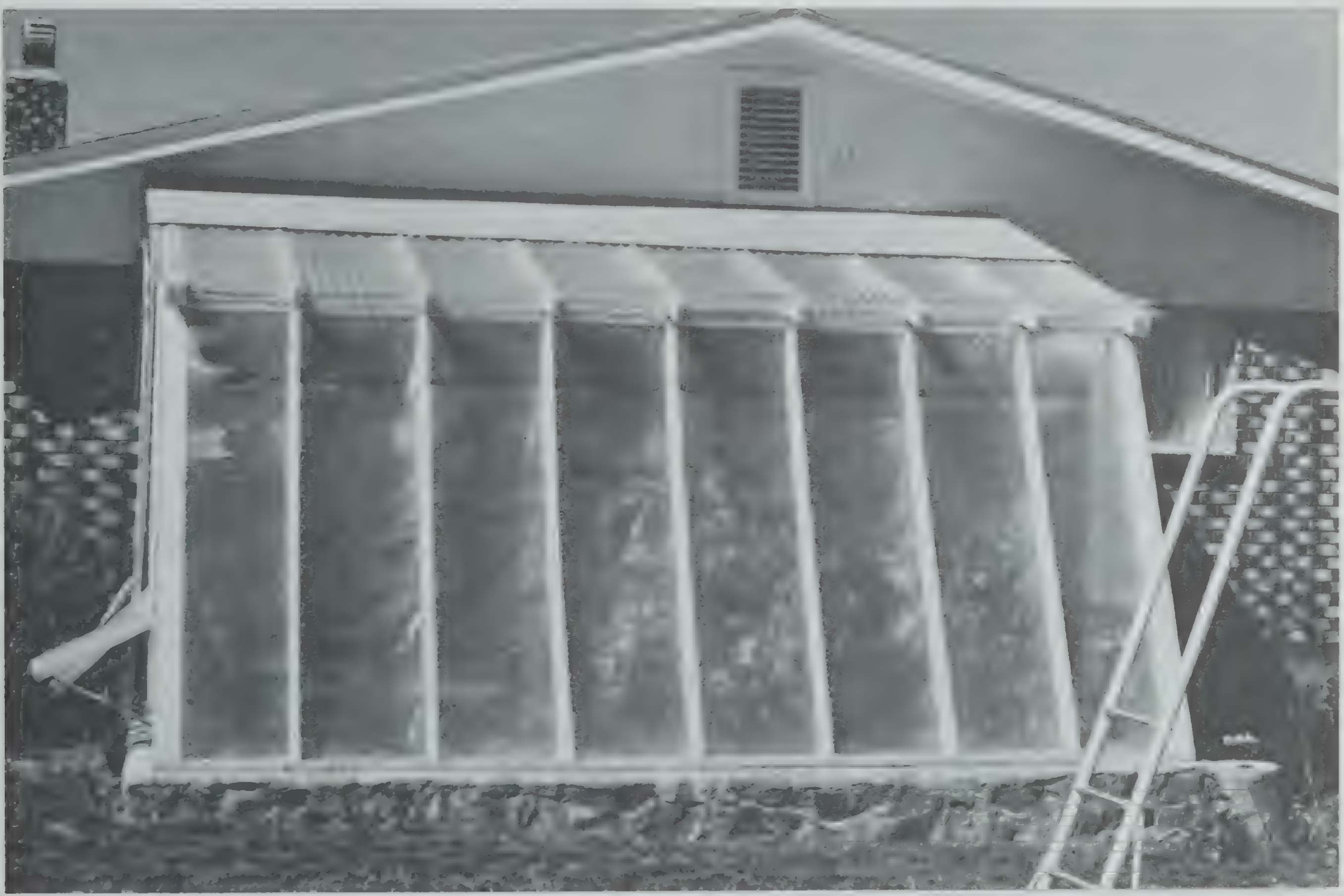

Of the 150 greenhouse owners interviewed, 81 percent said they built their greenhouses to save money on heating bills. Fifty-eight percent of the structures, like the one above, were retrofitted onto existing homes; 33 percent were integrated into the house design. The most popular greenhouse size reported was 150 to 200 ft^2 (14 to 19 m^2).

percent) or wood frame (25 percent). Various heat storage materials were used, particularly masonry walls, either existing or added, and water in containers (47 percent used 55-gal drums of water). Only 5 percent used isolated rock beds for heat storage, although use of this medium is growing. Five percent of the greenhouses included no thermal mass.

Thermal Performance

Good numerical data are often difficult to obtain from end-users of any technology, and solar greenhouse owners were no exception. Although 84 percent were using their greenhouses for heat collection and were almost universally happy with the results, few kept careful track of actual performance.

Forty-four percent of those surveyed claim to have kept at least some track of home fuel usage, but only 33 percent ventured to give percentage changes in home fuel use due to their greenhouses. Although answers varied widely, of course, due to different greenhouse-to-house size ratios, the average decrease in fuel usage was 31 percent. (See section on economics for further evaluation of these data.)

More people (65 percent) kept some track of temperatures in their greenhouses. Most of the respondents reported quite predictable temperature data for their particular greenhouse design. Typical winter lows generally ranged from 45° to 55° F (7° to 13°C) and winter highs from 75° to 85°F (24° to 29°C). The day-night temperature swing was generally about 35°F (19°C).

Very few homeowners reported consistently very high or very low temperatures, but a few (5 to 10 percent) did report unusually large day-night temperature fluctuations. These almost always occurred in greenhouses that had inadequate heat storage and/or a southwesterly orientation. When these conditions were combined, a few poor souls had day-night temperature swings of 28° to 100° F (–2° to 38° C) and 40° to 120° F (4° to 49° C). During the winter, some owners (6 percent) occasionally had to vent their greenhouses. Only 5 percent claimed to have had poor heat transfer to the house itself, but 23 percent used fans to help move hot air into the home.

Problems of frequent freezing in the greenhouse were rare (3 percent), although 8 percent of those surveyed did have occasional freeze problems. Even in well-designed structures, some measures must be taken to guard against freezing if plants are grown through midwinter. Twenty-one percent of the respondents used auxiliary heat, when necessary, and 33 percent left the connecting door to the house open. Fourteen percent grew only plants that could withstand cold temperatures; 13 percent let the greenhouse freeze. Although only 6 percent had no planting in the greenhouse during midwinter, there is some advantage to this approach. Because no heat has to be stored in the greenhouse for nighttime use, there is more daytime heat available for the house. This technique is more common in severe climates.

Summer temperatures reported in the greenhouses were very reasonable. Shading the glazing (especially roof glazing), venting, and extra watering were all common. Twenty-four percent of the owners used ventilating fans, resulting in temperatures generally close to those outside. In the few cases where inadequate precautions were taken, temperatures of 110° F (43° C) were reported. Only 5 percent of respondents felt they had severe overheating problems in their greenhouses, although 29 percent admitted to occasional overheating.

In many ways, temperatures and temperature fluctuations are good indicators of the "health" of a greenhouse. Based on the respondents who gave temperature data, it appears that about 90 percent of the greenhouses surveyed are in good shape. The problems encountered by the other 10 percent can be solved mostly through increased heat storage, proper weatherproofing, increased vent areas, and summer shading.

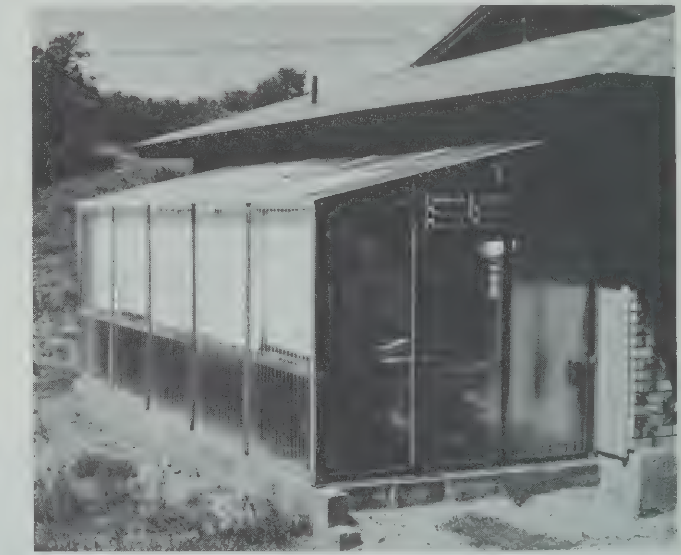

Shading glazing on the roof and south wall, venting, and increased watering were reported as common methods for preventing summer greenhouse overheating. In the few cases where inadequate precautions were taken, temperatures of 110°F (43°C) occurred.

During the survey, it became clear that many owners do not have a very good understanding of the heat transfer and storage principles involved in solar heating. They often try to avoid problems by taking the advice of friends and literature, but misunderstandings can lead to problems, particularly with the concept of heat storage. In one case, the owner had actually emptied all the water barrels that were purposefully placed in his greenhouse by a workshop crew. When questioned about his action, he said that every time he felt the barrels they were cold to the touch [probably about 65° to 70° F (18° to 21° C)] and "who wants a lot of cold water in the greenhouse?" After he emptied the barrels, he was unable to grow food during the critical winter months because of freezing.

Although most of the greenhouses were doing very well and provided substantial amounts of heat to the household, more complete education of the owners, with emphasis on what temperatures to expect in different locales, could result in even more effective thermal management of these heat-producing structures.

Flowers and Vegetables: Growing Issues

Most of the interviewees used their greenhouses for growing food and/or flowers in both summer and winter. In the northern section of the state, where growing seasons are short, tomatoes, melons, and cucumbers are often much better off in the greenhouse than in outside gardens. Of the homeowners interviewed, 57 percent were already gardeners before they built their greenhouses, and most of the respondents felt they had been successful in growing plants in their greenhouses. Previous gardening skills are transferred when gardeners go indoors, causing a large increase in the success rate. Forty-four percent of the respondents used the greenhouse to start seedlings for later outdoor transplanting. Comparing the greenhouse to the outdoor garden plot, 45 percent of the respondents felt the greenhouse plants needed to be watered less than those in outdoor gardens. In the Southwest, where water is very precious, intensive indoor gardening using very little water is becoming increasingly economical.

The major horticultural problem encountered by interviewees (44 percent) was excessive bugs. The types of pests most often encountered were white flies, in both summer and winter; spider mites, mainly in the winter; and aphids. Greenhouse pests were regulated through (1) biological control such as lady bugs (29 percent); (2) mechanical means including water sprays, sticky tapes, and vacuum cleaners (27 percent); and (3) botanical insecticides (22 percent). Other solutions included herbal sprays and companion planting; some interviewees had no luck at all. It is interesting to note that most of the pest control methods were natural rather than synthetic chemical pesticides. Since the greenhouse is essentially part of the house, people are becoming more aware of the health hazards of synthetic chemical sprays.

Interviewees went to friends (52 percent), garden books (43 percent), popular literature (30 percent), and horticultural specialists (20 percent) for help with greenhouse gardening problems. Most of the solar greenhouse owners (59 percent) did not feel it was difficult to find help with horticultural problems. In some towns throughout New Mexico, solar greenhouse owners have formed informal information networks to help each other with greenhouse gardening problems.

Besides excessive bugs, other gardening problems were excessive drying of plants (21 percent) and burned plants (17 percent). All of the horticultural concerns discussed here can be caused by many variables, including too much or too little humidity, insufficient air circulation and ventilation, and planting in the wrong place (e.g., cool-weather plants too close to the south face of the greenhouse).

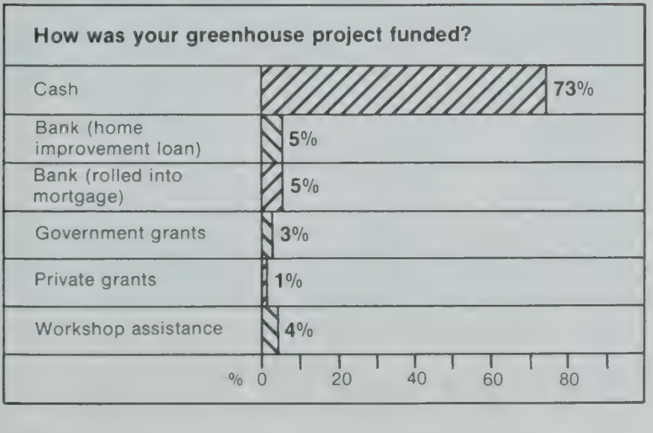

Recently, many greenhouse gardeners have been commenting that solar greenhouses are designed for thermal performance instead of growing plants. More information is needed on designing solar greenhouses for plants and on determining trade-offs involved in producing heat versus growing food.

Financing

Of the 133 owners who responded to the question of initial funding for the greenhouse, 82 percent paid cash without, apparently, even approaching a bank. Eleven percent obtained loans after mixed reactions from their bankers, and 4 percent financed their greenhouses primarily with private or government grants. That so many respondents paid cash does not necessarily reflect the wealth of the people sampled, but rather that they built greenhouses they could afford, whatever their income levels. The fact that an average of 60 percent of the labor, as well as many materials, was free or donated supports this conclusion. Interestingly, only 31 percent of the owners filed for available tax rebates.

Economics

Because of the multiple uses of greenhouses and the number of benefits derived (both tangible and intangible), hard economic evaluations are nearly impossible to make. Although 55 percent of the respondents listed "saving money on food" as one of their reasons for building a greenhouse, almost nobody ventured to attach a dollar amount to these savings. Even if they had, there is confusion as to how imputed labor costs, for instance, should be included in such an analysis.

Other very real, but difficult to quantify, benefits include the value of a pleasant sunspace, home value appreciation, environmental benefits due to decreased fossil fuel consumption, and stimulation of energy-conscious behavior on the part of homeowners.

During the early stages of this study, it was decided that only the fuel savings in the residence achieved by the solar heating aspects of the greenhouse were appropriate for economic analysis, and many questions were added to the questionnaire to deal with this issue. This was not done with the intent of diminishing the other benefits, which in some cases may even be greater than the heating benefits, but rather to present an analysis based on heat production to which the other benefits could be added.

Only 19 of the respondents gave data on construction costs and thermal performance sufficient for a proper analysis, but this was viewed as a suitable sample size. Each of the 19 greenhouses was analyzed by Scott Noll (an economist at Los Alamos Scientific Laboratory) to determine payback periods, average capital costs of annual energy savings, and net present value of lifetime energy savings. All calculations were based on conservative estimates of the annual fuel escalation rates for the actual fuels used by each home (generally about 10 percent, including inflation). Also, the calculations used estimated values for labor or materials that were "free or donated," so that capital costs were considered to be those that would have been incurred had all construction been paid for.

In all but 4 of the 19 cases, the greenhouses were estimated to produce a fuel savings equal to or greater than their initial capital cost plus maintenance costs over their expected lifespans (positive net present value). Costs per square foot of greenhouse floor area in these 15 designs ranged from \$4 to \$16.67 (\$44-\$185/m^2). The four greenhouses that were estimated not to pay back within their lifetimes were all expensive designs costing from \$23 to \$29/ft^2 (\$255-\$322/m^2).

Simple payback periods for the 15 "cost-effective" designs ranged from 3 to 10 years, with the majority (10) falling in the 4- to 8-year range. If these estimated dollar savings are discounted at the assumed homeowner opportunity cost of 7 percent (estimated opportunity cost on construction money had it been put into a savings account), the corresponding discounted payback periods increased by 1 to 3 years.

The average capital cost (AC) of annual energy savings is a good indicator of cost and performance. It is calculated by dividing the greenhouse capital cost by the level of annual energy savings stated in terms of displaced load (MMBtu per year). Fourteen of the 19 greenhouses analyzed had an AC in the range from \$31 to \$110/MMBtu per year (\$33-\$116/GJ per year). The four greenhouses estimated not to achieve economic paybacks (based on fuel savings alone) within their lifespans all had AC values greater than \$130/MMBtu (\$137/GJ) per year.

It becomes clear that after a certain point [\$10-\$12/ft^2 (\$111-\$133/m^2) in 1979\$], additional monies spent on greenhouse construction do not necessarily improve thermal performance. On the other hand, the more expensive greenhouse may well increase the aesthetic benefits and resale value of a home, offsetting the higher cost of annual energy saved. It should be noted that 83 percent of the 150 respondents indicated they thought the greenhouse had added as much, and generally more, to the market value of the house than had been invested in construction of the greenhouse.

Other factors aside, the economic analysis shows that the cost of heat produced by most of these structures in New Mexico competes favorably against most of the heating fuels available today.

Technology Transfer

Some of the more interesting results of the questionnaire survey were the answers to questions dealing with the transfer of information on solar greenhouse technology. Although early advocates of solar greenhouses clearly introduced the technology and should be given major credit, the waves they caused are now striking shores that may not be aware of the original source. Good ideas travel fast, and personal recommendations as well as popular literature have apparently become the prime vehicles of dissemination in New Mexico.

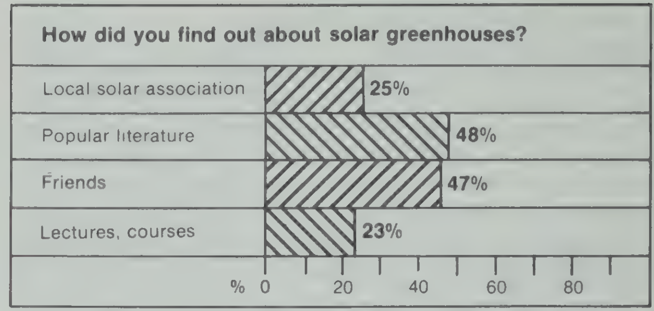

Although there were many multiple answers to the question, "How did you find out about solar greenhouses?", only 25 percent of the respondents credited local solar associations. Forty-eight percent cited popular literature, and 47 percent said they had learned through friends. For 23 percent, "lectures and courses" had been, perhaps, their first introduction.

Seventeen percent of the 150 respondents did attend some form of solar greenhouse workshop, which is quite significant, given that many of the "friends" referred to by others may also have participated. These workshops, mostly performed by the Yandas and NMSEA, have clearly had important and far-reaching effects.

Nineteen percent of the respondents indicated that they did have some trouble finding good design information, and 23 percent felt that it was difficult to find help with gardening problems. Again, most of the help seems to have come from friends and literature rather than from specialists. It should be recognized, however, that these are answers that were given in mid-1979 and that most of the greenhouses surveyed were built before 1978. As the number of solar greenhouses increases, so does the access to good information.

Solar greenhouses tend to bring people together. Homeowners generally rely on friends, neighbors, or popular literature for information.

Impacts

After having built a solar greenhouse and lived with it for a while, most (54 percent) of the interviewees said that they had plans for additional solar energy applications. Fourteen percent have already added other solar systems to their homes, a clear indication of the success of solar energy. Most

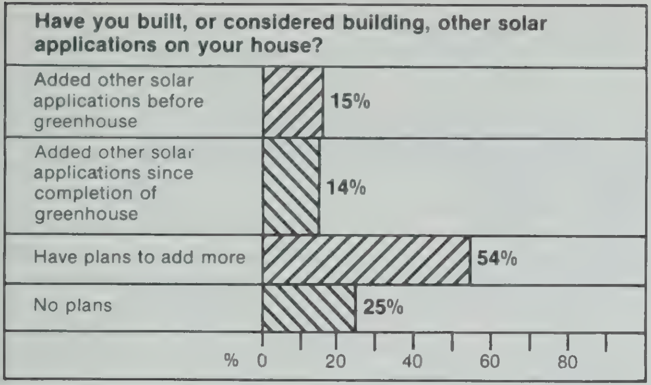

(88 percent) of the interviewees have recommended solar greenhouses to other people, and 52 percent said they knew of other greenhouses that were built as a result of their own. One of the best ways to develop interest in a new technology is through direct experience: "Seeing is knowing."

In response to questions concerning development of solar energy in their communities, 55 percent of the interviewees said that there should be more demonstration projects; 75 percent saw a need for more low-cost loans, tax rebates, and greater public education; and 55 percent said that more funds for research and small grants to individuals are needed. All of these factors are very important, especially if lower income people are going to be able to participate in the use of solar energy. Most of the interviewees said they had had no problems with building codes or zoning regulations. However, it is not known whether they had ever filed for a building permit.

Fifty-nine percent of the interviewees had very enthusiastic reactions to their solar greenhouses from friends and neighbors, and 41 percent said that their friends had been interested. Bill Yanda often comments that for every greenhouse workshop he conducted, 10 more greenhouses were built. This study estimates that there were 1000 solar greenhouses in New Mexico as of October 1979. Given a rough estimate of four persons per household, we estimate about 300,000 households in the state. This indicates that one of every 300 homes has a solar greenhouse (more in cold, mountainous regions). This is an impressive figure when it is noted that the technology emerged from its conception only about five years ago and has spread mostly through popular sources.

Eighty-eight percent of homeowners queried have recommended solar greenhouses to other people; 52 percent said they knew of other greenhouses built as a result of their own.

Another community impact of solar greenhouses, to which the questionnaire data do not directly refer, is the workshop component. Solar greenhouses tend to bring people together, either through workshop situations or in sharing pest control remedies or heat storage ideas. People naturally find others with like interests. Local solar associations have sprung up around the state because of this interchange.

Conclusions

The *New Mexico Solar Greenhouse Study* showed that the number of solar greenhouses in New Mexico is growing at a very rapid rate. This is primarily a result of people's needs to reduce fuel and food costs, although other factors, including an urge for self-reliance, have played an important role. The technology has spread primarily in an informal, "grassroots" fashion, and homeowners have designed and built these structures mostly themselves.

The intuitive belief that simple attached or integrated solar greenhouses pay for themselves in fuel savings alone has proven to be true in New Mexico. Aside from these very real heating benefits, solar greenhouses provide a very pleasant sunspace and an almost ideal year-round environment for growing food as well as flowers and other plants.

Although there is apparently some need for more information and education on the design and management of these systems, it is also clear that the use of solar greenhouses will continue to grow and flourish.

Acknowledgments

The study on which this paper is based was primarily funded by the Office of Technology Assessment, U.S. Congress. We would like to thank the following people for their help in conducting the survey.

Bruce Allen
Vince Burns
Scott and Libby Clark
Michael Coca
Able Davis
Barbara Escher
Kevin Leary
Joan Loitz
Beverley McGennis
David Miller
Susan Nichols
Scott Noll
B.T. Rogers
Greg Shenstone
Bristol Stickney
Ed Tyson
Frances Tyson
Paul Wilkerson
Alex Wilson
Ann Wonders

A copy of the results of the questionnaire survey upon which this article is based (17 pages) is available from the authors for the cost of copying and postage. A copy of the full final report (146 pages) is also available from the authors.

Natural Convection in Passive Solar Buildings: Experiments, Analysis, and Results*

Ashok Gadgil, Fred Bauman, and Ronald Kammerud
Passive Solar Analysis and Design Group
Lawrence Berkeley Laboratory
Berkeley, CA 94720

Abstract *Computer programs have been developed to simulate numerically natural convection in two- and three-dimensional room geometries. The programs have been validated using published data from the literature, results from a full-scale experiment performed at the Massachusetts Institute of Technology, and results from a small-scale experiment performed at LBL. One of the computer programs has been used to study the influence of natural convection on the thermal performance of a single zone in a direct-gain passive solar building. It is found that the convection heat transfer coefficients between the air and the enclosure surfaces can be substantially different from the values assumed in the standard building energy analysis methods, and can exhibit significant variations across a given surface. This study implies that the building heating loads calculated by standard building energy analysis methods may have substantial errors as a result of their use of common assumptions regarding the convection processes which occur in an enclosure.*

Nomenclature

A	Aspect ratio = H/L
C_p	Specific heat at constant pressure
Gr_L	Grashof number, = $g.\beta.\Delta T.L^3/\nu^2$
g	Acceleration due to gravity
H	Enclosure height
L	Enclosure length
$\overline{Nu}_L$	Average Nusselt number, $= gL/\Delta T \kappa$
$\overline{Nu}_{L_{IN}}$	Average Nusselt number on the hot wall
p	Dimensionless pressure
Pr	Prandtl number, = ν/α
q	Heat flux
Ra_L	Rayleigh number, = $Gr_L \cdot Pr$
$\widehat{Re}$	Dimensionless scale of time
T	Temperature
ΔT	Characteristic temperature difference, $= T_H - T_C$
ΔT^*	Maximum temperature on hot wall – minimum temperature on cold wall
t	Dimensionless time
T_{AIR}	Average temperature of air in the zone
T_{MRT}	Mean radiant temperature in the zone
T_C	Average temperature of the cold wall
T_H	Average temperature of the hot wall
$\vec{V}$	Dimensionless fluid velocity factor
X	Vertical axis (dimensionless)
Y	Horizontal axis (dimensionless)
α	Thermal diffusivity = $\kappa/\rho C_p$
β	Coefficient of volumetric expansion
δ_i^j	Kronecker Delta, $= \begin{matrix} 0 \text{ if } i \neq j \\ 1 \text{ if } i = j \end{matrix}$
θ	Dimensionless temperature
κ	Thermal conductivity
μ	Viscosity
ρ	Density
ν	Kinematic viscosity = μ/ρ

Introduction

In spite of the fundamental role it plays in both conventional buildings and passive solar systems, natural convection has received relatively little experimental or analytic attention within the building sciences. Within a single thermal zone†, natural convection and thermal radiation are jointly responsible for the distribution of heat from collection and/or storage media to the building occupants, to the occupied space, or to building elements having significant thermal mass but which do not receive direct sunlight. In general, several thermal zones are needed to characterize occupied buildings (e.g., buildings other than warehouses, airplane hangars, etc.); and convection processes contribute to the thermal transfers among these zones. Buoyancy-driven† convection is responsible for the air circulation producing a cooling effect in sunspaces, multistory atria, and in other thermal chimney designs. Finally, many passive solar concepts such as double envelope structures, thermocirculation systems, and air collection systems rely almost exclusively on natural convection for their operation.

Recent research results have emphasized the importance of natural convection processes. Analyses performed by the Los Alamos Scientific Laboratory (LASL) on the Balcomb house [1] have implied the importance of convective coupling of thermal zones as compared to radiative and conductive cou-

---

* This work was supported by the Research and Development Branch, Passive and Hybrid Division, Office of Solar Applications for Buildings, U.S. Department of Energy, under Contract No. 7405-ENG-48.

† See Glossary of Technical Terms.

plings in a multizone structure. Preliminary results from work performed at Lawrence Berkeley Laboratory (LBL) [2] indicate that the magnitude of the convection heat transfer coefficients on the inside surfaces of a typical direct gain building configuration can vary significantly with time. This result is consistent with an earlier study [3] which demonstrated that appreciable errors in prediction of building thermal loads can result from the common assumption that the total (convective + radiative) heat transfer coefficients are constant with time.

There is evidence that convective heat transfer processes are highly dependent on both the geometric configuration of the structure being studied (e.g., Ref. 2) and the range of thermal boundary conditions that might be encountered in the structure. Also, the natural convection processes that occur in passive systems are largely uninvestigated. Thus, there is a need to provide a sound technical basis for estimating the effects of convection on the performance of buildings. An unmanageably large number of experiments would be required to explore thoroughly natural convection phenomena in buildings empirically. The present study addresses this problem by focusing on the development of a general computerized numerical method for analysis of natural convection, and on the validation of the method using results from a few selected experiments. The computer code can then, with some confidence, be applied to a broad range of studies of natural convection in buildings. More specifically, the work reported here consists of (1) the development and validation of a numerical analysis technique for studying convective heat transfer in buildings and (2) the use of this analysis technique to study the quantitative role of natural convection in the thermal performance of a direct solar gain structure, and thereby to examine the accuracy of standard assumptions regarding convective heat transfer within a zone in a building.

Background

Past natural convection research [4] has dealt primarily with geometric configurations that do not typify rooms in buildings; as a result, these studies are of limited application in the building sciences. Convection heat transfer coefficients most often used in building energy analysis are largely based on experiments conducted 25 years ago [5-7]. This work was necessarily limited in the range of experimental parameters investigated. In addition, the lack of large computers and sophisticated experimental hardware prevented the researchers from thoroughly examining the sensitivity of their results to the experimental assumptions. This past research has not been extended, most likely due to three factors: (1) The historically low cost of energy used in buildings; (2) the emphasis on the use of forced convection wherever possible; and (3) the difficulty of conducting analytical, numerical, or experimental investigations of configurations representative of buildings.

More recently, there has been renewed interest in natural convection in the building sciences. Investigations of convective heat transfer within and between thermal zones have been reported by Buchberg [3], Nielsen [8], Honma [9], and Weber [10].

Problem Definition

In the published literature, the problem of natural convective heat transfer in an enclosure is typically simplified to the configuration illustrated in Fig. 1. In a two-dimensional rectangular enclosure, one vertical surface is maintained at a constant temperature T_H, and the opposite vertical surface is maintained at a lower constant temperature T_C. The horizontal surfaces are adiabatic (perfectly insulated). This was one configuration chosen for the numerical and experimental comparisons with published data. Heat input or extraction through one vertical surface of an enclosure is a reasonable model for many situations arising in buildings; for example, it may represent heat gain from an unvented Trombe wall or heat loss through windows in single- and multistory buildings. In addition, a previous study [11] indicates that in warm climates the heat losses through the walls and windows (the vertical surfaces) are larger than the losses through the floor and the ceiling (horizontal surfaces) in a well-insulated, single-story, residential building.

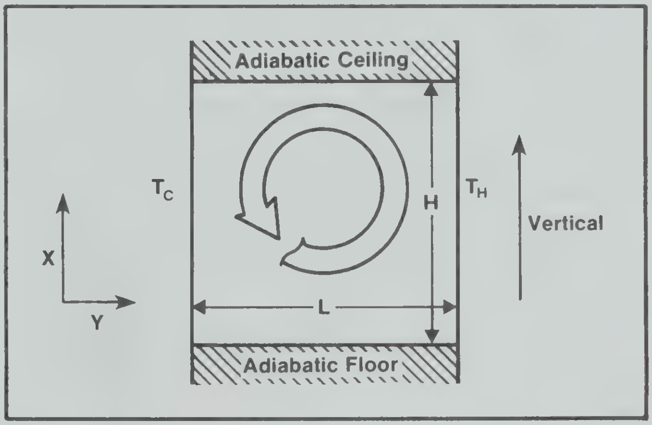

Fig. 1. Recirculating flow induced in a fluid inside a two-dimensional square cavity, defined by adiabatic floor and ceiling and isothermal walls, at tempertures T_H and T_C ($T_H > T_C$).

In the configuration illustrated in Fig. 1, variations in density drive the enclosed fluid up the heated wall, along the top horizontal surface, down the cooled wall, and along the bottom horizontal surface, completing the convective loop. The convective motion of the fluid is confined mostly to a thin region along all four internal surfaces, producing a rather large and fairly inactive central core region. Characteristics of the flow such as the mean air temperature, convection coefficients between air and walls, flow velocities, etc., are completely determined by specification of the three independent dimensionless parameters listed here:

- Aspect ratio: $A = H/L$ where H = enclosure height and L = enclosure length.
- Prandtl number: $Pr = \nu/\alpha$ where ν = kinematic viscosity and α = thermal diffusivity.
- Rayleigh number: $Ra_L = Gr_L Pr = g\beta\Delta T L^3 Pr/\nu^2$, where Gr_L = Grashof number, g = acceleration due to gravity, β = coefficient of thermal expansion, and ΔT = characteristic temperature difference = $T_H - T_C$.

These parameters include all relevant information regarding the enclosure geometry, the fluid properties, and the relative strength of buoyancy and viscous forces, respectively. For a rectangular room twice as long [5.5 m (18 ft)] as it is high [2.75 m (9 ft)] filled with air at 21°C (70°F) and with at least a 1°C (1.8°F) temperature difference between vertical walls, these parameters take the values:

$$A = 0.5,$$
$$Pr = 0.71, \text{ and}$$
$$Ra_L \geq 1 \times 10^{10}.$$

Analysis Description and Comparison with Published Data at Low Rayleigh Numbers

Little numerical work has been published on natural/buoyant convection at Rayleigh numbers in excess of 10^7. In this flow regime, fluid velocities become relatively large. If the popular Central Difference Scheme (CDS) is used for casting the equations governing the fluid flow into finite difference form, the large velocities necessitate an impracticably fine mesh size to ensure numerical stability of the solution procedure (e.g., Ref. 12). Spalding [13] has proposed a differencing scheme that overcomes this difficulty; it allows relatively coarse grid spacings without seriously compromising accuracy and solution stability [14]. Two computer programs, CONVEC2 and CONVEC3, were developed based on this differencing scheme. These programs respectively solve the coupled two- and three-dimensional conservation equations with the Boussinesq approximation:

Continuity: $\operatorname{div}(\vec{V}) = 0$,

Momentum:

$$\hat{Re}\;\frac{d\vec{V}}{dt} + (\vec{V}\cdot\vec{\nabla})\vec{V} = \nabla^2\vec{V} - \operatorname{grad} p + Gr\,\theta_i^3,$$

Energy:

$$\hat{Re}\;\frac{\partial\theta}{\partial t} + (\vec{V}\cdot\operatorname{grad})\,\theta = \frac{1}{Pr}\nabla^2\,\theta.$$

These computer programs can be applied to fluid flow problems driven by predefined temperature distributions on the enclosure surfaces and/or by pressure differentials between specified locations on the boundary. To date, a turbulence model has not been incorporated into either computer program, so the analyses are limited to steady (laminar) flows.* (For a more detailed description of the analysis technique, see Ref. 15 and references cited therein.)

Validation of the two computer programs CONVEC2 and CONVEC3 has been undertaken by comparing the calculated results to various published numerical and experimental efforts and to two recent experiments utilizing room geometries. The comparison to the low-Rayleigh-number data cited in the literature is described below; validations at the higher Rayleigh numbers characteristic of buildings are described in the next sections. The mesh sizes used for calculation in all validations were relatively coarse (the finest two-dimensional mesh size was 17 × 20). The grid lines were distributed evenly throughout the central region (interior of the fluid volume) with a concentration of grid lines near the enclosure boundaries; this permitted simulation of the sharp changes in flow properties associated with a developed boundary layer. Sensitivity analyses indicated that it was adequate for this purpose to position three grid lines parallel and adjacent to each enclosure surface.

A quantity of particular importance in the problem defined by Fig. 1 is the magnitude of convective heat transfer, measured by the Nusselt number. For a square enclosure ($H = L$ in Fig. 1), the average Nusselt number can be defined as:

$$\overline{Nu}_L = \frac{1}{T_H - T_C}\int_0^1 \left.\frac{\partial T}{\partial Y}\right|_{Y=0} dX$$

In Fig. 2, $\overline{Nu}_L$ calculated with the convection code, CONVEC2, is plotted as a function of Rayleigh number. On the same graph, relevant numerical and experimental results for $10^4 \leq Ra_L \leq 10^9$ from various investigators [16-22] have been superimposed; as shown, the agreement is quantitatively acceptable. Additional validation at low Rayleigh numbers has been presented in Ref. 15.

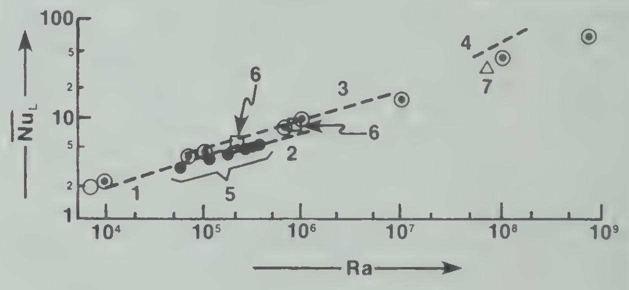

Curve **1:** de Vahl Davis, Calculations [16]
Curve **2:** Emery, Experimental Results [17]
Curve **3:** Portier et al., Calculations, Pr = 0.7 [18]
Curve **4:** Burnay et al., Data Reduced from Experiments, Pr = 0.7 [19]
Result **5:** Rubel and Landis, Calculations [20]
Result **6:** Quon, Calculations [21]
Result **7:** Fromm [22]
Points indicated by ◉ are from present calculations.

Fig. 2. Dependence of $\overline{Nu}_L$ on Ra, for two-dimensional flow inside a square cavity. Comparison with published results shows acceptable agreement.

Experiments and Analysis Validation at High Rayleigh Numbers

Existing experimental data have largely been limited to Rayleigh numbers of less than 10^9 — at least an order of magnitude below that which characterizes full-scale building geometries. In addition, most of the data are for large aspect ratios, typifying fluid flow in narrow vertical channels. Two recent experiments [2, 23] have expanded the data base into the geometric and kinematic region of interest to the buildings sciences. The experiments are described here and their results are compared to the predictions of the convection analysis code.

---

* For a room-shaped enclosure, buoyancy-driven convection will not become fully turbulent for Rayleigh numbers less than about 10^{11}. The wind-driven convection in a building is always turbulent.

Small-Scale Experiment

A small-scale experiment, coordinated with the analysis, is being carried out at Lawrence Berkeley Laboratory. The results from the first phase of this experiment are reported here.

A schematic cross-sectional view of the experimental configuration is shown in Fig. 3; the apparatus has inside dimensions of 12.7 cm (5 in.) high by 25.4 cm (10 in.) long and extended to a horizontal depth of 76.2 cm (30 in.) to minimize three-dimensional effects. Water was used as the working fluid; this allowed representative Rayleigh number values to be obtained in a small-scale apparatus. The range of parameters covered by this experiment are:

$$A = 0.5;$$
$$2.6 \leq Pr \leq 6.8; \text{ and}$$
$$1.6 \times 10^9 \leq Ra_L \leq 5.4 \times 10^{10}.$$

The opacity of water to thermal radiation implies that the experiment was not a direct, scaled approximation to a real room; using water in the experiment allowed measurement of the purely convective part of the heat transfer process being studied* and from this standpoint, was ideal for validating the convection analysis code.

In experimental modeling of convective heat transfer processes, the detailed behavior of a fluid with Prandtl number less than 1.0 cannot be accurately simulated with a working fluid having a Prandtl number much greater than 1.0 [24]. Therefore, the magnitude of the Nusselt number measured in this experiment is not numerically identical to that for an air-filled enclosure. However, the general fluid behavior and parametric relationship observed in the experiment can be expected to be representative of an air-filled cavity.

The heat transfer data obtained from the experiment are presented in the form of $\log_{10}(\overline{Nu}_{L_{IN}})$ vs. $\log_{10}(Ra_L)$ in Fig. 4. In this figure $\overline{Nu}_{L_{IN}}$ (Nusselt number) is a measure of the strength of the convective heat transfer at the heated wall. On the same figure, experimental results from a study by MacGregor and Emery [24] and predictions from an analytic study by Raithby et al. [25] are shown; the present experiment is in quantitatively good agreement with both of these previous results. (Note that at the high Rayleigh numbers shown in the figure, the Nusselt number is relatively insensitive to the aspect ratio [26, 27].)

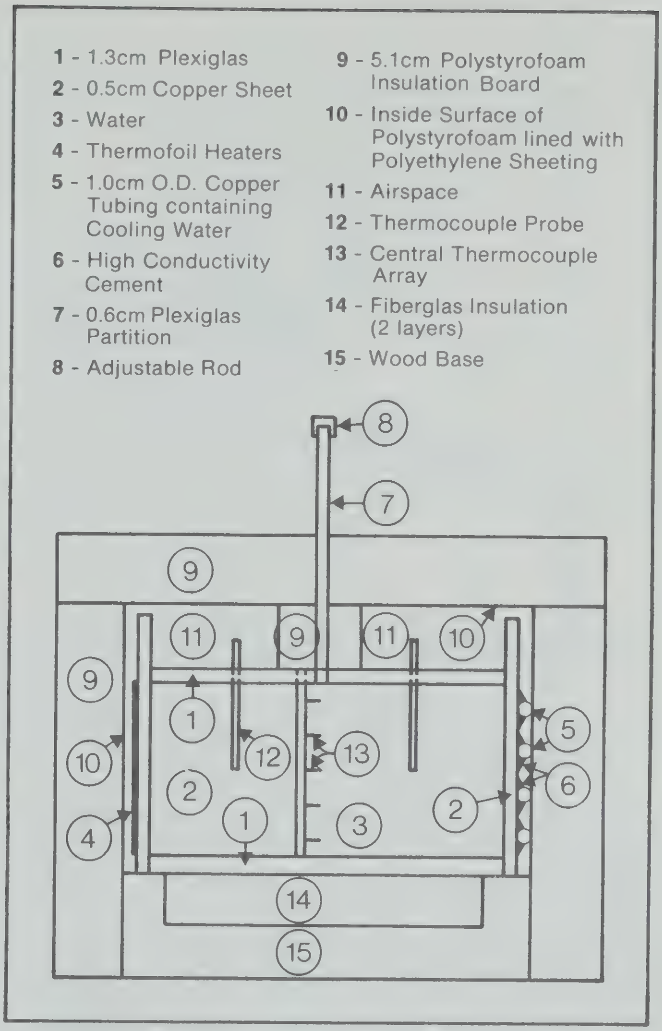
1 - 1.3cm Plexiglas
2 - 0.5cm Copper Sheet
3 - Water
4 - Thermofoil Heaters
5 - 1.0cm O.D. Copper Tubing containing Cooling Water
6 - High Conductivity Cement
7 - 0.6cm Plexiglas Partition
8 - Adjustable Rod
9 - 5.1cm Polystyrofoam Insulation Board
10 - Inside Surface of Polystyrofoam lined with Polyethylene Sheeting
11 - Airspace
12 - Thermocouple Probe
13 - Central Thermocouple Array
14 - Fiberglas Insulation (2 layers)
15 - Wood Base

Fig. 3. Schematic cross-sectional view of experimental configurations.

To use the data from this experiment for validation of the two-dimensional convection code, the computer program was modified to incorporate the temperature dependence of the physical properties of water. Sensitivity studies using the computer program demonstrated an increase of as much as 10 percent in the Nusselt numbers when the properties were allowed to vary with temperature rather than being fixed at their average values. Due to lack of sufficiently detailed experimental instrumentation, best estimates of some enclosure surface temperature profiles were necessary to complete the input to the analysis program. These surface temperature estimates are believed to have errors of less than ± 10 percent. To date, the sensitivity of the prediction of the computer code to these uncertainties has not been thoroughly investigated, pending the availability of data from an improved small-scale experiment in progress at LBL.

Comparisons of the predictions of the computer code with the experimental results for the extent of stratification in the core region are shown in Figs. 5 and 6. These figures show the temperature profiles along vertical and horizontal lines through the geometric centers of the enclosure for $Ra_L = 2.4 \times 10^9$ and $Ra_L = 4.7 \times 10^{10}$, respectively. The excellent agreement of the numerical prediction of the temperature profiles in the central core at the lower Rayleigh

---

* The maximum contribution of thermal radiation to the measured Nusselt number was calculated to be less than 2 percent.

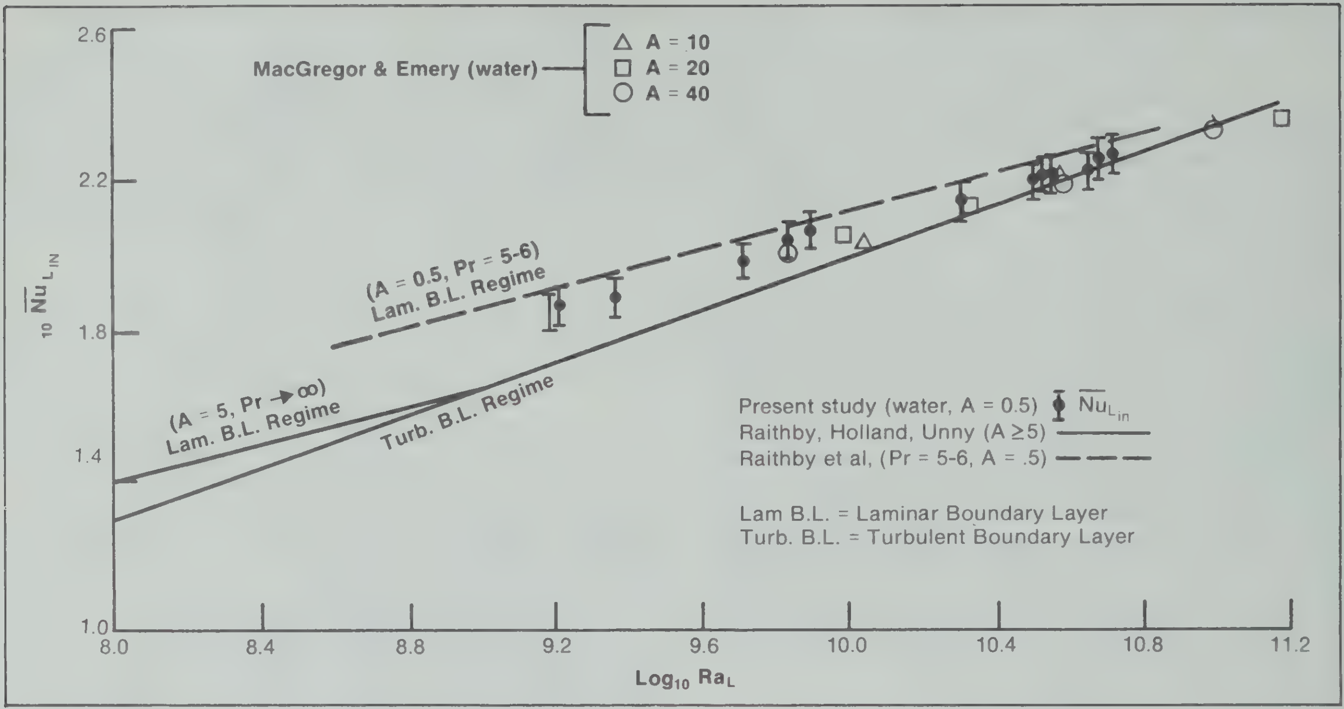

Fig. 4. Heat transfer results compared to previous results.

number (Fig. 5) indicates that the program is addressing the fundamental characteristics of the flow successfully at this Rayleigh number (2.4×10^9). The numerically predicted vertical centerline temperature profile at the higher Rayleigh number (4.7×10^{10}, Fig. 6) exhibits a shift to smaller temperature gradients in the central core region associated with an increased gradient near the horizontal surfaces. The most likely sources of this discrepancy are (1) the potential for transitional flow (between steady laminar and fully turbulent) at this value of Ra_L could contribute to the noted differences between experimental and numerical results; (2) due to increased convective effects at this higher Ra_L, the errors in the estimates of surface temperatures immediately upstream from the centerline region may have a significant effect on the magnitude of the calculated temperature profile at the centerline; or (3) the coarse mesh size used in the present numerical studies may also have been a contributing factor to the disagreement at this high value of Ra_L. Ongoing work is expected to shed some light on this question; until the source of the discrepancy is understood, however, the comparison of stratification profiles implies that the convection code properly represents the fundamental character of the flow for the smaller value of Ra_L and is qualitatively correct for all $Ra_L < 5 \times 10^{10}$.

The Nusselt number predictions made by the computer code are compared to the corresponding measurements in Table 1; the surface temperature distributions used in the simulations are also indicated in this table. The two numerical simulations (runs 2a and 2b) made at the higher Rayleigh number indicate the sensitivity of the predicted Nusselt number to differences in the details of a surface temperature specification. The disagreement in the Nusselt numbers at the lower Ra_L value is thought to be due to the sensitivity of the Nusselt number predic-

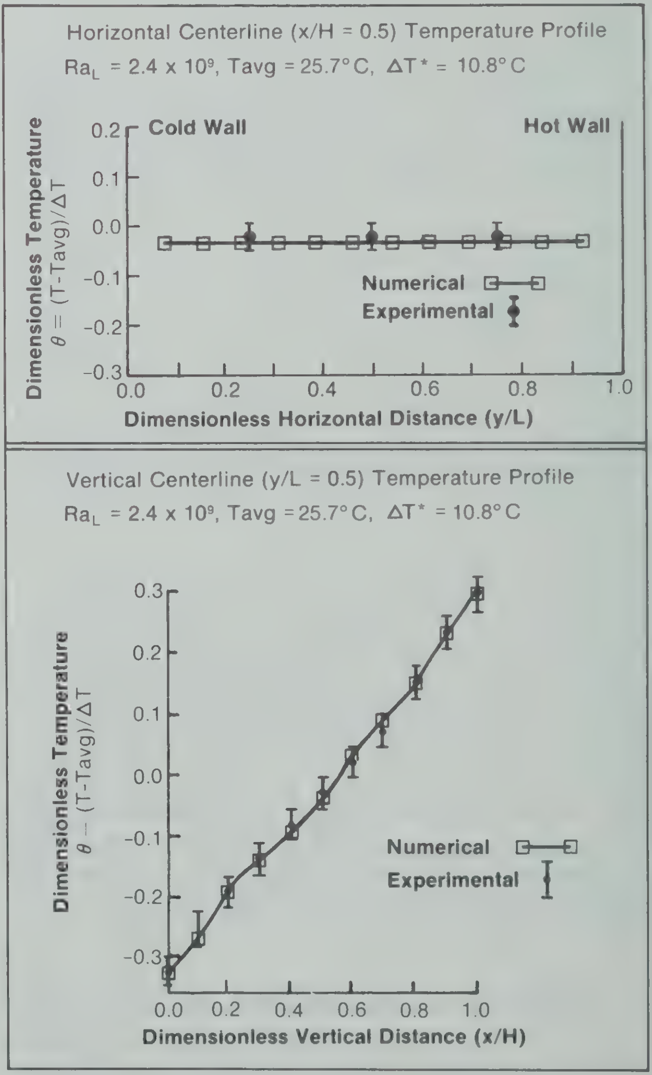

Fig. 5. Comparison of code predictions to experimental results for the extent of stratification in the core region for $Ra_L = 2.4 \times 10^9$.

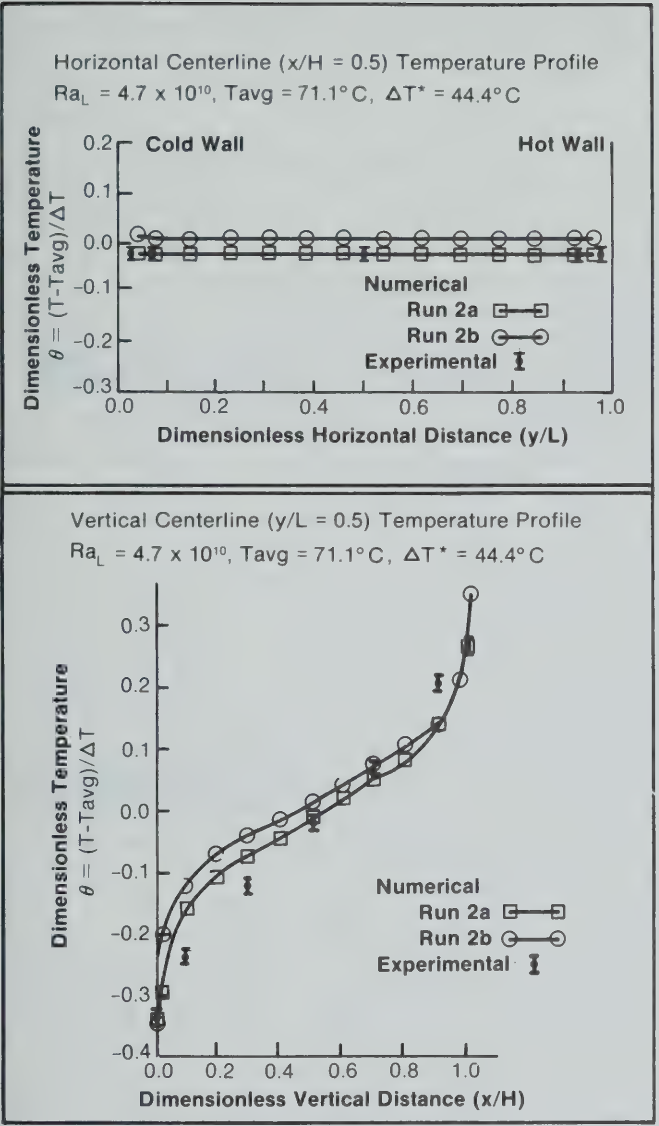

Fig. 6. Comparison of code predictions to experimental results for the extent of stratification in the core region for Ra_L = 4.7 x 10^6.

Run	Ra_L	Experi-mental	Numer-ical	Surface Temperatures for Numerical Simulations
1	2.4 x 10^9	79 ± 12	105	Estimated from Experiment
2a	4.7 x 10^{10}	165 ± 12	168	Estimated from Experiment
2b			201	Hot & Top Wall = T_H Cold & Bottom Wall = T_C

Table 1. Comparison of Hot Wall $\overline{Nu}_{L_{IN}}$.

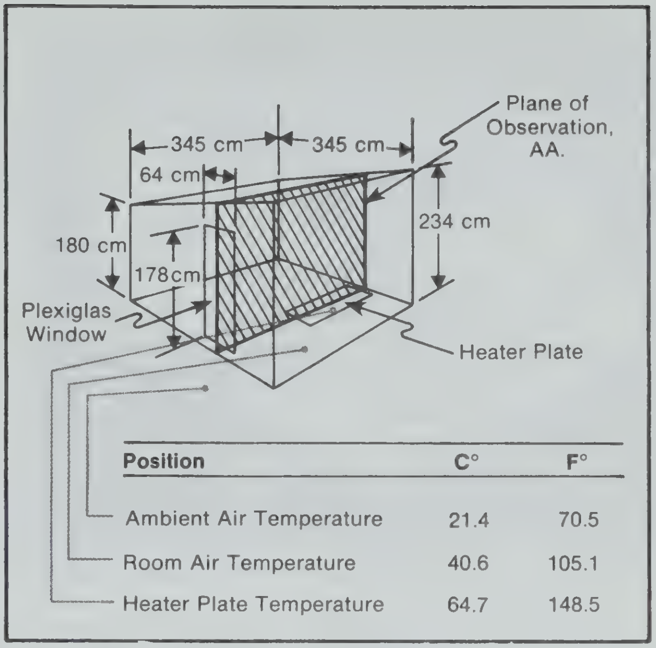

Position	C°	F°
Ambient Air Temperature	21.4	70.5
Room Air Temperature	40.6	105.1
Heater Plate Temperature	64.7	148.5

Fig. 7. Schematic diagram of Ruberg's full-scale test [23].

tion to the details of the (unmeasured) surface temperature distributions.

A Full-Scale Experiment

Natural convection was investigated by Ruberg [23] at the Massachusetts Institute of Technology in the full-sized test room shown schematically in Fig. 7. The conditions of this experiment correspond more closely to those in a real building. Heat was supplied to the test room by an electric resistance heater plate on the floor. A single-pane window was located on one wall of the enclosure. Though the window represents only 2 percent of the envelope area of the test room, it dominated the thermal load; 22 percent of the total heat loss was measured to be through this surface. Steady-state conditions were maintained by controlling the temperature of the air outside the test room to within ± 0.2° C (0.4° F) of its average value. The construction was sufficiently airtight that the effects of infiltration could be ignored.

The heater plate configuration was intended to represent a solar irradiated area on the floor; its rectangular shape and its size [1.16 m² (12.5 ft²)] were well matched to those of the 1.12-m² (12-ft²) window, and its heating capacity [448 W/m² (142 Btu/hr ft²)] was selected to approximate solar radiation falling on a dark-colored floor with low thermal capacity at noon on a clear day at 40° N latitude. The parameters for this experiment were:

$$A = 0.58,$$
$$Pr = 0.71, \text{ and}$$
$$Ra_L = 5 \times 10^{10}.$$

Convection observed in the test room was characteristic of the transition regime between laminar and turbulent flow. A schematic of the air flow patterns is shown in Fig. 8. Note the essentially three-dimensional character of the flow.

Air temperatures were measured with a vertical array of 11 thermistors mounted on a motorized boom which traversed the test room in the measurement plane. The array had 20-cm (8-in.) vertical spacings in the center and 10-cm (4-in.) spacings near the ceiling and floor; data were recorded at 20-cm (8-in.) horizontal intervals as the boom moved across the room. This resulted in a grid of 11 × 18 temperature data points in the measurement plane which perpendicularly bisects the window and the heater surfaces (plane AA in Fig. 7).

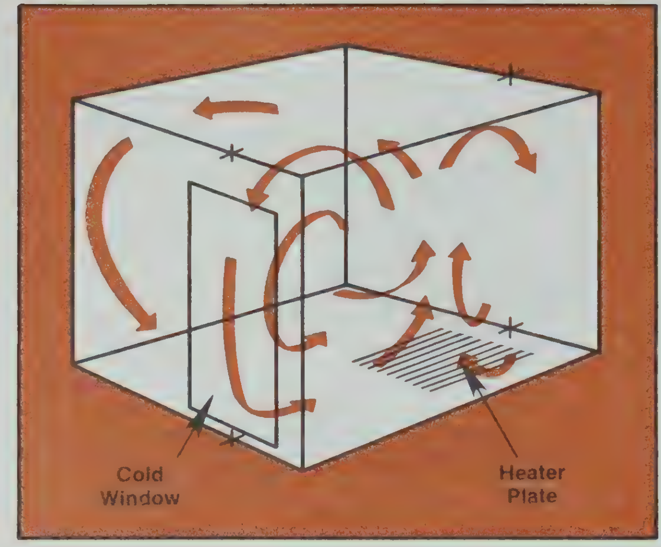

Fig. 8. Schematic of air-flow patterns in Ruberg's experiment [23].

Temperature measurements were converted to isotherms separated by intervals of 5 percent of the maximum surface-temperature difference in the room. The isotherms were referenced to the mean temperature of the room, indicated on Fig. 9 as 0.000. The three sets of isotherms represent data from three separate measurements of air temperatures under identical conditions. From the isotherms, the air flow patterns shown in Fig. 8 may be discerned: the plume over the heater plate, a layer of warm air at the ceiling, a cool air current at the window and along the floor, and a somewhat isothermal area in the center of the room. For more details of this experiment, see Ref. 23.

Data from this full-scale experiment were compared with the predictions from the three-dimensional version of the numerical code. The surface temperature profiles used in the analysis were estimated from the available data using a thermal balance technique. It is noted that the effects of radiation on the temperature probes are expected to bias the measured air temperatures toward higher values by an unknown amount. This effect was not accounted for in the thermal balance. This bias also affects the comparisons between the isotherms predicted by the numerical scheme (Fig. 10) and the experimental results (Fig. 9). Also, as noted above, the observed flow was in the transition regime (between laminar and fully turbulent), but was simulated with a numerical code assuming laminar flow. In light of these limitations, the agreement is satisfactory.

The validations described here have been performed with the available experimental data covering the range of interest of the important dimensionless parameters. The discrepancies between the predictions and the observations are thought to be understood, at least qualitatively. The computer program appears to simulate the convective flow correctly for $Ra_L < 5 \times 10^{10}$. The second phase of the ongoing small-scale experiment at LBL is expected to provide quantitatively a sound basis for further validation of the computer code at higher Rayleigh numbers.

The computer program, in its present validated form, has been used to study the influence of natural

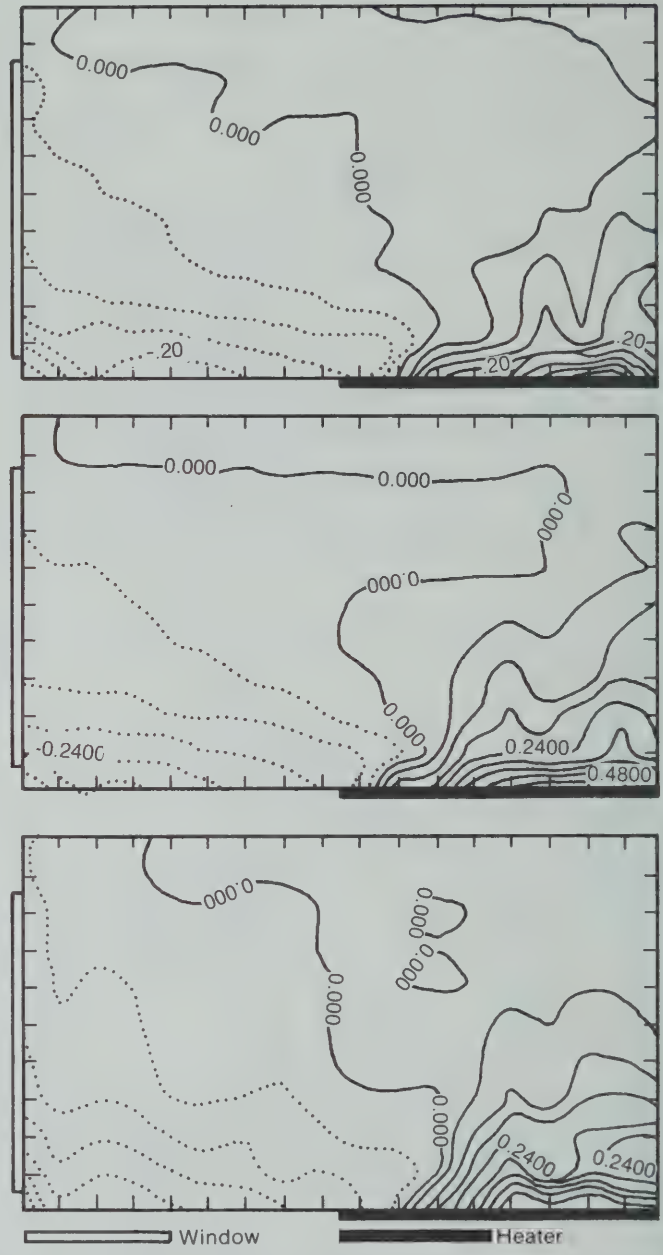

Fig. 9. Isotherms measured in Ruberg's experiment [23].

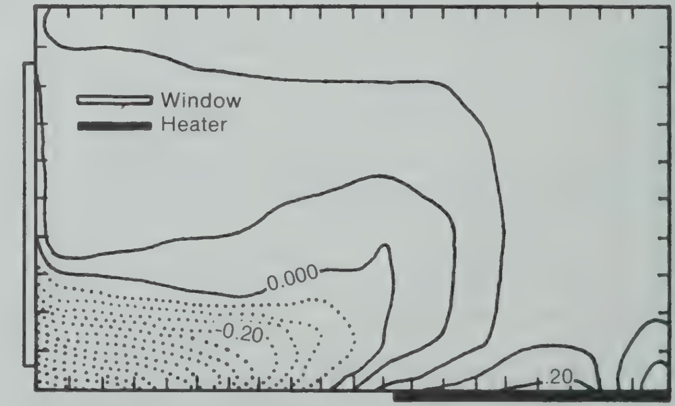

Fig. 10. Isotherms predicted by three-dimensional numerical code.

convection on the thermal performance of a single room in a direct gain passive solar building. This is described in the next section.

Convection Effects in Building Energy Analysis

Most building energy analysis techniques, including the most sophisticated computer codes (BLAST*, DOE-2†, etc.) and other passive solar system analysis programs, make the simplifying assumptions that (1) the air temperatures throughout the volume of the individual zones in the structure are uniform, and (2) the convection heat transfer coefficients for the surfaces of the building being analyzed are constants. These assumptions are largely consistent with the state of knowledge regarding convection at the time the codes‡ were developed. In a preliminary study [15], it was shown that convection coefficients at the surfaces of an enclosure are actually quite sensitive to the temperature distributions on the surfaces. To estimate the effects of this observation on the accuracy of results from the programs, the convection code was used iteratively with BLAST to obtain self-consistent surface temperature distributions and convection coefficients.**

The south-facing zone (S-zone in Fig. 11b) of a multizone building was studied. The floor plan of the building is shown in Fig. 11a. Figures 11b and 11c show the thermal zones used in the BLAST simulations. The building has been thoroughly described elsewhere [28]. This zone has dimensions of 3.7 m wide × 9.2 m long × 2.5 m high (12 ft × 30 ft × 8 ft). For the purpose of this study, the following modifications to the zone were made. The interior of the analyzed zone was made up of 14 surface segments. The two "end surfaces" (the east partition wall and the west exterior wall) measured 2.5 m × 3.7 m (8 ft × 12 ft) and were very highly insulated. The other four major surfaces (ceiling, slab floor, gypsumboard north partition wall, and the south exterior wall) were each divided into three equal subsurfaces (see Fig. 12). The individual subsurfaces extended the full 9.2-m (30-ft) length of the zone. The middle section of the south wall was specified as double-pane window. Iterative analyses were performed for both the nighttime (loss) and daytime (gain) modes for a selected winter design day.

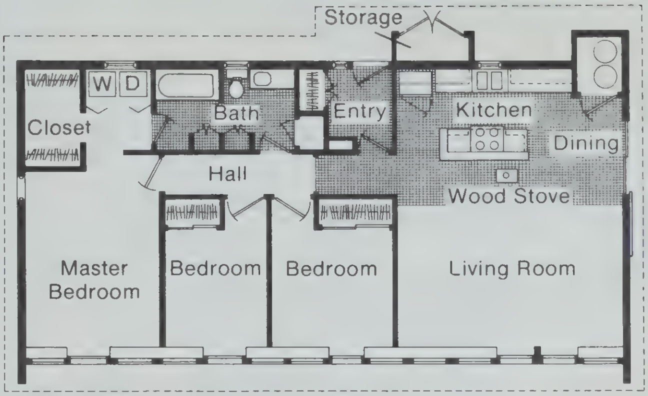

Fig. 11a. Floor plan of test building.

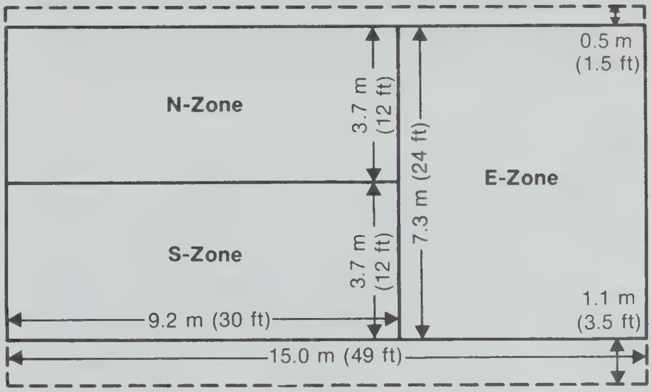

Fig. 11b. Floor plan showing thermal zones for BLAST simulation.

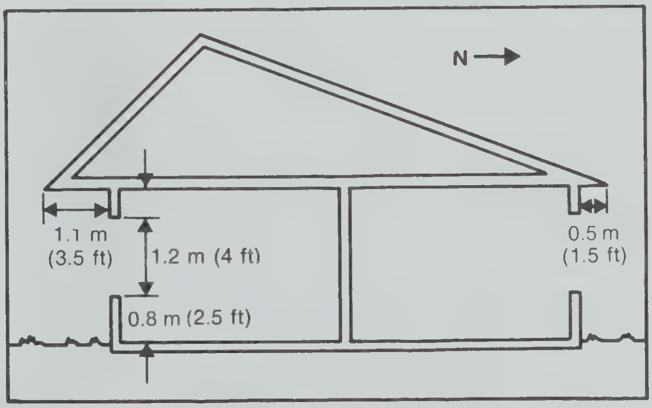

Fig. 11c. Cross-section for BLAST simulation.

For each iterative sequence of calculations, BLAST was first used to calculate the surface temperatures of each subsurface defining the zone for each hour of the design day using the standard constant convection coefficients. BLAST performs a full thermal balance on all surfaces of the zone under study and the zone air. The surface thermal balance accounts for thermal radiation between zone surfaces; convection between zone air and each surface; conduction through each surface; and radiative gains from occu-

---

* BLAST (Building Loads Analysis and System Thermodynamics) is copyrighted by the Construction Engineering Research Laboratory, U.S. Department of the Army, Champaign, Illinois.

† DOE-2 is a public domain program being developed by the Division of Communities and Building Energy Systems, U.S. Department of Energy.

‡ Some of the codes do utilize convection coefficients for nonvertical surfaces which are sensitive to the direction of heat flow, but not to the magnitude of the temperature difference between the room air and surface or to the possibly large effects induced by the differences in the temperatures of the different surfaces defining the zone.

** The convection heat transfer coefficient (CHTC) for a given surface is defined by the relation CHTC $= q/\Delta T$ where q = heat flux from the surface into the room air, ΔT = (average surface temperature) - (room air temperature).

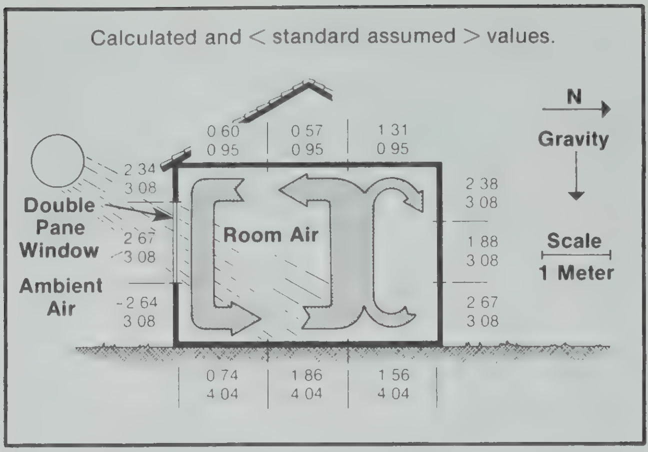

Fig. 12. Convection coefficients (W/m² °C) between the room air and the interior subsurfaces of a single zone in a house. Steady state (daytime) heat gain mode.

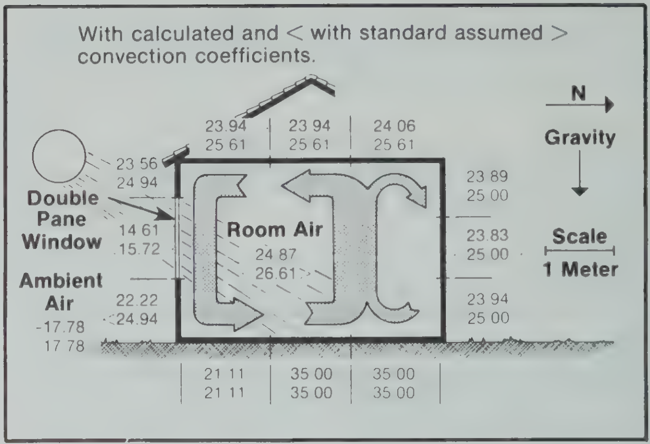

Fig. 13. Surface temperatures (°C) on the interior subsurfaces of 'a single zone in a house. Steady state (daytime) heat gain mode.

pants, lights, equipment, and transmitted solar energy. The thermal balance on the air accounts for convective gains from surfaces, occupants, lights, and equipment and for controlled and uncontrolled ventilation. For this study, the relevant output from BLAST was the distribution of temperatures of the subsurfaces defining the zone boundary. From the design day results, two hours were chosen for further analysis of convection: one hour at night when the zone is in the loss mode and one hour during midday when the zone is in the solar gain mode.

Because of the zone geometry and the distribution of the surface temperatures, the convective flow was expected to be two-dimensional. The subsurface temperatures calculated by BLAST were input to the two-dimensional convection code to simulate the details of the convection process and to calculate convection heat transfer coefficients for each subsurface. These coefficients were then used as input to BLAST to obtain the new subsurface temperatures. These temperatures were again used as input to the convection code, and the entire procedure was iterated until self-consistent results were obtained. Several features of the iteration process should be noted here.

- At this time, the convection code cannot account for sources and/or sinks of thermal energy in the air volume under study. Therefore, the BLAST simulation did not include auxiliary heating and/or cooling of the zone in which the convection was to be analyzed; the zone temperature was free-floating though adjacent zones were heated. This limitation led to the selection of an exterior dry-bulb temperature for the design day such that the zone air temperature would float near a typical daytime thermostat (nighttime thermostat setback) temperature. These temperatures are shown in Figs. 13 and 15.
- During the loss mode (nighttime) iterations, the north partition wall, representing a warm storage wall, and properly accounting for the existence of a conditioned zone to the north, was held at a constant temperature and was the primary heat source for the zone. During the gain mode (daytime), only the two subsurfaces of the slab floor closest to the north partition wall were irradiated by solar transmission through the south glazing. This configuration corresponds to midday conditions during the winter (solar altitude = 30°). These subsurfaces were the primary heat source for the zone, and their surface temperatures were held constant throughout the iteration process. Here, too, the effect of the adjacent conditional zones was properly accounted for by the BLAST analysis. The glass was also held at a constant surface temperature during the gain mode.
- A design day with varying ambient temperatures and other environmental parameters was used initially to calculate the starting points for the iteration scheme, but during the iterations steady-state external conditions were assumed to observe convergence more clearly. Since the BLAST simulations assumed no auxiliary heating or cooling in the zone being analyzed, the exterior temperature was selected to ensure that reasonable comfort conditions were maintained in the zone with the specified constant surface temperatures described.

The results of the detailed convection analysis are summarized in Figs. 12-15. The surface temperatures and convection coefficients obtained both with and without the iterative procedure using the convection code are shown in these figures. More detailed heat transfer data for the two modes are given in Tables 2 and 3. In these tables, subsurfaces are numbered sequentially around the zone; results for the thermal parameters for each subsurface appear in the table. Case I refers to standard assumptions, and Case II refers to the values after the iterations.

The convection coefficients are seen to change substantially from their standard assumed values for most of the surfaces. This is particularly true during the loss mode in which strong boundary-layer flows develop along both the warm north wall and the cold south window. During the gain mode, circulation induced by large, warm areas of the floor does not contain such strong boundary-layer flows. The balance point air temperature (mean radiant temperature) for the zone is observed to change by 0.51°C

Surface	Subsurface Number	Subsurface Location	Standard Building Energy Analysis Assumptions				Values After Iteration With Convection Code			
			Surface Temp. °C	Convection Coefficient W/m^2 °C	Convective Heat Flux From Zone To Surface W/m^2	Total Heat Flux From Zone To Surface W/m^2	Surface Temp. °C	Convection Coefficient W/m^2 °C	Convective Heat Flux From Zone To Surface W/m^2	Total Heat Flux From Zone To Surface W/m^2
South Exterior Wall	1	Top	20.11	3.08	2.53	7.46	19.72	4.27	2.99	6.91
	2	Middle/Window	11.22	3.08	29.91	83.87	10.06	1.97	20.41	77.18
	3	Bottom	20.11	3.08	2.53	7.46	18.61	−1.79	−3.24	7.03
Slab-On Grade Floor	4	South	20.89	4.04	0.16	0.57	20.39	7.18	0.22	0.28
	5	Middle	20.89	4.04	0.16	0.57	20.39	2.73	0.08	0.14
	6	North	20.89	4.04	0.16	0.57	20.39	1.64	0.05	0.11
North Partition Wall	7	Bottom	26.67	3.08	−17.68	−51.91	26.67	2.47	−15.44	−52.91
	8	Middle	26.67	3.08	−17.68	−51.91	26.67	1.60	−10.02	−47.49
	9	Top	26.67	3.08	−17.68	−51.91	26.67	1.15	−7.20	−44.67
Ceiling To Attic	10	North	20.56	0.95	0.35	2.67	20.17	8.90	2.22	3.55
	11	Middle	20.56	0.95	0.35	2.67	19.83	1.17	0.69	3.98
	12	South	20.56	0.95	0.35	2.67	19.83	0.85	0.50	3.79
			T_{AIR} = 20.93, T_{MRT} = 20.96				T_{AIR} = 20.42, T_{MRT} = 20.40			

T_{AIR} = Average Temperature of Air in the Zone, °C T_{MRT} = Mean Radiant Temperature in the Zone, °C

Table 3. Convective Analysis of a Single-Zone, Loss Mode (Figs. 14 and 15)

would be nearly twice as rapid as that from the top portions. Another interesting feature is the very large convection coefficient [8.9 W/m^2°C (1.56 Btu/hr ft^2°F)] for the portion of the cool ceiling directly warmed by the updraft from the warm north wall. Since the ceiling was well insulated, the temperature difference between this portion of the ceiling and the room air was decreased (by about 50 percent) with only a negligible change in the heat loss to the attic.

The results presented in Table 3 show that during the gain mode, the convective heat transfer from the floor to the air is reduced by about a factor of two when correct convection coefficients are used. This contributes to the observed lowering of the air temperature in the zone. Total heat transfer to the nonilluminated massive north partition wall is reduced by only approximately 20 percent. Also, losses from the south window are reduced by about 8 percent; this change is about equally split between reductions in convection and radiation.

During both modes of operation, the portion of the south wall directly below the double-pane window encounters a downdraft of cold air that has lost heat through the window. This downdraft of air is actually colder than the interior surface of the bottom portion of the south wall (this surface is warmed by radiative exchange with the other surfaces of the zone). Thus, although the bottom section of the south wall is actually cooler than the average room temperature, it deposits heat into the cold downdraft flowing across it. This has resulted in a negative convection coefficient for this subsurface (the convection coefficients are defined with respect to the average room air temperature).

From a practical viewpoint, convection coefficients and surface temperatures are of little real interest except as they influence comfort levels and/or thermal load. Here, the building load is a quantity of fundamental interest. To estimate the effect on the thermal load of a change in any building parameter, the accepted "exact" method (i.e., coheating) is described as follows: The building temperature is maintained at a constant level before and after the parametric change by introducing a heat source/sink of appropriate magnitude. The difference between the heat supplied/removed by the source/sink in the two cases gives the effect of the parametric change on the building load [29].

Since the BLAST simulations described here did not include heat sources/sinks, a less exact method based on the balance point air temperature was used to estimate the effect of the changed convection coefficients on the zone load. This method was calculated (using a radiation balance technique) to be in error by less than 2 percent (with respect to the results of the "exact" coheating method) for the configuration under study.

The zone under examination was simulated by BLAST with two different thermostat control profiles. The "base case" thermostat settings were (arbitrarily) set at 21.1°C (70°F) for daytime (gain mode) heating and 16.7°C (62°F) for nighttime (loss mode) heating. The base simulation assumed the same external weather conditions as used in the iteration procedures for the two modes of operation. Iterations with the convection code had predicted changes in the balance point air temperatures of 1.7°C (3°F) and 0.5°C (1°F) for the gain and loss modes respectively. The net effect of the balance point change would be to decrease the cooling load and/or increase the heating load. Therefore, during the second load calculation the second thermostat profile was set at

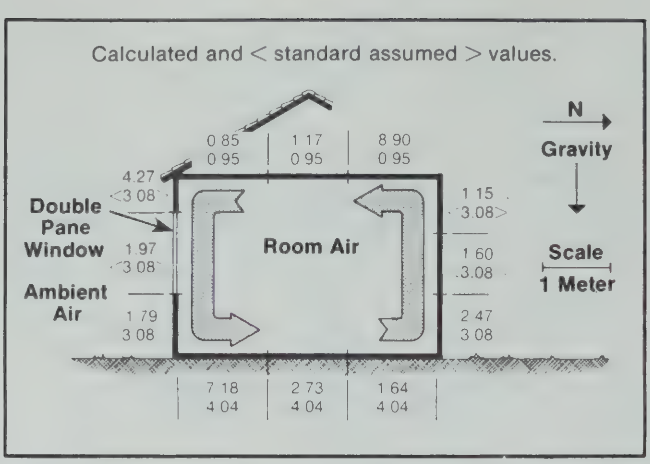

Fig. 14. Convection coefficients (W/m² °C) between the room air and the interior subsurfaces of a single zone in a house. Steady state (nighttime) heat loss mode.

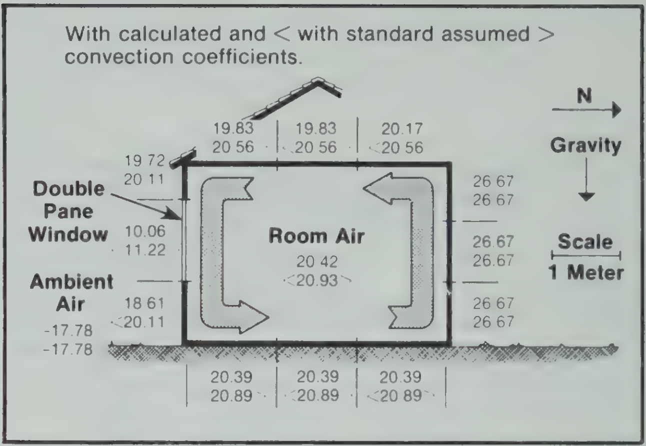

Fig. 15. Surface temperatures (°C) on the interior subsurfaces of a single zone in a house. Steady state (nighttime) heat loss mode.

(0.56°C) [1°F(1°F)] and 1.74°C (1.08°C) [3°F(2°F)] for the loss and gain modes, respectively.

The thermal behavior of the zone during the loss mode changes less than might be expected. The following considerations are relevant to this observation:

- The surfaces that are coupled to the room air through larger convection coefficients in Case II have smaller resulting temperature deviations from the room air temperature than in Case I. On the other hand, the surfaces that are coupled to the room air through smaller convection coefficients in Case II tend to have larger resulting temperature deviations from the room air than in Case I. This has a moderating influence on what otherwise would have been larger changes in the convective (and radiative) heat fluxes.
- Radiative exchange is of the same order of magnitude as convection in thermally coupling the zone surfaces to one another. For this reason, changes in the convective heat flux will have a smaller percentage effect on the total heat flux (convection + radiation) from a surface.

During the loss mode, the convective heat flux from the warm north wall shows a significant variation along its height [15.4 W/m² (4.9 Btu/hr ft²) from the bottom of the wall to 7.2 W/m² (2.3 Btu/hr ft²) from the top]. As cold air warms at the bottom of the north wall and rises, the upper portions of the wall encounter relatively warmer air and can contribute relatively less heat to this air. If this north wall were a heat storage system, in this configuration the convective recovery of heat from the bottom portions of the wall

Surface	Subsurface Number	Subsurface Location	Standard Building Energy Analysis Assumptions				Values After Iteration With Convection Code			
			Surface Temp. °C	Convection Coefficient W/m² °C	Convective Heat Flux From Zone To Surface W/m²	Total Heat Flux From Zone To Surface W/m²	Surface Temp. °C	Convection Coefficient W/m² °C	Convective Heat Flux From Zone To Surface W/m²	Total Heat Flux From Zone To Surface W/m²
South	1	Top	24.94	3.08	5.14	20.34	23.56	2.34	3.63	19.78
Exterior	2	Middle/Window	15.72	3.08	33.54	163.85	14.61	2.67	27.10	151.98
Wall	3	Bottom	24.94	3.08	5.14	20.34	22.22	-2.64	-7.81	19.21
Slab-On	4	South	21.11	4.04	22.22	60.46	21.11	0.74	2.98	44.64
Grade	5	Middle	35.00	4.04	-33.89	-159.89	35.00	1.86	-18.30	-142.94
Floor	6	North	35.00	4.04	-33.89	-159.89	35.00	1.56	-15.40	-137.30
North	7	Bottom	25.00	3.08	4.96	19.21	23.94	2.67	3.08	15.26
Partition	8	Middle	25.00	3.08	4.96	19.21	23.83	1.88	2.54	15.26
Wall	9	Top	25.00	3.08	4.96	19.21	23.89	2.38	2.98	15.26
Ceiling	10	North	25.61	0.95	0.95	11.86	24.06	1.31	1.45	11.86
To	11	Middle	25.61	0.95	0.95	11.86	23.94	0.57	0.65	11.86
Attic	12	South	25.61	0.95	0.95	11.86	23.94	0.60	0.69	11.86
			T_{AIR} = 26.61, T_{MRT} = 25.91				T_{AIR} = 24.87, T_{MRT} = 24.83			
T_{AIR} = Average Temperature of Air in the Zone, °C					T_{MRT} = Mean Radiant Temperature in the Zone, °C					

Table 2. Convective Analysis of a Single Zone, Gain Mode (Figs. 12 and 13)

22.8°C (73°F) (21.1°C + 1.7°C) for daytime heating and 17.2°C (63°F) (16.7°C + 0.5°C) for nighttime heating.

The results of the BLAST runs using these two different thermostat control profiles are shown in Table 4. The calculated percentage increase in the zone load for this particular case is seen to be quite large. It is noted that the small magnitude of the calculated thermal load represents the load through one external wall of one zone, and is only a fraction (about 20 percent) of the total building load.

Thermostat Settings		Corresponding Convection Coefficient Assumption	Calculated Thermal Load* kWh/Day
T_{Day} (7:00 am to 11:00 pm) °C	T_{Night} (11:00 pm to 7:00 am) °C		
21.1	16.7	Constant	1.97
22.8	17.2	Variable	2.93

*Assuming no internal loads and no infiltration

Table 4. Influence of Variable Convection Coefficients of Calculated Thermal Loads from BLAST.

The results presented here suggest that energy analysis of passive solar systems must include a more detailed representation of natural convection processes than current techniques allow. The iterative procedure described in this section has intentionally assumed somewhat oversimplified building occupancy and performance parameters (e.g., no internal loads, no infiltration, etc.). Though the example is not directly representative of real buildings, the simplifying assumptions are not expected to be the source of the observed discrepancies. These discrepancies are not expected to have been amplified by the simplifying assumptions unless the building is so dominated by occupant effects and operation that the natural convection processes become relatively small in comparison to forced convection. This is contrary to experience (e.g., Ref. 1) and to intuition. To more definitively assess the importance of convection effects on building loads, the convection analysis code described here will be modified. The new program will allow the addition of heat sources/sinks to the enclosure so that the balance point approach to calculating the change in building load can be replaced with the more exact coheating analysis. The capability of modeling turbulence is also planned.

Summary

A numerical technique for modeling natural convection in room geometries has been developed. The numerical predictions from this technique have been compared with various published data and demonstrate satisfactory agreement. The results from a small-scale and a full-scale experiment studying natural convection in room geometries have been presented. The numerical predictions are compared with the results of these experiments; the agreement is also satisfactory. The convection code has been used in conjunction with the BLAST computer program to investigate the thermal behavior of a realistic direct-gain zone configuration. The results indicate that:

- The detailed modeling of convection may have a significant effect on the zone air temperature and the mean radiant temperature.
- More carefully calculated values of the convection coefficients can be substantially different from the values currently assumed by the standard building energy analysis methods.
- The convection coefficients for a particular surface can have large diurnal variations.
- The convection coefficients can show a significant variation across a given zone surface.
- Such variations in convection coefficients can have substantial effects on thermal loads for a structure.

Glossary of Technical Terms

Buoyancy-Driven Convection: Convection driven by differences in the density of air at different temperatures within a space. This is sometimes also referred to as free or natural convection.

Zone: A room (or enclosure) in a building within which the air temperature (or comfort conditions) can be assumed to be homogeneous to an adequate approximation. These comfort conditions can then be calculated from the incident solar radiation, heat gain/loss through the exterior surfaces of the zone, internal heat gain within the zone, the rate of air exchanged with the outdoor environment and neighboring zones, etc.

References

1. Balcomb, J.D., Hedstrom, J.C., and Moore, S.W. *Performance Data Evaluation of the Balcomb Solar Home*. LASL/LA-UR-79-2659, 1979, Los Alamos Scientific Laboratory, Los Alamos, N.M.
2. Bauman, F. et al. "Buoyancy-Driven Convection in Rectangular Enclosures: Experimental Results and Numerical Calculations." *Proceedings, 19th National Heat Transfer Conference*. LBL-10257, 1980.
3. Buchberg, H. "Sensitivity of Room Thermal Response to Inside Radiation Exchange and Surface Conductance." *Building Science* 6:133. 1971.
4. Ostrach, S. "Natural Convection in Enclosures." *Advanced Heat Transfer* 8:161. 1972.
5. Rowley, F.B., Algren, A.B., and Blackshaw, J.L. "Surface Conductances as Affected by Air Velocity, Temperature, and Character of Surface." *Journal of the American Society of Heating and Ventilating Engineers* 2:501. 1930.
6. Rowley, F.B. and Eckley, W.A. "Surface Coefficients as Affected by Direction of Wind." *Journal of the American Society of Heating and Ventilating Engineers* 3:870. 1931.
7. *ASHRAE Handbook of Fundamentals*. Chapter 2. New York. 1977.
8. Nielsen, P.V. Ph.D. thesis, "Flow in Air-Conditioned Rooms." Technical University of Denmark, Copenhagen. 1974.
9. Honma, H. Ph.D. thesis, "Ventilation of Dwellings and Its Disturbances." Royal Institute of Technology, Stockholm, Sweden. 1975.
10. Weber, D.D. "Similitude Modeling of Natural Convection Heat Transfer Through an Aperture

in Passive Solar Heated Buildings." LASL/LA-8385-T, 1980, Los Alamos Scientific Laboratory, Los Alamos, N.M.

11. Wall, L.W. et al. "Conservation Options in Residential Energy Use: Studies Using the Computer Program TWOZONE." LBL-5271, 1977, Lawrence Berkeley Laboratory, Berkeley, Calif.
12. Roache, P.J. *Computational Fluid Dynamics.* Albuquerque, N.M.: Hermosa Publishers. 1972.
13. Spalding, D.B. "A Novel Finite Difference Formulation for Differential Expressions Involving Both First and Second Derivations." *International Journal of Numerical Methods in Engineering* 4:551-559. 1973.
14. Runchal, A.K. "Convergence and Accuracy of Three Finite Difference Schemes for a Two-Dimensional Conduction and Convection Problem." *International Journal of Numerical Methods in Engineering* 4:541-550. 1973.
15. Gadgil, A. Ph.D. thesis, "On Convective Heat Transfer in Building Energy Analysis." University of California, Berkeley. 1980.
16. de Vahl Davis, G. "Laminar Natural Convection in an Enclosed Rectangular Cavity." *International Journal of Heat and Mass Transfer* 11:1675. 1968.
17. Emery, A.F. "The Effect of a Magnetic Field upon the Free Convection of a Conducting Fluid." *Journal of Heat Transfer, Transactions of the American Society of Mechanical Engineers* 85:2. 1963.
18. Portier, J.J. and Arnas, O.A. *Heat Transfer and Turbulent Buoyant Convection.* Vol. II. Washington, D.C.: Hemisphere Publishing Corp. 1977.
19. Burnay, G., Hannay, J., and Portier, J. *Heat Transfer and Turbulent Buoyant Convection.* Vol. II. Washington, D.C.: Hemisphere Publishing Corp. 1977.
20. Rubel, A. and Landis, R. "Numerical Study of Natural Convection in a Vertical Rectangular Enclosure." *Physics of Fluids* Suppl. II, 12:II-208. 1969.
21. Quon, C. "High Rayleigh Number Convection in an Enclosure: A Numerical Study." *Physics of Fluids* 12:1. 1972.
22. Fromm, J.E. *A Numerical Method for Computing the Nonlinear, Time Dependent, Buoyant Circulation of Air in Rooms.* Building Science Series No. 39. Washington, D.C.: National Bureau of Standards, 1971.
23. Ruberg, K. Master's thesis, "Heat Distribution of Natural Convection: A Modeling Procedure for Enclosed Spaces." Massachusetts Institute of Technology, Cambridge. 1978.
24. MacGregor, R.K. and Emery, A.F. "Free Convection through Vertical Plane Layers — Moderate and High Prandtl Number Fluids." *Journal of Heat Transfer, Transactions of the American Society of Mechanical Engineers* 91:392-401. 1969.
25. Raithby, G.D., Hollands, K.G.T., and Unny, T.E. "Analysis of Heat Transfer by Natural Convection across Vertical Fluid Layers." *Journal of Heat Transfer, Transactions of the American Society of Mechanical Engineers* 99:287-293. 1977.
26. El Sherbiny, S.M., Raithby, G.D., and Hollands, K.G.T. "Heat Transfer by Natural Convection across Vertical and Inclined Air Layers." *Proceedings, 19th National Heat Transfer Conference.* 1980.
27. Shiralkar, G., Gadgil, A., and Tien, C.L. "High Rayleigh Number Convection in Shallow Enclosures with Different End Temperatures." Submitted for publication to *International Journal of Heat and Mass Transfer.*
28. Carroll, W.L., Place, W., and Curtis, B. "A Passive Solar Residential Prototype for Energy Modeling." LBL-10783, 1980, Lawrence Berkeley Laboratory, Berkeley, Calif.
29. Sonderegger, R.C., Condon, P.E., and Modera, M.P. "In-Situ Measurements of Residential Energy Performance Using Electric Co-Heating." LBL-10117, 1980, Lawrence Berkeley Laboratory, Berkeley, Calif.

Market Potential Indexing: A New Technique for Analyzing Solar Markets

Scott A. Noll, William M. Robson, and Marilyn K. Yeamans
Modeling and Economic Analysis Group (S-2)
Los Alamos Scientific Laboratory
Los Alamos, NM 87545

Abstract *A methodology for evaluating the relative market potentials of various solar technologies on a city-specific basis is presented. The methodology, selection of attributes and weighting factors, and the development of data bases for the model are described and analyses run for four regions of the country.*

Introduction

A significant number of economic analyses have been conducted in the last five years to try to predict the effects of solar energy use on the national energy economy. The work has focused on computer simulation models of the economic and engineering performance of various active solar technologies. Several models have attempted to predict the market penetrations of various solar technologies into the existing fossil fuel residential space and water heating market. These market penetration models rely on comparative cost data and logistic technology substitution curves. They are generally aggregated to a regional or national level and, therefore, have no benefit for analysis of local markets. Their primary focus is to evaluate policy decisions that are made at a national level, using theoretical economic behavior as their basis for prediction [1].

The high level of aggregation in these models makes them of little use to those trying to implement state or local programs to stimulate the use of solar energy. It is well recognized that local market conditions vary widely for various solar technologies and are based on many economic, technical, and sociological factors [2,3]. If policy makers and implementers are to make rational decisions that will efficiently increase the use of solar technology, they must have tools to evaluate local, state, and regional market conditions.

The Department of Energy (DOE) and the Regional Solar Energy Centers (RSEC) expressed a need for an evaluation method to determine the relative market potential of various solar technologies on a city-specific basis. To respond to this need, the Los Alamos Scientific Laboratory (LASL) Modeling and Economic Analysis Group (S-2) developed a Market Potential Indexing (MPI) technique to undertake city-specific comparisons [4-6]. The approach, based upon the management science technique of multiattribute decision analysis, hypothesizes that the market potential for passive solar energy in a given locale is a function of a fixed number of identifiable and quantifiable attributes. The attributes, varying according to building type (single-family, multifamily, mobile housing) and new or retrofit construction, are evaluated and scaled using either positive or negative sensed data and assigned a value (between 0 and 100) for each attribute in each city. Because each attribute has a different relative importance to passive solar market potential, weighting factors assigned to each attribute reflect these differences. The weighted attributes are then summed to provide a single index value for each of 220 clustered county solar performance regions.

This article describes the development of the Market Potential Indexing (MPI) methodology; the results obtained from several preliminary studies; and the future plans for research, implementation, and verification of the technique.

Discussion of Market Potential Indexing

Market Potential Indexing vs. Market Penetration Analysis

Market penetration analysis has been the primary technique used by economic modelers in their attempt to study the effects of various policy decisions on the current energy situation. These studies have attempted to predict how alternate energy sources could be made more attractive as substitutes for fossil fuel energy. The market research literature contains a wealth of information on the use of "logistic substitution curves" as predictive techniques for market penetration of alternative technologies [7,8].

The models are supposed to indicate how buyers will react to the relative economic competitiveness of a current technology as compared to a new one. The pattern of change is usually predicted solely on the basis of estimated economic advantage [9]. This model has some validity when applied to the commercial/industrial environment where most decisions are based primarily upon rational economic reasoning processes. When one is dealing with the public sector, however, many other factors enter into the decision processes [2], and the current market penetration models are not equipped to take these additional social/behavioral factors into account. Thus, their predictions may have no relevance for analysis of short-term, local market conditions [10].

At present, few market analysis tools other than the market penetration models are available to those charged with implementing passive solar energy usage goals, and the penetration models do not adequately define local markets for passive solar energy. If the DOE-established goal of stimulating the use of passive solar energy is to be realized, both the demand and supply sides of each local market must be analyzed to determine what measures will be most effective for stimulating the use and adoption of passive solar designs and components in the local housing market. In addition, the various local markets must be compared to determine where the maximum and minimum market potentials exist. This can be done through the technique of Market Potential Indexing.

During the past four years, members of the University of New Mexico (UNM) Resource Economics Group and staff from LASL have developed an economic performance code to evaluate the feasibility of residential passive solar space heating systems [11]. The model—LASL/UNM EASE III Economic Performance Code—is used to provide the technical, economic, and cost input data, as well as to structure the geographic market boundaries of the MPI model. The LASL/UNM model uses 220 clustered county regions, based on the SOLMET [12] weather data base, to define a set of highly disaggregated data bases. The LASL/UNM model is designed to operate with clustered county segments which cover the entire continental United States. These data are used as the starting point for the market potential indexing process (Fig. 1).

Each local market has a set of common attributes (e.g., weather characteristics, solar performance, building costs, fuel type usage and costs) which can be evaluated. The various attributes have different effects on the local market potentials. By using multiattribute decision analysis techniques, one can construct a quantitative market potential model which will allow comparison among the various local markets.

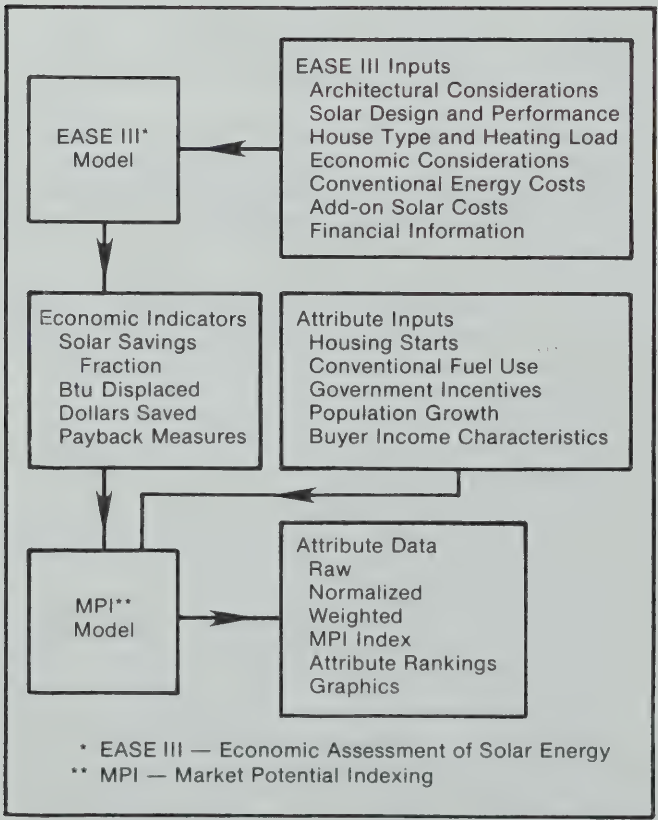

Fig. 1. Relationship between the EASE III and MPI models

Structure of the Methodology

The first step in any market analysis effort is to define the market(s) to be analyzed. This process, done on several levels, is typically called "Market Segmentation." Geographic boundary is the first level of market segmentation in the market potential indexing methodology. The structure of the LASL/UNM model divides the continental United States into 220 clustered county segments. This division process was dictated by the structure of the SOLMET weather data base and the LASL Q-11 load-collector-ratio (LCR) passive solar performance tables [13]. There is a reasonably good correlation between these clustered county segments and the population centers of the United States.

Once the national market is segmented geographically, the next steps of market segmentation become more complex. The goal of the segmentation process is to divide the market into units which can be analyzed for the potential of energy substitution by the use of solar technologies. Figure 1 illustrates the market segmentation structure used with LASL's market potential indexing methodology. Many other structures could be used, but this one was chosen because it fits best with the data structure of the LASL/UNM model.

As Fig. 2 illustrates, the next level of segmentation is the market sector split. At this level, the market is divided into three sectors: residential, commercial, and industrial/agricultural. These categories were chosen because they exhibit distinctly different patterns of building and plant energy equipment purchase, and financial motivation.

Residential building structures are usually characterized as having skin-dominated heating and cooling energy loads. The passive solar performance data generated by the LASL Q-11 Solar Energy Group are directly applicable to residential, skin-dominated building structures, so the separation of residential buildings as a market segment becomes quite sensible.

Most larger scale commercial buildings are internal-load dominated: that is, very often, cooling demands result from internal heat generated by lights, people, and operation of mechanical equipment. In addition, commercial buildings are usually characterized by multizone heating/cooling/lighting demands, so sophisticated distribution and ventilation HVAC equipment is installed to provide space conditioning. These factors, combined with the difficulty of collapsing performance data for passively tempered commercial buildings into simplified performance factors (as with the LCR method for residential applications), justify the separation of these building types as a distinct market segment.

A final market segment for building energy consumption is the industrial/agricultural sector. Although buildings in this sector do require space conditioning, the majority of energy use relates to process energy needs in the form of direct electric drive, direct heat, process steam, or hot water. The current structure of the LASL/UNM model and the primary emphasis of LASL S-2's passive solar work prohibit the consideration of the market potential for passive solar energy in this segment. However, with some reformulation and

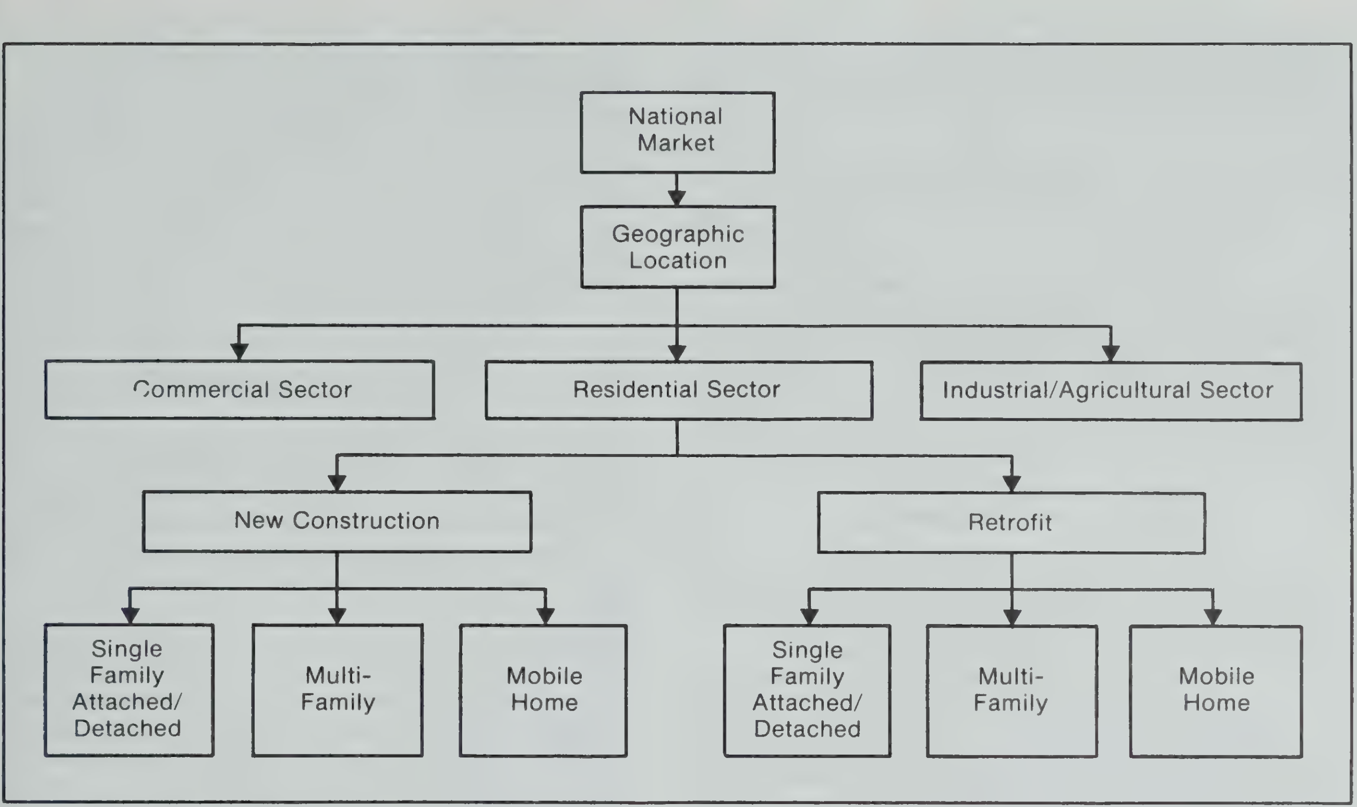

Fig. 2. Market segmentation structure of the MPI model

adequate solar performance data, market potential indexing could be applied to this sector as well.

The present emphasis of the market potential indexing methodology is on the residential sector, because of the availability of data from the LASL/UNM passive economic performance model. As more data are collected for the commercial sector, the scope of the methodology can be broadened.

The next level of segmentation within the residential sector divides the market into two segments: new construction and retrofit. The majority of engineering research and economic analysis of passive solar technology has been applied to new construction. This stands to reason since passive techniques are most effective when designed into a structure. However, if one looks at the amount of potential energy savings through new construction versus retrofitting the existing housing stock, it is clear that the retrofit market must be addressed. Retrofitting the existing housing stock with passive or hybrid techniques poses some unique engineering and economic problems; thus the market has some characteristics significantly different from those of the new construction market. The MPI methodology is divided into two sections to account for these differences.

Any analysis of the market potential for passive solar energy must consider the number of different designs and components available for collecting, storing, distributing, and controlling the energy. Each passive application has its own set of characteristics which makes it more or less adaptable to the various markets encountered. Some technologies are very adaptable to retrofit situations; others are appropriate only in new construction. This variation in characteristics can be integrated into the methodology so that market potentials can be evaluated for each of the various solar technologies.

The final level of market segmentation used in MPI is division by housing type: single family (both attached and detached), multifamily, and mobile home. These categories, used to segment both the new construction and retrofit markets, were chosen because they exhibit widely varying architectural design characteristics, ownership characteristics, and fuel consumption patterns.

Once this final level of market segmentation has been established, the goal of the analysis technique is to establish a market potential index for each residential segment in each geographic location.

Description of the Methodology

Use of Multiattribute Decision Analysis Techniques

The structure of the evaluation problem posed by market potential indexing fits very well into an area of management science known as "Multiattribute Decision Analysis." The mathematical techniques which come from this discipline are designed to evaluate decision processes in which there are multiple objectives, both quantitative and qualitative in nature, typically in conflict with each other. The problem is essentially one of making value tradeoffs of one objective against the other [14].

In the market potential indexing problem, 220 separate geographic market segments are to be evaluated. A set of common characteristics (attributes) can be determined which apply to all of the market segments. Knowledge of the status of each of these attributes for a particular market will help to determine the market potential for that segment as compared to the other market segments. Some attributes will affect the market potential more than others; therefore, a method for weighting the value of each attribute is incorporated in the value function.

Development of the Primary Value Function

Review of the decision analysis literature revealed that the most applicable form of a value function is the additive form [14,15]. This form is basically the same technique used by the Solar Energy Research Institute (SERI) for the value function in its Commercial Readiness Assessments Methodology [16]. Equation 1 is the primary value function for the market potential indexing methodology.

$$P_i = \sum_{j=1}^{n} W_j V_j (A_{ij}) \text{ where,} \qquad (1)$$

$V_j (A_{ij})$ = The value function of the j^{th} attribute for the i^{th} market segment

W_j = The weighting factor for the j^{th} attribute

Equation 2 gives an additional constraint on the weighting factors. This constraint is based on the assumption that each attribute contributes a fractional portion to the total index value, thus the weighting factors specify that fractional portion. Since the total of all fractional parts can be no greater than the whole, this constraint must be imposed.

$$\sum_{j=1}^{n} W_j = 1 \qquad (2)$$

Development of the Attibutes and Their Value Functions

A set of common characteristics (attributes) can be determined which, when evaluated, will provide insight to the operation of any market region. Many attributes affect the operation of a market system. For MPI analysis, we have divided these attributes into "objective" and "subjective" categories. Objective attributes are readily identifiable, accurately measured or predicted, and not directly influenced by subjective conditions in the marketplace. Subjective attributes, on the other hand, are usually identifiable but are most difficult to measure and/or quantify. Examples of each type of attribute are presented in Table 1.

In a general sense, the objective factors would determine both market potential and rates of diffusion in a perfectly rational economic marketplace. However, many of the subjective factors can have a tremendously strong impact on both potential and penetration and therefore should be considered in a thorough MPI analysis. The difficulty, of course, is to translate these subjective attributes into quantifiable terms and to conduct the actual data collection in a cost-effective manner.

Attribute Identification

The initial step in developing the MPI methodology was to establish a set of objective attributes using the data available in the LASL/UNM EASE III model and other commonly available sources. This set of attributes covers only the new construction, single-family, residential market sector.

Market research field studies currently being conducted by Market Facts, Inc., SERI, and the RSECs will help define the nature and magnitude of the subjective attribute influences. Data collected in the Household/Builder market surveys will be used to formulate initial quantitative values for the subjective attributes and will form the basis for further MPI analysis. The value functions for each of the objective attributes are described below.

A_{i1} Solar Performance ($W_1 = 0.18$)

$$A_{i1} = \sum_{k=1}^{4} \frac{TCSOL_i}{SFDISP_{ik}} \cdot FF_{ik} \text{ where,}$$

A_{i1} = Solar Performance attribute value (\$/MMBtu/year/home)

k = Fuel types (1 = natural gas, 2 = heating oil, 3 = electric resistance, 4 = electric heat pump)

$TCSOL_i$ = Total cost of solar system (\$) in the i^{th} market region

$SFDISP_{ik}$ = Annual solar savings (MMBtu/year/home)

FF_{ik} = Fraction of newly constructed homes in the i^{th} market region using fuel type k

Objective	Subjective
Predicted Solar Cost/Performance	Aesthetic Preference of Designs
Housing Starts	Grassroots Networking
Housing Stock	Political Climate
Insulation Levels	Social Advantage - "Snob Appeal"
Fuel Use Patterns	Investment Decision Criteria
Current Fuel Prices	Resale Value
Income Levels	Risk Perception
Predicted Population Growth	Utility Policies/Attitudes
Tax Incentives	
Solar Investment Cash Flow	
Tax Burdens	
Zoning/Building Codes	

Table 1. Examples of Objective and Subjective MPI Attributes in the Residential Buildings Sector

The solar performance attribute describes the amount of energy savings that can be achieved per dollar of solar investment, taking into consideration the total cost of the specified solar system, the annual solar savings, and the fractional breakdown of housing by fuel type.

A_{i2} Energy Market Share ($W_2 = 0.25$)

$$A_{i2} = TNS \cdot HS_i \cdot \sum_{k=1}^{4} \frac{SFDISP_{ik}}{CONVF_k} \cdot FF_{ik} \text{ where,}$$

A_{i2} = Energy Market Share attribute value (MMBtu/market/region/year)

TNS = Total national housing starts per year

HS_i = Fraction of total national housing starts in the ith market region

$SFDISP_{ik}$ = Annual solar savings (MMBtu/year/home)

$CONVF_k$ = Energy conversion efficiency factor (MMBtu output/MMBtu input)

FF_{ik} = Fraction of newly constructed homes in the ith market region using fuel type k

The energy market share attribute describes the potential energy savings for a market region if the total market penetration is achieved. (Data Sources: LASL/UNM EASE III Solar Economic Performance Model; National Association of Home Builders)

A_{i3} Consumer Liquidity ($W_3 = 0.18$)

$$A_{i3} = \sum_{k=1}^{4} YRDP_{ik} \cdot YNCF_{ik} \cdot FF_{ik} \text{ where,}$$

A_{i3} = Consumer Liquidity attribute value

$YRDP_{ik}$ = Years to recover down payment

$YNCF_{ik}$ = Years of negative annual cash flow

FF_{ik} = Fraction of newly constructed homes in the ith market region using fuel type k

The consumer liquidity attribute describes the consumer's financial obligations and benefits. It measures how soon the consumer starts to reap the benefits of investment in a solar system. The time to recover down payment and years of negative cash flow are the basis of this attribute. (Data Source: LASL/UNM Solar Economic Performance Model)

A_{i4} Consumer Financial Parameters ($W_4 = 0.05$)

$$A_{i4} = \frac{MIR_i \cdot PTXR_i}{FSLTXR_i} \text{ where,}$$

A_{i4} = Consumer Financial Parameters attribute value

MIR_i = Mortgage interest rate for the ith market region

$PTXR_i$ = Effective property tax rate for the ith market region

$FSLTXR_i$ = Effective federal, state, and local income tax rate for the ith market region

The consumer financial parameters attribute is structured to compare negative tax and interest effects to the offsetting income tax deduction benefit. (Data Sources: Internal Revenue Service; H & R Block, Inc.)

A_{i5} Government Incentives ($W_5 = 0.12$)

$$A_{i5} = ICIT_i + ICIP_i + ICIL_i \quad \text{where,}$$

A_{i5} = Government Incentives attribute value

$ICIT_i$ = Incentives index for income tax credits and deductions for the ith market region (Laws giving income tax credits were allowed two points for each \$1000 of tax credit. Deductions were allowed from two to four points depending upon the law structure.)

$ICIP_i$ = Incentives index for property tax deferments for the ith market region [Property tax incentives usually are written as exemptions with the value of the property assessed as the value of the property less the value of the solar system. Two points were given for an exemption up to five years, three points for an unknown length of years (we could not assume the law would hold indefinitely), and four points for up to 20 years.]

$ICIL_i$ = Incentives index for low-interest loans and grants (In states where they are available, loan and grant incentives are usually applied to retrofit solar designs. No points were given for retrofit. If a grant or loan is available for a new construction design, one point is allowed.)

This attribute measures the value of government incentives available in the selected market segment for installation of passive solar equipment. These incentives, from the federal, state, and local levels, take the forms of tax credits, tax deductions, grants, and other cost deferments. (Data Sources: U.S. Department of Housing and Urban Development; U.S. Department of Commerce)

A_{i6} Household Income Characteristics ($W_6 = 0.07$)

A_{i6} = $AHIC_i$ where,

$AHIC_i$ = Average Household Income Characteristics for the ith market region

The household income characteristics attribute measures the ability of families within the market region to afford new housing. Since passive solar houses usually carry a premium cost, there is a correlation between income and the number of passive solar houses built in a region. (Data Source: U.S. Bureau of the Census)

A_{i7} Population Growth ($W_7 = 0.15$)

$$A_{i7} = POP_i \cdot GR_i \text{ where,}$$

POP_i = The 1980 projected population of the ith market region

GR_i = The 1980 projected population growth rate of the ith market region

The population growth attribute is a proxy for new household formation. The market potential for newly constructed passive solar houses will obviously be highest where the level of new construction starts is highest. (Data Source: U.S. Bureau of the Census)

Additional Attributes

This list of attributes is by no means totally representative of all of the factors affecting the market potential for passive solar technologies. The list was chosen because the data are readily available and easily manipulated using the existing LASL/UNM EASE III code. Tasks in the next phase of development for the methodology will add additional subjective attributes and associated data bases to develop a more complete model.

Attribute Normalization

By reviewing the list of attributes, one can readily see that they are measured in many different dimensions. Each measurement must be transformed into a dimensionless utility number that reflects its "goodness" or "badness." This is done by developing a transformation function for each set of attribute data. The data set for a particular attribute is assembled from each of the 220 market segments. The maximum and minimum values are determined for the data set, and a range of values is defined over which the value of the utility function can vary from 0 to 100. Finally, a functional relationship is developed which allows a utility number to be evaluated from any measured value in the attribute data set. For this version of the methodology, a linear transformation function is assumed. The transformation process involves shifting the zero point and scaling the data to conform with the 0 to 100 range of the utility values.

Two versions of the linear transformation function are used. The first version is used with "positive" data (i.e., data in which the lowest value is equivalent to a utility value of 0 and the highest value is equivalent to a utility value of 100). The second version is used with "negative" data (i.e., data in which the highest value is equivalent to a utility value of 0 and the lowest value is equivalent to a utility value of 100). Equations 3 and 4 give these transformation functions.

The transformation function for positive-sensed data is given by:

$$V_{ij} = 100 \cdot \frac{A_{ij} - Min_j}{Max_j - Min_j}, \qquad (3)$$

whereas the transformation function for negative-sensed data is given by:

$$V_{ij} = 100 \cdot \frac{Max_j - A_{ij}}{Max_i - Min_j} \text{ where,} \qquad (4)$$

V_{ij} = The utility value, range 0 to 100

A_{ij} = Attribute value, ranges from Min to Max

Min_j = The minimum value from the data set

Max_j = The maximum value from the data set

Attribute Weighting Factors

Selection of the attribute weighting factors is a critical process in the model development. It is a subjective process with no single set of weights being optimum. To determine the weights for the study presented in the following section, we combined the results of independent weightings performed by members of the LASL Modeling and Economic Analysis Group who have been active in the passive solar economic and marketing analysis program. Key tasks for the future are to develop a process to determine the attribute weights and to conduct a series of sensitivity analyses to test the responsiveness of the MPI model to alternative weighting distributions.

An Example of an MPI Study

To illustrate the use of the MPI methodology, a study was run on the 220 market regions of the continental United States. The direct gain with night insulation system was chosen for analysis, and four separate MPI runs were done for the study. The first two runs used solar savings fractions of 20 percent and 40 percent and did not take conservation optimization into consideration. The second two runs also used solar savings fractions of 20 percent and 40 percent, but assumed optimal conservation and passive solar energy for those specific solar savings fractions [17].

Maps 1-4 illustrate the results of the direct gain study. The areas of highest potential are generally located in the northern portion of the United States. Particularly heavy concentrations of high-potential areas are located in the Midwest and the Northwest. The low-potential areas are located primarily in the southeastern portion of the nation. This distribution of potentials can be attributed to the cost of prevalent fuels, solar performance, and heat loads. It must be remembered that this study pertains only to residential space heating and that a substantial energy savings potential can be realized, particularly in the southern latitudes, through the use of passive cooling techniques.

Caution must be exercised when analyzing these data because they are based only on one set of weighting factors. A low relative potential does not mean that passive solar systems are ineffective in that area; it simply means that the total market for other areas has a greater potential for development.

Tables 2-5 list the raw and normalized attribute data for the highest ranked locations to give an indication of the MPI analysis procedure. This study is an example of the types of analyses which can be done with the MPI model. Variables such as solar savings fraction, conservation level, system type, and attribute weights can be changed to determine the shifts in market potential that result. Market regions exhibiting high potential can be pointed out using this methodology.

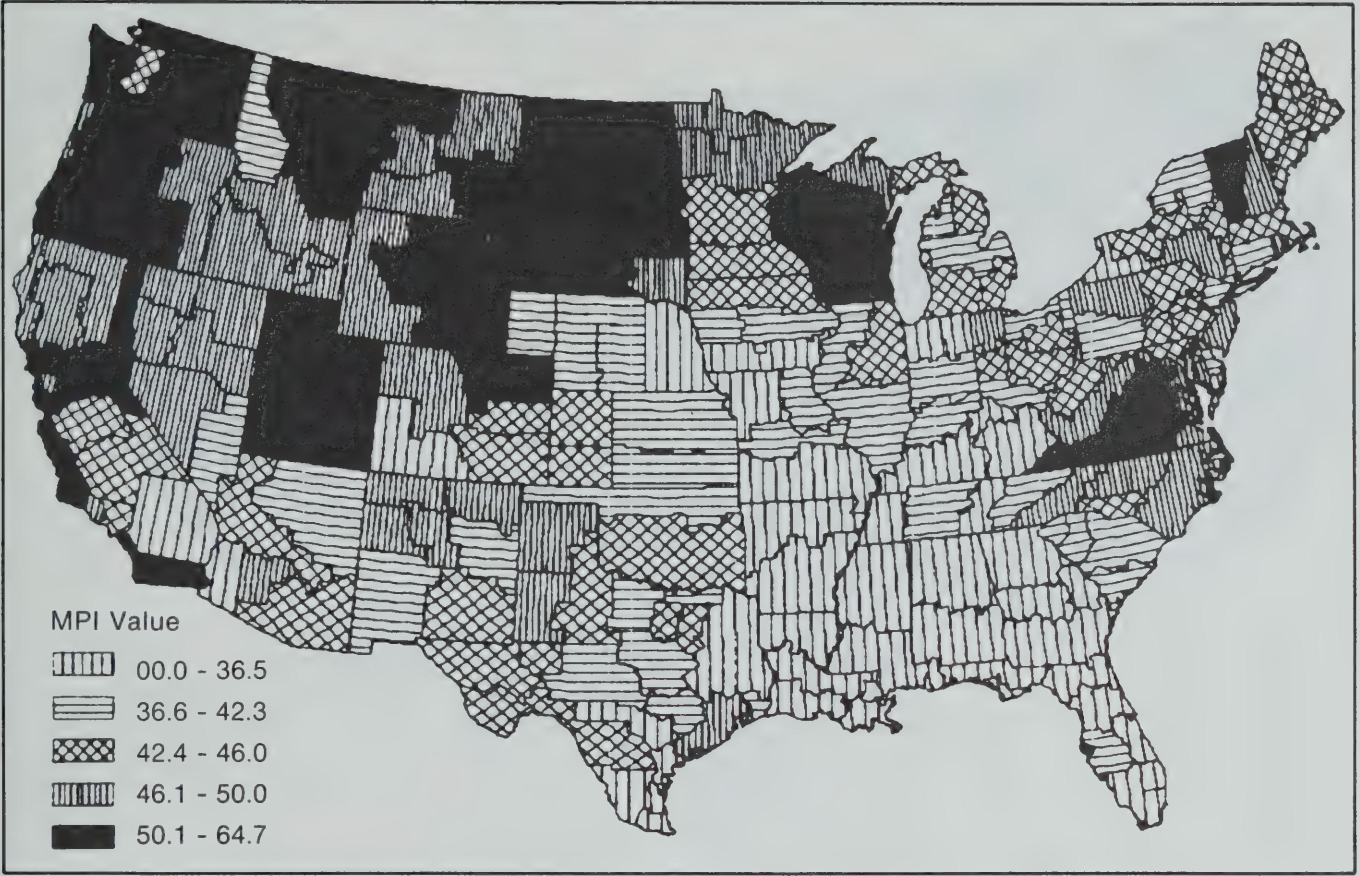

Map 1. MPI Values for Residential Direct Gain Systems with Night Insulation (Solar Savings Fraction - .20)

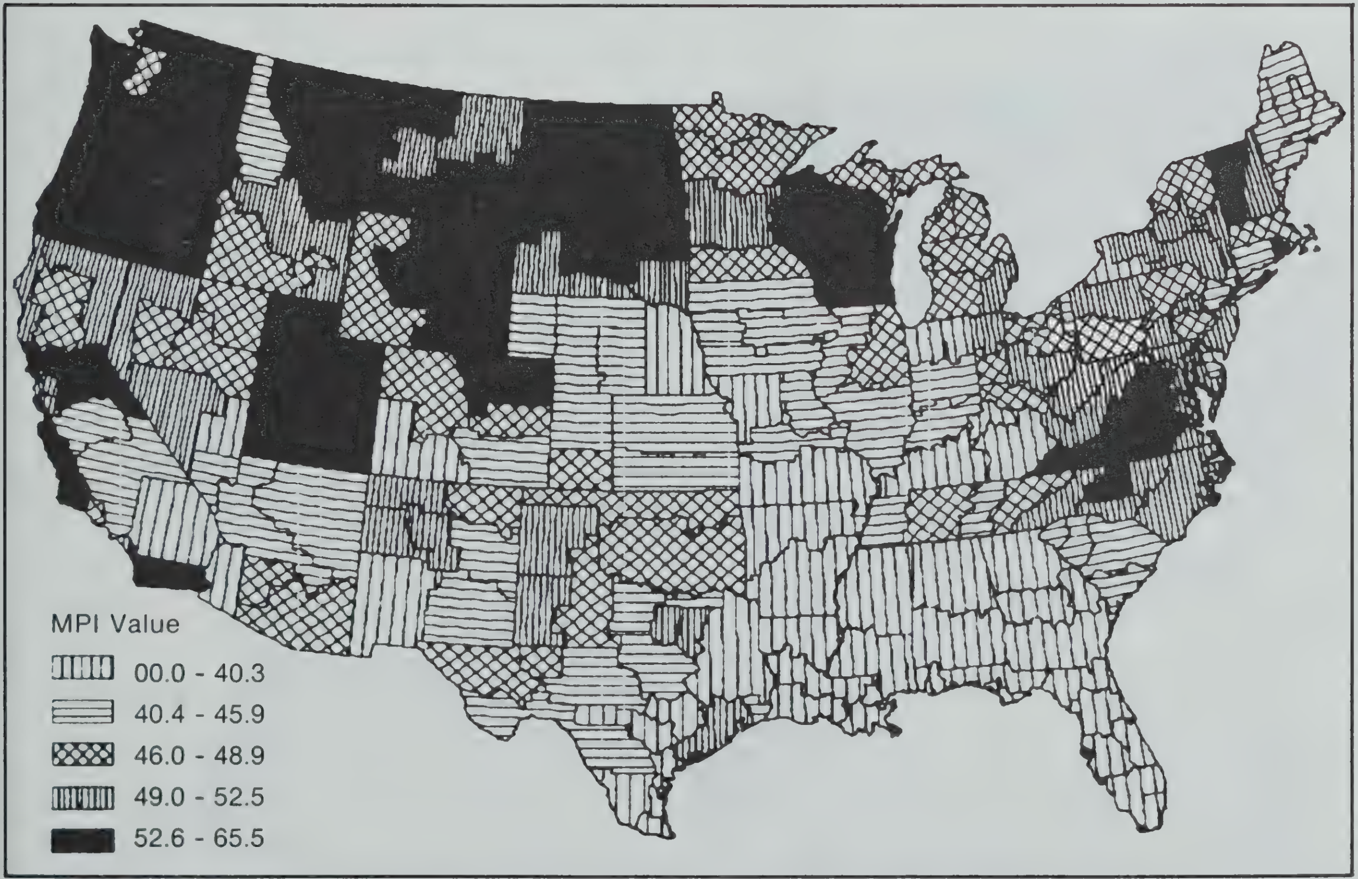

Map 2. MPI Values for Residential Direct Gain Systems with Night Insulation (Solar Savings Fraction - .20; conservation option included)

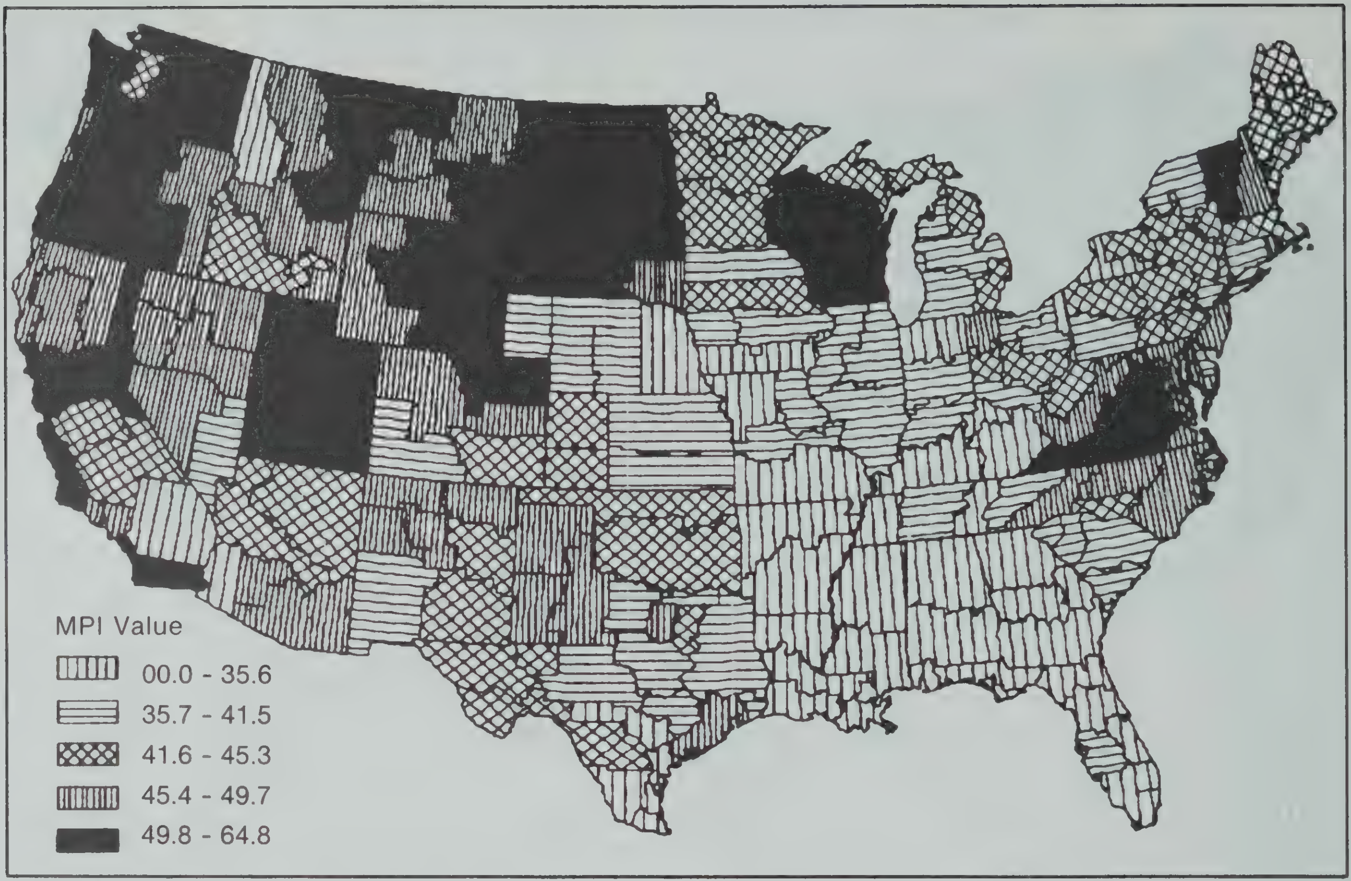

Map 3. MPI Values for Residential Direct Gain Systems with Night Insulation (Solar Savings Fraction - .40)

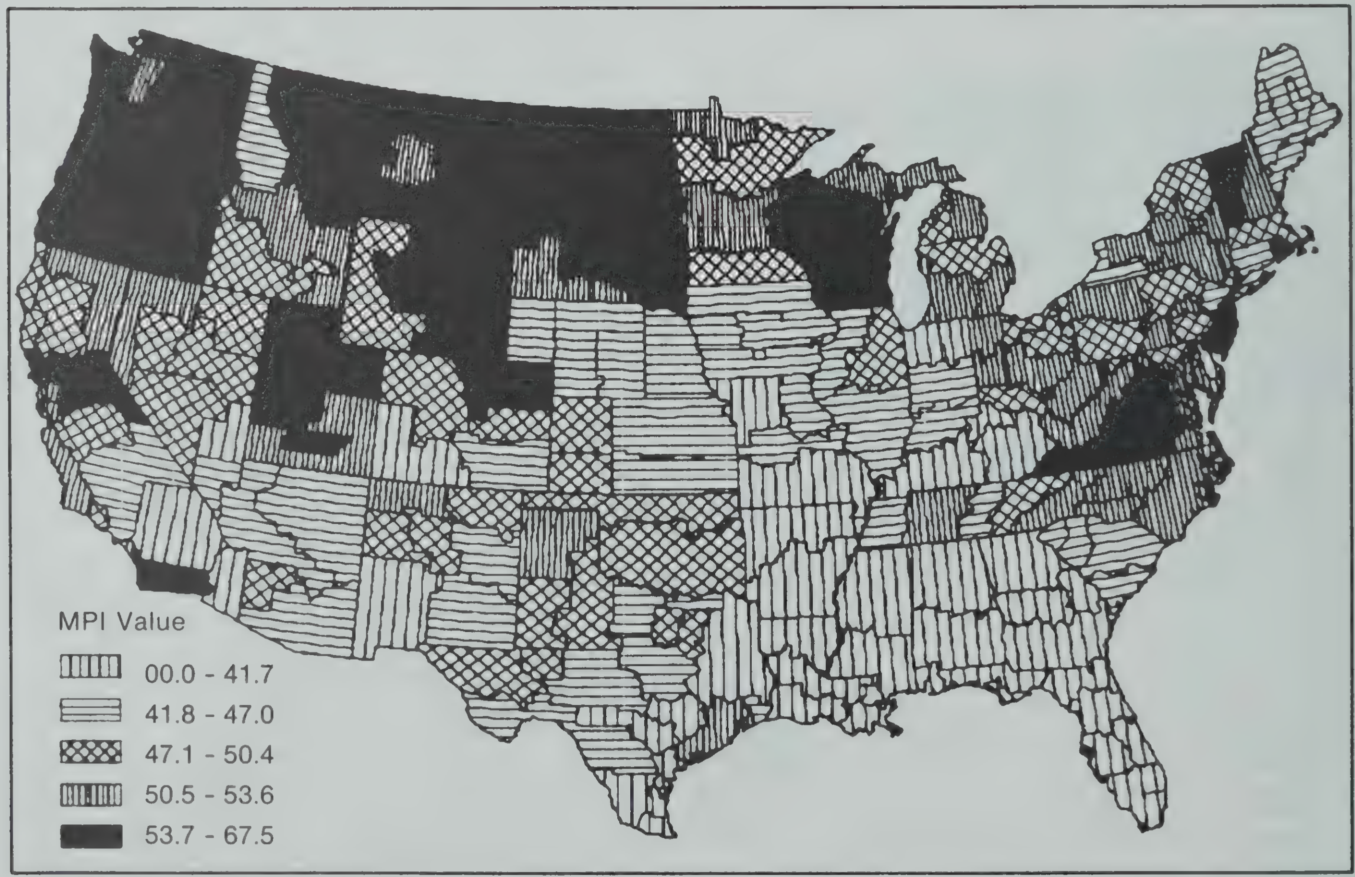

Map 4. MPI Values for Residential Direct Gain Systems with Night Insulation (Solar Savings Fraction - .40; conservation option included)

Sorted Raw Attribute Data
System Type = **6** **SSF** = **.20**

Weight				.180	.250	.180	.050	.120	.070	.150
				Attribute						
Location	Rank	MPI	Region	1	2	3	4	5	6	7
Bryce Canyon, Utah	1	64.7	198	84.2	47307.	21.	.6	0.0	22692.	4366.
Madison, Wisconsin	2	62.2	215	149.2	49427.	69.	1.5	3.0	22057.	6978.
Cheyenne, Wyoming	3	60.7	218	105.5	45933.	67.	1.4	0.0	25762.	1545.
Green Bay, Wisconsin	4	60.2	213	144.1	49546.	164.	1.2	3.0	21706.	10508.
Casper, Wyoming	5	60.2	217	102.9	46975.	164.	1.2	0.0	28907.	3788.

Sorted Normalized Attribute Data
System Type = **6** **SSF** = **.20**

Weight				.180	.250	.180	.050	.120	.070	.150
				Attribute						
Location	Rank	MPI	Region	1	2	3	4	5	6	7
Bryce Canyon, Utah	1	64.7	198	69.9	94.0	95.9	86.9	0.0	49.8	23.7
Madison, Wisconsin	2	62.2	215	46.6	98.2	86.8	52.3	33.3	45.3	26.0
Cheyenne, Wyoming	3	60.7	218	62.3	91.3	87.1	57.4	0.0	71.5	21.2
Green Bay, Wisconsin	4	60.2	213	48.4	98.4	68.4	64.6	33.3	42.8	29.1
Casper, Wyoming	5	60.2	217	63.2	93.3	68.4	62.6	0.0	93.7	23.2

Table 2. Direct Gain with Night Insulation (conservation not considered)

Sorted Raw Attribute Data
System Type = **6** **SSF** = **.20**

Weight				.180	.250	.180	.050	.120	.070	.150
				Attribute						
Location	Rank	MPI	Region	1	2	3	4	5	6	7
Madison, Wisconsin	1	67.5	215	90.3	148045.	7.	1.5	3.0	22057.	6978.
Green Bay, Wisconsin	2	66.2	213	90.4	147937.	62.	1.2	3.0	21706.	10508.
La Crosse, Wisconsin	3	65.1	214	96.6	147525.	7.	1.7	3.0	19871.	3905.
Eau Claire, Wisconsin	4	64.0	212	86.6	138927.	7.	1.8	3.0	18155.	8721.
Burlington, Vermont	5	63.8	201	98.7	145277.	30.	2.9	5.0	18777.	5589.

Sorted Normalized Attribute Data
System Type = **6** **SSF** = **.20**

Weight				.180	.250	.180	.050	.120	.070	.150
				Attribute						
Location	Rank	MPI	Region	1	2	3	4	5	6	7
Madison, Wisconsin	1	67.5	215	61.6	100.0	98.5	52.3	33.3	45.3	26.0
Green Bay, Wisconsin	2	66.2	213	61.6	99.9	86.6	64.6	33.3	42.8	29.1
La Crosse, Wisconsin	3	65.1	214	58.9	99.6	98.5	45.0	33.3	29.8	23.3
Eau Claire, Wisconsin	4	64.0	212	63.2	93.8	98.5	41.4	33.3	17.7	27.5
Burlington, Vermont	5	63.8	201	58.0	98.1	93.6	1.2	55.6	22.1	24.8

Table 3. Direct Gain with Night Insulation (conservation considered)

Sorted Raw Attribute Data
System Type = **6** **SSF** = **.40**

Weight				.180	.250	.180	.050	.120	.070	.150
				Attribute						
Location	Rank	MPI	Region	1	2	3	4	5	6	7
Bryce Canyon, Utah	1	64.8	198	90.8	92851.	25.	.6	0.0	22692.	4366.
Madison, Wisconsin	2	61.2	215	177.1	97331.	95.	1.5	3.0	22057.	6978.
Cheyenne, Wyoming	3	60.6	218	116.8	90470.	85.	1.4	0.0	25762.	1545.
Casper, Wyoming	4	60.3	217	116.8	92653.	191.	1.2	0.0	28907.	3788.
Sheridan, Wyoming	5	59.1	220	134.2	95482.	216.	1.3	0.0	29018.	3292.

Sorted Normalized Attribute Data
System Type = **6** **SSF** = **.40**

Weight				.180	.250	.180	.050	.120	.070	.150
				Attribute						
Location	Rank	MPI	Region	1	2	3	4	5	6	7
Bryce Canyon, Utah	1	64.8	198	70.7	93.7	96.0	86.9	0.0	49.8	23.7
Madison, Wisconsin	2	61.2	215	42.8	98.2	85.0	52.3	33.3	45.3	26.0
Cheyenne, Wyoming	3	60.6	218	62.3	91.3	85.5	57.4	0.0	71.5	21.2
Casper, Wyoming	4	60.3	217	62.3	93.5	69.7	62.6	0.0	93.7	23.2
Sheridan, Wyoming	5	59.1	220	56.7	96.3	65.7	60.4	0.0	94.5	22.7

Table 4. Direct Gain with Night Insulation (conservation not considered)

Sorted Raw Attribute Data
System Type = **6** **SSF** = **.40**

Weight				.180	.250	.180	.050	.120	.070	.150
				Attribute						
Location	Rank	MPI	Region	1	2	3	4	5	6	7
Madison, Wisconsin	1	65.5	215	112.1	171707.	25.	1.5	3.0	22057.	6978.
Bryce Canyon, Utah	2	63.6	198	70.9	151802.	14.	.6	0.0	22692.	4365.
Green Bay, Wisconsin	3	63.5	213	113.8	172146.	100.	1.2	3.0	21706.	10508.
La Crosse, Wisconsin	4	63.1	214	120.5	169676.	19.	1.7	3.0	19871.	3905.
Eau Claire, Wisconsin	5	62.0	212	110.7	161114.	23.	1.8	3.0	18155.	8721.

Sorted Normalized Attribute Data
System Type = **6** **SSF** = **.40**

Weight				.180	.250	.180	.050	.120	.070	.150
				Attribute						
Location	Rank	MPI	Region	1	2	3	4	5	6	7
Madison, Wisconsin	1	65.5	215	57.6	97.8	94.7	52.3	33.3	45.3	26.0
Bryce Canyon, Utah	2	63.6	198	73.2	86.5	97.1	86.9	0.0	49.8	23.7
Green Bay, Wisconsin	3	63.5	213	56.9	98.0	78.7	64.6	33.3	42.8	29.1
La Crosse, Wisconsin	4	63.1	214	54.4	96.6	96.0	45.0	33.3	29.8	23.3
Eau Claire, Wisconsin	5	62.0	212	58.1	91.8	95.2	41.4	33.3	17.7	27.5

Table 5. Direct Gain with Night Insulation (conservation considered)

Conclusion

The fundamental purpose of MPI analysis is to aid decisionmakers in allocating scarce resources among competing uses. In a sense, the information gained from MPI analysis is helpful in reducing the risk of uncertainty in decisionmaking. Members of trade associations can use MPI results to narrow the number of test market areas for newly initiated product marketing campaigns. Local planners from the Regional Solar Energy Centers can use MPI results to help guide allocation of commercialization monies within their region. DOE program managers can use MPI results to target regional budget allocations or to develop marketing and information strategies.

The Market Potential Indexing methodology is still in the early stages of development. To complete the single-family, new construction version of the model, the sensitivity studies for the weighting factors must be run for a number of additional solar technologies including Trombe wall, water wall, and sunspaces. These multiple studies will provide a set of characteristics for the model which will allow verification studies to begin.

The next phase of development, currently underway, establishes additional sets of attributes, data bases, and weighting factors for evaluating the multifamily, manufactured housing, and retrofit residential market sectors. The computer code, currently operational, is easily adapted to different MPI configurations.

Early experience with the Market Potential Indexing concept shows that it is potentially useful in numerous market evaluation applications areas such as active solar, wind energy conversion, and photovoltaics. Once the markets are characterized by MPI, a series of validation experiments must be designed to test the accuracy of the results [18]. By correlating actual market penetration of passive solar in alternative cities with a cross-sectional/time series analysis of attribute valuations, a more defensible basis for market penetration estimates will have been established.

Acknowledgments

We are indebted to the following individuals who helped prepare this article: Katie Greiner and Alexine Martinez for computer graphics, Pat Aragon for data collection, and Grace Roybal for typing.

References

1. Schiffel, D. et al. *The Market Penetration of Solar Energy: A Model Review Workshop Summary.* SERI-16, 1978, Solar Energy Research Institute, Golden, Colo.
2. Sparrow, T. et al. "Socioeconomic Factors Affecting the Adoption of Household Solar Technology: Preliminary Findings." Presented at the Symposium on Social and Behavioral Implications of the Energy Crisis. University of Houston. June 1977.
3. Nall, D. H. *Economic Performance and Market Penetration for Passive Solar Technologies to the Year 2000.* Prepared for the U. S. Department of Energy, Energy Information Administration. July 1979.
4. Noll, S. A. and Robson, W. M. *Market Potential Indexing for Passive Solar Technologies.* LASL/LA-UR-80-1025, 1980, Los Alamos Scientific Laboratory, Los Alamos, N.M.
5. Robson, W. M. and Yeamans, M. *Market Potential Indexing in Support of Solar Action Week.* LASL/LA-UR-80-1698, 1980, Los Alamos Scientific Laboratory, Los Alamos, N.M.
6. Robson, W. M., Noll, S. A., and Yeamans, M. "Market Potential Indexing for Passive Solar Heating: Single Family New Construction in the Mid-American Region." *Proceedings of the 5th National Passive Solar Energy Conference.* 1980.
7. Mansfield, E. "Technical Change and the Rate of Imitation." *Econometrica.* 29 (4), 1961.
8. Fisher, J. C. and Pry, R. H. "A Simple Substitution Model of Technological Change." *Technological Forecasting and Social Change.* Sept. 1971, pp. 75-88.
9. Stern, M. O. et al. "A Model for Forecasting the Substitution of One Technology for Another." *Technological Forecasting and Social Change.* Vol. 7, 1975, pp. 57-79.
10. Warren, E. H., Jr. *Solar Market Penetration Models: Science or Number Mysticism?* Sept. 1979, Jet Propulsion Laboratory, Pasadena, Calif.
11. Roach, J. F. et al. "The LASL/UNM Solar Economic Performance Code: A Basic Primer." *Proceedings of the 4th National Passive Solar Energy Conference.* 1979.
12. Cinquemani, V., Owenby, J. R., Jr., and Baldwin, R. G. *Input Data for Solar Systems.* Prepared for the U.S. Department of Energy. Nov. 1978.
13. Balcomb, J. D. et al. *Passive Solar Design Handbook: Volume Two.* DOE/CS-0127/2, Appendix F. Jan. 1980.
14. Keeney, R. L. and Raiffa, H. *Decisions with Multiple Objectives: Preferences and Value Tradeoffs.* New York: John Wiley and Sons. 1976.
15. Dyer, J. S. and Sarin, R. K. "Measurable Multiattribute Value Functions." *Operations Research.* Vol. 27, No. 4, July-August 1979, pp. 810-822.
16. Benson, W. and Hewett, R. *Commercial Readiness Assessments: Working Paper Description of Study Methodology.* Prepared for the U. S. Department of Energy. Aug. 1979, Solar Energy Research Institute, Golden, Colo.
17. Balcomb, J. D. "Conservation and Solar: Working Together." *Proceedings of the Systems Simulation and Economic Analysis Conference.* Jan. 1980.
18. Noll, S. A., Robson, W. M., and Roach, J. F. *Market Potential Indexing for Solar Technologies: A Strategy Plan for Research, Implementation, and Verification.* LASL/LA-UR-80-2660, 1980, Los Alamos Scientific Laboratory, Los Alamos, N. M.

Heat Exchangers Effective in Radon Control

This report summarizes research conducted by staff of the Energy and Environment Division at Lawrence Berkeley Laboratory. The complete text of "The Use of Mechanical Ventilation with Heat Recovery for Controlling Radon and Radon-Daughter Concentrations" (William W. Nazaroff, Mary L. Boegel, Craig D. Hollowell, and Gary D. Roseme) appeared in the March 1981 issue of Atmospheric Environment (Vol. 15). — *Ed.*

Ongoing research at Lawrence Berkeley Laboratory (LBL) suggests that, in many American energy-conserving homes, mechanical ventilation systems using air-to-air heat exchangers may provide cost-effective control of indoor radon buildup.

Radium 226, part of the uranium 238 decay chain, constantly decays into a radioactive noble gas (radon 222), which in turn decays into four daughters. Present in almost all soil and rock radium presents a nearly inescapable source of potential radon contamination. Soil around a structure's foundation, building materials, natural gas, and well water may all emanate radon into a building's living space, where prolonged exposure to the substance may threaten occupant health.

LBL researchers selected an energy research home in Carroll County, Md., to test the effectiveness of a mechanical ventilation system with heat recovery as an energy-efficient radon control technique. A single-story structure with a full basement, the test house relies on energy-conserving strategies to reduce infiltration, reduce heat loss through the building envelope, and reduce energy consumption by appliances. The house is heated with a heat pump; air in both the main floor and basement is conditioned. The air distribution system circulates air from the basement through registers into the main living space.

Measured infiltration rates in the test house ranged from 0.05 to 0.15 air changes per hour (ach), in contrast to the typical range of 0.5 to 1.5 ach in conventional U.S. homes. These low rates resulted from standard weatherization measures (caulking and weatherstripping) and placement of a continuous plastic vapor barrier behind the drywall. All electric outlets and lighting fixtures were surface-mounted (avoiding penetration of the walls and subsequent air leakage); bathroom exhaust fan ducts were dampered.

Air quality problems, including excessive humidity and formaldehyde levels, were observed shortly after the house was completed. High concentrations of radon and radon daughters within the house proved to be the most serious concern. Spot measurements of radon consistently showed concentrations in excess of 20 picocuries/liter, significantly high levels even for houses in locations with known high radon sources. Current Canadian and U.S. regulatory guidelines call for remedial action when the average indoor radon-daughter level exceeds 0.02 working levels (WL) in some high-radon locales. (Typically, 150-300 picocuries/liter of radon yield one working level.)

A mechanical ventilation system consisting of a large counterflow air-to-air heat exchanger, ductwork, and two small fans was installed. Variable transformers are used to vary the speed of the fans in order to supply the desired ventilation rate. The exchanger contains 20 air-flow passages and, depending on air-flow rates, recovers up to 75 percent of the heat from exhausted air.

Radon concentrations were monitored with a continuous radon monitor (CRM) and through analysis of approximately 50 grab samples of interior air. Grab sampling apparatus, calibrated using a National Bureau of Standards radium solution, was used as a secondary standard for CRM calibration. The uncertainty of this calibration is 10 percent (one standard deviation of the ratio of

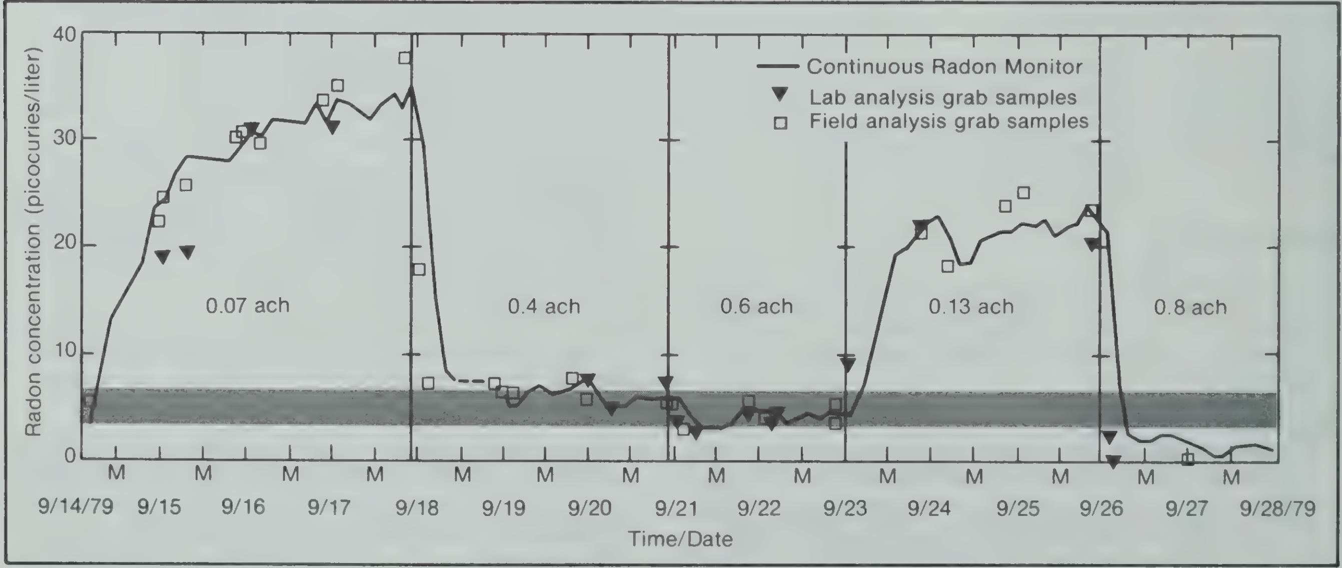

Fig. 1. Radon concentration in the Carroll County, Md., test home as a function of time for five ventilation rates. Ventilation conditions were changed every 2 to 4 days of the 2-week test period by adjusting the flow through the heat exchanger. Shaded area indicates the approximate range of radon-daughter working levels cited by U.S. and Canadian environmental guidelines (3-6 picoucries/liter).

radon concentration measured by grab sampling to counts per interval in the CRM). A Residential Radon Daughter Monitor developed at LBL was used to make measurements of radon-daughter concentrations during daylight hours. Uncertainty in the individual daughter concentrations is about 20 percent at concentrations of 1 picocurie/liter.

The mechanical ventilation system operating at low, medium, and high fan speeds yielded air-exchange rates of 0.4, 0.6, and 0.8 ach, respectively. When the system was operated at low fan speed, with intake and exhaust openings almost completely taped over, the air exchange rate was 0.13 ach. The fifth ventilation condition was infiltration with no mechanical ventilation (0.07 ach). The ventilation rate was measured several times under each condition. Because the range of values obtained for a given condition was small (on the order of 10 percent or less), the ventilation rate was considered constant for any of the five conditions.

Figure 1 shows radon concentration plotted as a function of time at the five selected ventilation rates. For purposes of analysis, the output of the CRM was averaged over 3-hour intervals. Radon concentration ranged from a high of 35 picocuries/liter to less than 1 picocurie/liter. Concentration outside the house was measured several times during the 2-week period and at no time exceeded 0.5 picocurie/liter. A dramatic effect of ventilation rate on radon concentration was displayed: The variations in radon concentration under a given ventilation condition are much smaller than the variations that occur when the ventilation condition is changed.

Radon-daughter working level plotted as a function of time reveals the same general dependence on ventilation. Within a given ventilation condition, however, the working level shows more variability than the radon concentration, indicating that radon-daughter concentrations depend on factors other than radon concentration and ventilation rate.

LBL researchers further examined the radon source magnitude between the test house and the general housing stock. Although published data on this question are limited, results of studies in England [1] and the United States [2] show source values spanning nearly three orders of magnitude (Fig. 2). When compared to these studies, the test house source values rank from the 60th to the 93d percentile against the U.S. study and from the 84th to the 95th percentile against the English study. Thus, while the source magnitude at the test house is high, it is not unique.

Study data were also examined against the fraction of houses that might have radon problems if constructed tightly. LBL research indicates that 36 percent of English homes and 75 percent of the homes in the United States would have radon concentration exceeding 5 picocuries/liter when closed if (1) all houses were constructed to achieve infiltration rates of 0.1, and (2) source magnitudes were distributed as in Fig. 2. With assumed ventilation rates raised to 0.5 ach, the corresponding percentages would be 5 percent in England and 7 percent in the United States. These estimates reflect "worst case" conditions, with all doors and windows in the house remaining closed. Under normal occupancy conditions (doors opened throughout the year and windows open for some portion of it), a considerably lower percentage of houses could be expected to show average radon concentrations in excess of 5 picocuries/liter.

LBL studies have also calculated expected dollar and energy savings gained by using mechanical ventilation systems with air-to-air heat exchangers. It was shown that, at current prices, the use of heat exchangers in gas-heated homes does not appear to be economical for most of the country. In homes heated with oil or electricity, however, incorporating heat exchangers in tightly built houses appears cost-effective in all regions but those with temperate climates.

References

1. Cliff, K.D., (1978) "Assessment of Airborne Radon Daughter Concentrations in Dwellings in Great Britain," *Physics of Medicine and Biology* 23, pp. 696-711.
2. "Radon Measurements and Emanation Studies," *Energy and Environment Division Annual Report*, LBL-11650, Oct. 1980, Lawrence Berkeley Laboratory, Berkeley, Calif.

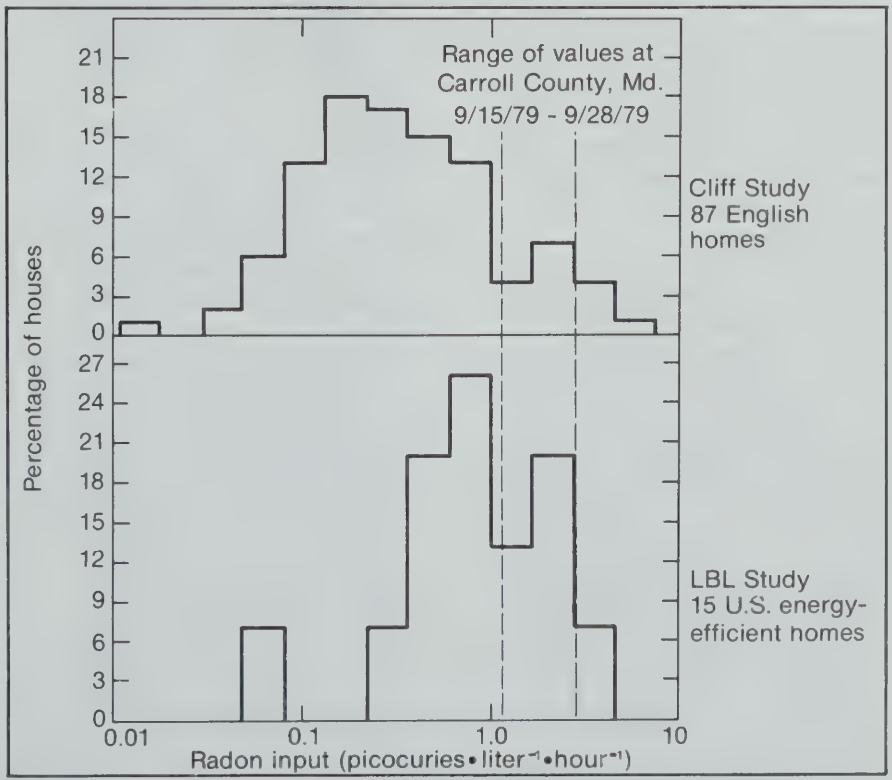

Fig. 2. Histograms of radon source magnitude in houses. The values obtained for the Maryland test house, though well above the geometric mean, are by no means unique.

Overview: Procedures for Validating BEAS

David Wortman, Bob O'Doherty, and Ron Judkoff

Building Systems Division
Solar Energy Research Institute
1617 Cole Boulevard
Golden, CO 80401

Building Energy Analysis Simulation Codes (BEAS) are being used with increasing frequency in the building design process, both directly and as the basis for simplified design tools and guidelines. As the demand for more energy-efficient buildings continues to grow, the use of BEAS and their spinoffs will increasingly impact the design, construction, and operation of buildings in the United States. To date, however, there has been little or no systematic effort to ensure that the various BEAS provide accurate, or even intuitively reasonable, results.

Researchers at the Solar Energy Research Institute (SERI) are developing a procedure for validating these codes. The procedures developed so far are limited to BEAS having time-steps on the order of one hour and using hourly values of radiation, ambient temperature, and other environmental data. More detailed information on the procedures is presented in Refs. 1 and 2. Up-to-date information is available from the authors.

The validation procedure is divided into three parts. In the first, Comparative Study, each BEAS analyzes the same building using the same set of weather data input files. Building designs and weather data can be chosen to test the parameters having the greatest impact on building performance. This also allows sampling of the different combinations of parameters before measured data are available. This technique is useful for finding large errors that are counterintuitive or that consistently produce results different from those of other codes. However, this procedure does not necessarily reveal all errors and gives little indication of the source of the discovered errors. It also provides little information on how to reconcile results caused by differences that cannot be construed as errors but rather as different approaches or mechanisms.

The second part of the validation procedure, Analytical Verification [2], is useful in diagnosing errors in heat transfer mechanisms in the BEAS. It is used with the Comparative Study to locate and correct problems in the specific mechanisms that are most important in building energy use [1].

The third phase of the validation procedure is Empirical Validation with carefully monitored test cells and buildings. Full-scale building data will be obtained from a national monitoring program for this purpose; test-cell data will be collected from five two-zone cells at SERI. The successful implementation of this procedure on the BEAS should greatly enhance the trust and utilization of the BEAS by the user community.

Description of the BEAS

The first and second parts of the validation procedure have been used to test four different main-frame, computer-based BEAS: SUNCAT 2.4, DEROB 4, DOE 2.1, and BLAST 3.0. (DEROB 3, an earlier version of DEROB, was also tested with the analytical verification procedure.)

These codes were chosen because of their potentially wide use in the building energy analysis industry and because of their differing modeling approaches. SUNCAT 2.4 [3] is a thermal network code that requires explicit information from the user on the lumped thermal properties of the building. With the exception of window tilt and azimuth, SUNCAT 2.4 does not consider building geometry in its building model.

DEROB 4 [4] is also a network model but is much more rigorous than is SUNCAT 2.4. DEROB 4 uses a geometric building model and contains an internal radiation heat transfer network. It also can calculate convective heat transfer coefficients at each hourly time-step, and position nodes through the thickness of massive wall components.

DOE 2.1 [5] uses a response factor model for heat transfer through massive surfaces. It does not use an internal radiation network, but rather a combined convective/radiative heat transfer coefficient between internal surfaces and the room air.

BLAST 3.0 [6] uses transfer functions for heat transfer through massive components. It contains more mechanisms for passive solar processes and is more rigorous in its internal energy distribution model than is DOE 2.1. Both BLAST 3.0 and DOE 2.1 have much more extensive plant, equipment, and system capabilities than the other two codes. However, the validation procedures presented here do not attempt to evaluate the extended capabilities.

Comparative Study

In the Comparative Study, the BEAS were used to calculate the annual heating and cooling loads for a simple direct-gain building in two different climates. The building was specified to be representative of typical passive designs. It is well insulated, with 1500 ft^2 (139 m^2) of floor space and 350 ft^2 (32.5 m^2) of vertical, south-facing, double-glazed windows. Two variations of the building were studied: a high-mass case and a low-mass case. The low-mass case used 0.5 in. (1.27 cm) of gypsum board for the ceiling and the walls; the high-mass case used the same ceiling but 8 in. (20.32 cm) of concrete for the walls. The building was operated with the heating set point at 75°F (23.9°C) and the cooling set point at 65°F (18.3°C) for the entire year. Two very different climates were chosen for the study: Madison, Wis., has a climate in which the loads are dominated by losses to the ambient air; Albuquerque, N.M., has a climate in which the loads are primarily driven by solar radiation gains. Typical Meteorological Year (TMY) weather data for these two cities were used in the simulations.

The results of the Comparative Study for the four BEAS are

	Madison, Wis.				Albuquerque, N.M.			
	Heating		Cooling		Heating		Cooling	
	High Mass	Low Mass	High Mass	Low Mass	High Mass	Low Mass	High Mass	Low Mass
BLAST 3.0	44	60	18	31	7	25	45	64
DEROB 4	72	90	14	30	24	46	44	68
DOE 2.1	52	70	17	34	8	33	37	66
SUNCAT 2.4	60	81	17	37	13	42	41	74

Table 1. Annual Heating and Cooling Loads (Million Btu)

shown in Table 1. Differences in the calculated loads are evident. However, the relative position for each BEAS is consistent throughout the set of test cases. In particular, DEROB 4 consistently calculates the highest heating loads, and BLAST 3.0 calculates the lowest heating loads. One can speculate on the causes of these differences by discussing the various modeling techniques used in the BEAS, but few substantive conclusions can be reached without more rigorous testing.

Analytical Verification

The Comparative Study procedure points out potential problems in a BEAS but gives no indication as to their causes. The Analytical Verification technique was developed to pinpoint the source of these problems. This procedure consists of several tests, each of which verifies a combination of mechanisms in a BEAS. These tests were chosen because they verify the algorithms for the mechanisms that are the most important in predicting the thermal performance of buildings. The selected mechanisms are:

- steady-state and dynamic heat conduction and thermal storage of mass walls,
- glazing transmittance and conductance,
- heat load caused by infiltration, and
- response of mass walls to solar radiation.

Variations in the tests for these mechanisms have also been developed to examine the effects on the BEAS of changes in mass, insulation, glazing type, and other parameters.

In general, implementation of the Analytical Verification technique on the four BEAS showed no apparent discrepancies. However, one of the BEAS — DEROB 3 — showed a slower than expected response in internal temperature to a step-function change in external temperature (Fig. 1). A similar slow response to solar radiation was also exhibited by this code.

These slow responses are similar to what would be expected from models of buildings with higher thermal mass than that described in the input files of these codes. As a result of the slow responses, building designers might use less thermal mass in their building designs than correctly working BEAS would suggest. The problem in DEROB 3 was traced to the solution technique used in the code. After the technique was corrected, the thermal responses predicted by DEROB 3, as well as by DEROB 4, agreed well with the expected results.

The Analytical Verification technique also revealed differences between the BEAS in the effect of changes in infiltration rate on heating and cooling loads, and differences in the thermal characteristics which each BEAS contains for a variety of internally determined window models (i.e., a double-glazed window in one BEAS is not necessarily the same as one used in another BEAS). For example, DEROB 4 includes substantially higher glass conductances than the other BEAS do.

In summary, the Analytical Verification technique and the Comparative Study have proved to be valuable in locating problems and differences in the BEAS. Since the BEAS exhibit a broad range of calculated loads for the same sets of conditions, caution must be exercised when using the absolute energy consumption

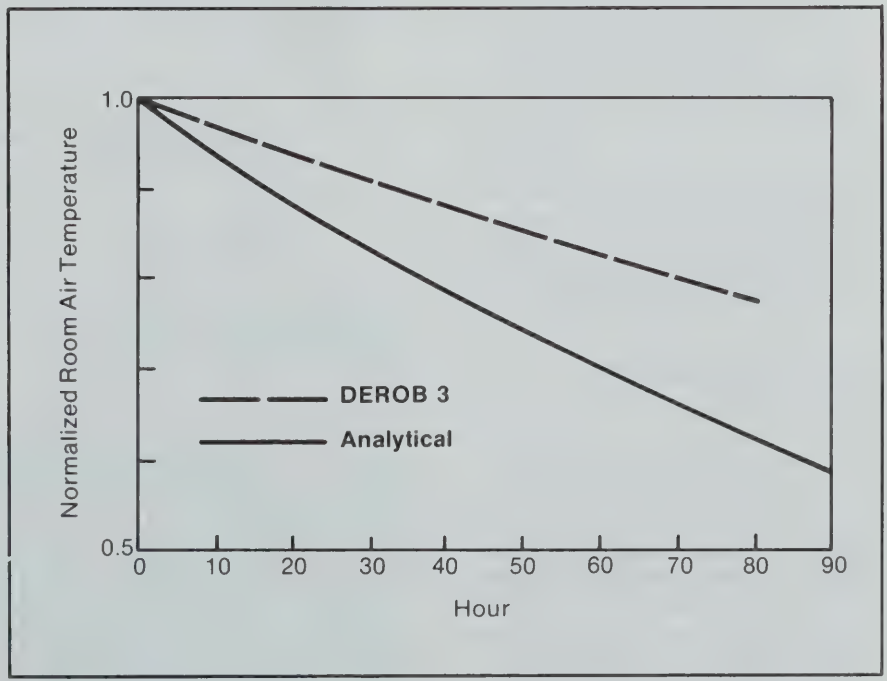

Fig. 1. High-mass temperature decay test using the original version of DEROB. Problems with the solution technique used in the code were corrected in subsequent DEROB version. The discrepancy in the BLAST results have been accounted for and corrected.

calculated by a single BEAS. The practice of using results from a single BEAS to generate design guidelines or simplified tools or input for economic analyses, or to develop policy, is questionable.

References

1. Judkoff, R. et al. "A Comparative Study of Four Passive Building Simulations: DOE 2.1, BLAST, SUNCAT 2.4, DEROB 3," *Proceedings of the 5th National Passive Solar Conference.* Amherst, Mass.: 1980.
2. Wortman, D. et al. "The Implementation of an Analytical Verification Technique on Three Building Energy Analysis Codes: SUNCAT 2.4, DOE 2.1, and DEROB 3." ASME/SSEA Conference: 1981.
3. Palmiter, L. "SUNCAT Version 2.4 User Notes." Unpublished.
4. Arumi-Noe, F. and Wysocki, M. *DEROB 3, the DEROB System.* Vols. 1-8. 1979.
5. York, D. A. and Tucker, E. F., eds. *DOE-2 Reference Manual (Version 2.1).* LA-7689-M, 1980, Los Alamos Scientific Laboratory, Los Alamos, N.M.
6. Hittle, D.C. *The Building Loads Analysis and System Thermodynamics Program, Volume 1: User's Manual.* U.S. Army Construction Engineering Research Laboratory, Champaign, Ill. Dec. 1977.

Details of the Comparative Study and the Analytical Verification technique are available from the authors, who are also preparing information on the application of these validation techniques to other untested BEAS.

Trinity Develops Efficient AC Unit

An energy-efficient air conditioner designed to both cool and dehumidify residences and commercial buildings in humid regions is being tested at Trinity University's Passive Test Facility, San Antonio, Tex.

By incorporating an air-to-air heat exchanger with an efficient air conditioner, researchers hope to optimize the dehumidification function of the cooling system and decrease dependence on a heat pump for cooling — an exchange of sensible for latent cooling. Thus, high-efficiency air conditioners will use the heat pump capacity almost entirely for dehumidification rather than primarily for cooling.

Conventional mechanical dehumidifiers use a heat pump cycle, generally exhibiting coefficients of performance (COP) less than 1. Conventional air conditioners generally have dehumidification COP of about 1; in contrast, the Trinity system appears to be capable of COP approaching 3.

Figure 1 illustrates the Trinity process. In a heat exchanger attached to the air conditioner inlet and outlet, cold air leaving the air conditioner is used to precool incoming air. Under nomal operating conditions, the incoming air reaches dew point while still in the exchanger, using the previously wasted cooled air from the conditioner.

Since dew point is reached while air is inbound through the exchanger, some condensation or dehumidification takes place. The evaporative coil continues dehumidification, further reducing air stream dew point. Condensation occurs during the entire time air is in contact with the coil and not just intermittently as is the case with an air conditioner operating alone.

Temperatures measured during a test run on 1 April 1980 indicate the effect of the heat exchanger on the airstream temperature. The exchanger precooled incoming air to 58°F (14.4°C) — nearly as cold as the 55°F (12.8°C) output from the air conditioner operating alone. With a "headstart" on cooling from 77° to 58°F (25°-14.4°C), the air conditioner produced the significantly lower saturated air temperature of 43°F (6.1°C) compared to 55°F (12.8°C) from the air conditioner alone. Air exited the exchanger into the room at 71°F (21.7°C) — nearly as warm as the ambient 77°F (25°C), but drier and more comfortable.

Phase I of the project, which includes system design and development of operating strategies, is under contract with the U.S. Department of Energy and extends through December 1981. Phases 2 and 3 involve production line design, field testing, market strategy development, and the actual distribution and sales of the product to carefully defined target groups.

■ E.S. Doderer, Assistant Professor, Engineering Science, Trinity University

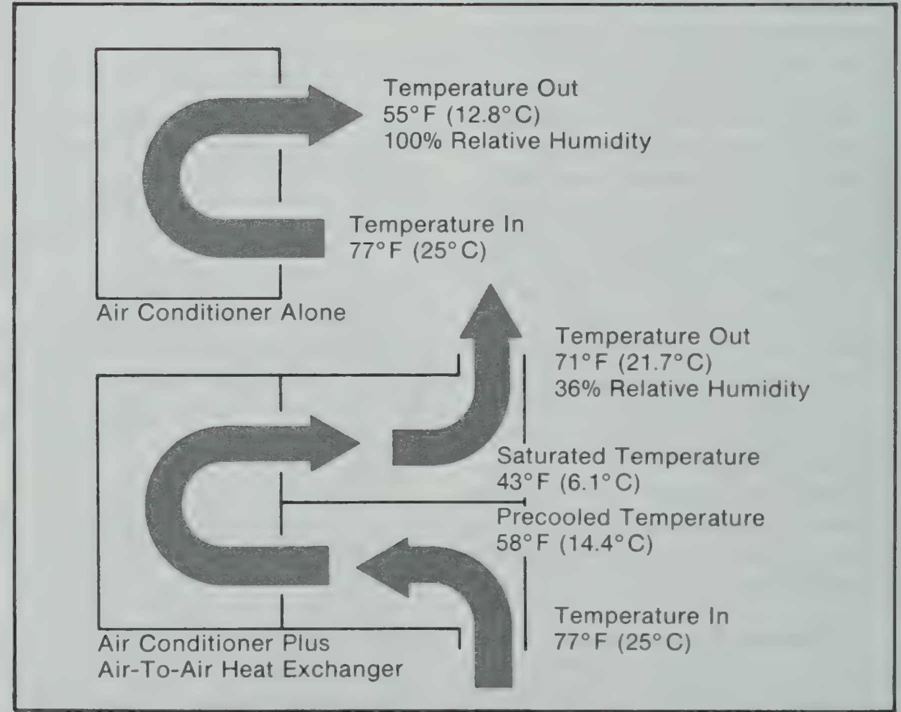

Fig. 1. Temperature measurements taken April 1980 at Trinity University illustrate the effect of a heat exchanger on air conditioner airstream temperature.

SERI to Publish Monitoring Results

Initial data gathered as part of a nationally coordinated effort to evaluate the performance of passive/hybrid systems will be published this summer by the Solar Energy Research Institute (SERI). The publication, tentatively titled *Passive Solar at Work,* will present mostly qualitative data collected for 20 homes in the U.S. Department of Energy's (DOE) Passive and Hybrid Systems Performance Evaluation Program.

SERI researchers managing the program for DOE say the booklet will be the culmination of Class C monitoring efforts to acquire noninstrumented performance data from a large sample of passive/hybrid buildings. Results from the Class C effort, as well as from the progressively more quantitative studies of Classes A and B, will help define research and development needs suggested by commonly cited design problems.

As part of the Class C effort, DOE contracted the four Regional Solar Energy Centers (RSECs) to study a total of 400 existing passive/hybrid homes. Local contractors audited homes to determine the relationship of such factors as glazing, thermal mass, and user interaction with the building to solar performance. A self-administered form for homeowners yielded attitudinal information regarding design and purchase rationale, perceived performance, and satisfaction.

The Memphremagog Group, Newport, Vt., and Market Facts, Inc., Washington, D.C., were contracted by SERI to review and process the nontechnical data on the homes; Total Environmental Action, Harrisville, N.H., assisted the RSECs in evaluating the technical data.

Preliminary Class C findings indicate that passive solar designs differ according to region (i.e., homes in the West are more sophisticated; eastern homes are generally owner-built, simple, direct-gain systems) and that solar heat contributions vary significantly according to locale.

The Class B phase of the program involves more intensive monitoring of 15 of the Class C homes in each region. Class B test homes received Data Acquisition Systems (microprocessor-based) which will monitor up to 22 sensors every 15 seconds to compute Btu requirements and Btu contributions of passive solar features. Testing began in May and will continue for one year.

The Class A performance evaluation will rely on data gathered for six passive/hybrid homes throughout the country. Class A monitoring, based on 100 or more sensors installed in each home, will determine detailed thermal performance of "generic" and innovative homes to obtain "hard" data for validating computer simulation codes and to determine the thermal performance and thermal mechanisms operating in innovative building systems.

■ Sharyn Towle, Program Manager, Class C Monitoring; Don Frey, Program Manager, Class B Monitoring; Ken Ortega, Program Manager and Principal Scientist, Class A Monitoring, Solar Energy Research Institute

Double-Envelope Evaluation Begun

Engineers and scientists from the Solar Energy Research Institute (SERI) are monitoring a double-envelope house near Denver to determine its thermal performance and to collect fundamental data regarding the thermal mechanisms operating in this passive design. The house is one of six buildings slated for extensive monitoring in the U.S. Department of Energy's Passive and Hybrid Systems Performance Evaluation Program.

SERI plans extensive monitoring of this double-envelope house.

To date, it has generally been assumed that air heated in a south greenhouse flows in a pattern around the inside of the envelope's outer skin, transferring its heat to interior living spaces in the process. However, by monitoring all thermal characteristics of the house, SERI scientists expect to provide researchers, builders, and consumers with new data on double-envelope performance.

Testing procedures will determine overall building heating load and associated UA-value; infiltration from inside to outside, from inside to plenum air space, and from plenum to the outside environment; and energy flow paths. The latter test will determine how heat enters the structure, where it is stored, where it is transferred, and where it is lost to the environment.

Testing will progress in two stages. In the first stage, all windows and openings will remain covered for several days to block sunlight and empty the house of all retained heat. The amount of auxiliary heat needed to maintain the house at a set temperature overnight will be measured, and the steady-state conductive value of the house calculated. Subsequently, the rate of temperature decay will be tested to determine overall conductance and capacitance of the envelope. To determine decay rate, the house will be heated to 70°F (21°C) before auxiliary heat is turned off, and consequent drop in temperature will be measured.

In the second stage of testing, data will be collected with the house in normal operation and the results used to validate a computer thermal model of the double-envelope house. Changes in basic design can then be introduced via computer to test their effect on thermal performance of the double-envelope.

■ Ken Ortega, Principal Scientist, Solar Energy Research Institute

New Prototype of Transwall Tested

Transwall, a second-generation prototype waterwall developed at Ames Laboratory, Iowa State University, is undergoing design performance testing to provide data to support commercialization.

Transwall resembles a series of water-filled, aquarium-like, glass containers, each 4 to 6 in. (10.2 - 15.2 cm) wide, supported atop each other by aluminum frames. The Transwall system, conceived to combine popular Trombe wall and direct-gain solar heating systems, reduces window obstruction, photodegradation of interior furnishings, and overheating problems found in conventional systems. It also reduces interior light intensity and peak temperatures without disturbing the visual and daylighting functions of windows. Its water-based thermal storage cuts weight and space requirements by factors of at least four and two, respectively, relative to commonly used concrete.

Because a large fraction of solar energy is absorbed within the water storage, high temperatures do not occur on the exterior facing wall surface as is the case for Trombe walls. This reduces radiative losses as well as the need for circulating air between the glazing and the wall to transfer heat to the interior.

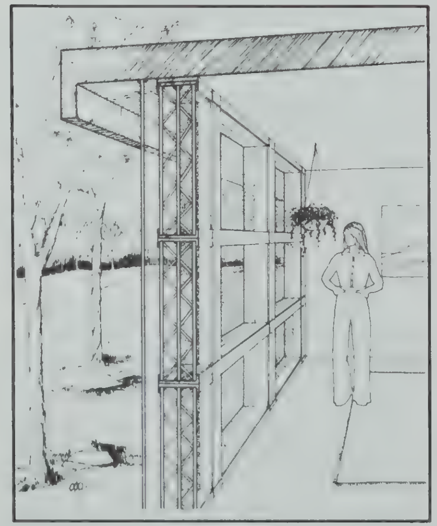

New Transwall prototype alleviates Trombe wall, direct-gain problems of daylight and view obstruction, photodegradation, and heat loss from exterior surfaces.

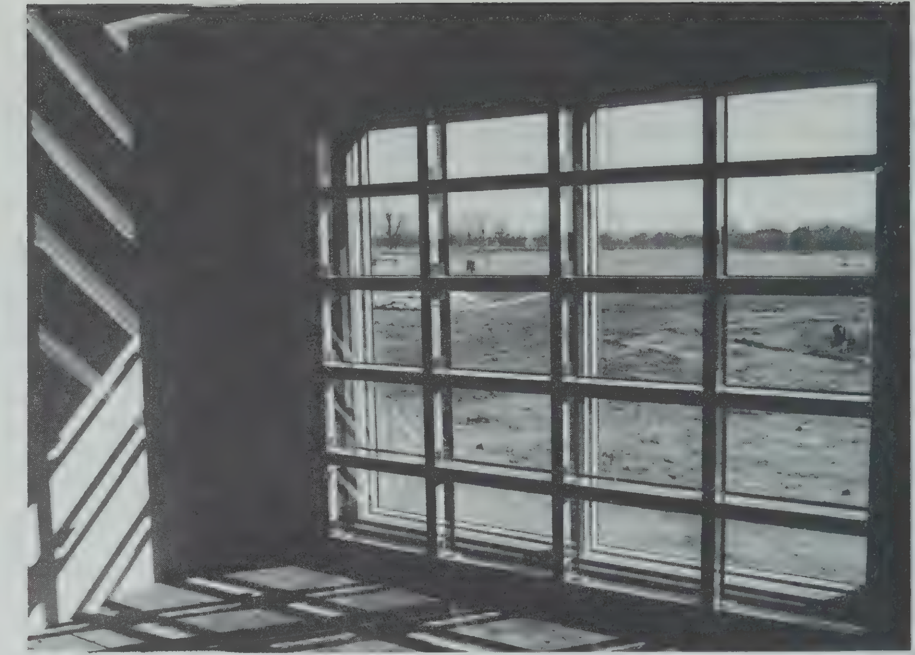

Transwall modules and aluminum support are designed for compatibility with economical mass production methods. The second-generation prototype is nearing commercialization readiness.

Transwall delivers solar heat to a building in the following manner: The near-infrared portion of incident solar energy passes through the front glass surface and is absorbed within the first inch (2.5 cm) of water. Approximately 65 percent of incident sunlight reaches the Transwall absorber plate, where a fraction, depending on the plate's transmissivity, is absorbed. The remaining visible portion of solar energy passes through the rear Transwall into the building interior, providing illumination and some direct-gain heating. Solar radiation is absorbed within the Transwall, raising the temperature of the modules. Part of this thermal energy is then transmitted to the building via radiation, convection, and conduction from the Transwall surface facing the interior.

Transwall exhibits one major advantage over conventional Trombe systems because Transwall stores most solar energy in its interior rather than at the front surface facing the windows. Hence, Transwall avoids the thermal losses associated with hot exterior-facing surfaces.

Module specifications were developed through computer simulation and consultation to the following outer dimensions: 52-in. wide, 23-in. high, and 7-in. thick (132 x 58.4 x 17.8 cm). Fabricated of acrylic plastic plates 3/8-in. (0.95 cm) thick, the modules require that three vertical rib braces be cemented inside each plate to prevent bowing under hydrostatic pressure. An absorber plate, located halfway between the two face plates, is supported by pairs of vertical strips cemented to each end plate. An aluminum retainer lid caps each module to prevent movement in face plates due to hydrostatic pressure and to reduce water evaporation and contamination. Water mass contained within each module is approximately 238 lb (30 gal). An additive inhibits biological growth inside the modules.

The modules and aluminum support structure are expected to be compatible with economical methods of mass production. Data on Transwall summer performance, currently being collected from a test building at the laboratory, should complete year-round performance summaries needed by potential commercial manufacturers.

Testing of Transwall prototypes by a range of commercial organizations will begin in Winter 1981.

■ John F. McClelland, Associate Physicist, Ames Laboratory, Iowa State University

Review

Passive Solar Design Handbook

Volume One: Passive Solar Design Concepts

Volume Two: Passive Solar Design Analysis

Total Environmental Action and Los Alamos Scientific Laboratory for the U.S. Department of Energy, 1980

Reviewers: Jeffrey Cook, Bill Wright, William A. Shurcliff

Few publications in the field have elicited stronger sentiments of praise and criticism than has this one. The prodigious work was begun shortly before the 1978 Second National Passive Conference in Philadelphia; originally envisioned as a 5-month task, the project ultimately spread over 2 years. Widely hailed upon publication, the handbook and its contents have been the subject of increasing scrutiny. Bill Shurcliff, one of our featured reviewers, states well the breadth of the reviewer's dilemma: "This book is an excruciating challenge. It is a mammoth contribution, yet it has scores of serious defects. Should the reviewer stress the pros or the cons? Should he hail the blazing of important new trails toward simplified calculations of thermal performance? Or should he scold the authors for badly worded and edited captions to graphs? Should he judge just the book, or judge the entire rationale propounded?" Critiques are presented here by a panel of three reviewers whose views are solely their own. The significance of the handbook practically cries out for ongoing interchange. Thus, feedback is welcome and encouraged. - - Ed.

Available from the National Technical Information Service (NTIS), 5285 Port Royal Road, Springfield, VA 22161 (DOE/CS-0127/1,/2; $13.25/$14.00; $3.00 each in microfiche)

There is a long tradition of handbooks within the building professions. Since the Renaissance, small manuals that could slip into a pocket have been tools for architects, civil engineers, surveyors, and "clerks of the works." As information about building construction expanded, so did the size of the reference. But even in the late 20th century, crisp communication and compact format are the standard.

Unfortunately, these two volumes from the Government Printing Office conform in no way to that tradition. They fit in no one's pocket, and their soft covers mean they are not stiff enough to stand on a shelf. A prudent professional with guts should attempt to read them and copy those essential pages that are indeed handy to his/her practice. Since there is no index, this is the only way to discover what is there and the only way to make things useful.

Volume One: Concepts was produced by Total Environmental Action. It contains typographic errors, awkward sentences, and many white spaces. However, the language is generally readable. Bruce Anderson, the prime author, in the foreword recognizes the "large size and disparate nature" of the work and that *Volume One: Concepts* is an introduction of qualitative information for the uninitiated.

Volume One begins with a definition of "passive" that relates only to "heating and cooling buildings or for heating domestic water" in which the key phrase is "by natural means." The implication is that pumps or fans are "unnatural," and that thermal and other energy tasks not tied into heating and cooling buildings are outside the definition.

A weak definition of "active" solar systems follows in which the concept of off-site power or parasite dependency is missed. The use of active solar systems as a benchmark for passive systems is a curious fetish left over from another age. As related to buildings, passive applications should be compared with the norm or standard environmental control systems of the times — fossil-fueled forced air and hot water radiators.

The text proceeds with a certain uncertainty: "The proper semantic cataloging of these techniques is unimportant compared with the concepts they try to communicate." Unfortunately, what the authors call concepts are really systems. Perhaps it is a reflection of the entire passive community that a conceptual schema of the interaction of the simple functions or components has not been articulated, at least in the United States. Rather, we are stuck with a limited number of application samples stylized here as:

1. Direct Gain
2. Convective Loops
3. Thermal Storage Walls
4. Thermal Storage Roofs and
5. Attached Sunspaces.

For architects used to dealing with component manipulation, this limited number may be adequate since each has a simple physical and architectural image. In general, they cover the prototypes of today's practice. However, this description is inadequate as a conceptualization of the field. (For those professionals self-confident enough to start with Volume Two, the same schema is again described but with some clarity and brevity.)

Although the definitions in Volume One of such thermal processes as "radiation" and "thermosiphoning" are weak, the descriptions and discussion of the five basic system types are adequate for all except thermal storage roofs, where prejudice shows. For instance, "structural support for the heavy mass" should really not represent much of a disadvantage. Since 6 in. of water is typically quite adequate for thermal mass, that weight is well below the 40 and 50 lb/ft^2 snow load required by code for structures in many locations.

And why "the heavy weight of thermal mass above the ceiling might be psychologically unacceptable (especially in an earthquake-prone area)"? The psychological acceptance of heavy construction cannot be found in any professional discussion of such building types as apartment houses or office buildings. Indeed, independent structural analyses of "Skytherm" construction using water bags on steel decking in earthquake zones show that such construction is superior to almost any other because of the diaphragm structural action of the roof plane and the value of the water in various disaster modes.

> **"Categorical statements without qualification are part of the simplification syndrome..."**

In the "Basics of Solar Building Design," the simplistic approach of Volume One is exposed where "energy conservation" is equated with "adding insulation." Only later is there a conceptual suggestion of comfort/climate as the basis for prescribing walls and their performance, composition, or heat transfer characteristics.

Then, there is that fascinating phenomenon "natural daylight" (p. B-71) that causes us to wonder about other forms of daylight. Categorical statements without qualification are part of the simplification syndrome: "In an air conditioned office (daylighting) reduces the electric lighting load on the air conditioning system by 93 percent." Presumably, this is a maximum possible figure which makes no account of the potential heating and cooling load added by increased glazing.

> **". . . information available . . . is impressive and yet is largely unused."**

Certainly, while some architects would agree with the authors that "there is a dearth of knowledge regarding solar gain through windows," not all researchers would. The quantity of information available in the technical literature, both in the United States and abroad, is impressive and yet is largely unused. The lack of use is then the responsibility of intermediaries, educators, writers, profession leaders, and of forward professional literature such as Volume One attempts to be.

An insufficient understanding of convection is revealed in the statement that "up to 20 percent of the heat gained during a sunny day can be lost through" reverse siphoning by the next day. It is very easy to design a convective system in which 100 percent or more of the heat gained can be lost. Similarly, a statement that "poorer performance and lower comfort levels may result whenever systems are designed to provide over 30 percent of the seasonal load" ignores successful systems that provide enviable comfort levels with 80 percent and higher of the seasonal load.

The use of the term "thermal storage walls" in such a set of major publications is sloppy semantics — since every wall has thermal characteristics. In particular, there is some confusion whether the phrase refers to thermal compositions such as Morse-Trombe-Michel walls, (where solar gain, thermal storage, and thermal delivery functions are directly coupled and are built as a constructional assembly) vs. thermal storage walls as separated temperature stabilizing features of an interior or exterior. Especially in passive design, the thermal characteristics of all surfaces must be designed — whether solar or otherwise. It would be an unfortunate, distorted definition if "thermal walls" would become standard nomenclature.

Diagrams intending to show ideal configurations show less than ideal relationships. A convective air heater is shown with air passing only on the back side. Without explanation, vents in a vented Trombe wall are shown in other than customary top and bottom wall locations. Trombe vents are also shown directly opposite each other rather than staggered for exhaust and supply functions. The preference of stain over paint for masonry collector surfaces is not mentioned.

Confusion of terms and generic types continues in "Thermal Storage Roofs" (p. C4-194). Obviously, there is a more basic type of roof pond than the distorting definition: "waterbed-like transparent bags filled with water." Indeed, ponded roof construction had many built examples during the 1940s and 1950s. The description of a "south sloping" pond is misleading to anyone who does not already know the subject. The inclusion of a discussion of south-sloping glazing in the Atascadero description confuses both subjects. In general, the description of roof ponds reveals some ignorance of both Skytherm experiences as well as related construction.

> **". . . one of the better researched and written chapters is 'Passive Solar Cooling' . . ."**

Useful knowledge to professionals is included, however, such as the methods of arriving at quantifiable value judgments. One such exercise economically compares the number of glazings and various movable insulations as related to annual heating degree days.

Surprisingly, one of the better researched and written chapters is "Passive Solar Cooling" — an odd title for a somewhat nonsolar function. Safely, very little is said about natural ventilation and the design of airflow using windows. The experimentally derived models by the Olgyays and Givoni are difficult to summarize as well as to apply to real building design situations. The only factual flaw in the chapter is in the respective attributions of Yellott and Hay regarding the Skytherm system. Both made earlier and perhaps more generic studies and contributions than the water-bagged roof. The calculation methods for stack-effect and for analyzing radiative cooling are straightforward and useful.

"The review of glazings is first-class . . ."

A series of Appendixes provides more useful information, although the materials are perhaps more appropriate to Volume Two, the reference text. The review of glazings is first class, although there is some conjecture in the application details of plastic films. Sunshine maps, conversion factors, energy costs, and R-values are included, but rules of thumb distributed through the text of Volume One are never gathered into one place for reference.

If the contents of Volume One seem familiar, it's probably because they are. References confirm that information is heavily borrowed from previous Anderson, TEA, and other publications. If there is some confusion about content, it may be because of some dependence on secondary sources rather than on original documents or research reports. If the quality of illustrations is mixed, it is because some have been lifted and some have been traced, and some have been generated from scratch.

In spite of these flaws (all of which could be a reflection of the processes of executing such a contract), the sum may be somewhat better than any of the separate documents from which the book borrows.

In its current state, *Volume One: Concepts* is just another report. With technical and editorial screening and a real publisher, it could be a neat introduction to the field. But that is only a promise.

Jeffrey Cook, Professor
College of Architecture
Arizona State University

It seems important to place criticism on Volume Two of this handbook in perspective relative to the state of development of the technology. We are still in the toddler stage of our understanding of passive buildings. In another 20 years, surely passive design will be old hat, and passive design handbooks will be four-color with crisp *Scientific American*-style illustrations. We are not there yet, but Volume Two is a step in that direction. One usually critiques handbooks based on their completeness, presentation, depth of material, and so on. In this case, the field itself is still forming and thus criticism must include definition and methodology.

". . . the likely reaction of those earning a living by design will be to ignore the monthly method."

In its presentation, Volume Two needs help. That frank description is the summary of comments from designers who reviewed copies. The organization is confusing and really penetrable only through diligent effort. However, it *can* be penetrated — it just takes a substantial amount of effort. Reorganization and repackaging by a technical publisher would multiply the utility and readability by severalfold. The sections on rules of thumb and the Load Collector Ratio (LCR) method have real potential, if repackaged properly. However, the monthly Solar Savings Fraction (SSF) method (which takes a minimum of 30 minutes to complete and for many situations requires an hour to grind through — all for a single point of performance) is simply unusable to the majority of practicing designers. Although a few dedicated innovators may well grind for a few hours to find out how a given building design is penalized by off-axis orientation, the likely reaction of those earning a living by design will be to ignore the monthly method.

"Mass and number of glazings would have been very useful to include . . ."

In terms of completeness, it is important to note that Volume Two gives no information on natural lighting, heating-cooling interactions, or overheating calculations for conventional frame construction retrofits. A major omission is a direct gain calculation for triple-glazed systems without night insulation. Including direct gain in the LCR tables as a dead loss for most of the northern tier is not terribly useful, whereas the sensitivity curves suggest that triple-glazing is a possible means of implementing direct-gain systems, which are so popular with consumers. Similarly, the sensitivity curves for mass correction are not confidently applied to a particular design, and yet mass is a critical cost item in conventional construction. Mass and number of glazings would have been very useful to include in the correlations so that individual systems could have been evaluated for these important design parameters. To be sure, these omissions are not so much oversights on the part of the Volume Two authors as they are an indication of the state of available information.

On the other hand, the completeness in terms of the number of levels of computation effort available, the geography covered, and the number of system types presented represents a major contribution to our current state of understanding. The backup material for methods and calculations would have been better presented in some appendix volume in which the models used and PASOLE could have been thoroughly documented for those who cared. As it stands, much of the backup material requires prior knowledge of other LASL papers and memos and thus could be better presented in a separate companion volume.

"The completeness . . . represents a major contribution to our current understanding."

One area in the methodology which poses major concern is the definition of Solar Savings Fraction (SSF). The SSF definition, although simple, arbitrarily places passive solar in a difficult light. In Appendix D, the LASL authors say, "The definition of passive solar used in this handbook is fairly generally accepted now and it is hoped that the definition of other terms employed herein will also come to be accepted." It is perhaps oversell to say that SSF "is fairly generally accepted"; rather, it is probably more accurate to say that the pros and cons of the several definitions have caused considerable confusion resulting in *no* generally accepted solar fraction definitions.

The SSF is troublesome because it computes savings with respect to a fictitious reference which is only relevant to a fraction of the population. The notion is that savings can't be calculated with respect to the solar building because the passive aperture is more "lossy" than a "conventional" wall and therefore has an abnormally high load. Thus, the fact that the actual passive building may be 75 percent heated by the sun is considered a "misrepresentation." The issue is thus whether or not the resident would have chosen to purchase the solar building regardless of savings. The indication that direct gain and live-in sunspaces are the most popular passive designs is really a reflection of the high value consumers place on visual aesthetics. For the consumer who would have purchased the passive solar house even if it faced north, the savings are with respect to the *actual* house, not the "net" reference.

Additionally, before the energy crunch, most consumers lived in winter temperatures in excess of 70°F. The free choice temperature (and therefore, heat of high value) was *above* that temperature which LASL selected as cutoff for inclusion in the load. Thus, the warming effect of 72° to 78°F was *devalued* to zero.

While this technique makes calculation simple, the current SSF definition cancels two primary passive ingredients which give the consumer what he or she wants — comfort. The discussion is not specious, because the magnitude of the effect on savings is large. For example, in upstate New York, a passive design which yields actual savings of 18.5 million Btu is reduced to 7.1 million Btu — a penalty of 62 percent. The higher number gives no credit for heat which takes the building above 65 percent, and so the SSF is understated even more.

"The SSF is troublesome . . . "

Arguments such as these lead to a belief that the current SSF definition cannot be generally accepted if passive is to survive. A definition of savings which reflects the composite current lifestyles of consumers is needed. In some cases, the savings will be minimal due to consumer preferences that are similar to the LASL reference. In many cases, however, consumer preferences will shift the savings to a multiple of the SSF definitions and hence allow passive design to proliferate.

All in all, Volume Two of the handbook is a major contribution, representing the first offering which makes a real attempt at a comprehensive integration of our understanding of passive buildings. As a mirror of the current level of understanding, the book makes starkly apparent the distance which we have yet to travel. Nonetheless, the LASL team is to be congratulated for this pioneering achievement.

Bill Wright, Manager
Technology Development
Division
Northeast Solar Energy Center

At the very start, the reader is thrown off by the book's subtitle, *Passive Solar Design Analysis.* The book deals, in fact, with only a small fraction of passive solar design analysis. A concisely delimiting and truly descriptive subtitle might be *Proposed Simplified Method of Predicting the Wintertime Thermal Performance of a Simple Small Building that (1) Employs, on the South Side, Direct Solar Gain or a Trombe Wall and (2) Receives Little or No Energy via the Non-South Windows or from Occupants, Light Bulbs, Etc.*

If the subtitle were thus delimited, readers would know what not to expect. They would be forewarned that the book deals only with analysis, specifically with analysis of thermal performance, and more specifically with an analysis method that is (judged by those who use it routinely) simple but not outstandingly accurate.

They would know that the book deals only with wintertime thermal performance — despite the fact that some design features that are excellent for winters may be bad for summers. They would recognize that (1) complicated buildings (as in those that are not merely clean-cut rectangular boxes with clean-cut thermal properties, clean-cut windows that either are, or are not, solar windows, etc.) are given little attention; (2) indirect passive solar heating is given little attention; (3) emphasis is on the south wall only, despite the fact that east and west windows can play important roles in supplying wanted solar energy in winter and unwanted solar energy in summer; and (4) intrinsic heat from humans, light bulbs, cooking stoves, etc., is assumed to be negligible, despite the fact that in very well-insulated houses, such heat can supply a large fraction of winter heat needs.

The central rationale, plan, or procedure specified in this book seems almost grotesque. Suppose, for example, you intend to design a direct-gain passive solar house with 300 ft^2 of south windows. The recommended procedure is for you to (1) complete your tentative design; (2) take the large backward step of deleting the solar gain; (3) compute the thermal performance of this emasculated and purely imaginary house; (4) estimate the fractional reduction in auxiliary heat need when the solar gain is restored; and (5) with this information in hand, estimate the actual amount of auxiliary heat needed.

"The central rationale, plan, or procedure . . . seems almost grotesque."

Why is this procedure near-grotesque? First, there is no satisfactory way to specify how the solar gain is to be eliminated. Should one imagine that the entire house is covered by a big black cloth so that no sunlight can reach it? Or should just the windows be covered? Instead of using a black cloth, should one use an extremely thick plate of Styrofoam® so that no energy can flow in or out of the windows? Should exceptions be made for windows that are triple-glazed or equipped with high-R nighttime shutters? What about infiltration through the windows? What about doors in the south wall — how are they to be treated?

The authors scarcely address these questions. They refer vaguely to omitting or covering "the solar collection wall" or "solar aperture," but do not define these vague terms. They suggest, alternatively, invoking a "normal wall" (not specified) which, they expect, or *hope,* will have "an exactly null effect on the average" so that gains and losses here will "exactly balance."

"Surely a well-conceived passive solar home is a nicely balanced combination of features."

At this point, the reader may well feel lost. What *average* is meant? Average throughout one 8-hour sunny day? Throughout a 24-hour typical day in January? And what does "exactly balance" mean? Balance during a sunny day, a sunless day, complete month of April, full winter, or what? Balance assuming that the furnace is never used? And what is meant by "normal wall"? Normal as to thickness? Materials? Normal in the context of 1930 design, 1970 design, or 1980 design?

A second flaw with the analysis method is that the authors improperly ascribe much significance to the Step 4 result: the estimate of fractional reduction in auxiliary heat use. One reads on p.10 that this fraction (called the Solar Savings Fraction or SSF) "is of primary interest in evaluating the energy-effectiveness and cost-effectiveness" of the proposed solar house. Actually, it is of little or no interest. Worse, it can be highly misleading.

Why is SSF of little or no interest? Because it is computed with respect to an imaginary, emasculated, nonsensical, unlivable house. Surely a well-conceived passive solar home is a nicely balanced combination of features: The designer strives to match the heat-saving features to the various heat inputs (solar input via windows and inputs from human bodies, light bulbs, etc.) and the thermal mass. What happens if a designer is forced to wipe out a proposed 300-ft^2 south window area? The match is destroyed. The design is an atrocity. With no south windows — and no natural illumination or view — the house is unlivable.

Notice also that such SSF values do not correlate with design merit. For example, they do not correlate with actual amounts of auxiliary heat needed. In extreme situations, an SSF-80 percent house might, for example, use *more* auxiliary heat than an SSF-60 percent house. If a client, or a banker considering making a mortgage loan, were impressed with a high-SSF value, he might later realize he has been misled.

What really *is* of importance? The actual annual auxiliary heating and cooling needs, for starters. More important yet is the combined present-value of capital cost of the building as a whole and of the lifetime cost of auxiliary heat in winter and cooling in summer. These quantities receive little attention in this book. Much importance is ascribed to relatively trivial questions such as, "Will the annual cost of auxiliary heat be \$50 or \$100?" Little importance is ascribed to the far more important question, "What is the overall cost of the building, and will it require a \$4,000 auxiliary heating system, or can it get by with one costing \$400, or only \$40?"

"Much importance is ascribed to relatively trivial questions . . ."

One more general criticism must be made. If the book were written clearly and included carefully phrased definitions and had an index (so that the reader could quickly locate the definitions), the strengths and weaknesses of the computational procedures recommended could be understood. But because there is no index, and the definitions are vague and scattered, and many of the tables and graphs are near-inscrutable, the typical reader may be unable to achieve real understanding, unable to bring his judgment into play. (Incidentally, it is unfortunate that the authors have not assigned a name to their procedure. It is difficult for a reader to discuss the procedure with friends if it has no name.)

"Perhaps 'solar savings increment' is what the book is about."

Having read carefully only a small fraction of the book, I am left in some doubt as to whether the authors' general method, the second step of which is a big backward step introducing an ill-defined, fictitious comparison house, is in fact ill-conceived, or whether it has merely been improperly explained and wrongly focused.

Perhaps the authors' real intent is to show how to compare different passive design features, i.e., how to estimate the auxiliary heat savings that can be made by small changes in south window area, in amount of thermal mass, and in other design elements.

Perhaps "solar savings increment" is what the book is about. Perhaps the authors could abandon the fictitious comparison house and abandon the contention that solar savings fraction itself has any simple significance. It is the increments provided by various intelligently chosen changes in passive design that are of interest — not the absolute value relative to a fictitious and unlivable house.

Could it be that the (nameless) method described in this book should be used only for evaluating the effects of small changes in passive design, and that designers interested in the absolute values of overall heat loss and overall auxiliary heat need should switch to a direct calculation using a high-capacity computer — the method that has been given the degrading name "simulation"? On p. 261, the authors state that simulation gives especially accurate results and, with the proliferation of high-capacity, low-cost computers, may soon be the preferred method.

A final worry: Does the authors' nameless method stack the cards against superinsulated houses? Such houses are, in a very real sense, direct-gain passive houses. They are easy to design and build, and to calculate their thermal performance is especially simple. Their superb thermal performance in winter and summer has been well demonstrated. Why, then, does this book scarcely mention them? Where, in this book, does one find recognition that (1) it is now easy to insulate a building so well that conductive heat loss in winter (and heat gain in summer) is relatively trivial; (2) intrinsic heat amounts to a considerable fraction of the total wintertime heat need; (3) the intrinsic thermal mass of a house, with no resort to concrete floors or walls, is impressively large (on the order of 15 tons); and (4) a house that takes advantage of these facts may need no substantial backup system, with savings that may amount to $1,000 to $4,000?

"The present book is without parallel . . ."

By any chance, would the superinsulated house be the ideal house for use as a reference house? Now that designers are learning how to reduce auxiliary heat need further and further, has not the time come to do an about-face and compare performance with the top of the scale (complete freedom from furnace) instead of the bottom of the scale (atrocious design and great dependence on furnace)?

I have mentioned only a very few of the book's good features. I have not mentioned the enormous number of fact-filled tables and graphs or the 19 kinds of correction factors that can be used to extend the overall method to a wide variety of direct-gain and Trombe-wall designs and to many other designs. As everyone knows, the Los Alamos group has done an enormous amount of work in constructing, testing, and analyzing passive solar structures and has done valuable pioneering work in correlating the results and compiling, for widespread use, short-cut calculational procedures. The present book is without parallel and fills, or makes a strong beginning at filling, a big void. Let us hope that a revised edition, with clearer logic and better writing, will be prepared soon.

William A. Shurcliff, Physicist
19 Appleton St.
Cambridge, MA 02138

Passive Solar Journal

Heating, Cooling, Hybrid Technologies and Strategies for Sustainable Design

ON ARCHITECTURAL CENTER
RY
NEWBURY ST.
ON, MA. 02115

Volume 1, Number 2 Spring 1982

Official Journal of the Passive Systems Division of the American Solar Energy Society,® Inc.

PASJDF 1(2) 65-128(1982) ISSN: 0277-6456

Passive Solar Journal

Editor-in-Chief:
Jeffrey Cook, Department of Planning, College of Architecture, Arizona State University, Tempe, Arizona

Associate Editors:
John Hayes (Book Review Editor), Marlboro College, Marlboro, Vermont
William A. Wright (Design Tools Review Editor), Cambridge Energy Corporation, Cambridge, Massachusetts
J. Douglas Balcomb, Los Alamos National Laboratory, Los Alamos, New Mexico
Michael Holtz, Architect, Boulder, Colorado
Fred Nelson, Sunset Magazine, Menlo Park, California

Managing Editor:
Cyndi Meagher, Passive Solar Journal, Tempe, Arizona
Assistant Editor, consulting:
Heidi Osselaer, Scottsdale, Arizona
Typesetting:
Paradise Valley Typesetting Studio, Paradise Valley, Arizona
Chief Artist, consulting:
Mark Woodruff, Glendale, Arizona

Director of Publications:
Albert Henderson, ASES, Bridgeport, Connecticut
Publications Production Manager:
Barbara Bradley, ASES, Newark, Delaware

Executive Director, ASES:
Lee Salmon, Boulder, Colorado

This issue of the Passive Solar Journal was produced in offices kindly donated by Allen & Philp Architects, Inc., formerly Associate Design Group/Architecture, of Phoenix, Arizona.

Submission of Manuscripts

Manuscripts will be invited; however, those proposed for publication are also welcome. They must be original and unpublished, although previously published data will be permitted. Manuscripts and accompanying illustrations are subject to peer review and editing.

Although this is the official journal of the Passive Systems Division, ASES, manuscripts are accepted from solar researchers and professionals throughout the world. Authors may or may not be members of ASES.

Manuscripts must be written in English and include illustrations and references. Four copies are required. All must be typed and double spaced on one side of white paper 8½ x 11 in. (22 x 28 cm) with ample margins. All pages should be numbered consecutively with abstract (up to 150 words), text with subtitles, acknowledgements, appendix, references, notes, figure captions and illustrations. Manuscripts should be prepared according to the "Style Manual" of the American Institute of Physics, 335 East 45th Street, New York, 10017. All materials will be published using both units of measure: Imperial (English) and SI. The units of the original research will take precedence (with the equivalents in parentheses). Manuscripts from a dot matrix printer will not be accepted.

Manuscripts should be sent to the Editor, **Passive Solar Journal**, Department of Planning, College of Architecture, Arizona State University, Tempe, Arizona 85287.

Cover: The relationships of nature, buildings and people form the basis for the study and practice of passive/hybrid solar research and design.

Photos: Boulder Energy Conservation Center, Bruce Flynn, Henry Mueller and Sharyn Towle.

Passive Solar Journal

The Official Journal of the Passive Systems Division
of the American Solar Energy Society.®
The United States Section of the International Solar Energy Society

SPRING 1982 Volume 1, Number 2

CONTENTS

DESIGN TOOLS

67 **Expanding the SLR Method:**
J. Douglas Balcomb, Robert W. Jones, Robert D. McFarland and William O. Wray develop correlation constants for 94 passive heating configurations.

RESEARCH METHODS

91 **Passive Solar Test Modules:**
Fuller Moore reviews the use of test boxes, rooms and building in the United States and Canada, including an introduction to the use of test modules.

BUILDING EVALUATION

109 **Non-Instrumented Performance Evaluation of Passive Solar Homes:**
Beth Sachs, Blair Hamilton, Katherine Clough and Ron Alward present selected results from a Class C survey of more than 300homesin the United States.

BASIC RESEARCH

121 **Thermal Impedance in Multi-Pane Windows:**
Joseph K.E. Ortega reports the computer modeled results of changing surface emissivity and placement, and of reducing free convection and gas conduction.

REVIEWS/BOOKS

128 Alex Wilson evaulates *Easy to Build Solar Bath Heater, Thermosiphoning Air Panel* and *Retrotrombe,* three manuals from the Total Environmental Action Foundation.

Publisher: The Passive Solar Journal is published by the American Solar Energy Society, Inc. (ASES): The United States Section of the International Solar Energy Society, 110 West 34th St., New York 10001. Quarterly: Winter, Spring, Summer, Fall. It is the official journal of the Passive Systems Division of ASES. (Solar Energy Society is a registered trademark.)

ASES assumes no responsibility for the statements and opinions advanced by contributors to the society's publications. Editorial views do not necessarily represent the official position of ASES.

This publication contains accounts of work sponsored by the United States Government. Neither the United States nor the United States Department of Energy, nor the American Solar Energy Society, nor any of their employees, nor any of their contractors, subcontractors, or their employees, makes any warranty, express or implied, or assumes any legal liability or responsibility for the accuracy, completeness, or usefulness of any information, apparatus, product, or process disclosed or represents that is use would not infringe privately owned rights.

Subscription rates: ASES individual members, 1982, one year, U.S. $20.00, foreign, $28.00; Corporate/Nonmembers, one year, U.S. $80.00, foreign, $88.00. Members of the Passive Systems Division receive the Passive Solar Journal as a benefit of membership. Individual member rates are for personal use only, paid with personal funds.

For membership information, write to ASES, 1230 Grandview Ave., Boulder, Colorado 80302.

Business correspondence:

Changes of address should be sent by members and subscribers to ASES' offices at 1230 Grandview Ave., Boulder, Colorado 80302. Allow six weeks for the notification to become effective. All communications should include both old and new addresses with zip codes and should be accompanied by a recent mailing label.

Claims for missing issues will not be allowed if received more than 90 days from date of mailing plus the time normally required for postal delivery of the issue and claim. No claims will be allowed because of failure to notify a change of address or because a copy is "missing from files."

Editorial correspondence:

The editorial office of the Passive Solar Journal may be contacted through Editor-in-Chief Jeffrey Cook, Dept. of Planning, College of Architecture, Arizona State University, Tempe, Arizona 85287.

Access: The Passive Solar Journal is covered by *Engineering Index* (monthly and annual), *Energy Abstracts* and *Energy Information Abstracts.*

Copyright © American Solar Energy Society, Inc.

It is a condition of publication that manuscripts submitted to this journal have not been published and will not be simultaneously submitted or published elsewhere. By submitting a manuscript, the authors agree that the copyright for their article is transferred to the publisher if and when the article is accepted for publication. However, assignment of copyright is not required from authors who work for organizations which do not permit such assignment. The copyright covers the exclusive rights to reproduce and distribute the article, including reprints, photographic reproductions, microform or any other reproductions of similar nature and translations. No part of this publication may be reproduced, stored in a retrieval system or transmitted in any form or by any means, electronic, electrostatic, magnetic tape, mechanical, photocopying, recording or otherwise, without permission in writing from the copyright holder.

U.S. COPYRIGHT LAW APPLICABLE
TO USERS IN THE USA

The Article Fee Code on the first page of an article in this journal indicates the copyright owner's consent that, in the U.S.A., copies may be made for personal or internal use provided the stated fee for copying beyond that permitted by Section 107 or 108 of the United States Copyright Law, is paid. The appropriate remittance should be forwarded with a copy of the first page of the article to the Copyright Clearance Center Inc., 21 Congress Street, Salem, MA 01970 U.S.A. If a code does not appear, copies of the article may be made without charge, provided permission is obtained from the publisher. The copyright owner's consent does not extend to copying for general distribution, for promotion, for creating new works or for resale. Specific written permission must be obtained from the publisher for such copying.

Reviewers

The Passive Solar Journal gratefully acknowledges the contribition of these and other professionals who have agreed to review articles before publication.

Donald Abrams
Cambridge Energy Corporation
Atlanta, Georgia

Bruce Anderson
Total Environmental Action, Inc.
Harrisville, New Hampshire

Dennis Andrejko
State University of New York at Buffalo

George Arnold
Tennessee Valley Authority
Knoxville, Tennessee

Steve Baer
Zomeworks Corp.
Albuquerque, New Mexico

Raymond J. Bahm
Raymond Bahm and Associates
Albuquerque, New Mexico

Paul Berdahl
Lawrence Berkeley Laboratory
Berkeley, California

Stanley Boghosian
Mechanical Engineering Consultant
East Palo Alto, California

Arthur Bowen
University of Miami
Coral Gables, Florida

Lester Boyer
Oklahoma State University
Stillwater, Oklahoma

James Brown
Donald J. Reeves & Associates, AIA
San Diego, California

Harvey Bryan
Massachusetts Institute of Technology
Cambridge, Massachusetts

Subrato Chandra
Florida Solar Energy Center
Cape Canaveral, Florida

Bing Chen
University of Nebraska
Omaha, Nebraska

Eugene Clark
Trinity University
San Antonio, Texas

James Clinton
Solar Energy Analysis Lab
San Diego, California

Alvin Converse
Dartmouth College
Hanover, New Hampshire

Earl Doderer
Trinity University
San Antonio, Texas

Fred S. Dubin
Dubin-Bloome Associates
New York, New York

Benjamin Evans
Virginia Polytechnic Institute and
State University
Blacksburg, Virginia

Philip Fairey
Florida Solar Energy Center
Cape Canaveral, Florida

Baruch Givoni
Ben Gurion University of the Negev
Israel

William Glennie
Princeton Energy Group
Princeton, New Jersey

Harry Gordon
Burt Hill Kosar Rittelmann Associates
Washington, D.C.

John Griffiths
Texas A & M University
College Station, Texas

Keith Haggard
Consultant
Denver, Colorado

John Hill
Southern Solar Energy Center
Atlanta, Georgia

Peter Hollander
Booz, Allen & Hamilton
Bethesda, Maryland

Bruce Hunn
Los Alamos National Laboratory
Los Alamos, New Mexico

Ralph Johnson
NAHB Research Foundation
Rockville, Maryland

David Johnston
Potomac Energy Group
Alexandria, Virginia

Ralph Jones
Brookhaven National Laboratory
Upton, Long Island, New York

Douglas Kelbaugh
Kelbaugh and Lee Architects
Princeton, New Jersey

Sanford Klein
National Bureau of Standards
Washington, D.C.

Kenneth Labs
Undercurrent
New Haven, Connecticut

William K. Langdon, AIA
Asheville, North Carolina

Andrew Lau
Southern Solar Energy Center
Atlanta, Georgia

Richard Levine
University of Kentucky
Lexington, Kentucky

Fred M. Loxsom
Trinity University
San Antonio, Texas

Peter Lunde
New Energy Resources, Inc.
Simsbury, Connecticut

Thomas Mancini
New Mexico State University
Las Cruces, New Mexico

Marlo Martin
Lawrence Berkeley Laboratory
Berkeley, California

Robert McFarland
Los Alamos National Laboratory
Los Alamos, New Mexico

Marietta Millet
University of Washington
Seattle, Washington

Stephen C. Moore
National Association of Home Builders
Washington, D.C.

W. Scott Morris
Researcher
Santa Fe, New Mexico

Philip Niles
California State Polytechnical University
San Luis Obispo, California

Harold Olin
U.S. League of Savings and Loans
Chicago, Illinois

Joseph K.E. Ortega
University of Colorado at Denver
Denver, Colorado

Larry Palmiter
Ecotope Group
Seattle, Washington

John Peck
Environmental Research Laboratory
Tucson, Arizona

Peter Pfister
Architectural Alliance
Minneapolis, Minnesota

Donald Prowler
South Street Design
Philadelphia, Pennsylvania

Victor Reno
Total Environmental Action, Inc.
Harrisville, New Hampshire

Benjamin T. Rogers
Consulting Engineer
Embudo, New Mexico

Beth Sachs
The Memphremagog Group
Newport, Vermont

Robert San Martin
Department of Energy
Washington, D.C.

Stephen Selkowitz
Lawrence Berkeley Laboratory
Berkeley, California

John Spears
National Solar Data Network
Silver Spring, Maryland

Steven Strong
Solar Design Associates, Inc.
Lincoln, Massachusetts

Krishnappa Subbarao
Solar Energy Research Institute
Golden, Colorado

Paul Sullivan
Cambridge Energy Corp.
Cambridge, Massachusetts

Herbert Wade
Ministry of Energy
Fiji Islands

George Way, AIA
Houston, Texas

Bruce Wilcox
Berkeley Solar Group
Berkeley, California

C. Byron Winn
Colorado State University
Fort Collins, Colorado

Francis de Winter
Altas Corp.
Santa Cruz, California

David Wolcott
New York Energy Research
& Development Authority
Albany, New York

David Wortman
Solar Energy Research Institute
Golden, Colorado

William Wray
Los Alamos National Laboratory
Los Alamos, New Mexico

John Yellott
Arizona State University
Tempe, Arizona

Performance Analysis of Passively Heated Buildings: Expanding the SLR Method

By J. DOUGLAS BALCOMB, ROBERT W. JONES, ROBERT D. McFARLAND and
WILLIAM O. WRAY
Los Alamos National Laboratory, Mail Stop K571, Los Alamos, New Mexico 87545

ABSTRACT

Correlation methods for the analysis of solar system performance are described and the Solar Load Ratio (SLR) method applied to passive systems is presented in detail. Reference designs are defined and correlation constants are given for 94 cases representing a variety of direct gain, thermal storage wall and sunspace configurations. A method of handling internal heat generation through the use of a balance point temperature for the degree-day base is described, and an example of the monthly calculation process is presented. Solar radiation correlations for quickly estimating monthly solar radiation absorbed, as needed to use the method, are described.

INTRODUCTION

It is now generally accepted that computer simulation analysis using a validated thermal network mathematical representation of energy flows can accurately represent the thermal performance of passive solar buildings. The analysis generally uses hourly solar and weather data and is desirable if the designer has the necessary computer equipment, time and money. Most designers want simpler techniques to use with hand calculators or desktop microcomputers which can generate estimates in a few minutes.

Such simplified correlation techniques can be reasonably accurate and are particularly useful early in the design process when quick feedback is essential. They can be applied to either residential or commercial buildings.

This paper focuses on both a monthly calculation, the Solar Load Ratio (SLR) method, and an annual calculation, the Load Collector Ratio (LCR) method, which were developed at Los Alamos National Laboratory. The annual method uses tables precalculated by the SLR technique and is more appropriate to hand analysis, while the monthly method is more versatile and appropriate to programmable calculator or microcomputer-aided analysis.

CORRELATION METHODS

In a correlation technique, one seeks to relate a desired result to one or more correlating parameters (generally dimensionless). Success is much more likely if the chosen correlating parameters preserve some essence of the overall physics governing the energy balances. The F-chart technique, developed at the University of Wisconsin for active solar systems, is an example of a correlation technique.[1] In that case, two correlating parameters

---

This work was performed under the auspices of the Office of Solar Heat Technologies of the U.S. Department of Energy.

were used. Researchers at the Los Alamos National Laboratory independently developed the SLR method for active systems, which utilizes one correlating parameter, the solar load ratio.[2] The ratio essentially relates the monthly net solar energy available to the building to the monthly net heating load that would be experienced by a comparable building without the passive solar element. Since then, the SLR method has been applied extensively to passive solar systems, and the University of Wisconsin has developed the un-utilizability method for passive systems.[3]

The un-utilizability and SLR methods have two things in common. First, they use monthly weather data to predict monthly performance. A month has been found to be a particularly useful time interval, being long enough that statistical variations tend to average out, and short enough that the basic weather statistics are stationary. Furthermore, only 8 to 12 monthly heating calculations are required to predict annual performance. The SLR prediction of monthly performance leads to relatively high errors (typically ±8%) but annual performance is predicted using LCR with an error of only ±3%, typically (compared to the simulation results). This is adequate for design purposes, being significantly less than the year-to-year variation in weather that can be anticipated.

A second common feature of the methods is that the correlations are derived using "data" developed from hour-by-hour computer simulations. The Transient System Analysis (TRNSYS) program generated the data used for the F-chart method and the PAssive SOLar Energy[4] (PASOLE) program generated the data for the passive SLR correlations. In short, the correlation techniques are second-generation analytical procedures, intended to give reasonably good correspondence with simulation analyses. Their results are intrinsically no better than those obtained from simulations. The correlations techniques, however, require several thousand times fewer calculations to complete a yearly estimate and require no more expensive equipment than a hand-held calculator.

THE SLR METHOD APPLIED TO PASSIVE HEATING SYSTEMS

The SLR method has been applied extensively to a variety of passive heating systems. A different correlation is required for each different passive system configuration such as sunspace or Trombe wall. The method is the basis for the design techniques described in Volume Two of the *Passive Solar Design Handbook*[5] and widely used within the passive solar design community. Varied hand-held calculator and microcomputer programs have been written using the methodology, and many are for sale.[6]

As noted, the parent set of monthly performance data for the SLR correlations has been generated using the PASOLE[4] hour-by-hour computer simulation code. The original method used a single correlating parameter (SLR) defined as follows:

$$\mathrm{SLR} = \frac{\text{solar energy absorbed}}{\text{building heating load}} \qquad (1)$$

Different definitions of "solar energy absorbed" and "building heating load" have been used in the past; this paper develops more precise, current definitions. The correlation time is 1 month so that each of the parameters in the above equation is for a 1-month period. Both the numerator and denominator of SLR are in energy units so that SLR itself is dimensionless.

The parameter that is correlated to the SLR is the solar savings fraction (SSF) defined as follows:

$$\mathrm{SSF} = 1 - \frac{\text{auxiliary heat}}{\text{net reference load}}. \qquad (2)$$

In this equation the net reference load is equal to the degree-day load of the nonsolar elements of the building as follows:

$$\text{Net reference load} = (\mathrm{NLC}) \cdot (\mathrm{DD}) \qquad (3)$$

where NLC is the net load coefficient. The NLC is computed leaving out the solar elements of the building. This is the "building load coefficient" or BLC in Volumes Two and Three of the *Passive Solar Design Handbook*.[5], [7] The change is to emphasize by the word "net" that only the nonsolar elements are included. The nominal units are Btu/°F day *(Wh/°C day)*. The quantity DD is the degree-days computed for an appropriate base temperature, as will be discussed later. (See Eq. 14.) A building energy analysis based on the SLR correlations would then begin with a calculation of the monthly SSF values. The monthly auxiliary heating requirements are then calculated by inverting Eq. 2:

$$\text{Auxiliary heat} = (\mathrm{NLC}) \cdot (\mathrm{DD}) \cdot (1 - \mathrm{SSF}). \qquad (4)$$

The annual auxiliary heat is the sum of the monthly values.

By definition (Eq. 2), SSF is the fraction of the degree-day load of the nonsolar portions of the building that is saved by the solar element. To place this definition in a concrete context, a nonsolar reference building was defined in Volume Two of the *Passive Solar Design Handbook*[5] as a basis for defining an annual energy savings due to the solar elements. This definition of a reference building provided a useful model in a simple analysis, but it unnecessarily complicated the method and was often misinterpreted as limiting the analysis to comparisons with that particular reference building. Therefore we recommend that expressing the analysis in terms of a particular reference building be discarded in favor of either of two approaches.

1. The first approach is more convenient and easier to use than the second but is less accurate. It is based on the observation that if the

solar elements of the building (south-facing walls and windows) were to be replaced by other elements such that the net annual flow of heat were zero, then the annual heat consumption would be the net reference load. The savings achieved by the solar elements would therefore be the net reference load (Eq. 3) minus the auxiliary heat (Eq. 4):

$$\text{Solar savings} = (\text{NLC}) \cdot (\text{DD}) \cdot (\text{SSF}). \quad (5)$$

Although very simple, this is a reasonable approximation because in many situations and climates it is approximately true that a "normal" solar-facing wall, with a normal complement of opaque walls and windows, will have an approximately null effect taken over the whole heating season. Thus the term "solar savings fraction," while having the precise definition given in Eq. 2, also is a reasonable indicator of the actual savings (as a fraction of the net reference load) that can be expected.

The difference between this approach (which is the one used later in an example) and the procedure outlined in Volume Two of the *Passive Solar Design Handbook*[5] is the calculation of DD. In the handbook two types of DD were determined, one for the solar building and one for the nonsolar building. The latter type was used only to define an annual SSF. This distinction is now dropped and only one type of degree days is used, as will be discussed later.

2. In the second alternative one defines a nonsolar comparison building in any desired way (although it is often difficult to obtain agreement on a single definition). The the auxiliary for this comparison building can be calculated using the SLR method to estimate the direct gain solar effect. In this case "solar savings" is the difference between the auxiliary heat of the nonsolar and solar buildings. This method requires a second complete building calculation.

In any case, SSF is not a figure of merit in itself, but is more appropriately considered as a convenient correlation parameter useful as an intermediate number needed in the process of estimating the required auxiliary heat.

Glossary

Auxiliary heat—Conventional heat delivered by space heating equipment to the building as a supplement to solar heat.

Base temperature—A fixed temperature in the definition of degree days.

Clearness ratio (K_T)—The ratio of monthly total horizontal to monthly extra-terrestrial horizontal radiation.

Degree days (DD)—Also heating degree days or degree days above a base temperature. The summed differences between a fixed base temperature and the daily mean outdoor temperatures. Only positive differences are counted, that is, when the outdoor mean is less than the base temperature. The daily mean is traditionally computed as the mean of the daily minimum and maximum temperatures.

Floating band—The temperature range between the heating and cooling thermostat setpoints.

Gross reference load—Steady state heat loss from a building assuming a constant indoor temperature. Both solar and nonsolar portions of the building are included.

Internal heat—Heat generated inside the building by sources other than the solar system or the space heating equipment such as appliances, lights and people.

Net load coefficient (NLC)—Net reference load per degree of indoor-minus-outdoor temperature difference per day.

Net reference load—Steady-state heat loss from the nonsolar portions of the building assuming a constant indoor temperature. See Eq. 3.

PASOLE—PAssive SOLar Energy, an hour-by-hour computer simulation program for passive solar energy systems.

Reference loads—See net reference load and gross reference load.

Solar load ratio (SLR)—Ratio of solar gain to heat load used in SLR correlations. See Eq. 9.

Solar savings fraction (SSF)—The fraction of the net reference load that is met by solar heat. See Eq. 2.

SOLMET weather data—A compilation of solar radiation and meteorological data for solar system analysis.

SUNSPOT—An hour-by-hour computer simulation program for direct gain passive solar energy systems derived from PASOLE.

Total load coefficient (TLC)—Gross reference load per degree of indoor-minus-outdoor temperature difference per day.

Typical meteorological year (TMY)—A composite year of hourly solar radiation and meteorological data used for solar system analysis. The years were constructed by combining typical months selected from the period of record for each of 26 locations in such a way as to represent typical years.

Reference Designs

The hour-by-hour simulations that are used as the basis for the SLR correlations are done with a detailed model of the building in which all the different design parameters are specified. (The only design parameter that remains variable is the load collector ratio (LCR), defined in Eq. 10.)

The correlations allow the designer to estimate performance variations due to changes in a certain limited group of design parameters. These are the thermostat setpoint, the internal heat generation rate, the glazing orientation and configuration, shading and other modifiers of the solar radiation. There is no allowance, however, for estimating the effect of changes in the many other design parameters. Thus the correlations relate only to the reference designs used in the simulations.

One way to overcome this difficulty is to use sensitivity calculations that have been done using the hour-by-hour simulation codes. The procedure is to perform a series of year-long simulations for different values of one of the design parameters, holding all other parameters at the reference level. These results are generally presented in graphic form and allow the designer to see the effect of changing one particular design parameter. This procedure is followed for each of the different design parameters. Major parts of Volumes Two and Three[5], [7] are taken up with such sensitivity studies.

Another possibility is to provide enough different SLR correlations for different selections of design parameters that one can come reasonably close to the intended design or bracket the calculation with two SLR estimations. This approach is quite practical. Since the publication of Volume Two,[5] the number of configurations for which correlations have been developed has been expanded from the original 6 to 94. (See appendices B and C.) These results are presented in Volume Three.[7]

Nine different direct-gain correlations have been developed representing different numbers of glazings, different values of storage-surface-to-glazing-area ratios and different wall thicknesses. Fifty-seven different thermal storage wall correlations have been developed representing Trombe wall and water wall, use or nonuse of night insulation, different numbers of glazings, use or nonuse of a selective surface, different Trombe wall thicknesses and thermal conductivities, different water wall masses, and both vented and unvented

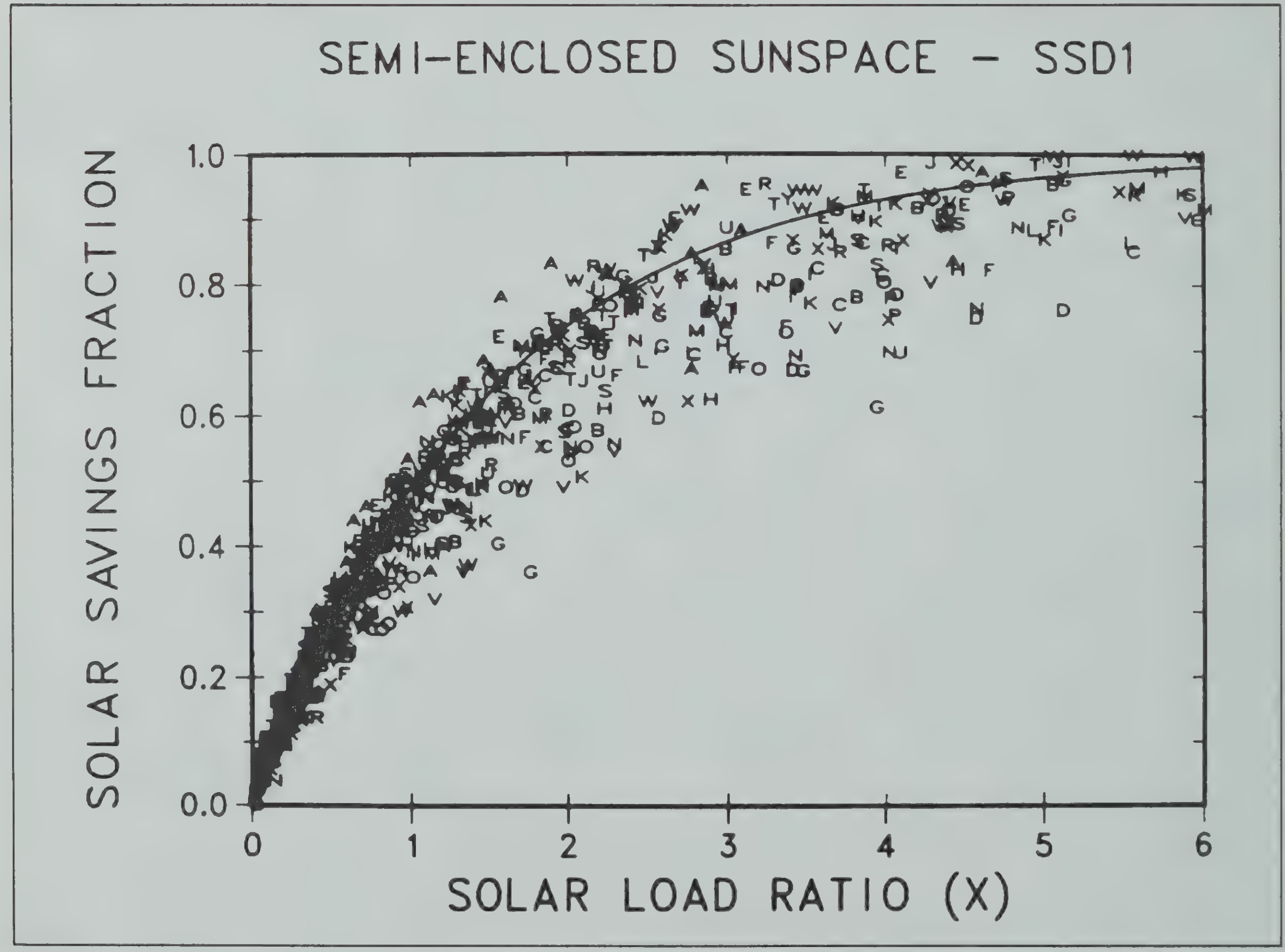

Graph: L.A.N.L.

Figure 1: Solar load correlation for passive system SSD1. Individual values of SSF and SLR resulting from the hourly simulations are shown for months having greater than 100 degree days F (56 degree days C). See Fig. 2 for city identification. The curve is the SLR correlation, chosen to yield a minimum square error in annual SSF.

Trombe walls. Twenty-eight different sunspace correlations have been developed representing five different configurations, glazed and unglazed end walls on the linear configurations, use or non-use of night insulation, and masonry wall or water drum storage. (See Appendix A for a summary of the reference design characteristics.)

Example of an SLR Correlation

As an example of the correlation results, we give simulation results in Fig. 1 and the corresponding correlation accuracy in Fig. 2 for one reference design, the case of a semi-enclosed sunspace with 50° sloped glazing, masonry thermal storage between sunspace and house, and no night insulation. This is system type SSD1. (See Appendices A and B for the system characteristics.)

Procedure

A solar load ratio (SLR) correlation is generated by a statistical least-squares fit of an ensemble of monthly data points that represent the monthly performance of a particular passive solar system. These points are computed using a detailed hour-by-hour computer thermal network simulation model of the passive system. Each model has been validated based on comparisons with test room data. The PASOLE computer code[4] and its derivative, SUNSPOT,[8] are the codes used. Annual simulations are done using typical meteorological year (TMY) data for ten or more cities representing a broad spectrum of U.S. climate types. Typically, hour-by-hour simulations are performed over a full year for each city for five different values of LCR (defined in Eq. 10). This gives a reasonably diverse ensemble of data points. The functional form of the SLR correlation allows for the selection of several different coefficients. The entire set of monthly simulation results is used to determine a set of coefficients that results in a minimum square error in the prediction of the annual solar savings expressed as a dimensionless solar savings fraction.

The scatter in the monthly points (Fig. 1, for example) appears severe, but the greatest deviations are for the warmer months (larger SLRs) that have little effect on the annual results. The standard deviation of the error in prediction of the annual solar savings fraction, compared to the hour-by-hour simulations, is typically 2 to 4%.

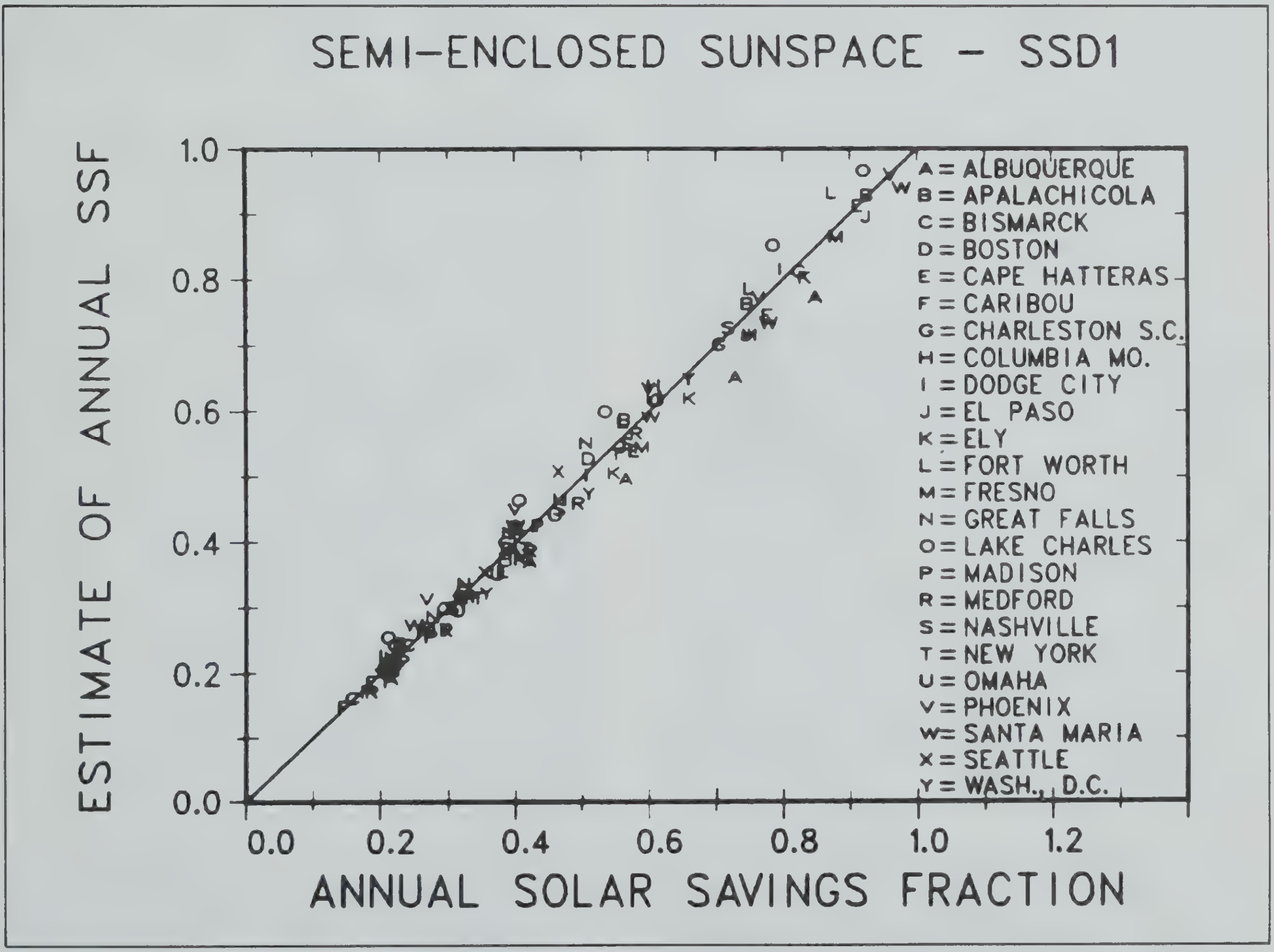

Graph: L.A.N.L.

Figure 2: Comparison of correlation vs. simulation results for passive system SSD1. The x-axis is the simulation result and the y-axis is the result of the SLR monthly method using the SLR curve on Fig. 1. The root-mean-square error of these 120 points is 2.8%. The city identification is the same for Fig. 1 and Fig. 2.

Initially, two SLR correlation forms were used, one for direct gain and another for all other systems. To avoid confusion, a general, slightly more complicated correlation form has been adopted that encompasses both. The monthly SSF is given by

$$\mathrm{SSF} = 1 - (1 - \mathrm{F})\mathrm{K} \qquad (6)$$

where

$$\mathrm{K} = 1 + \frac{\mathrm{G}}{\mathrm{LCR}} \qquad (7)$$

and

$$\mathrm{F} = \begin{cases} \mathrm{B} - \mathrm{C}\exp(-\mathrm{D}\cdot \mathrm{X}) & \text{when } \mathrm{X} > \mathrm{R} \\ \mathrm{A}\cdot \mathrm{X} & \text{when } \mathrm{X} < \mathrm{R} \end{cases} \qquad (8)$$

Equation 8 requires the additional condition that the maximum value of F is 1. The quantity X is the generalized solar load ratio,

$$\mathrm{X} = (\mathrm{S}/\mathrm{DD} - \mathrm{LCR_s}\cdot \mathrm{H})/(\mathrm{LCR}\cdot \mathrm{K}). \qquad (9)$$

Values for the correlation coefficients A, B, C, D, G and H for 94 passive system types are given in Appendix C. Note that H = O for direct gain, and for all other systems B = 1, G = 0 and R = -9 (which means that the second line of Eq. 8 is not used). System identifications are given in Appendix B. Reference designs are described in Appendix A.

The quantity LCR has the same meaning as in the design handbook:[5], [7]

$$\mathrm{LCR} = \frac{\text{net load coefficient}}{\text{projected area}} = \frac{\mathrm{NLC}}{\mathrm{A_p}} \qquad (10)$$

where "net load coefficient" (NLC) refers to the load coefficient of all of the building except the solar radiation aperture (same as "building load coefficient" or BLC in the handbook[5], [7]). The "projected area" (A_p) is the area of the net solar glazing as projected on a vertical plane (same as collection area, A_c, in the handbook[5], [7]). This is the same as the area measured on an elevation drawing normal to the glazing azimuth.*

The parameter LCR_s is the load collector ratio of just the solar aperture. Nominal values of LCR_s are given in the correlation coefficient tables, however LCR_s can be modified in practice to reflect changes in system design compared to the reference design. The dimensionless parameter H was determined at Los Alamos in the course of developing the correlations.

The parameter S is the solar radiation absorbed in the building per month per unit of projected area. It can be estimated using the solar radiation correlations described below (see Eq. 11) or by more complex trigonometic relations given in the literature.

Note that the correlations in this paper are the same as those in the third volume of the handbook[7] but are slightly different than those given in the second.[5] The changes are due to the change in correlation form, to changes in reference designs, and to minor inconsistencies in the earlier analytical models. These new correlations show somewhat improved performance compared to those of Volume Two.[5]

With minor exceptions, there are no known non-random variations in the SLR correlation results compared to the simulation results. The exceptions are some non-night insulated sunspace and thermal storage wall correlations at SLR less than 0.3. The result is that the correlations may overpredict SSF by a few percent for LCR values greater than 100. These correlations may be modified slightly in the future but for now one can test for these errors by calculating the performance of a comparable night-insulated case; if the performance of the non-night insulated case is greater, then reduce SSF to the night-insulated value.

SOLAR RADIATION CORRELATIONS

Solar radiation correlations are determined in a similar fashion to those for solar heating but by use of only the hourly solar radiation processor part of the computer simulation code. The hourly total horizontal and direct normal solar radiation from the 26 typical meterological year (TMY) cities are used to determine the solar radiation incident on and transmitted through glazings of various orientations. The diffuse sky radiation is assumed to be isotropic. The ground is assumed to have a diffuse reflectance of 0.3. Correlations are then determined for the monthly totals. The results are more accurate than the earlier correlations published in Volume Two[5] due to the use of two correlating parameters, the latitude minus the midmonth solar declination (L - D) and clearness ratio, K_T, rather than just L - D. The improved accuracy is most notable in cloudy climates where the earlier correlations led to errors up to 20%.[9] The accuracy now is adequate for use with the SLR process.

The desired result is S, the solar radiation absorbed in the building per month per unit of pro-

---

*It is recognized that using projected area is less convenient than using actual area. The advantage occurs when one wants to analyze a sunspace configuration that does not exactly correspond to one of the five reference design types. If actual area were to be used, significant error could result, whereas using projected area gives better accuracy for a wide variety of possible configurations. It is equally possible to use the actual area; however it is necessary to be consistent throughout. Each of the variables in the equation for X must be normalized to the same area. Thus in calculating S, LCR and LCR_s, be sure to use the same convention. Note that the solar radiation correlations given in Appendix F are defined in terms of the projected area, as defined herein, and those with tilted glazing would need to be modified by an appropriate constant if actual area were to be used instead. Also, the last column in Appendix C, which gives values of SSF for LCR = 20 (*113 Wh/°C day m²*), is based on an LCR calculated with the projected area.

jected area. To estimate S, it is convenient to use the following product of factors:

$$S = N \cdot HS \cdot \frac{A}{A_p} \cdot \frac{\text{incident}}{\text{horizontal}} \cdot \frac{\text{transmitted}}{\text{incident}} \cdot \frac{\text{absorbed}}{\text{transmitted}} \quad (11)$$

where

N = number of days per month,

HS = average daily total solar radiation on a horizontal surface, Btu/ft^2 day, (*Wh/m^2 day*), and

A/A_p = actual area/projected area.

If there is more than one glazing orientation, this formula can be used to estimate the contribution to S from each.

The last three ratios in the above equation for S are usually of the form used in Volume Two of the handbook[5]:

$$\text{Ratio} = C_1 + C_2 \cdot (L - D) + C_3 \cdot (L - D)^2 \quad (12)$$

except that now the correlation coefficients C_1, C_2 and C_3 are themselves linear in the clearness ratio, K_T:

$$\begin{aligned} C_1 &= B_1 + B_4 \cdot K_T \\ C_2 &= B_2 + B_5 \cdot K_T \\ C_3 &= B_3 + B_6 \cdot K_T \end{aligned} \quad (13)$$

For two of the transmittance correlations it was necessary to extend the correlation out to the $(L - D)^6$ term.

The general solar radiation correlations are given in Appendix E. Twelve correlations are given for the ratio incident/horizontal for different azimuths and tilts. Also given are 13 correlations for the ratio transmitted/incident for each case of single, double and triple glazing. The ratio absorbed/transmitted is not a simple function; tables for this are given in Volume Three[7] but are too voluminous to be reproduced here. Values of the absorbed/transmitted ratio for the Trombe wall, water wall, and direct gain reference designs are given in Appendix D.

For the special case of a south-facing solar aperture, it is convenient to combine three or four of the ratios in Eq. 11 into one. This can be done with the reference designs because then the geometry, azimuth and tilt are all specified. For the Trombe wall, water wall and direct gain cases, the first three ratios are combined into one: transmitted/horizontal. The absorptance can then be obtained from Appendix D. For the sunspace cases, all four ratios are combined into one: S/horizontal. These combined correlations are given in Appendix F. They are not exactly equivalent to the more general products, but are reasonably accurate.

PERFORMANCE TABLES FOR PARTICULAR LOCATIONS (ANNUAL METHOD)

Because the correlation curves are developed using weather data from a variety of different locations, these curves can be used in locations that have a climate type encompassed by the data for the original cities. However, an annual solar savings fraction calculation involves summing up the results of twelve monthly calculations. For a particular city, the resulting SSF depends only on LCR (the ratio of the net load coefficient to projected area), the system type and the temperature base used in the calculation of the degree days. Thus it is possible to make up tables for a particular city that relate SSF to LCR for the various systems, assuming one particular degree-day base temperature. These tables are easier for hand analysis than are the SLR correlations.

Annual SSF vs LCR tables have been made up for 209 different locations in the U.S. based on the SOLMET weather data[10, 11] and 10 cities in southern Canada. These are given in Volume Three.[7] These tables form the basis of a simplified design procedure—the LCR method—described in Volumes Two and Three. [5, 7]

MIXED SYSTEMS

A simple methodology has been developed for dealing with designs that have more than one passive type when using the SLR method.[5] The technique treats the building net load coefficient as if it were divided into portions in the same ratio as the relative projected areas of the various passive system types. This amounts to the simple assumption that each of the system types serves a portion of the load with no exchange of heat across an imaginary boundary within the building. Normally one would expect that transfers which do take place would be beneficial and, therefore, the calculations based on this assumption might be somewhat conservative.

The procedure is as follows:

1. Calculate one LCR for the entire building, using NLC for the entire building and the sum of all projected areas for A_p.
2. Calculate individual values of SSF for each passive type using the appropriate correlation or table and the LCR determined in step one, above. In this calculation use the appropriate separate values of S in Eq. 9 for each system. (Note that this treatment of S departs from the procedure recommended in Volume Two.[5])
3. Calculate the whole building SSF by computing an area-weighted average of all of the SSFs determined in step two, above.

ACCOUNTING FOR INTERNAL HEAT

Energy generated within the building by people, appliances, lights and equipment partially offsets the need for auxiliary heat. A convenient method to account for this interal heat is to make the base temperature for calculating degree days equal to the balance point temperature. The procedure is as follows:

$$T_{base} = T_{balance\ point} = T_{set} - \frac{\text{daily internal heat}}{\text{total load coefficient}} . \qquad (14)$$

"Daily internal heat" is the total internal energy deposited during one day in the building, and the "total load coefficient" is the net load coefficient, NLC, plus the steady-state heat load coefficient of the solar aperture. The average thermostat setting is T_{set}.

For this procedure to be accurate, it is important to include only that portion of the internal heat that stays in the building. The heating and ventilating system may discharge some of the internal heat directly, in which case this should not be counted.

In practice, the reduction in annual auxiliary heat requirements that results from an increase in internal heat is often less than one-half of the annual internal heat. It is normally more efficient to use just auxiliary heat when needed and to put internal heat into the building only as necessary for lighting and other vital functions—not to put in internal heat as, in effect, an auxiliary heat source itself.

For clarity, this paper includes an example of these procedures as they would be applied to a building in Denver, Colorado.

Continued on page 78

Example

Consider a commercial building located in Denver, Colorado with 3000 ft² *(280 m²)* of usable space and a sunspace entry foyer. The projected area (A_p) is 420 ft² *(39 m²)*. A sketch and preliminary plan are shown in Fig. 3. Note that the metric and English unit versions of the example are not exact conversions of each other. They are, instead, approximately the same example but with building parameters chosen as round numbers. Preliminary estimates of the heat load coefficients are shown in Table 1.

In order to calculate a load coefficient, a factor of 24 is needed to convert from Btu/°F h to Btu/°F day *(W/°C toWh/°C day)*. The net load coefficient, NLC, is computed without the solar aperture:

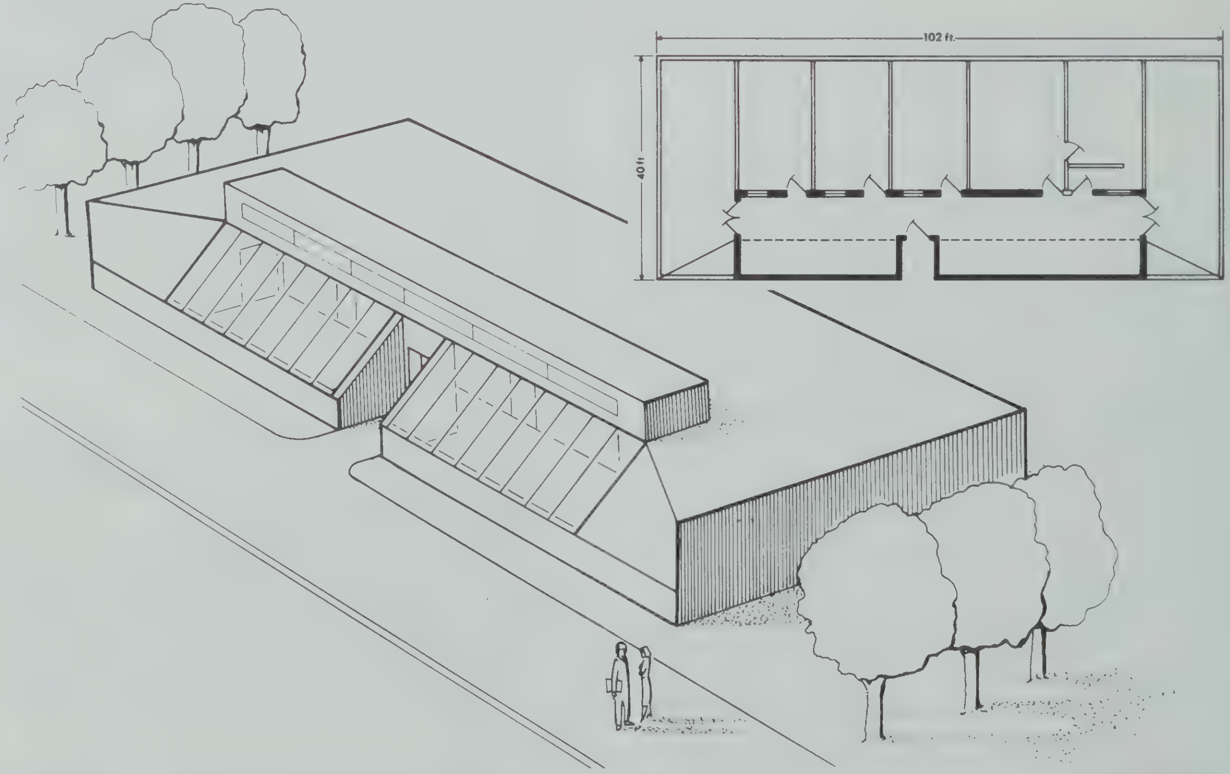

Drawing: L.A.N.L.

Figure 3: Floor plan and perspective drawing for the commercial building used as an example. The long sunspace on the south side serves both as the building main entrance and hallway. Distribution of solar heat to the offices is primarily by convection through the doorways from the sunspace. The principal mass in the building is in the common wall that separates the sunspace from the offices and in the sunspace floor. Miscellaneous doors and windows on the east, west and north facades are not shown.

Example

Estimated Heat Load Coefficients for Example Building

Metric Area A (m^2)	Metric U-value U ($W/m^2 {}^\circ C$)	Metric U x A ($W/{}^\circ C$)		English Area A (ft^2)	English U-value U ($Btu/h\ ft^2 {}^\circ F$)	English U x A ($Btu/h {}^\circ F$)
186	0.23	42.8	Opaque wall	2000	0.04	80
280	0.17	47.6	Ceiling	3000	0.03	90
280	0.23	64.4	Floor (over crawl space)	3000	0.04	120
10	3.15	31.5	Windows (E, W, N)	100	0.55	55
		186.3	Subtotal			345
		95.2	Infiltration			180
		281.5	Subtotal			525
		110.5	Sunspace (treated as unheated space calculated later)			209
		392.0	Total			734

Table 1: ASHRAE procedures are approximated with V = volume, ft^3; c = heat capacity of Denver air, $Btu/ft^3 {}^\circ F$; ACH = air changes/h; equivalent U x A for infiltration = V x c x ACH. In this instance, V = 24,000 ft^3, c = 0.015 $Btu/ft^3 {}^\circ F$, ACH = 0.5. (In the metric, V = 680 m^3, c = 0.28 $Wh/m^3 {}^\circ C$, ACH = 0.5.)

$$\mathrm{NLC} = 24 \cdot (525) = 12{,}600\ \mathrm{Btu/{}^\circ F\ day}$$
$$(\mathit{NLC} = 24 \cdot (281.5) = 6756\ \mathit{Wh/{}^\circ C\ day})$$

and the total load coefficient, TLC, includes the solar aperture:

$$\mathrm{TLC} = 24 \cdot (734) = 17{,}620\ \mathrm{Btu/{}^\circ F\ day}$$
$$(= 24 \cdot (392.) = 9408\ \mathit{Wh/{}^\circ C\ day}).$$

The load collector ratio, LCR, is

$$\begin{aligned} \mathrm{LCR} &= \mathrm{NLC}/\ A_p \\ &= 12{,}600/420 = 30\ \mathrm{Btu/ft^2\ {}^\circ F\ day} \\ &(= 6756/39 = 173\ \mathit{Wh/m^2\ {}^\circ C\ day}). \end{aligned}$$

Suppose that the daily internal heat is 141,000 Btu/day *(41.8 kWh/day)* and that the average thermostat setting is 68 °F *(20 °C)*. Then:

$$T_{\mathrm{base}} = 68 - 141{,}000/17{,}620 = 60\ {}^\circ\mathrm{F}$$
$$(= 20 - 41800/9408 = 15.5\ {}^\circ C\ ).$$

Thus, degree days are to be calculated for a 60 °F *(15.5 °C)* base temperature.

In this example the solar system is type SSD1. This is a semi-enclosed sunspace with a 50°-tilted double glazing and a 12-in. *(30-cm.)* masonry wall between the sunspace and the remainder of the building. In this commercial building, the sunspace is used as an entry foyer and main east-west hallway and contains only a few decorative plants. Therefore, to achieve a projected area of 420 ft^2 *(39 m^2)* requires an actual net glass area of 420/sin 50° = 548 ft^2 *(39/sin 50° = 50.9 m^2)*. Note that the sunspace area is not included in the 3000 ft^2 *(280 m^2)* floor area nor are any heat flow paths from the main building into the sunspace included in the calculation of the net load coefficient.

The nominal value of LCR_s for Type SSD1 is 17.8 Btu/ft^2 °F day *(101 Wh/m^2 °C day)*; however, small changes from the nominal value may be accounted for by calculating LCR_s for the actual building. LCR_s should include only heat flow paths from the sunspace to the outside. Table 2 presents an example.

As developed in Table 2,

$$\mathrm{LCR_s} = 23.5\ \mathrm{Btu/ft^2\ {}^\circ F\ day}$$
$$(= 135\ \mathit{Wh/m^2\ {}^\circ C\ day}).$$

Using the constants of Appendix C, the SLR formulas become

$$\begin{aligned} X &= (S/DD - 23.5 \times 0.84)/30 \\ &(= (S/DD - 135 \times 0.84)/173) \\ \mathrm{SSF} &= 1 - 0.9889 \exp(-0.6643\ X). \end{aligned}$$

Values of S and DD need to be determined for each month. For S we can use the solar radiation correlation for SSD1 from Appendix F assuming a due south building orientation and no shading. An example will be carried through for January.

Parameters needed to apply the correlations of Appendix F are (L - D), the latitude minus the mid-month solar declination; and K_T, the average monthly clearness ratio. These parameters are

Example

LCR_S Calculation for Example Building

Metric Area A (m^2)	U-value ($W/m^{2\circ}C$)	U x A ($W/^\circ C$)		**English** Area A (ft^2)	U-value ($Btu/h\ ft^{2\circ}F$)	U x A ($Btu/h^\circ F$)
50.9	3.18	161.9	Glass (double)	548	0.55	301
5.1	0.23	1.2	Opaque Wall	55	0.04	2
1.8	1.13	2.0	Door	20	0.20	4
53.9	0.17	9.2	Roof	580	0.03	17
		174.3	Subtotal			324
		36.8	Infiltration			70
		9.0	Perimeter loss			17
		220.1	Total			411

Therefore, $LCR_S = 24 \times 411/420 = 23.5\ Btu/ft^2\ ^\circ F$ day. (In the metric, $LCR_S = 24 \times 220.1/39 = 135\ Wh/m^{2\circ}C$ day).

Equivalent U x A for infiltration = V x c x ACH, where V = volume, ft^3; c = heat capacity of Denver air, $Btu/ft^{3\circ}F$; ACH = air changes/h. In this example, V = 9300, c = 0.015, ACH = 0.5. (In the metric, V = 263 m^3, c = 0.28 $Wh/m^{3\circ}C$, ACH = 0.5.)

Equivalent U x A for perimeter loss = L x f, where L = length of exterior sunspace perimeter, ft., f = perimeter heat loss coefficient per foot of perimeter. In this example, L = 72, f = 0.24. The value f = 0.24 corresponds to R12 perimeter insulation. (In the metric, L = 22 m., f = 0.41 perimeter heat loss coefficient per meter of perimeter, a value which corresponds to U = 0.47 $W/m^{2\circ}C$ for perimeter insulation.)

Notes:

On glazing:

The sunspace is double glazed, with a ¼ in. (6 mm.) gap. The recommended U-value is 0.55 $Btu/h^\circ F\ ft^2$ (3.18 $W/m^{2\circ}C$).

For other glazing considerations, the U-value may be estimated by use of the formula $U = 1.083/(N + 1.517t - 0.4295)$, $Btu/h^\circ F\ ft^2$, where N is the number of glazing layers and t is the thickness of the glazing air gap in inches. If $t > 0.5$, use $t = 0.5$. (In the metric, $U = 6.14/(N + 0.059/t - 0.4295)$, $W/m^{2\circ}C$, where N is the number of glazing layers and t is the thickness of the glazing air gap in millimeters. If $t > 12$, use $t = 12$.)

These values are recommended, not necessarily because they give the best estimates of actual glazing heat loss, but because they are consistent with the LCR_S values used to develop the sunspace SLR correlations. In the case of night insulation, use the time-weighted average U-value.

On the load coefficient:

The steady-state load coefficient of the building through the sunspace, treating the sunspace as unheated, can be estimated as the effect of two conductances in series. Taking the average U-value of the common wall between the sunspace and the adjacent building to be 0.424 $Btu/h\ ft^{2\circ}F$ and the common wall area to be 1005 ft^2, the load coefficient from the building into the sunspace is U x A = 0.424 x 1005 = 426 $Btu/h^\circ F$. This, in series with the 411 $Btu/h^\circ F$ from sunspace to outside yields $1/(1/411 + 1/426) = 209$ $Btu/h^\circ F$. (In the metric, if average U-value of the common wall is 2.4 $W/^\circ C\ m^2$ and the area is 92.5 m^2, then the load coefficient from the building into the sunspace is U x A = 2.4 x 92.5 = 222 $W/^\circ C$. This, in series with the 221.1 $W/^\circ C$ from sunspace to outside, yields $1/(1/220.1 + 1/222) = 110.5$ $W/^\circ C$.)

This was needed in the earlier calculation of the TLC.

Table 2: ASHRAE procedures are approximated as in Table 1. See this table's notes for further explanation of sunspace glazing and finding the steady-state load coefficient of the building through the sunspace, treating the sunspace as unheated.

tabulated for 219 U.S. and Canadian locations in Volume Three[7]. Alternatively, they can be calculated as follows. For solar declination, we can use the approximate formula:

$$\begin{aligned} D &= 23.3 \cos(30\ N - 187.1);\ N = \text{ month} \\ &= 23.3 \cos(30 - 187.1) = -21.46 \text{ degrees.} \end{aligned}$$

$$\text{Latitude} = 39.7;\ \text{therefore L-D} = 61.16.$$

For estimating K_T, the clearness ratio, we first need to estimate the horizontal extraterrestrial solar radiation. Convenient formulas are:

$$\begin{aligned} I &= 427\ (1 - 0.0316 \sin(30\ N + 252)) \\ &= 440.2\ Btu/ft^2\ h \\ &(= \mathit{1346}\ (\mathit{1} - \mathit{0.0316} \sin(\mathit{30}N + \mathit{252})) \\ &= \mathit{1388}\ W/m^2), \end{aligned}$$

$$\begin{aligned} Sha &= \cos^{-1}(-\tan(L)\tan(D)) = 70.95^\circ, \\ Y &= (24/\pi)(\cos(L)\cos(D)\sin(Sha)) \\ &\quad + (Sha)(\pi/180)\sin(L)\sin(D)) = 2.959. \end{aligned}$$

The average January horizontal solar radiation in Denver is 840 Btu/ft^2 day *(2647 Wh/m^2 day)* (see Ref. 10 or 11).

$$\begin{aligned} K_T &= Q_{horiz}/(I \cdot Y) = 840/1302 = 0.645 \\ &(= Q_{horiz}/(I \cdot Y) = \mathit{2647}/\mathit{4107} = \mathit{0.645}). \end{aligned}$$

Example

Heating Performance Analyses for Example Building

English

Heating Month	S (Btu/ft²)	DD (°F day)	S/DD (Btu/ft²°F day)	SSF	Net Ref. Load (10^6 Btu)	Solar Savings (10^6 Btu)	Aux. Heat (10^6 Btu)
Sep	52,108	51	1022.0	1.000	0.64	0.64	0.00
Oct	52,223	261	200.0	0.982	3.29	3.23	0.06
Nov	40,598	618	65.7	0.643	7.79	5.00	2.79
Dec	38,212	849	45.0	0.435	10.70	4.65	6.05
Jan	43,670	933	46.8	0.457	11.76	5.37	6.39
Feb	45,491	762	59.7	0.592	9.60	5.68	3.92
Mar	53,705	713	75.3	0.711	8.98	6.39	2.59
Apr	49,695	379	131.1	0.916	4.78	4.38	0.40
May	49,515	143	346.3	0.999	1.80	1.80	0.00
Jun	49,538	23	2154.0	1.000	0.29	0.29	0.99
		4732			59.63	37.43	22.20

Annual SSF = 37.43/59.63 = 0.63

Metric

Heating Month	S (kWh/m²)	DD (°C day)	S/DD (Wh/m²°C day)	SSF	Net Ref. Load (kWh)	Solar Savings (kWh)	Aux. Heat (kWh)
Sep	164.2	28	5866	1.000	190	190	0
Oct	164.6	145	1135	0.980	980	960	20
Nov	128.0	343	373	0.634	2320	1470	850
Dec	120.4	472	255	0.426	3190	1360	1830
Jan	137.6	518	266	0.448	3500	1570	1930
Feb	143.4	423	339	0.583	2860	1670	1190
Mar	169.3	396	428	0.703	2680	1880	800
Apr	156.6	211	742	0.912	1430	1300	130
May	156.1	79	1951	0.999	530	530	0
Jun	156.1	13	12007	1.000	90	90	0
		2628			17770	11020	6750

Annual SSF = 11020/17770 = 0.62

Table 3: SLR method calculations produce performance analyses shown here for the Denver, Colorado, commercial building used as an example. See Fig. 4 for a bar chart of these results.

In these formulas, I is the extraterrestrial direct normal solar radiation, Sha is the sunset hour angle, Y is a multiplier such that I · Y is the extraterrestrial daily horizontal solar radiation, and Q_{horiz} is the measured average daily horizontal solar radiation.

Now S can be estimated using the appropriate solar radiation correlation from Appendix F:

$$\begin{aligned} \text{ratio} = {} & (0.73147 - 0.15276\ K_T) \\ & + (-0.15418 + 0.14608\ K_T) \cdot (L\text{-}D)/100 \\ & + (0.50763 + 3.6950\ K_T) \cdot [(L\text{-}D)/100]^2 \\ = {} & 1.677. \end{aligned}$$

Therefore,

$$\begin{aligned} S &= (31) \cdot (840) \cdot (1.677) \\ &= 43{,}670\ \text{Btu/ft}^2 \\ (&= (31) \cdot (2647) \cdot (1.677) \\ &= 137600\ \text{Wh/m}^2). \end{aligned}$$

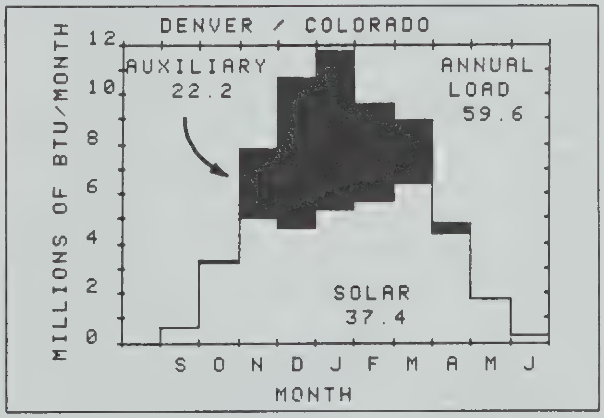

Graph: L.A.N.L.

Figure 4: Bar chart of the SLR results for the example building. The chart shows that the solar savings are relatively constant from November through April for this building in Denver and that the auxiliary peaks strongly in December and January. The chart is an output from a typical microcomputer routine.

Example

Degree days for various base temperatures are tabulated for numerous locations in Volumes Two and Three of the *Passive Solar Design Handbook*[5, 7] and from the National Climatic Center, Asheville, North Carolina.[12] They can also be estimated using the method of Thom[13] and a standard deviation estimate given by Erbs, et al.[14] The value from Volume Three[5] for a base temperature of 60 °F *(15.5 °C)* for January in Denver is 933 *(518)* degree days.

Then:

$$\begin{aligned} S/DD &= 43{,}670/933 = 46.8\ \mathrm{Btu/ft^2\ {}^\circ F\ day} \\ X &= 0.902,\ \text{and} \\ SSF &= 0.457. \end{aligned}$$

Therefore for January:

$$\begin{aligned} \text{Net reference load} &= (933)\cdot(12{,}600) \\ &= 11.76\ \text{million Btu}, \\ \text{Solar savings} &= (11.76)\cdot(0.457) \\ &= 5.37\ \text{million Btu, and} \\ \text{Auxiliary heat} &= 11.76 - 5.37 \\ &= 6.39\ \text{million Btu} \end{aligned}$$

(Or in the metric,

$$\begin{aligned} S/DD &= 137600/518 = 265.5\ \mathrm{Wh/m^2\,{}^\circ C\ day} \\ X &= 0.879,\ \text{and} \\ SSF &= 0.448. \end{aligned}$$

Therefore for January:

$$\begin{aligned} \text{Net reference load} &= (518)\cdot(6756) = 3500\ \mathrm{kWh}, \\ \text{Solar savings} &= (3500)\cdot(0.448) = 1570\ \mathrm{kWh},\text{and} \\ \text{Auxiliary heat} &= 3500 - 1570 = 1930\ \mathrm{kWh}.) \end{aligned}$$

This calculation can be repeated for the other months with the results shown in Table 3.

A bar graph of these results is shown in Fig. 4.

Many people will inevitably insist on knowing the solar *heating* fraction, SHF. Although there are various possible definitions of SHF, one easily obtained value is a "reference SHF" computed for a degree-day load at a reference temperature equal to the building balance point temperature. In this case

$$SHF = 1 - \frac{\text{auxiliary heat}}{\text{gross reference load}}$$

where

$$\begin{aligned} \text{gross reference load} &= (TLC)\cdot(DD) \\ &= 83.4\ \text{million Btu annually}, \\ &(= 24720\ \mathrm{kWh}\ \text{annually}) \\ SHF &= 0.73. \end{aligned}$$

The actual measured SHF should be larger than this because the building will occasionally be warmer than the thermostat setting of 68 °F *(20 °C)* due to solar gains. A good estimate of the actual SHF would require a simulation analysis, but this is probably not warranted because SHF is not an important result. The important result is the annual auxiliary, which is accurately estimated.

The annual solar savings of 37.4 million Btu *(11020 kWh)* is also an important result if one needs to justify the expense of the sunspace on the basis of its energy savings. Of course, the amenity and utility values of the sunspace must also be taken into account in the justification. Note that the sunspace is a good performer, saving 68,000 Btu/ft² *(217 kWh/m²)* each year.

Continued from page 74

SHADING AND OTHER CONSIDERATIONS

Shading and other factors that might modify the solar energy absorbed, S, although not accounted for in the example, can easily be included in the calculational procedure by modifying the monthly value of S. These modifying factors may be any of the following:

1. Orientation different than due south or tilt other than the reference value
2. Ground reflectance different than the assumed value of 0.3
3. Shading by building overhangs or fins
4. Shading by neighboring buildings or trees
5. Addition of a reflector to enhance solar gain
6. Glazing transmittance other than that assumed in the reference design
7. Building absorptance other than that assumed in the reference design.

Each of these effects can be estimated using various graphs and other available tools.[5, 7, 15–16]

COMPLEXITY

Working through the accompanying example with a hand-held calculator is tedious and would certainly not be considered a "simplified method" by most designers. However, a variety of inexpensive calculating machines is now available that can convert this to a very fast process. Hand-held programmable calculators can be programmed to calculate repetitively and quickly the clearness ratio, solar radiation correlation, and SLR correlation. A desktop microcomputer provides another step-up in speed and convenience at modest cost and can be programmed to complete an annual SLR estimate in 4 to 10 seconds. Either approach can provide a very useful tool for estimating the auxiliary heating implications of design decisions.

Another approach is to use tables that give the results of SLR calculations for various values of LCR for a particular climate. This is the "annual method" mentioned earlier. The advantage is that a simple four-function calculator is quite adequate, and one can complete an estimate in just a few minutes —again quickly enough to be useful as a design aid. Such tables are given in the second and third volumes of the handbook.[5, 7] The disadvantage is that fewer parameters can be varied. The tables require that the orientation, degree-day base and LCR_S all be specified and do not allow one to assess the implications of shading. Nonetheless, they are useful and provide an easy way to assess differences in performance for the various system options. A very limited example is given in Appendix C where SSF is listed for LCR = 20 *(113 Wh/°C day m²)* for Denver for a 65 °F *(18.3 °C)* base.

PERFORMANCE VARIATION DUE TO LIVING HABITS

All of the simulation analyses used to develop the correlations are based on a building that is used in a very specific and regular manner. The auxiliary heating thermostat is assumed to be set at a particular fixed level. A 10 °F *(5.5 °C)* floating band is assumed. If the temperature in the building exceeds the thermostat setting by more than 10 °F *(5.5 °C)*, then it is assumed that the excess energy is vented so as to maintain the temperature less than or equal to the upper setting. This energy is not stored and is therefore lost.

It is well known that the manner in which the building is operated greatly affects the energy consumption. The thermostat setting for auxiliary heat is by far the most important effect. This shows up clearly in a sensitivity analysis. For example, if the thermostat setting were to be increased from 68 °F to 73 °F *(20 °C to 23 °C)* in the preceding example, the auxiliary heat required would be increased by 50% *(54% for 3 °C increase)*. See Table 4.

Therefore, in interpreting the results from monitored buildings, or in stating the predicted performance of new buildings, one must be very careful to specify the operating conditions.

Other operating characteristics of the building can also be important, such as:

1. If movable insulation is provided, then it is important to know how it is operated;
2. A building with a large traffic in and out may experience larger infiltration due to multiple door openings;
3. A building with doorways connecting the heated areas and a sunspace might be much more comfortable and use less auxiliary heat if some attention is paid to the appropriate opening and closing of these doors;
4. The internal heat can have a major effect on the required auxiliary.

DESIGN ANALYSIS VERSUS PERFORMANCE PREDICTION

As pointed out in the previous section, various aspects of the operation of a building have an important effect on the auxiliary heat requirement. Likewise, various building construction characteristics and the weather to which the building is exposed will have important effects on the building's auxiliary consumption. Because many of these things are only approximately predictable, analysis tools like the SLR method cannot predict the performance of a particular building during a particular year. Instead, the analysis estimates the average annual performance using long-term normal weather statistics and certain building and operation assumptions.

DECIDING BETWEEN CONSERVATION AND PASSIVE SOLAR OPTIONS

A simple technique has been developed that can be used to determine the optimum mix between conservation and solar strategies.[17] In order to obtain an answer, one needs the cost characteristics of both the passive solar system and the energy conservation features. This information will generally be in the form of the cost per R per ft^2 *(m^2)* for the wall and ceiling insulation, the cost per additional glazing for windows, the cost of reducing infiltration (including the cost of adding an air-to-air heat recovery unit if needed) and also the cost per ft^2 *(m^2)* for the passive solar collection aperture. Given this information, the method provides simple equations that can be used to trace out

The Effect of a Thermostat Setting Change on SLR Method Results

Metric			**English**	
20°C	23°C	Thermostat setting	68°F	73°F
15.5°C	18.5°C	Balance point	60°F	65°F
2628°C days	3403°C days	Degree days	4732°F days	6018°F days
17770 kWh	22990 kWh	Net reference load	59.6 x 10⁶ Btu	75.8 x 10⁶ Btu
.62	.55	SSF	.63	.56
11020 kWh	12590 kWh	Solar savings	37.4 x 10⁶ Btu	42.5 x 10⁶ Btu
6750 kWh	10400 kWh	Auxiliary heat	22.2 x 10⁶ Btu	33.3 x 10⁶ Btu

Table 4: Changing the thermostat setting for auxiliary heat produces significantly different SLR method results.

the economic optimum-mix line for a particular locale.

COOLING CONSIDERATIONS

The important issues of summer comfort and cooling loads have not been addressed in the work reported here. Nevertheless, *year-round* comfort and energy efficiency is the goal of a balanced passive solar design. A passive solar heating system may aggravate the summer discomfort or cooling load because of excessive solar gains through the solar aperture, but suitable summer solar controls can largely alleviate this potential problem. Indeed, some of the elements of a good passive solar design for heating also enhance summer comfort, namely, mass for thermal storage and conservation measures in the building envelope. Other important controls are shading and ventilation. It is a significant design challenge to tastefully and effectively integrate the necessary controls with the passive solar heating system and the rest of the building so that the heating system performance is not unnecessarily compromised, yet does not significantly aggravate summer discomfort or cooling loads.

CONCLUSIONS

Correlation methods of analysis have advantages in greatly simplifying the time and complexity of performance analyses. Their accuracy is generally adequate for design purposes provided they are applied to buildings that correspond reasonably closely to the reference designs used in developing the correlations. The most simplified correlation procedures can be used with hand calculators, especially if precalculated tables are available that include the influence of the weather for the location of interest. When reporting the results of these calculations, the designer should be especially careful to specify the assumptions made in the analysis, especially as pertains to both operating characteristics and design parameters.

Correlation techniques like the SLR method are especially amenable to use in microcomputer routines that can be used in a design office. Very quick answers can be obtained during the schematic design and design development phases of a building to aid in deciding among different designs. This would include trade-offs between various conservation and passive solar options.

REFERENCES

1. Beckman, W.A.; Klein, S.A.; Duffie, J.A. 1977. *Solar Heating Design by the F-Chart Method.* New York: Wiley-Interscience.
2. Solar Energy Group, Los Alamos Scientific Laboratory. November 1976. *ERDA's Pacific Regional Solar Heating Handbook.* Available from: U.S. Government Bookstore; Stock No. 060-000-0024-7.
3. Monsen, W.A.; Klein, S.A.; Beckman, W.A. 1981 (May). "The Un-utilizability Design Method for Collector-Storage Walls." *Proceedings of the 1981 Annual Meeting of AS/ISES.* Philadelphia, Pennsylvania; 26-30 May 1981.
4. McFarland, R.D. 1978 (October). *PASOLE: A General Simulation Program for Passive Solar Energy.* Los Alamos National Laboratory Report LA-7433-MS.
5. Balcomb, J.D.; Barley, D.; McFarland, R.D.; Noll, S.; Perry Jr., J.E.; Wray, W.O. 1980 (January). *Passive Solar Design Handbook—Volume Two: Passive Solar Design Analysis.* Prepared for: U.S. Department of Energy; DOE/CS-0127/2.
6. Nordham, D. 1981 (February). *Microcomputer Methods for Solar Design and Analysis.* Solar Energy Research Institute, SERI-SP-722-1127.
7. Jones, R.W., editor; Balcomb, J.D.; Kosiewicz, C.E.; Lazarus, G.S.; McFarland, R.D.; Wray, W.O. *Passive Solar Design Handbook—Volume III: Passive Solar Design Analysis (Addendum).* Prepared for the U.S. Department of Energy (to be published) ; DOE/CS-0127/3.
8. Wray, W.O. 1981 (June). *Design and Analysis of Direct Gain Solar Heated Buildings.* Los Alamos National Laboratory Report LA-8885-MS.
9. Straub, D.; Palmiter, L. "A Comparison of Empirically-Based Solar Radiation Models." *Proceedings of the 1980 Annual Conference of SESC I.* Vancouver, B.C., Canada; 6-10 August 1980.
10. Cinquemani, V.; Owenby, J.R.; Baldwin, R.G. 1978 (November). *Input Data for Solar Systems.* Asheville, North Carolina: National Climatic Center.
11. Knapp, C.L.; Stoffel, T.L.; Whitaker, S.D. 1980 (October). *Insolation Data Manual.* Solar Energy Research Institute, SERI/SP-755-789.
12. National Climatic Center. U.S. Department of Commerce. *Degree Days to Selected Bases.* Asheville, North Carolina. Unpublished but available.
13. Thom, H.C.S. 1954 (May). "Normal Degree Days Below Any Base." *Monthly Weather Review.* Vol. 82 (No. 5).
14. Erbs, D.G.; Beckman, W.A.; Klein, S.A. 1981 (September). "Degree Days for Variable Base Temperatures." *Proceedings of the Sixth National Passive Solar Conference of the AS/ISES.* Portland, Oregon; 8-12 September 1981.
15. Sharp, K. 1980 (October). "Analytical Integration of the Insolation on a Shaded Surface at Any Tilt and Azimuth." *Proceedings of the Fifth National Passive Solar Conference of the AS/ISES.* Amherst, Massachusetts; 19-26 October 1980.
16. Mazria, E. 1979. *The Passive Solar Energy Book.* Rodale Press.
17. Balcomb, J.D. 1980 (October). "Conservation and Solar: Working Together." *Proceedings of the Fifth National Passive Conference.* Amherst, Massachusetts; 19-26 October 1980.

ACKNOWLEDGEMENT

The authors gratefully acknowledge the assistance of Gloria Lazarus and Claudia Kosiewicz in developing the correlations.

Appendix A: Reference Design Characteristics

Masonry properties	**English**	**Metric**
thermal conductivity, direct gain and sunspace	1.0 Btu/h ft °F	1.73 W/m °C
density	150 lb/ft^3	2403 kg/m^3
specific heat	0.2 Btu/lb °F	0.836 kJ/kg °C
infrared emittance of normal surface	0.9	0.9
infrared emittance of selective surface	0.1	0.1

Solar absorptances		
water wall	0.95	0.95
masonry, Trombe wall	0.95	0.95
direct gain and sunspace	0.8	0.8
sunspace: water containers	0.9	0.9
lightweight common wall	0.7	0.7
other lightweight surfaces	0.3	0.3

Glazing properties		
transmission characteristics	diffuse	diffuse
orientation	due south	due south
index of refraction	1.526	1.526
extinction coefficient	0.5 in^{-1}	0.2 cm^{-1}
thickness of each pane	⅛ in	3.2 mm
air gap between panes	½ in	12.7 mm
infrared emittance	0.9	0.9

Control range		
room temperature	65 °F to 75 °F	18.3 °C to 23.9 °C
sunspace temperature	45 °F to 95 °F	7.2 °C to 35.0 °C
internal heat generation	0	0

Thermocirculation vents (when used)		
vent area/projected area (sum of both upper and lower vents)	0.06	0.06
height between vents	8 ft	2.44 m
reverse flow	none	none

Night insulation (when used)		
thermal resistance (or conductance, in the metric)	R9	0.63 W/m^2 °C
in place, solar time	5:30 pm to 7:30 am	5:30 pm to 7:30 am

Solar radiation assumptions		
shading	none	none
ground diffuse reflectance	0.3	0.3
lightweight absorption fraction	0.2	0.2

Other sunspace characteristics		
opaque wall thermal resistance (or conductance) (both insulated wall and end walls, if any)	R20	0.28 W/m^2 °C
infiltration, ACH	0.5	0.5
masonry wall thickness (masonry wall cases)	12 in	30.5 cm
water container heat capacity (insulated wall cases) (per unit of projected area)	62.4 Btu/ ft^2 °F	1274 kJ/ m^2°C

Appendix B: System Identifications

DIRECT GAIN

Metric						English	
Nominal Wall Thickness (cm)	Thermal Storage Capacity (kJ/°C m^2)	**Designation**	Mass-to-Glazing-Area Ratio	No. of Glazings	Night Insulation	Thermal Storage Capacity (Btu/ft^2°F)	Nominal Mass Thickness (in.)
5.1	612	**A1**	6	2	no	30	2
5.1	612	**A2**	6	3	no	30	2
5.1	612	**A3**	6	2	yes	30	2
15.2	919	**B1**	3	2	no	45	6
15.2	919	**B2**	3	3	no	45	6
15.2	919	**B3**	3	2	yes	45	6
10.2	1225	**C1**	6	2	no	60	4
10.2	1225	**C2**	6	3	no	60	4
10.2	1225	**C3**	6	2	yes	60	4

VENTED TROMBE WALL

Metric							English		
ρck (kJ^2/s m^4°C^2)	Nominal Wall Thickness (cm)	Thermal Storage Capacity (kJ/°C m^2)	**Designation**	No. of Glazings	Wall Surface	Night Insulation	Thermal Storage Capacity* (Btu/ft^2°F)	Nominal Wall Thickness (in.)	ρck (Btu^2/h ft^4°F^2)
3.48	15.2	306	**A1**	2	normal	no	15	6	30
3.48	22.9	459	**A2**	2	normal	no	22.5	9	30
3.48	30.5	612	**A3**	2	normal	no	30	12	30
3.48	45.7	919	**A4**	2	normal	no	45	18	30
1.74	15.2	306	**B1**	2	normal	no	15	6	15
1.74	22.9	459	**B2**	2	normal	no	22.5	9	15
1.74	30.5	612	**B3**	2	normal	no	30	12	15
1.74	45.7	919	**B4**	2	normal	no	45	18	15
0.87	15.2	306	**C1**	2	normal	no	15	6	7.5
0.87	22.9	459	**C2**	2	normal	no	22.5	9	7.5
0.87	30.5	612	**C3**	2	normal	no	30	12	7.5
0.87	45.7	919	**C4**	2	normal	no	45	18	7.5
3.48	30.5	612	**D1**	1	normal	no	30	12	30
3.48	30.5	612	**D2**	3	normal	no	30	12	30
3.48	30.5	612	**D3**	1	normal	yes	30	12	30
3.48	30.5	612	**D4**	2	normal	yes	30	12	30
3.48	30.5	612	**D5**	3	normal	yes	30	12	30
3.48	30.5	612	**E1**	1	select.	no	30	12	30
3.48	30.5	612	**E2**	2	select.	no	30	12	30
3.48	30.5	612	**E3**	1	select.	yes	30	12	30
3.48	30.5	612	**E4**	2	select.	yes	30	12	30

Thermal storage is per unit of projected area. Nominal wall thickness is for the particular case of $\rho c = 30$ Btu/ft^3°F(or $\rho c = 2010$ kJ/m^3°C).

Appendix B: System Identifications (cont.)
UNVENTED TROMBE WALL

Metric							English		
ρck ($kJ^2/s\,m^4\,{}^\circ C^2$)	Nominal Wall Thickness (cm)	Thermal Storage Capacity ($kJ/{}^\circ C\,m^2$)	**Designation**	No. of Glazings	Wall Surface	Night Insulation	Thermal Storage Capacity ($Btu/ft^2\,{}^\circ F$)	Nominal Wall Thickness (in.)	ρck ($Btu^2/h\,ft^4\,{}^\circ F^2$)
3.48	15.2	306	**F1**	2	normal	no	15	6	30
3.48	22.9	459	**F2**	2	normal	no	22.5	9	30
3.48	30.5	612	**F3**	2	normal	no	30	12	30
3.48	45.7	919	**F4**	2	normal	no	45	18	30
1.74	15.2	306	**G1**	2	normal	no	15	6	15
1.74	22.9	459	**G2**	2	normal	no	22.5	9	15
1.74	30.5	612	**G3**	2	normal	no	30	12	15
1.74	45.7	919	**G4**	2	normal	no	45	18	15
0.87	15.2	306	**H1**	2	normal	no	15	6	7.5
0.87	22.9	459	**H2**	2	normal	no	22.5	9	7.5
0.87	30.5	612	**H3**	2	normal	no	30	12	7.5
0.87	45.7	919	**H4**	2	normal	no	45	18	7.5
3.48	30.5	612	**I1**	1	normal	no	30	12	30
3.48	30.5	612	**I2**	3	normal	no	30	12	30
3.48	30.5	612	**I3**	1	normal	yes	30	12	30
3.48	30.5	612	**I4**	2	normal	yes	30	12	30
3.48	30.5	612	**I5**	3	normal	yes	30	12	30
3.48	30.5	612	**J1**	1	select.	no	30	12	30
3.48	30.5	612	**J2**	2	select.	no	30	12	30
3.48	30.5	612	**J3**	1	select.	yes	30	12	30
3.48	30.5	612	**J4**	2	select.	yes	30	12	30

WATER WALL

Metric						English	
Wall Thickness (cm.)	Thermal Storage Capacity ($kJ/{}^\circ C\,m^2$)	**Designation**	Wall Surface	No. of Glazings	Night Insulation	Thermal Storage Capacity ($Btu/ft^2\,{}^\circ F$)	Wall Thickness (in.)
7.6	318	**A1**	normal	2	no	15.6	3
15.2	637	**A2**	normal	2	no	31.2	6
22.9	955	**A3**	normal	2	no	46.8	9
30.5	1274	**A4**	normal	2	no	62.4	12
45.7	1911	**A5**	normal	2	no	93.6	18
61.0	2548	**A6**	normal	2	no	124.8	24
22.9	955	**B1**	normal	1	no	46.8	9
22.9	955	**B2**	normal	3	no	46.8	9
22.9	955	**B3**	normal	1	yes	46.8	9
22.9	955	**B4**	normal	2	yes	46.8	9
22.9	955	**B5**	normal	3	yes	46.8	9
22.9	955	**C1**	select.	1	no	46.8	9
22.9	955	**C2**	select.	2	no	46.8	9
22.9	955	**C3**	select.	1	yes	46.8	9
22.9	955	**C4**	select.	2	yes	46.8	9

Thermal storage capacity is per unit of projected area. Nominal wall thickness is for the particular case of $\rho c = 30$ $Btu/ft^3\,{}^\circ F$ (or $\rho c = 2010$ $kJ/m^3\,{}^\circ C$).

Appendix B: System Identifications (cont.)
SUNSPACE GEOMETRIES

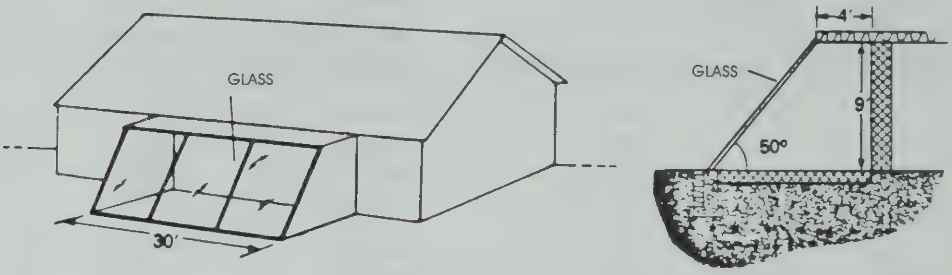

Attached (A)

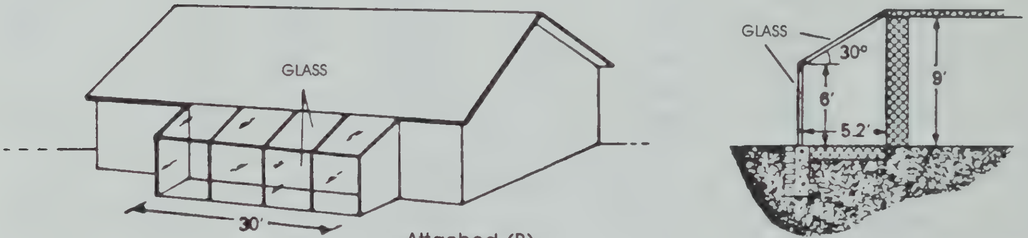

Attached (B)

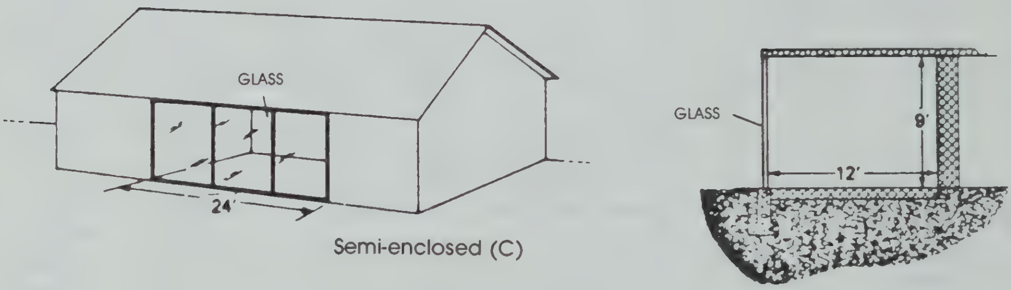

Semi-enclosed (C)

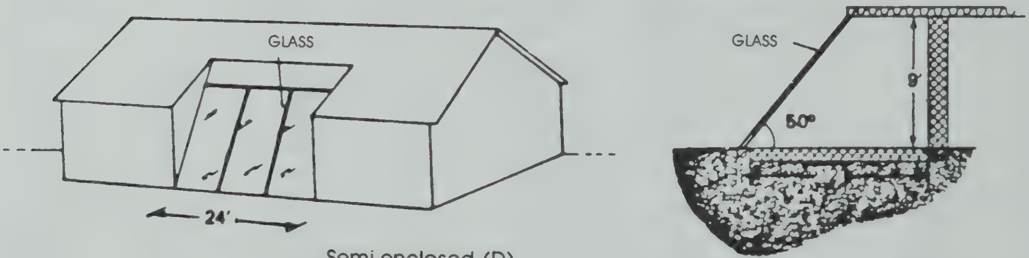

Semi-enclosed (D)

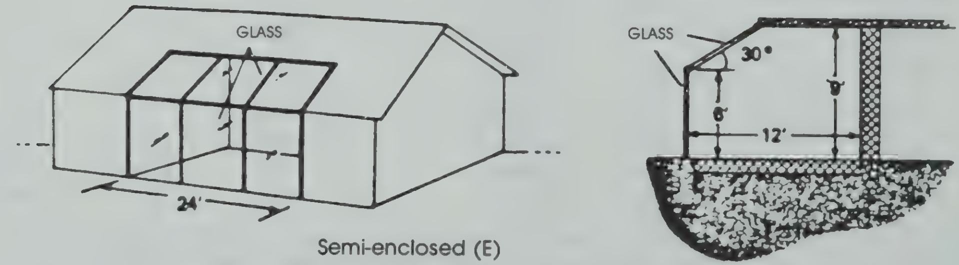

Semi-enclosed (E)

Appendix B: System Identifications (cont.)
SUNSPACE

Designation	Type	Tilt (degrees)	Common Wall	End Walls	Night Insulation
A1	attached	50	masonry	opaque	no
A2	attached	50	masonry	opaque	yes
A3	attached	50	masonry	glazed	no
A4	attached	50	masonry	glazed	yes
A5	attached	50	insulated	opaque	no
A6	attached	50	insulated	opaque	yes
A7	attached	50	insulated	glazed	no
A8	attached	50	insulated	glazed	yes
B1	attached	90/30	masonry	opaque	no
B2	attached	90/30	masonry	opaque	yes
B3	attached	90/30	masonry	glazed	no
B4	attached	90/30	masonry	glazed	yes
B5	attached	90/30	insulated	opaque	no
B6	attached	90/30	insulated	opaque	yes
B7	attached	90/30	insulated	glazed	no
B8	attached	90/30	insulated	glazed	yes
C1	semi-enclosed	90	masonry	common	no
C2	semi-enclosed	90	masonry	common	yes
C3	semi-enclosed	90	insulated	common	no
C4	semi-enclosed	90	insulated	common	yes
D1	semi-enclosed	50	masonry	common	no
D2	semi-enclosed	50	masonry	common	yes
D3	semi-enclosed	50	insulated	common	no
D4	semi-enclosed	50	insulated	common	yes
E1	semi-enclosed	90/30	masonry	common	no
E2	semi-enclosed	90/30	masonry	common	yes
E3	semi-enclosed	90/30	insulated	common	no
E4	semi-enclosed	90/30	insulated	common	yes

All systems are double glazed.

Appendix C: Solar Load Ratio Correlation Constants and SSFs
DIRECT GAIN

	A	B	C	D	R	G	**Metric** G	H	LCR$_S$	**Metric** LCR$_S$	SSF
A1	.5650	1.0090	1.0440	.7175	.3931	9.36	(53.1)	0.00	0.0	0.0	.406
A2	.5906	1.0060	1.0650	.8099	.4681	5.28	(29.9)	0.00	0.0	0.0	.535
A3	.5442	.9715	1.1300	.9273	.7086	2.64	(15.0)	0.00	0.0	0.0	.681
B1	.5739	.9948	1.2510	1.0610	.7905	9.60	(54.5)	0.00	0.0	0.0	.480
B2	.6180	1.0000	1.2760	1.1560	.7528	5.52	(31.3)	0.00	0.0	0.0	.600
B3	.5601	.9839	1.3520	1.1510	.8879	2.38	(13.5)	0.00	0.0	0.0	.731
C1	.6344	.9887	1.5270	1.4380	.8632	9.60	(54.5)	0.00	0.0	0.0	.591
C2	.6763	.9994	1.4000	1.3940	.7604	5.28	(29.9)	0.00	0.0	0.0	.686
C3	.6182	.9859	1.5660	1.4370	.8990	2.40	(13.6)	0.00	0.0	0.0	.802

Solar Savings Fractions (SSF) are for Denver, Colorado; LCR = 20 Btu/ft^2 °F day, T_{base} = 65 °F (in metric, LCR = Wh/m^2 °C day, T_{base} = 18.3 °C). This information is provided primarily to provide a check point so that users can verify that the correlation constants are entered and used correctly.

Appendix C: Solar Load Ratio Correlation Constants and SSFs (cont.)
TROMBE WALL—VENTED & UNVENTED

									Metric	
	A	B	C	D	R	G	H	LCR_S	LCR_S	SSF
A1	0.0000	1.0000	.9194	.4601	-9.0000	0.00	1.11	13.0	73.7	.460
A2	0.0000	1.0000	.9680	.6318	-9.0000	0.00	.92	13.0	73.7	.557
A3	0.0000	1.0000	.9964	.7123	-9.0000	0.00	.85	13.0	73.7	.596
A4	0.0000	1.0000	1.0190	.7332	-9.0000	0.00	.79	13.0	73.7	.608
B1	0.0000	1.0000	.9364	.4777	-9.0000	0.00	1.01	13.0	73.7	.477
B2	0.0000	1.0000	.9821	.6020	-9.0000	0.00	.85	13.0	73.7	.548
B3	0.0000	1.0000	.9980	.6191	-9.0000	0.00	.80	13.0	73.7	.559
B4	0.0000	1.0000	.9981	.5615	-9.0000	0.00	.76	13.0	73.7	.534
C1	0.0000	1.0000	.9558	.4709	-9.0000	0.00	.89	13.0	73.7	.481
C2	0.0000	1.0000	.9788	.4964	-9.0000	0.00	.79	13.0	73.7	.501
C3	0.0000	1.0000	.9760	.4519	-9.0000	0.00	.76	13.0	73.7	.479
C4	0.0000	1.0000	.9588	.3612	-9.0000	0.00	.73	13.0	73.7	.430
D1	0.0000	1.0000	.9842	.4418	-9.0000	0.00	.89	22.0	124.8	.424
D2	0.0000	1.0000	1.0150	.8994	-9.0000	0.00	.80	9.2	52.2	.657
D3	0.0000	1.0000	1.0346	.7810	-9.0000	0.00	1.08	8.9	50.5	.707
D4	0.0000	1.0000	1.0606	.9770	-9.0000	0.00	.85	5.8	32.9	.762
D5	0.0000	1.0000	1.0721	1.0718	-9.0000	0.00	.61	4.5	25.5	.765
E1	0.0000	1.0000	1.0345	.8753	-9.0000	0.00	.68	12.0	68.1	.760
E2	0.0000	1.0000	1.0476	1.0050	-9.0000	0.00	.66	8.7	49.3	.765
E3	0.0000	1.0000	1.0919	1.0739	-9.0000	0.00	.61	5.5	31.2	.855
E4	0.0000	1.0000	1.0971	1.1429	-9.0000	0.00	.47	4.3	24.4	.835
F1	0.0000	1.0000	.9430	.4744	-9.0000	0.00	1.09	13.0	73.7	.458
F2	0.0000	1.0000	.9900	.6053	-9.0000	0.00	.93	13.0	73.7	.532
F3	0.0000	1.0000	1.0189	.6502	-9.0000	0.00	.86	13.0	73.7	.555
F4	0.0000	1.0000	1.0419	.6258	-9.0000	0.00	.80	13.0	73.7	.543
G1	0.0000	1.0000	.9693	.4714	-9.0000	0.00	1.01	13.0	73.7	.455
G2	0.0000	1.0000	1.0133	.5462	-9.0000	0.00	.88	13.0	73.7	.497
G3	0.0000	1.0000	1.0325	.5269	-9.0000	0.00	.82	13.0	73.7	.487
G4	0.0000	1.0000	1.0401	.4400	-9.0000	0.00	.77	13.0	73.7	.435
H1	0.0000	1.0000	1.0002	.4356	-9.0000	0.00	.93	13.0	73.7	.428
H2	0.0000	1.0000	1.0280	.4151	-9.0000	0.00	.83	13.0	73.7	.414
H3	0.0000	1.0000	1.0327	.3522	-9.0000	0.00	.78	13.0	73.7	.372
H4	0.0000	1.0000	1.0287	.2600	-9.0000	0.00	.74	13.0	73.7	.300
I1	0.0000	1.0000	.9974	.4036	-9.0000	0.00	.91	22.0	124.8	.387
I2	0.0000	1.0000	1.0386	.8313	-9.0000	0.00	.80	9.2	52.2	.622
I3	0.0000	1.0000	1.0514	.6886	-9.0000	0.00	1.01	8.9	50.5	.666
I4	0.0000	1.0000	1.0781	.8952	-9.0000	0.00	.82	5.8	32.9	.731
I5	0.0000	1.0000	1.0902	1.0284	-9.0000	0.00	.65	4.5	25.5	.745
J1	0.0000	1.0000	1.0537	.8228	-9.0000	0.00	.65	12.0	68.1	.739
J2	0.0000	1.0000	1.0677	.9313	-9.0000	0.00	.62	8.7	49.3	.739
J3	0.0000	1.0000	1.1153	.9831	-9.0000	0.00	.44	5.5	31.2	.834
J4	0.0000	1.0000	1.1154	1.0607	-9.0000	0.00	.38	4.3	24.4	.813

Solar Savings Fractions (SSF) are for Denver, Colorado; LCR = 20 Btu/ft^2 °F day, T_{base} = 65 °F (in metric, LCR = Wh/m^2 °C day, T_{base} = 18.3 °C). This information is provided primarily to provide a check point so that users can verify that the correlation constants are entered and used correctly.

Appendix C: Solar Load Ratio Correlation Constants and SSFs (cont.)

WATER WALL

									Metric	
	A	B	C	D	R	G	H	LCR_S	LCR_S	SSF
A1	0.0000	1.0000	.9172	.4841	-9.0000	0.00	1.17	13.0	73.7	.465
A2	0.0000	1.0000	.9833	.7603	-9.0000	0.00	.92	13.0	73.7	.609
A3	0.0000	1.0000	1.0171	.8852	-9.0000	0.00	.85	13.0	73.7	.660
A4	0.0000	1.0000	1.0395	.9570	-9.0000	0.00	.81	13.0	73.7	.687
A5	0.0000	1.0000	1.0604	1.0387	-9.0000	0.00	.78	13.0	73.7	.714
A6	0.0000	1.0000	1.0735	1.0827	-9.0000	0.00	.76	13.0	73.7	.728
B1	0.0000	1.0000	.9754	.5518	-9.0000	0.00	.92	22.0	124.8	.481
B2	0.0000	1.0000	1.0487	1.0851	-9.0000	0.00	.78	9.2	52.2	.713
B3	0.0000	1.0000	1.0673	1.0087	-9.0000	0.00	.95	8.9	50.5	.794
B4	0.0000	1.0000	1.1028	1.1811	-9.0000	0.00	.74	5.8	32.9	.821
B5	0.0000	1.0000	1.1146	1.2771	-9.0000	0.00	.56	4.5	25.5	.816
C1	0.0000	1.0000	1.0667	1.0437	-9.0000	0.00	.62	12.0	68.1	.815
C2	0.0000	1.0000	1.0846	1.1482	-9.0000	0.00	.59	8.7	49.3	.806
C3	0.0000	1.0000	1.1419	1.1756	-9.0000	0.00	.28	5.5	31.2	.885
C4	0.0000	1.0000	1.1401	1.2378	-9.0000	0.00	.23	4.3	24.4	.860

SUNSPACE

									Metric	
	A	B	C	D	R	G	H	LCR_S	LCR_S	SSF
A1	0.0000	1.0000	.9587	.4770	-9.0000	0.00	.83	18.6	105.5	.628
A2	0.0000	1.0000	.9982	.6614	-9.0000	0.00	.77	10.4	59.0	.774
A3	0.0000	1.0000	.9552	.4230	-9.0000	0.00	.83	23.6	133.9	.574
A4	0.0000	1.0000	.9956	.6277	-9.0000	0.00	.80	12.4	70.3	.757
A5	0.0000	1.0000	.9300	.4041	-9.0000	0.00	.96	18.6	105.5	.572
A6	0.0000	1.0000	.9981	.6660	-9.0000	0.00	.86	10.4	59.0	.769
A7	0.0000	1.0000	.9219	.3225	-9.0000	0.00	.96	23.6	133.9	.494
A8	0.0000	1.0000	.9922	.6173	-9.0000	0.00	.90	12.4	70.3	.743
B1	0.0000	1.0000	.9683	.4954	-9.0000	0.00	.84	16.3	92.5	.562
B2	0.0000	1.0000	1.0029	.6802	-9.0000	0.00	.74	8.5	48.2	.723
B3	0.0000	1.0000	.9689	.4685	-9.0000	0.00	.82	19.3	109.5	.525
B4	0.0000	1.0000	1.0029	.6641	-9.0000	0.00	.76	9.7	55.0	.706
B5	0.0000	1.0000	.9408	.3866	-9.0000	0.00	.97	16.3	92.5	.485
B6	0.0000	1.0000	1.0068	.6778	-9.0000	0.00	.84	8.5	48.2	.712
B7	0.0000	1.0000	.9395	.3363	-9.0000	0.00	.95	19.3	109.5	.430
B8	0.0000	1.0000	1.0047	.6469	-9.0000	0.00	.87	9.7	55.0	.687
C1	0.0000	1.0000	1.0087	.7683	-9.0000	0.00	.76	16.3	92.5	.593
C2	0.0000	1.0000	1.0412	.9281	-9.0000	0.00	.78	10.0	56.7	.713
C3	0.0000	1.0000	.9699	.5106	-9.0000	0.00	.79	16.3	92.5	.478
C4	0.0000	1.0000	1.0152	.7523	-9.0000	0.00	.81	10.0	56.7	.646
D1	0.0000	1.0000	.9889	.6643	-9.0000	0.00	.84	17.8	101.0	.727
D2	0.0000	1.0000	1.0493	.8753	-9.0000	0.00	.70	9.9	56.2	.853
D3	0.0000	1.0000	.9570	.5285	-9.0000	0.00	.90	17.8	101.0	.660
D4	0.0000	1.0000	1.0356	.8142	-9.0000	0.00	.73	9.9	56.2	.835
E1	0.0000	1.0000	.9968	.7004	-9.0000	0.00	.77	19.6	111.2	.659
E2	0.0000	1.0000	1.0468	.9054	-9.0000	0.00	.76	10.8	61.3	.797
E3	0.0000	1.0000	.9565	.4827	-9.0000	0.00	.81	19.6	111.2	.556
E4	0.0000	1.0000	1.0214	.7694	-9.0000	0.00	.79	10.8	61.3	.751

Solar Savings Fractions (SSF) are for Denver, Colorado; LCR = 20 Btu/ft² °F day, T_{base} = 65 °F (in metric, LCR = Wh/m² °C day, T_{base} = 18.3 °C). This information is provided primarily to provide a check point so that users can verify that the correlation constants are entered and used correctly.

Appendix D: Solar Absorptance Factors for the Reference Designs

		Ratio of absorbed/transmitted
Direct gain system with	mass-area-to-glazing-area ratio = 3,	0.948
	mass-area-to-glazing-area ratio = 6,	0.976
Trombe wall and water wall systems with	single glazing,	0.957
	double glazing,	0.962
	triple glazing,	0.964

Trombe wall and water wall ratios are based on surface absorptance = 0.95

Appendix E: General Solar Radiation Correlations

Coefficients for Transmitted/Incident Equations of Form:

$$T/I = B_1 + B_2Y + B_3Y^2 + K_T(B_4 + B_5Y + B_6Y^2)$$

Where $Y = (LAT - DEC)/100$

1 Glazing

TILT	AZIM	B_1	B_2	B_3	B_4	B_5	B_6
0	0	0.7646	0.2637	-0.4133	0.0640	-0.1718	-0.0349
30	0	0.7766	0.1372	-0.1614	0.0442	-0.1075	0.1715
30	30	0.7766	0.1334	-0.1689	0.0473	-0.0989	0.1389
30	60	0.7731	0.1413	-0.2101	0.0577	-0.1078	0.1027
30	90	0.7729	0.1342	-0.2378	0.0525	-0.0396	-0.0952
60	0	0.7735	0.0970	-0.0568	-0.0354	0.2104	-0.1189
60	30	0.7761	0.0713	-0.0414	-0.0032	0.1268	-0.0821
60	60	0.7754	0.0620	-0.0796	0.0343	0.0210	-0.0121
60	90	0.7722	0.0742	-0.1474	0.0394	0.0218	-0.0850
90	0	See Subsequent Table					
90	30	See Subsequent Table					
90	60	0.7728	0.0154	-0.0251	-0.0136	0.1710	-0.1321
90	90	0.7728	0.0087	-0.0350	0.0117	0.1094	-0.2094

2 Glazings

TILT	AZIM	B_1	B_2	B_3	B_4	B_5	B_6
0	0	0.6331	0.3094	-0.4862	0.0759	-0.2092	-0.0221
30	0	0.6471	0.1596	-0.1862	0.0521	-0.1214	0.1884
30	30	0.6476	0.1537	-0.1945	0.0551	-0.1094	0.1525
30	60	0.6434	0.1643	-0.2449	0.0678	-0.1264	0.1220
30	90	0.6432	0.1565	-0.2766	0.0624	-0.0531	-0.0966
60	0	0.6429	0.1186	-0.0727	-0.0375	0.2257	-0.1159
60	30	0.6467	0.0844	-0.0496	-0.0026	0.1454	-0.0947
60	60	0.6456	0.0763	-0.0971	0.0404	0.0263	-0.0153
60	90	0.6450	0.0672	-0.1409	0.0436	0.0516	-0.1418
90	0	See Subsequent Table					
90	30	See Subsequent Table					
90	60	0.6436	0.0174	-0.0275	-0.0148	0.1946	-0.1459
90	90	0.6431	0.0115	-0.0392	0.0156	0.1215	-0.2342

Continued on next page

3 Glazings

TILT	AZIM	B_1	B_2	B_3	B_4	B_5	B_6
0	0	0.5397	0.3355	-0.5234	0.0766	-0.2504	0.0516
30	0	0.5594	0.1422	-0.1649	0.0454	-0.0998	0.1580
30	30	0.5600	0.1357	-0.1718	0.0482	-0.0876	0.1230
30	60	0.5553	0.1503	-0.2254	0.0617	-0.1137	0.1081
30	90	0.5520	0.1665	-0.2900	0.0610	-0.0796	-0.0454
60	0	0.5542	0.1125	-0.0709	-0.0366	0.2092	-0.1014
60	30	0.5582	0.0776	-0.0455	-0.0038	0.1365	-0.0882
60	60	0.5571	0.0699	-0.0903	0.0356	0.0319	-0.0234
60	90	0.5568	0.0590	-0.1280	0.0389	0.0547	-0.1440
90	0	See Subsequent Table					
90	30	See Subsequent Table					
90	60	0.5553	0.0134	-0.0238	-0.0155	0.1853	-0.1405
90	90	0.5549	0.0084	-0.0344	0.0126	0.1205	-0.2304

Coefficients for Transmitted/Incident Equations of Form:

$$T/I = B_1 + B_2Y + B_3Y^2 + B_4Y^3 + B_5Y^4 + B_6Y^5 + K_T(B_7 + B_8Y + B_9Y^2 + B_{10}Y^3 + B_{11}Y^4 + B_{12}Y^5)$$

Where $Y = (LAT - DEC)/100$

1 Glazing

TILT	AZIM	B_1	B_2	B_3	B_4	B_5	B_6
		B_7	B_8	B_9	B_{10}	B_{11}	B_{12}
90	0	0.7899	0.5388	-5.868	19.912	-26.876	12.777
		0.0098	-3.5791	24.622	-63.976	74.729	-32.865
90	30	0.8130	0.0561	-3.151	13.473	-20.389	10.529
		-0.1433	-0.3334	8.718	-30.567	41.434	-19.727

2 Glazings

TILT	AZIM	B_1	B_2	B_3	B_4	B_5	B_6
		B_7	B_8	B_9	B_{10}	B_{11}	B_{12}
90	0	0.6465	0.7766	-7.157	22.771	-29.310	13.294
		0.0523	-4.2457	26.952	-65.486	71.106	-28.793
90	30	0.6863	0.1325	-4.078	16.838	-25.266	13.027
		-0.1539	-0.5816	11.321	-38.883	52.567	-25.112

3 Glazings

TILT	AZIM	B_1	B_2	B_3	B_4	B_5	B_6
		B_7	B_8	B_9	B_{10}	B_{11}	B_{12}
90	0	0.5497	0.8103	-6.904	21.070	-26.118	11.345
		0.0730	-4.2675	25.534	-58.122	57.904	-20.849
90	30	0.5967	0.1515	-4.225	17.334	-26.076	13.513
		-0.1504	-0.7208	12.499	-42.924	58.527	-28.285

Appendix E: General Solar Radiation Correlations (cont.)

Coefficients for Incident/Horizontal Equations of Form:

$$I/Q_h = B_1 + B_2Y + B_3Y^2 + K_T(B_4 + B_5Y + B_6Y^2)$$

Where $Y = (LAT - DEC)/100$

TILT	AZIM	B_1	B_2	B_3	B_4	B_5	B_6
30	0	0.9786	-0.1895	0.4573	-0.0918	0.1596	2.5034
30	30	0.9935	-0.2581	0.4834	-0.1134	0.3354	1.9329
30	60	0.9937	-0.2691	0.3902	-0.1155	0.4634	0.8290
30	90	0.9959	-0.3156	0.3208	-0.1217	0.5485	-0.4429
60	0	0.8682	-0.4587	0.9788	-0.2817	0.4051	4.0989
60	30	0.8850	-0.5729	1.0557	-0.2689	0.6560	3.0255
60	60	0.8749	-0.5617	0.8552	-0.2151	0.9028	1.0646
60	90	0.8710	-0.5943	0.7018	-0.1966	1.0178	-0.7940
90	0	0.6866	-0.6623	1.3269	-0.4458	0.3090	4.7776
90	30	0.7183	-0.8937	1.5666	-0.3680	0.6415	3.2484
90	60	0.7203	-0.9037	1.3357	-0.2920	1.2595	0.5969
90	90	0.6749	-0.6051	0.7595	-0.1959	1.0720	-0.7838

Appendix F: Solar Radiation Correlation Coefficients for the Reference Designs

transmitted/horizontal

$$TRANS/QH = B_1 + B_2 \cdot Y + B_3 \cdot Y^2 + K_T(B_4 + B_5 \cdot Y + B_6 \cdot Y^2)$$

TYPE	B_1	B_2	B_3	B_4	B_5	B_6
WW, TW, DG - 1 GL	0.5136	-0.4020	0.9059	-0.3306	-0.3787	5.1344
WW, TW, DG - 2 GL	0.4146	-0.2847	0.7160	-0.2817	-0.4251	4.5913
WW, TW, DG - 3 GL	0.3484	-0.1610	0.4980	-0.2049	-0.6715	4.4288

absorbed/horizontal

$$S/QH = B_1 + B_2 \cdot Y + B_3 \cdot Y^2 + K_T(B_4 + B_5 \cdot Y + B_6 \cdot Y^2)$$

TYPE	B_1	B_2	B_3	B_4	B_5	B_6
SS - A1, 2, 5, 6	0.72008	-0.15181	0.49973	-0.15039	0.14384	3.6374
SS - A3, 4, 7, 8	0.81554	-0.23988	0.60252	-0.16445	0.33730	3.1695
SS - B1, 2, 5, 6	0.58932	-0.09693	0.38955	-0.14699	-0.39149	3.9171
SS - B3, 4, 7, 8	0.62569	-0.13941	0.43331	-0.14982	-0.26401	3.5685
SS - C1, 2, 3, 4	0.39436	-0.21103	0.58815	-0.24083	-0.60746	4.6546
SS - D1, 2, 3, 4	0.73147	-0.15418	0.50763	-0.15276	0.14608	3.6950
SS - E1, 2, 3, 4	0.61661	-0.10127	0.40733	-0.15367	-0.40940	4.0969

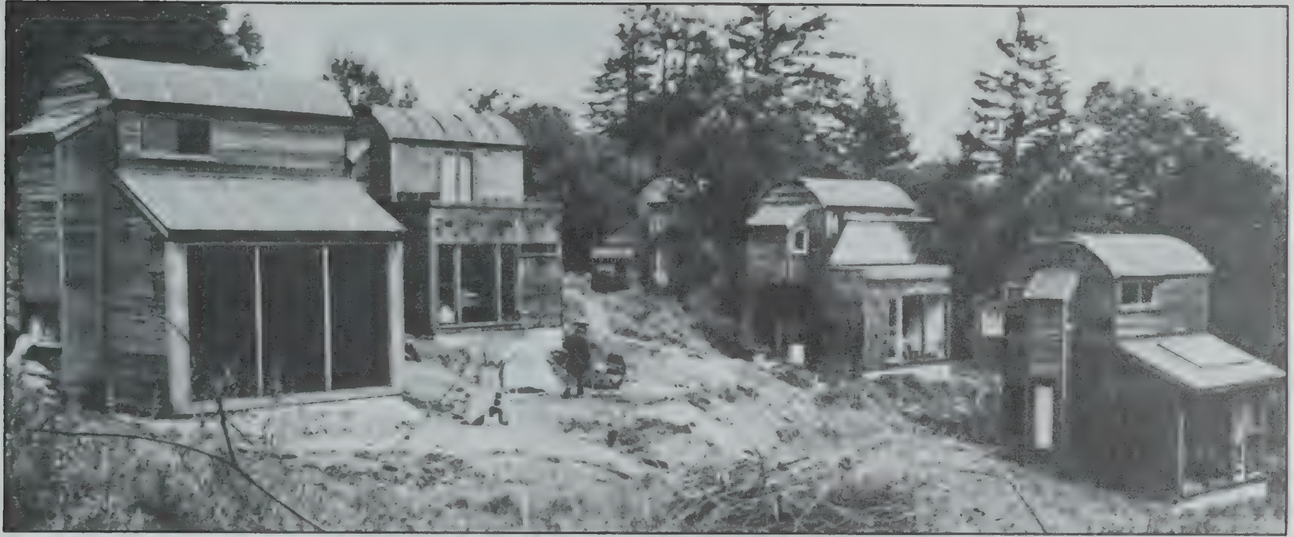

Photo: Suzan Brower

Figure 1: Test buildings at the Farallones Institute in California eventually became shelters for guests.

Passive Solar Test Modules

A Definition and Survey of the Canadian and American Experience

By FULLER MOORE
Department of Architecture, Miami University, Oxford, Ohio, 45056

ABSTRACT

This report reviews the use of test boxes, rooms and buildings for passive solar research in the United States and Canada. In addition to presenting a thorough survey, this report provides an introductory guide to experimental methods in passive solar heating for researchers who have limited familiarity with test-module design. The experimental uses and physical characteristics of test modules are discussed and existing facilities are described.

INTRODUCTION

Physical test modules have been useful for research in passive solar heating of buildings. These test modules range in size and sophistication from small insulated test boxes to rooms and full-scale multi-room buildings. The principal advantages of test modules are that their cost is low (compared to full-scale testing of occupied buildings) and that data can be taken under carefully controlled conditions.

Harold Hay used small-scale insulated test boxes in early experiments to prove the concept of his "Skytherm" system. Using a foam box filled with water, Hay removed the lid to receive sunlight during the day and replaced the lid at night to reduce heat loss. The measured increase in water temperature demonstrated the heating potential of the system. By covering the box during the day and uncovering at night, the cooling potential was similarly demonstrated.[1]

Since 1975 the Solar Energy Group at Los Alamos National Laboratory (L.A.N.L.) has used small boxes for comparative testing and to validate computer simulations. These studies have led to field-testable thermal models of multi-zone buildings.[2, 3]

Test rooms, typically full scale in height, permit the observation of vertical convection effects that approximate those of actual buildings. This advantage, coupled with easier interior access and dimensional similarity to actual buildings, accounts for the extensive use of test rooms in passive solar research. Well insulated, of wood frame construction, approximately 9 ft. high by 5 ft. wide by 8 ft. deep *(2.7 by 1.5 by 2.4 m.)*, with south vertical glazing and minimum permanent internal mass, such

---

The author worked on this survey while he was a guest scientist at Los Alamos National Laboratory. The work was performed under the auspices of the Office of Solar Heat Technologies of the U.S. Department of Energy and supported by Miami University.

©Passive Solar Journal 0277-6456/82/0102-0091$3.00/0

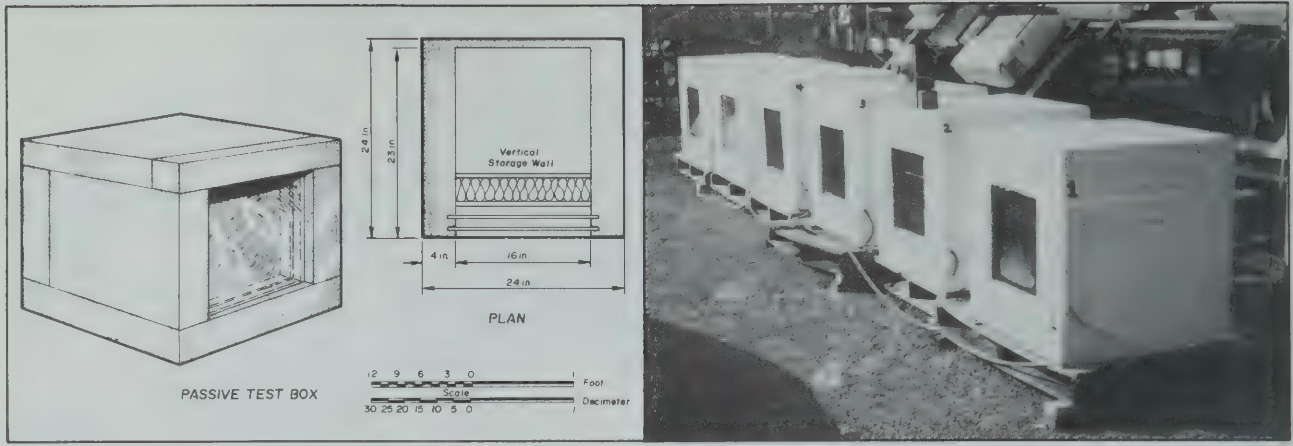

Drawing source: L.A.N.L.

Figure 2: The Los Alamos test boxes are designed as thermal models, and do not duplicate conventional building techniques. Their construction and placement allow air to circulate freely to all exterior surfaces.

rooms have been used extensively for passive heating research at Los Alamos,[4] the National Center for Appropriate Technology (N.C.A.T.),[5] University of Nebraska,[6] and the Solar Energy Research Institute (S.E.R.I.).[7]

Test buildings (as the term is used in this study) are similar in size and construction to actual buildings, but are designed and constructed for test purposes only and not intended for occupancy. Such buildings offer the opportunity for multizone testing as well as direct analogy to actual building performance. Installations include those at Trinity University,[8] the Solar Energy Analysis Laboratory[9] and the Environmental Research Laboratory at Tucson, Arizona.[10] Monitored buildings that were designed for concurrent occupancy are beyond the scope of this study.

Test modules can be used to accomplish a variety of experimental objectives. Small, simple modules can be used for proof-of-concept demonstration and operational testing (i.e., "Does this work?"). Comparative testing of components or systems involve matched test modules (i.e., "Which works best?"). Single test modules can be used to empirically measure heat transfer values for entire systems (i.e., "Why does this perform as it does?"). Test modules can be used for computer model validation (i.e., "How well can a computer simulate the measured conditions of a test module, given similar weather data as input?"). Finally, test modules can be used as direct physical analogs of actual buildings (i.e., "How will an actual building perform in terms of comfort and auxiliary energy usage?").

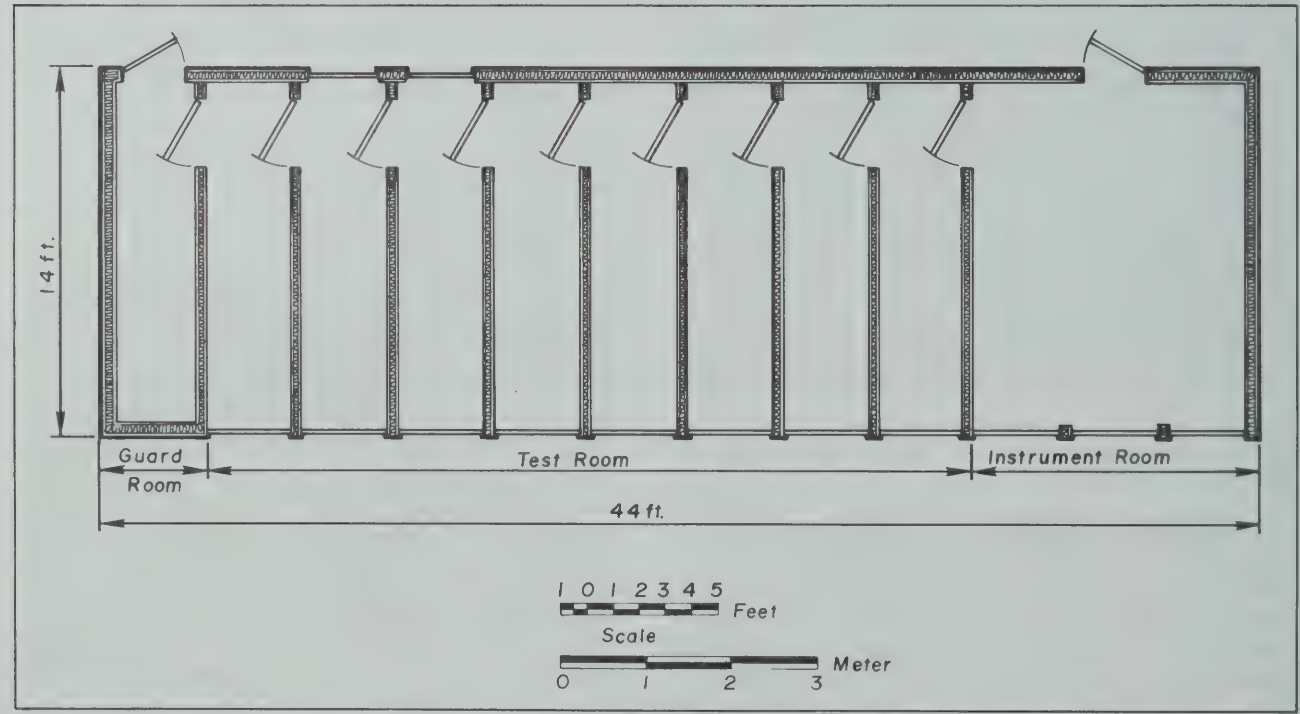

Figure 3: These reconfigurable test rooms at M.I.T. were designed to keep heat transfer between rooms to a minimum. North wall insulation is variable to permit adjustment of thermal load.

TEST MODULE TYPES AND EXAMPLES

Boxes

Test boxes are used primarily for comparative testing where convective flow is not a parameter. Because the principal concern is thermal similarity between competing boxes, the boxes are typically constructed of foam insulation with removable glazing. The ratio of heat loss to collector area should be similar to that of a passive building. The result is a thick-walled box with little similarity in appearance to a scale building model.

Grimmer[3] has described the use of cubic test boxes, 24 in. *(60 cm.)* on a side, at Los Alamos for direct comparison with each other as well as for normalized, indirect comparison with test rooms. (See Fig. 2).

Grimmer[2] has examined theoretically and with computer modeling the use of small test boxes to represent multi-room passive solar designs. His discussion includes realistically massive walls, thermocirculation, infiltration effects, edge-effect corrections, and microclimate shading effects in terms of how each responds to dimensional analysis and scaling.

Morris[11] has described the use of four natural air convection test boxes (two tilted, two vertical) with integral water thermal storage. Approximately 24 in. wide by 36 in. deep by 72 in. high *(60 by 90 by 180 cm.)*, these boxes were used to compare directly the performance of four convective systems.

Rooms

Test rooms usually have the following physical characteristics:

- full-scale height, reduced-scale width and depth
- permanent construction deliberately of low mass
- ratio of heat loss to collection area similar to that of actual passive buildings
- reconfigurable solar aperture size, tilt and glazzing
- reconfigurable thermal mass
- continuously monitored or constant infiltration rate.

One of the earliest examples of the use of test rooms for passive solar research was the Massachusetts Institute of Technology (M.I.T.) facility described by Dietz and Czapek[12] and Hollingsworth.[13] Constructed in 1947 in Cambridge, Massachusetts, the single structure housed six reconfigurable test rooms, a direct gain low mass room for a control, and an instrument room. The rooms were vertically glazed, measured 6 ft. by 14 ft. *(1.8 by 4.2 m.)* and featured a reconfigurable *north* wall to permit adjustment of heat loss, along with auxiliary heat, movable insulation, and a variety of reconfigurable water storage walls. (See Fig. 3.)

In 1967, a test room was constructed by Harold Hay and John Yellott to investigate roof pond cooling and heating. The 10-by-12 ft. *(3 by 3.6 m.)* structure was constructed in Phoenix, Arizona, and heavily instrumented for monitoring during 1967-1968.[1] (See Fig. 4.)

At Los Alamos National Laboratory, a total of 14 test rooms are being used primarily for validation of the PAssive SOLar Energy (PASOLE) simulation code developed at L.A.N.L. by McFarland. They are also used for comparison testing and heat transfer measurements.[14] Each of seven test structures contains two south-facing, single-zone rooms separated by an insulated partition. In addition to fiberglass insulation in the wood-frame construction, each interior is completely lined with 1 in. *(2.5 cm.)* of extruded polystyrene foam insulation to minimize the effect of the mass of the test cell itself. The thermal load can be varied by changing the rate of fan-forced infiltration that is controlled by a damper and measured periodically using an ASTM-type calibrated nozzle. The accuracy of this measurement has been validated using SF^6 tracer-gas tests. Because the interiors are maintained under positive pressure, the effects of temperature difference and wind speed on the infiltration rate are small. (See Fig. 5.)

When required, auxiliary heat is added using incandescent light bulbs. These are controlled by the same computer used to monitor and record data. Auxiliary power is monitored by a relay-controlled on/off status sensor connected to the computer. It is calculated from a one-time measurement of electrical consumption of typical bulbs.

A pair of rooms (virtually identical to those at Los Alamos) has been constructed and operated at both the National Center for Appropriate Technology (N.C.A.T.), Butte, Montana,[5] and at the University of Pennsýlvania, Philadelphia, Pennsylvania.[15] In addition, two retrofit, two attached greenhouse and two detached greenhouse test rooms have been constructed at N.C.A.T.

An extensive test-module program is being conducted at S.E.R.I.[7] The program includes two test boxes, 10 test rooms, and one proposed test building. The test boxes are cubes measuring 3 ft. 4 in. *(1 m.)* with 4-in.- *(10-cm.-)* thick expanded polysytrene foam sides. One side is glazed and one side is a black-coated, copper radiation plate with re-

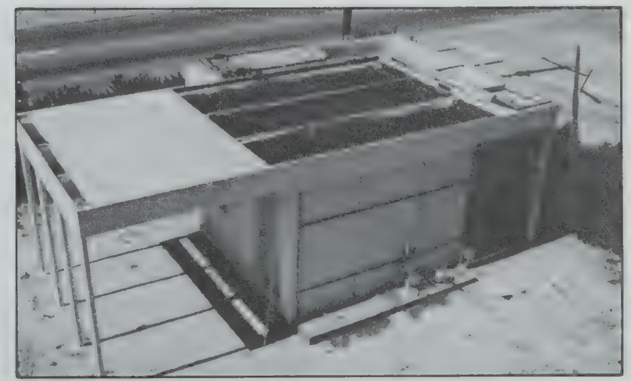

Photo: J.I. Yellott

Figure 4: The roof pond test room of Hay and Yellott in Phoenix, Arizona, used insulation that could be moved manually. Data were also manually collected and reduced.

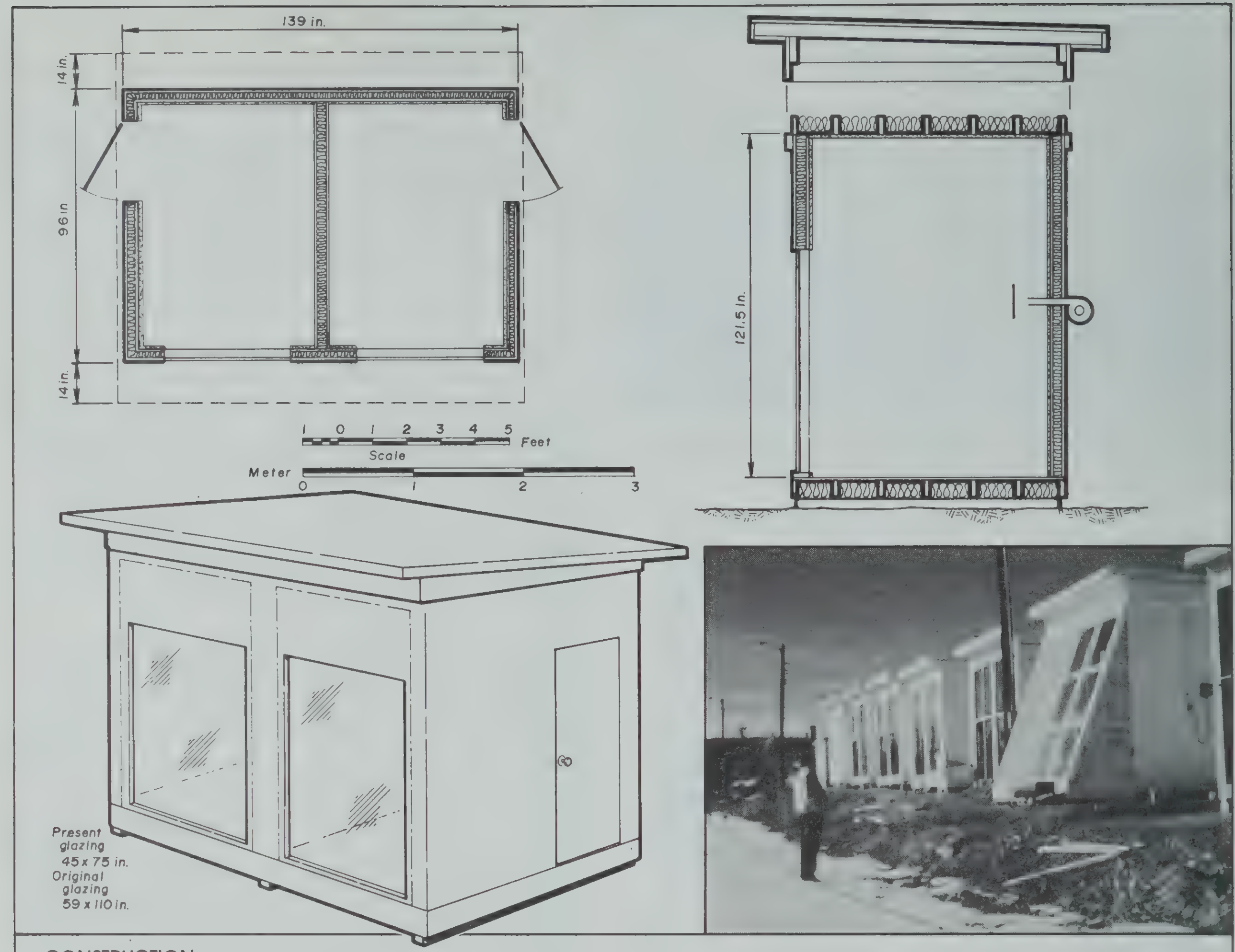

CONSTRUCTION:

Removable roof:	Ceiling:	Walls:	Floor:
90 lb. rolled roofing 2 x 4 rafters 16 in. on center	2 x 4 joists 16 in. on center 26 ga. corrugated metal 7 in. fiberglass insulation 1 in. extruded polystyrene foam	⅝ in. plywood (painted white) 2 x 4 studs 16 in. on center 3.5 in. fiberglass insulation 1 in. extruded polystyrene foam forced infiltration fan with deflector	⅝ in. plywood 2 x 6 joists 16 in. on center 7 in. fiberglass insulation ¼ in. plywood 4 x 4 sleepers

Photo: L.A.N.L.

Figure 5: The impact of data derived from the Los Alamos test rooms makes them among the most influential of passive solar facilities. Each of the seven test structures is divided into two single-zone rooms.

movable insulation (allowing the use of radiative cooling for varying thermal load). The boxes are used for preliminary experiments before employing the test rooms.

The ten S.E.R.I. rooms are configured in pairs (similar to the earlier Los Alamos rooms) for a total of five structures. The units are 10 ft. by 12 ft. *(3 by 3.6 m.)* and completely reconfigurable (suitable for two zones) as well as portable. Fixed mass and infiltration are minimized and auxiliary heat is available in the form of monitored, portable, electric resistance heaters. They are principally used for comparison testing and computer code validation. (See Fig. 6.)

The proposed test building is designed like a conventional, frame construction house, to be installed at the site. The unoccupied structure will be reconfigurable and tested as five systems (control, waterwall, waterwall/greenhouse, low mass/greenhouse, air convection). The building will be used for thermal equilibrium co-heating experiments as well as for code validation. The S.E.R.I. data acquisition system is very extensive (currently 1700 channels with expansion capability to 3000), including 80 heat flux transducers.

Chen[6] has described the six passive solar test rooms constructed at the University of Nebraska. (See Fig. 7). The modules are used to directly com-

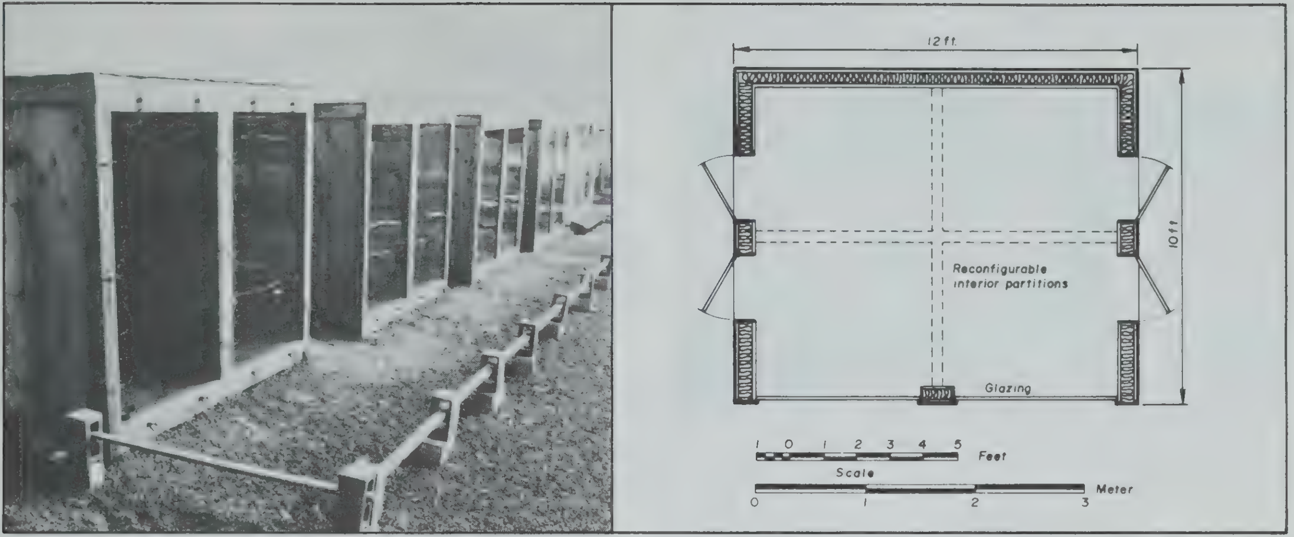

Photo: S.E.R.I.

Figure 6: The Solar Energy Research Institute's test rooms at Golden, Colorado, are built with reconfigurable interior partitions to permit two-zone experiments.

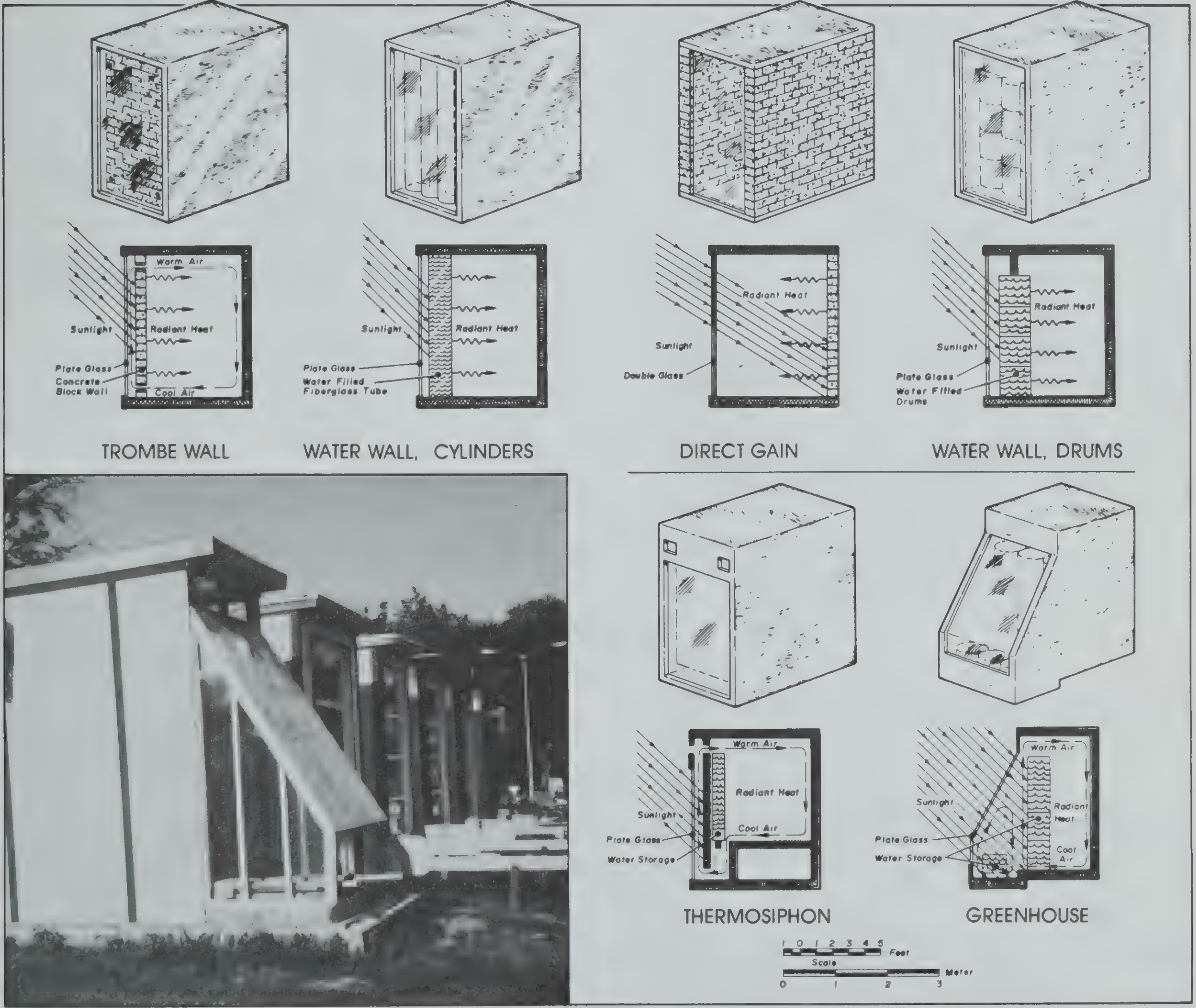

Photo: J.D. Balcomb Drawing source: U. of N.

Figure 7: Rooms at the University of Nebraska can be used to test passive cooling as well as heating. The six modules and their instrumentation were constructed by undergraduate students, with emphasis on the economical acquisition of reliable test data.

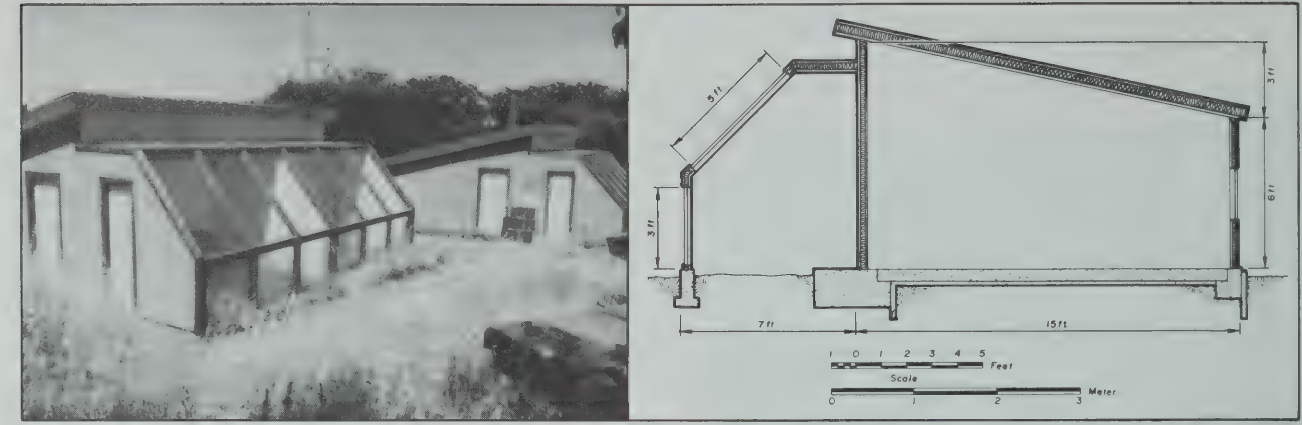

Photo and drawing source: Habitat Center

Figure 8: The four test rooms of Habitat Center in Walnut Creek, California, are contained in two buildings devoted entirely to testing retrofit sunspaces. Their construction is typical of northern California housing.

pare direct gain, Trombe wall, waterwall, double envelope, earth sheltered, greenhouse, and direct gain/ceiling systems. They are also used to validate the Princeton Circuit Analysis Program (P.C.A.P.) developed at Princeton Univerity.[16] This sophisticated and rigorous U. of N. research program is being accomplished almost completely by undergraduate students under faculty direction. The test rooms were constructed by building construction students; the instrumentation and data acquisition system were designed, constructed and installed by electrical engineering and physics students; signage and demonstration graphics were executed by graphic design students; and materials were donated by local sources. The program is considered exemplary not only as an integrated, test room research program, but also as a successful example of the fulfillment of diverse undergraduate educational objectives through a research effort.

Four test rooms were constructed by the Habitat Center, Walnut Creek, California, to compare indirectly the performance of retrofit greenhouses. The units were configured to include a "dwelling" room with an attached greenhouse. Each of the two buildings measured 26 ft. wide by 22 ft. deep by 9 ft. high *(7.8 by 6.6 by 2.7 m.)* and contained two adjacent test units separated by an insulated wall. One unit served as the control, while the common walls (between the greenhouse and dwelling) were varied in the other three during the various test periods. No auxiliary heat was used during the tests.[17] (See Fig. 8.)

Morris[18] has described a pair of natural convection collector test modules constructed at Los Alamos. The unit is reconfigurable, capable of varying collector height, collector tilt, air-flow channel depth, glazing type, absorber type, heat transfer to simulated storage, air-flow resistance, pressure drop through storage, and operating temperature of the collector system. (See Fig. 9.)

Eleven passive greenhouse test modules (four

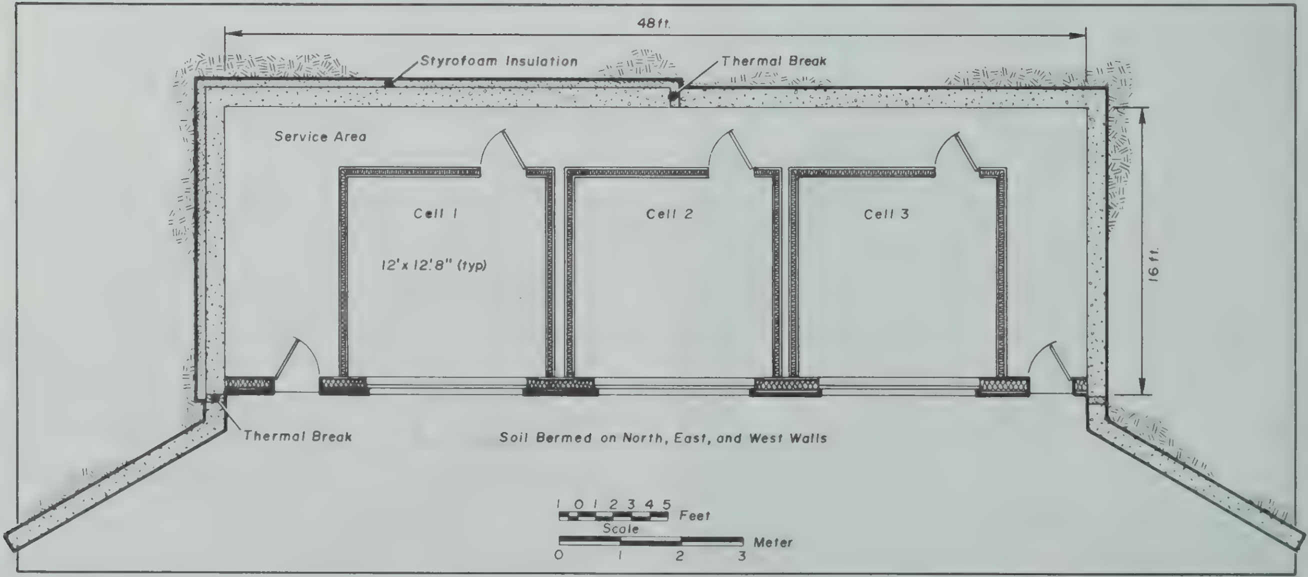

Drawing source: Ames Laboratory

Figure 10: Ames Laboratory at Iowa State University uses rooms to test its own passive designs, such as the water wall it has patented. The rooms are earth-sheltered and insulated by work spaces on three sides, providing for control of the test environment.

Addresses for Test Module Facilities in the United States and Canada

A. Harold Hay, Skytherm Processes & Engineering, 2424 Wilshire Blvd., Los Angeles, California 90057 (J. Yellott, Phoenix, Arizona)

B. Environmental Research Laboratory, Tucson International Airport, Tucson, Arizona 85706 (J. Peck)

C. Pacific Gas & Electric, Department of Engineering Research, San Ramon, California 94583 (H. Seilstad)

D. Farallones Institute, Sonoma County, California (P. Calthorpe, 55c Gate 5 Rd., Sausalito, California 94965)

E. Solar Energy Analysis Laboratory, San Diego County, California (J. Clinton, 4325 Donald, San Diego, California 92117)

F. Habitat Center, 2293 Olympic Blvd., Walnut Creek, California 94595 (M. Martin)

G. Solar Energy Research Laboratory, 15/3, 1617 Cole Blvd., Golden, Colorado 80401 (K. Harr)

H. Massachusetts Institute of Technology, Department of Building Engineering Construction, Cambridge, Massachusetts (F. Hollingsworth)

I. National Center for Appropriate Technology, R/D Branch, P.O. Box 3838, Butte, Montana 59701 (L. Palmiter)

J. University of Nebraska, Department of Electronics and Engineering Technology, 60th & Dodge, Omaha, Nebraska 86182 (B. Chen)

K. Florida Solar Energy Center, 300 State Road 401, Cape Canaveral, Florida 32920 (P. Fairey)

L. Los Alamos National Laboratory, P.O. Box 1663, M/S 571, Los Alamos, New Mexico 87545

L-1. L.A.N.L. (D. Balcomb, rooms)
L-2. L.A.N.L. (D. Grimmer, boxes)
L-3. L.A.N.L. (S. Morris, convective collector)

M. Solar Room Company, Taos, New Mexico 87541 (S. Kenin)

N. Wessling Consulting, Albuquerque, New Mexico (F. Wessling, Tennesee Valley Authority, Solar Applications, Chattanooga, Tennessee)

O. Scott Morris, P.O. Box 4815, Santa Fe, New Mexico 87501

P. Ghost Ranch, Abiquiu, New Mexico (B. Rogers, Embudo, New Mexico 87531)

Q. Purdue University, College of Architecture, W. Lafayette, Indiana 47907.

R. Ames Laboratory, Iowa State University, Ames, Iowa 50011 (R. Mercer)

S. Waterwall Engineering, New Paris, Ohio (F. Moore, 118 Beachpoint, Oxford, Ohio 45056)

T. Pennsylvania State University, Department of Agricultural Engineering, State College, Pennsylvania (J. White)

U. University of Pennsylvania, Department of Architecture, Philadelphia, Pennsylvania (D. Prowler)

V. Tennessee Valley Authority, Solar Applications Division, 340 Credit Union Building, Chattanooga, Tennessee (D. Kuberg)

W. Trinity University, Department of Engineering Science, 715 Stadium Drive, San Antonio, Texas 78284 (G. Clark)

X. University of Alberta, Department of Mechanical Engineering, Edmonton, Alberta, Canada (R. Gilpin)

Y. Lakehead University, Department of Physics, Thunder Bay, Ontario, Canada (R. Jones)

Table 2: Addresses for test module facilities include the reporting author or contact person at the time of this report.

United States and Canada

ue	of, R-value	Attached greenhouses	Glazing area, ft²	Reconfigurable mass	Reconfigurable glazing	Reconfigurable partitions	Auxiliary heat type Electric Resistance or Fan Coil	Auxiliary heat control Data acquisition system or Thermostat	Infiltration Forced or Minimized	Reference	Remarks
			120				FC	T	M	1	roof pond
			104		Y				M	10	coding experiments
			64	Y			ER	D	M	28	
			V						M	37	occupied during testing
		1	V				FC	D	M	9	two zone; scheduled to close Jan. '84.
		4	117	Y					M	17	
			40	Y	Y	Y	ER	T	M	7	test boxes approx. 4 ft./side
			32	Y	Y	Y	ER	T	M	12	variable north wall insulation
		2	35	Y	Y		ER	T	M	5	plus 2 retrofit, 2 detached greenhouses
		1	30	Y	Y	?			?	6	infiltration monitored continuously; removable walls; cooling experiments
			V	Y	Y	Y	ER	D	M	24	
		2	36	Y	Y	Y	ER	D	F	4	
			1.7	Y	Y	Y	ER		M	2	
			V	Y	Y				M	18	convective collector experiments
		3	96				ER	T	M	20	product development
		3	V						M	19	retrofitted to residence
			12	Y					M	11	convective collector experiments
			V				ER	T	M	26	adobe construction
			112/41	Y			ER	T	M	22	1830 ft² floor area
			45	Y					M	19	
			32	Y	Y				F		product development
		4	V	Y			ER	D	M		plus detached greenhouses
			36	Y	Y				M	15	
			35	Y		/Y	ER	D	M	21	
			800	Y	Y	Y	FC	D	M	8	roof pond; cooling experiments
			119	Y		Y	ER	T	M	25	1 passive solar; 5 conservation
			7/10	Y	Y		ER	T	M	30	

Test Module Facilities in the

		Year operational	Discontinued	Boxes	Rooms	Buildings	Modules per structure	Height, ft.	Width, ft.	Depth, ft.	Walls, R-value	Floor, R-va	R
A.	Skytherm Processes & Engineering	'67	Y		1		1	9	10	12	?	S	P
B.	Environmental Research Laboratory	'81				4	1	12	40	24	V	V	V
C.	Pacific Gas & Electric	'77			4		2	9	10	10	20	20	20
D.	Farallones Institution	'76	'78			5	1	16	14	12	11	S	19
E.	Solar Energy Analysis Laboratory	'81				8	1	9	16	16	11	S	19
F.	Habitat Center	'79	'81		4		2	10	14	22	14	16	30
G.	Solar Energy Research Institute	'81		2	10		2	9	6	10	25	25	25
H.	Massachusetts Institute of Technology	'47	'50		6		6	10	6	14	14	14	14
I.	National Center for Appropriate Technology	'78	'80		4		2	10	5	8	19	24	24
J.	University of Nebraska	'78			6		1	10	5	8	22	18	28
K.	Florida Solar Energy Center	'81				1	1	24	40	40	V	S	V
L-1.	Los Alamos National Laboratory	'75			14		2	10	5	8	19	19	19
L-2.	Los Alamos National Laboratory	'75		8			1	2	2	2	32	32	32
L-3.	Los Alamos National Laboratory	'80			2		2	20	40	1	40	40	4
M.	Solar Room Company	'77			4		4	9	8	22	40	40	40
N.	Wessling Consulting	'77	'78		4		4	8	8	8	V	V	V
O.	Scott Morris	'77	'79	4			1	6	2	3	9	18	9
P.	Ghost Ranch	'76	'77			4	1	10	40	17	22	25	25
Q.	Purdue University	'45				2	1	8	?	?	12	?	?
R.	Ames Laboratory	'79			3		1	8	12	12	28	28	24
S.	Waterwall Engineering	'80	'82		2		1	9	6	4	14	20	20
T.	Pennsylvania State University	'80	'81		4		4	8	12/16	8/12	10	G	2
U.	University of Pennsylvania	'77			2		2	10	5	8	19	19	19
V.	Tennessee Valley Authority	'81			4/2		1/2	8	5/12	8	19	19	25
W.	Trinity University	'81				2	1	10	40	20	?	S	V
X.	University of Alberta	'78				6	1	12	24	22	20	?	40
Y.	Lakehead University	'79	'80	2			2	4	4	4	20	20	32

Y = yes G = gravel P = pond S = slab V = varies ? = information unavailable

Table 1: Formal test module facilities in the United States and Canada have existed since the 1940s. See Table 2 for addresses

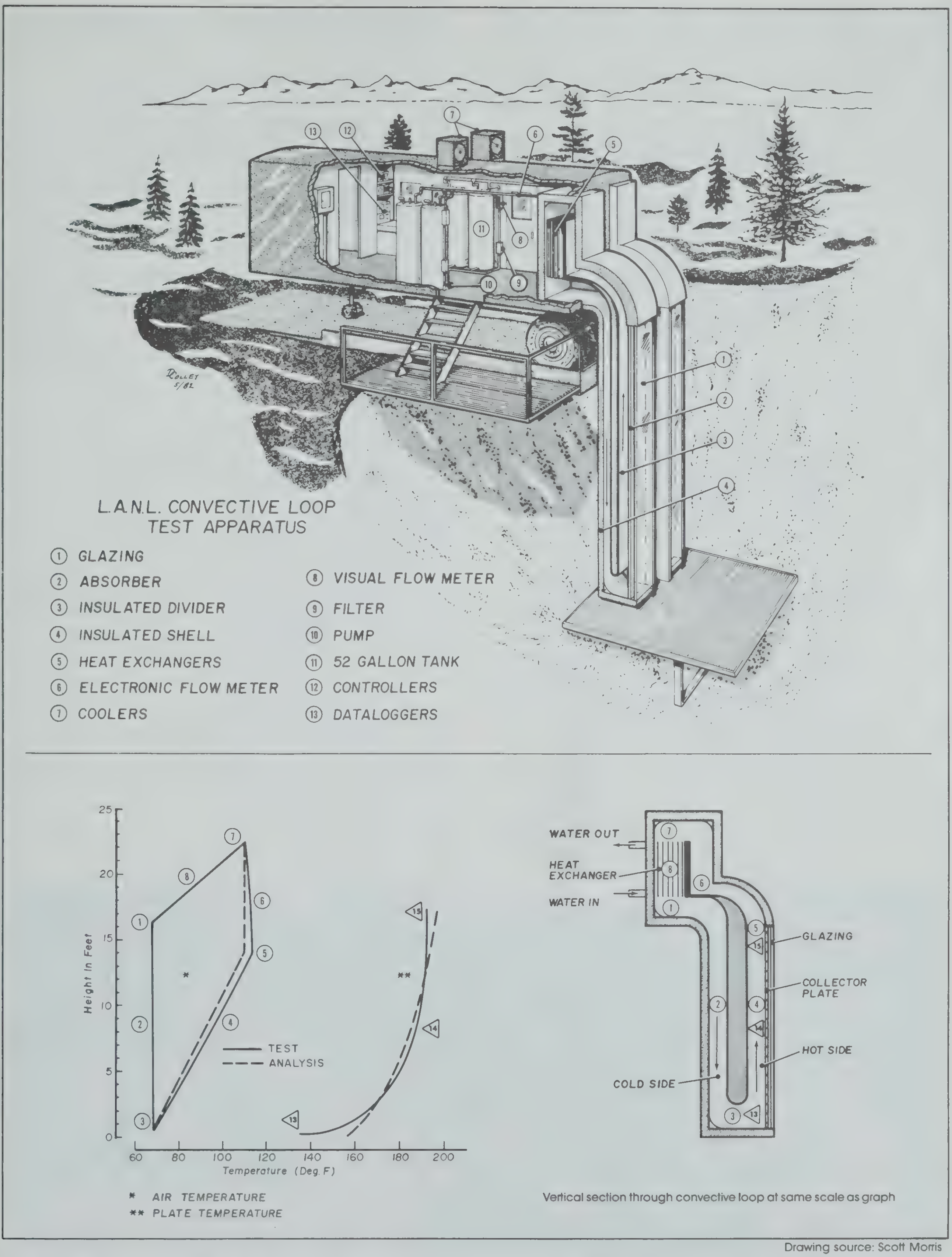

Vertical section through convective loop at same scale as graph

Drawing source: Scott Morris

Figure 9: The two convective heating test modules at Los Alamos are designed for maximum flexibility of configurations. The instrumentation is in a movable trailer, while the convective test chamber projects downward from a platform at one end. The graphs show air and collector plate temperatures at various heights within the chamber during a sample test. The efficiency correlation for this test was within one percentage point of the efficiency correlation derived from a computer simulation analysis.

attached to buildings, seven isolated for crop growing only) have been constructed at the Department of Agricultural Engineering of Pennsylvania State University, University Park, Pennsylvania. Each encloses 1400 ft^2 *(130 m^2)* of floor area and is reconfigurable in mass and glazing.

Three passive solar rooms measuring 12 ft. by 12 ft. by 8 ft. *(3.6 by 3.6 by 2.4 m.)* were constructed at the Passive Technologies Test Facility, Ames Laboratory, Iowa State University. The three rooms are thermally isolated and housed in a single insulated, earth-sheltered envelope.[19] (See Fig. 10.)

Four attached greenhouse test rooms were constructed in Taos, New Mexico, by the Solar Room Company[20] for the direct comparison of various storage media in double-wall inflated greenhouses. The four rooms formed one structure, with the adjacent rooms isolated with an R-40 wall.

Four rooms, 5 ft. by 8 ft. *(1.5 by 2.4 m.)* and two rooms, 12 ft. by 8 ft. *(3.6 by 2.4 m.)*, are being used by the Solar Applications Division of the Tennessee Valley Authority in Chattanooga, Tennessee. The smaller rooms are separate, whereas the modules measuring 12 ft. *(3.6 m.)* wide can accommodate a north/south partition.[21]

Buildings

One of the earliest examples of passive solar test buildings was the installation of two test houses at Purdue University, as described by Hutchinson.[22-31] Constructed in Lafayette, Indiana, in 1945, one house was used as a control and the other for comparative direct gain experiments.

Test buildings currently range from small, reconfigurable, two-zone structures (only slightly larger than test rooms) to full-size, uninhabited residences. Because most were designed to meet specific research objectives, they share only a few common characteristics. In addition to being unoccupied, most have at least limited reconfigurability of aperture, mass and zones.

Eight two-zone test buildings have been constructed in San Diego as part of a passive solar research program at the Solar Energy Analysis Laboratory.[9] The buildings were constructed by two local utilities; monitoring, analysis and simulation studies were supported by the utilities and the U.S. Department of Energy. The buildings measure 16 ft. by 16 ft. *(4.8 by 4.8 m.)* and are permanent structures in order to reflect standard construction practices (at some expense to ease of reconfigurability). These structures are among the few available for full-scale analysis of the effects of controls (fans, remote storage) on the performance of multi-zone passive structures. The data are being used by the Solar Energy Analysis Laboratory and by Sebald[32, 33] and University of California, San Diego (U.C.S.D.) graduate engineering students for code validation and simplified design tool development. (See Figs. 11a and 11b.)

Two identical reconfigurable test buildings have been constructed at Trinity University, San Antonio, Texas. Doderer, et al.[8] have described the facilities, which are primarily intended for code validation and heat transfer coefficient measurement in passive cooling systems. Each building can be configured into the following systems: 1.) roof pond with movable insulation, 2.) trickle roof, 3.) low mass roof, and 4.) plenum roof. (See Fig. 12.)

Four test buildings have been constructed at the Environmental Research Laboratory, Tucson, Arizona. The structures are primarily intended to allow study of various cooling strategies in hot, arid climates; however, some passive heating study is included. The size, mass, configuration and thermal load is different for each structure.[10] (See Fig. 13.)

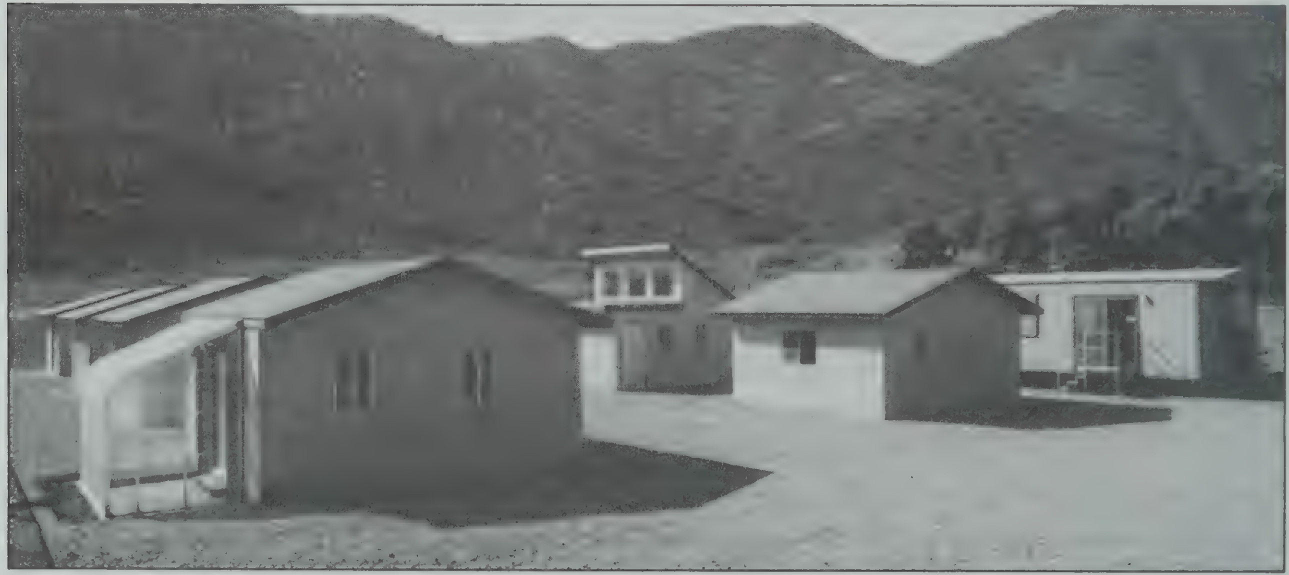

Figure 11a: Test buildings of the Solar Energy Analysis Laboratory in San Diego reflect local construction practices. Each building contains a north and south room and tests both heating and cooling.

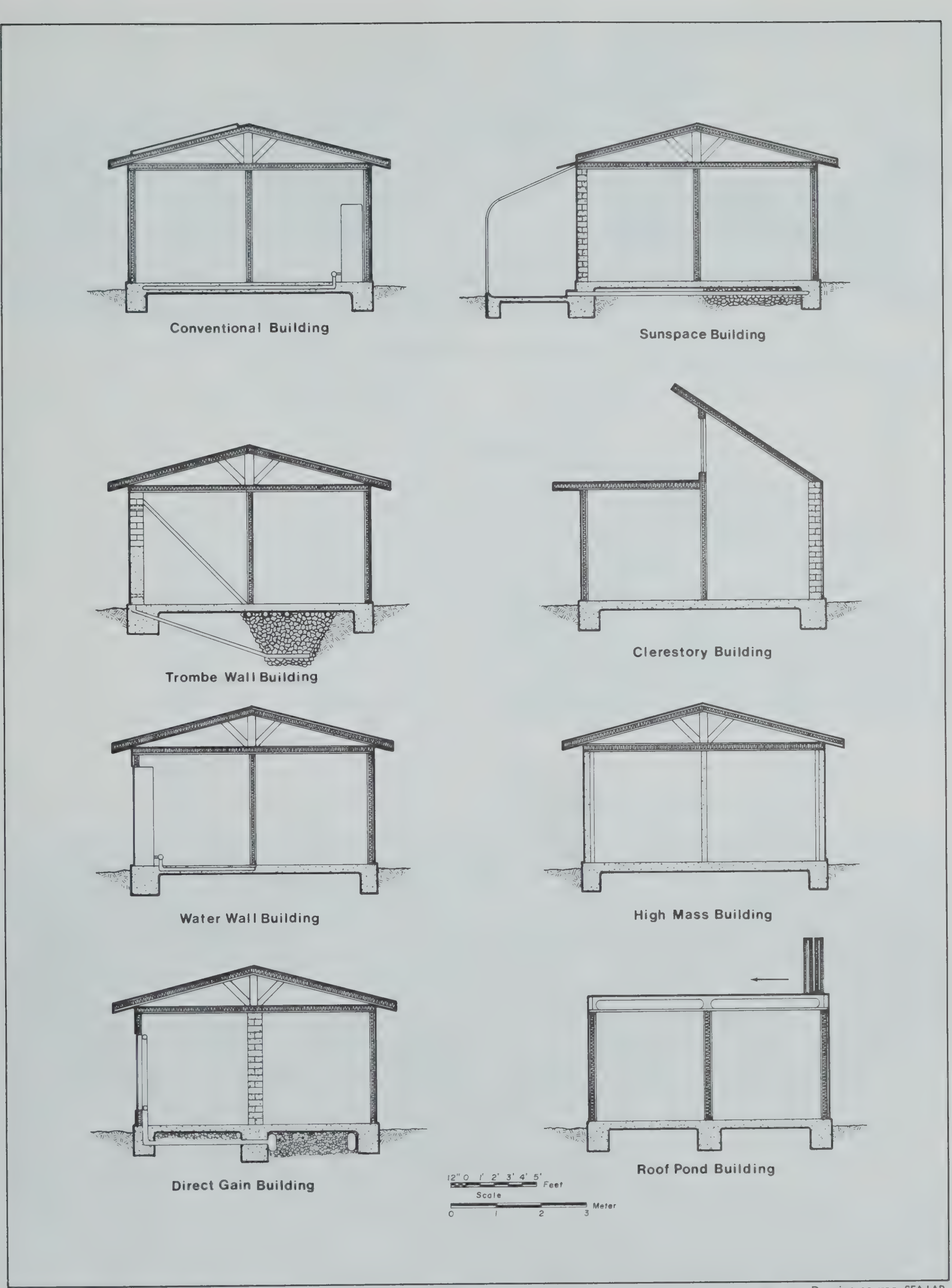

Drawing source: SEA-LAB

Figure 11b: The SEA-LAB buildings' construction is uninsulated concrete slab on grade, 2x4 stud frame walls and truss-framed roof with a ½ in. drywall ceiling. Each building has a double entrance door with a 3 ft. by 3 ft. air lock chamber to minimize air replacement. Regular windows are single glazed; solar glazing is double.

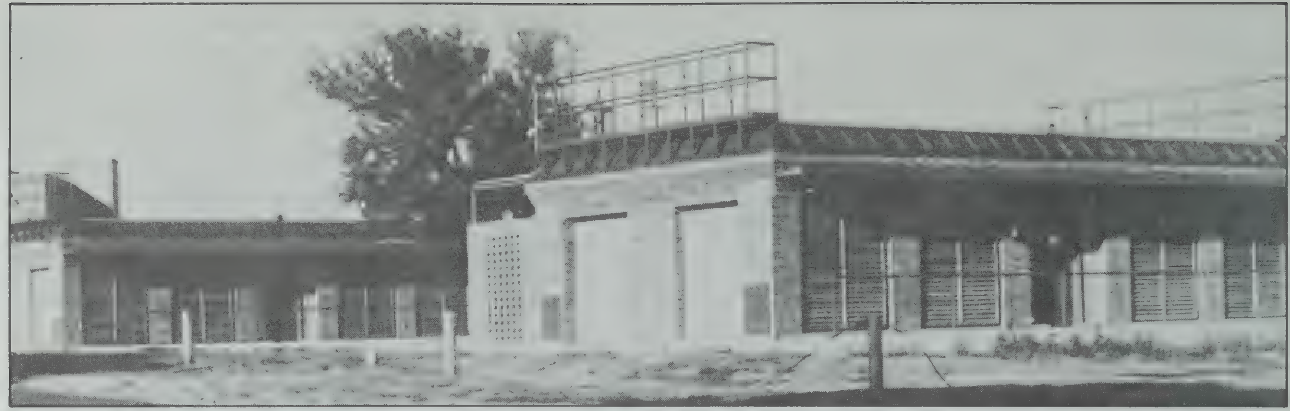

Photo: Trinity University

Figure 12: The two test buildings at Trinity University in Texas provide comparative facilities for research on passive cooling, especially roof radiation.

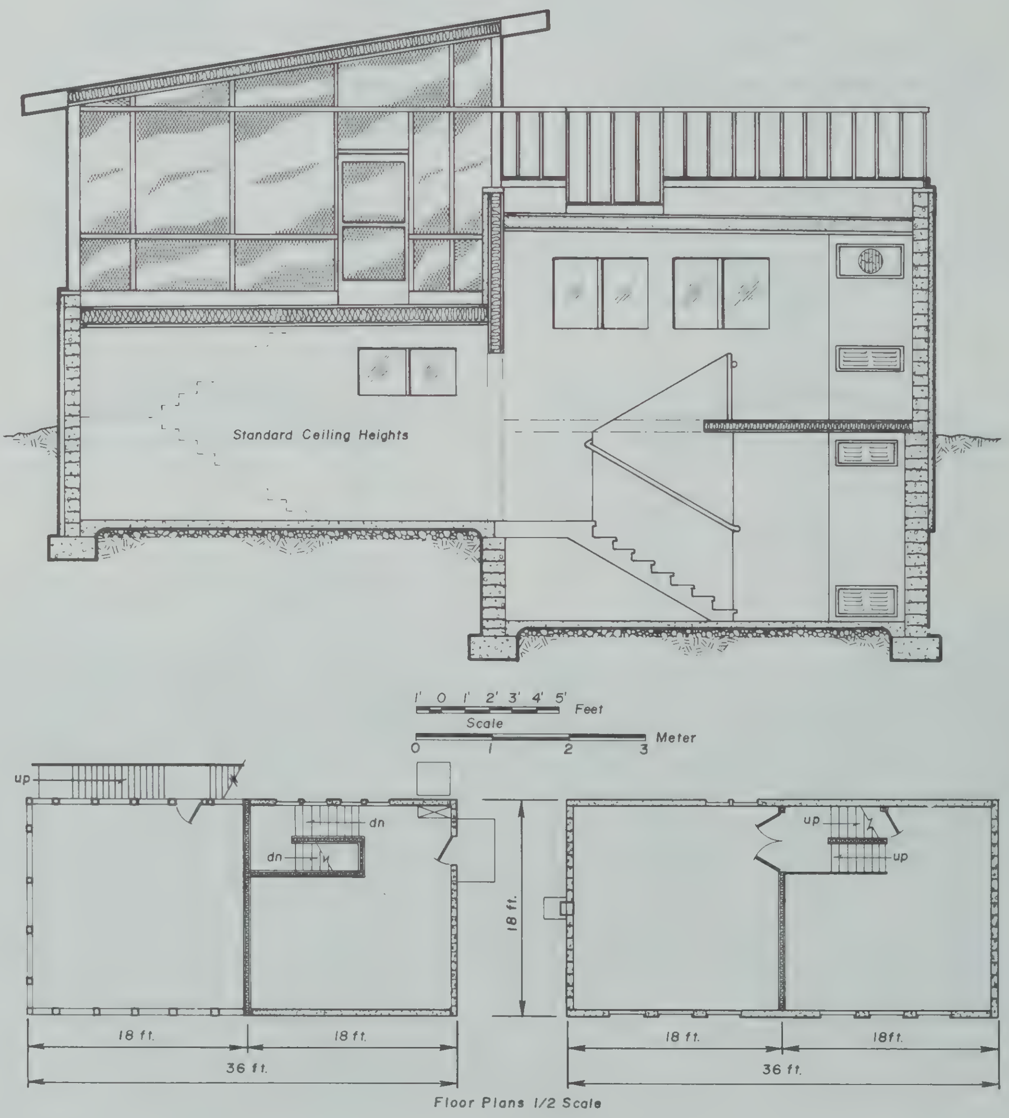

Drawing source: Environmental Research Laboratory

Figure 13: One of several test buildings at the Environmental Research Laboratory in Tucson, Arizona, contains five different zones, including several with cooling approaches. The ceiling of the screened porch is insulated to permit its eventual enclosure.

The Florida Solar Energy Center in Cape Canaveral has constructed a building module for cooling experiments. The structure is unique in that all (including exterior) walls are reconfigurable. One configuration involved the investigation of thermal stack spaces 24 ft. *(7.2 m.)* high. The concrete-slab floor is supported by hollow concrete masonry blocks on a second slab allowing reconfigurable air distribution and thermal storage.[34] (See Fig. 14.)

A set of six test buildings was constructed at the University of Alberta, Edmonton, Alberta, Canada to compare the thermal performance of standard construction to that of four alternatives (conservation, passive solar, active air solar, active liquid solar). A sixth building was used for short-term testing. The building measured 22 ft. by 24 ft. *(6.6 by 7.2 m.)* and used frame construction, roof trusses, single-zone above grade and basement.[35]

Four, two-room, single-zone adobe test buildings were constructed at Ghost Ranch, Abiquiu, New Mexico. One is a standard construction control unit; the other three test sunspace, direct gain and Trombe wall construction. Designed by Peter van Dresser and built using unskilled labor, these buildings measured 17 ft. by 40 ft. *(5.1 by 12 m.)* and were not reconfigurable. They were extensively monitored by Los Alamos until they were occupied as guest units at the ranch.[36] (See Fig. 15.)

A set of five frame-construction test buildings are located at the Farallones Institute, northern California. Calthorpe[37] has described the design and performance of these occupied test structures; experimental objectives included direct comparison and demonstration. (See Fig. 1.)

Four test rooms measuring 9 ft. high by 10 ft. wide by 10 ft. deep *(2.7 by 3 by 3 m.)* are being used by the Pacific Gas and Electric Company (Department of Engineering Research) at their San Ramon, Cal-

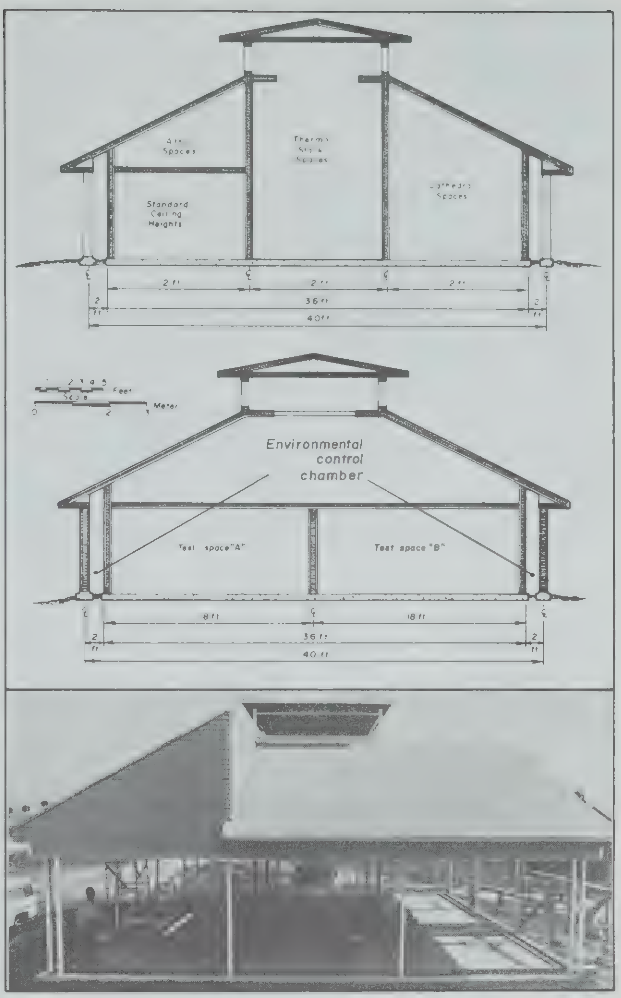

Photo and drawing source: F.S.E.S.

Figure 14: The Florida Solar Energy Center's test building at Cape Canaveral evaluates convective cooling by means of a reconfigurable space.

Photo: L.A.N.L.

Figure 15: The adobe test buildings of the Ghost Ranch at Abiquiu, New Mexico, were monitored prior to occupancy and continue to provide data while functioning as guest quarters.

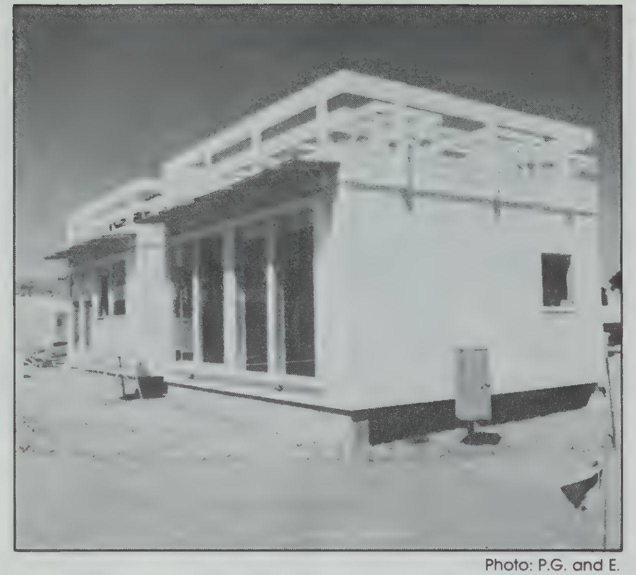

Photo: P.G. and E.

Figure 16: The Pacific Gas and Electric Company test rooms in San Ramon, California, provide measurements of weather, interior temperatures and, most importantly, rooftop radiation. This passive solar test facility is a demonstration project for the utility and part of its energy research.

ifornia Passive Solar Test Facility. (See Fig. 16.)

Table 1 lists the test-module facilities in the United States and Canada. See Table 2 for addresses.

USES OF TEST MODULES IN PASSIVE SOLAR RESEARCH

Proof-of-Concept Experiments

Such experiments are often used by innovators in order to determine whether further, more rigorous testing is justified. The objective here is to isolate the principle under investigation and minimize unrelated variables. In the interest of expediency and economy, there is a temptation to proceed with the experiment before adequate theoretical analysis. Care must be exercised to prevent unrelated variables from overpowering the principle to be demonstrated. Reconsider, for example, the early heating experiment by Hay using the water-filled foam box. It is easy to imagine a set of conditions (low sun angle, rapid air movement, low humidity) that actually would have resulted in a cooling effect rather than the heating anticipated.

Conversely, early (even premature) physical experimentation can be conducive to enhancing the intuitive process. Many innovators gain most of their insights while working with such physical models, while others favor sketching or theoretical calculations.

Another important use of proof-of-concept experiments is for educational purposes. As a college professor, the author has found single-purpose test modules to be particularly valuable for demonstrating passive solar principles to students. Several such demonstrations are described by Benton and Akridge.[38]

Comparative Experiments

Comparative experiments may be direct (where two or more systems are compared in one experiment under identical conditions) or indirect (where two or more systems are compared in separate experiments using a control system). In the latter, some method of normalization is required to provide a basis of comparison between the competing experimental systems.

In direct comparison experiments, the objective is to compare the performance of two competing components or systems through simultaneous test-

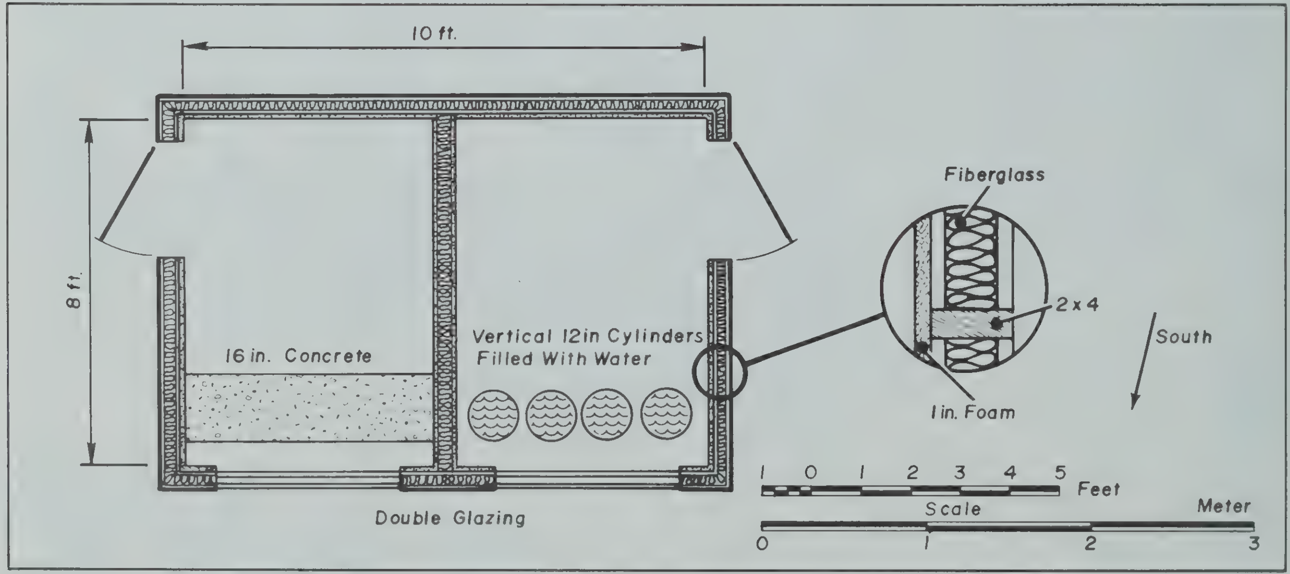

Figure 17: An early experiment at Los Alamos used adjacent test rooms to directly compare water tube and masonry wall thermal storage systems.

ing. The experiment should isolate the difference(s) of the two systems, minimizing the unrelated variables so performance differences will be a result of the differing system characteristics under study. The more generalized the desired result, the more important is the isolation of differences.

For example, an early experiment[39] at Los Alamos directly compared a masonry thermal storage wall system and a water tube thermal storage system in adjacent test rooms. Several comparative experiments were run while changing such parameters as the vents in the masonry wall and blocking the space between the storage tubes. This gave a direct comparison of overall system performance for the particular configurations tested. (See Fig. 17.)

Note, however, that it is not possible to draw general conclusions from this experiment about masonry vs. water as a thermal storage medium. In this experiment, readily available standard components were used (i.e., fiberglass water tubes 12 in. by 8 ft. *(30 by 240 cm.)* and solid masonry 16 in. *(40 cm.)* thick). The resulting thermal storage capacities were similar—35 Btu/°F ft^2 water vs. 32.5 masonry *(715 kJ/°C m^2 vs. 664)*. However, this thermal storage limitation resulted in spacing the water tubes 2.4 in. *(6 cm.)* apart and leaving a 24 in. *(60 cm.)* gap above the tubes. Foam insulation was inserted into the spaces between and above the water tubes (in order to reduce the convective air transfer between the glazing and room interior). This prevented any direct solar gain between the tubes at mid-day, and partially blocked sun from the sides of the tubes in the morning and afternoon.

If the experimental objective had been to compare thermal storage media, the following characteristics (unrelated to medium type) should have been identical: exposed mass area and shape, venting, thermal storage capacity and interior mass area and shape. This would have implied a very non-standard configuration of at least one of the systems (i.e., round concrete cylinders or flat waterwall).

An example of indirect comparative testing is the experiments at Los Alamos reported by Hyde.[40] In this series, the performance of various experimental thermal storage wall systems (varying storage medium, glazing, surface selectivity and night insulation) was compared with that of a control sys-

Sample Performance Summaries, Indirect Comparison Test Room Experiments, Normalized on the Basis of $Q_{solar}/Q_{solar, control}$. ($Q_{solar, control} = Q_8$.)

Cell wall, black collection surface, glazing, insulation	Q_{solar} Btu/Day	Q_{aux} Btu/Day	Load Btu/Day	Ambient Temp. °F	Insolation Btu/ft²/Day	SSF	Q_{solar}/Q_8
1 Trombe, flat, SG	11400	19700	30900	32.4	1630	0.38	0.63
2 Trombe, chrome, SG	19100	13100	31800			0.59	1.05
5 water, chrome, SG	25500	10100	34900			0.68	1.40
6 water, flat, SG	15200	20400	34800			0.36	0.83
7 Trombe, flat, DG, NI	22100	10500	32100			0.67	1.31
8 Trombe, flat, SG	16900	15400	31800			0.52	1.00
1 Trombe, flat, SG, NI	13700	14600	28400	37.6	1214	0.49	0.91
2 Trombe, chrome, SG	15100	12800	27900			0.55	1.01
5 water, chrome, SG	17800	12500	30300			0.56	1.19
6 water, flat, SG, NI	22800	9900	32700			0.65	1.52
7 Trombe, flat, DG, NI	18200	11200	29400			0.61	1.31
8 Trombe, flat, DG	13900	13600	27600			0.52	1.00
1 Trombe, flat, DG	11400	17200	28600	37.4	1430	0.40	0.92
2 Trombe, chrome, DG	14700	13100	27800			0.54	1.19
5 water, chrome, DG	19900	10100	30000			0.65	1.61
6 water, flat, DG	14400	15900	30300			0.44	1.16
7 Trombe, flat, DG, NI	MALFUNCTION IN BEAD SYSTEM						
8 Trombe, Flat, DG	11500	16200	27700			0.43	1.00
1 Trombe, flat, DG	22400	16400	38800	23.5	1950	0.57	1.00
2 Trombe, chrome, DG	28500	10400	38900			0.72	1.27
5 water, chrome, DG	40000	3500	43500			0.91	1.78
6 water, flat, DG	37400	5600	44100			0.82	1.67
7 Trombe, flat, DG, NI	29900	10000	39800			0.74	1.44
8 Trombe, flat, DG	20800	18000	38800			0.53	1.00

SG — single glazed, DG — double glazed, NI — night insulation, SSF — solar savings fraction.

Table 3: Example of test room use in comparative experiments at Los Alamos National Laboratory.[40]

tem (double glazed, flat black, unvented Trombe wall, no night insulation). The basis for comparing the systems was Q_{solar} (net thermal energy delivered through the south wall). This was calculated from the energy balance: Q_{solar} + aux. heat = load. Auxiliary heat was measured directly and the load was calculated from the measured room heat loss coefficient, the measured average room temperature and the measured ambient temperature.

The control Trombe wall system (Room No. 8) was operated for the duration of all test periods, while the various experimental systems were tested during shorter periods (see Table 3). Note that all experimental systems were not directly compared with each other (due to the limited number of rooms available). Instead, the various experimental systems were normalized against the control, i.e., the ratio of a test room's net energy to the control room's net energy (Q_{solar}/Q_8) was used as a direct basis of performance comparison. (See Fig. 18.)

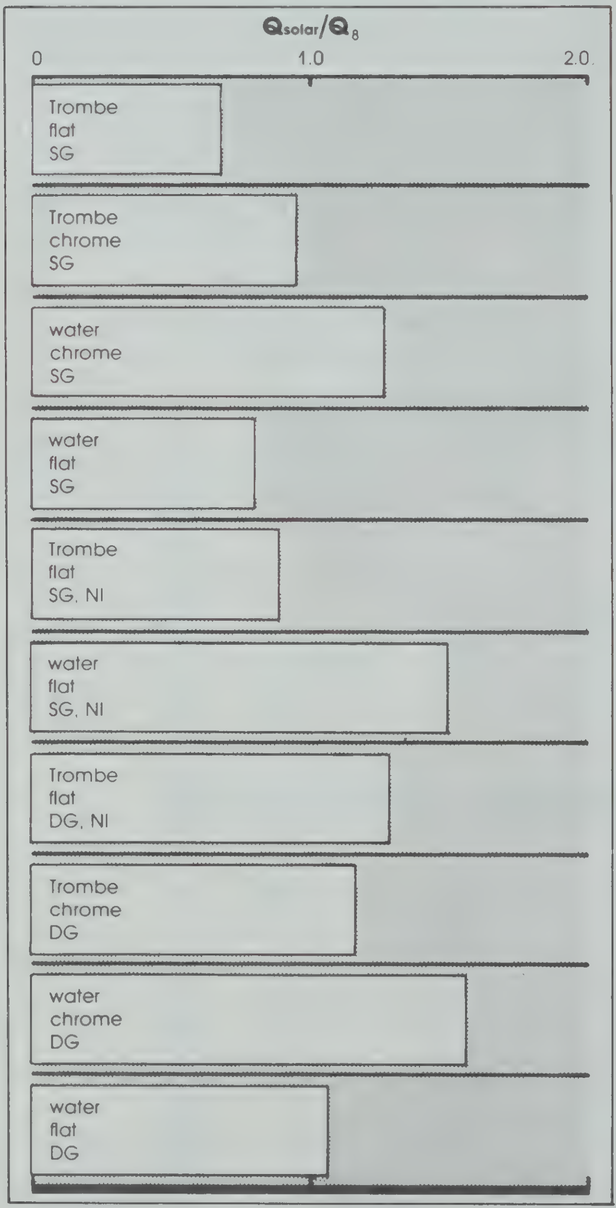

SG: single glazed, DG: double glazed, NI: night insulation

Graph: Johanna Bertoldo

Figure 18: Comparative test room performance (varying cell wall type, black collection surface, glazing and insulation) as measured by $Q_{solar}/Q_{solar,\ control}$.[40]

In order for such indirect comparisons to be valid, the ratio (Q_{solar}/Q_8 for a given system must remain constant over changing weather conditions. Hyde validated the normalization parameter by operating each of the experimental systems in at least two periods. A comparison of Q_{solar}/Q_8 (Table 3) for a given experimental system in two different test periods provides a measure of the validity of this normalization method for each of the various systems.

Test-module indirect comparison experiments are frequently used by commercial manufacturers as a method of comparing the performance of competing systems while using a minimum number of test modules. Usually, only two modules are employed; however, using three makes it possible to monitor continuously the validity of the normalization measure ($Q_{exper.}/Q_{control}$ in the Hyde experiments). It should be noted that an accurate normalization procedure (in either direct or indirect comparisons) raises the level of results from "Which is better?" to "How much better?".

The instrumentation typically required for comparative experiments is shown in Fig. 19.

Theoretical Model Validation Experiments

Traditionally, steady-state calculation methods[40] have been used for determining heat loss in buildings. Although acceptable for buildings of low thermal mass, they are not capable of accounting for the lag effect associated with massive construction under changing thermal conditions. Thermal network models have become widely accepted as an accurate technique for simulating the dynamic performance of massive buildings.[42-50] This technique breaks down continuous parameters (time, temperature, solar radiation, mass, thermal resistance) into many small increments that are solvable by numerical calculation. These increments can be conceptually illustrated by analogy as an electrical network.

In a thermal network diagram of a passive solar building, a series of nodes are used to represent selected points and various elements in a building such as windows or wall assemblies. If there is any thermal transfer (convection, radiation, conduction) between these building elements, a resistance symbol •–⋀⋀⋀⋀–• is used to represent the connection between nodes. The thermal transfer rate between the elements (U-value x Area, or equivalent) is represented by this resistance symbol. All of the mass (capacitance) of the building element is assumed to be concentrated at the node. Heat can be added to the system at any node (e.g., sun on the surface of a Trombe wall), or the temperature of any node can be assigned (e.g., outside air temperature).

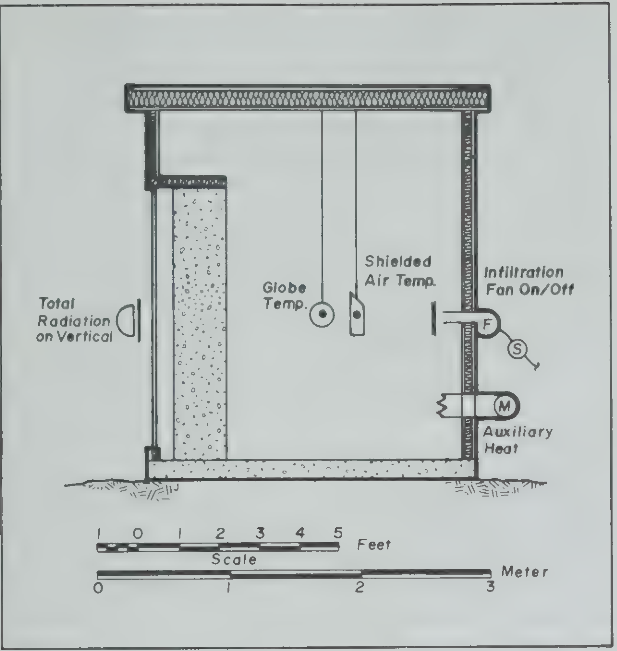

Figure 19: Instrumentation typically required for comparison experiments measures the total radiation on the vertical, globe temperature, and shielded air temperature as well as monitoring and recording auxiliary heat and an infiltration fan.

The initial temperature of each node must be specified (see Fig. 20). A series of calculations are performed to determine the temperature at each node after an increment of time. Based on new known temperature inputs (i.e., outside air) and heat inputs (i.e., solar radiation, auxiliary heat), and the new calculated temperatures, the procedure is repeated for the next time increment. The effect of the initial assumed temperature diminishes with each repetition and eventually vanishes. Increasing the number of nodes and decreasing the time increment increases the accuracy of the simulation at the expense of increasing calculation time.

At Los Alamos, PASOLE, a generalized FORTRAN program, was developed by McFarland to run hour-by-hour thermal network simulations of passive solar buildings using weather data input.[46] Others have developed similar codes.[44, 47–50] This allows the thermal performance of a building to be predicted in any climate for which hourly weather data are available. From correlations derived from these simulations, a simplified procedure was developed by Balcomb at Los Alamos for predicting the monthly requirements for auxiliary heat in various types of passive buildings in over 200 cities in the U.S. and Canada.[51]

Before a computer model can be accepted as an accurate simulation of the thermal behavior of a building, it must be validated against the actual performance of a monitored structure. Typically, the actual building performance data are directly compared with the simulation results obtained using the recorded test period weather data. Statistical techniques are employed to measure the accuracy of the comparison. Such comparisons provide a basis for refining the model. Although the basic calculational procedure used by the model is simple, the determination of some of the system parameters may not be. Some parameters (such as the effective mass of an interior room) may be difficult to calculate; some are non-linear and vary with time (i.e., night insulation) or heat transfer rates (convection in a Trombe wall). Test module operating data and one-time measurements are used to determine these coefficients.

Test modules typically provide the best basis for this validation process for several reasons:

- They are easily reconfigurable.
- They facilitate sensor placement.
- The effects of unrelated variables can be minimized or easily measured.
- They are unoccupied.
- They can be used with or without auxiliary heat.

Although test boxes and test buildings have been used for code validation, full height, small test rooms are the most widely used; in fact, in many research programs, code validation is the primary purpose of these rooms.

Because of the detailed scrutiny that code validation data will ultimately receive, the most rigorous experimental procedures are typically employed. Sensor placement has a direct correspondence to simulation node selection. Not only must sensor location be planned to maximize its value for future reference, but placement must be precise and accurately recorded. In addition, the experimenter must ensure that each sensor does not significantly perturb the experiment. For example, conduction along the stem of a thermocouple can alter the local temperature.

Code validation requires that the experimental objective be extended beyond "How well does it perform?" to ask "Why does it perform as it does?". This requires many temperature sensors to validate simulation node conditions, as well as a large number of one-time measurements to accurately determine the heat transfer coefficients for the simulation. (Coefficients obtained from literature values are sometimes not considered sufficiently accurate for code validation purposes.) (See Fig. 21.)

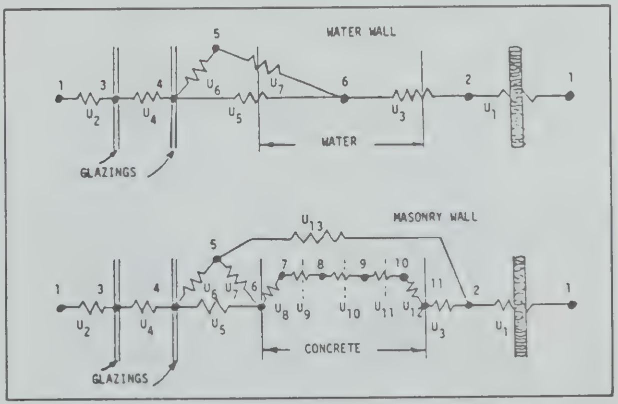

Drawing: L.A.N.L.

Figure 20: Thermal network diagrams show thermal transfer between elements in water wall and Trombe wall test rooms.

Component Performance

Test modules can be used to obtain data on component performance under realistic operating conditions. This might include evaluating the effectiveness of a night insulation system or measuring the effective heat loss coefficient of a selective surface.

Building Performance Experiments

When test modules are to be used as a direct analog of an occupied building, typically the primary measures of performance are human thermal comfort and auxiliary heating performance over an extended period. The objective of direct simulation of thermally complex, occupied buildings requires that the size and zonal configuration of the test module exceed the capabilities of a test room and approach the characteristics of an actual building. Because of these difficulties, it may be preferable to monitor an occupied building. This is the focus of the S.E.R.I. Class B Passive Solar Buildings Monitoring Program.[52] However, the monitoring of occupied buildings presents a number of measurement and control problems that make it difficult to draw general conclusions from specific experiments. These include:

- variation in infiltration rate (due to operation of doors and windows, and exhaust fan operation)
- variation in net contribution of auxiliary heat from heat pumps, wood stoves, fireplaces, oil or gas furnaces, etc.
- unmeasurable miscellaneous heat gain from internal sources (water heaters, cooking, bathing, laundry, lighting, occupant body heat, etc.)
- inaccessibility of the building for measurement and observation
- configuration permanence.

The experimental alternative to monitored occupied buildings is unoccupied, full-scale test buildings. In such a facility, the above-named variables can be controlled and measured.

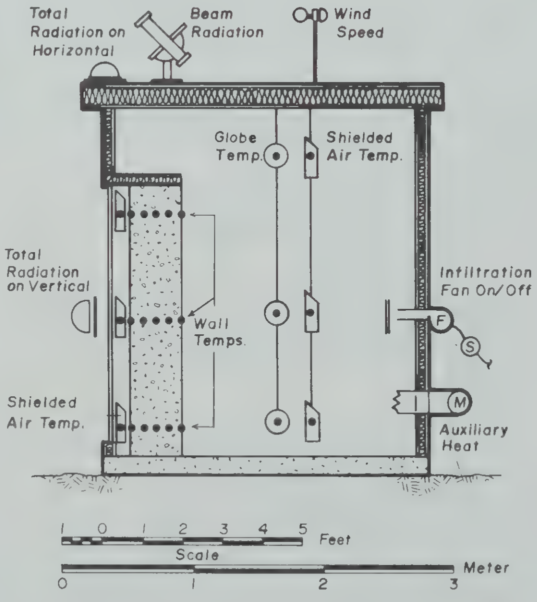

Figure 21: A schematic section through a Trombe wall test room shows typical instrumentation required for computer code validation.

SPECIAL CONSIDERATIONS

Auxiliary Heating

A fundamental option in passive test modules is the use of auxiliary heating. Most proof-of-concept experiments (i.e., "Does it work?") are "free running" (no auxiliary heat). The choice is less clear for comparison and code validation experiments; studies concerning heat transfer coefficients and building performance usually employ auxiliary heat. "Free running" experiments may allow easier isolation of a particular thermal behavior in a component; however, this type of investigation may distort the overall behavior of a passive system because of lower operating temperatures. For example, in a Los Alamos experiment on the effect of reverse thermosiphoning in vented Trombe walls, it was found that the use of a check-valve (to prevent reverse thermosiphoning) made little difference in thermal performance if the system was "free running," but significantly increased performance if auxiliary heat was used.

Perhaps the biggest advantage of auxiliary heating is that it provides a direct measure (without any simulation) of the primary performance indicator of passive building (i.e., amount of auxiliary heat required). The principal advantages of free running systems include the use of internal temperature as a performance indicator—laymen are usually able to interpret temperatures on a thermometer more easily than quantities of heat (Btu or kilowatt/hours). The second advantage is the simplicity of free running systems. Control of auxiliary heat is a problem, because standard wall thermostats are often inaccurate; Los Alamos has found control by the data acquisition system to be more reliable when using room air-temperature sensors as the control input.[53] Electric resistance heat is preferred because of its ease of measurement. Los Alamos uses standard incandescent light bulbs[54] while S.E.R.I. uses portable resistance heaters with a destratification fan.[55]

Test-Module Calibration

If test modules are to be used only for direct comparison experiments, it is sufficient to ensure that the various parameters (heat loss, aperture, size, tilt, glazing, etc.) are identical. This can be done by identically configuring the modules, and monitoring interior temperatures after an initial stabilization period.

However, if test modules are to be used for code validation purposes, the value of all parameters affecting performance must be known by direct measurement, and this purpose requires a precise calculation procedure.

Typically, the following one-time measurements are made:

- absorber surface characteristics (emissivity and absorptivity)
- glazing characteristics (transmissivity, absorptivity, reflectivity, area, tilt, orientation)
- thermal storage characteristics (surface area, mass, specific heat)
- heat loss coefficient (including infiltration) of entire test cell, excluding solar wall (solar wall is covered with heavily insulated panel and auxiliary heat consumption is monitored)
- infiltration rate.

Heat loss in buildings caused by infiltration is dependent on the following factors: the difference between the inside and outside temperatures, the specific heat and density of the air, and the infiltration rate. The infiltration rate is not constant, varying with wind speed, direction and temperature difference (stack effect). Because of the expense and complexity of continuously monitoring the infiltration rate in test rooms, at Los Alamos the rate is fixed by using a fan to pressurize the room slightly, overpowering the natural variables of wind speed and temperature difference. The fan is positioned on the outside of the room, supplying air through a duct.

SUMMARY

This representative selection of test modules identifies prototypical and influential experiments.

Additional experimental practices will be described in subsequent issues of *Passive Solar Journal.*

REFERENCES

1. Hay, H.R.; Yellott, J.I. 1970 (January). "A Naturally Air-Conditioned Building." *Mechanical Engineering.* Vol. 32 (No. 1): pp. 19-23.
2. Grimmer, D.P.; McFarland, R.D. and Balcomb, J.D. 1979. "Initial Experimental Tests on the Use of Small Passive-Solar Test-Boxes to Model the Thermal Performance of Passively Solar-Heating Building Designs." *Solar Energy.* Vol. 22: pp. 351-354.
3. Grimmer, D.P. 1979. "Theoretical Considerations in the Use of Small Passive-Solar Test-Boxes to Model the Thermal Performance of Passively Solar-Heated Building Designs." *Solar Energy.* Vol. 22: pp. 343-350.
4. Balcomb, J.D.; McFarland, R.D.; Moore, S.W. 1977 (June). "Simulation Analysis of Passive Solar Heated Buildings—Comparison with Test Room Results." *Proc. American Section of the International Solar Energy Society, 1977 Annual Meeting;* Orlando, Florida; 6-10 June 1977. (AS/ISES, Cape Canaveral, Florida,) Vol. 1, Sec. 11, pp. 5-9. (LA-UR-77-939).
5. Palmiter, L.; Wheeling, T.; Corbett, B. 1980 (October). "Performance of Passive Test Units in Butte, Montana." *Proc. 5th National Passive Solar Conference*; Amherst, Massachusetts; 19-26 October 1980. Vol. 2, 5.2, pp. 591-595.
6. Chen, B.; Maloney, J.; Thorp, J.; Pederson, K.; Holmes, W.; Sedlacek, C.; Sash, R.; and Hollingsworth, E. 1979 (May). "Preliminary Winter Comparison Results of Four Passive Test Cells in Omaha, Neb." *Proc. International Solar Energy Society,* Atlanta, Georgia, pp. 1583-1587.
7. Andrews, M. 1980 (May). "SERI Passive Solar Test Cell Drawing No. AA-0842-01," Solar Energy Research Institute, Golden, Colorado.
8. Doderer, E., Bentley, D., and Allen, C. 1981 (May). "A Flexible Test Facility for Passive Cooling and Solar Heating." *Proc. American Section of the International Solar Energy Society*; Philadelphia, Pennsylvania, 26-30 May 1981, pp. 941-945.
9. Clinton, J.R. 1980. "The Sea-Lab Passive Test Building Project." *Proc. Second Systems Simulation and Economic Analysis Conference*; San Diego, California, pp. 91-94.
10. Peck, J.F.; Kessler, H.J. 1981 (November). "A Passive Cooling Experimental Facility for a Hot/Arid Climate." *Proc. International Passive and Hybrid Cooling Conference*; Miami Beach, Florida, 10-12 November 1981, pp. 437-441.
11. Morris, W.S. 1978 (March). "Natural Convection Solar Collectors." *Proc. Second National Passive Solar Conference.* Philadelphia, Pennsylvania, 16-18 March 1978, pp. 596-601.
12. Dietz, A.G.H.; Czapek, E.L. 1950 (March). "Solar Heating of Houses by Vertical South Wall Storage Panels," *Heating, Piping, and Air Conditiong*; pp. 118-125.
13. Hollingsworth, F.N.. 1947 (May). "Solar Heat Test Structure at M.I.T.," *Heating and Ventilating.*
14. Balcomb, J.D. 1981 (September). "Dynamic Measurement of Heat Loss Coefficients Through Trombe Wall Glazing Systems," *Proc. Sixth National Passive Solar Conference*; Portland, Oregon 8-12 September 1981 (LA-UR-812223).
15. Prowler, D. 1978 (March). "Testing and Simulation of Passive Solar Systems." *Proc. Second National Passive Solar Conference*; Philadelphia, Pennsylvania, 16-18 March 1978, pp. 581-587.
16. Chen, B.; Maloney, J.; Thorp, J. 1979 (May). "Modeling Thermal Networks with PCAP." *Proc. International Solar Energy Society;* Atlanta, Georgia, pp. 1630-1633.
17. Martin, M.; Nelson, L.; Wexler, A.; Schiller, S.R. 1981 (September). "Results of a Retrofit Sunspace Testing Program." *Proc. Sixth National Passive Solar Conference*; Portland, Oregon, 18-20 September 1981, pp. 778-782.
18. Morris, W.S. 1980 (October). "Development of an Experimental Test Apparatus for Natural Convection Solar Collectors." *Proc. Fifth National Passive Solar Conference*; Amherst, Massachusetts, 1926 October 1980 (LA-UR-80-2329), pp. 1032-1036.
19. Mercer, R.; McClelland, J.; Hodges, L.; Szydlowski, R. 1981 (September). "Recent Developments in the Transwall System." *Proc. Sixth National Passive Solar Conference*; Portland, Oregon, 18-20 September 1981, pp. 178-182.
20. Kenin, S.R.; Betz, W.B. 1978 (March). "The \$2.50/ft^2 Solar Collector: A Description and Cost Analysis." *Proc. Second National Passive Solar Conference*; Philadelphia, Pennsylvania, 16-18 March 1978, pp. 558-590.
21. Kuberg, D. 1981 (Mary 19). "Calibration of Test Cells." Tennessee Valley Authority, Solar Applications Branch Test Plan No. 804002; 300 Credit Union Bldg.; Chattanooga, Tennessee 37401.
22. Hutchinson, F.W. 1947 (May). "The Solar House: Analysis and Research." *Progressive Architecture*; pp. 90-94.

23. Hutchinson, F.W.; Chapman, W.P. 1946 (July). "A Rational Basis for Solar Heating Analysis." *Heating, Piping, and Air Conditioning.*

24. Hutchinson, F.W. "Heat Gain from Winter Sunshine in the U.S." 1946 (March). *Heating and Ventilating.*

25. Hutchinson, F.W. 1946 (March). "The Solar House: A Research Progress Report." *Heating and Ventilating.*

26. Parmalee, George V. 1945 (October-November). "The Transmission of Solar Radiation Through Flat Glass Under Summer Conditions." *Heating, Piping, and Air Conditioning.*

27. Hand, Irving F. 1937. "Review of U.S. Weather Bureau Solar Radiation Investigations." *Monthly Weather Review.* Vol. 65: pp. 441.

28. Moon, Parry. 1940 (November). "Proposed Standard Solar Radiation Curves for Engineering Use." *Journal of the Franklin Institute.* Vol. 230 (No. 5): p. 605.

29. Wexler, C.H. 1934. "Turbidites of American Air Masses and Conclusions Regarding Seasonal Variation in Atmospheric Dust." *Monthly Weather Review.* Vol. 62: pp. 397-402.

30. *Monthly Weather Review.* 1945 (January). Climatological Data Section. Vol. 73 (No. 1).

31. Hutchinson, F.W. 1945 (September). "The Solar House: A Full-Scale Experimental Study." *Heating and Ventilating.*

32. Sebald, A.V.; Vered, G. 1981. "On Extracting Useful Building Performance Characteristics Without Simulation." *Proc. American Section of the International Solar Energy Society*; Philadelphia, Pennsylvania. Volume 2, pp. 1016-1020.

33. Carroll, J.A.; Clinton, J.R. 1980 (October). "A Thermal Network Model of a Passive Solar House." *Proc. Fifth National Passive Solar Conference*; Amherst, Massachusetts, 19-26 October, 1980. pp. 257-261.

34. Fairey, P.W. "A Passive Cooling Experimental Facility for Warm Humid Climates." Published by the Florida Solar Energy Center; 300 State Road 401; Cape Canaveral, Florida 32920.

35. Dale, J.D.; Ackerman, M.; Gilpin, R.R.; Forest, T. 1980 (August). "The Alberta Home Heating Research Facility Update I—The 1979-1980 Heating Season." *Proc. National Conference Solar Energy Society of Canada, Inc.*; Vancouver, British Columbia, 6-10 August 1980, pp. 693-7011.

36. Rogers, B.T. 1980 (June). "Preliminary Report on Sundwelling Passive Units at the Ghost Ranch." *Proc. American Section of the International Solar Energy Society*; Phoenix, Arizona, 2-6 June 1980, pp. 46-52.

37. Calthorpe, P. 1978 (March). "The Farallones Institute Study of Five Passive and Hybrid Space Heating Systems." *Proc. Second National Passive Solar Conference;* Philadelphia, Pennsylvania, 2-6 June 1980, pp. 146-152.

38. Benton, C.C.; Akridge, J.M. 1981 (January). "Interim Report: Passive Solar Curriculum Development Project." Department of Architecture, Georgia Institute of Technology; Atlanta, Georgia, Lab No. 2, pp. 7-10.

39. Balcomb, J.D., et al. 1977. "Passive Solar Heating of Buildings." Los Alamos Scientific Laboratory report LA-UA-77-1162.

40. Hyde, J.C. 1980 (October). "Performance of Night Insulation and Selective Absorber Coatings in L.A.S.L. Test Cells." *Proc. Fifth National Passive Solar Conference;* Amherst, Massachusetts, 19-26 October 1980, (LA-UR-80-2268), pp. 277-281.

41. MacPhee, C.W., editor. *ASHRAE Handbook of Fundamentals* American Society of Heating, Refrigerating, and Air Conditioning Engineers, Inc., New York, Chapter 24.

42. Perry, J.E., Jr. 1977 (October). "Mathematical Modeling of the Performance of Passive Solar Heating Systems." Presented at the Mediterranean Working Group of the NATO Committee on the Challenge of Modern Society, Nice, France, 10-12 October 1977 (LA-UR-77-2345).

43. Wray, W.O. 1980 (October). "A Quantitative Comparison of Passive Solar Simulation Codes. *Proc. Fifth National Passive Solar Conference*; Amherst, Massachusetts, 19-26 October 1980 (LA-UR-80-2267), pp. 118-131.

44. Clinton, J.R. 1979 (October). "The Sea-Pass Passive Simulation Program." *Proc. Fourth National Passive Solar Conference*, Kansas City, Missouri, 3-5 October 1979, pp. 202-206.

45. Sebald, A.V. 1981. "Efficient Simulation of Large, Controlled Passive Solar Systems: Forward Differencing in Thermal Networks." Final Report, U.S. Department of Energy, Contract Number DE AC04-79AL10891. University of California, San Diego, California.

46. McFarland, R.D. 1978 (October). "PASOLE: A General Simulation Program for Passive Solar Energy," Los Alamos Scientific Laboratory LA-7433MS.

47. Kohler, J.T.; Sullivan, P.W. 1979. TEANET User's Manual Total Environmental Action, Inc., Harrisville, New Hampshire.

48. Arumi-Noe, F. 1978 (March). "A Model for the DEROB/PASOLE System." *Proc. Second National Passive Solar Conference*; Philadelphia, Pennsylvania, 16-18 March 1978, pp. 529-533.

49. Abrash, M., et al. 1978 (March). "Modeling Passive Buildings Using TRNSYS." *Proc. Second National Passive Solar Conference*; Philadelphia, Pennsylvania, pp. 398-403.

50. Judkoff, R., et al. 1980 (October). "A Comparative Study of Four Passive Building Energy Simulations: DOE-2.1, BLAST, SUNCAT-2.4, DEROB-III." *Proc. Fifth National Passive Solar Conference*, Amherst, Massachusetts, 19-26 October 1980, pp. 126-130.

51. Balcomb, J.D., et al. 1980. *Passive Solar Design Handbook*: Vol. II Passive Technical Information Service, Springfield, Virginia.

52. Frey, D.; McKinstry, M. 1980. *Installation Manual: SERI Class B Passive Solar Data Acquisition System.* Solar Energy Research Institute, Golden, Colorado.

53. D'Albora, E.G. 1981 (August). "Performance Results of Passive Test Rooms." Pacific Gas and Electric Company, Department of Engineering Research Report 005-81.2, San Ramon, California.

54. Wessling, F.G. 1978 (March). "Solar Retrofit Test Modules." *Proc. Second National Passive Solar Conference*; Philadelphia, Pennsylvania, 16-18 March 1978, pp. 445-449.

55. Jones, R.E., Jr. 1978 (August). "Results from Passive Solar Test Room Investigations in a Cold Climate." *Proc. American Section of the International Solar Energy Society Conference;* Denver, Colorado, Vol. 2.2, pp. 53-58.

ACKNOWLEDGEMENTS

The author wishes to thank Douglas Balcomb for his guidance and encouragement, Joe Perry and Bob McFarland for their many helpful discussions on heat transfer and simulation methods and Stan Moore and Lee Dalton for their help on measurement and data acquisition.

Drawings are by Dennis Colley of COL-TEC, Phoenix, Arizona, based on illustrations supplied by the author as indicated.

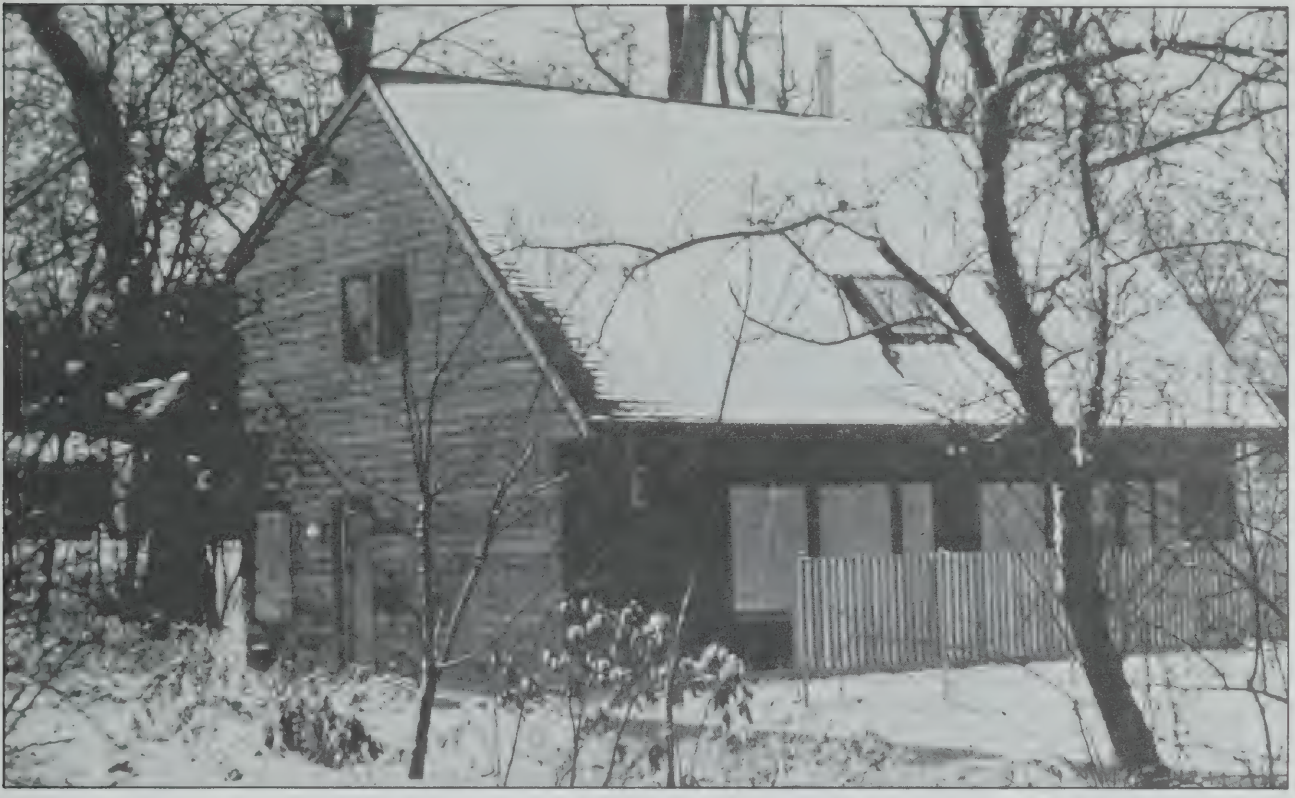

Figure 1: This survey house in Highland Park, Illinois, is heated by a simple direct gain system with a tile-covered storage floor. Movable window insulation reduces heat loss; louver shades prevent excessive heat gain.

Non-Instrumented Performance Evaluation of Passive Solar Homes in the United States

Selected Results from a Class C Survey of more than 300 Homes

By BETH SACHS, BLAIR HAMILTON, KATHERINE CLOUGH and RON ALWARD
The Memphremagog Group, P.O. Box 456, Newport, Vermont 05855

ABSTRACT

Class C is one of three levels of passive solar performance evaluation which have been carried out as part of a systematic national effort sponsored by the U.S. Department of Energy. The Class C approach attempts to determine as much as possible about the performance of passive solar buildings without instrumentation. This article reports selected results regarding the system characteristics and performance of more than 300 passive solar homes throughout the United States. All results are based on Class C data from new or retrofitted houses occupied for one full year.

INTRODUCTION

How well do passive solar homes work? A number of buildings around the country have been instrumented and monitored individually to begin answering that question; however, for the most part these evaluations have not followed a single comprehensive and systematic plan and, even if they had, providing such evaluation for all types of passive systems in all the diverse climates of the United States would be prohibitively expensive. Furthermore, even instrumented evaluation can not fully address the more qualitative aspects of performance which are perceived by the occupants, such as heat distribution and overall thermal comfort.

The D.O.E. Plan

In response to these circumstances, in late 1979 the U.S. Department of Energy (D.O.E.) commissioned a comprehensive program with standardized evaluation methods at three levels of precision. Class A, the highest level of instrumentation and accuracy, provides data to validate computer models and to answer the question of why a particular system works, and how its separate design elements contribute to the performance of the whole. Class B, a more moderate level of instrumentation, determines how well a particular system works—what energy savings can be attributed to the passive features in a specific time frame. Class C, the non-instrumented level, attempts to learn as much as possible at the least possible cost about the performance of a large number of passive solar buildings.

Surveying the large number of sites made possible by the relative simplicity and low cost of the Class C level provides a statistically important data base. A large data base is the only practical basis from which to draw conclusions about such factors as the relative performance of several systems under different climate or use conditions, or about the average performance of passive solar buildings in general. Non-instrumented data are useful in the aggregate, even though the individual building information may not be as precise or as scientifically accurate as that supplied by evaluations using instruments.

Class C data also has a wide variety of other uses. Indoor temperatures perceived by the occupants, identified problems and comments by occupants can be used to assess the relative comfort and discomfort levels being achieved, in passive solar homes. Cost and energy consumption data can provide feedback on the degree to which passive solar cost and performance goals are being met. The frequency and seriousness of problems encountered in existing passive solar homes provides critical identification of areas where further research and development may be necessary. Comparisons of auxiliary energy consumption with non-solar homes can be made to estimate the impact of passive solar residential construction on national energy consumption.

Accordingly, D.O.E. funded each of the four Regional Solar Energy Centers (R.S.E.C.s) to collect and analyze data in their respective areas and the Solar Energy Research Institute (S.E.R.I.) in Golden, Colorado, to analyze the data nationally. S.E.R.I., in turn, subcontracted management and technical analysis work to the Memphremagog Group, a nonprofit research, technical assistance and consulting organization specializing in programs leading to community self-reliance.

METHODS

Site Selection

The selection of sites was subject to various needs associated with different end uses of the data. All of the sites had to meet two minimum criteria:

- that the system had been fully operational and the home occupied for at least one full year, and

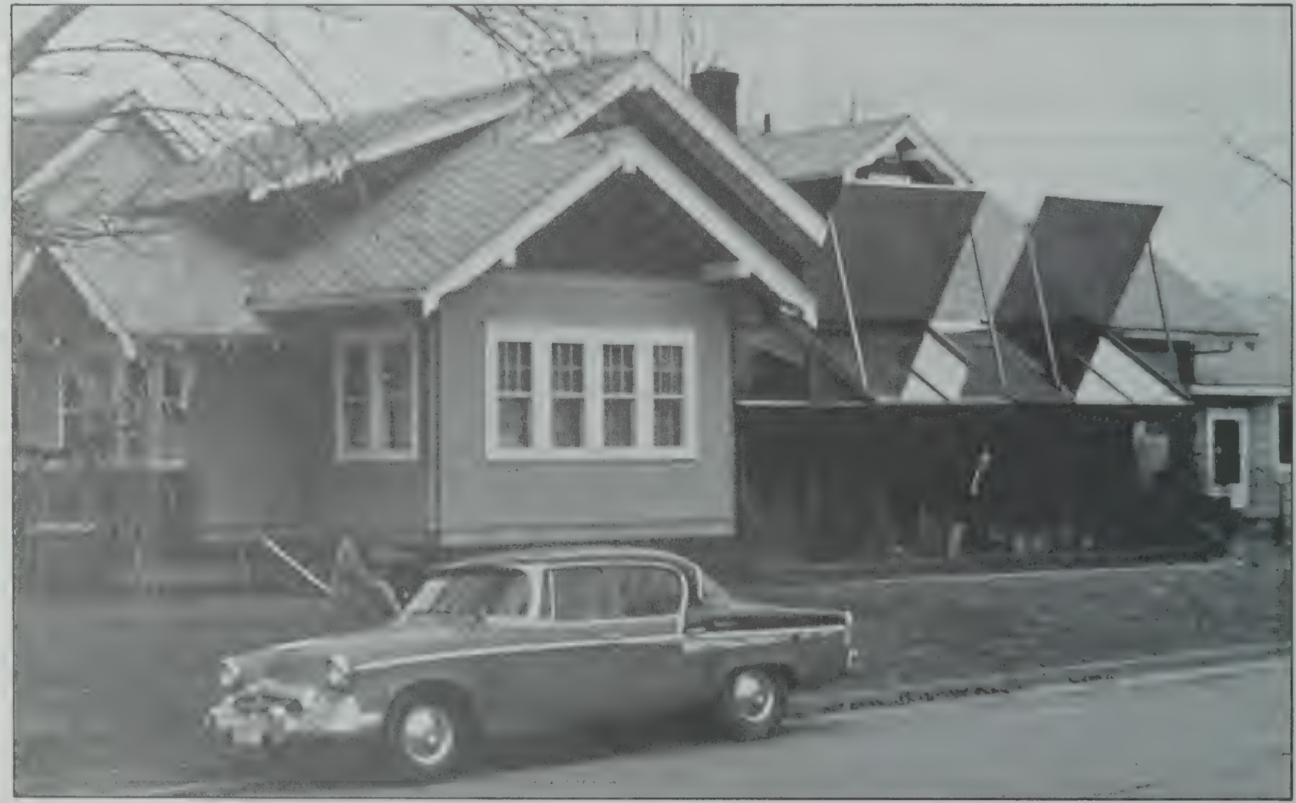

Figure 2: In Vermillion, South Dakota, the survey included a retrofit greenhouse, located off of the kitchen and dining areas. The house is also heated by direct gain through additional south-facing windows.

- that a full year of complete energy consumption records be obtainable.

In addition, each of the R.S.E.C.s had its own priorities for site selection related to its programs in technical assistance, public information and other aspects of commercialization of passive solar technology.

Data Collection

Both the observations of trained auditors and the perceptions of occupants were used to collect the data. Two questionnaires were used to gather this information. The questionnaire that was filled out by the occupants gathered information on:

- why a passive solar home or retrofit was chosen;
- what information sources were used and how useful they were;
- perceived incremental cost of passive solar;
- kinds of problems encountered and their seriousness;
- perceived passive system performance;
- overall satisfaction level;
- demographics.

The second questionnaire, completed by auditors who visited each site, was designed to provide an objective thermal description of the house and covered the following areas:

- the environment in which the house is situated, including site, solar access, wind exposure and local weather data;
- a thermal description of the building in enough detail to calculate overall heat loss and gain;
- information on internal heat gains such as appliances, furnaces, water heaters, lighting and occupants;
- a detailed description, including sketches, of all of the passive solar heating and cooling systems;
- information on how auxiliary energy is used, including details on equipment and its operation;
- information on auxiliary energy sources and use (fuel or utility bills supplied by the occupant or utility) for at least one year.

Auditors with technical backgrounds and familiarity with passive solar systems were hired by each of the regional centers and trained by The Memphremagog Group in a coordinated program to reduce inconsistencies in data gathering. Both the training sessions and the audit form were designed to minimize auditor-specific influence on the data. The auditors visited each site to administer the occupant questionnaire and gather the technical data specified on their forms. Three hours of an auditor's time were required to complete a typical audit.

Analysis of Audit Data

The data from the occupant questionnaires were tabulated and analyzed regionally by the R.S.E.C.s and Market Facts, Inc., a market research firm based in Chicago, Illinois. The national analysis of the occupant responses was completed by S.E.R.I. Preliminary results of both regional and national analyses were presented in two papers published last year.[1, 2]

This paper provides selected results from Memphremagog's analysis of the data collected by auditors. A national report covering all results from the Class C evaluation program is expected to be published by S.E.R.I.[3]

RESULTS

General Description of the Sample

All of the sites audited as part of the Class C program are residential buildings. (See Fig. 1 for an example.) Of the total of 321* sites, 24 sites (7%) are retrofits. (See Fig. 2.) Ninety-seven percent of the homes were described as single-family detached and 76% were custom-built. The type of construction was primarily—76%—wood frame. The mean heated floor area was 2136 ft^2 *(198.4 m^2)*.

Ninety-seven of the sites were located in the Northeast, 86 sites in the South, 72 in Mid-America and 66 in the West.

Eighty-eight percent of the audited homes were built and occupied within the time period 1977 to 1980. The remaining 12% were built between 1900 and 1976—primarily after 1974.

Indoor Temperature

Unlike conventionally-heated houses, many of the sites did not have thermostats and therefore the indoor temperature figures reported on the audit form were based on the occupants' perception of the temperature. In some cases, occupants' estimations were aided by measurements they had made with a thermometer. While occupant perceptions can be quite different from actual indoor temperatures, this information is still useful, as it provides the occupants' evaluation of one aspect of thermal comfort.

Average temperatures reported are time- and space-weighted. The average indoor temperature for all sites was 65.5 °F *(18.6 °C)*, average daytime temperature 68.1 °F *(20.1 °C)* and average nighttime temperature 63.1°F *(17.3°C)*. These data are summarized in Fig.3,and invite closer scrutiny and comparison with similar data for non-solar homes. Seventy-seven percent of the sites maintain an average daytime temperature of between 64 °F *(17.8 °C)* and 72 °F *(22.2 °C)*. Those with cooler houses often had some explanation such as the

---

*The sample number varies between data items because all audits were not able to complete all questions.

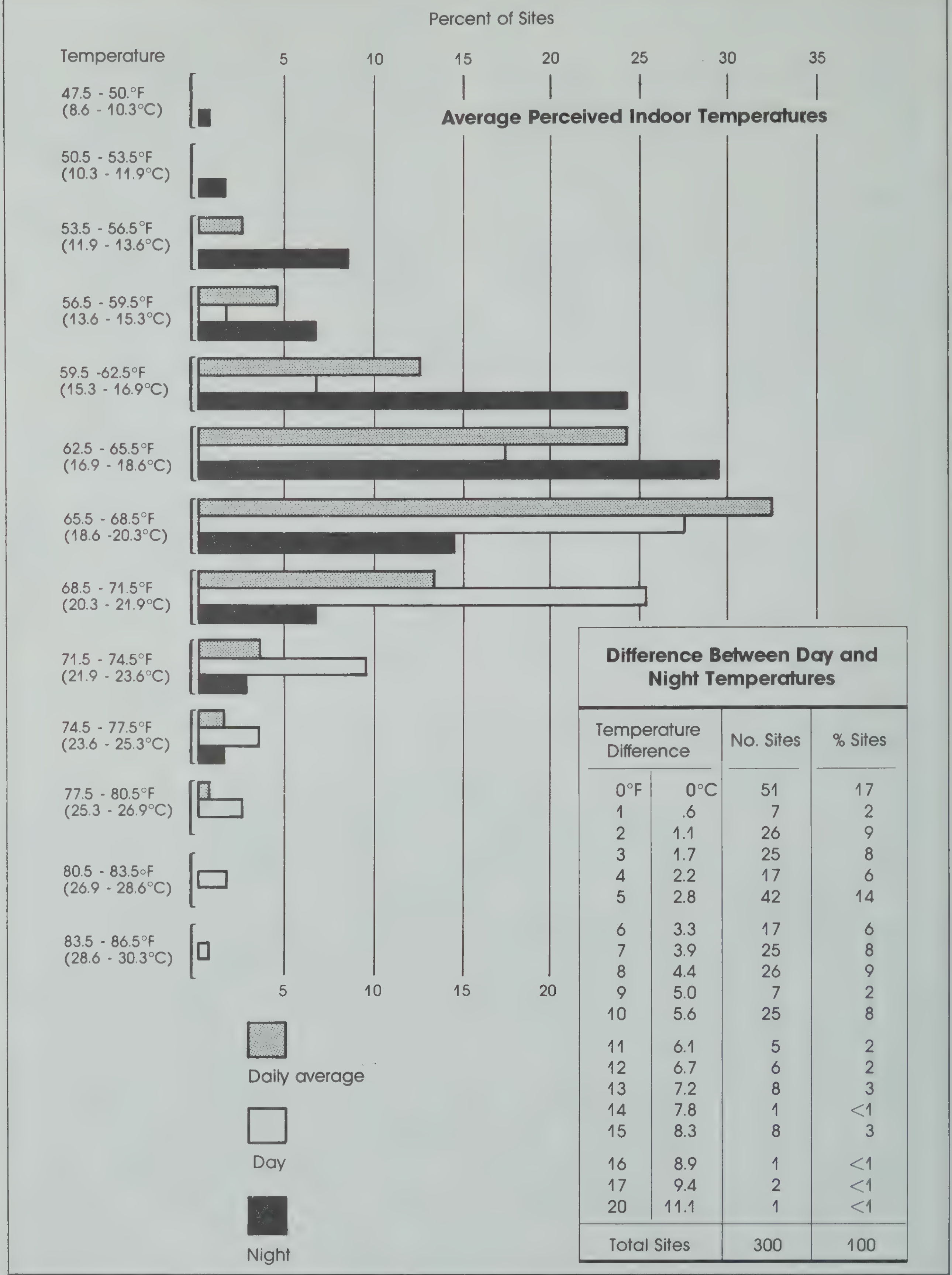

Difference Between Day and Night Temperatures

Temperature Difference		No. Sites	% Sites
0°F	0°C	51	17
1	.6	7	2
2	1.1	26	9
3	1.7	25	8
4	2.2	17	6
5	2.8	42	14
6	3.3	17	6
7	3.9	25	8
8	4.4	26	9
9	5.0	7	2
10	5.6	25	8
11	6.1	5	2
12	6.7	6	2
13	7.2	8	3
14	7.8	1	<1
15	8.3	8	3
16	8.9	1	<1
17	9.4	2	<1
20	11.1	1	<1
Total Sites		300	100

Figure 3: The passive solar homes included in the Class C evaluation tended to have average temperatures perceived by occupants to be between 61° and 72°F (15° and 22°C) for daytime, nighttime and 24-hour daily periods. More than 25% of the sites had day-night differences of less than 3°F (1.7°C).

house being unoccupied during the day or for some of the winter months. In spite of the enormous climatic differences between sites, there was no difference between mean indoor temperatures among regions.

One of the limitations to comfort in a passive solar house can be the swings in temperature experienced on sunny days in the spring and fall. These differences can be buffered by insulation and auxiliary heating and cooling. The data for daytime minus nighttime temperature are shown in Fig. 3. Seventeen percent of the sites recorded no difference between day and nighttime temperatures. Thirty-nine percent of the sites had a 5°-9°F *(2.8°-5°C)* difference and 19% a difference of 10°F *(5.6°C)* or more.

Aperture to Floor Area Ratio

Figure 4 shows the data on the ratio of total area of solar aperture to total floor area of living space, where living space is defined as all areas of the house which always remain within 10°F of the temperature in the primary living area.

The mean ratio for all sites is 0.14. The regional ratios are close to the national mean except for the western region, where it is considerably higher—0.17.

The ratios are quite low and many sites did not meet the study's selection criterion of 0.10 ratio. In most cases, this is because the estimates of floor area made by the occupants during site recruitment excluded the heated basements, which were included in the figures reported by the auditor. The apparently low ratios also reflect the fact that most of the audited homes fall into the low-aperture/low-mass/well-insulated category of solar homes rather than high-aperture/high-mass category.

Solar Heating System Types

The direct gain wall was the most common system type found in audited homes. The direct gain wall classification includes both south-facing window systems and sunspace systems when the sunspace is part of the living space and not separated from the rest of the living space by a storage wall. Three-quarters of the homes monitored had this type. The data on frequency of primary heating system types is presented in Table 1.

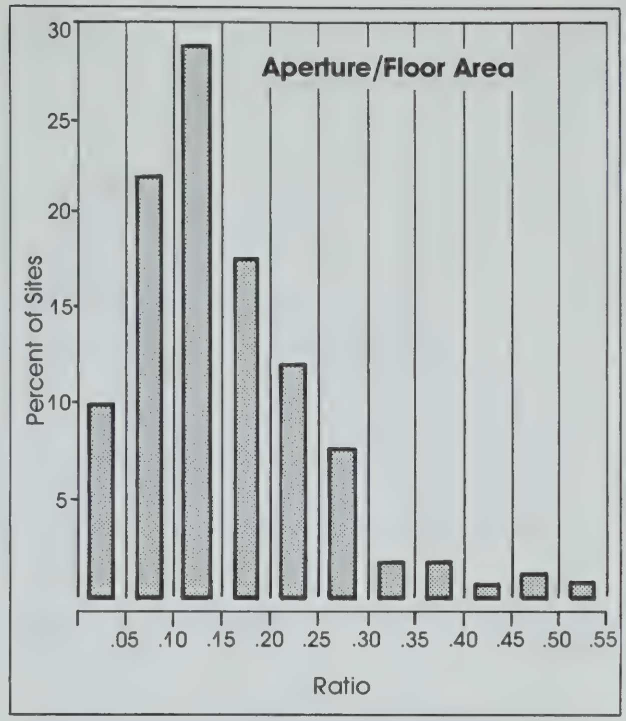

Figure 4: The solar aperture to floor area ratio is generally low. Many of the audited survey homes were of the type featuring small aperture, low mass and high insulation values.

Information was also obtained on the configuration of the primary thermal mass in each home. A variety of configurations were found, with the most common one being the directly sunlit storage floor. The configurations found in the audited

Passive Solar Heating System Types

System Type	No. Sites	% Sites
Direct gain wall, e.g. south-facing windows	240	76
Storage wall, e.g. Trombe wall	33	10
Isolated storage wall/floor, e.g. storage insulated from living space	25	8
Collection wall, e.g. thermosiphoning hot-air collector	10	3
Direct gain roof, e.g. skylight	8	2
Storage roof, e.g. roof pond	1	< 1
Other	1	< 1
Total Sites	318	100

Table 1: Direct gain walls, the most common system type found in audited homes, included both south-facing window systems and sunspace systems not separated from the living space by a storage wall.

Primary Mass Configuration

Configuration	No. Sites	% Sites
Mass is directly sunlit floor of living space, e.g. floor slab	75	32
Mass is directly sunlit wall of living space, e.g. brick wall sunlit through clerestory	39	17
Mass is located remote from living space, e.g. rock bin	31	13
Mass is wall of living space sunlit on outside surface, e.g. Trombe wall	29	13
Mass is in sunspace with controlled air flow to inside living space, e.g. greenhouse with vents into house	25	11
Mass is floor, walls or ceiling of living space which receives only reflected solar radiation, e.g. brick chimney which is never directly sunlit	21	9
Mass is floor, walls or ceiling of living space which does not receive either direct or reflected solar radiation, e.g. masonry walls in north rooms	12	5
Total Sites	232	100

Table 2: In homes which had thermal mass, the directly sunlit storage floor was the most common.

homes are presented in Table 2. This table only includes the sites where thermal mass was present.

Cooling

Table 3 shows the dominant types of passive cooling in audited homes. Seventy-eight percent of the sites were classified as being primarily cooled by direct convection cooling (e.g. windows or vents) and 11% had shading of the aperture classified as the dominant passive cooling mechanism. The distribution of system types in the southern region and nationally is similar.

Auxiliary Heating

Three hundred and twelve of the sites monitored used some form of auxiliary heating and the most striking feature to emerge from the data is a strong preference for wood as an auxiliary heating fuel. Most home owners burn wood in a stove or fireplace; a few use wood furnaces. The data on types of auxiliary heating equipment are presented in Table 4. (See Fig. 5 for example.)

These figures are most meaningful when clumped according to auxiliary energy type. Fig. 6 shows the auxiliary energy types used in the audited passive solar homes on a regional basis. The differences from region to region reflect the availability of different fuels, e.g. oil in the Northeast, and gas in Mid-America. The preference for wood is most marked in the Northeast and Western regions. In the South and in Mid-America, while wood is not the predominant source of auxiliary heat, presumably because of availability, it is still

Dominant Passive Cooling System Types

System Type	No. Sites in South	% Sites in South	No. Sites Nationally	% Sites Nationally
Natural ventilation through the building, e.g. open windows or vents	40	59	180	79
Shading of solar aperture, e.g. overhangs or vegetation	16	24	26	11
Coupling of the building to the ground, e.g. earth-sheltered building	9	13	16	7
Cooling of the outside of the building by wind- or thermal-driven ventilation or evaporation, e.g. evaporative cooling of roof	2	3	3	1
Radiation to the sky, e.g. storage roof cooled by night-sky radiation	1	1	2	<1
Cooling of remote storage mass by natural convection, e.g. regenerative rock bed	0	0	1	<1
Total Sites	68	100	228	100

Table 3: The largest percentage of audited sites featured passive cooling by natural ventilation. The South did not differ significantly from the national preferences in passive cooling.

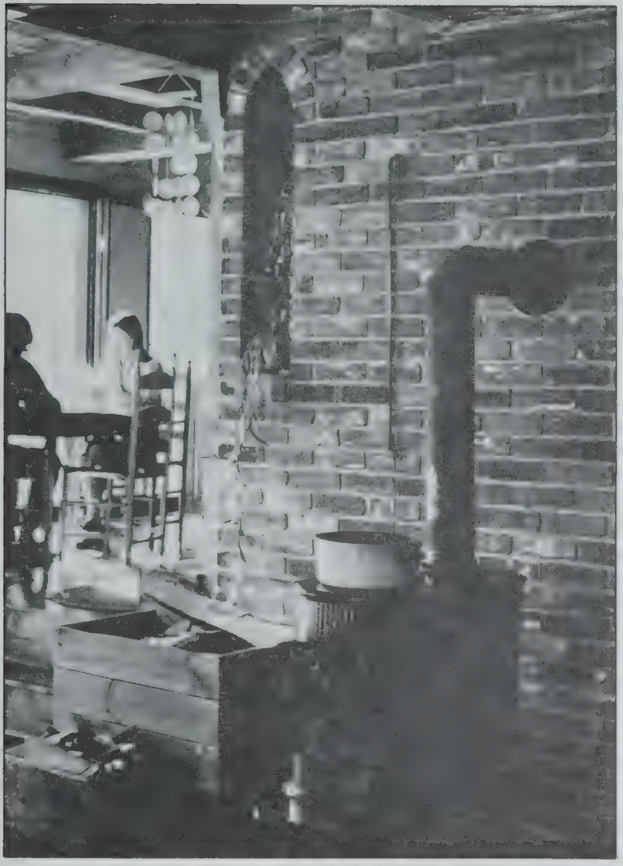

Figure 5 (above) and **Table 4** (at right): Passive solar home owners in the survey most frequently chose fireplaces or woodstoves as their auxiliary heating equipment. The stove above in a house in Yarmouth, Maine, is typical of airtight construction.

Types of Auxiliary Heating Equipment

Type of Equipment	No. Sites	% Sites
Oil-fired hot air furnace	14	4
Oil-fired hydronic space heat	3	1
Oil-fired hydronic space & water heat	7	2
Gas-fired central hot air furnace	56	18
Gas-fired space heater	2	<1
Gas-fired hydronic space heater	9	3
Electric hot air furnace	10	3
Electric resistance heating	18	6
Electric radiant heating	5	2
Heat pump	43	14
Wood-fired hot air furnace	7	2
Wood-fired hydronic space & water heat	2	<1
Woodstove or fireplace	132	42
Woodstove and water heat combination	4	1
Total Sites	312	100

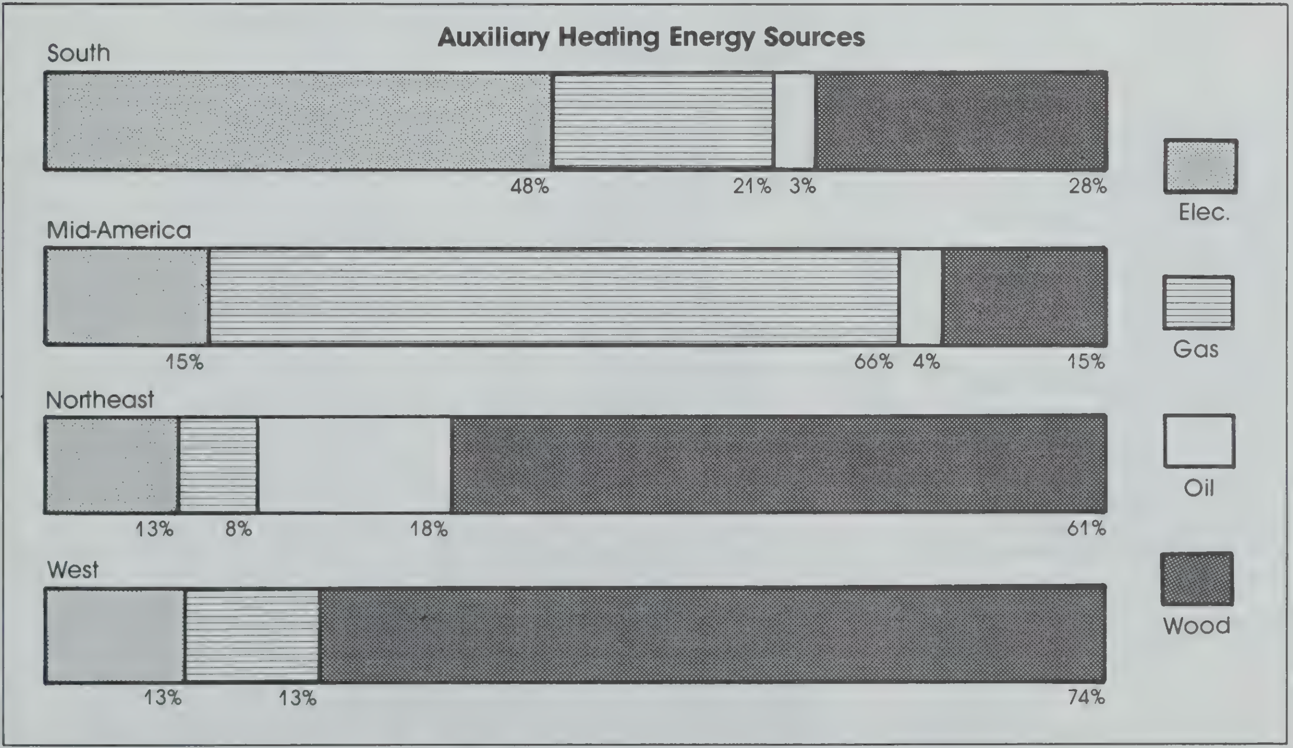

Figure 6: Preferred sources of auxiliary heating energy varied considerably by region, with wood favored in the West and Northeast, gas in Mid-America and electricity in the South.

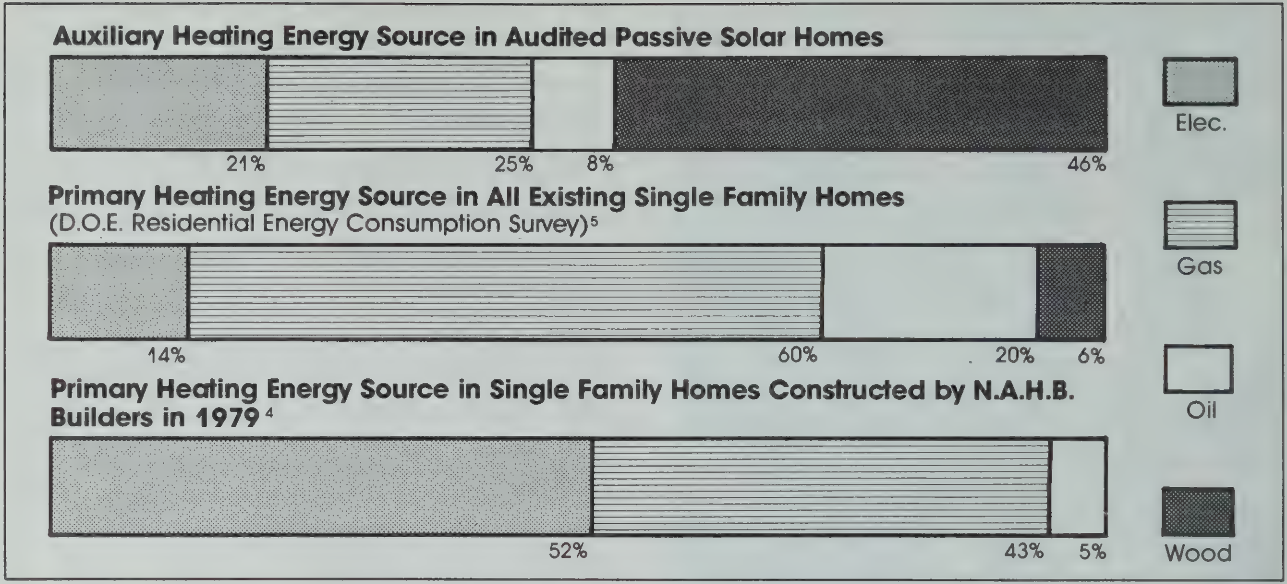

Figure 7: National preferences in sources of heating energy varied considerably between auxiliary heat used in the survey's passive homes and primary heat used in conventional homes.

used in a significant number of the homes. In the South, electricity is the most popular source of auxiliary heat; it is gas in Mid-America.

Nationally, as shown in Fig. 7, wood is the predominant auxiliary energy source, being used in 46% of the audited passive solar homes. Also shown in Fig. 7 is information from two different sources on the types of heating energy used in all single family dwellings in 1979. The data reported by The National Association of Home Builders Research Foundation[4] is from their survey of 3,073 NAHB builders. They show the energy source of the primary heating systems installed by NAHB builders in 63,754 single family dwellings completed in 1979. The data from the Department of Energy's Residential Energy Consumption Survey[5] show the mix

Figure 8 (at right): Total net heat loss ranged between 300 and 600 Btu/hour°F (100 and 300 W/°C) in the greatest percentage of passive solar homes surveyed. Heat loss results were calculated by the auditors based on their inspection of the homes and the use of a standardized technique. This was developed from ASHRAE practices and the Department of Energy Model Audit for the Residential Conservation Service.

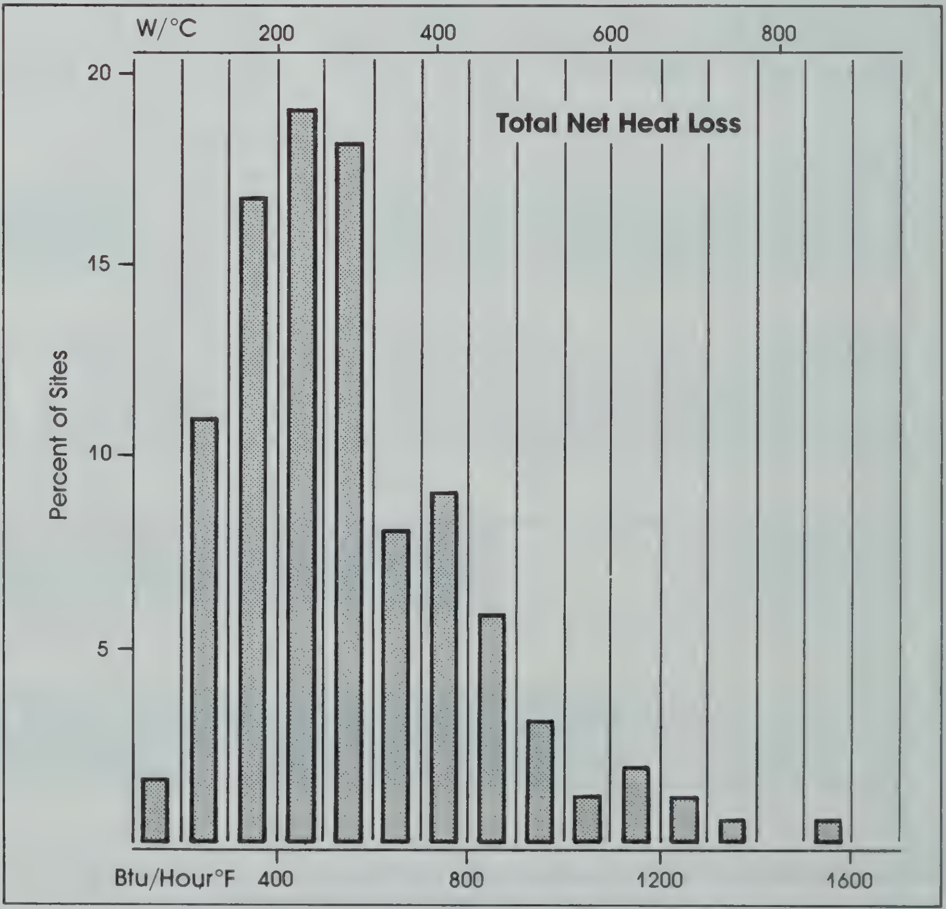

of heating sources for the entire stock of single family dwellings existing in 1979.

Heat Loss

The data on heat loss can be considered to be a measure of the degree of insulation and the tightness of the house. Two aspects of heat loss are presented: a) total net heat loss, expressed in Btu per hour per °F *(W per °C)*, (Fig. 8) and b) normalized loss factor expressed in terms of net heat loss per unit floor area (Fig. 9). Heat loss and infiltration were calculated by the auditors based on their inspection of the homes and the use of a standardized technique. The technique used for these calculations was developed from standard ASHRAE practices and the Department of Energy Model Audit for the Residential Conservation Service.

The mean value of the normalized loss factor for all sites is 0.26 Btu/ft^{2}hour °F *(1.48 W/m^2°C)*. Draftier homes, e.g. those with a higher infiltration rate, have a mean normalized loss factor of 0.31 Btu/ft^2 hour °F *(1.76 W/m^2°C)*, whereas tighter houses with lower infiltration rates have a mean normalized loss factor of 0.23 Btu/ft^2 hour °F *(1.31 W/m^2°C)*. The net household heat loss in colder areas is about the same as in warmer areas.

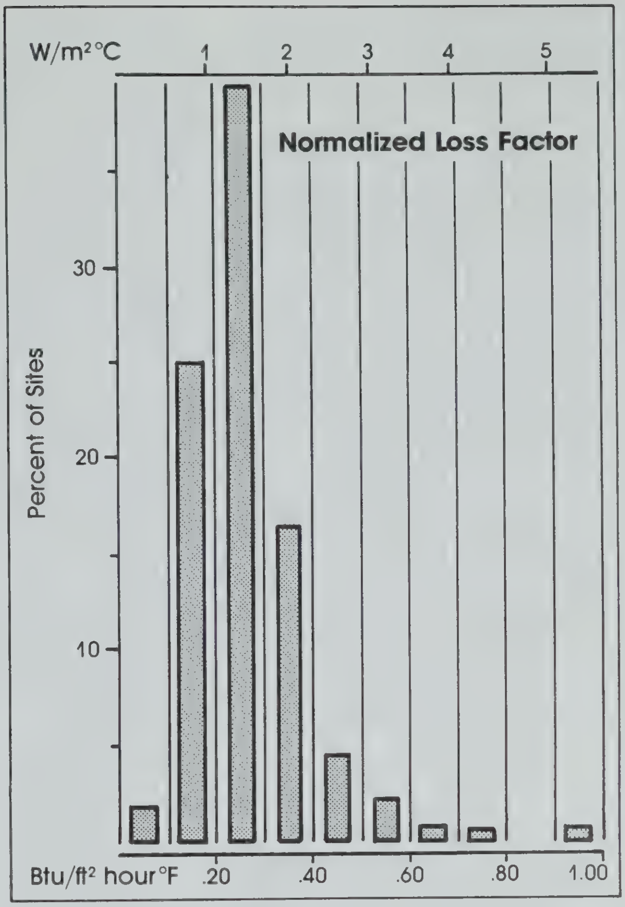

Figure 9 (at right): The normalized loss factor is expressed in terms of net heat loss per unit of floor area. The mean value of the normalized loss factor is 0.26 Btu/ft^2 hour°F (1.48 W/m^2°C).

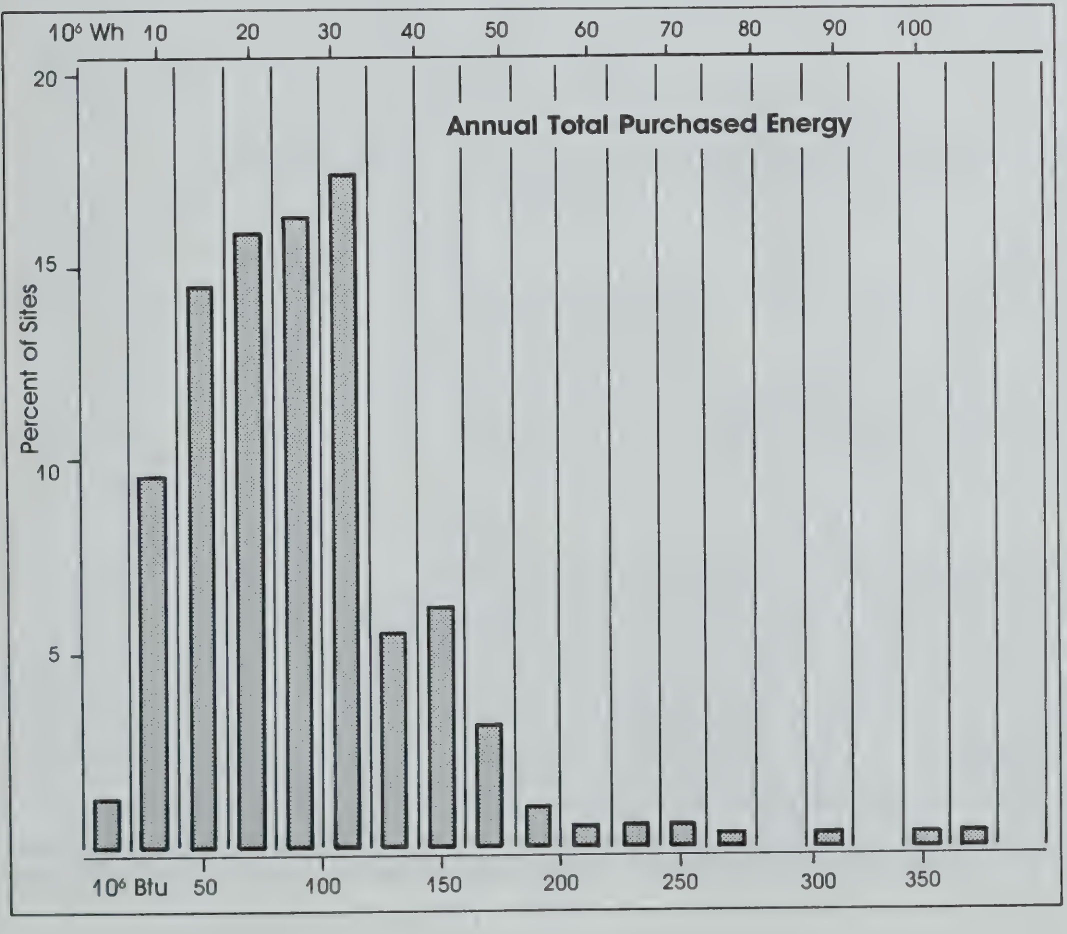

Figure 10 (at left): Annual total purchased energy for 244 audited sites was gathered from occupant records, utilities and/or fuel suppliers. The data are measured energy consumption, with the exception of wood, which was estimated by the homedwellers to the nearest quarter of a cord. See Table 5 for the mean total purchased energy for all audited homes.

Total Purchased Energy

Total purchased energy is defined as the annual total of energy supplied to the building for *all* uses. It is expressed in Btu *(or Wh)* and is the sum of the energy contents of all supplied fuels. See Fig. 10 for the total purchased energy figures for all of the audited sites. This information was gathered from occupant records, utilities and/or fuel suppliers. The data are *measured* energy consumption, with the exception of wood, which was estimated by the homedwellers to the nearest quarter of a cord. Sites were eliminated where the occupants could not confidently estimate their wood use to the nearest quarter of a cord.

Because total purchased energy is a measure of energy *supplied*, buildings which use mostly electricity, for instance, will tend to have lower values for total purchased energy than those which use substantial amounts of oil, gas or wood, where only a fraction of their energy value is delivered to the load due to conversion inefficiencies.

Table 5 shows the mean total purchased energy for all audited homes and a regional comparison.

Total Purchased Energy

Metric		English
10^6 Wh	Region	10^6 Btu
27.8	National	95
29.3	Northeast	100
29.3	South	100
26.7	Mid-America	91
20.5	West	70

Table 5: The national and regional mean values for total purchased energy are based on the annual total of energy supplied to each building for all uses.

Building Performance Index

Building performance index is defined as the total purchased energy normalized by dividing it by floor area. Because the floor area of these audited passive solar homes is larger than average homes, this normalization makes the comparison of solar and non-solar homes more reasonable, as well as providing an index for comparing passive solar homes of different sizes.

Histograms of building performance index for sites in each region are presented in Fig. 11. A histogram of building performance index for all sites is shown in Fig. 11. In Table 6, the building performance index for selected dependencies is presented. The mean annual building performance index for all sites is 47.3 x 10^3 Btu/ft^2 *(149 kWh/m^2)* per year. The highest regional value is 54.0 *(170)* in the Northeast and the lowest is 38.0 *(120)* in the West.

The relatively large standard deviation for sites in the Northeast—28.4 *(89.6)*—suggests a greater variability in the success of passive solar buildings in this region with respect to achieving low levels of building energy consumption. The histogram of building performance index for this region supports this suggestion, showing a cluster of sites with very high building performance indices. Inspec-

Building Performance Index (B.P.I.) for Various Dependencies

Metric				English	
Mean B.P.I. kWh/m^2	Standard Deviation	Dependency	No. Sites	Mean B.P.I. 10^3 Btu/ft^2	Standard Deviation
149	73.8	All sites	244	47.3	23.4
170	89.6	Northeast region	86	54.0	28.4
137	65.6	Mid-America region	56	43.4	20.8
150	58.7	Southern region	66	47.6	18.6
120	55.2	Western region	36	38.0	17.5
151	63.4	Sites with active systems	18	47.9	20.1
141	71.6	Norm. loss factor 0 - 0.3 Btu/ft^2 hr°F (0 - 1.7 W/m^2 °C)	176	44.6	22.7
171	74.1	Norm. loss factor 0.3 - 1.0 Btu/ft^2 hr°F (1.7 - 5.7 W/m^2°C)	73	54.3	23.5
148	56.1	Restricted solar access	19	46.8	17.8
171	72.2	Sites with wood heat	146	54.2	22.9

Table 6: The building performance index is defined as the total purchased energy normalized by dividing it by floor area.

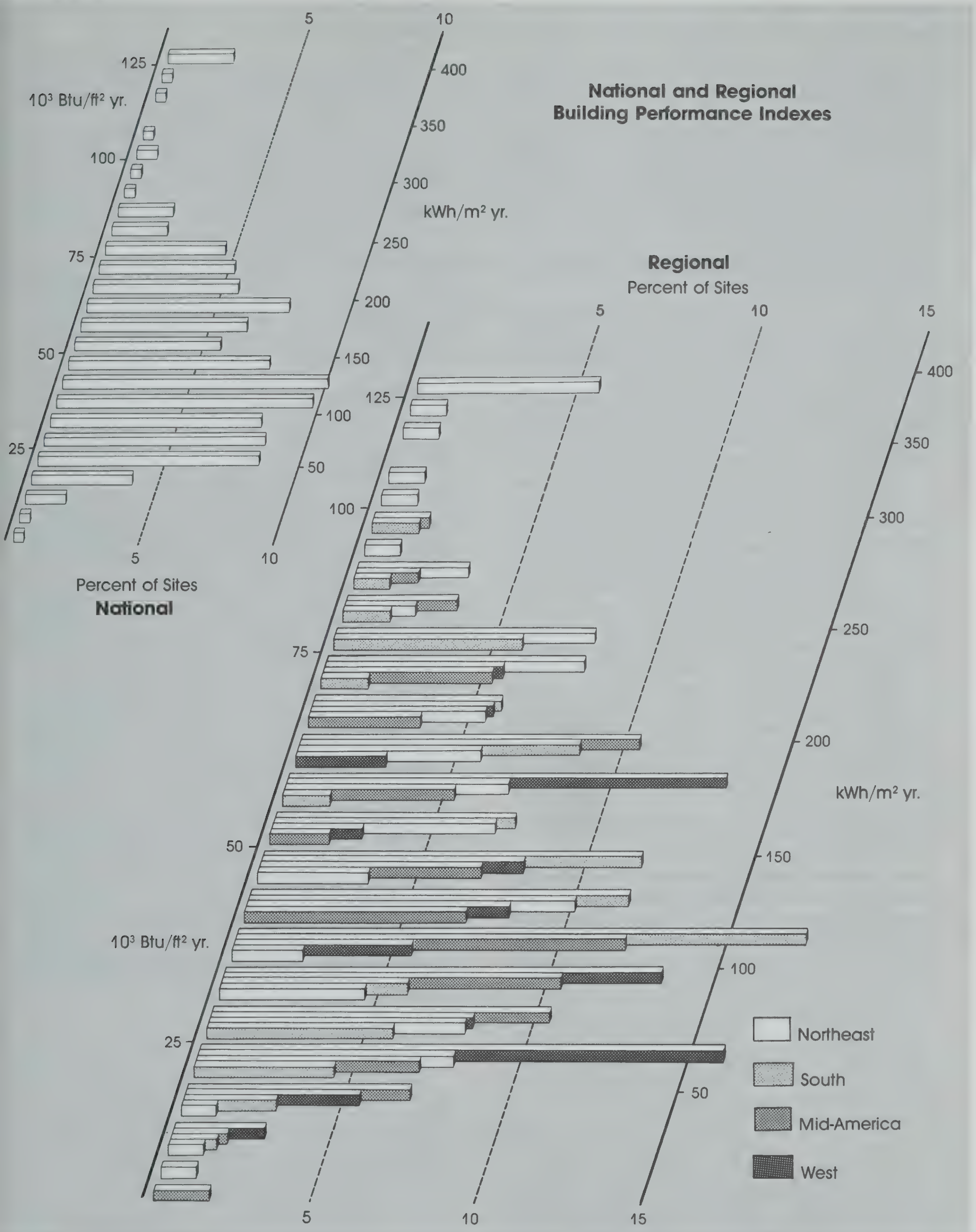

Figure 11: Building performance indexes are compared by region. (Total sites for each region are 36 in the West, 56 in Mid-America, 66 in the South and 86 in the Northeast.) The national building performance index is presented at top left.

tion of the individual audits for these sites reveals that most of them were homes where the auditors noticed major flaws in design or construction. In most cases, these also appear to be early examples, when design principles may not have been well understood.

The average building performance index for sites which also have active space heating systems does not differ from those with passive systems alone. Sites with lower normalized loss factors use less energy than those with higher normalized loss factors. As might be expected, this indicates that the "lossiness" of a house is a significant factor affecting the performance of the audited passive solar homes.

Sites with restricted solar access use no more energy than those with good access, suggesting that their designs compensated for this with larger apertures or higher levels of conservation.

Sites using wood as their primary auxiliary heating source use a higher amount of energy than other sites. The most likely explanation is the lower efficiency with which wood is burned.

It would obviously be very desirable to compare the building performance index of passive solar and non-solar homes. Unfortunately, the D.O.E. Residential Energy Consumption Survey[5] previously referenced does not detail the energy use and size of recently-built, single-family dwellings and the authors have been unable to find any other source for such data. D.O.E. is presently conducting a new survey which should include the data necessary to develop a value for building performance index for reference non-solar homes, making such a comparison possible in the near future. In any case, the results reported here provide a useful yardstick against which designers and analysts can compare the performance of other solar and non-solar homes.

CONCLUSIONS

An audit technique has been developed and demonstrated to be useful in obtaining non-instrumented performance data on passive solar residential buildings. This technique was used to establish a data base of quantitative and qualitative information on various aspects of passive solar home performance.

Generally, the Class C evaluation program confirms that passive solar homes are achieving high levels of thermal comfort. They are using small amounts of auxiliary heat, which is reflected in the relatively low average building performance index. They are also tight and well-insulated homes, as indicated by the low average normalized heat loss factor.

Other significant findings of the survey are that direct gain was the most common passive heating system type, and that the most common primary thermal storage configuration was the directly sunlit storage floor. The dominant passive cooling system, whether in the warmer South of the cooler North, was natural ventilation. In addition, passive solar home owners revealed a strong preference for wood as the primary source of whatever auxiliary heat they required.

REFERENCES

1. Hamilton, B.; Sachs, B.; Alward, R.; Lepage, A. 1981 (September). "Non-Instrumented Performance Evaluation of 335 Passive Solar Homes." *Proceedings of the Sixth National Passive Solar Conference*; Portland, Oregon; 8-12 Sept. 1981.
2. Towle, S.; Thomas, T. 1981 (May). "The Class C Performance Evaluation Program." *Proceedings, U.S. Department of Energy Passive and Hybrid Solar Energy Program Update*; Washington, D.C.; 1981.
3. *Class C Performance Evaluation of Passive Solar Homes—National Report* (Draft), to be published by SERI; Golden, Colorado; 1982.
4. National Association of Home Builders, Research Foundation. *1981 Research Results Report*. Rockville, Maryland, 1981.
5. *Residential Energy Consumption Survey: 1979-1980; Consumption and Expenditures, Part 1: National Data*. U.S. Department of Energy, DOE/EIA-0262/1, 1981.

ACKNOWLEDGEMENTS

Graphs for this article were drawn by Johanna Bertoldo of Tempe, Arizona, based on materials supplied by the authors.

Thermal Impedance of Multi-Pane Windows

Computer Models Assess the Effects of Changing Surface Emissivity, Location and Spacing Between Panes, and of Reducing Free Convection and Gas Conduction

By JOSEPH K.E. ORTEGA
Mechanical Engineering Department, University of Colorado at Denver,
Denver, Colorado 80202

ABSTRACT

In this paper, the thermal impedance (R values) for multi-pane window systems are determined by computer modeling as a function of the emissivity of the surface of the window panes, the location and number of low-emissive surfaces in the system and the spacing between window panes. Also, the effect of reduced free convection and gas conduction between window panes is determined. The results demonstrate that only a small increase in thermal impedance is associated with the addition of each pane of ordinary glass. On the other hand, a significant increase in thermal impedance can be obtained with the use of a low-emissive coating applied to the surface of the window pane. Further improvements can be obtained by reducing or eliminating free convection and gas conduction heat transfer between window panes with low-emissive surfaces that have a partial or total vacuum between panes.

INTRODUCTION

Most buildings lose a significant amount of heat through windows. In the northern half of the United States, 15% to 35% of the total heat loss during winter from a typical house is through the windows.[1] Windows are thermal leaks because of poor insulation qualities. Comparison of the thermal impedance (R value) of a normal double-pane window— $R \simeq 0.4\ (\mathrm{W/m^2\ °C})^{-1}$—to the R value of most building walls— $1.8\ (\mathrm{W/m^2\ °C})^{-1} \leq R \leq 3.5\ (\mathrm{W/m^2\ °C})^{-1}$—clearly demonstrates this fact. *(In English units, $R \simeq 2.0(\mathrm{Btu/h\ ft^2 °F})^{-1}$ for the windows and $10(\mathrm{Btu/h\ ft^2\ °F})^{-1} \leq R \leq 20(\mathrm{Btu/h\ ft^2\ °F})^{-1}$ for the walls.)* The difference in R values is very important in conventional building designs, but is critical in passive solar building designs where windows comprise a significant portion of the building shell.

Investigators have proposed many methods to improve the thermal impedance of windows.[1, 2, 3, 4, 5] Similar methods have been proposed for flat-plate collector glazings; a review of this work is presented by Duffie and Beckman[6] and Kreith and Kreider.[7] For windows, the methods vary from adding window shutters and shades,[1] to applying selective radiation coatings to the window panes and introducing low-conduction/convection fill gas between panes.[2, 3, 4] The amount of insulation provided (i.e. the largest R value) is an important criterion in selecting a window system, and one that is vital in predicting cost effectiveness. The R values of different systems are frequently calculated or determined with different boundary conditions and different evaluation/testing techniques, however; this lack of standardization introduces variability in the determined R value for any system, and also makes it difficult to compare system performance. Little information exists that correlates the thermal impedance of window systems to different boundary conditions (e.g., external wind speeds). Silverstein[2] presented data in tabular form correlating the window thermal impedance to a variety of wind velocities on the external glass pane. However, because he used semiempirical convective formulae in the calculations, Silverstein estimates that the accuracy of the conductance calculations are approximately 15% of the absolute value.

In the present investigation, an approach is taken that accounts for the variability of the boundary condition caused by changing external wind conditions. The present analytical investigation is based on a theoretical configuration consisting of a

---

This work was performed while the author was principal scientist in the Building Systems Branch of the Solar Energy Research Institute, Golden, Colorado.

hot-plate and cold-plate, with the window system placed between the plates. This configuration is advantageous for a number of reasons:

- It provides constant and well-defined boundary conditions for numerical thermal simulations.
- All of the convection couplings are the same and are well-defined (empirical relationships for free convection within enclosures are used).
- Validation of the analysis by experimental investigation is simplified.
- Maximum and minimum values for the thermal impedance provided by any window system due to variable wind conditions can be determined.

Analytical and experimental investigations resulting in the determination of maximum and minimum values for thermal impedance would benefit both designer and researcher. The designer could take into consideration minimum values of thermal impedance provided by a window system, and the researcher could examine practical ways to achieve maximum values of thermal impedance in real building applications.

Both Silverstein[2] and Selkowitz[3] consider methods to reduce convective heat transfer between window panes. For example, both consider using a variety of fill gases to reduce pane-to-pane convective heat transfer. In general, these methods can improve the insulation characteristics of multipane window systems, and as the results of the present investigation show, reduced pane-to-pane convective heat transfer is most effective when thermal radiation exchange between panes is significantly reduced. The effect of the absence of free convection and gas conduction heat transfer between window panes as a function of radiation exchange between window panes was also investigated to determine the upper theoretical limit of thermal impedance that various window systems can provide.

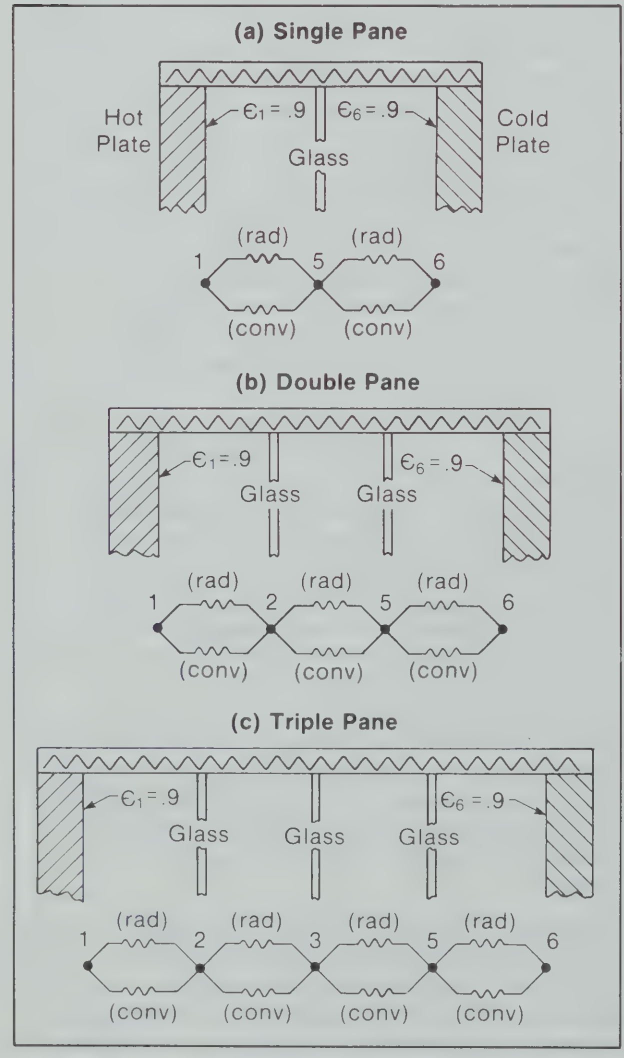

Figure 1: Single-, double- and triple-pane window systems are represented in nodal thermal models.

MATERIALS AND METHODS

The thermal impedance provided by double-pane and triple-pane window systems was evaluated as a function of surface emissivities and window pane spacing using numerical nodal thermal models. The nodal thermal models representing single-pane, double-pane and triple-pane window systems are presented in Fig. 1. In all systems, nodes 1 and 6 are constant temperature boundary nodes. Node 1 represents a hot plate with a fixed surface emissivity of 0.9, maintained at 26.7 °C *(80°F)*. Node 6 represents a cold plate with a fixed surface emissivity of 0.9, maintained at 4.4 °C *(40°F)*. In the single-pane window (a), the glass pane is represented by node 5. Glass panes for all window systems considered here are represented by a single node because previous investigations[2, 8] have determined that the surface-to-surface temperature gradient is very small. The resultant impedance provided by solid conduction through the glass pane is much smaller and is insignificant compared to the impedance provided by convection and radiation exchange between surfaces. Nodes 2 and 5 represent the glass panes for the double-pane window system (b). Nodes 2, 3 and 5 represent the glass panes for the triple-pane window system (c). In all cases, the glass panes are considered to be totally opaque to thermal radiation.

The Martin Interactive Thermal Analysis System (MITAS), a heat transfer computer program, was used to obtain a steady-state solution for node temperatures and heat flows between nodes.[9] Subroutines were written and used in the solution to calculate gas conduction and free convection as a function of the temperature of the surfaces and the enclosed gas, and the spacing between surfaces. The subroutines used empirical relationships for the Nusselt number Nu, as a function of the Rayleigh number Ra and spacing b between the two surfaces[10]:

$$Nu_1 = 0.0605\ Ra_b^{1/3}$$

$$Nu_2 = (1 + \{\,0.104\ Ra_b^{0.293}/[1 + (6310/Ra_b)^{1.36}]\}^3)^{1/3}$$

$$Nu_3 = 0.242\ (Ra_b/AR)^{0.272}$$

$$Nu_b = (Nu_1,\ Nu_2,\ Nu_3)_{max} \qquad (1)$$

The values for kinematic viscosity and thermal conductivity as functions of temperature were put in the program as arrays and were used by the subroutines in the solution technique.

User input for the MITAS program's radiation conductors is in the form $\sigma A_i \pounds_{ij}$, where σ is the Stefan-Boltzmann constant, A_i is the surface area, and $\pounds_{ij}$ is the Hottel script F or gray body radiation interchange factor. For this investigation, the hot and cold plates were simulated to be parallel to the glass surfaces. The spacing between glass panes was varied. £ was calculated for two parallel gray planes with different values for total surface emissivity ϵ:

$$\pounds_{ij} = \left(\frac{1-\epsilon_i}{\epsilon_i} + \frac{1-\epsilon_j}{\epsilon_j}\left[\frac{A_i}{A_j}\right] + \frac{1}{F_{ij}}\right)^{-1}. \qquad (2)$$

F_{ij} is the radiation shape factor, and A_i and A_j are the respective areas of the panes.

The values for radiation and free convection conductors and for heat fluxes were calculated using a surface area of 0.836 m^2 *(9 ft^2)*. The total impedance R_T was calculated from Eq. 3:

$$R_T = \frac{(T_1 - T_6)\,A}{Q}\,. \qquad (3)$$

The surface-to-surface impedance R_S was calculated from Eq. 4:

$$R_S = \frac{(T_2 - T_5)\,A}{Q}\,. \qquad (4)$$

The test configuration described here (a window system between a hot plate and cold plate) will produce easily reproducible boundary conditions for any window system tested, a major advantage for establishing evaluation standards and validating analytical results with experimental results. Also, because the resulting heat transfer coefficient h on both the interior and exterior window surface will be smaller than in actual building applications, the maximum thermal impedance of the window system can be determined. For example, the value of h on the inside window surface in a normal building will be between 1.7 and 4.0 W/m^2 °C *(0.3 and 0.7 Btu/h ft^2°F)*. In the present test configuration, h varied between 1.1 and 2.0 W/m^2 °C *(0.20 and 0.35 Btu/h ft^2°F)*. On the outside surface h can vary between 2.8 and 34.0 W/m^2 °C *(0.5 and 6.0 Btu/h ft^2°F)*. Again in the present test configuration, h varied between 1.1 and 2.0 W/m^2 °C *(0.20 and 0.35 Btu/h ft^2°F)*. Thus R_T presented for this configuration represents a "best" case value, or the maximum thermal impedance the window system can produce.

The minimum value of thermal impedance provided by the window system can be calculated when there is an infinite conductance from the inner and outer surfaces ($h_{12} = h_{56} = \infty$) to the hot plate and cold plate. Another way to calculate the minimum impedance is to treat the inner and outer surfaces as the hot and cold plates, and use these temperatures to calculate ΔT. Thus the inner surface to outer surface thermal impedance (or surface-to-surface thermal impedance R_S) represents

Nomenclature and Glossary

A = surface area.

AR = aspect ratio, L/b.

b = spacing between window pane.

c = specific heat = J/kg K *(Btu/lb$_m$ F)*.

E_C/E_T = normalized convection energy exchange.

E_N = normalized energy exchange.

E_R/E_C = radiation-to-convection ratio.

E_R/E_T = normalized radiation energy exchange.

F = radiation shape factor.

g = acceleration of gravity = m/sec^2 *(ft/hr^2)*.

Gr_b = Grashof number = $\beta\, g\, b^3\, \Delta\, T/\gamma^2$ (dimensionless). The Grashof number is a measure of the relationship of the buoyant to viscous forces.

h = heat transfer coefficient.

k = thermal conductivity = W/m K *(Btu/hr ft °F)*.

L = window height.

Nu_b = average Nusselt number based on b.
= hb/k (dimensionless). The Nusselt number is a coefficient of heat transfer.

Pr = Prandtl number = $c_p\mu/k$ or γ/α (dimensionless). The Prandtl number is a measure of how rapidly momentum is dissipated compared to the rate of diffusion of heat through a fluid.

Q = heat flow rate.

Ra_b = Rayleigh number = Gr_bPr (dimensionless).

R = thermal impedance.

T = temperature.

α = thermal diffusivity = $k/\rho c$ = m^2/sec *(ft^2/h)*.

β = temperature coefficient of volume expansion = 1/°R *(1/K)*.

γ = kinematic viscosity, μ/ρ = m^2/sec *(ft^2/hr)*.

σ = Stefan-Boltzman constant. The Stefan-Boltzmann constant is the ratio of the emissive power of a black body per unit of area and time to the absolute temperature of the body.

μ = absolute viscosity = N sec/m^2 *(lb$_m$/ft sec)*.

N = newton, the unit of force required to accelerate a mass of one kilogram one meter per second per second.

ρ = mass density = kg/m^3 *(lb$_m$/ft^3)*.

ϵ = total surface emissivity.

£ = Hottel script F or gray body radiation interchange factor. $\pounds_{ij}$ is the fraction of the energy emitted by surface i and absorbed by surface j.

Subscripts:

i, j, 1, 2, 3, 5, 6 = surface or node i, j, 1, 2, 3, 5, 6.

S = surface to surface value, calculated between nodes 2 and 5.

T = total value, calculated between nodes 1 and 6.

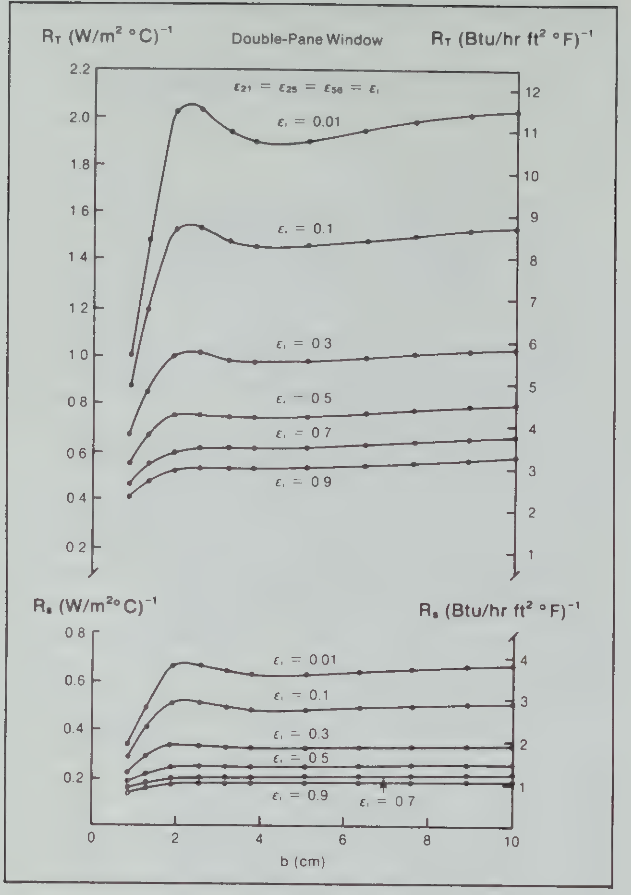

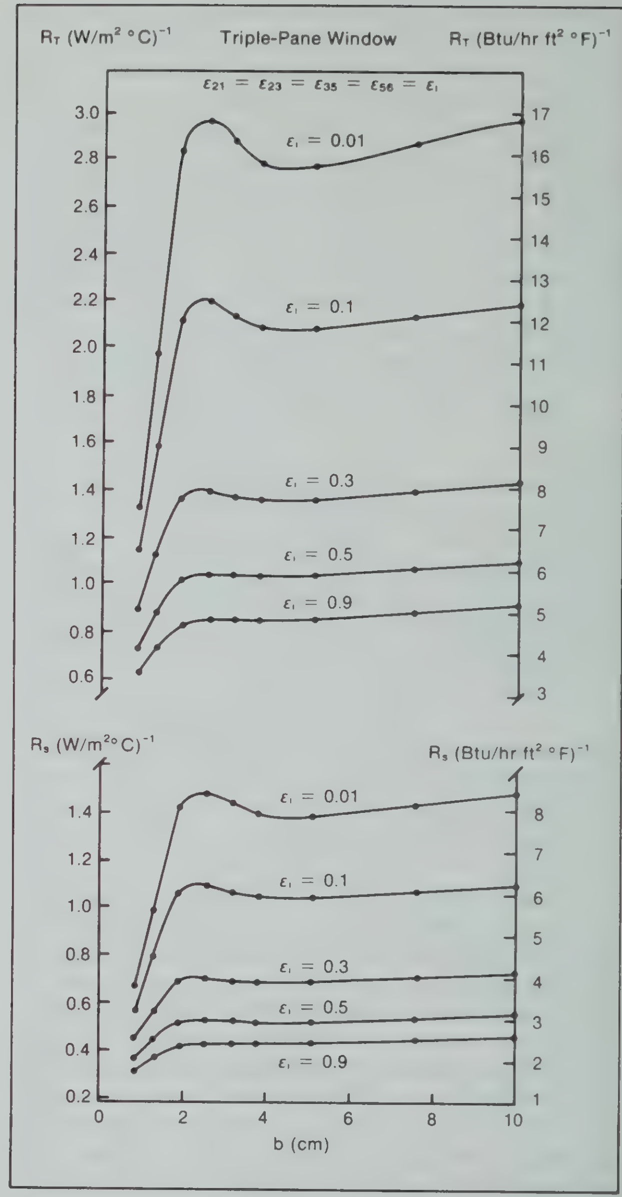

Figure 2 (above) **and 3** (at right): R_T and R_S are shown as a function of spacing b for double-pane (above) and triple-pane (at right) windows. ϵ_{21} is the emissivity of the inner glass pane surface (node 2) facing the hot plate, ϵ_{25} is the emissivity of the inner glass pane surface (node 2) facing the outer glass pane (node 5), ϵ_{56} is the emissivity of the outer glass pane surface (node 5) facing the cold plate, ϵ_{23} and ϵ_{35} are the surface emissivities of nodes 2 and 3 facing nodes 3 and 5, respectively.

the minimum thermal impedance expected from a window system.

DISCUSSION

The total thermal impedance R_T and surface-to-surface thermal impedance R_S are plotted in Figs. 2 and 3 as a function of the spacing between window panes b, for double-pane and triple-pane window systems with varying surface emissivities. The results demonstrate that when the window surface emissivity is large ($\epsilon_i = 0.9$), R_T and R_S are nearly constant for window spacings larger than 2 cm. For smaller spacings —$b < 2$ cm. *(<0.8 in.)*—R_T and R_S decrease. When the window surface emissivity is small — ϵ_i = 0.01 — the thermal impedance is much larger. When window spacings are between 2 cm. and 3 cm. *(0.8 in. and 1.2 in.)* in both double-pane and triple-pane window systems, R_T and R_S reach a maximum value; R_T and R_S decrease rapidly when window spacings are less than 2 cm. *(0.8 in.)*.

Figures 4 and 5 plot R_T and R_S versus $£_{ij}$ for double-pane and triple-pane windows, respectively. Spacings between glass panes, the hot plate or cold plate, and the adjacent pane, were 2.54 cm. *(1.0 in.)*. Since the radiation shape factor F_{ij} is nearly 1.0 for this configuration, and the areas of the glass panes, hot plate, and cold plate are the same—0.836 m² *(9 ft²)*— £ (on the horizontal axis) varies only with the emissivity of the glass panes according to Eq. 5:

$$\pounds_{ij} \simeq \left(\frac{1}{\epsilon_i} + \frac{1}{\epsilon_j} - 1 \right)^{-1} . \qquad (5)$$

Figure 4 plots R_T and R_S as a function of $£_{ij}$ for a double-pane window. R_T and R_S increase as the surface emissivity of the glass panes decreases. Various cases are also shown in Fig. 4. If only the emissivity of the surface between the glass panes varies ($£_{25} = £_{ij}$; $£_{12} = £_{56} = 0.785$), maximum values of $R_T \simeq$ 0.9 (W/m² °C)$^{-1}$ and $R_S = 0.53$ (W/m² °C)$^{-1}$ *(or $R_T \simeq 5$*

and $R_S \simeq 3(Btu/h\ ft^2{}^\circ F)^{-1}$) are reached when $£_{25} = 0.01$. We can obtain $£_{25} = 0.01$ with $\epsilon_{25} = 0.01$ and $\epsilon_{52} = 0.9$, with $\epsilon_{25} = 0.9$ and $\epsilon_{52} = 0.01$, or with $\epsilon_{25} = \epsilon_{52} = 0.02$. Similarly, maximum values of $R_T \simeq 1.4\ (W/m^2\ {}^\circ C)^{-1}$ and $R_S \simeq 0.6\ (W/m^2\ {}^\circ C)^{-1}$ *(or* $R_T \simeq 8$ *and* $R_S \simeq 3.4(Btu/h\ ft^2{}^\circ F)^{-1}$) are reached when $£_{12} = £_{25} = 0.01$. If the hot plate (surface 1) has a constant surface emissivity of 0.9, then ϵ_{21} (facing surface 1) must be 0.01. The largest total impedance for a double-pane window, $R_T \simeq 2.0\ (W/m^2\ {}^\circ C)^{-1}$ *(or* $R_T \simeq 11.4(Btu/h\ ft^2{}^\circ F)^{-1}$), is obtained when $£_{12} = £_{25} = £_{56} = 0.01$.

Figure 5 plots R_T and R_S versus $£_{ij}$ for a triple-pane window. Four different cases are plotted here. First, R_T and R_S are functions of a variable $£_{23}$ between surfaces 2 and 3 ($£_{23} = £_{ij}$; $£_{12} = £_{35} = £_{56} = 0.785$). Second, R_T and R_S vary as $£_{23}$ and $£_{35}$ vary ($£_{23} = £_{35} = £_{ij}$; $£_{12} = £_{56} = 0.785$). Third, R_T and R_S vary as $£_{12}$, $£_{23}$ and $£_{35}$ vary ($£_{12} = £_{23} = £_{35} = £_{ij}$; $£_{56} = 0.785$). Finally, R_T and R_S vary as $£_{12}$, $£_{23}$, $£_{35}$ and $£_{56}$ vary ($£_{12} = £_{23} = £_{35} = £_{56} = £_{ij}$).

By plotting R_T and R_S as a function of $£_{ij}$, many window systems and configurations can be characterized by just a few curves. Furthermore, these plots provide a great deal of flexibility to the user in assessing various window systems. The user can vary the number, the location and the value of the low-emissive surface coatings for double-pane and triple-pane window systems, and interpolate from Figs. 4 and 5 the maximum and minimum thermal impedance provided by the window systems.

A few simple examples may help to illustrate the benefits and flexibility provided by plotting R_T and R_S as a function of $£_{ij}$. Consider a double-pane window with two low-emissive coatings applied to the inner and outer panes so that they face each other. The surface emissivity of these coatings is 0.15 ($\epsilon_{25} = \epsilon_{52} = 0.15$). All other pane surfaces have their normal emissive value of about 0.9 ($\epsilon_{21} = \epsilon_{56} = 0.9$). To determine the maximum and minimum thermal impedance (R_T and R_S), we simply calculate $£_{25}$ from Eq. 5 and interpolate R_T and R_S from the last curve labeled $£_{25} = £_{ij}$; $£_{12} = £_{56} = 0.785$ on Fig. 4. Using Eq. 5, $£_{25}$ is calculated to be 0.081, and $R_T \simeq 0.8\ (W/m^2$

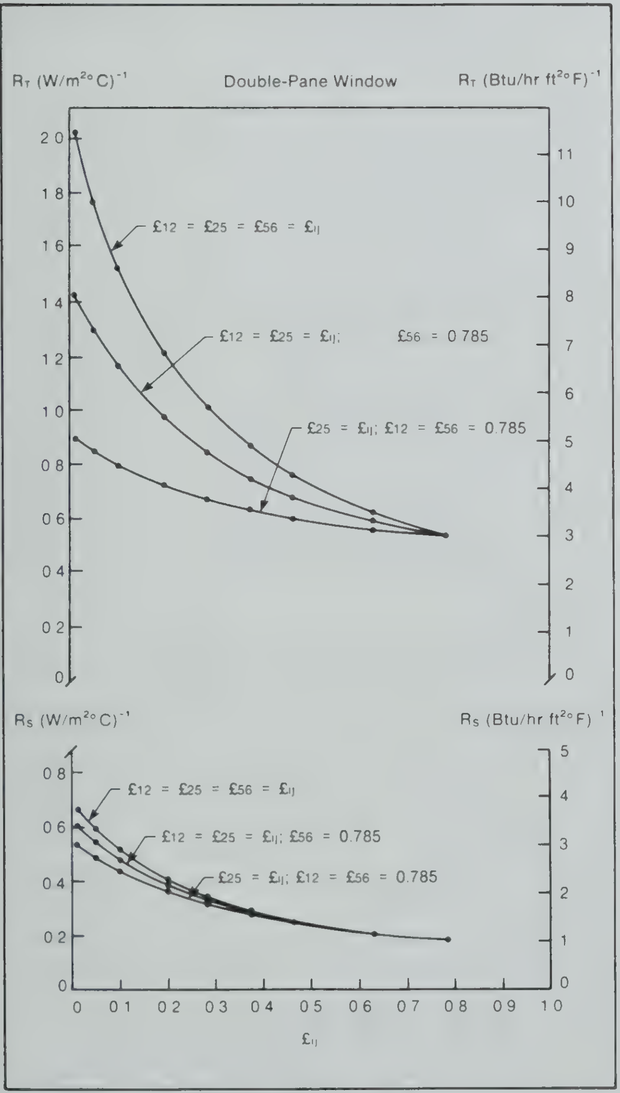

Figure 4: R_T and R_S are plotted versus $£_{ij}$ for a double-pane window. Subscripts indicate the surface or nodes for which £ was calculated.

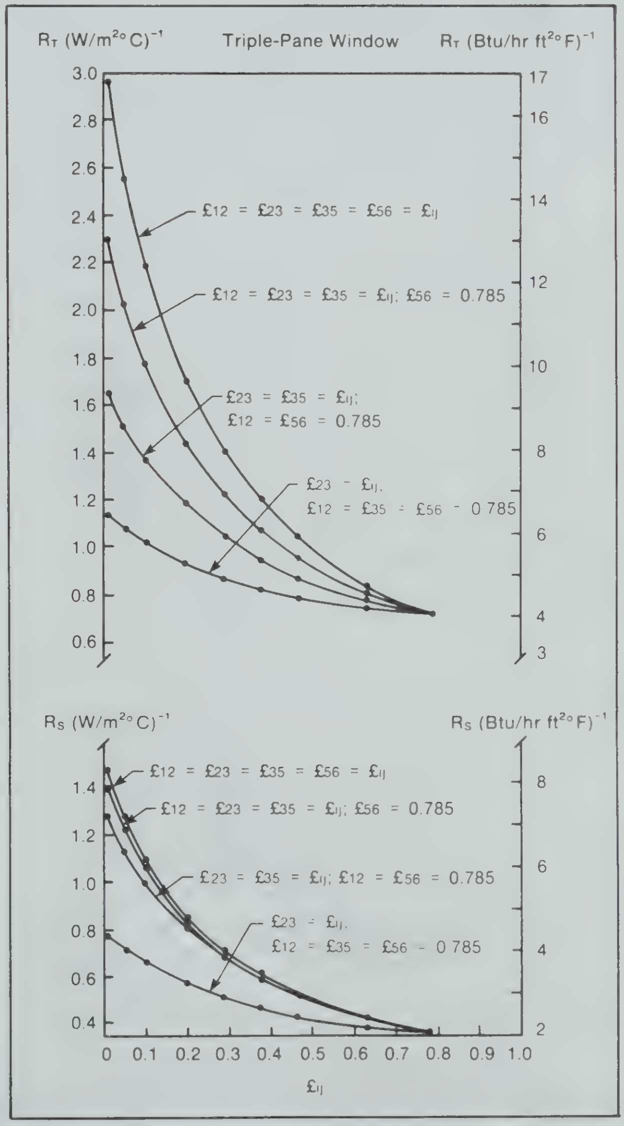

Figure 5: R_T and R_S are plotted versus $£_{ij}$ for a triple-pane window, as in Fig. 4.

Three Manuals 'Succeed Admirably'

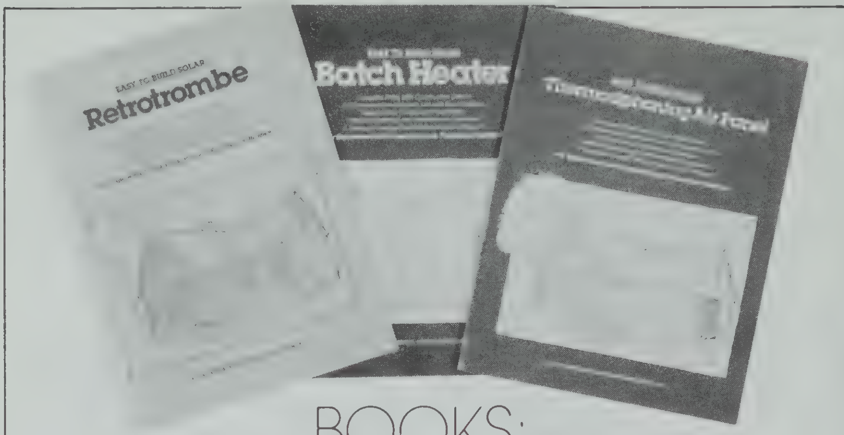

BOOKS:

Easy to Build Solar Batch Heater, Thermosiphoning Air Panel and Retrotrombe. Total Environmental Action Foundation, Harrisville, New Hampshire, 1981. Each manual 16 pp., illus., $7.95.

These three construction manuals (and one to come on sunspaces) are a welcome addition to the solar literature. The retrofitter can spend less time with on-site experimentation if the manuals are followed carefully.

These are the clearest, most straight-forward, construction manuals available for batch solar water heaters, thermosiphoning air panels, and Trombe wall retrofits. A particularly exciting feature is that for relatively low material costs, the end results are crisp, aesthetically pleasing products with glass as the glazing material in all three cases. Each has a few problems, to be sure, but they are a refreshing improvement over most available retrofitting details.

Reviewed by Alex Wilson, executive director of the New England Solar Energy Association and former workshop program director of the New Mexico Solar Energy Association. He is the author of the Thermal Storage Wall Design Manual.

All three manuals have the same basic format:

- Concise introduction of the system and its applicability
- Good discussion of energy conservation as the first step
- Discussion of system performance with energy and dollar savings
- Pre-construction checklist
- Detailed materials list with cost estimates
- Necessary tools
- Step-by-step construction sequence
- Operation and maintenance information
- Short bibliography.

The accompanying blueprints are full-sized, clear and professionally done.

Most of the problems are fairly minor, but noteworthy. With all three manuals, the cost information will go out of date almost immediately, depending on actual inflation rates and the state of the construction industry. In addition, building material prices vary from place to place, and this is not discussed. With a little digging, however, accurate price information should be readily obtainable.

Nothing is mentioned in the batch heater and retrotrombe manuals about selective absorber surfaces, a potential modification which could significantly boost performance at relatively low cost.

More should be said in the batch heater manual about obtaining assistance from professional plumbers. In many states and communities, a license is required to tap into the domestic hot water system. In addition, several plastic adapters are specified while all other plumbing is copper. Having had poor luck with plastic fittings and adapters in solar water heaters, most installers now avoid them.

Most thermosiphoning air panel designs provide inadequate vent areas. This one provides enough, finally, but the recommended plastic or Frisket paper back-draft dampers might provide too much air resistance, especially with reduced linear flow rates caused by the large vents. Also, it is questionable whether such back-draft dampers are all that successful at preventing reverse thermosiphoning.

Neither the thermosiphoning air panel nor retrotrombe manuals provides enough information on overheating. The only option mentioned is covering the glazing with a tarp, which is surprising given the obvious desire to provide an aesthetically pleasing end product. Overhangs and exterior vents should at least be discussed as options.

Both wall-collector manuals paint a rosy picture of existing wall attachment ease. From my own experience, I know that one can seldom count on having flat walls or studs perfectly aligned on 16 or 24 inch centers. Consequently, a wall-collector retrofit site should always be approached with a wide variety of fasteners on hand, from lag bolts, toggle bolts and lead anchor shields to screws and Hilti-Hit Anchors.

Nevertheless, these are still the best manuals available which, for a modest price, will produce functional, aesthetically pleasing retrofit Trombe walls, thermosiphoning air panels and batch water heaters. They are intended to be construction manuals, not treatises on every nuance of design. As construction manuals, they succeed admirably.

Passive Solar Journal

Heating, Cooling, Hybrid Technologies and Strategies for Sustainable Design

ARCHITECTURAL CENTER
LIBRARY

Volume 1, Number 3: Summer 1982

B. Givoni: **cooling** by longwave radiation; R.F. Jones and G. Dennehy: **performance** of a double-envelope house; and T.E. Johnson: **new materials** used in MIT's Solar Building No. 5; **book reviews** by R.O. Smith and R.G. Derickson, and a **design tool review** by W.A. Wright.

Official Journal of the Passive Systems Division of the American Solar Energy Society,® Inc.

PASJDF 1(3) 129-192(1982) ISSN: 0277-6456

Passive Solar Journal®

Editor-in-Chief:
Jeffrey Cook, Department of Planning, College of Architecture, Arizona State University, Tempe, Arizona (602) 965-6210

Associate Editors:
John Hayes (Book Review Editor), Marlboro College, Marlboro, Vermont
William A. Wright (Design Tools Review Editor), Cambridge Energy Corporation, Cambridge, Massachusetts
J. Douglas Balcomb, Los Alamos National Laboratory, Los Alamos, New Mexico
Michael Holtz, Architect, Boulder, Colorado
Fred Nelson, Sunset Magazine, Menlo Park, California

Managing Editor:
Cyndi Meagher, Passive Solar Journal, Tempe, Arizona
Assistant Editors:
Heidi Osselaer, Scottsdale, Arizona / Peter Brown, Phoenix, Arizona
Typesetting:
Paradise Valley Typesetting Studio, Phoenix, Arizona
Chief Artist, consulting:
Mark Woodruff, Glendale, Arizona

Director of Publications:
Albert Henderson, ASES, New York, New York (212) 736-8227
Publications Production Manager:
Barbara Bradley, ASES, Newark, Delaware

Executive Director, ASES:
G. Lee Salmon, Boulder, Colorado (303) 492-6017

This issue of the Passive Solar Journal was produced in offices kindly donated by Allen & Philp Architects, Inc., formerly Associate Design Group/Architecture, of Phoenix, Arizona.

Submission of Manuscripts

Manuscripts proposed for publication are solicited. They must be original and unpublished, although previously published data will be permitted. Articles and reviews are also initiated by invitation of the editors. All materials and illustrations are subject to peer review and editing.

Although this is the official journal of the Passive Systems Division, ASES, manuscripts are accepted from solar researchers and professionals throughout the world. Authors may or may not be members of ASES.

Manuscripts must be written in English and include illustrations and references. Four copies are required. All must be typed and double spaced on one side of white paper 8½ x 11 in. (22 x 28 cm) with ample margins. All pages should be numbered consecutively with abstract (up to 150 words), text with subtitles, acknowledgements, appendix, references, notes, figure captions and illustrations. Manuscripts should be prepared according to the "Style Manual" of the American Institute of Physics, 335 East 45th Street, New York, 10017. All materials will be published using both units of measure: Imperial (English) and SI. The units of the original research will take precedence (with the equivalents in parentheses). Manuscripts from a dot matrix printer will not be accepted.

Manuscripts should be sent to the Editor, **Passive Solar Journal**, Department of Planning, College of Architecture, Arizona State University, Tempe, Arizona 85287.

Cover: The relationships of nature, buildings and people form the basis for the study and practice of passive/hybrid solar research and design. Photos by Bruce Flynn, Henry Mueller and Sharyn Towle.

Passive Solar Journal

The Official Journal of the Passive Systems Division
of the American Solar Energy Society.®
The United States Section of the International Solar Energy Society

SUMMER 1982 Volume 1, Number 3

CONTENTS

COOLING

131 **Cooling by Longwave Radiation**

Baruch Givoni of the Jacob Blaustein Institute for Desert Research reviews the design options for radiant cooling and the equations necessary for their evaluation, and discusses practical implications for research.

BUILDING EVALUATION

151 **The Mastin Double-Envelope House**

Ralph F. Jones and Gerald Dennehy of Brookhaven National Laboratory evaluate the performance of a double-envelope house built in Middletown, Rhode Island. In supplementary comment, J. Douglas Balcomb of Los Alamos National Laboratory compares the Brookhaven results to a Solar Load Ratio analysis of a double-envelope design.

MATERIALS

175 **MIT Solar Building No. 5's Third Year Performance**

Timothy E. Johnson presents measurements indicating that new materials can overcome the overheating and glare associated with many direct-gain buildings.

REVIEWS/BOOKS

185 Robert O. Smith evaluates *Passive Solar Heating Design* by Ralph M. Lebens, and Russell G. Derickson considers *Air-to-Air Heat Exchangers for Houses* by William A. Shurcliff.

REVIEWS/DESIGN TOOLS

188 William A. Wright, the *Journal's* design tools editor, describes a system he proposes for evaluating a design tool.

Credit: In Volume 1, Number 2, the cutaway perspective drawing of the LANL convective loop test apparatus was based on original work by W. Scott Morris; the loop section beneath it was based on work by Franz A. Biehl.

Publisher: The Passive Solar Journal is published by the American Solar Energy Society, Inc. (ASES): The United States Section of the International Solar Energy Society, 110 West 34th St., New York 10001. Quarterly: Winter, Spring, Summer, Fall. It is the official journal of the Passive Systems Division of ASES. (Solar Energy Society is a registered trademark.)

ASES assumes no responsibility for the statements and opinions advanced by contributors to the society's publications. Editorial views do not necessarily represent the official position of ASES.

This publication contains accounts of work sponsored by the United States Government. Neither the United States nor the United States Department of Energy, nor the American Solar Energy Society, nor any of their employees, nor any of their contractors, subcontractors, or their employees, makes any warranty, express or implied, or assumes any legal liability or responsibility for the accuracy, completeness, or usefulness of any information, apparatus, product, or process disclosed or represents that is use would not infringe privately owned rights.

Subscription rates: ASES individual members, 1983, one year, U.S. $20.00, foreign, $28.00; Corporate/Nonmembers, one year, U.S. $90.00, foreign, $98.00. Members of the Passive Systems Division receive the Passive Solar Journal as a benefit of membership. Individual member rates are for personal use only, paid with personal funds.

For membership information, write to ASES, 1230 Grandview Ave., Boulder, Colorado 80302.

Business correspondence:

Changes of address should be sent by members and subscribers to ASES' offices at 1230 Grandview Ave., Boulder, Colorado 80302. Allow six weeks for the notification to become effective. All communications should include both old and new addresses with zip codes and should be accompanied by a recent mailing label.

Claims for missing issues will not be allowed if received more than 90 days from date of mailing plus the time normally required for postal delivery of the issue and claim. No claims will be allowed because of failure to notify a change of address or because a copy is "missing from files."

Editorial correspondence:

The editorial office of the Passive Solar Journal may be contacted through Editor-in-Chief Jeffrey Cook, Dept. of Planning, College of Architecture, Arizona State University, Tempe, Arizona 85287.

Access: The Passive Solar Journal is covered by *Engineering Index* (monthly and annual), *Energy Abstracts* and *Energy Information Abstracts*.

Copyright © American Solar Energy Society, Inc. 1982

It is a condition of publication that manuscripts submitted to this journal have not been published and will not be simultaneously submitted or published elsewhere. By submitting a manuscript, the authors agree that the copyright for their article is transferred to the publisher if and when the article is accepted for publication. However, assignment of copyright is not required from authors who work for organizations which do not permit such assignment. The copyright covers the exclusive rights to reproduce and distribute the article, including reprints, photographic reproductions, microform or any other reproductions of similar nature and translations. No part of this publication may be reproduced, stored in a retrieval system or transmitted in any form or by any means, electronic, electrostatic, magnetic tape, mechanical, photocopying, recording or otherwise, without permission in writing from the copyright holder.

U.S. COPYRIGHT LAW APPLICABLE
TO USERS IN THE USA

The Article Fee Code on the first page of an article in this journal indicates the copyright owner's consent that, in the U.S.A., copies may be made for personal or internal use provided the stated fee for copying beyond that permitted by Section 107 or 108 of the United States Copyright Law, is paid. The appropriate remittance should be forwarded with a copy of the first page of the article to the Copyright Clearance Center Inc., 21 Congress Street, Salem, MA 01970 U.S.A. If a code does not appear, copies of the article may be made without charge, provided permission is obtained from the publisher. The copyright owner's consent does not extend to copying for general distribution, for promotion, for creating new works or for resale. Specific written permission must be obtained from the publisher for such copying.

Reviewers and Advisors

In addition to the reviewers recognized in Vol. 1 No. 2, the Passive Solar Journal gratefully acknowledges the contributions of the following who have agreed to review articles before publication, as well as advisors who have contributed to the editorial direction.

Donald W. Aitken
San Jose State University
San Jose, California

Maria Argyropolous
Architect & Planner
London, England

George Arnold
Architectural Design Branch, TVA
Knoxville, Tennessee

Medhi N. Bahadori
University of Waterloo
Ontario, Canada

Tom Barr
Mad Dog Construction
Tallahassee, Florida

William A. Beckman
University of Wisconsin
Madison, Wisconsin

Bob Besant
University of Sasketchewan
Saskatoon, Canada

Mark Blanpied
Trinity University
San Antonio, Texas

Thomas Bligh
Massachusetts Institute of Technology
Cambridge, Massachusetts

Richard L. Casperson
Energy Engineering Group
Golden, Colorado

Richard Crenshaw
National Bureau of Standards
Washington, D.C.

Larry Degelman
Texas A & M
College Station, Texas

Russell G. Derickson
Solar Consultant
Fort Collins, Colorado

Jane Drew
Fry, Drew & Creamer
London, England

Joseph Farber
Solar Research Systems
Costa Mesa, California

Pliny Fisk
Center for Maximum Potential
Building Design
Austin, Texas

Harrison Fraker
Princeton, New Jersey

Gregory Franta
Lakewood, Colorado

E. Maxwell Fry
Fry, Drew & Creamer
London, England

Frank W. Gilleland
Owens Corning Fiberglas
Toledo, Ohio

Drew Gillett
R.G. Vanderweil Engineers, Inc.
Boston, Massachusetts

James W. Griffith, P.E.
Dallas, Texas

M.C. Gupta
Indian Institute of Technology
Madras, India

Kenneth Haggard
San Luis Obispo Solar Group
Santa Margarita, California

Harold Hay
Los Angeles, California

Blair Hamilton
The Memphremagog Group
Newport, Vermont

Robert Hammond
Mobile-Tyco Solar Energy Corp.
Concord, Massachusetts

Everado Hernandez
Universidad Nacional Autonoma
de Mexico
Mexico City, Mexico

Bengt Hidemark
Royal Institute of Technology
Stockholm, Sweden

Timothy Johnson
Massachusetts Institute of Technology
Cambridge, Massachusetts

Robert Jones
Los Alamos National Laboratory
Los Alamos, New Mexico

Ron Judkoff
Solar Energy Research Institute
Golden, Colorado

Helen Kessler
Environmental Research Lab
Tucson, Arizona

Ken-Ichi Kimura
Waseda University Shinjuku
Tokyo, Japan

Bill B.P. Lim
University of Singapore
Singapore

Sergio Los
Instituto Universitario di Architettura
Venice, Italy

Eric Mayer
Universidad Simon Bolivar
Caracas, Venezuela

Edward Mazria
Mazria/Schiff & Associates, Inc.
Albuquerque, New Mexico

Charles Michal
Equinox, Inc.
Peterborough, New Hampshire

Murray Milne
University of California, Los Angeles
Los Angeles, California

Fuller Moore
Miami University
Oxford, Ohio

Harold Orr
National Research Council
Saskatoon, Canada

Cristian F. Otto
Cornell University
Ithaca, New York

John K. Page
University of Sheffield
Sheffield, England

John Reynolds
University of Oregon
Eugene, Oregon

Michael Riordan
Cheshire Books
Palo Alto, California

Richard Rittelmann
Burt Hill Kosar Rittelmann Associates
Butler, Pennsylvania

Claude Robbins
Solar Energy Research Institute
Golden, Colorado

Stephen W. Sawyer
University of Maryland
College Park, Maryland

A.A.M. Sayigh
Kuwait Institute for Scientific Research
Safat, Kuwait

James W. Scalise
Arizona State University
Tempe, Arizona

John T. Schenbly
Thermal Technology Corp. of Aspen
Broomfield, Colorado

Greg Schoenan
University of Sasketchewan
Saskatoon, Canada

Rick Schwolsky
Sunrise Builders
Grafton, Vermont

Dennis Sharp
Architect & Design Consultant
Hertford, England

Robert Shibley
State University of New York at Buffalo
Buffalo, New York

Tony Siebauld
Solar Energy Analysis Lab
San Diego, California

Robert O. Smith
Robert O. Smith & Associates
Newton, Massachusetts

J.F. van Straaten
National Bldg. Research Institute
Pretoria, South Africa

Steve Szokolay
University of Queensland
St. Lucia, Australia

Robert D. Taylor
Solar Energy Research Institute
Golden, Colorado

Michael Utzinger
University of Wisconsin
Milwaukee, Wisconsin

Francis Wessling
Solar Applications Branch, TVA
Chattanooga, Tennessee

James I. Williams
Brattleboro Design Group
Brattleboro, Vermont

Alex Wilson
New England Solar Energy Association
Brattleboro, Vermont

Steven Winter
Steven Winter Associates, Inc.
New York City, New York

David Wright
Solar Environmental Architect
Nevada City, California

Bill Yanda
Brother Sun
Santa Fe, New Mexico

Simos Yannas
Architectural Association
London, England

Review and Evaluation

Cooling by Longwave Radiation

By BARUCH GIVONI
KATZEF Professor of Solar Energy at the Jacob Blaustein Institute for Desert Research, Ben-Gurion University of the Negev, Sede Boqer Campus, Israel

ABSTRACT

Theoretical and experimental studies are summarized in a review, and the design options for using radiant cooling are evaluated. The various components involved in the radiant exchange of longwave (nocturnal) radiation between radiators and the atmosphere are analyzed. The basic equations by which these components can be evaluated are presented. The techniques by which the heat loss due to longwave radiant exchange can be used, are discussed, as well as their practical implications.

INTRODUCTION

Any material surface emits electromagnetic radiation with a wavelength inversely related to its temperature. The radiation emitted from the surface of the sun, referred to as shortwave, has a spectral range from about .25 to 3 microns (one-thousandth of a millimeter) with a peak radiation of about .5 microns. The radiation emitted from surfaces on the earth with natural temperatures, called longwave, is in the spectral range of 5 to 30 microns with peak radiation at about 10 microns. Constant exchange of radiant energy in the longwave spectrum takes place between a building and the atmosphere. Any element of the external envelope of a building which "sees" the sky is emitting longwave radiation toward it, continuous over the spectral range. Since the roof is the building element exposed the most to the sky, it is the most effective location for a longwave radiator.

The emission of longwave radiation from building surfaces takes place continuously, day and night. However, during the daytime the radiating surface is exposed to solar radiation. The solar radiation absorbed at the surface (which depends on its solar absorptivity, i.e., its color) produces heat which, in most cases, outweighs the cooling effect produced by the emission of longwave radiation.

Research and development on special surfaces, highly reflective in the solar spectrum and with high emissivity in the longwave range (5 to 30 microns) may change this situation. However, with the materials presently available, radiant cooling can be obtained only during the night hours. For this reason it is often referred to as nocturnal radiation.

The temperature of deep space beyond the atmosphere is near absolute zero, about 4 K. However, the atmosphere forms a screen between the ground and deep space. Some constituents of the atmosphere emit longwave radiation toward

---

This research is supported jointly by the Israeli Ministry of Energy and Infrastructure and the U.S. Department of Energy. Principal investigators were B. Givoni, A. Manor, and M. Mostrel.

Nomenclature

C = convective heat exchange between radiator and ambient air.
C_a and C_n = cloud correction factors.
F = flow rate of radiator.
h_c = convective coefficient.
h_{in} = cooled air.
h_{out} = heat transfer.
k = thermal conductivity.
l = length.
n = cloud cover.
NC = net cooling.
Pr = Prandtl number, a measure of how rapidly momentum is dissipated compared to the rate of diffusion of heat through a fluid.
Q = heat loss.
Q_c = convective heat exchange with ambient air.
Q_{net} = overall heat balance of a nocturnal radiator.
R_{abs} = absorbed sky radiation.
RC = radiant cooling.
Re = Reynolds number, the ratio of inertia forces to viscous forces in fluid flow.
R_{emit} = emitted radiation.
R_{net} = net radiant heat loss of a radiator.
R_{sky} = atmospheric incoming radiation.
T = temperature of radiator.
T_a = temperature of ambient air.
$\Delta T_{a\,s}$ = depression of sky temperature below ambient air under clear sky conditions.
T_{av} = average temperature.
T_{dp} = ambient dew point temperature.
T_o = initial reference temperature.
T_{out} = air outlet temperature.
T_r = surface temperature of a radiator.
T_{rs} = radiative surface stagnation temperature.
ΔT_{rs} = temperature depression of ambient air.
T_{sky} = effective sky temperature.
T_{stag} = stagnation temperature.
U_c = convective-conductive coefficient.
U_R = radiative heat loss coefficient.
σ = Stefan-Boltzmann constant, the ratio of the emissive power of a blackbody per unit of area and time to the absolute temperature of the body.
ϵ_1 = absolute emissivity.
ϵ_r = emissivity of the radiator.
ϵ_s = variable sky emissivity.

$$°C = \frac{°F-32}{1.8}$$

K = °C + 273.15 (one degree Celsius equals one kelvin, but temperatures in °C and kelvin are not equal).

the ground and this radiation partially counteracts the outgoing longwave radiation emitted from the building, or from specialized radiators used to collect "nocturnal cold." There are some differences in the energy flux and the spectral distribution of the radiation emitted by the building and that emitted by the atmosphere, resulting in net radiant heat loss from the building.

Under clear sky conditions, the incoming radiant flux has two distinct peaks, at about 7 and 15 microns, with a "deep," the so-called sky, or atmospheric window, clearly evident between 8 and 13 microns, where the atmospheric back radiation is appreciably weaker. As the moisture and clouds in the air increase, radiation in the 8 to 13 micron range increases, as can be seen in Fig. 1. Under cloudy conditions, the spectral distribution is close to that of a graybody, namely, a continuous spectrum peaking at about 10 microns.

In a comment on this manuscript, one of the reviewers has pointed out that "dust particles and other atmospheric aerosols do not contribute much to the longwave atmospheric radiation unless they act as nucleation centers for moisture condensation."

The net radiant heat loss from a radiator placed on the roof of a building is the balance between the energy flux emitted by the radiator and the incoming atmospheric radiation which is absorbed by the radiator. It can be up to about 70 W/m^2 *(22 Btu/ft^2 h)* from a radiator with an ordinary surface under a clear sky on a calm night in the desert. The net radiant loss decreases with cloudiness and humidity of the ambient air.

In calculating the net radiant heat loss, it is convenient to make use of the concept of the "effective sky temperature." It is defined as the temperature of a blackbody which radiates toward the ground with a continuous spectrum, and at the same flux as the measured atmospheric radiation under the given climatic conditions. The effective sky temperature depends mainly on cloudiness conditions and ambient humidity. It also varies across the sky vault, being lowest at the zenith and highest near the horizon, where it practically equals the ambient air temperature.

As long as the emitting surface is at a higher temperature than the ambient air, it can use all the potential of radiant heat loss, together with additional convective cooling. This can be the case when, for instance, a concrete roof is used as the radiating surface, or when a lightweight, uninsulated roof is in thermal contact with the indoor space. This "thermal contact" should be eliminated, of course, during the daytime hours in summer, and throughout the winter at all times.

The emittance of longwave radiation may lower the temperature of the radiating surface below the ambient air level. In this case, a convective heat gain from the air counteracts the radiant heat loss until an equilibrium is reached between the heat gain and loss. The convective heat gain depends on the wind speed near the emitting surface so that as the wind speed increases, the temperature of the emitting surface is closer to that of the ambient air.

In humid climates, during warm nights with clear skies, radiant heat loss may be the major force for cooling of buildings. With suitable design it is possible to cool a storage mass (the roof itself or a specialized storage layer, such as pond on the roof) to a temperature below the wet bulb, or even below the dew point. In such cases condensation may take place on the radiating surface, which might be the limiting factor for dropping the temperature.

Under ordinary conditions the cooling effect resulting from the net radiant heat loss by the external surface of the roof cannot be used directly for cooling the building because of the thermal resistance of the roof. Almost all of the cold produced is expended to cool the ambient air in contact with the roof, unless the radiating surface is at a temperature higher than the ambient air.

In order to use the cooling effect of the nocturnal radiation, ways have to be found by which the cold produced can be transferred into the building's interior. Different approaches for using the radiant heat loss for cooling the interior of the building are discussed later on.

Three types of problems are involved in the design of systems for using nocturnal longwave radiation for cooling:

- The first problem involves the estimation of the meteorological potential for radiant heat loss. It includes estimation of the effective sky temperature, or its emissivity, and the convective heat exchange as bases for calculating the net radiant and total heat losses of ordinary surfaces.
- The second type of problem involves development and application of techniques for augmenting the net radiant loss from the radiating surface above its natural level, and reducing the convective heat gain from the ambient air by such means as infrared (IR) transparent windscreens and the use of IR selective surfaces. In considering these problems, attention should be paid to the possibilities of deviations from the theoretical ideal performance due to such factors as dew formation and dust settling on the radiator's surface, as well as the durability of the windscreen materials and the structural details of its application.
- The third type of problem is related to using the cold produced by the nocturnal radiation, that is, the transfer of this cold to the building and the way in which it is used to provide the required indoor comfort conditions. In practice it means the choice and design of the type of cooling system, whether direct cooling of the cold storing mass (e.g., a roof), or the use of a heat transfer medium and a specialized longwave radiator.

The actual choice and design of the cooling system depends on the type of building (e.g., single story or multistory) and the temperatures attainable by the radiator under the given climatic conditions. This choice may also be influenced by the desirable mode of indoor cooling (e.g., conductive or convective heat transfer). This last point also greatly affects the comfort sensations of the occupants because it determines the role of radiative and convective heat exchange between the human body and the indoor environment.

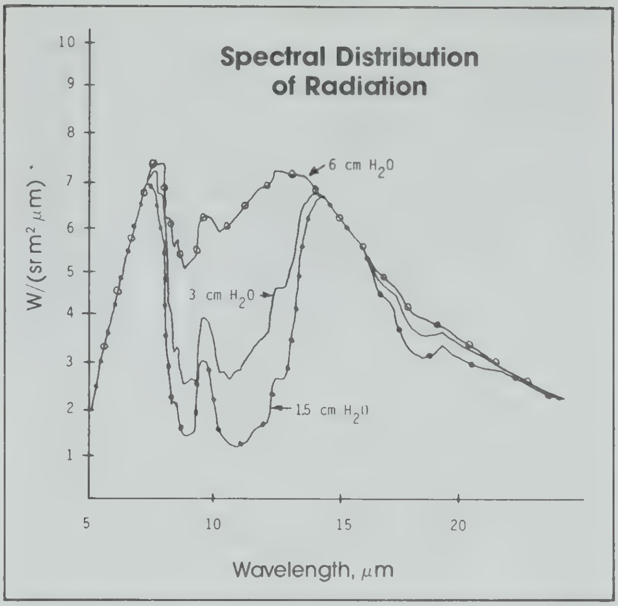

Figure 1: As moisture and clouds in the air increase, radiation in the 8 to 13 micron band increases.

This paper is, on the one hand, a summary of the state of the art in radiant cooling, based on a review of the literature and, on the other hand, a personal evaluation of the material.

Detailed information on the results of the experimental studies on radiant cooling by the author is presented in a research report by Mostrel and Givoni.[1]

HEAT EXCHANGE IN RADIANT COOLING

All systems of cooling buildings by nocturnal longwave radiation involve four components of heat transfer:

- the radiation emitted by the atmosphere and absorbed by the radiating surface;
- the longwave radiation emitted by the radiator;
- the convective heat exchange between the radiator and the ambient air;
- the heat transfer from the building (or the cold storage) to the longwave radiator, during the night hours (i.e., the used cold energy).

Atmospheric Radiation

As known, the atmosphere consists mainly of nitrogen (about 78%) and oxygen (about 21%), with only minute quantities of other constituents, mainly water vapor, carbon dioxide, and dust. Oxygen and nitrogen neither absorb nor emit longwave radiation and thus are transparent to this part of the radiation spectrum. However, water vapor emits and absorbs radiation at wavelengths around 6.6 and 18.0 microns while carbon dioxide emits and absorbs radiation at around 15 microns. The radiation emitted by these gases downward towards the earth is defined as the atmospheric back radiation.

---

*The steradian, sr, is defined by ASHRAE as the unit of measure of a solid angle with its vortex at the center of a sphere and enclosing an area of the spherical surface equal to that of a square with sides equal in length to the radius.

As mentioned above, the atmospheric back radiation depends mainly on the level of cloudiness. Under clear sky conditions and low humidity, the atmospheric radiation is concentrated in the 3 to 8 micron and in the 13 to 20 micron bands. As the water vapor content of the air increases, the intensity of the atmospheric back radiation in the 8-13 micron band, or atmospheric window, also increases, resulting in a stronger total atmospheric back radiation toward the earth (see Fig. 1).[2]

Clouds, especially low clouds, emit radiation throughout the whole longwave spectrum so that under an overcast sky, the phenomenon of the sky window practically disappears. Thus, under cloudy sky conditions the atmospheric radiation reaches its maximum, and consequently the net radiant heat loss is reduced to its minimum.

There are two ways by which the atmospheric back radiation can be expressed quantitatively. The first is to assume that the sky emits radiation as a blackbody, with a given effective sky temperature. The atmospheric emissivity is then taken as unity ($\epsilon_s = 1.0$). The other way is to assume that the atmosphere has the same temperature as the air near the ground, but its emissivity is less than unity (like radiation emitted from a graybody). The lower sky emissivity is used to express quantitatively the reduced intensity of the atmospheric radiant flux.

Emitted Radiation

The intensity of the longwave radiation emitted by specialized radiators, or by the roof itself when it serves as the radiating surface, depends, from the physicist's viewpoint, only on two factors: the absolute temperature of the radiating surface, T_r, and its emissivity, ϵ_r. The emissivity of any given radiating surface is a physical property which, theoretically, does not vary with the way in which the radiator is being used, although it might change with time (e.g., by oxidation). In practice, however, when the temperature of a selective radiator drops below the dew point of the ambient air and dew is formed over it, its effective emissivity might approach that of an ordinary surface.

On the other hand, the temperature of a radiator used at night, and especially its relation to the ambient air temperature, depends on its mass and on the way in which it is used. This factor is very significant in determining the total energy loss from the radiator (the combined net radiant loss and convective exchange). In particular, the thermal contact between the radiator and the building to be cooled can affect the temperature of the radiator and its overall efficiency. This point is discussed in detail later.

Convective Heat Exchange with Ambient Air

In all cases of radiant cooling there is also a convective component of heat exchange interacting with the radiative processes. For exposed longwave radiators the convective exchange is a function of the convective coefficient, which depends on the wind speed near the radiator and is proportional to the temperature difference between the radiator and the ambient air.

The convective coefficient, however, is one of the most difficult factors to estimate accurately. It depends on the wind speed near the radiating surface and on whether the air flow next to the surface is laminar or turbulent. Realistically, any value assumed for the air speed should be considered as only a rough estimate. A building's known wind parameters are usually only the wind speed and direction determined at some meteorological station which is not always close to the building. Furthermore, the wind fluctuates constantly both in direction and speed, so that the relationship between the wind conditions at the measuring point and next to the radiator changes constantly. Thus, there is no way to know with any reasonable accuracy the nature and speed of the wind next to the radiating surface, and it should be realized that any value assigned in the equations of the convection coefficient is only a rough estimate.

If it is assumed that most of the night the temperature of the radiating surface will be greater than the ambient air temperature (e.g., when a massive concrete roof or a water pond on the roof serves directly as a radiator) then a high wind speed may assist the cooling rate by increasing the convective heat loss.

However, in those systems of radiant cooling where the radiator's temperature is planned to be below that of the ambient air, special IR transparent windscreens can be applied to minimize the convective heat gain from the warmer air.

Net Energy Loss

The net energy loss from a radiator is the balance between three components of heat exchange: the radiation emitted by the surface, the atmospheric radiation which is absorbed by the radiator (which together determine the net radiant loss), as well as the convective heat exchange between the radiator and the ambient air. Whether the convective heat exchange provides heat to or extracts heat from the radiator depends of course on the temperature relationship between the radiator and the ambient air. In those systems where the radiating surface can be kept at a higher temperature than the ambient air during the night while collecting nocturnal cold, as mentioned above, convective heat loss is used together with the net radiant loss to provide a cooling effect. In such systems the total cooling rate of the building is highest. However, such systems can be applied only if the roof is insulated during the daytime hours.

On the other hand, when the radiator has to be at a lower temperature than the ambient air in order to provide the necessary cooling effect, which is the case whenever specialized radiators are used, then the convective heat exchange counteracts the radiant loss, resulting in a lower total heat loss compared with that obtainable in the first case.

Cold Energy Used—Net Cooling, NC

For the net cooling to be useful, a heat flow path is required to transfer heat from the building, or from a cold-storing medium, to the radiator so that it can be dissipated through the net radiant loss.

Such a heat transfer can be made by several means, the choice of which determines the type of radiant cooling system to be used.

These heat transfer means include, among other things:

- forced convection, by air or water flow between the building (or storage) and the radiator; and
- conduction of heat from the indoor space to the radiating surface, (e.g., through the roof structure). When this mode of heat transfer is applied the roof itself serves as the radiator. In this case insulation should be provided during the daytime hours, either above the roof or between the roof and the cooled indoor space.

The heat transfer at night from the building (or the store) to the longwave radiator is the net cooling effect (NC) produced by the radiant cooling process.

BASIC EQUATIONS OF RADIANT COOLING

A comprehensive review and analysis of the basic physical factors affecting the potential for radiant cooling are presented in a paper by Clark and Berdahl[3] summarizing the works at Trinity University and at Lawrence Berkeley Laboratory. This paper by Clark and Berdahl is based on results which were presented previously in several publications. The following treatment in this chapter of the equations related to the components of the exchange is based to a large extent on this work. The convective heat gain from the ambient air and the net cooling utilized by the building are discussed in the next chapter.

The general equation expressing the overall heat balance of a nocturnal radiator is:

$$Q_{net} = R_{net} \pm C \qquad (1)$$

where Q_{net} is the net cooling utilized by the buildings, R_{net} is the net radiant heat loss of the radiator and C is the convective heat exchange between the radiator and the ambient air.

Net Radiant Loss, R_{net}

The net radiant heat loss R_{net} from an exposed radiator made of ordinary nonselective surface materials (a graybody) is the balance between the longwave flux emitted by the radiator, R_{emit}, and the incoming atmospheric radiation which is absorbed by the radiator, R_{abs}. The absorbed radiation is the product of the radiation emitted by the sky, R_{sky}, and the absorptivity of the radiator's surface, which equals its emissivity for the same radiation spectrum, ϵ_r.

Thus:

$$R_{net} = R_{emit} - R_{abs}. \qquad (2)$$

Emitted Radiation, R_{emit}

The longwave radiation emitted by a gray radiator (or a roof surface) depends on its absolute temperature, T_r, and emissivity, ϵ_i. The radiator's longwave emissivity depends mainly on whether the surface is metallic or nonmetallic. For metallic surfaces exposed to the weather with some oxidation, the emissivity of the surface, ϵ_r, is about 0.1 to 0.2. Nonmetallic materials, such as concrete, plaster, glass, wood, and so on, have emissivities of about 0.9. It should be noted, however, that the emissivities of metallic surfaces and those containing metallic ingredients depend on the degree of oxidation, which may vary with time. Therefore, they should be considered only as approximate values.

Thus:

$$R_{emit} = \sigma \, \epsilon_r \, T_r^4 \qquad (3)$$

where σ is the Stefan-Boltzmann constant, whose value depends on the units which are used:

$\sigma = 5.67 \cdot 10^{-8}$ (W/m^2 K^4), in SI units;
$\sigma = 4.88 \cdot 10^{-8}$ (k cal/m^2 h K^4), in metric units;
$\sigma = 0.17 \cdot 10^{-8}$ (Btu/ft^2 h R^4), in English units.

Atmospheric (Sky) Radiation, R_{sky}

The atmospheric incoming longwave radiation can be expressed in two ways. The first way is to estimate the effective sky radiant temperature, T_{sky}, assuming the sky emissivity as 1.0 (blackbody radiation). Then the atmospheric incoming radiation is given by:

$$R_{sky} = \sigma \, T_{sky} \qquad (4a)$$

The second approach is to estimate the atmospheric radiation in terms of the ambient air temperature (near the ground), T_a, assuming a variable sky emissivity,

$$R_{sky} = \sigma \, \epsilon_s \, T_a^4. \qquad (4b)$$

Both of these methods disregard the spectral distribution of the sky incoming radiation and deal only with the total flux of radiant energy, assumed with a continuous spectrum. These methods can be applied when the radiating surface is a graybody which absorbs indiscriminately the different wavelengths of the sky thermal radiation. A different approach may be preferred when the radiating surface is a selective one.

Emissivity of Clear Sky, ϵ_s

The concept of atmospheric sky emissivity relates the radiant loss directly to the ambient air temperature, a meteorological measurement which is available in most locations. Since the sky emissivity can be estimated for clear sky conditions by a simple formula, it is useful to discuss separately the radiant heat loss under clear sky conditions.

Under clear sky conditions, the main factor which affects the radiant heat loss, R_{net}, and hence the emissivity of the sky and its radiant temperature, is the absolute humidity level, expressed in terms of the vapor pressure or the dew point.

Clark and Berdahl[3] compare different equations and measurements of the emissivity of clear sky as a function of the dew point. Clark and Allen[4] have suggested the following formula for the emissivity of clear sky, as a function of the dew point (in °C):

$$\epsilon_s = 0.787 + 0.0028\ T_{dp}\ . \qquad (5)$$

Effective Sky Temperature, T_{sky}

Clark and Berdahl[3] suggest that, as the two ways mentioned above express the same incoming sky radiation, together they enable us to estimate the effective sky temperature in terms of the ambient air temperature, by equating the two expressions:

$$R_{sky} = \sigma T_s^4 = \sigma\ \epsilon_s T_a^4.$$

$$\text{Hence:}\quad T_{sky} = \epsilon_s^{1/4}\ T_a. \qquad (6a)$$

Values of ϵ_s for different dew points are given in Table 1.

Clark and Allen[4] have analyzed measurements of the net radiant cooling in San Antonio, Texas. Berdahl and Fromberg[5] have analyzed data from Gaithersburg, Maryland; Tucson, Arizona; and St. Louis, Missouri. Each of them has developed correlations between the depression of the sky temperature below ambient air under clear sky conditions, $\Delta T_{a\text{-}s}$ as a function of the ambient dew point, ΔT_{dp}.

Emissivity of Clear Sky at Varying Dew Points

(°F)	(°C)	ϵ_s	$\epsilon_s^{1/4}$
32	0	0.74	0.93
41	5	0.77	0.94
50	10	0.80	0.95
59	15	0.83	0.95
68	20	0.86	0.96
77	25	0.89	0.97
86	30	0.92	0.98
95	35	0.95	0.99

Table 1: Values of clear sky emissivity, ϵ_s and of $\epsilon_s^{1/4}$ are given for eight dew points, T_{dp}.

Sky Temperature Depression as a Function of Dew Point

English		Metric	
T_{dp} (°F)	$\Delta T_{a\text{-}s}$ (°F)	T_{dp} (°C)	$\Delta T_{a\text{-}s}$ (°C)
32	34.2	0	19
41	31.0	5	17.2
50	27.7	10	15.4
59	24.5	15	13.6
68	20.5	20	11.4
77	16.6	25	9.2

Table 2: The depression of sky temperature below ambient air under clear sky conditions, $\Delta T_{a\text{-}s}$, is shown as a function of the ambient dewpoint T_{dp}.

The results can be expressed in tabular form (see Table 2) and by an average formula (in degrees centigrade) derived by the author:

$$\Delta T_{a\text{-}s} = 19 - 0.36\ \ T_{dp}\ . \qquad (7)$$

Hence, the sky temperature under clear sky conditions which is calculated in Eq. 6a also can be estimated by the formula:

$$T_{sky} = T_a - T_{a\text{-}s} = T_a - (19 - 0.36\ T_{dp}). \qquad (6b)$$

Absorbed Sky Radiation, R_{abs}

The atmospheric sky radiation, R_{sky}, is absorbed by the earth surface and buildings' surfaces according to absorptivity. For any given wavelength the absorptivity of a surface equals its emissivity, ϵ_r.

The general formula of the absorbed sky radiation is:

$$R_{abs} = \sigma\cdot\epsilon_r \cdot R_{sky}. \qquad (8a)$$

The specific formula by which to calculate the absorbed sky radiation depends on the form in which the sky radiation is expressed.

When the sky radiation is expressed in terms of the sky temperature (Eq. 3), then the absorbed radiation is given by:

$$R_{abs} = \sigma\cdot\epsilon_r \cdot R_{sky}. \qquad (8a)$$

When the atmospheric radiation is expressed in terms of the ambient temperature, T_a, and the sky emissivity, ϵ_s, the absorbed atmospheric radiation is:

$$R_{abs} = \sigma\cdot\epsilon_r \cdot \epsilon_s \cdot T_a^4\, . \qquad (8b)$$

Net Radiant Loss, R_{net}

The net radiant heat loss is given by:

$$R_{net} = \sigma \cdot\epsilon_r\ (T_r^4 - T_s^4) = \sigma\cdot\epsilon_r(T_r^4 - \epsilon_s\cdot T_a^4) \qquad (9a)$$

where T_r equals the surface temperature.

Clark and Berdahl[3] state that if a reference temperature, T_o, of about 20°C (293 K) is assumed, then the net radiant heat loss can be expressed by a linear function of the difference between the temperatures of the radiator and the sky (in K)

$$R_{net} = \epsilon_r \, 4\sigma T_o^3 \, (T_r - T_s). \qquad (9b)$$

The expression ($4\sigma T_o^3$) is a constant. Its value is approximately 5.7 in SI, 4.9 in metric, and 1.00 in English units. Assuming for ordinary surfaces that $\epsilon_r = 0.9$, the net radiant loss becomes:

$$R_{net} = \text{constant} \, (T_r - T_s) \qquad (9c)$$

where the constant is 5.11 in SI units, 4.4 in metric units, and 0.9 in English units.

The linear form of the formula for the net radiant loss, when it is expressed in terms of the effective sky temperature, facilitates greatly the related calculations. However, the sky temperature has to be evaluated separately, for example, by Eq. 6a or 6b.

Net Radiant Cooling under Clear Sky

The preceding equations enable the estimation of the net nocturnal radiant heat loss from a radiator with a given surface temperature, T_r, when the ambient air and dew point temperatures are known, following the procedure applied by Clark and Berdahl.[3] The steps are:

1) Estimate the sky emissivity, ϵ_s, from the dew point (by Eq. 5).
2) Estimate the sky temperature, T_s, from the air temperature and the sky emissivity (by Eq. 6a or Eq. 6b).
3) Estimate the net radiant heat loss, R_{net}, (by Eq. 9c):

$$R_{net} = 5.11 \, (T_r - T_s), \text{ in SI units.}$$

Clark and Allen [4, 5, 6] have measured the net radiant loss at different humidity conditions under clear skies. They have expressed the net radiant loss as a function of the ambient air temperature, T_a, assuming variable sky emissivity, ϵ_s.

The sky emissivity itself was expressed by Clark and Allen as a function of the ambient dew point temperature, T_{dp}. The formulas they used are:

$$R_{net} = \epsilon_s \, \sigma \, (T_r^4 - \epsilon_s \cdot T_a^4)$$

where ϵ_r is the radiator's emissivity, and where $\log_e$ is the natural logarithm

$$\epsilon_s = 0.787 + 0.764 \log_e \left(\frac{T_{dp}}{273} \right).$$

Effect of Cloud Cover on Atmospheric Radiation

Clouds, especially low clouds, increase greatly the incoming sky radiation and thus reduce the net radiant heat loss. High altitude clouds have little effect because of their low temperatures. Cloudy conditions at night often are estimated visually by observers at weather stations, and results reported in terms of n, tenths of the sky dome obscured (ranging from 0 for clear sky to 10 for completely overcast sky).

Cloudiness and Sky Radiation

Clark and Allen have measured the sky back radiation for different cloudiness conditions.[4] In order to express quantitatively the increase in the atmospheric radiation caused by the clouds, they have defined a cloud correction factor, C_a. This correction factor is the ratio of the measured back radiation of a cloudy sky to the computed clear sky radiation, by Eq. 4a or 4b given above. The cloud cover is expressed by n, tenths of opaque sky cover. Thus:

$$C_a = \frac{\text{measured cloudy sky atmospheric radiation}}{\text{computed clear sky atmospheric radiation}}.$$

Based on their measurements, Clark and Allen have developed a regression formula, expressing the dependence of the cloud correction, C_a, on the cloud over, n:

The regression they arrived at is:

$$C_a = 1 + 0.0224n - 0.0035n^2 + 0.00028n^3 \quad (10)$$

With overcast sky (n = 10) the value of C_a is 1.154.

The value of C_a for different sky cover conditions, according to this formula, is given in Table 3. It should be noted that although the effect of cloudiness on the total atmospheric back radiation is small, increasing it under overcast sky by only 15% above the clear sky level, its effect on the net radiant loss is much greater. This is caused because the difference in the fluxes of the emitted radiation and the sky incoming radiation is very small in comparison with the actual levels of the radiation fluxes.

Therefore, even a small decrease in the overall flux of the incoming radiation which occurs under clear sky conditions due to the atmospheric window increases greatly the difference between the emitted radiation and the incoming sky radiation.

Effect of Cloud Cover on Net Radiant Heat Loss

Instead of computing the net radiant heat loss under cloudy sky conditions as the balance between

Cloud Correction Factors at Different Cloud Covers

n	0	1	2	3	4	5	6	7	8	9	10
C_a	1	1.019	1.033	1.111	1.052	1.060	1.069	1.081	1.099	1.122	1.154

Table 3: Values are given for the cloud correction factor, C_a, at different amounts of cloud cover, n.

the emitted outgoing radiation and the incoming corrected sky radiation, it is possible to express the net radiant heat loss under cloudy sky directly as the ratio of the net radiant heat loss under cloudy sky to the net radiant loss under clear sky conditions.

Clark and Allen have thus defined another cloud correction factor, C_n, which is defined by the ratio:

$$C_n = \frac{\text{cloudy sky net radiation}}{\text{clear sky net radiation}} . \qquad (11)$$

The measured values of the net radiation under the different cloud conditions were used by Clark and Allen to generate a formula for C_n. The general regression formula that Clark and Allen got for their data (all types of clouds) is:

$$C_n = (1 - 0.056n) \qquad (11a)$$

which means that under overcast sky the net radiant loss is less than half of that occurring under clear sky conditions.

Clark and Allen also estimated C_n for different types of clouds:

1) for low clouds, altitude 0–3 km (*0–9,000 ft*)
   C_n (low) $= 1 - 0.059n$, (11b)
2) for medium clouds, altitude 4–7 km (*12,000–21,000 ft*)
   C_n (medium) $= 1 - 0.039$ n, (11c)
3) for high clouds, altitude 8–12 km (*24,000–36,000 ft*)
   C_n (high) $= 1 - 0.029n$. (11d)

Effective Temperature of Cloudy Sky

Putting together the formulas for the sky emissivity, ϵ_s (Eq. 5) and the cloud correction factor, C_a, Blanpied[7] has estimated the effective (cloudy) sky temperature as derived from the ambient air temperature:

$$T_{sky} = (\epsilon_s C_a)^{1/4}\, T_a . \qquad (12)$$

TECHNIQUES TO INCREASE NET HEAT LOSS

Two techniques can be used, separately or jointly, to increase the rate of the net heat loss from radiators, namely:

1) applying a windscreen, transparent to longwave radiation, to reduce the convective heat gain from the ambient air; and
2) applying a selective surface to the radiator, which emits mainly in the spectrum of the sky window and is reflective in the rest of the longwave spectrum, and preferably also in the shortwave (solar) spectrum.

Nocturnal Convection as Related to Radiant Cooling

Depending on whether the radiator's temperature is above or below that of the ambient air, convective heat transfer either assists or counteracts the radiant cooling process.

The nature of the convection coefficient, whether forced or thermal, depends, of course, on the wind conditions. Nights in many places are relatively calm and therefore the question of free convection, induced by thermal differences, deserves special attention in dealing with the effect of convection on the performance of nocturnal radiators.

When the radiator's temperature is above ambient air, the heat flow is in the upwards direction. Consequently, the free convection coefficient is much higher than when the radiator is cooler than the ambient air, and a stagnant, cooled layer of air is formed over its surface.

The general formula for convective heat exchange, Q_C, is:

$$Q_c = h_c\,(T_r - T_a). \qquad (13)$$

Clark and Berdahl[3] suggest the following values for the convective coefficient, h_c, under the different conditions of wind speed and the relationship between the temperatures of the radiator and the ambient air (in SI units):

1) radiator warmer than the ambient air and wind speed below 0.45 m/sec
   $h_c = 3.5$ W/m²°C, (13a)
2) radiator cooler than ambient air and wind speed below 0.076 m/sec
   $h_c = 0.8$ W/m²°C, (13b)
3) wind speed below 1.35 m/sec

$$h_c = \frac{(0.054\, Re^{0.8}\, Pr^{0.33})k}{L} \qquad (13c)$$

where

$$Re = \frac{L_s}{\mu}\;V \qquad \text{and} \qquad Pr = \frac{\mu C_p}{k}$$

4) wind speed (V) between 1.35 - 4.5 m/sec
   $h_c = 1.8 + 3.8$ V. (13d)

As stated above, the actual wind speed next to the radiating surface is typically unknown so the convective coefficient and resulting convective heat exchange rate should be considered as only rough estimates. Therefore, a simple, single formula can provide the rough estimation of the convection coefficient. Analysis of the values obtained by Clark and Berdahl has provided the following formula, suggested by the author for estimating h_c, when the radiator is cooler than the ambient air:

$$h_c = 1 + 6\, V^{0.75} . \qquad (13e)$$

This single formula provides reasonable representation of the convective coefficient over the wind speed range experienced in practice when the radiator temperature is below the ambient air.

Temperature Depression and Net Heat Loss Due to Nocturnal Radiation

When the radiant heat loss is not used (stagnation conditions) there is a balance between the heat loss from the radiator (which is at a lower temperature than the air) and the heat gain by convection from the ambient air. This balance results in a temperature depression of the radiating surface below the ambient air in which the heat loss by radiation equals the heat gain by convection.

Under these conditions the temperature difference between the ambient air and the radiating surface is highest (assuming stable conditions in the wind and cloudiness). The temperature thus attained is termed the stagnation temperature, T_{rs}.

This balance between the net radiant loss and the convective gain yields the formulas:

$$R_{net} = h_c \, (T_a - T_{rs}) \tag{14}$$

$$\Delta T_{rs} = \frac{R_{net}}{h_c} \tag{15}$$

and

$$T_{rs} = \quad h_c \cdot T_a - \frac{R_{net}}{h_c} \tag{16}$$

where

R_{net} is the net radiant heat loss,
h_c = the convective coefficient,
T_a = ambient air temperature,
T_{rs} = radiative surface stagnation temperature.

Combining the equations for the emitted radiation, R_{emit}, (Eq. 3), the absorbed sky radiation, R_{abs}, (Eq. 8a), and that of the convective coefficient for a radiator which is below ambient air, h_c, (Eq. 13) the following general formula can estimate the temperature depression, ΔT_{rs}, of a radiator under stagnation conditions (in all compatible units):

$$\Delta T_{rs} = \frac{(R_{emit} - R_{abs})}{h_c} \ . \tag{17}$$

Thus, it is possible to estimate the stagnation temperature depression, which expresses the potential for radiant cooling for any climatic conditions. The climatic data which is required to compute these formulas are:

- outdoor air temperature;
- dew point;
- cloud cover (by the n scale);
- wind speed.

Transient Pattern of the Radiator's Temperature

Gordon and Zarmi[8] have shown that the relaxation time of a radiator can be computed by the formula (in any compatible system of units):

$$T = \frac{mC}{(U_c + 4U_R \, T_a^{\,3})} \tag{18}$$

and that

$$-\frac{t}{T} = \log_e \frac{(T - T^*)}{(T_o - T^*)}$$

where

mC = heat capacity of the radiator;
U_c and U_R = convective-conductive and radiative heat loss coefficient, respectively;
T = temperature of the radiator;
T_o = initial temperature;
T^* = stagnation temperature;
T_{av} = average temperature between T_o and T^*;
t = time;
T = relaxation time of a radiator.

The relaxation time, T, can be determined experimentally from the slope of the straight line obtained by plotting $\log_e (T - T^*)/(T_o - T^*)$ versus time, t.

Convection Suppression by Infrared Transparent Windscreens

The convective heat exchange increases with the wind speed. Therefore, in cases when it is desired to lower the radiator's temperature well below the ambient level it would be desirable to minimize convection without interfering too much with the emission of longwave radiation. (This is always the case when a specialized nocturnal radiator is used and when a heat exchange medium rather than the thermal storage mass itself is being cooled.)

An inexpensive material which is transparent (by 60 to 80%) to longwave radiation (IR transparent) is polyethylene film without UV inhibitors. If a thin sheet of polyethylene is firmly supported over the radiator, either by air pressure or by tension so that it does not flutter in the wind, a stagnant cold air layer will be formed over the radiator. The stagnant air layer serves as transparent insulation, minimizing the convective heat gain and producing a lower temperature of the radiator.

Radiative properties of polyethylene film (without UV inhibitors) were measured by Clark and Blanpied.[9] These includes its IR transmission, reflectivity, and emissivity. Typical weighted averages (for the different angles of incidence) are:

transmissivity = 0.75;
reflectivity = 0.10;
emissivity = 0.15.

Even a single layer of polyethylene reduces by about 25% the emitted radiation because of its imperfect transmissivity. However, when the radiator's temperature is below that of the ambient air, the convective heat gain is reduced to a much greater extent, especially under windy conditions. Thus, the net effect is to increase the amount of the radiator's depression below ambient air temperature.

Two layers of polyethylene further reduce the convective heat gain from the ambient air, but at the same time the radiant heat loss is also reduced. Higgs and Hand[10] have found no difference between the cooling rates with single and double polyethylene layers.

In Arlington, Texas, Higgs and Hand measured the radiant heat loss (cooling rate) from a horizontal radiator with the radiator either exposed or covered by a polyethylene windscreen. As expected, when the radiator's temperature was at or above ambient air, the cooling rate from the exposed radiator was higher. Only when the radiator's temperature was more than 2°C *(3.6°F)* below the ambient air was the cooling rate from the screened radiator higher than that from the exposed one. Higgs and Hand have suggested the following two formulas for estimating the rate of heat loss, Q, from a nocturnal radiator (either exposed or screened) as a function of the temperature difference between the radiator, T_r, and the ambient air, T_a. For exposed radiators with ordinary surfaces the suggested formula is:

$$\begin{aligned} Q &= 125 - 24(T_a - T_r), \text{ in SI units (W/m}^2\text{ C)} \\ &= 100 - 21(T_a - T_r), \text{ in metric units (k cal/h m}^2\,^\circ\text{C)} \\ &= 40 - 8(T_a - T_r), \text{ in English units (Btu/h ft}^2\,^\circ\text{F).} \end{aligned} \tag{19}$$

For an ordinary radiator covered with polyethylene windscreen, the suggested formula is:

$$\begin{aligned} Q &= 93 - 10(T_a - T_r), \text{ in SI units} \\ &\simeq 80 - 9(T_a - T_r), \text{ in metric units} \\ &\simeq 30 - 3(T_a - T_r), \text{ in English units.} \end{aligned} \tag{20}$$

These formulas suggest that under the relatively humid climate conditions prevailing in Arlington, Texas, the average temperature depression of an exposed ordinary radiating surface, when the cooling effect is not used, is about 5°C and that of a radiator with a windscreen is about 9°C. These values represent the potential for radiant cooling in that region. Temperature depressions of 5° to 7°C have been measured in the coastal city of Haifa, Israel, with exposed radiators.[11]

In San Antonio, Texas, Manning[12] measured the net heat loss rate from a radiator with a 4-mil-thick polyethylene film at different temperature depressions below the ambient air level (T_a - T_r) under different cloudiness conditions. Some of his results are summarized in Table 4.

At the Institute for Desert Research in Sede Boqer, Israel, the effect of a polyethylene windscreen on the stagnation surface temperature depression below the ambient air was measured in a lengthy experimental series.[1] The measurements have revealed a phenomenon which is not taken yet into account in estimating the effect of the polyethylene windscreen.

Measurements were taken of the surface temperature of panels made of thin steel sheets insulated from below. One panel was exposed and the other one was protected by polyethylene film, placed 2 cm *(0.8 in)* above surface. It was observed that in the evenings the radiating surface which was protected by the polyethylene had cooled faster and attained a lower temperature than the exposed surface. However, on most nights, condensation started to form on the polyethylene sheet at about midnight, or even earlier, and then the difference between the exposed and the protected radiating areas practically disappeared. Furthermore, the two surfaces were very sensitive to passing clouds. Whenever the sky became cloudy the temperature of the two radiators rose and the difference between the exposed and the covered areas was greatly reduced.

The two phenomena are shown in Figs. 2, 3, and 4, which show the temperature patterns during three nights of the experimental series. The conditions of the sky cloudiness and the onset of condensation are stated also in these figures. Results similar to those shown in Fig. 3 were observed most nights.

Discussion and Implications

Dew formation over the polyethylene windscreen is bound to occur at night whenever the temperature of the film drops below the ambient dew point. The polyethylene film itself, being mostly transparent to infrared radiation, has a low emissivity, and thus would not cool significantly by radiant heat loss. However, when the radiator, under the windscreen, is cooled sufficiently below ambient air, a layer of stagnant cold air is formed between the radiator and the windscreen.

The polyethylene film is then cooled by conduction and its temperature may drop below the ambient dew point. When the film's temperature drops below that, condensation of dew is initiated.

Net Heat Loss from a Radiator: Manning's Results in San Antonio

English (Btu/ft^2 h)					Metric (W/m^2)			
0	3	6	10	$T_a - T_r = \Delta T$	0	3	6	10
23	17	11	7	Clear sky	72	53	35	22
16	11	7	3.5	Partly cloudy	50	35	22	11
11	5.5	3	—	Cloudy	35	17	9	—

Table 4: Some results are summarized from an experiment in San Antonio, Texas by Manning.[12] He measured the rate of net heat loss from a radiator with a 4-mil-thick polyethylene film at different temperature depressions below the ambient air level, T_a - T_r, under different cloudiness conditions.

Once condensation starts to occur over the polyethylene, it is a self-accelerating process: water absorbs longwave radiation and therefore has very high emissivity. The water film over the polyethylene becomes the radiating surface, and because of its very low heat capacity (due to its thinness) its temperature drops rapidly, accelerating the rate of dew formation until the polyethylene film and the radiator underneath reach the stagnation temperature of an ordinary exposed radiator.

When cold is withdrawn from the radiator, by cooling either air or water, its temperature is closer to that of the ambient air in comparison with a stagnant radiator. However, the overall benefit of the windscreen decreases greatly when the temperature difference between the ambient air and the radiator is decreased.

In practice, when the nocturnal radiator is used to cool a heat transfer medium (air or water), the temperature difference between the radiator and the ambient air might be about 2° to 5°C *(3.6°-9°F)*, depending on cloudiness and humidity. In this situation the net effect of the windscreen may be so small as to be insignificant or even counterproductive.

Analysis of Polyethylene Windscreens Under Use Conditions

Although the attainable temperature of a radiator with polyethylene under stagnation is significantly lower than that attainable by an exposed

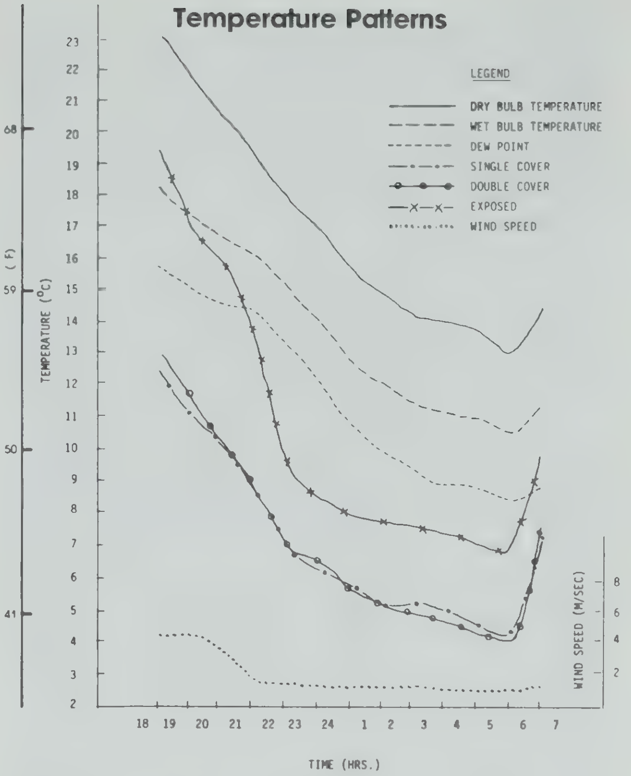

Figure 2: A graph of the night of Oct. 13-14, 1981, shows the effect of a clear, dry night on temperature patterns for exposed and protected radiators, as well as climatic conditions. In the evenings, the surfaces protected by polyethylene cooled faster and attained lower temperatures than the exposed surface.

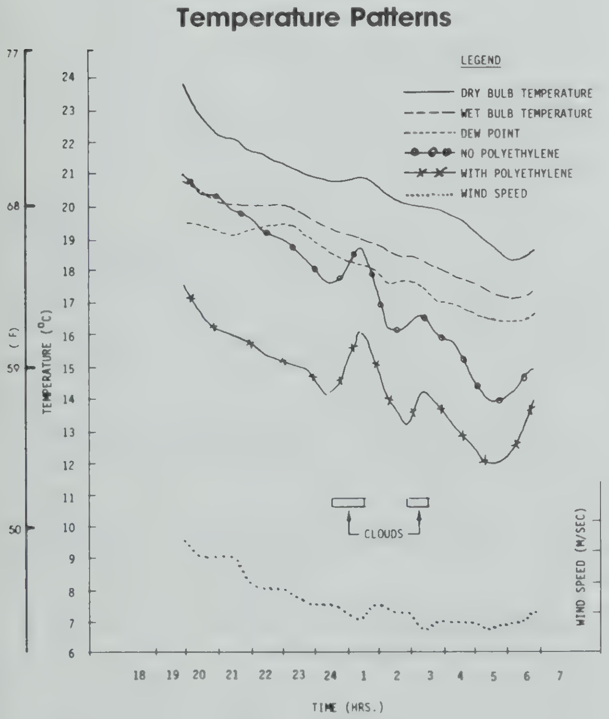

Figure 3: A graph of the night of Aug. 28-29, 1981, shows the effect of cloudiness during a dry night on temperature patterns for exposed and protected radiators, as well as climatic conditions.

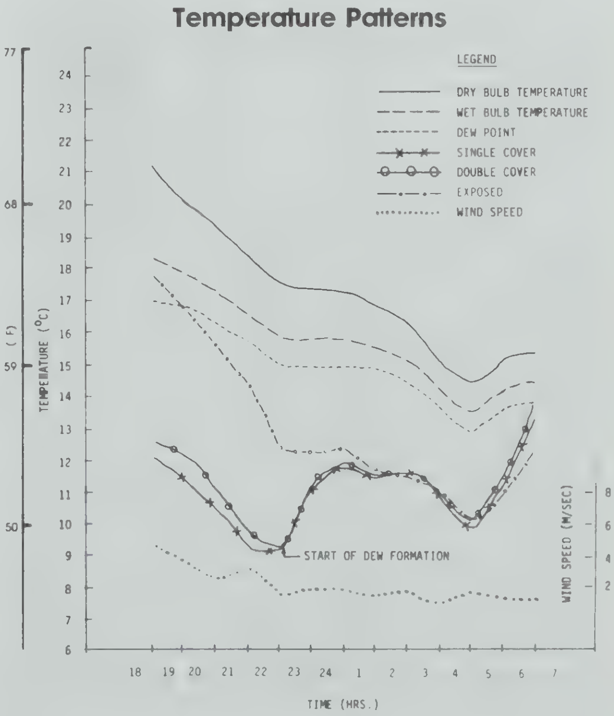

Figure 4: A graph of the night of July 12-13, 1981, shows the combined effect of dew formation and cloudiness on temperature patterns for exposed and protected radiators, as well as climatic conditions.

radiator, the net radiant loss is lower because of the partial transparency of polyethylene to longwave radiation. The lower stagnation temperature results from the fact that while the radiant loss is reduced to about 75%, the convective heat gain from the ambient air is reduced to about 30% under slight windy conditions, and to 40% on still nights.

The heat sink for any nocturnal radiator is the sky with an effective sky temperature which is usually below the ambient air temperature. The depression of the sky temperature below the ambient one depends only on the ambient dew point and the cloud cover.

The sky temperature is a meteorological parameter, although an imaginary one, useful only for calculating the expected net radiant heat loss from the radiator. It is, of course, completely unaffected by the temperature of the radiator itself.

On the other hand, the net radiant heat loss from the radiator decreases as its temperature decreases and approaches the sky temperature. Therefore, anything which lowers the radiator's temperature reduces the total radiant loss, although the temperatures attainable for use in cooling of buildings are lower.

The application of a polyethylene windscreen reduces the net radiant heat loss in two ways: first, the lower radiator temperature reduces the net radiant loss from the radiator. Second, because the polyethylene is only partially transparent to longwave radiation, less energy is radiated towards the sky.

In fact, the reduced convective heat gain from the ambient air, which is the reason for the application of the windscreen in the first place, does not compensate for the reduction in the net radiant loss, so that the useable cooling is also reduced.

Examples based on the experimental results of the energy balances of exposed and screened radiators can illustrate the effect of polyethylene when the radiator is used to cool the ambient air. With ambient temperatures of about 20°C *(68°F)* and dew points of about 10°C *(50°F)*, typical depressions of the stagnation temperatures under clear skies and without condensation were about 6°C *(10.8°F)* for exposed and 11°C *(19.8°F)* for windscreened radiators. The calculated net radiant loss from the exposed radiator is 64 W/m² *(20 Btu/ft² h)*, yielding an effective convective coefficient of about 11 W/m² °C *(1.94 Btu/ft² h°F)*.

Assuming 75% transparency of the polyethylene windscreen, the net radiant loss from the screened radiator (with the lower temperature) was about 45 W/m² *(14 Btu/ft² h)*, yielding an effective convective coefficient of about 4 W/m²°C *(0.7 Btu/ft² h°F)*.

When outdoor air is blown under the radiator to cool it, the total net radiant loss and the convective heat gain coefficient remain about the same. The average temperature of the radiator is stabilized at some level between the ambient and the stagnation temperatures, depending on the air flow rate under the radiator. The total radiant cooling is partitioned between the convective heat gain from the ambient air and that used to cool the air flowing under the radiator. The heat balance of a radiator, in use, is given as:

$$Q_{net} = R_{net} \pm C \qquad (1)$$

but typically, because of the influence of air, the equation is:

$$Q_{net} = R_{net} - h_c\,(T_a - T_r). \qquad (21)$$

Calculating the Radiator's Temperature, T_r

The following calculation examples will cover three conditions of the radiator's temperature:

1) a radiator at ambient temperature (when no radiant cooling effect materializes because the ambient air can be used directly without the radiator);
2) a radiator at stagnation (no cooling used);
3) in use, when ambient air is drawn under the radiator and cooled to a lower temperature. The radiator's average temperature is assumed halfway between the ambient air and the stagnation temperature. This assumed temperature is arbitrary but represents realistic conditions obtained in experimentation.

Assumed conditions for the calculations include:

- clear sky;
- ambient air temperature, T_a = 20°C *(68°F)*;
- dew point, T_{dp} = 10°C *(50°F)*;
- light wind, about V = 2 m/sec *(4.7 mi/h)*;
- radiator's temperature depression, when used, equals one-half of stagnation depression.

Equations for basic calculations (in SI units):

$T_{sky} = T_a - (19 - 0.36\ T_{dp})$, (6b)
$R_{net} = 5.11\ (T_r - T_s)$, for an exposed surface,
$R_{net} = 0.7 \cdot 5.11\ (T_r - T_s)$, for a surface under polyethylene, (9c)
$h_c = 11$ for an exposed radiator, and 4 W/m^{2}C for a screened one (*1.9 and 0.7 Btu/ft² h °F*).

Sample Heat Balances for a Nocturnal Radiator Under Various Conditions

- Exposed ordinary radiator at ambient temperature:
  T_r = 20°C;
  radiant heat loss = 70 W/m²;
  convective heat gain = 0;
  utilized cooling = 0.
- Exposed radiator under stagnation:
  T_r = 14°C, from experimental data;
  radiant heat loss = 64 W/m²;
  convective heat gain = 64 W/m²;
  utilized cooling = 0.

- Exposed radiator in use:
  $T_{r,\ av}$ 17°C, $T_{emit} = 16°C$;
  radiant heat loss = 67 W/m²;
  convective heat gain = 33 W/m²;
  utilized cooling = 67 — 33 = 34 W/m².
- Screened ordinary radiator at ambient temperature:
  transparency = 75%;
  T_r= 20°C;
  radiant heat loss = 0.75 ≃ 52 W/m²;
  convective heat gain = 0;
  utilized cooling = 0.
- Screened ordinary radiator under stagnation:
  T_r= 9°C, from experimental data;
  radiant heat loss = 45 W/m²;
  convective heat gain = 45 W/m²;
  utilized cooling = 0.
- Screened ordinary radiator in use under two conditions:
  1) When T_r = 17°C
     radiant heat loss = 50 W/m²;
     convective heat gain = 12 W/m²;
     net cooling = 38 W/m²;
  2) When T_r = 14.5°C
     radiant heat loss = 48 W/m²;
     convective heat gain = 22 W/m²;
     net cooling = 26 W/m².

The above calculations indicate that even without condensation (which nullifies the effect of the IR transparent windscreen), the effect of the screening on the useable radiant cooling is very small (when the radiator's temperature is kept at the same level as the exposed one) or even negative, when the radiator's temperature is lower.

It should be pointed out, however, that under stronger winds the relative performance of the screened radiator would be better, although the net cooling of both radiators would be smaller.

The results of the experimental data and the calculations may suggest far reaching implications for the application of convection suppression by IR transparent screens, as well as for the use of IR selective surfaces (to be discussed later).

The fact that even in arid regions like Sede Boqer condensation has negated the effect of the polyethylene on most of the summer nights may suggest that in more humid climates the practicality of using IR transparent screens is even more questionable.

Although from the physicist's viewpoint, and in laboratory and simulation studies, IR transparent windscreens seem to enhance the obtainable radiant cooling, there are some problems related to its application which may further reduce the efficiency of a polyethylene windscreen. In many cases even its desirability may be questionable.

Whenever the storage mass itself (e.g., a concrete roof or a roof water pond) is cooled at night, its temperature during most of the night is usually above the ambient air.

When a specialized radiator is being cooled at night by IR radiation its temperature is usually below that of the ambient air and an IR transparent windscreen may improve its performance. However, even in this case a distinction should be made between the laboratory case of a stagnant radiator and the situation when radiant heat loss from the radiator has to be used to cool a building. Whenever the radiator is used to cool a heat transfer medium, either air or water, its temperature is higher in comparison with the stagnant situation and closer to the ambient air. Consequently, the effect of the windscreen on the convective heat gain decreases and the reduction in the emitted radiation becomes more significant.

Another factor which may reduce the effectiveness of polyethylene windscreens is dust accumulation on the film. Polyethylene tends to exhibit static attraction of dust and, even without it, dust which ordinarily exists in the air may settle on the film and reduce its transmissivity. Furthermore, the dust particles may serve as nucleation centers for condensation, and thus enhance the formation of dew over the film.

It should also be pointed out, in summary, that the provision of a polyethylene windscreen in a full-scale building (or specialized radiators) increases greatly the cost of the cooling system due to the support and tensioning requirements. In reality there is a quantum jump in the cost of a radiator when an exposed one is transformed into a screened one. This factor may determine the economic viability of the system.

SELECTIVE LONGWAVE RADIATORS

To maximize the net longwave radiant heat loss, the radiative surface theoretically should reflect away the incoming atmospheric radiation (from the water, carbon dioxide, and the dust particles in the air) while emitting strongly at the longwave spectrum of the atmospheric window.

An ideal longwave radiator should have high absorptivity (and, therefore, high emissivity) in the 8-13 wave band and high reflectivity (and, therefore, low absorptivity) above and below this band. In particular, it would be desirable to have a surface with high reflectivity also in the solar spectrum (0.4 to 3.0 microns) so that radiant cooling will continue also during the daytime. Theoretical discussion of the potential for radiant cooling which can be obtained by a selective surface was presented by Catalanotti, et al.[13] The selective surface consisted of an aluminum layer evaporated on to a 0.1-mm Tedlar sheet, adhered to the aluminum radiator. A windscreen of thin polyethylene film minimized the convective gain. A stagnation temperature depression of about 12°C *(21.6°F)* was recorded. Daytime radiative cooling, with the radiator shaded from the direct solar radiation, yielded temperature depressions of up to 15°C *(27°F)*. Selective surfaces with similar properties are being developed.

Experimental comparisons of the radiant cooling obtainable by a graybody emitter and a selective emitter has been done by Mitchell in Australia,[14] by Sakkal, Martin, and Berdahl of the Lawrence Berkeley Laboratory,[15] and by Miller and Bradley of the Desert Research Institute in Nevada,[16] and by Landro and McCormick in Australia.[17]

Results of Experimental Studies

Mitchell[14] reported an extensive series of experiments which were carried out at the Commonwealth Scientific and Industrial Research Organization (CSIRO) in Australia in which the performance of radiators with various selective surfaces was measured. The radiators were either exposed to the sky or shaded from the sun. Shading was provided by a sheet of insulation mounted with a tilt of approximately 70° facing south (in the Southern Hemisphere). The inner layer of the shade was lined with bright rolled aluminum foil. In this way the radiating surface was shaded from the sun most of the daytime hours while "seeing" the sky. The surfaces tested as radiators included:

- anodized aluminum of 4 and 10 microns;
- aluminum with sodium silicate layer;
- aluminized Tedlar sheet;
- white paint;
- black paint.

In addition, several types of plastic sheets were tested for their IR transmission for evaluation as windscreens. The radiators were placed near the top of an insulated box and protected by a windscreen of polyethylene film.

The diurnal patterns of the radiator's surface temperature were measured and the temperature difference with respect to the ambient air computed and plotted. All tests were conducted under stagnation conditions.

No data on the meteorological conditions during the tests were given in the report (wet bulb temperature, wind) except for general comments on cloudiness. Nevertheless, the results enable general evaluation of the performance of the selective surfaces compared to ordinary black and white paints. In particular, as anodized aluminum was compared in many tests to other surfaces on the same days, the differences in temperature depressions between anodized aluminum and the other surfaces can serve as a basis for a more general evaluation.

At night the temperature depression of the anodized aluminum radiator without shading ranged from about 6° to 10°C *(10.8° to 18°F)*. During the day the temperature elevation of the radiator, above ambient air, ranged from 15° to 20°C *(27° to 36°F)*.

At night the temperature depressions of the anodized aluminum radiator with fixed shading and viewing the sky (directly and via a reflector) were around 7°C *(12.6°F)*. During the daytime hours the radiator's temperature was most of the time about 2° to 3°C *(3.6° to 5.4°F)* below the ambient air. No difference was found between anodizing thicknesses of 4 and 10 microns.

At night the temperature depression of the aluminum radiator with sodium silicate and shading was about 4°C *(7.2°F)*. Thus, it is less efficient than anodized aluminum.

The temperature depression of the aluminized Tedlar radiator with shading was about 6°C *(10.8°F)* at night, the same as that of anodized aluminum under the same climatic conditions. Thus, it seems that the two surfaces have about the same efficiency as longwave radiators.

At night the temperature pattern of a radiator painted black and without shading was the same as that of anodized aluminum, both with a depression of about 8.5°C *(15.3°F)*. Therefore, the spectral selectivity of anodized aluminum did not result in a higher total radiant heat loss. This point is discussed further later on.

The temperature depression of a radiator painted white and with shading at night was about 6°C *(10.8°F)*. No direct comparison with another surface was reported.

The experimental study of Sakkal et al.[15] at Berkeley consisted of exposing two horizontal plates covered with polyethylene windscreens to a clear night sky and allowing them to cool down until equilibrium temperature was achieved. The graybody emitter was an aluminum plate, 0.8 mm *(0.03 in.)* thick, painted white.

During the experimental comparison the ambient air temperature was 12.5°C *(54.5°F)* and the dew point 8°C *(46.4°F)*.

The white radiator was cooled to an equilibrium temperature of 3.5°C *(38.3°F)* while the selective emitter reached 3.3°C *(38°F)*. Thus, the stagnation temperature depression with both surfaces was about 8.5°C *(15.3°F)*. When the temperature depression of the radiators below ambient air was less than 5°C *(9°F)*, the ordinary surface actually cooled down faster than the selective one. Only at temperature depressions of more than 5°C *(9°F)* did the selective surface attain a somewhat lower temperature than the ordinary surface. The actual difference between them was negligible.

From the results of this experiment, the added efficiency of this selective emitter as compared to an ordinary painted aluminum plate was negligible. Another observation in this experiment was the condensation of dew on the upper surface of the polyethylene windscreen.

In the study of C. Miller[16] at the Nevada Desert Research Institute, the performance of ordinary surfaces (painted black and white) was compared to that of a selective surface made of anodized aluminum. At night, with still ambient air temperature of 5°C *(41°F)*, the selective surface reached a stagnation temperautre of -12°C *(10.4°F)*, the white surface reached -11°C *(12.2°F)*, and the black surface about -10°C *(14°F)*.

Also, in experiments which were reported by Kruskopf et al.[18] from Lawrence Berkeley Laboratory where the performance of an aluminized PVF was compared with that of white paint, very little difference was observed when the surface temperatures were about 6°C *(10.8°F)* below ambient air. The comparison was less favorable at higher radiator's temperatures.

Landro and McCormick[17] compared the radiant heat loss from a radiator painted flat black and a radiator made of aluminized PVF, under clear sky conditions. The regression lines of their measured results, expressing the radiant cooling (RC) as a function of the temperature difference between ambient air, T_a, and the radiator, T_r, (calculated by the author of this paper) were:

- for the black radiator:
  $RC = 90 - 9(T_a - T_r)\ \ W/m^2$;*(28.5 − 1.584* $(T_a - T_r)$ *Btu/ft² h °F;)*
- for the selective (PVF) radiator;
  $RC = 80 - 5.7(T_a - T_r)\ \ W/m^2$;*(25.4 − 1.0* $(T_a - T_r)$ *Btu/ft² h °F.)*

They also gave results of the radiant heat loss from the aluminized PVF under different absolute humidities, ranging from 8.7 to 11.6 gr/m³, at constant ambient temperature (292 K), and under different ambient temperatures, ranging from 288 K to 303 K at constant absolute humidity (8 gr/m³).

All these data were obtained with radiators screened by a thin polyethylene film, apparently without any dew formation over the polyethylene film.

Evaluation of the Performance of Selective Radiators

The results of all the studies mentioned above have demonstrated that, with the selective surfaces tested, no distinct advantage was observed in their radiant cooling potential over radiators with ordinary surfaces.

Taking into account the fact that the small effects of selectivity were obtained in all these studies under stagnation conditions, without any use of the cooling, the practicality of using selective surfaces (which always will be more expensive than ordinary surfaces) is questionable, at least in the present state of the technology of these surfaces.

When the radiating surface temperature is closer to the ambient air, as is usually the case when the roof itself serves as a combined radiator and cold-storage element, a selective radiator might even be less effective than an ordinary surface.

Another point which should not be overlooked is the probable effect of condensation on the performance of selective surfaces. The lower temperature attained by such surfaces may increase the likelihood of condensation over the selective surface itself. However, once the selective surface is covered by a water film it may lose its selective radiative properties. This point deserves experimental examination.

As research on the development of new materials for selective surfaces continues, it may be that eventually materials with performance closer to the ideal one will be available.

Additional Notes on Selective Surfaces

The disappointing results concerning the effect of selective surfaces on the performance of longwave radiators, which were obtained in practically all the studies where selective radiators were compared with ordinary ones, may suggest that something was wrong with the basic assumptions.

The concept that a selective radiator has an advantage over an ordinary one is based on the assumption that the intensity of the atmospheric back radiation, in the spectral regions below 8 microns and above 13 microns, is higher than the radiation emitted by an ordinary surface in these spectral regions. This situation can occur only when the sky temperature is higher than that of the ordinary radiator. As long as the radiator's temperature is higher than that of the sky, the emitted radiation (in the absence of any solar radiation) will exceed that of the atmospheric radiation at all wavelengths.

Therefore, a selective radiator can have an advantage over an ordinary one only when its temperature is actually lower than the effective sky temperature. This means that the depression of the radiator's temperature below ambient air must be greater than the difference between the ambient air and the sky temperatures for the selective radiator to be advantageous.

Such conditions may occur very rarely, even under stagnation conditions, when there is strong temperature inversion near the ground. However, when the radiator is used (e.g., by blowing air to be cooled under it), its temperature is higher than that which occurs under stagnation with the same meteorological conditions. In most likelihood, the radiator temperature, when used, will be closer to the ambient air temperature.

It may very well be that an inexpensive ordinary radiator might out-perform the more expensive selective one. Only experiments where a selective radiator is compared directly with an ordinary one under cold use conditions can resolve this question.

One of the reviewers of this article has made a comment disagreeing with this point. He has stated:

> Sky temperature is defined as the temperature of a horizontal blackbody surface in radiative equilibrium with the sky. Under such conditions the radiator experiences a net outward flux (radiative loss) in the spectral region between 8 and 13 microns, and an inward flux (radiative gain) outside this range of wavelengths such that the loss equals the gain. It is not always true that the emitted radiation will exceed that of the atmospheric radiation at all wavelengths when the radiator exceeds the

> sky temperature. This is true only if the radiator temperature exceeds the ambient air temperature. Selective emitters are in principle advantageous at all radiator temperatures below that of the ambient air.

This comment is of basic theoretical importance in understanding the spectral nature of radiant cooling. If this is true then it follows that a vertical radiator, which "sees" the earth and the lower layer of the atmosphere, which emits most of the atmospheric radiation below 8 microns and above 13 microns, will have no net radiant loss.

However, in previous experiments by the author,[11] as well as an experimental study on radiant cooling to be reported in a subsequent paper, temperature depressions measured on vertical ordinary exposed radiators amounted to about 40% of the temperature depression of a horizontal radiator at the same time.

Thus, it seems that this point of discussion deserves a detailed experimental/spectral investigation to clarify it.

DESIGN ISSUES AND APPROACHES IN RADIANT COOLING USE

The issues related to the design and application of cooling systems using nocturnal longwave radiation include several decisions:

1) to either apply direct cooling of a cold storage mass (usually the roof) or to cool a specialized lightweight and insulated radiating surface in contact with a heat transfer medium (air or water);
2) to select the type of radiating surface: either an ordinary (gray radiator) or a selective one;
3) to use or omit a convection suppression layer (usually a polyethylene film); and
4) to determine the suitability of radiant cooling under different climatic conditions and building types.

Some of the problems involved in applying different options to these design issues are discussed below.

Direct Cooling of the Cold-Storing Mass

Direct cooling of the cold-storing mass, by exposing it to the sky during the night while protecting it from the sun and the hot ambient air during the daytime, can be achieved in two ways:

1) by application of an operable insulation so that the roof itself (or a water pond above the roof) is exposed to the sky during the night and insulated during the daytime; and
2) by pumping water over the roof to create a pond above an insulating layer to be cooled during the nighttime, and draining the water below the insulating layer (but above the roof itself and in thermal contact with it) during the daytime.

Operable insulation can be in the form of horizontal movable panels (as in the Skytherm system) or hinged panels which are positioned vertically during the night so as to expose the roof mass below. These hinged panels should be covered on both sides with a reflective layer (e.g., aluminum foil) so that the radiation emitted in an oblique direction will be reflected toward the sky.

Horizontally movable panels require an area at the roof level for their storage while the roof is exposed. The area allocated to this function may take about one-quarter of the roof area and the area itself cannot be cooled by radiation. In small buildings the garage or a porch area can be allocated for the storage of the panels when the roof is exposed. In large buildings, an area has to be set aside for this function. Hinged panels, on the other hand, can expose effectively the whole roof area when in a vertical position. Although physically they cover an area corresponding to their thickness (about 5 to 10% of their height), it is possible to minimize this blocking effect by covering the two sides of the panels with a reflective layer (e.g., aluminum foil). Experiments by the author have demonstrated that with reflective vertical panels the roof effectively is exposed to the whole sky vault: the radiant cooling from a completely exposed roof and from a roof with such reflective panels above it was practically the same. Consequently such hinged panels seem more suitable than horizontal movable insulation for large buildings.

When the storage mass (the roof itself, a water pond, or pumped water) is cooled directly by outgoing longwave radiation, the temperature of the radiating body is higher than is the case with radiation from lightweight and insulated specialized radiators. The minimum temperatures which are attained by direct radiation are not as low as those of specialized radiators, but more heat is lost by radiation and more cold thus can be stored. The ceiling of the radiating roof can serve directly as a cooling panel and a heat sink for the space below it, and, thus, there is no need for heat exchangers.

Using the roof (or a water pond above it) as a longwave radiator and for cold storage with daytime insulation enables it to achieve temperatures well below the daytime outdoor air. Table 5 illustrates the typical results obtained in test cells at the Institute for Desert Research of the Ben-Gurion University in Israel.[19]

It is of interest to note that although the experiments were carried out in a desert and the water pond was exposed from sunset to sunrise, almost no observable net evaporation took place and the water level remained constant over several weeks. In fact, on most nights water evaporated until about midnight, but afterwards the water temperature dropped below the dew point with the result that condensation took place, balancing the previous evaporation.

Radiant Cooling by a Specialized Radiator

Instead of cooling the mass of the storage itself by outgoing longwave radiation, it is, of course, possible to cool a specialized longwave radiator to temperatures below those attainable when the storage mass is cooled directly. The radiator should be lightweight and insulated underneath to obtain rapid cooling without heat flow to the radiator from the roof below.

A heat transfer medium (air or water) flowing above, under, or within the radiator is cooled. The temperature to which the heat transfer medium can be cooled is always higher than the stagnation temperature of an unused radiator. The higher the flow rate of heat transfer medium per unit area of the radiator, the smaller the temperature depression of the heat transfer fluid below its initial temperature. Thus, there exists an inverse relationship between the flow rate and the temperature depression of the heat transfer medium.

Air Cooling

When the medium is outdoor air which flows under the nocturnal radiator (insulation prevents heat flow to the air stream from below), then the air temperature will gradually approach the stagnation temperature. If the stagnation temperature of the radiator is T_{stag}, its length *l*, and the flow rate per m² of radiator is F, then the air outlet temperature, T_{out}, will be:

$$T_{out} = T_a - (T_a - T_{stag})\ \mathrm{exp}\ \left(\frac{-kF}{l}\right) \cdot \quad (22)$$

The value of k depends on the ratio of the coefficients of heat transfer between the radiator and the ambient air, h_{out} and between the radiator and the air flowing under it, h_{in}. It can be determined experimentally.

In practice it means that the higher the velocity of the cooled air at a given flow rate (e.g., by decreasing the depth of the stream) relative to the ambient wind speed, the more efficient the cooling system. On the other hand, a higher velocity for a given flow rate requires more fan power to produce the required air flow. When the heat transfer medium is water then the inlet water temperature, T_{in}, should be substituted for T_a in the above formula.

The cold which is delivered from the radiator to the heat transfer fluid has to be transferred again to a thermal storage mass. When the heat transfer medium is air, then it is usually blown through a rock bin to cool the rocks. The cooled rocks are later used as a heat sink for the heat from the building during the following day by circulating the indoor air through the rock bin. In this way the rocks serve both as a storage mass and as a heat exchanger.

When water is used as the heat transfer medium it can be used also as the cold storage mass. However, with a water cold storage there is a need for a specialized water-to-air heat exchanger in order to cool the building. There is a temperature difference between the water in the storage and the cooled air, which in turn cools the building. In many cases the temperature of the water may be too high for the use of a heat exchanger. Consequently, air systems seem more suitable than water systems when specialized radiators are used.

Cooling of water by nocturnal radiation can be accomplished by the application of unglazed solar water heaters. During the night, the solar panels are cooled by the outgoing radiation to a temperature which is lower than the ambient air. The water flowing through the panels is also cooled down, and subsequently can be used for cooling buildings.

The temperatures attainable by radiant cooling usually are too high for application of conventional heat exchangers, such as fan coils. One possibility is to use them in cooling concrete floors, which then serve as combined cold storage and radiant convectors cooling panels. Such a system was applied in Davis, California, in the Trident Energy Systems, as reported by B. Juchau.[20]

In this system, water is cooled at night while flowing through unglazed solar collectors. The water circulates by polybutylene tubes embedded in the concrete floor. The concrete floor, in turn,

Cooling Performance of Roof

English (°F) Minimum	English (°F) Maximum		Metric (°C) Minimum	Metric (°C) Maximum
58	80.6	Outdoor air	14.5	27.0
		Roof 10-cm concrete:		
53.6	66.7	roof surface	12.0	19.3
57.2	70.3	indoor air	14.0	21.3
		Roof 4.5-cm concrete covered by water pond:		
53.6	65.3	roof surface	12.0	18.5
56.3	69.0	indoor air	13.5	20.5

Table 5: Some typical results are shown from test cells at The Institute for Desert Research at The Ben-Gurion University in Israel. Using the roof (or water pond above it) as a longwave radiation radiator and for cold storage with daytime insulation enables it to achieve temperatures well above the daytime outdoor air.

serves as a heat sink during the day.

The effect of nocturnal radiant cooling of the floor was evaluated under two conditions: one week with natural ventilation at night, and another week without night ventilation. The temperature in the house cooled by the radiant floor was about 2°C lower than in a similar control house. This cooling effect was delivered at an average energy efficiency ratio (EER) of 7.4 (with night ventilation) and an EER of 9.7 (without night ventilation).

Proposed Scheme for a Building Cooled by Nocturnal Radiation

Considering the application problems and cost of selective surfaces and of windscreens, it is the opinion of the author that, at least in the present state of the relevant technology, exposed ordinary radiators are the only ones suitable for immediate application.

Any metallic deck placed a few centimeters above an insulated, nearby, flat roof, can serve as the radiator. It should be painted to provide it with a high emissivity. The expected temperature depression of the radiator, under stagnation conditions, would be from about 4° to 5°C *(7.2° to 9°F)* (in humid regions) to about 6° to 7°C *(11° to 12.6°F)* (in desert regions).

Assuming the conditions for an exposed radiator in use, the utilized radiant cooling would be about 34 W/m^2 *(10.8 Btu/ft^{2}h)*. With an air flow rate, F, of 30 m^3/h per one m^2 of the floor area (3,000 m^3/h for a building of 100 m^2 and net volume of 250 m^3), the temperature depression of the air would be about 3.8°C *(6.8°F)* below the ambient night temperature. If this cooled air is used to cool the building by ventilation, the air change rate would be (3,000/250 = 12 air changes per hour, quite adequate for ventilation cooling.

It would be of interest to compare this radiant/convective cooling with pure convective cooling by ambient night air. Typical differences between the indoor air and the outdoor air at night, in buildings which are ventilated at night, are about 3° to 4°C *(5.4° to 7.2°F)*. As the temperature depression of the air cooled by nocturnal radiation is also about 3° to 4°C *(5.4° to 7.2°F)*, it means that the radiant cooling can double the net convective cooling achieved by nocturnal ventilation.

In regions where night winds with a known direction are available in summer, it is possible to induce the air flow under the radiator and through the building by the wind force, augmented by the thermosyphonic effect. This can be achieved by providing an air inlet, for the flow under the radiator, facing the prevailing night air. The wind then can force the flow under the radiator and into the building (e.g., through a small covered courtyard).

Warmer indoor air can be exhausted through a chimney, assisted by outlet details which produce a venturi suction effect, so that the same wind force produces pressure at the inlet to the nocturnal radiator and suction at the outlet for the indoor air.

In regions lacking persistent night winds, the air flow can be induced, of course, by a fan. A scheme of the system is shown in Fig. 5.

The color of the radiator (white or dark) does not affect its performance as a nocturnal radiator. Its choice would depend on whether or not it is intended for use in winter as a preheater of air in a solar space heating system. If winter heating is not contemplated, then the preferred color would be white, to minimize the heat load on the building. If winter heating is contemplated, then the color of the radiator would be dark, so it could serve as an exposed solar air heater.

Although the efficiency of an exposed horizontal solar collector is rather low, in many places it can provide very effective preheating of the ventilation air, which can then further be heated by glazed, vertical, or inclined solar air collectors.

CONCLUSION

From the theoretical analysis and the experimental studies summarized above, it is possible to estimate the performance which can be expected from various systems using nocturnal radiation as the cooling source.

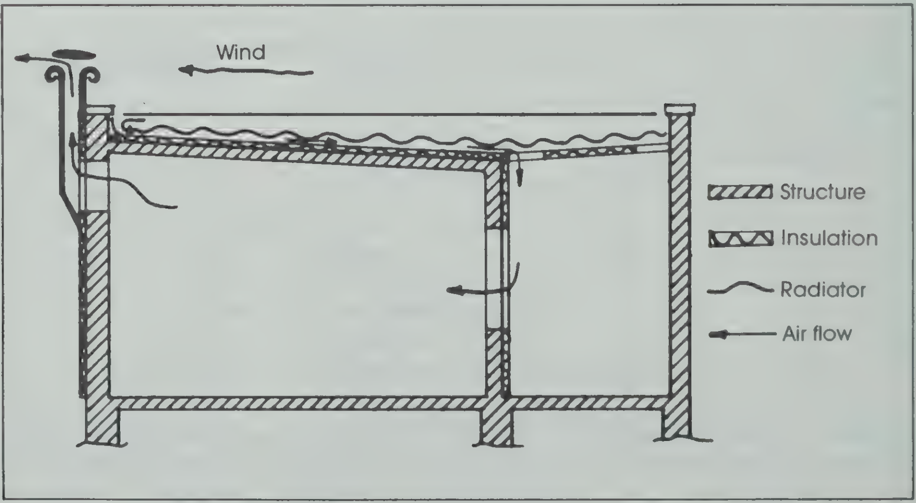

Figure 5: Warm indoor air can be exhausted when air is forced under the radiator, into the building, and then out again through a chimney. The air flow may be induced either by wind force or a fan.

Systems which directly cool the cold-storing mass (the roof itself or a roof water pond) operate generally at temperatures which are above the ambient night temperatures. As a result, they can use the whole radiant cooling effect together with some convective cooling. The total heat loss by such systems, over 10 hours of a night, can be about 1,000 W/m^2 night *(about 320 Btu/ft^2 night)* in arid regions, and about half that in humid regions. In such systems, the roof is made of conductive materials (concrete or steel) so that the ceiling acts as a radiant/convective panel for the space below. A temperature gradient of 2° to 3°C *(3.6° to 5.4°F)* between the ceiling and the indoor air temperatures is usually sufficient to provide the necessary cooling effect. In addition, the roof (or the pond) provides the thermal storage. However, an integral component of such systems is usually some form of movable insulation, so that the radiating surface is not exposed to the sky during the day. Existing systems of operable insulation are expensive and may require maintenance. Consequently, systems which directly cool the roof or a water pond are also expensive at present.

On the other hand, simple inexpensive systems exist which use nocturnal longwave radiation to cool the ambient night air for building ventilation. Just putting a metallic deck over an insulated roof, or using metal plates as the roof cover layer itself, can provide the nocturnal radiator. When outdoor air is blown under such a metallic deck it can be cooled by about 2° to 4°C *(3.6° to 7.2°F)* below the ambient temperatures in humid or arid regions, respectively.

When the cooling is required mainly during the evening and the night hours (e.g., in many residential buildings), such systems can provide the cooling effect at relatively modest cost. If the building has high heat capacity and is well insulated, it is possible also to use the cooled air for cooling the structural mass thus storing the night cold for the next day.

However, when specialized storage is required, such as a gravel bin, the usefulness and economic viability of radiant cooling may be questionable, especially in humid regions.

Concerning the selective surfaces and polyethylene windscreens, it is the opinion of the author that, with the present state of the relevant technology, there is no justification for their application, either on the basis of energy performance or cost. It seems that at present the use of ordinary low-cost materials for the radiating elements is the most reasonable approach.

It should be pointed out that existing mathematical models developed for predicting the performance of radiant cooling systems did not take into account the effect of the dew formation on the performance of the radiator. Furthermore, the existing models deal only with stagnation conditions and do not take into account the performance of the system when it is used. More theoretical work is required to take the above factors into account in predicting the performance of radiant cooling systems.

PROPOSED DIRECTIONS FOR FUTURE RESEARCH

In view of the higher performance of systems which directly cool the cold-storing mass and the present high cost of operable insulation which is presently essential for such systems, it seems to the author that research for using nocturnal radiation for cooling should be in developing systems with fixed insulation which can cool directly the cold-storage mass.

Another direction should be the development of inexpensive operable insulation for flat roofs or water ponds.

If any of these directions would yield satisfactory results, nocturnal radiation could provide effective cooling for single-story buildings in most climatic regions.

REFERENCES

1. Givoni, B; Mostrel, M. 1982. "Experimental Study and Model Validation of Radiant Cooling." Research report to the Israeli Ministry of Energy and the U.S. DOE. Institute for Desert Research, Ben-Gurion University of the Negev, Sede Boqer Campus, Israel.
2. Givoni, B. 1981 (Nov.). "Cooling Buildings by Passive Systems." *Passive Cooling: Proceedings of the International Passive/Hybrid Cooling Conference*. Edited by Arthur Bowen, Eugene Clark, and Kenneth Labs. Miami, Florida; Nov. 6-16, 1981. Newark, Delaware: American Section of the International Solar Energy Society, Inc. (AS/ISES), University of Delaware; pp. 588-596.
3. Clark, E.; Berdahl, P. 1980. "Radiative Cooling: Resource and Applications." *Passive Cooling Handbook: Proceedings of the Passive Cooling Workshop*. Edited by Harry Miller. Amherst, Massachusetts; Oct. 20, 1980. Berkeley, California: Center for Energy Efficient Design; pp. 177-212.
4. Clark, E.; Allen, C. 1978. "Estimation of Atmospheric Radiation for Clear and Cloudy Skies." *Proceedings of the Second National Passive Solar Conference*. 2.2 Edited by Don Prowler. Philadelphia, Pennsylvania; March 16-18, 1978. Newark, Delaware: AS/ISES, University of Delaware; pp. 675-678.
5. Clark, E.; Allen, C. 1979. "Sensible and Latent Cooling Requirements of Conventional and Passively Cooled Residences in American Climates." *Proceedings of the International Energy Commission, European Community*. Boston, Massachusetts; pp. 269-273.
6. Clark, E.; Allen, C. 1979a. "Supplemental Cooling Requirements of Passively Cooled Buildings in Selected American Cities." *Proceedings of the Third National Passive Solar Conference*. Edited by Harry Miller, Michael Riordan, and David Richards. San Jose, California; Jan. 11-13, 1979. Newark, Delaware: AS/ISES, University of Delaware; pp. 344-349.
7. Blanpied, M. 1979. "A Model of Radiative Cooling Using I.R. Transparent Windscreens." Dept. of Engineering Science, Trinity University, San Antonio, Texas.

8. Gordon, J.; Zarmi, Y. 1981. "Transient Behavior in Radiative Cooling." *Solar Energy*. Vol. 27, No. (1): 77-79.
9. Clark, G.; Blanpied, M. 1979. "The Effect of IR Transparent Windscreens on Net Nocturnal Cooling from Horizontal Surfaces." *Proceedings of the Fourth National Passive Solar Conference*. Edited by Gregory Franta. Kansas City, Missouri; Oct. 3-5, 1979. Newark, Delaware: AS/ISES, University of Delaware; p. 509.
10. Higgs, F.S.; Hand, J.W. 1979. "Assessing the Viability of the Sky as a Heat Sink for Passive Cooling in North Central Texas." SAED, University of Texas at Arlington.
11. Givoni, B. 1968. *Man, Climate and Architecture*. London: Applied Science Publishers.
12. Manning, R., et al. 1980. "Measurements and Simulations of Radiative Cooling Through IR Transparent Windscreens." *Proceedings of the Fifth National Passive Solar Conference*. 5.2. Edited by John Hayes and Rachel Snyder. Amherst, Massachusetts; Oct. 19-26, 1980. Newark, Delaware: AS/ISES, University of Delaware; pp. 717-719.
13. Catalonotti, S., et al. 1975. "The Radiative Cooling of Selective Surfaces." *Solar Energy*. Vol. 17:83.
14. Mitchell, D. 1976. "Selective Radiation Cooling: Another Look." University of Melbourne, Parksville, Victoria, Australia.
15. Sakkal, F., et al. 1979. "Experimental Test Facility for Selective Radiative Cooling Surfaces." *Proceedings of the Fourth National Passive Solar Conference*. Edited by Gregory Franta. Kansas City, Missouri; Oct. 3-5, 1979. Newark, Delaware: AS/ISES, University of Delaware; pp. 483-487.
16. Miller, W.C.; Bradley, J.O. 1979. "Radiative Cooling with Selective Surfaces in a Desert Climate." *Proceedings of the Fourth National Passive Solar Conference*. Edited by Gregory Franta. Kansas City, Missouri; Oct. 3-5, 1979. Newark, Delaware: AS/ISES, University of Delaware; pp. 480-482.
17. Landro, B.; McCormick, P.G. 1980. "Effect of Surface Characteristics and Atmospheric Conditions on Radiative Heat Loss to a Clear Sky." *Int. Heat Mass Transfer*. Vol. 23:613-620.
18. Kruskopf, M., et al. 1980. "Radiative Cooling Test Facility and Performance Evaluation of 4-Mil. Aluminized Polyvinyl Fluoride and White Paint Surfaces." Lawrence Berkeley Lab.
19. Givoni, B. 1980. "Experimental Studies on Passive Cooling at the Institute for Desert Research, Israel." *Proceedings of the International Solar Energy Symposium*. Nice, France; Dec. 1980; pp. 296-300.
20. Juchau, B. 1981. "Nocturnal and Conventional Space Cooling Via Radiant Floors." *Passive Cooling: Proceedings of the International Passive/Hybrid Cooling Conference*. Edited by Arthur Bowen, Eugene Clark, and Kenneth Labs. Miami, Florida; Nov. 6-16, 1981. Newark, Delaware: AS/ISES, University of Delaware; pp. 256-260.

ADDITIONAL READINGS

Atwater, M.A.; Ball, J.T. 1978. "Computation of I.R. Sky Temperature and Comparison with Surface Temperature." *Solar Energy*. Vol. 21:211.

Berdahl, P.; Fromberg, R. 1981. "An Empirical Model for Estimating the Thermal Radiance of Clear Skies." Submitted to *Solar Energy*.

Berdahl, P.; Martin, M. 1971. "Spectral Measurements of I.R. Sky Radiance." *Proceedings of the Third National Passive Solar Conference*. Edited by Harry Miller, Michael Riordan, and David Richards. San Jose, California; Jan. 11-13, 1979. Newark, Delaware: American Section of the International Solar Energy Society, Inc. (AS/ISES), University of Delaware; pp. 443-447.

Givoni, B. 1977. "Solar Heating and Night Radiation Cooling by a Roof Radiation Trap." *Energy and Buildings*. Vol. 1:141.

Givoni, B. 1979. "Passive Cooling by Natural Energies." *Energy and Buildings*. Vol. 2.

Givoni, B. 1981a. "Conservation and the Use of Integrated Passive Energy Systems in Architecture." *Energy and Buildings*. Vol. 3:213.

Givoni, B. 1981b. "Experimental Studies on Radiant and Evaporative Cooling of Roofs." *Passive Cooling: Proceedings of the International Passive/Hybrid Cooling Conference*. Edited by Arthur Bowen, Eugene Clark, and Kenneth Labs. Miami, Florida; Nov. 6-16, 1981. Newark, Delaware: AS/ISES, University of Delaware; pp. 279-283.

Hansen, D.G.; Yellott, J.I. 1978. "A Study of Natural Cooling Process in a Hot, Arid Region." *Passive Solar State of the Art*. Vol. 2. Mid-Atlantic Solar Energy Association. Philadelphia, Pennsylvania; p. 653.

Hay, H.R. 1978. "A Passive Heating and Cooling System from Concept to Commercialization." *Proceedings of the 1978 Annual Meeting of the American Section of ISES*. Newark, Delaware: AS/ISES, University of Delaware.

Martin, M.; Berdahl, P. 1979. "Radiative and Passive Cooling." *Proceedings of the Third Annual Solar Heating and Cooling Research and Development Branch Contractors Meeting*. Washington, D.C.

Sayigh, A.A.M. 1976. "Summer Night Sky Cooling in Saudi Arabia. *Proceedings of Solar and Heating: A National Forum*. Miami Beach, Florida; Dec. 13-17, 1976; p. 271.

Yellott, J.; 1979. "Historical and International Perspective for Passive Solar Heating and Cooling." *Proceedings of the Third National Passive Solar Conference*. Edited by Harry Miller, Michael Riordan, and David Richards. San Jose, California; Jan. 11-13, 1979. Newark, Delaware: AS/ISES, University of Delaware; pp. 508-511.

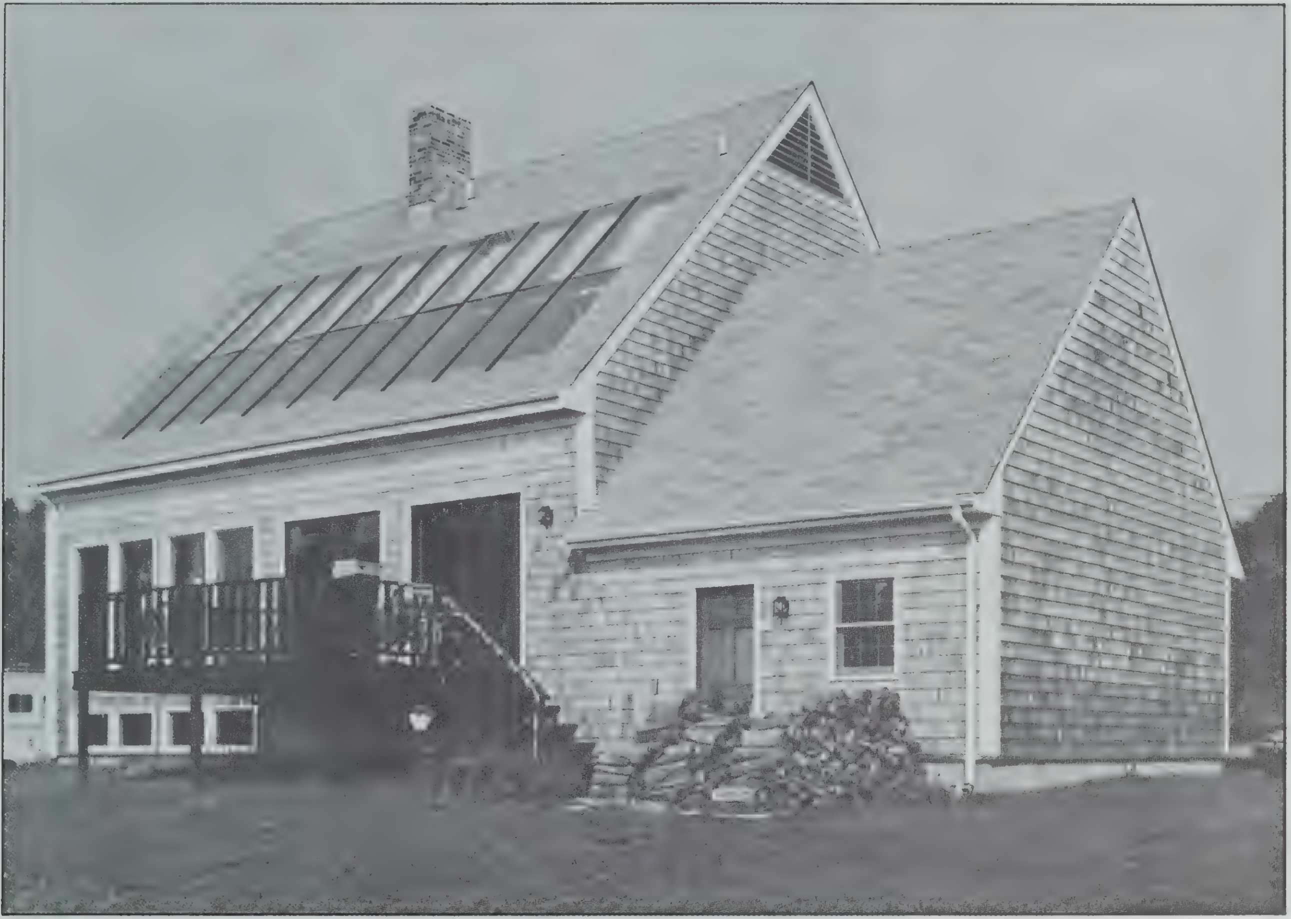

Figure 1: A southeast view of the Mastin house shows the solarium exterior and massive roof glazing.

The Mastin Double-Envelope House: A Thermal Performance Evaluation

By RALPH F. JONES and GERALD DENNEHY
Brookhaven National Laboratory, Upton, New York 11973

ABSTRACT

An evaluation is made of the thermal performance of a double-envelope house of Ekose'a design built by Robert Mastin in Middletown, Rhode Island. The home has two shells with an air space between through which air can circulate. Monitoring of the house in the heating season showed that the requirements for auxiliary heat are very low, about 2.1 Btu per square foot of floor space per Fahrenheit degree-day *(43 kJ/m² °C-DD)*. Design changes are identified which could reduce the heating requirement even further. This ranks the house among the most energy-efficient building designs available today. It is concluded that the low heating needs of the house are due primarily to the excellent insulative value of the double shell.

Figure 2 (below): A sectional view of the Mastin house shows the relationship of the inner and outer shells.

Figure 3 (at right): The balcony into the solarium from the second floor can be seen at the back of the interior view above.

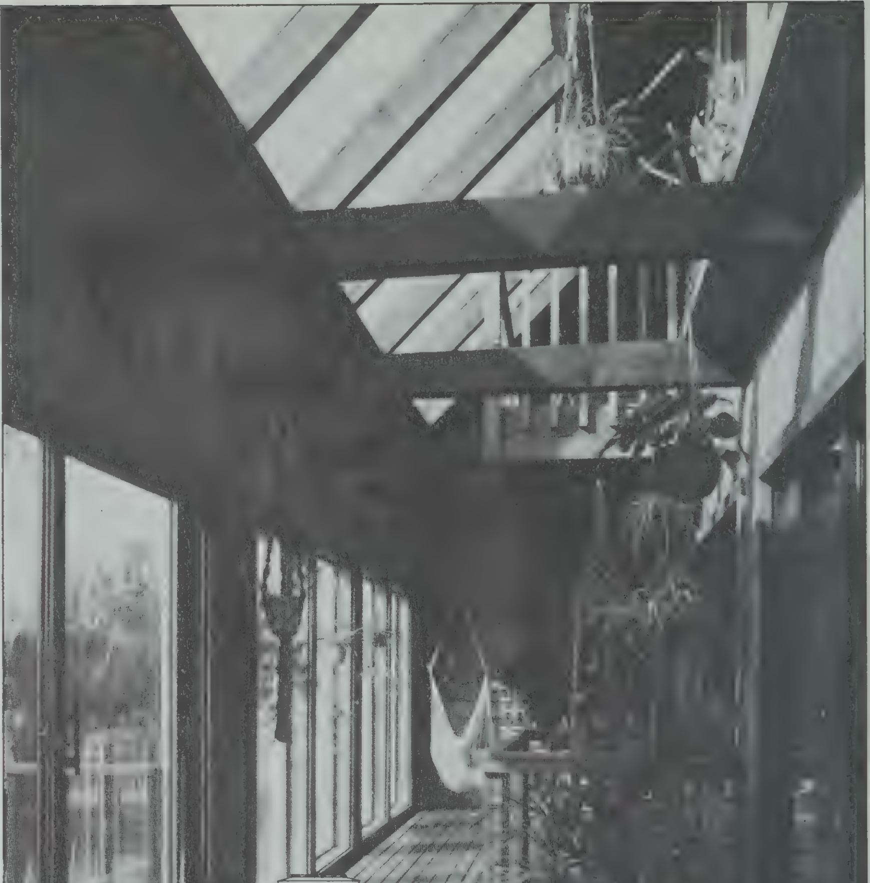

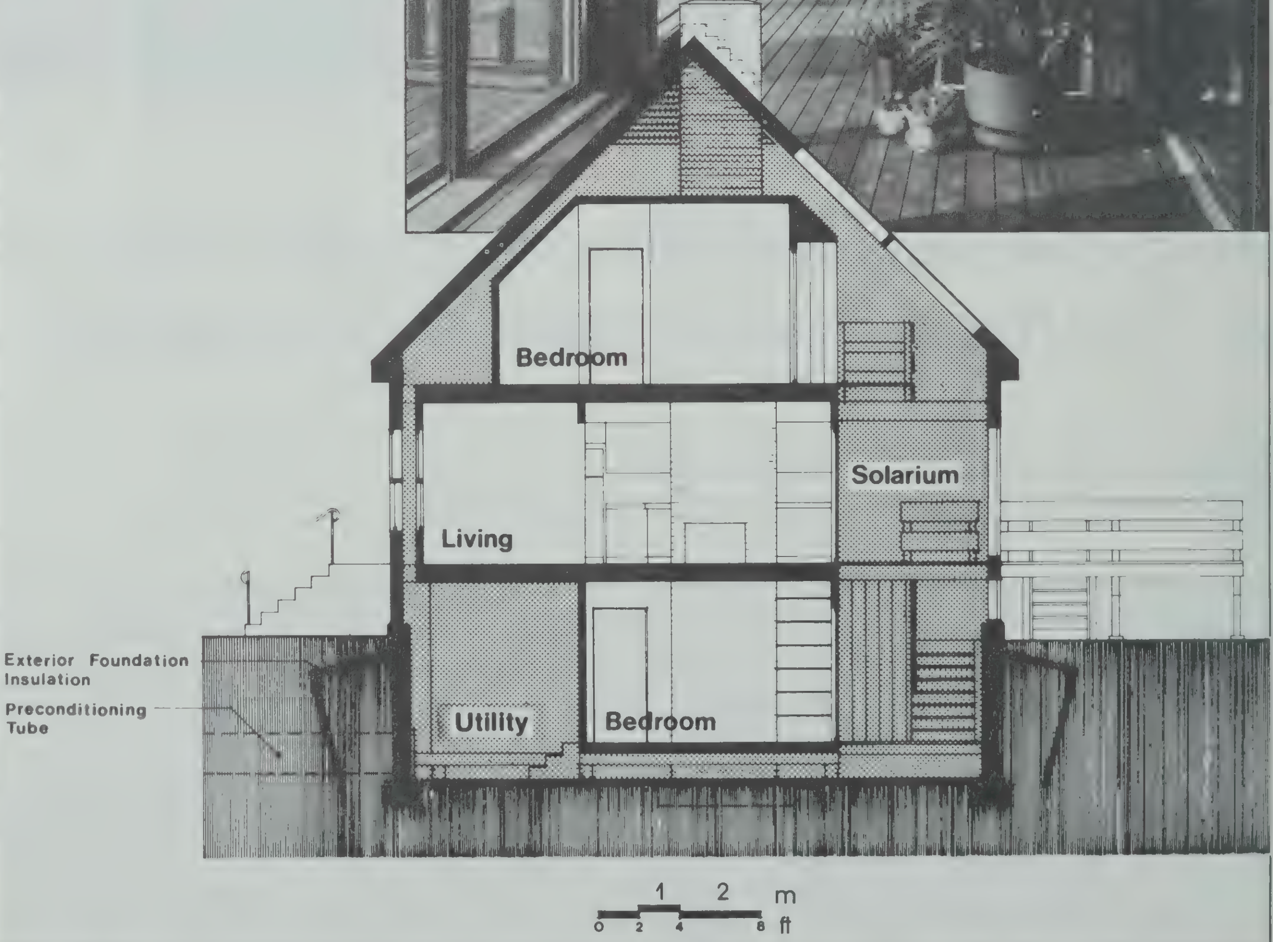

INTRODUCTION

The "double-envelope house" has received a lot of attention in the last few years. It is also referred to as "double-wall," "double-shell," "thermal envelope," "air envelope," "buffering air envelope," or simply "envelope house." If the word "envelope" is taken to mean "shell," then "double envelope" is a more accurate description than "envelope." Those using the term envelope house apparently consider the air space between the shells to be an envelope.

Whatever it's called, the design is basically a house within a house. Typically, a double-envelope house is one with an inner and outer roof, two walls on the north side, an attached sunspace on the south side, and a crawl space below the basement. Both shells are insulated. Air is presumed to flow through these spaces in what has been called a "convective loop." Articles on double-envelope houses have appeared in trade journals and newsletters, popular magazines, and major city and local newspapers. Most articles emphasize the claim that these houses can be heated by the sun, the earth, and the heat given off by occupants, appliances, and a fireplace, and require no conventional heating system.

Several hundred double-envelope homes have been built or are under construction around the country. One of the first architects to market the concept successfully is Lee Porter Butler. His firm, Ekose'a, located in San Francisco, has designed over 100 double-envelope homes to date, including one built by Robert Mastin in Middletown, Rhode Island.

Brookhaven National Laboratory (BNL) made preliminary experimental measurements at the Mastin house in January, February, and March 1980. This article provides an analysis of the data taken during that winter period and during subsequent short-term testing. The Mastin house was recommended to BNL for evaluation in consultation with Lee Porter Butler, who felt it was generally representative of Ekose'a designs in its thermal performance. The proximity of the house to BNL was also a factor in the choice. Butler cooperated in the preparation of the study by providing background information and drawings of the Mastin house.

DESCRIPTION OF THE HOUSE

The Mastin house is a double-envelope design with relatively traditional Cape Cod styling (except for the south elevation) built in Middletown, Rhode Island, in late 1978 and early 1979. The house has three stories including basement, with approximately 2,000 ft^2 *(186 m^2)* of living area, or 2,600 ft^2 *(242 m^2)* including the solarium and its space below. The top floor holds two bedrooms and a bathroom. On the main level an open space comprises living, dining, and kitchen areas. There is also an air-lock foyer and a bathroom. Both the top and main floors face the two-story solarium to the south. The solarium floor consists of 2 x 4 in. *(50 x 100 mm)* wood decking with 3/16 in. *(4.8 mm)* slots between boards. On the second floor, a balcony of similar construction projects into the solarium. The lower, or basement, floor contains a bedroom (which Mastin uses as an office), a bath, an all-purpose family room, a utility room, and an unassigned space under the solarium floor. All floors are accessible to the others through a large, central stairwell. Sliding doors on the main floor and in one of the bedrooms on the upper floor permit opening the inner space to the solarium. There is an attached garage on the east side.

A photograph of the southern elevation of the house appears in Fig. 1. The house is shown in cross section in Fig. 2, with the convective loop space shaded. Figure 3 provides a view of the main level in the solarium and the balcony extending from the upper level. Construction details of the north wall are shown in Fig. 4.

The Mastin building site is relatively flat with a view of the Atlantic Ocean to the south. The location is approximately 41° 30′ north latitude and 71° 15′ west longitude with about 5,800 heating degree-days, base 65°F *(3,220 °C-DD, base 18°C)*. Nearby Narragansett Bay and the Atlantic Ocean raise winter temperatures enough that many storms precipitate rain rather than snow. Sea breezes cool the summers, and dense fogs occur often in both summer and fall and occasionally in winter. The mean daily solar radiation is approximately 300 Langleys or 1.1 x 10^3 Btu/ft^2 *(12.5 MJ/m^2)* on an annual basis.

The house is of frame construction with single walls of 2 x 6 in. *(50 x 150 mm)* studs, insulated with R-19 fiberglass batts on the east and west. The double north wall is constructed of 2 x 4 in. studs on the inside and 2 x 6 in. studs on the outside, *(50 x 100 mm and 50 x 150 mm)*, with a clear air space of 8 in. *(200 mm)* between. Fiberglass batt insulation is R-11 *(R_{SI}-1.9)* on the inside and R-19 *(R_{SI}-3.3)* on the outside. Kraft paper on the batts is used as a vapor retarder, oriented towards the warm side. The top floor ceilings (the floor of the attic) are insulated with R-11 *(R_{SI}-1.9)*, and the roof (or attic ceiling) is insulated with R-19 *(R_{SI}-3.3)*. The roof and exterior walls are sheathed with plywood over which asphalt roof shingles or cedar shingles are applied. There is about 520 ft^2 *(48 m^2)* of double-glazed south window area, two-thirds of which is on the 45° roof. The other three elevations have minimal glazing. Urethane foam insulation is installed in the ground outside the foundation perimeter. The convective loop is 8 ft *(2.4 m)* wide in the solarium and 8 in. *(200 mm)* wide on the north side of the house.

The double north wall is connected to a 12 in. *(300 mm)* high sub-basement crawl space through the utility room on the north. A 4 in. *(100 mm)* concrete floor slab was poured on the excavated sub-basement earth grade, and wood joists supported by 8 in. *(200 mm)* concrete block form the final

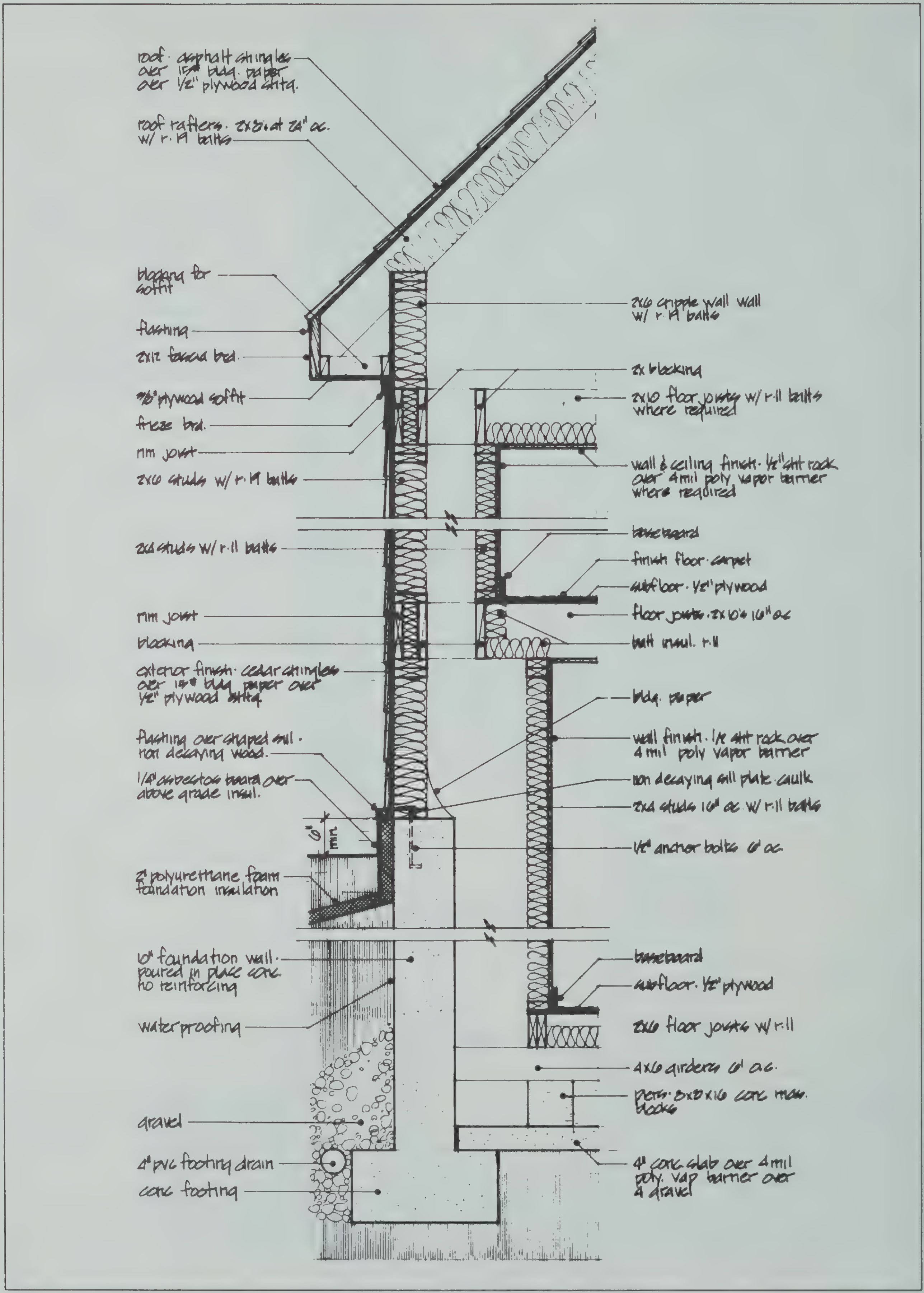
roof · asphalt shingles over 15# bldg. paper over 1/2" plywood shtg.
roof rafters · 2x8's at 24" oc. w/ r·19 batts
blocking for soffit
flashing
2x12 fascia bd.
5/8" plywood soffit
freeze bd.
rim joist
2x6 studs w/ r·19 batts
2x4 studs w/ r·11 batts
rim joist
blocking
exterior finish · cedar shingles over 15# bldg paper over 1/2" plywood shtg.
flashing over shaped sill · non decaying wood.
1/4" asbestos board over above grade insul.
6" min.
2" polyurethane foam foundation insulation
10" foundation wall · poured in place conc. no reinforcing
waterproofing
gravel
4" pvc footing drain
conc footing
2x6 cripple wall wall w/ r·19 batts
2x blocking
2x10 floor joists w/ r·11 batts where required
wall & ceiling finish · 1/2" sht rock over 4 mil poly vapor barrier where required
baseboard
finish floor · carpet
subfloor · 1/2" plywood
floor joists · 2x10's 16" oc
batt insul. r·11
bldg. paper
wall finish · 1/2 sht rock over 4 mil poly vapor barrier
non decaying sill plate · caulk
2x4 studs 16" oc · w/ r·11 batts
1/2" anchor bolts 6' oc.
baseboard
subfloor · 1/2" plywood
2x6 floor joists w/ r·11
4x6 girders 6' o.c.
piers · 8x8x16 conc mas. blocks
4" conc slab over 4 mil poly. vap barrier over 4" gravel

Figure 4: Construction details are visible in a section through the north wall.

structure for the finished floor above that crawl space. The basement wood floor joists are insulated with R-11 *(R_{SI}-1.9)* fiberglass batts.

Several of the appliances—an electric water heater, a freezer, a clothes washer, and a dryer—are located in the utility room, which is a part of the convective loop. There is no central heating system and no ductwork for air distribution. Two small electric baseboard heaters of 3,000 watts total capacity are installed on the lower level, however. (These were added by Mastin as a retrofit.) In addition, there are two wood-burning fireplaces, which draw combustion air from the convective loop. Mastin installed a wood stove in the fireplace on the lower level after his first year in the house.

For summer ventilation, a large louver is provided at each end of the roof peak. These are hinged and can be opened and closed by a system of ropes. In addition, there is a 21 in. *(533 mm)* diameter metal cooling tube installed under the north lawn with a riser to ground level near the property line. This tube goes through the foundation in the utility room. By opening a cover, air cooled by the ground can be admitted to the convective loop.

THERMAL PERFORMANCE EVALUATION

Scope of Analysis

The decision to proceed with monitoring the performance of the Mastin house was made in December 1979. Plans were made to proceed at once in order to obtain cold weather performance data during the winter of 1979-80. This decision dictated use of monitoring equipment already on hand, which consisted of data recorders of the type that provide printed records on paper tape. Because the reduction of data recorded in this manner is very time consuming, continuous testing for

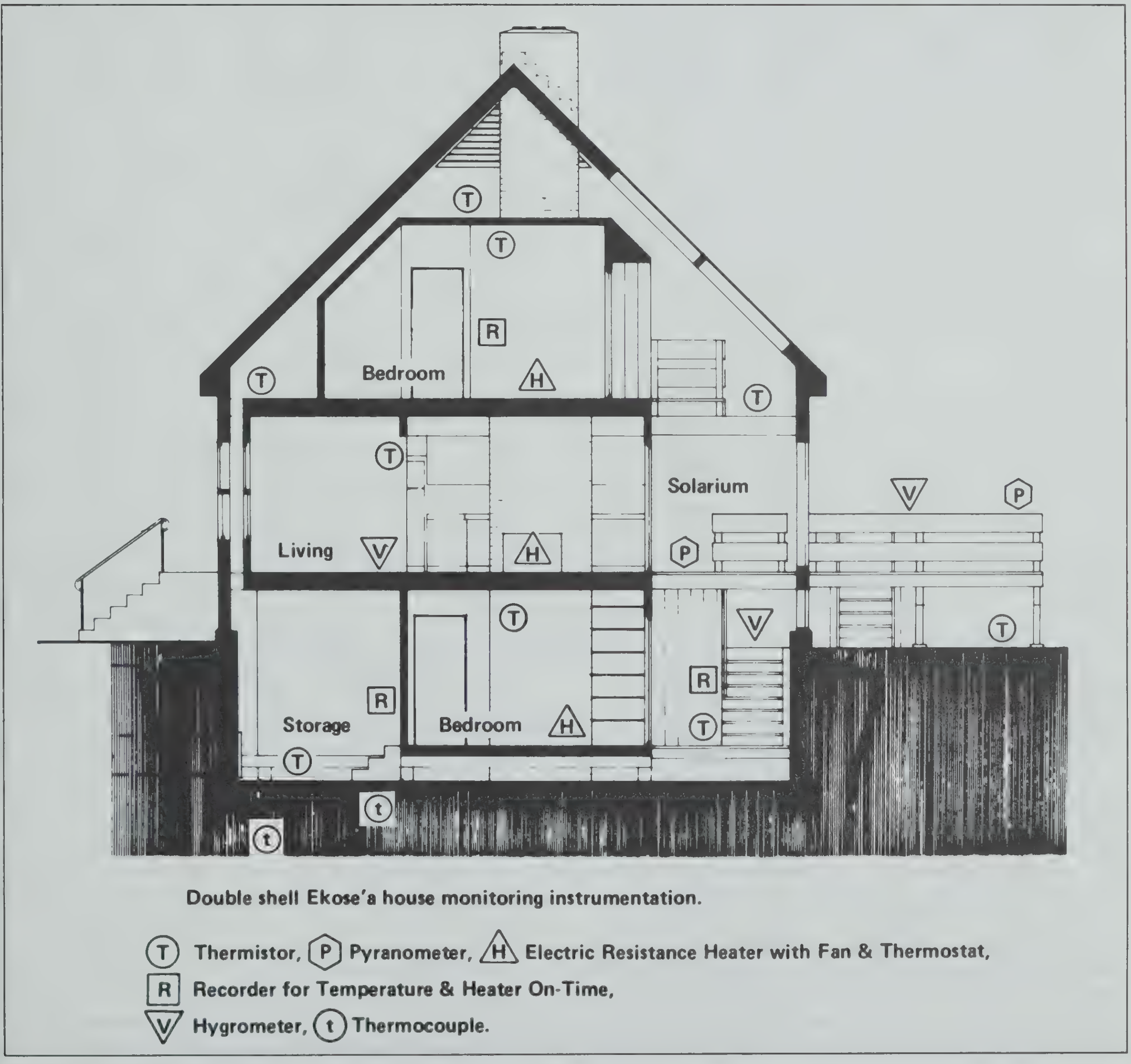
T
T
R
Bedroom
H
T
T
T
Solarium
V
P
Living
V
H
P
T
V
R
Storage
R
Bedroom
H
T
T
t
t
T
Double shell Ekose'a house monitoring instrumentation.
T Thermistor, P Pyranometer, H Electric Resistance Heater with Fan & Thermostat,
R Recorder for Temperature & Heater On-Time,
V Hygrometer, t Thermocouple.

Figure 5: Instruments were located throughout the house as shown.

a long period was not planned. Short-term testing was scheduled for periods in January, February, and March 1980 to determine the extent to which the house required auxiliary heating in order to maintain comfortable indoor temperatures. The short-term test results were to be used to estimate the need for auxiliary heat over a full heating season. After identifying the basic performance of the house in those terms, further tests were to be considered to identify and analyze the contribution of individual features of the house, such as ground thermal coupling.

Instrumentation Employed

Instrumentation used in the initial monitoring included nine thermistors for temperature measurement, three recording hygrometers for relative humidity, and two recording pyranometers for insolation on the horizontal plane. The location of this equipment in the house is shown in Fig. 5.

A 1,500-watt electric heater with a wall-mounted thermostat was installed centrally on each floor. The precise wattage of each heater had been determined in the laboratory and the three heaters were to be used as the sole source of auxiliary heat during the test periods. Three data loggers were installed, one on each floor. Each data logger recorded the readings of three of the thermistors at 20-minute intervals, along with the number of seconds of operation of one of the heaters during the previous 20-minute period. A Fluke data logger was used for thermocouples which were installed later in the testing for monitoring temperatures in the slab below the house and in the cooling tube.

Approach to Preliminary Testing

During the winter test periods, the heater thermostats were set to provide a nominal temperature of 65°F *(18°C)* on each level of the house at all times. By recording the "on time" for each heater during each 20-minute period, it was possible to determine reasonably accurately the kWh consumed and the amount of auxiliary heat required by the house. The electric consumption of the heater and its fan is converted to Btus at 100% efficiency. The procedure is called the electric coheating method[1] of identifying a building's auxiliary heating needs.

The house was occupied during the test periods by Robert and Elizabeth Mastin. In double-envelope houses and other houses with a solarium, thermal performance depends on an interaction of the occupants with the building. During the heating season, doors connecting the solarium to the inner space are normally opened on sunny winter mornings as soon as the solarium temperature exceeds the temperature in the living space, typically between 9 and 11 a.m. Heat is then transferred from the solarium to the house by free convection. These doors are closed in the late afternoon when the solarium temperature drops to the house temperature or when the indoor temperature has risen to a comfortable level.

Since the primary purpose of the preliminary tests was to establish the amount of auxiliary heat required to keep the house comfortable during winter months, fireplaces were not intended to be used during the test period. Nevertheless, the Mastins used the fireplace a few times during the test period. The electric auxiliary heat was adjusted upward on the days when a fire was lit, as recorded in a detailed log he maintained, by the amount of heat estimated to have been provided by the wood fire. If the testing had not been performed, the occupants would probably have met a significant part of the auxiliary heating requirement during the test period by burning wood, as a matter of personal choice.

Observed Hourly Performance, January 20 to 26, 1980

Figure 6 provides an hour-by-hour record of selected performance data for the seven-day period, January 20 to 26, 1980. This period was representative in that it included days with high and low insolation and with a range of outside temperatures typical of Rhode Island mid-winter weather.

The first two days of the period (January 20 and 21) had high insolation and outside temperatures in the range of 23° to 42°F *(-5° to 6°C)*. The final three days (January 24 to 26) also had high insolation, but were somewhat colder, in the 18° to 38°F range *(-8° to 3°C)*. In between, there were two days (January 22 and 23) with low insolation and temperatures in the range of 23° to 41°F *(-5° to 5°C)*.

On sunny days, the temperature at the top of the loop exceeded 90°F *(32°C)*. It reached 106°F *(41°C)* on January 25 and 26. The peak was reached in all cases between noon and 3 p.m. The temperature at the bottom of the loop remained in the range of 45° to 55°F *(7° to 13°C)* for the entire period. On cloudy days, it remained in a narrow range of 48° to 52°F *(9° to 12°C)*. The time of the peak temperature at the bottom of the loop generally coincided with the time of the peak at the top of the loop on four of the sunny days but lagged by a few hours on the other sunny day (January 21). The time of the trough of the temperature at the bottom of the loop on sunny days coincided almost exactly (within one hour) with the temperature at the peak of the loop.

The average indoor temperature remained generally in the 63° to 65°F *(17° to 18°C)* range during the seven-day period, but rose to the 68° to 71°F *(20° to 22°C)* range in midafternoon on the sunny days. As mentioned earlier, the electric heater thermostats were set at a nominal 65°F *(18°C)*. Mastin set them a degree or two lower on the upper floors, however, during part of the test period, as a matter of comfort.

The daily and hourly requirement for auxiliary electric heat are shown toward the bottom of Fig. 6. The daily requirement ranged from 115 x 10^3 Btu to 176 x 10^3 Btu *(33.7 to 51.6 kWh)*. As would be expected, it was lowest on a sunny day (January 20) and highest on a cloudy day (January 22). On January 25, a sunny day, the auxiliary heat was the same 160 x 10^3 Btu *(46.9 kWh)* as on January 23, a cloudy day, but the average outside temperature was 22.9°F *(-5.1°C)* on the sunny day versus a warmer 32.4°F *(0.2°C)* on the cloudy day.

The total use of auxiliary heat during the seven days was 1,032 x 10^3 Btu. This equates to 302 kWh or a cost of only about $11.00 at the kWh rate (.036). Mastin was paying for his hot water electric service at the time the test was conducted. For comparison, if the house had been heated by an oil heating system with an efficiency of 75%, the oil use for this typical winter week would have been only 10 gallons *(38 l)*. For a gas heating system with a 70% efficiency, the gas use would have been only about 15 therms *(42 m^3)*. This is less than a quarter of the oil or gas use of typical older houses with the same floor space.

The bars in Fig. 6 showing hourly auxiliary heating demands provide a basis for several observations. On the two cloudy days, the demand was relatively constant at about 7 x 10^3 Btu/h *(2.05 kW)* throughout the 24-hour period. On sunny days, the demand was relatively high in the hours from midnight to 8 a.m. and relatively low in the hours from 6 p.m. to midnight. The hourly average on sunny days ranged from 5 x 10^3 Btu/h to 6.75 x 10^3 Btu/h *(1.5 kW to 2.0 kW)*. Some heat was always needed in the noon to 6 p.m. period, even on clear days. This was due to stratification of air in the three levels of the house, discussed below.

The outside temperatures in the midnight to 6 a.m. period were essentially the same on January 24 and January 25 (19.7°F *(-6.8°C)* and 18.1°F *(-7.7°C)*, respectively). January 25 followed a sunny day, while January 24 followed a cloudy day. Designers of double-envelope houses claim that heat captured in the convective loop on sunny days is stored in the ground (or the structure) and released to the loop at night. If this is true, one would expect the midnight to 6 a.m. auxiliary heat requirement to be lower on January 25 than on January 24. Actually, the requirement in those six hours was 57.9 x 10^3 Btu *(17.0 kW)* on January 25 and 62.2 x 10^3 Btu *(18.2 kW)* on January 24. The difference is so small that it suggests that no significant storage and release of heat is taking place over that time span. The principal release of heat stored in the loop dur-

Observed Hourly Performance, January 20 to 26, 1980

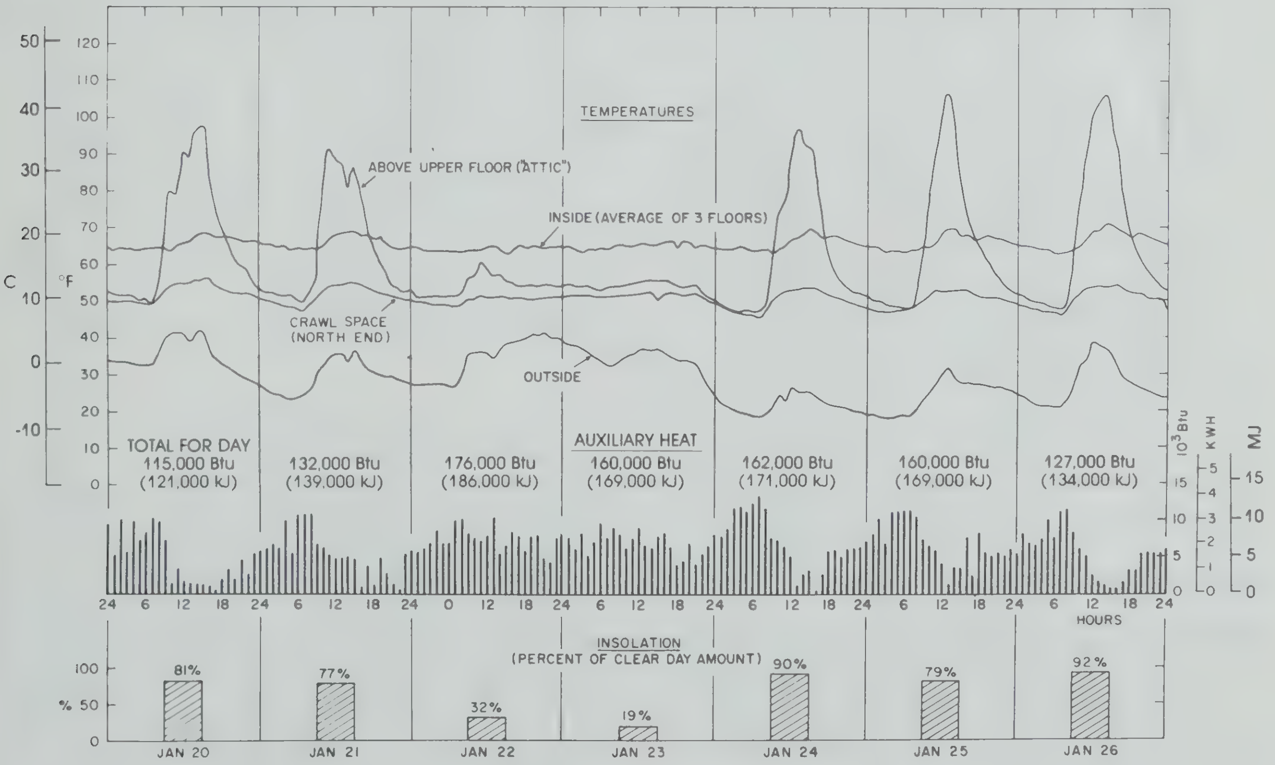

Figure 6: Observed hourly performance includes two sets of information. The first, at the top of figure, is air temperature. Curves are plotted for outside and inside temperatures and for temperatures at the top (attic) and bottom (crawl space) of the convective loop on the north side. The second, shown in narrow vertical bars, is the use of auxiliary heat during each hour. Also shown, at the bottom of the figure, is each day's insolation available as a percentage of the clear sky insolation available on that date in Middletown.

Air Temperature and Heater Use by Levels: January 25 to 26, 1980

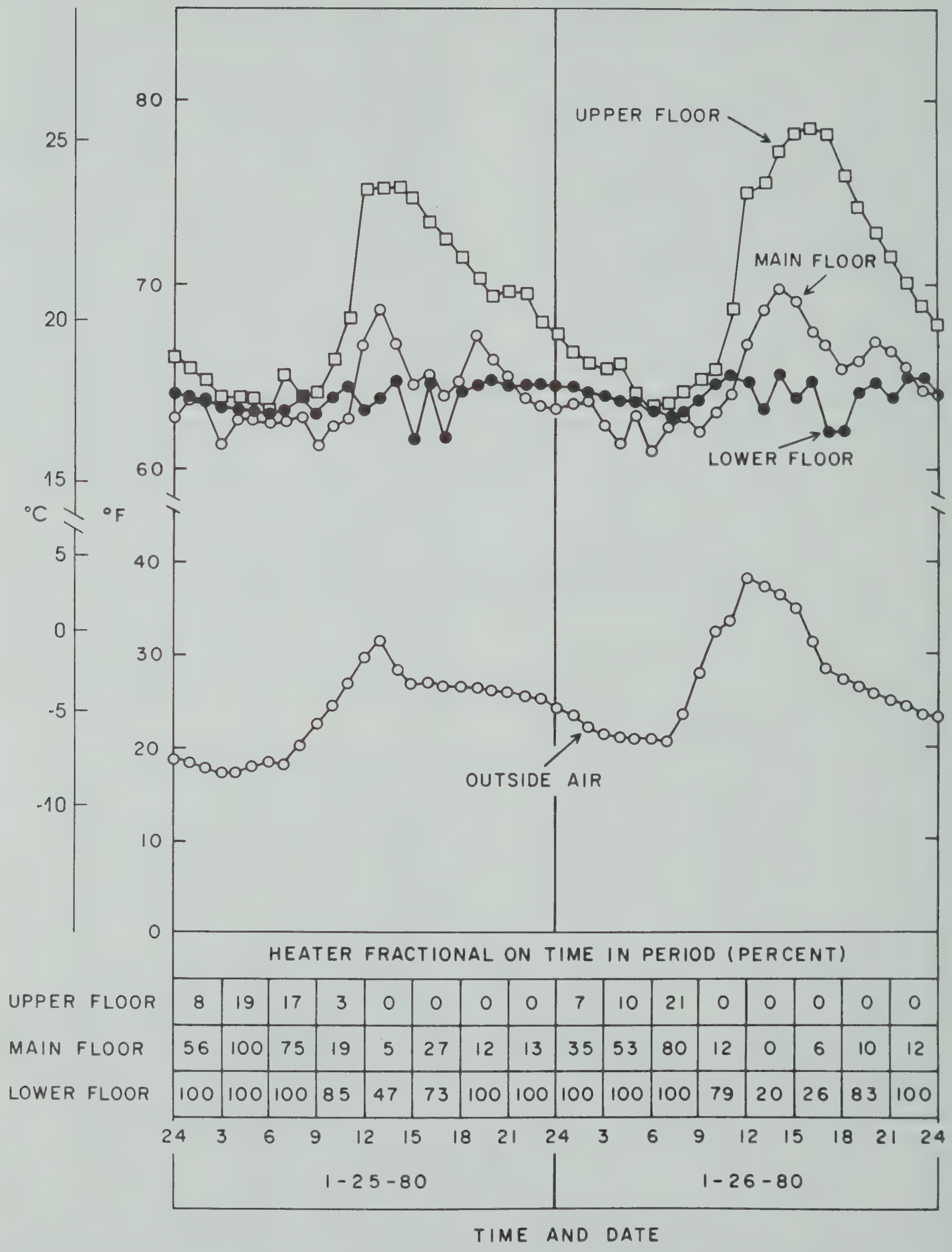

HEATER FRACTIONAL ON TIME IN PERIOD (PERCENT)

UPPER FLOOR	8	19	17	3	0	0	0	0	7	10	21	0	0	0	0	0
MAIN FLOOR	56	100	75	19	5	27	12	13	35	53	80	12	0	6	10	12
LOWER FLOOR	100	100	100	85	47	73	100	100	100	100	100	79	20	26	83	100

Figure 7: Hourly air temperatures are plotted for the outside and for each of the three floors inside. At the bottom of the figure, running times are tabulated for each of the three auxiliary heaters, expressed as the percentage of each three-hour period that a floor's heater was on. Note the difference between the lower and upper floors.

ing the day appears to take place in the evening hours.

As noted above, some auxiliary heat was always used, even in the afternoons on sunny days when the average house temperature rose to a range of 68° to 71°F *(20° to 22°C)*. The reason for this is evident from examination of Fig. 7. This figure provides a plot of hourly temperatures on each of the three levels of the house for the sunny two-day period January 25 and 26, 1980. Outside air temperature is also plotted. At the bottom of the figure, the running time of each of the electric heaters is tabulated. The heater running times are listed for each three-hour period, expressed in terms of the percent of time that the heater was operating in that period.

On the first day, the upper floor temperature rose to 75°F *(24°C)* by noon and remained there until 3 p.m. when it started to drop slowly. It was not until 3 a.m., however, that it reached 65°F *(18°C)*, at which temperature the auxiliary heater would come on. On the second day, which was milder—38°F *(3°C)* high versus 32°F *(0°C)*— the upper floor temperature rose to 78°F *(26°C)* by 3 p.m. By midnight it had fallen only to 68°F *(20°C)*. The heater on this level operated only 5% of the time during the two days.

The lower level temperature, in contrast, never exceeded 65°F *(18°C)* during the entire two-day period. The heater on this level was on most of the time, including periods (such as 6 p.m. to 11 p.m., January 25) when the average house temperature was above 65°F *(18°C)*. The lower level heater was on 82% of the time in the two-day period, and the main floor heater was on 32% of the time.

The lack of forced circulation in the house results in stratification of the air. This results in a situation where auxiliary heat is needed on the lower level even when the upper level is overheated. If some mixing of the air on the three levels could be achieved, the auxiliary heating requirement would be even lower than that measured in this test.

Heating Load Calculation

A calculation of the heating load of the inner space of the house was made, according to ASHRAE, in order to permit comparison with observed performance. The existence of the convective loop space does not present any special problems in this calculation. The ASHRAE procedure provides for treatment of adjacent unheated spaces, such as attics.

In calculating the heating load of the inner space, a value was assumed for the air temperature in the convective loop about midway between the assumed inside and outside air temperatures, which were 68° and 0°F *(20° and -18°C)* respectively.* A similar assumption was made for the garage. The losses to the convective loop from the house were tabulated separately from losses directly to the outside (as at the east and west walls) and to the garage. The losses from the convective loop to the outside were also tabulated. The losses to the convective loop should, of course, be equal to the losses from the convective loop. In the first calculation, they were not equal. A new temperature was selected for the convective loop and losses were calculated again. This procedure was repeated until an equality of losses was obtained. A summary tabulation of the results is shown in Table 1. The equilibrium temperature in the convective loop was just under 37°F *(3°C)*.

The heating load calculated for the inner space, according to this method, is 28.227 x 10^3 Btu/h *(8,272 W)*. This is equal to a "normalized heating requirement" (NHR) of about 411 Btu/h°F *(217 W/°C)*. Of the total heat load, 21.637 x 10^3 Btu/h *(6,341 W)*, or 77%, is lost to the convective loop, and 21.637 x 10^3 Btu/h *(6,341 W)* is lost from the convective loop to the outside.

In making the heating load calculation, an air infiltration rate of 0.5 air changes/h (ACH) was used for the inner building. Infiltration tests were performed with the assistance of the Princeton Center for Environmental Studies using a simplified sulfur hexafluoride gas concentration decay method in which the samples are returned to Princeton for analysis. Two readings, under winds of 5 mph and 12 mph *(2 m/s and 5 m/s)*, each showed about 0.5 ACH.

It is interesting to note that the roof glazing accounts for a heat loss of some 10.819 x 10^3 Btu/h *(3,171 W)* at 68°F *(20°C)* Δ T, or 50% of all heat lost by the convective loop.

Calculated Heat Loss
0°F (-18 °C) Outside Temperature,
68 °F (20 °C) Inside Temperature

	English (Btu/h)	**Metric** (W)
Heat loss from inner space:		
To convective loop	21,637	6,341
Other losses	6,590	1,931
Total loss	28,227	8,272
NHR	=411 Btu/h°F	=217 W/°C
Heat loss from convective loop:		
Through roof glazing	10,819	3,171
Other losses	10,818	3,170
	21,637	6,341

NHR: Normalized heating requirement

Table 1: Tabulation of heat loss is based on an equilibrium temperature in the convective loop of just under 37°F (3°C).

---

*The outside temperature of 0°F *(-18°C)* was selected as being representative of many locales in the Northeast. The ASHRAE winter design temperature for Middletown, Rhode Island, is actually 5°F *(-15°C)*.

Estimated Internal Heat

Metric (W) Appliances and Lighting	Metric (W) Occupants	Metric (W) Total	Space	English (Btu/day) Appliances and Lighting	English (Btu/day) Occupants	English (Btu/day) Total
387	131	518	Inner space	31,660	10,700	42,360
525		525	Convective loop	43,000		43,000
912	131	1,043	Total	74,660	10,700	85,360

Table 2: Heat available to the inner space is estimated from records of meter readings for the three months prior to January 1980 and from location and estimated use of lighting and appliances. Heat available to the convective loop is based on estimates from appliances and lights located in the loop, and on readings of the separate meter for the domestic hot water heater in the loop.

Daily Performance Analysis, January 17 to February 16, 1980

Continuous performance monitoring of the house took place from mid-January to mid-February, except on January 31 when suitable data were not obtained. Each day's performance was analyzed to determine the need for auxiliary electric heat in relationship to the outside air temperature (Δ T) and the amount of insolation available to heat the house on that day.

The pyranometer on the deck outside the house recorded insolation on the horizontal plane. The horizontal insolation was converted to a "weighted insolation" available to the outside of the house, taking account of the inclination of the house's south-facing glass. About 32% of that glazing is vertical and 68% (that part in the roof) is at an angle of 45° from the horizontal. In order to arrive at a weighted value, the observed horizontal insolation in Btu/ft^2 h was converted to insolation in the vertical and 45° planes, using standard ratios for 40° latitude, and these values were combined in a 32/68 ratio.

The auxiliary heating requirement also was normalized for the difference between inside and outside temperatures (Δ T), in order to deal with only two variables, normalized auxiliary heating requirement and weighted insolation. To do this, Δ T for each day was adjusted downward to account for the internal heat from occupants, lighting, and appliances. This is necessary because internal heat is essentially constant and is not related to degree-days. The need for auxiliary and solar heat depends on heating degree-days after crediting for internal heat.

The Mastin house has separate electric meters for the domestic hot water heater and all other uses. Referring to records of meter readings for the three months prior to January 1980 and the location and estimated usage rates of lighting and appliances, an estimate was made of the heat available to the inner space. This turned out to be about 282 kWh per month of electricity, which equates to 31.66 x 10^3 Btu/day. (The water heater, freezer, clothes washer and dryer, and some lights, are located in the convective loop. Their rejected heat is not directly available to the inner space.)

Occupancy during the test period included Mr. Mastin and a construction worker on weekdays during working hours, and Mr. and Mrs. Mastin in the evenings and about half of weekend hours. This converts, at 250 Btu per person per hour, to 10.7 x 10^3 Btu/day *(131 W)*. The total estimated internal heat available to the inner space is, therefore, 42.36 x 10^3 Btu/day *(518 W or 12.42 kWh/day)*.

Heat available to the convective loop was estimated to include the balance of the non-hot-water electric usage and one-half of the electricity used by the water heater. The other half of the water heater energy was assumed to leave the house with drain water. The internal heat estimates are summarized in Table 2.

The reduction of "breakeven" or "balance" temperature of the inner house due to internal heat can be estimated by applying the NHR for the house calculated in Table 1, as follows:

$$\text{NHR} = 411 \text{ Btu/h°F}$$

$$NHR = 217\ W/°C$$

$$\Delta\text{T} = \frac{42,360}{411 \cdot 24} = 4.29°\text{F } (2.4°C).$$

The temperature data recorded for each day was analyzed on an hour-by-hour basis. The average outside temperature for an hour was subtracted from the average inside temperature (on the three levels) to obtain a degree-hour figure. These were summed over 24 hours to obtain a degree-hour total for the day. These figures were then converted to degree-days (based on actual inside temperatures) and reduced by 4.3°F *(2.4°C)* to obtain degree-day figures adjusted for the internal heat available to the inner space.

The adjusted degree-day figures for the January 17 to February 16 period are shown in Table 3, along with the daily auxiliary electric heating requirement (as determined from the running time of the three heaters), and the auxiliary heating requirement normalized on an adjusted degree-day basis.

Also tabulated is the weighted insolation figure for each day, whose calculation was described earlier.

The normalized auxiliary heating requirement for each day in this period is plotted against weighted insolation in Fig. 8. A best-fit straight line is drawn through the points, using a linear regression analysis. The correlation coefficient, .79, indicates a reasonably good correlation between these two variables. The amount of auxiliary heat needed drops significantly, but not drastically, as insolation increases. On days with ample sunlight the auxiliary heating requirement is about 30% less than on days with slight insolation. This relatively small difference may suggest that a true southerly orientation of the sunspace is not critical for the double-envelope house.

Extrapolating the line in Fig. 8 to the ordinate indicates that the house would need about 7.6 x 10^3 Btu/°F-DD *(4.0 kWh/°C-DD)* (adjusted for internal heat) in the absence of sun. This amount is compared to the heat loss calculated by the ASHRAE method in Fig. 9, for a 30°F *(-1°C)* outside temperature and a 68°F *(20°C)* inside temperature.

The design heat load calculated in Table 1, 28.227 x 10^3 Btu/h *(8,272 W)* corresponds to a NHR of 411 Btu/h °F *(217 W/°C)*. At a ΔT of 38°F *(21°C)*, the load would be 411 · 38 · 24 *(217 · 21 · 24)* or 375 x 10^3 Btu/day *(395 MJ/day)*. The internal heat available to the inner space, 42.36 x 10^3 Btu/day *(44.7 MJ/day)*, can be subtracted from the calculated heat load, leaving a net load of 332.64 x 10^3 Btu/day *(350.3 MJ/day)*. The indicated auxiliary heating re-

Daily Auxiliary Heat, Adjusted Degree-Days, and Insolation; English

				Auxiliary Electric Heat		
Day	Date	Degree-Hours (°F)	Adjusted Degree-Days (°F)	Daily Amount (10^3 Btu)	Per Adjusted Degree-Day (Btu/DD)	Weighted Insolation (Btu/ft^2 day)
1	Jan. 17	861	31.6	227.9	7,214	417
2	18	703	25.0	187.5	7,501	666
3	19	635	22.2	147.3	6,637	542
4	20	728	26.0	114.8	4,415	1,429
5	21	860	31.5	132.4	4,702	1,352
6	22	733	26.2	176.2	6,726	559
7	23	751	27.0	160.4	5,939	346
8	24	1,051	39.5	161.9	4,099	1,617
9	25	987	36.8	160.2	4,354	1,437
10	26	907	33.5	127.3	3,799	1,678
11	27	835	30.5	111.3	3,651	1,633
12	28	861	31.6	102.9	3,256	1,545
13	29	905	33.4	173.4	5,190	712
14	30	1,058	39.8	196.5	4,938	1,729
15	Feb. 1	1,098	41.5	213.0	5,134	1,655
16	2	1,093	41.2	188.9	4,584	1,934
17	3	1,048	39.4	189.7	4,815	1,871
18	4	1,006	37.6	168.1	4,471	1,823
19	5	996	37.2	170.1	4,574	1,589
20	6	919	34.0	153.6	4,518	1,608
21	7	870	32.0	244.9	7,653	686
22	8	837	30.6	174.8	5,712	1,917
23	9	886	32.6	148.5	4,554	1,364
24	10	909	33.6	154.6	4,600	1,402
25	11	914	33.8	219.2	6,485	756
26	12	807	29.3	136.4	4,657	1,496
27	13	861	31.6	119.1	3,769	1,753
28	14	762	27.5	132.3	4,813	1,237
29	15	792	28.7	97.8	3,407	1,595
30	16	829	30.3	217.3	7,172	536

Degree-days adjusted downward by 4.3 °F to account for 42.36 x 10^3 Btu/day of internal heat available to the inner space. Data for Jan. 31 were not suitable, and therefore are not reported here.

Table 3a: Adjusted degree-day figures are shown for the January 17 to February 16 test period, along with the auxiliary heat required daily and the auxiliary heat normalized on an adjusted degree-day basis. The weighted insolation figure for each day is also shown. See Table 3b for metric equivalents.

quirement in the absence of sun, 7.6 x 10^3 Btu/adjusted °F-DD *(4.0 kWh/°C-DD)*, would be 256.12 x 10^3 Btu/day *(270 MJ/day)*.* This is about 23% less than the calculated load less internal heat.

As indicated in Table 2, about 43 x 10^3 Btu/day *(45.3 MJ/day)* of heat from lighting and appliances is released to the convective loop. This heat tends to reduce the need of the inner space for auxiliary heat. If it contributes to reducing the heat loss of the inner space at a ratio of one Btu for each two Btu of internal heat, the difference of 76.32 x 10^3 Btu/day *(80.5 MJ/day)* in Fig. 9 would be reduced by 21.5 x 10^3 *(22.7)*, to 54.82 x 10^3 Btu/day *(57.8 MJ/day)*. The remaining difference would be about 16.5% of the calculated heat load less internal heat. In other words, the thermal performance of the house in the absence of sun is about 16.5% better, in terms of auxiliary heat required, than would be expected from an ASHRAE heat loss calculation. Many observers feel that the ASHRAE factors are often conservative by 10% to 20%.

The auxiliary heat required during the full 30 days of testing in January and February was about 4.91 x 10^6 Btu *(1,439 kWh or 5,181 MJ)*. The degree-days for the period totaled 1,051 *(584)*. This was somewhat more than the average for the period, which is about 990 *(550)* for Middletown. Insolation on the horizontal plane averaged 806 Btu/ft^2 day *(9.15 MJ/m^2)*, also somewhat above the average for the period, which is about 760 *(8.63)*. Thus, the period was a bit colder than normal but had more sun than normal. In terms of heating load, it was probably quite close to normal. The auxiliary heat needed for the 30-day period is summarized in Table 4.

---

*7,600 (68 - 4.3 - 30) = 256,120, where 4.3 is the inside temperature adjustment associated with internal heat.

Daily Auxiliary Heat, Adjusted Degree-Days, and Insolation; Metric

Day	Date	Degree-Hours (°C)	Adjusted Degree-Days (°C)	Auxiliary Heat Daily Amount (kWh)	Auxiliary Heat Per Adjusted Degree-Day (kWh/DD)	Weighted Insolation ($MJ/m^2/day$)
1	Jan. 17	478	17.5	66.79	3.82	4.74
2	18	391	13.9	54.95	3.95	7.56
3	19	353	12.3	43.17	3.51	6.16
4	20	404	14.4	33.65	2.34	16.23
5	21	478	17.5	38.80	2.22	15.35
6	22	407	14.6	51.64	3.54	6.35
7	23	417	15.0	47.01	3.13	3.93
8	24	584	21.9	47.45	2.17	18.36
9	25	548	20.4	46.95	2.30	16.32
10	26	504	18.6	37.31	2.01	19.06
11	27	464	16.9	32.62	1.93	18.55
12	28	478	17.5	30.16	1.72	17.55
13	29	503	18.6	50.82	2.73	8.09
14	30	588	22.1	57.59	2.61	19.64
15	Feb. 1	610	23.0	62.43	2.71	18.80
16	2	607	22.9	55.36	2.42	21.96
17	3	582	21.9	55.60	2.54	21.25
18	4	559	20.9	49.27	2.36	20.70
19	5	553	20.6	49.85	2.42	18.05
20	6	511	18.9	45.02	2.38	18.26
21	7	483	17.7	71.78	4.06	7.79
22	8	465	17.0	51.23	3.01	21.77
23	9	492	18.1	43.52	2.40	15.49
24	10	505	18.6	45.31	2.44	15.92
25	11	508	18.8	64.24	3.42	8.59
26	12	448	16.3	39.98	2.45	16.99
27	13	478	17.5	34.91	1.99	19.90
28	14	423	15.2	38.77	2.55	14.05
29	15	440	15.9	28.66	1.80	18.11
30	16	461	16.8	63.69	3.79	6.09

Degree-days adjusted downward by 2.4 °C to account for 12.42 kWh/day of internal heat available to the inner space. Data for Jan. 31 were not suitable, and therefore are not reported here.

Table 3b: Metric equivalents are given for Table 3a.

Auxiliary Heating Requirement vs. Insolation: January 17 to February 16, 1980

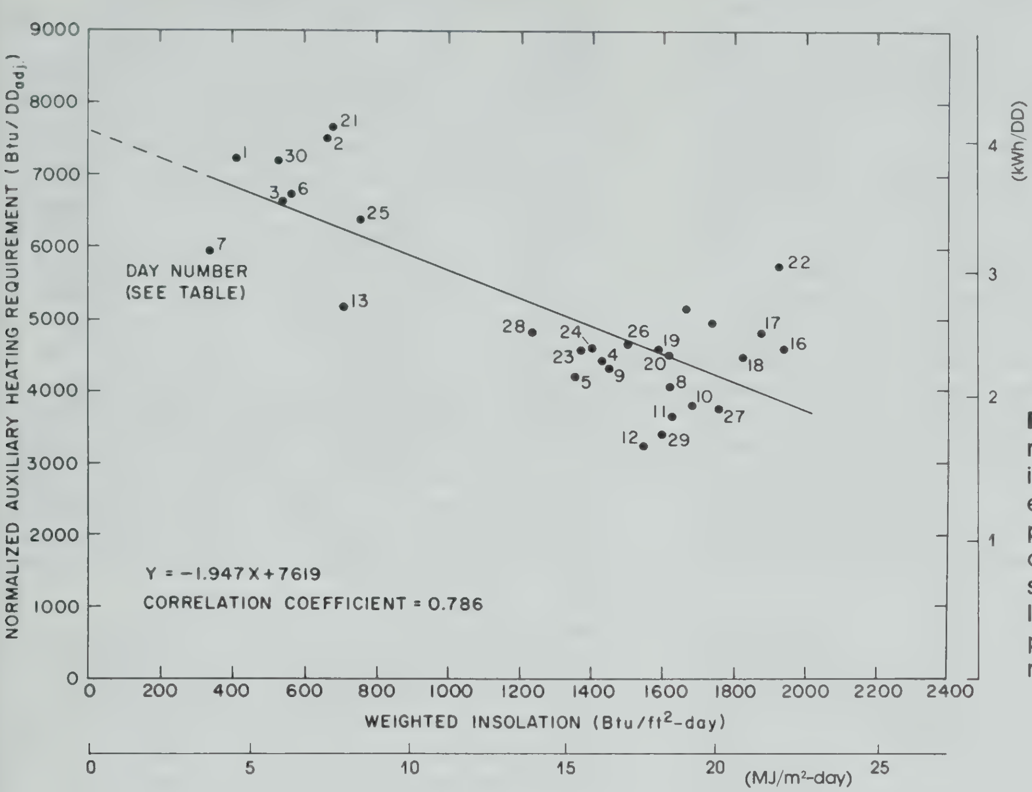

Figure 8 (at left): A normalized auxiliary heating requirement for each day of the test period is plotted against weighted insolation, with a best-fit line drawn through the points, using a linear regression analysis.

Auxiliary Heating Requirement, Internal Heat and Calculated Heating Load with No Solar Heating

Figure 9 (at right): Heat loss calculated by the ASHRAE method is compared to the auxiliary heating requirement extrapolated from Fig. 8.

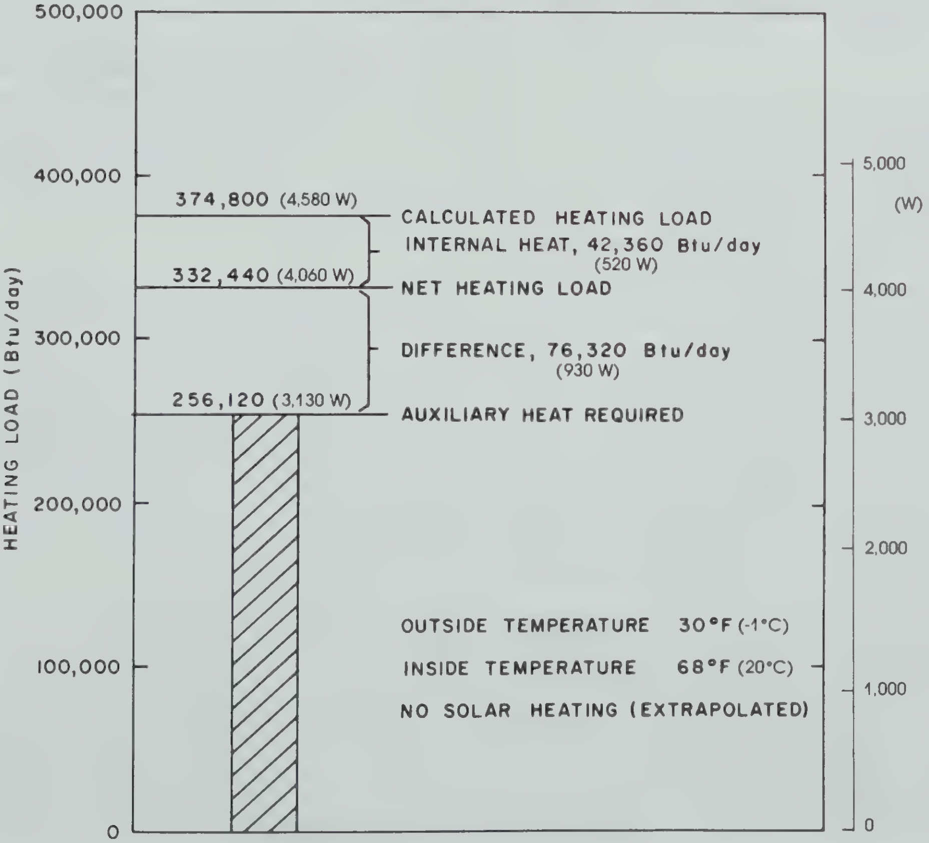

The auxiliary heat use for the 30-day period agrees closely with the use discussed earlier for the January 20 to 26 period. It is less than a quarter of the purchased energy needed for space heat in conventional, recently built houses with equivalent floor space. The average inside temperature was about 64°F *(18°C)* during this period, but it tended to be higher than this on the upper floors during the daytime, as discussed previously. No night temperature setback was used during the test period. The 64°F *(18°C)* 24-hour average temperature can be thought of (and roughly equated to in terms of heat required) as a day temperature of 66°F *(19°C)* and a night temperature of 60°F *(16°C)*.

The daily auxiliary heat required by the house in this period is related to insolation in Fig. 10. The requirement varies from about 3 Btu/ft^2 °F-DD *(61 kJ/m^2 °C-DD)* under conditions of light insolation to about 2 Btu/ft^2 °F-DD *(41 kJ/m^2 °C-DD)* on cloudless days. Under average conditions of insolation, the house can be characterized as having a mid-winter auxiliary heating requirement of about 2.5 Btu/ft^2 °F-DD *(51 kJ/m^2 °C-DD)*. Over the entire heating season the figure would probably be even lower, perhaps close to 2.0 *(41)*. This is true because, while degree-day tables show degree-days in all months, even summer months in which the hourly temperature is below 65°F some of the time, the solar and thermal storage features of houses like the Mastin house tend to preclude the need for auxiliary heat in these marginal heating months (i.e., May, June, September, and October).

The balance point temperatures of the Mastin house, based on the preceding analysis, are shown in Fig. 11. The temperatures are about 58°F *(14°C)* on overcast days and 48°F *(9°C)* on clear days, for a 68°F *(20°C)* inside temperature. Expressed another way, the house can be expected to maintain an average indoor temperature 10°F *(6°C)* above the ambient temperature on overcast days and 20°F *(11°C)* above the ambient temperature on clear days, with no auxiliary heating. The actual performance is probably better than this, because the actual heating load of the house appears to be about 16.5% lower than the calculated NHR of 411 Btu/h °F *(217 W/°C)*, which was used in estimating the balance points, as discussed earlier (see Fig. 9).

Auxiliary Heat Required
January 17 to February 16, 1980

Metric		English
5,181 MJ	Total for period	4,910 x 10^3 Btu
173 MJ	Daily average	164 x 10^3 Btu
	Equivalent electricity	
5,181 MJ	Period	1,439 kWh
173 MJ	Per day	48 kWh
	Equivalent gas	
198.0 m^3	Period	70.0 therms
6.6 m^3	Per day	2.3 therms
	Equivalent oil	
178.0 l	Period	47.0 gal
6.1 l	Per day	1.6 gal

Equivalent gas is based on a gas heating system operating at 70% efficiency. Equivalent oil is based on an oil heating system operating at 75% efficiency.

Table 4: The auxiliary heat requirements occurred during a 30-day test period that was somewhat colder than normal for Middletown, and also somewhat sunnier than normal.

Auxiliary Heating Requirment vs. Insolation
30°F (-1°C) Outside Temperature

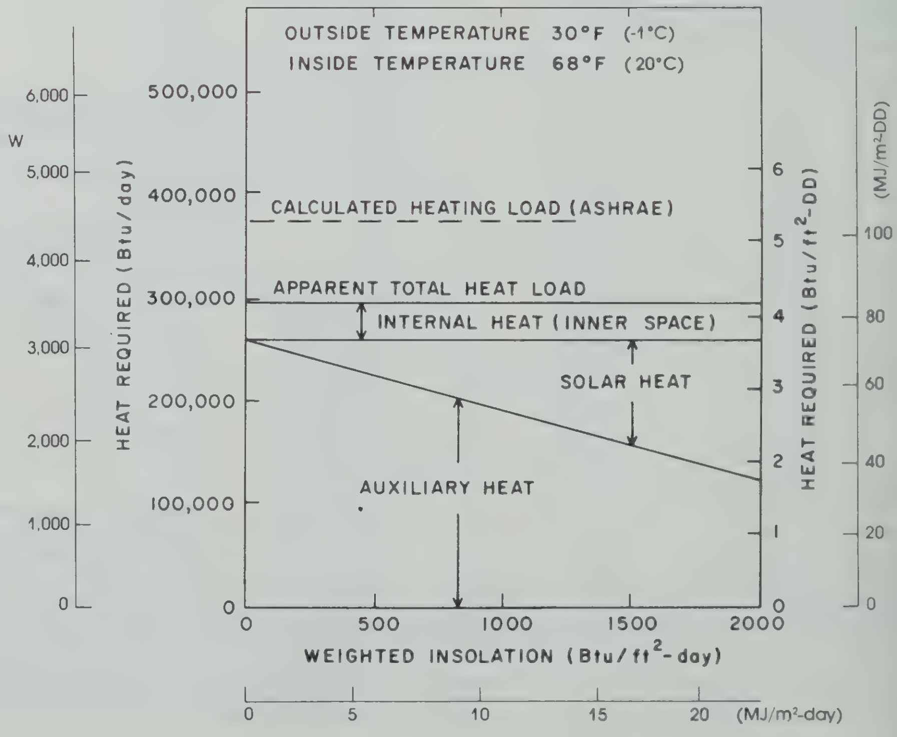

Figure 10 (at right): Auxiliary heat requirements are plotted against weighted insolation. Heating requirements in the absence of insolation are those shown in Fig. 9. The reduction of auxiliary heat required as insolation increases is based on Fig. 8. At the right side, a second scale shows the heat requirements in terms of Btu per square foot of floor space per degree-day. This scale is calculated on the basis of the standard usage of degree-days, i.e., temperatures below 65°F (18°C). The scale is based on 2,027 ft^2 (188 m^2) of living space, which is the space within the inner building shell. It does not include the main level of the solarium, which can be classified as usable living space during daylight on most days, even in midwinter.

Performance of Convective Loop

In evaluating the thermal performance of a double-envelope house, the contribution of convective airflow in the space between the shells is difficult to assess. Some readings of airflow in the loop were attempted using a hand-held ionized corona probe, but the results were not conclusive. The velocities were very low, less than 90 ft/min *(.46 m/s)* and multidirectional. A simple test was then devised to try to isolate the benefit of the circulation to the auxiliary heating requirement of the house.

For the test the flow of air around the loop was physically blocked by closing the opening from the bottom of the solarium to the crawl space. Building paper was installed at this location, using staples. This effectively blocked close to 100% of the area at this point in the loop.

This barrier was installed in February 1980 after completion of the initial testing, and data were collected for the period from February 17 through February 28. The results are plotted in Fig. 12. The normalized auxiliary heating requirement is plotted for each day against weighted insolation, as was done for the earlier test data plotted in Fig. 8. The best-fit straight line, using linear regression analysis, shows a high correlation coefficient of about .95.

The best-fit line for the days with the loop blocked and that for the earlier test period are plotted in Fig. 14, which is presented later. A comparison shows that the blockage caused no increase in the auxiliary heat required. If anything, the auxiliary heat needed was *lower* by about 5% to 20% with the loop blocked, depending on insolation. This difference is not large enough to be conclusive, considering the experimental errors. However, it does seem to support the conclusion that blocking the loop had no deleterious effect.

Some observers feel that air circulation in the between-shells space takes the form of two separate loops, one in the sunspace and one in the north wall. These flows would not be impaired greatly

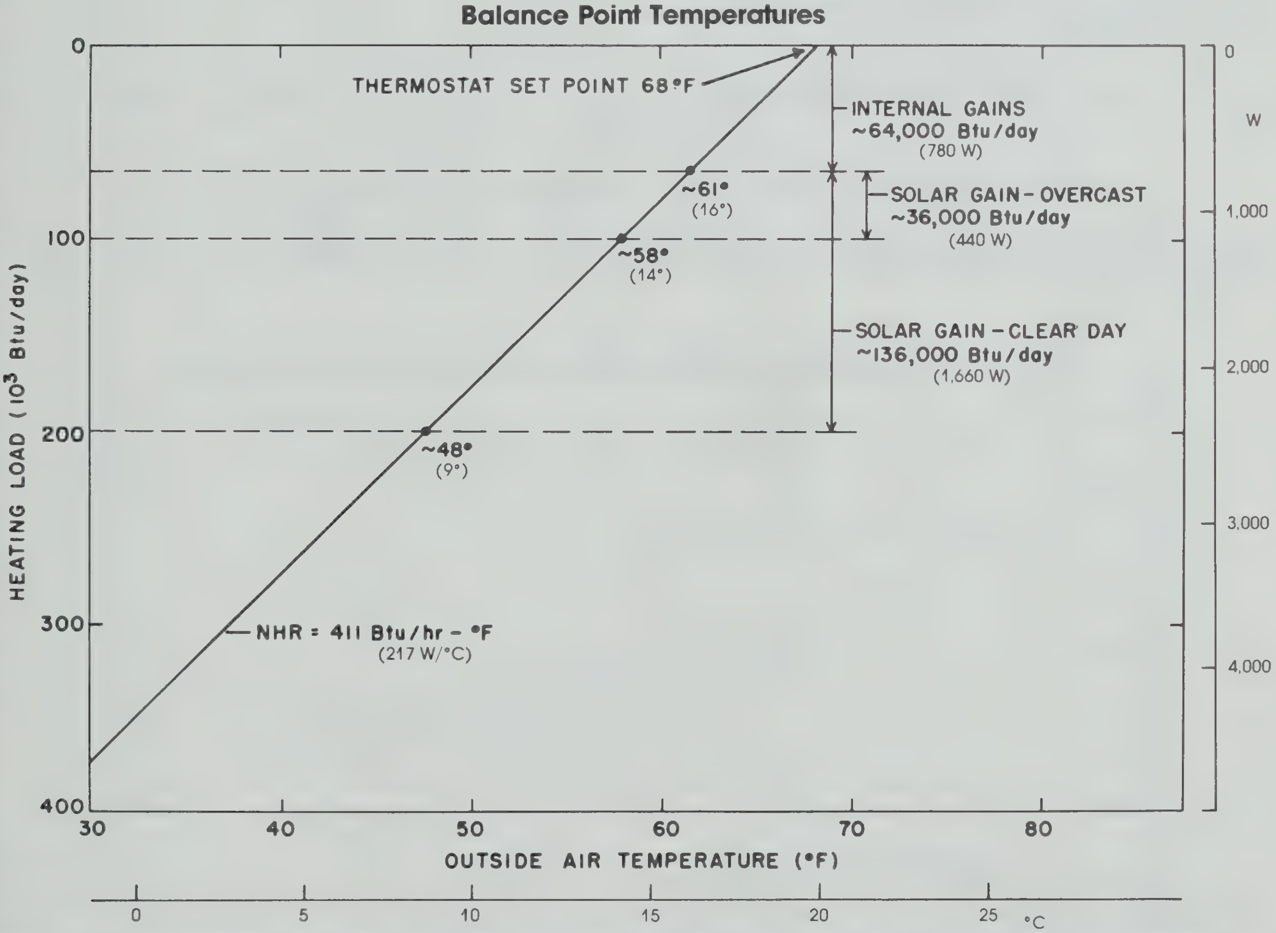

Figure 11: Balance point temperatures of the Mastin house are shown. Assuming a 68°F (20°C) interior thermostat setting, the heating load of the house can be read on the left scale as a function of outside air temperature. This is based on Table 1's calculated heat load, 411 Btu/h F (217 W/°C). In preparing this figure, an internal gain of 64,000 Btu/day (782 W) was used. Internal heat provided to the inner space is estimated at 42,360 Btu/day (518 W), plus one-half of the 43,000 Btu/day (525 W) internal heat provided to the convective loop (see Table 2). The allocation of half of the loop heat as a contribution toward meeting the heating needs of the inner space is arbitrary, but probably reasonably accurate. The benefit of solar gain on overcast days is estimated from the mean of the cluster of points at the left in Fig. 8. The clear day benefit is estimated from the right cluster of points.

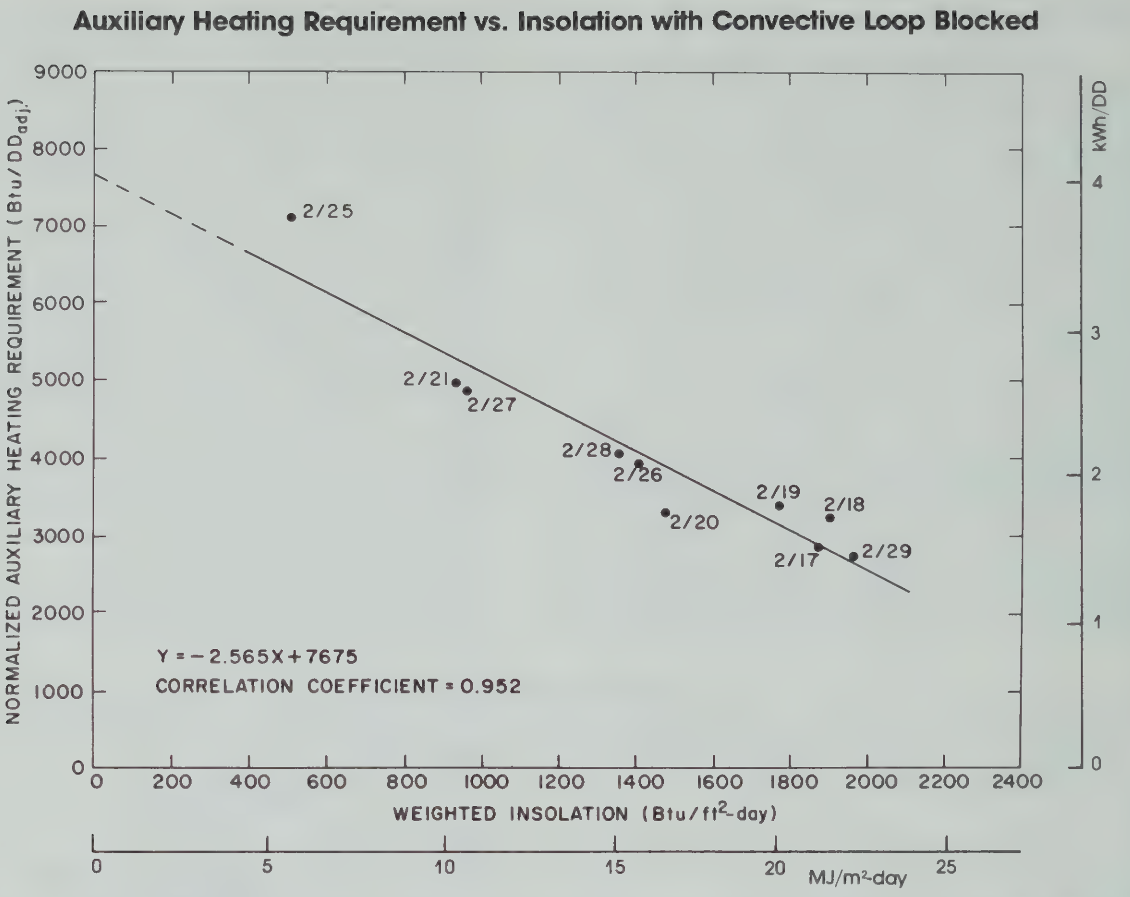

Figure 12: The auxiliary heating requirement is plotted against insolation with the convective loop blocked by paper at the south end of the crawl space.

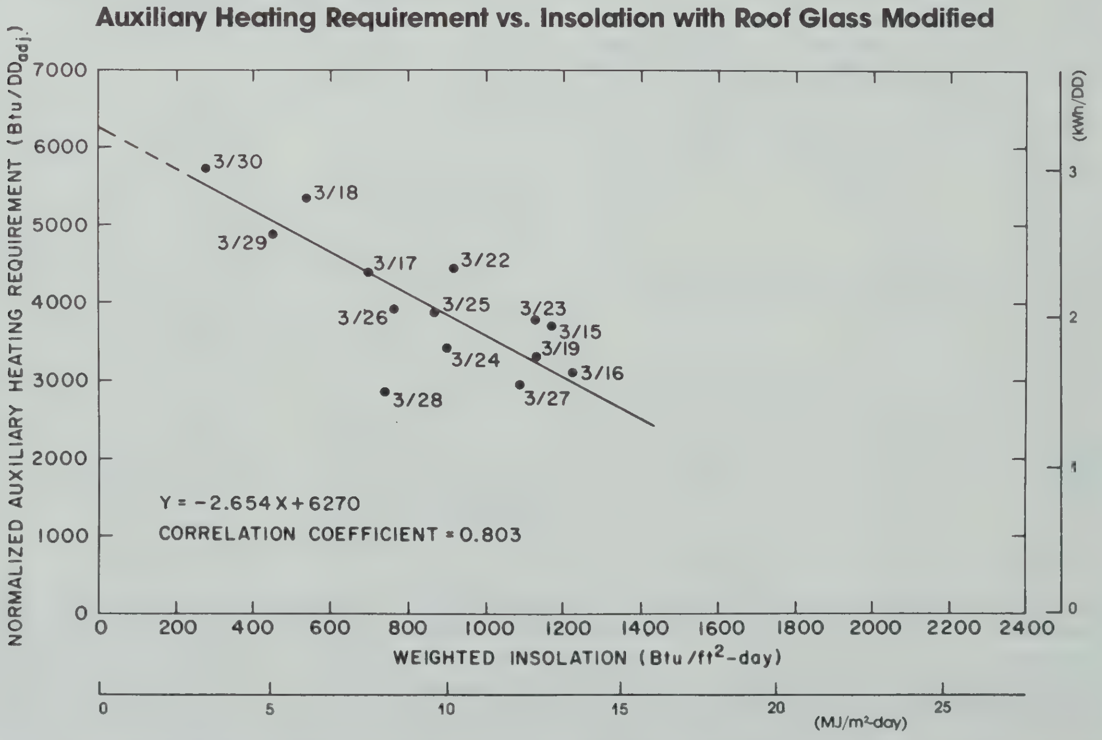

Figure 13: The auxiliary heating requirement is plotted aginst insolation with the upper row of roof glass blocked and insulated as in Fig. 1.

by the barrier that was installed for this test. Lee Butler, in the first edition of *Ekose'a Homes*,[2] shows circulation of air all the way around the loop in the "heat gain" mode. In the second edition,[3] however, he shows two separate circulation paths, one on the south side and the other on the north side. He states that the actual paths are unique and variable in every case, but that the two paths are "what appear to be predominant air movement patterns."

Performance with Reduced Roof Glazing

After the test with the loop blocked, Robert Mastin suggested that the house be modified by covering the upper row of glazing in the roof, which he felt might improve the thermal performance. This was done by installing batts of fiberglass insulation under the glass, performing the triple function of blocking solar gain and radiation losses and greatly reducing the conductive heat loss. This insulation can be seen in the photograph in Fig. 1, which was taken in March 1980, after the installation was made.

A third period of testing was then performed, from March 15 to March 30, to identify the effects of this change. (The barrier to airflow in the loop was removed before these tests started.) The results are plotted in the same format as for the other test periods in Fig. 13. In this case the correlation was also quite good, with a coefficient of .80, and the auxiliary heat required was reduced significantly, by 25% to 50%, as compared with the first test period. The best-fit line of normalized auxiliary heating requirement versus weighted insolation is compared with that for the base period in Fig. 14.

The observed reduction in auxiliary heat associated with reducing the roof glazing is about 2 x 10^3 Btu per adjusted degree-day under average insolation. This amounts to about 67 x 10^3 Btu/day *(70.7 MJ/day)* or 2.8 x 10^3 Btu/h *(821 W)* on a 30°F *(-1°C)* day. The roof glazing has an area of 358.9 ft^2 *(33.3 m^2)* and a U-value of .830 *(4.7)*. The heat loss from the convective loop through half of the glass, at 30°F *(-1°C)* outside temperature, (when the loop temperature would be about 50°F *(10°C)* is about 3 x 10^3 Btu/h *(879 W)*. Insulated, it would drop to about 180 Btu/h *(53 W)*. The reduction in auxiliary heat needed for the inner space (2.8 x 10^3 Btu/h or *821 W*) is of the same magnitude at the calculated reduction in heat load of the convective loop (2.82 x 10^3 Btu/h or *826W*) associated with blocking and insulating half of the roof glass.

The results of this test would seem to indicate

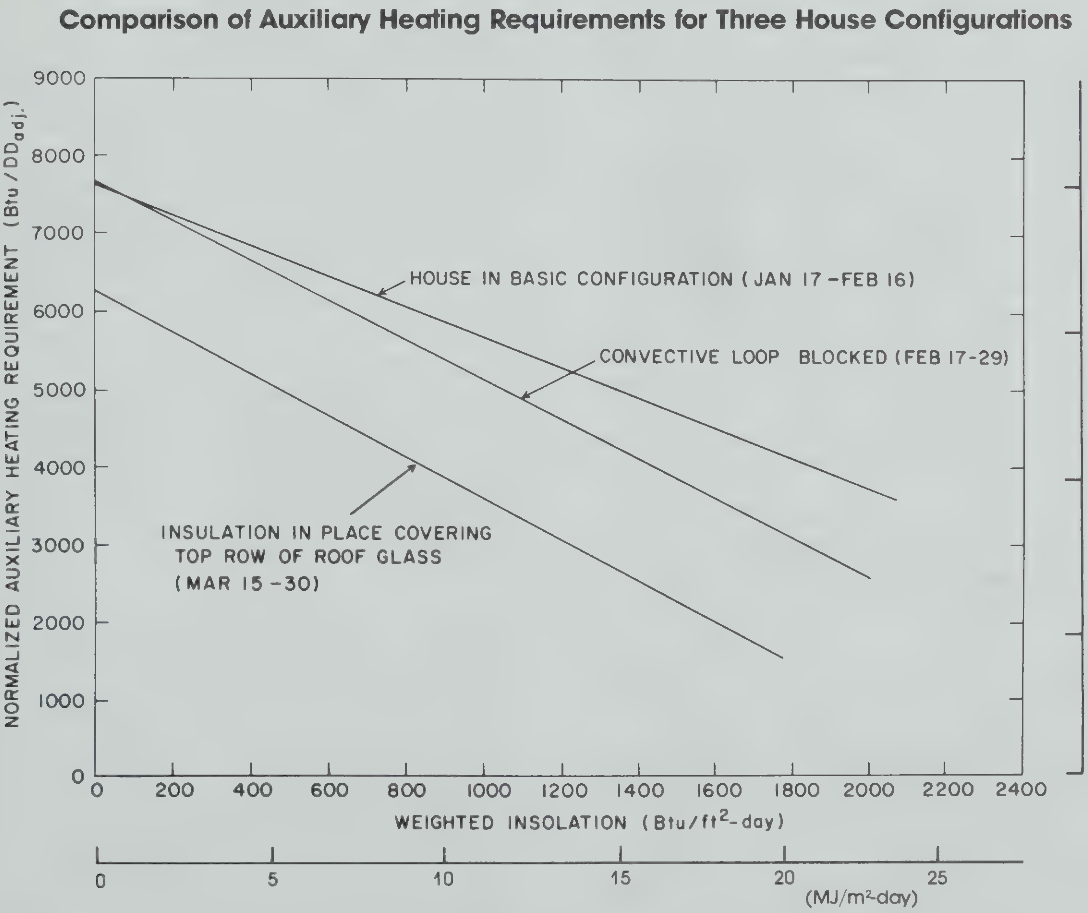

Figure 14: The effects of convective loop and roof glass modifications on auxiliary heat requirements are compared with the requirements of the original house configuration.

that most or all of the benefit derived from solar gain through the upper row of roof glass is offset by radiative heat loss through the glass on a daily cycle. This is without regard for conductive heat loss through the glass. It appears quite possible that this conclusion would apply to the lower row of roof glass as well. The lower row in the Mastin house permits a water view to the south from the upper level, however, so it would not be reasonable to eliminate it, though its area could be reduced.

Analysis of Ground Thermal Coupling

After the original testing period, January to March 1980, thermocouples were installed to monitor the heat flow in the concrete slab beneath the crawl space. Four Type J thermocouples were installed, one on the surface, one ½ in. *(13 mm)* down in the slab, one 3 in. *(76 mm)* down, and the other at the bottom of a hole 6 in. *(152 mm)* below the surface of the slab, in the supporting gravel. These were connected to the Fluke data logger.

The temperature profiles in the slab were analyzed for an 11-day period in January 1981 (the following winter). The hourly measured temperatures were averaged to obtain a daily average for each thermocouple. The daily averages were then averaged for the 11-day period. The results, shown in Table 5, indicate a small gradient from the temperature 6 in. *(152 mm)* below the slab to a slightly cooler (0.52°F or *.29°C* difference) temperature on the surface of the slab. The slab surface temperature averaged 50.1°F *(10.1°C)* in the period.

Using standard ASHRAE material properties for concrete and gravel, a steady-state heat flux of about 0.7 Btu/ft^2 h *(2.2 W/m^2)* was calculated for this temperature gradient. This corresponds to about 700 Btu/h *(205W)* or 16.8 x 10^3 Btu/day *(17.7 MJ/day)* for the 1,005 ft^2 slab area. While not insignificant, it is a small amount as compared with the 43 x 10^3 Btu/day *(45.4 MJ/day)* available to the convective loop from appliances, and the inner space NHR of 411 Btu/h °F *(217 W/°C)*.

A second analysis was made to identify the periodic heat flow into and out of the slab on a daily basis. The surface temperatures were inspected to find a day within the 11-day period when the non-steady-state heat flow was close to being periodic. January 12 met this criterion, and had a surface temperature amplitude $[(T_{max} - T_{min}/2]$ of 1.15°F *(.64°C)*, which is near the average for the period. Using theoretical solutions for periodic heat transfer in an infinite slab, the amount of energy stored or released in a half cycle is calculated to be less than 25 Btu/ft^2 *(.28 MJ/m^2)* or about 25 x 10^3 Btu *(26 MJ)* for the area of the slab. In other words, on a representative day about 25 x 10^3 Btu *(26 MJ)* is stored in the slab during the day and released at night. This is also a relatively small amount when compared, for example, with the 256 x 10^3 Btu/day *(270 MJ/day)* needed by the house from solar and auxiliary heat on a 30°F *(-1°C)* day (Fig. 9).

Average Slab Temperatures
January 3 to 14, 1981

Metric		**English**
Average Temperature (°C)	Thermocouple Location	Average Temperature (°F)
10.34	6 in. below surface	50.62
10.26	3 in. below surface	50.47
10.17	0.5 in. below surface	50.31
10.06	On slab surface	50.10

Table 5: Average temperatures for the concrete slab below the crawl space were derived from hourly measurements made during an 11-day period in 1981.

Performance with Auxiliary Heaters Disconnected

A short test was conducted in March 1981 with no auxiliary heating to determine the inside temperature at which the house would "float." The results are plotted in Fig. 15.

The three portable electric heaters were inactivated and the thermostat for the ground floor electric baseboard heaters was turned down at 10 a.m. on March 9. The outside temperature was about 43°F *(6°C)*. By midnight, when the outside temperature was 35°F *(2°C)*, the upper floor temperature had dropped only to about 65°F *(18°C)*. The ground floor temperature, however, had fallen to 58°F *(14°C)*. The average temperature dropped at a rate of only about 0.4°F *(0.2°C)* per hour with a ΔT of about 25°F *(14°C)*. This is comparable to the night temperature lapse rate reported for other energy efficient houses such as the Balcomb and Burns houses, and for well-designed, superinsulated houses.

The inside temperatures continued to fall until 8 a.m. the next day when the upper floor was 62°F *(17°C)* and the ground floor was 56°F *(13°C)*. The house started to warm by 9 a.m., however, even though the day was overcast (insolation for the day was 580 Btu/ft^2 or *6.6 MJ/m^2*), and the inside temperatures had risen by about 5°F *(3°C)* by mid-afternoon.

On the second morning, March 11, even though it was a few degrees colder outside, the low temperatures reached inside were only a degree below those measured on the first morning after the heaters were turned off. Thus, the house appears to have reached an average inside equilibrium temperature of about 59°F *(15°C)* in the mornings and 63° to 64°F *(17°C)* in the afternoons with outside temperatures averaging 35° to 40°F *(2° to 4°C)*. This was accomplished under conditions of light insolation, suggesting that the balance point temperature under such conditions may be more like 20°F *(11°C)* above ambient temperature than the 10°F *(6°C)* shown in Fig. 11.

The crawl space air temperature (not plotted), which was about 53°F *(12°C)* at the start of this test, remained in a 50° to 55°F *(10° to 13°C)* range for the entire two-day test period. The crawl space temperature was 52.3°F *(11.3°C)* at the end of the test at noon on March 11. The temperatures at other points in the convective loop were in the same 50° to 55°F *(10° to 13°C)* range during night hours, but were warmer than that during daylight hours.

On the third day, a fire was started in a wood stove on the ground level shortly after noon, when the average inside temperature was about 59°F *(15°C)*. The stove was very effective in raising the temperature on all three levels of the house. Within two hours the ground floor temperature was 72°F *(22°C)* and the other two floors were about 63°F *(17°C)*. The average house temperature was 67°F *(19°C)* and reached 71°F *(22°C)* by 5 p.m.

Performance with Auxiliary Heaters Disconnected

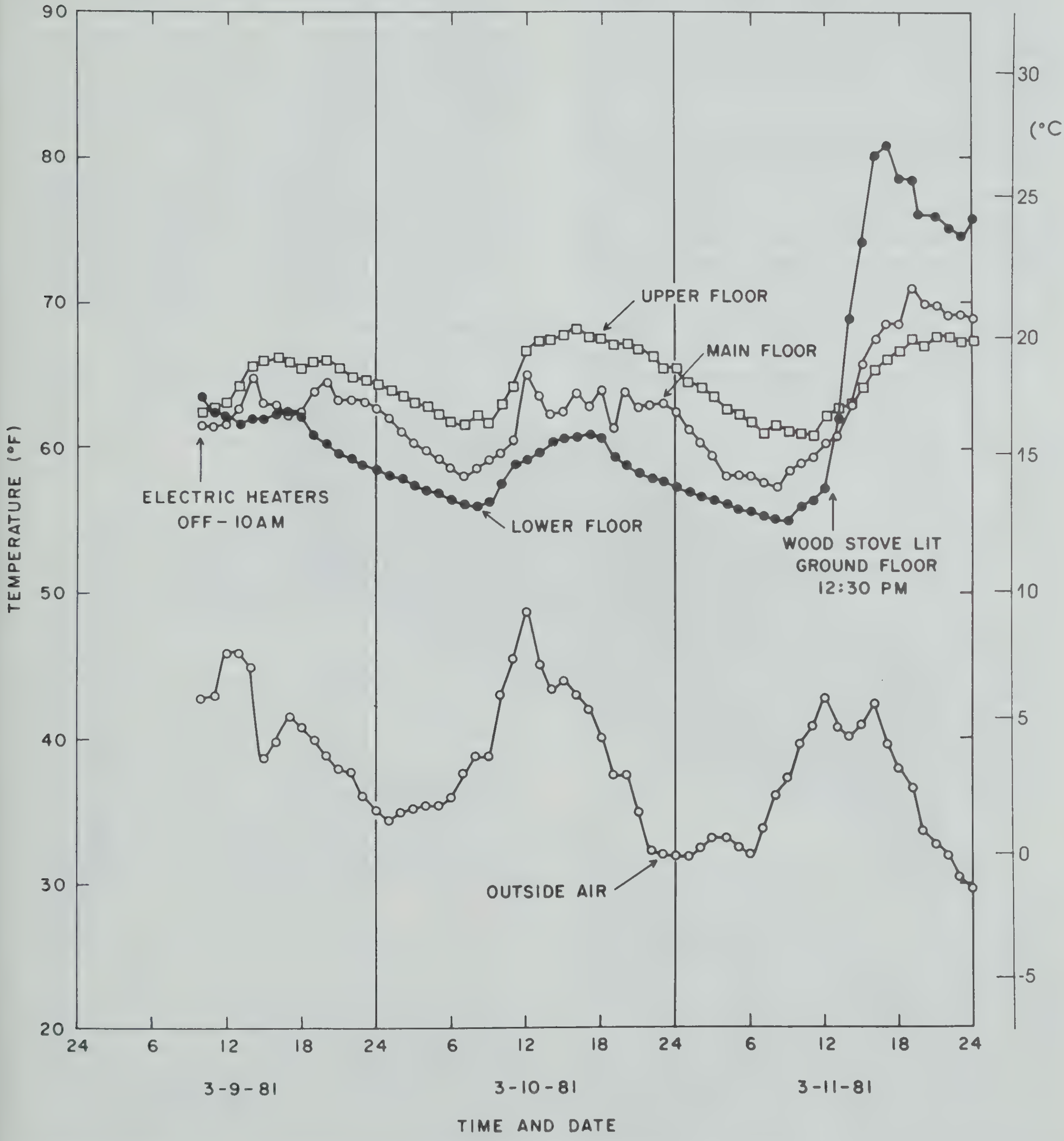

Figure 15: The inside air temperature of the house at three levels is shown with the auxiliary heaters off. Outside air temperature is also shown.

Summer Ventilation and Cooling

As discussed earlier, the Mastin house benefits from the prevailing southwest winds which bring cool air from the Atlantic Ocean to the Rhode Island coast on most summer afternoons. It relies on natural ventilation and the protection from solar gain provided by the outer shell to maintain comfortable inside temperatures in the summer. No air conditioners are installed.

The triangular screened and louvered attic vents described earlier are kept open for most of the summer. The 50-ft *(15-m)* long, 2-ft *(.61-m)* diameter cooling tube, running underground from a capped opening on the north lawn to the utility room, is intended to be used in conjunction with the attic vents to ventilate and cool the air envelope space.

In Brookhaven's monitoring of the house, several temperature sensors were installed inside the cooling tube and some limited data were collected. However, the tests were not conclusive. Air appeared to be flowing from the envelope space through the tube to the outside, rather than being drawn into the envelope space when the testing was performed.

Mastin observes that the cooling tube is not entirely effective. He feels that the best ventilation is normally achieved by opening only the east gable vent, which is on the low pressure side of the house with the prevailing southwest winds. With the sliding doors from the envelope space to the outside also open, the envelope space is pressurized slightly and ventilated very effectively. Under these conditions, Mastin finds that the airflow in the tube is often in the wrong direction. If the sliding doors were closed, the airflow in the tube would be generally in the right direction (into the house), but the solarium would heat up too much.

DISCUSSION OF BUILDING PERFORMANCE

Auxiliary Heat Requirement

Testing during the initial period in January and February 1980 showed that the Mastin house needs very little auxiliary heat to maintain comfortable conditions in the living space. The average daily requirement was only 164 x 10^3 Btu *(173 MJ)*, as indicated in Table 4, or a little over 2 Btu/ft² °F-DD *(41*

Comparative Annual Heating Loads

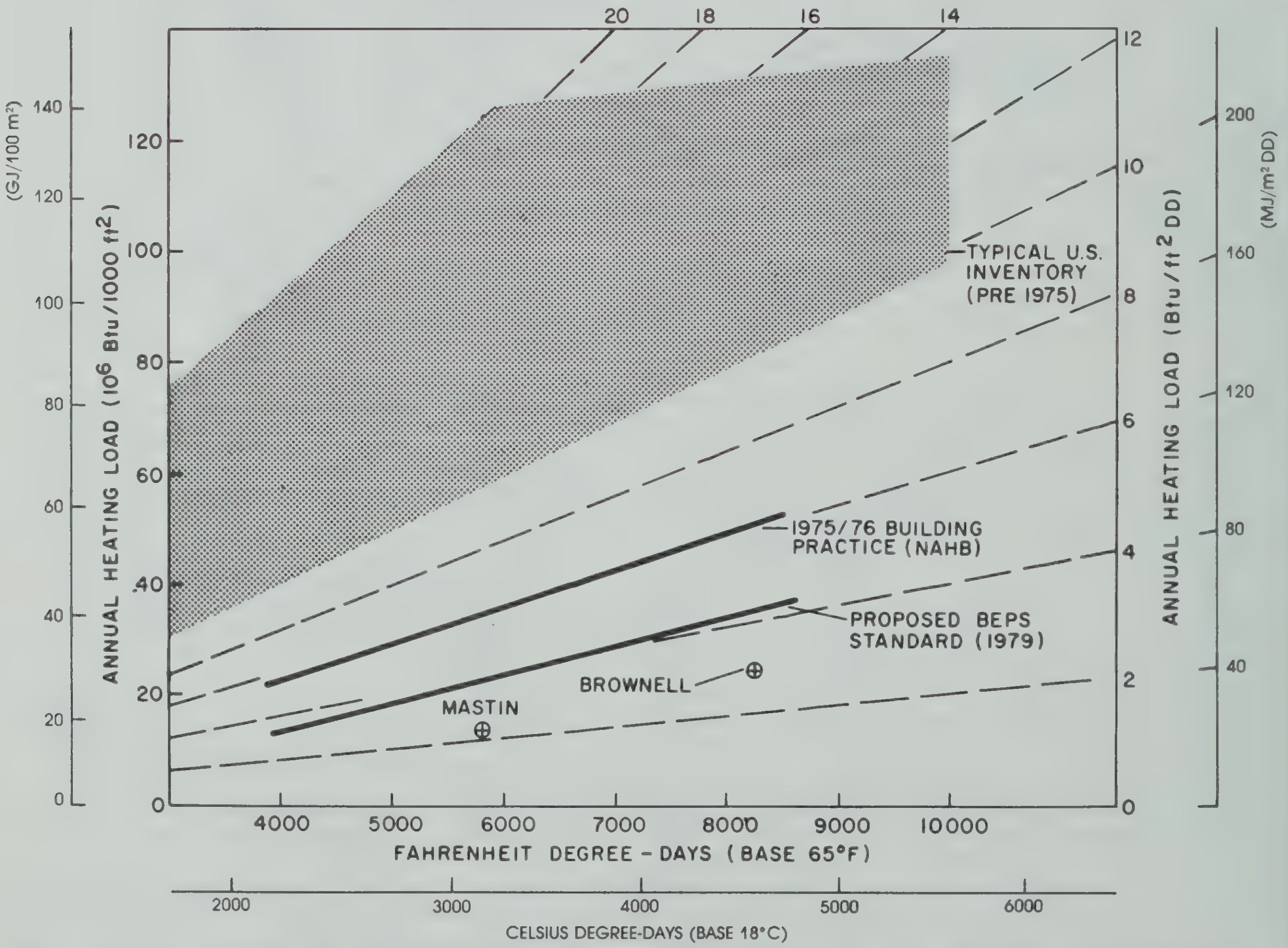

Figure 16: The estimated annual heating load of the Mastin house is compared with those of typical inventory houses and other construction.

kJ/m² °C-DD). A comparison of the estimated annual heating load of the house with that of typical inventory houses and other construction is provided in Fig. 16. The Mastin house load of about 2.1 Btu/ft² °F-DD *(43 kJ/m² °C-DD)* compares with about 4 *(82)* under the Department of Energy's proposed Energy Performance Standards for New Buildings (BEPS), 6 *(122)* for 1975-1976 building practice as surveyed by the National Association of Home Builders, and 10 to 20 *(204 to 408)* for the typical U.S. housing stock built before 1975. Also indicated is a reference point for the Brownell house described in an earlier BNL case study.[4]

The low heating requirement of the Mastin house reflects the balance point temperature associated with its low thermal losses, internal heat, and the benefit of insolation. Fig. 11 shows the estimated balance point temperatures to be in the 48° to 58°F *(9° to 14°C)* range (for a 68°F *or 20°C* interior temperature), depending upon the amount of insolation. However, on the basis of the test conducted with no auxiliary heating (see Fig. 15), it appears that the balance point temperatures are even lower, probably in the range of 40° to 50°F *(4° to 10°C)*, depending on insolation. Auxiliary heat (other than a small amount needed for the basement level) probably would not be required except when the outside temperature is below the 40° to 50°F *(4° to 10°C)* range, assuming the availability of a normal amount of internal heat. This means that, under average Rhode Island temperature conditions, auxiliary heat would seldom be required except in the period from early December to late March.

Measurement of the amount of auxiliary heat required by energy-efficient houses, for purposes of making a quantitative comparison with other houses, requires that the inside temperature be maintained at a controlled level. This was done in evaluating the Mastin house. Thermostats on three levels of the house turned electric heaters on to prevent the temperature on each level from falling below 65°F *(18°C)* approximately. The auxiliary heat requirement reflected the maintenance of this level of comfort. It is evident that an energy-conserving house without such automatic temperature control could use less auxiliary heat than measured by this test procedure, because the occupants might allow the inside temperature to drop below 65°F *(18°C)* at some times of the day on some levels of the house.

Circulation in Convective Loop

No conclusions can be drawn from our simple measurements of air velocities in the loop, except that the flows were quite low (less than 90 ft/min *or .46 m/s*) and variable. Tests by others have shown that the velocities in the most restricted part of the loop are typically in the 10 ft/min to 50 ft/min *(.05 m/s to .26 m/s)* range when flow exists.[5, 6] Some of these tests show evidence of periodic reversal of the direction of the airflow while others show that reversal does not take place.[6]

Low air velocities should not be taken to mean that heat movement is insignificant because the air volumes are large. The area of the north wall cavity in the Mastin house is about 20 ft² *(1.8 m²)*. A leisurely flow velocity of 50 ft/min *(.26 m/s)* (about one-sixth of an average person's walking speed) corresponds to a transport rate of about 1,000 ft³/min *(28 m³/min)*. Air flowing at 1,000 ft³/min *(28 m³/min)* moves about 10 x 10³ Btu/h *(2,930 W)* of heat energy from one point in the loop to another for each 10°F *(6°C)* drop in the temperature of the airstream.

Our tests of the Mastin house with the loop blocked showed no adverse effect on house performance. However, it is possible that this was true because the flow in the loop is not continuous, but instead takes place in the form of separate circulatory paths in the north and south loop spaces. Clearly, additional experimental measurements of the loop airflow should be made in double-envelope houses.

Some analysts of double-envelope houses believe that performance would be improved by introducing forced circulation in the loop. This could be done quite easily in the Mastin house by closing the loop at the south end of the crawl space (where we closed it as an experiment) and installing several small fans in openings in the partition. The fans could be thermostatically controlled (in the heating season) to come on when the attic temperature exceeded 80°F *(27°C)* or so. Based on the calculation above, 1,000 ft³/min *(28 m³/min)* of fan-induced circulation, with an attic temperature of 80°F *(27°C)* and a crawl space temperature of 50°F *(10°C)* would transport 30 x 10³ Btu/h *(8,792 W)* to the crawl space. This is approximately equal to the total calculated hourly heat loss of the house at a 0°F *(-18°C)* outside temperature.

Having a more uniform temperature in the loop (due to forced circulation) might not significantly reduce the total heat loss from the loop, but it would seem to have two other advantages. It would shift more of the loss to the basement slab and the earth below, from which it could be retrieved at night, and it would reduce the tendency toward overheating of the upper floor bedrooms in the afternoons.

Ground Heat Storage and Retrieval

The BNL tests showed the ground coupling of the Mastin house in a mid-winter (January) period to be weak. There was, however, a heat flow from the ground during the test period of about 17 x 10³ Btu/day *(17.9 MJ/day)*. Superimposed on this flow was a diurnal transfer to and release from the earth of about 25 x 10³ Btu/day *(26.4 MJ/day)*. These flows, while not negligible, are small compared with the heat loss of the house, which is about 300 x 10³ Btu/day *(317 MJ/day)* under the test conditions. For another comparison, solar heating provides some 100 x 10³ Btu/day *(106 MJ/day)* to the inner space on clear days in January, according to our analysis, or about six times the heat flow from the ground.

Performance monitoring of some other double-envelope houses has produced similar conclusions about ground coupling. A report on testing of the Tom Smith house in Lake Tahoe concludes that "it appears that heat transfer from the crawl space to storage does not constitute a major heat transfer mechanism."[5] Testing of the Ekose'a-designed Stokes house in Canton, Georgia, produced a conclusion that "energy storage in the crawl space was not evident."[6] The test report on a house near Ottawa concluded that "if thermosyphoning does move some sunspace heat usefully through the upper jacket and finally into and across the basement, it appears that the basement does not store it and release it usefully."[7]

A "thermal-envelope-concept test room" has been built at the University of Nebraska. In a preliminary winter condition test report, earth coupling is discussed. The authors state, "The initial conclusions indicate that air circulation does occur albeit at rather low flow rates. Apparently little energy is transferred from the greenhouse to mass storage via the plenum route."[8]

Observed versus Calculated Heating Requirements

As discussed earlier, and plotted in Fig. 9, the heat load calculated for the Mastin house, using standard ASHRAE procedures, agrees reasonably closely with the heat available in the form of auxiliary electric heat, solar gain, and internal sources of heat. The heat required was 16.5% less than the calculated heating requirement. In making this comparison, the 17×10^3 Btu/day *(17.9 MJ/day)* heat flow from the ground was not considered. Counting this gain, and subtracting the heat loss through the basement floor used in the heat loss calculation, the agreement is even closer, within about 11%. Thus, there do not appear to be any significant unexplainable phenomena contributing to the good thermal performance of the house.

Cooling Performance

The Mastin house remains quite comfortable in the summer months because of the breeze that comes in from the ocean on most afternoons. Because of the availability of this source of ventilation, the cooling tube is not used often. In other double-envelope houses, the cooling tube would probably play a greater role in maintaining comfortable conditions in the living space.

Earth cooling tubes have been modeled recently at the Southern Solar Energy Center and the Georgia Institute of Technology's College of Architecture. This work was reported at the Fifth National Passive Solar Conference.[9] The authors also measured the cooling tube performance of the Stokes double-envelope house in Georgia. They state in the introduction to their paper, "Offering the lure of unsophisticated hardware, low operating energy and theoretical simplicity, the earth cooling tube concept has been eagerly embraced by the energy-conscious popular media and public." They conclude that earth cooling tubes do provide a workable method of space cooling, but that "the potential output is lower and the design difficulty higher than generally suspected." They add, "It is doubtful that a typical earth cooling tube can be justified as a replacement for conventional air conditioning on economics alone in the near future."

CONCLUSIONS

The Mastin double-envelope house, which is believed to be generally representative in its thermal performance of houses of the type designed by Ekose'a and others, has a very low auxiliary space heating requirement of about 2.1 Btu per square foot of floor area per Fahrenheit degree-day *(43 kJ/m² °C-DD)* in northern climates. This ranks it among the most energy-efficient new housing designs offered today in terms of heating energy needs. The house also remains comfortable in summer months without need for mechanical air conditioning; this is due in part to the cool afternoon ocean breezes which are prevalent at the building site on the Rhode Island coast.

The basis for the good thermal performance of double-envelope houses remains somewhat controversial. It is clear that strong circulatory flow of air in the convective loop does not take place, and that there is only a small amount of interchange of heat with the ground below. We conclude that the low energy needs of the house are attributable mainly to the excellent insulative value of its double shell.

The double-shell construction of the house results in very low air infiltration, even on windy days. (The infiltration is readily controllable, however, by opening inside windows.) This leads to higher, more comfortable interior humidity levels during cold weather. The combination of low infiltration, comfortable humidity, and reduced body heat loss through radiation provides a comfortable level at 65°F *(18°C)* inside air temperature which probably approaches that at 70°F *(22°C)* in conventional houses.[10] Another benefit of the house is the sound attenuation achieved. Several people have remarked that the house is unusually quiet inside, probably due to the surrounding air plenum and the heavily insulated east and west end walls.

As compared to other thermally efficient houses, such as superinsulated designs and houses constructed partially underground, the double-envelope house has certain aesthetic advantages. Their importance is subjective, depending on the interests and priorities of the homeowner. First among these is the ability to provide large areas of south-facing glass without the usual heat loss associated with glazing. This is particularly desirable if the house site offers attractive views, as is the case with the Mastin house. The house also offers excellent natural daylighting and an attractive solarium which can be enjoyed in all seasons. Further, the double-envelope design can maintain the living space temperature above freezing for extended periods with no auxiliary heat. This could be important if the house is used as a vacation home.

REFERENCES

1. Sonderegger, R.C.; Condon, P.E.; Modera, M.P. 1979. "In-Situ Measurements of Residential Energy Performance Using Electrical Co-Heating." LBL-10117.
2. Butler, L.P. 1978. *Ekose'a Homes*. San Francisco, California: Ekose'a, Inc.
3. Butler, L.P. 1980. *Ekose'a Homes*, 2nd edition. San Francisco, California: Ekose'a, Inc.
4. Jones, R.F.; Krajewski, R.F.; Dennehy, G. 1979 (May). "Case Study of the Brownell Low Energy Requirement House." BNL 50968.
5. Chen, B., et al. 1980 (Oct.). "Performance Results of the Tom Smith Double Shell Residence, Lake Tahoe, California." *Proceedings of the Fifth National Passive Solar Conference*. Vol. 5.1. Edited by John Hayes and Rachel Snyder. Amherst, Massachusetts; Oct. 19-26, 1980. Newark, Delaware: American Section of the International Solar Energy Society, Inc. (AS/ISES), University of Delaware; pp. 528-532.
6. Akridge, J.M.; Benton, C.C. 1980 (May). "Performance Study of a Thermal Envelope House—Final Report, Phase I." College of Architecture, Georgia Institute of Technology.
7. Milne, W.C.; Platts, R.E. 1980 (Oct.). "Double Shell Passive Solar House—A Proof of Concept Test." *Proceedings of the Fifth National Passive Solar Conference*. Vol. 5.1. Edited by John Hayes and Rachel Snyder. Amherst, Massachusetts; Oct. 19-26, 1980. Newark, Delaware; AS/ISES, University of Delaware; pp. 533-537.
8. Chen, B., et al. 1980 (June). "Preliminary Winter Results of the Thermal Envelope Concept Test Room." *Proceedings of the 1980 Annual Meeting, AS/ISES.* Vol. 3.2. Edited by Gregory E. Franta and Barbara H. Glenn. Phoenix, Arizona; June 2-6, 1980. Newark, Delaware: AS/ISES, University of Delaware; pp. 928-932.
9. Abrams, D.W.; Benton, C.C.; Akridge, J.M. 1980 (Oct.). "Simulated and Measured Performance of Earth Cooling Tubes." *Proceedings of the Fifth National Passive Solar Conference.* Vo. 5.1. Edited by John Hayes and Rachel Snyder. Amherst, Massachusetts; Oct. 19-26, 1980. Newark, Delaware; AS/ISES, University of Delaware; pp. 732-736.
10. *ASHRAE Handbook: 1981 Fundamentals.* 1981. New York: American Society of Heating, Refrigerating and Air-Conditioning Engineers, Inc.; pp. 8.1-8.26.

The Mastin Double-Envelope House: Comparing The Brookhaven Results to an SLR Analysis

By J. DOUGLAS BALCOMB
Los Alamos National Laboratory, Los Alamos, New Mexico 87545

In the Brookhaven National Laboratory report, "Case Study of the Mastin Double-Envelope House" (BNL-51460, May 1981), the authors take the right data and analyze it in a way that provides useful insights into the nature of the building's performance. Furthermore, the report is both informative and easy to read.

As I read the report, I became curious about how the building might be expected to perform if it were treated as a simple sunspace design without a convective loop and how this would compare with the results that Brookhaven obtained. Such a comparison should provide further insight as to whether the sunspace and its associated convective loop is an effective passive solar element.

In order to make the comparison, I calculated the heat load coefficients of the house, assuming that the various cavities associated with the convective loop were dead airspaces, and then performed a solar load ratio analysis using the appropriate sunspace correlation for Los Alamos sunspace type SSB5.[1, 2] I used the actual measured solar gains and degree-days (corrected for internal loads) in this analysis. I also did an annual performance analysis based on long-term data. My observations based on these calculations are as follows.

1. The following comparison is obtained between predicted and measured auxiliary for the 30-day period January 17 to February 16, 1981:
   Predicted = 2.5 x 10^6 Btu *(732 kWh),*
   Measured = 4.91 x 10^6 Btu *(1,438 kWh).*
   The difference could result either from too little heat storage or from stratification. As Jones and Dennehy acknowledge, stratification in the house would tend to cause the auxiliary to be greater than predicted since the solar heat is essentially not available to the lower level.
2. The prediction yields a solar heating fraction (SHF) of 51% for the same period, compared to 33% inferred from the slope of the auxiliary-vs.-solar least-squares fit developed by BNL.
3. The predicted solar savings fraction (SSF) is 16% for this period. This means that the sunspace would be expected to contribute 16% of the net heat requirements of the rest of the building during this period plus all the sunspace heat requirements.
4. On an annual basis in a normal year an SSF of 21% is predicted (SHF = 55%) and the predicted

---

This work performed under the auspices of the U.S. Department of Energy, Office of Solar Technologies.

annual auxiliary requirement is 19.9 x 10^6 Btu *(5,828 kWh)* with the thermostat set at 65°F *(18.3°C)* and the same internal heat. This is all predicated on a sunspace model (Los Alamos Type SSB5) that seems to predict somewhat better performance than the actual Mastin house achieves (as indicated in Item 1 above). The annual prediction is based on long-term average data for nearby Providence, Rhode Island.

5. The total load coefficients predicted by BNL (9,864 Btu/DD) and me (9,822 Btu/DD) are both substantially higher than the apparent no-solar load coefficient of 7,600 Btu/DD inferred from the BNL correlation of aux.-vs.-solar. Is this difference due to double-envelope mystique or simply an overestimate of various coefficients? It may be due in small part to ground coupling, although this represents only 7-8% of the predicted loss coefficient. I suspect that it is due in part to reduced infiltration because of the double-stage barrier.
6. BNL feels that performance was enhanced by blocking the convective loop based on its brief experiment. This also would explain the differences observed in Items 1 and 2 above. The SHF implied by BNL's measurement with the loop blocked is 43%, in much better agreement with my prediction of 51%.
7. Sunspace storage mass is much less than the Los Alamos reference design used for the solar load ratio correlation—which leads to the speculation that the performance should also be less. The effect of the decreased mass is hard to assess due to the direct-gain nature of solar penetration into the main house through the house sunspace glazing (or openings). Based on our sensitivity curves, it could easily explain a 10% reduction in SSF.
8. Overall, it appears that the Mastin house solar performance is not as good as would be predicted, based on the sunspace model, given the same glazed area and building load coefficient. This suggests that the sunspace is not functioning as well as it could. The deficiency is probably inadequate heat storage mass and inadequate solar heat distribution. I tend to agree with the Brookhaven conclusion that the house works well primarily because of its superinsulated character and not particularly because of solar gains or the double-envelope design.

REFERENCES

1. Balcomb, J. Douglas; Jones, Robert W.; McFarland, Robert D.; Wray, William, O.; "Performance Analysis of Passively Heated Buildings: Expanding the SLR Method." *Passive Solar Journal.* Vol. 1 (No. 2): pp. 67-89.
2. Jones, R.W., editor. Balcomb, J.D.; Kosiewicz, C.E.; Lazarus, G.S.; McFarland, R.D.; Wray, W.O. 1982. *Passive Solar Design Handbook—Volume Three: Passive Solar Design Analysis (Addendum).* Prepared for the U.S. Department of Energy. DOE/CS-0127/3.

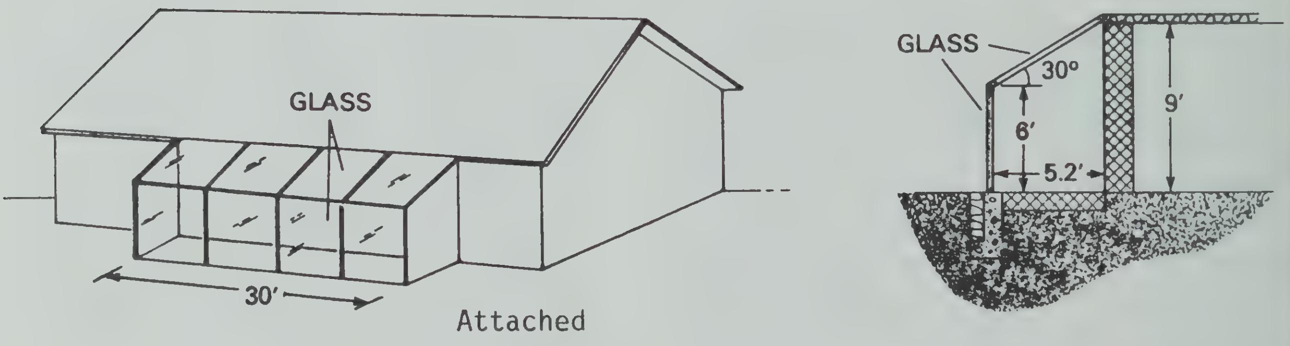

Figure 1: A simple sunspace design (SSB5) at Los Alamos is used for comparison with the Mastin Double-Envelope House to see if the convective loop is an effective passive solar element.

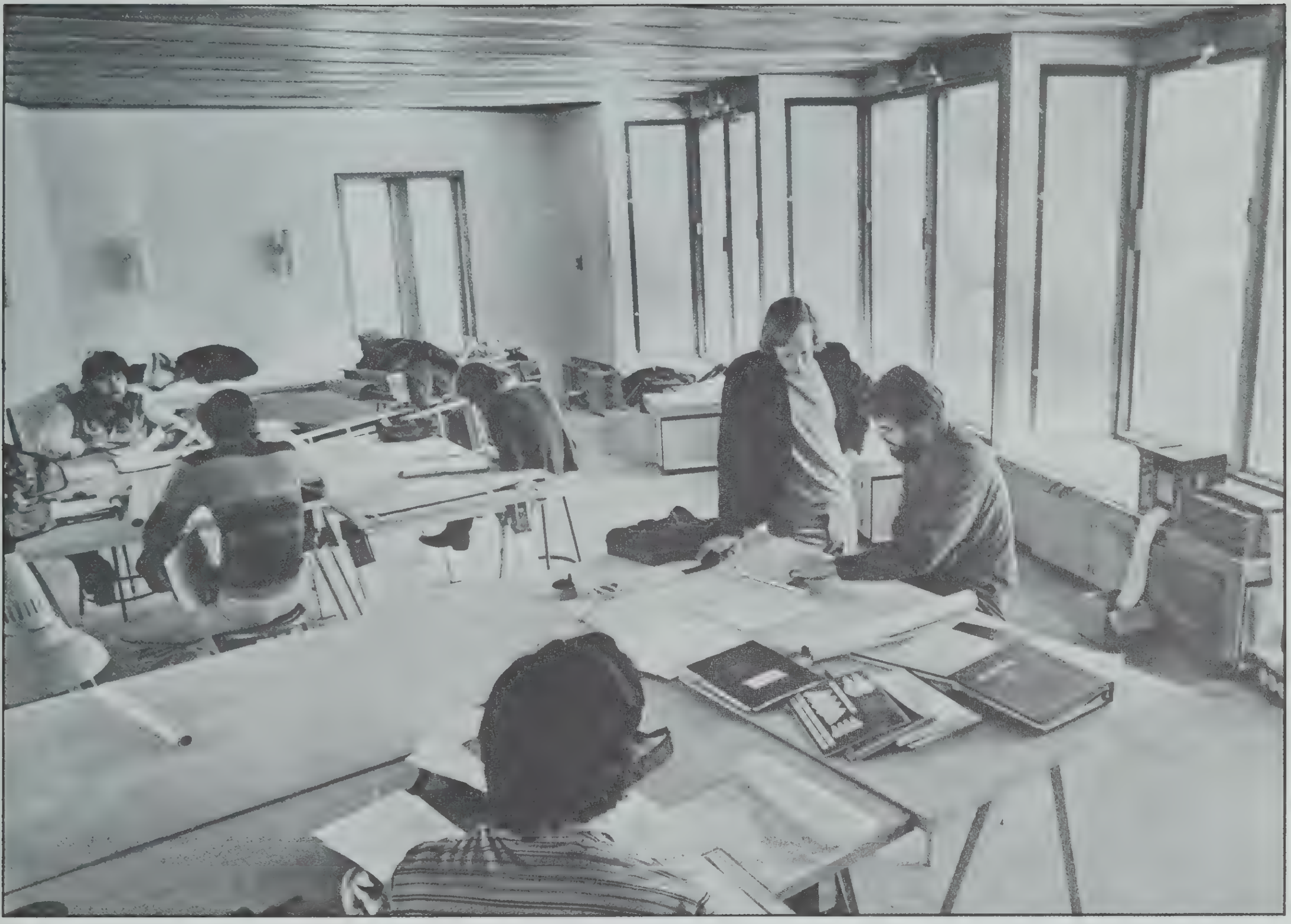

Figure 1: The one-story Solar Building No. 5 is used as an experimental studio and classroom.

MIT Solar Building No. 5: The Third Year Performance

By TIMOTHY E. JOHNSON
Department of Architecture, Massachusetts Institute of Technology,
Cambridge, Massachusetts 02139

ABSTRACT

MIT Solar Building No. 5 has shown that the overheating and glare problems associated with many direct-gain residences can be overcome using three new architectural finish materials: (1) a superinsulating window, (2) a glare-modulating and light-directing louver, and (3) a ceiling tile that stores heat latently.

The latest 1979-80 thermal measurements indicated that the sun supplied 67% of the building's seasonal heating requirement while an additional 12% of the load was met by the lights. This was done by glazing only 45% of the south wall (or 22% of the heated floor area) and not using movable window insulation. The indoor air temperature never exceeded 76°F *(24.5°C)* during the heating season.

Even with Solar 5's large window area, auxiliary energy use was as low as that of many superinsulated homes with double-thick walls and small windows.

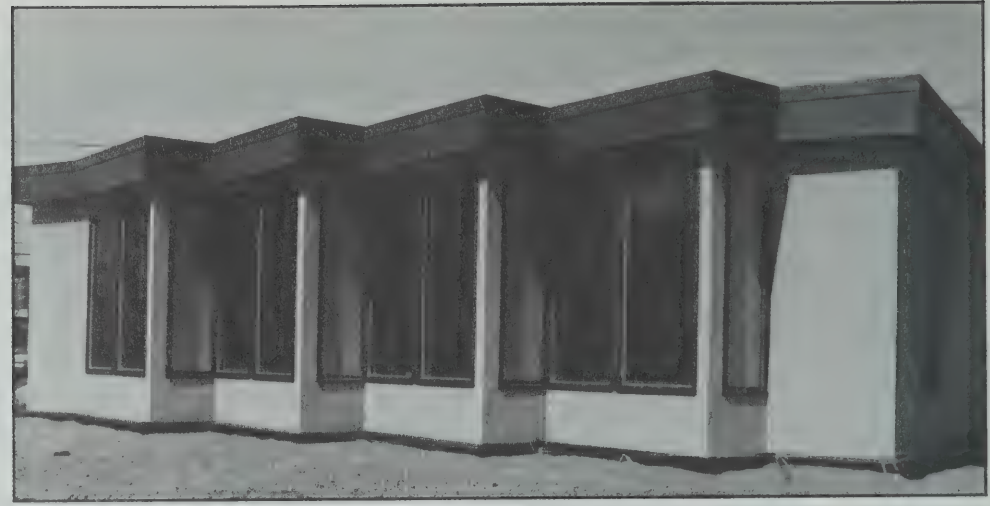

Figure 2: The four window bays of Solar Building No. 5 on the MIT Cambridge campus face south.

INTRODUCTION

The 1979-80 MIT Solar 5 heating season registered a more interesting thermal performance than the two previous monitoring seasons.[1, 2] It was in the third year that the glass coated for low emissivity and higher transmissivity was substituted for the original heat-mirror-coated plastic used in the south-facing windows, and wall-to-wall carpeting was installed over the concrete floor slab.

This experimental building has shown that the sunny winter day overheating, short carry through, and high glare problems associated with many direct-gain residences can be overcome with new architectural finish materials that emphasize their thermal-physical properties. Three new building components are demonstrated in the structure: (1) a view window that insulates twice as well as ordinary double glazing with little loss in solar transmission, (2) a glare-reducing and light-directing louver, and (3) a phase change material (PCM) ceiling tile that regulates the interior air temperature fluctuation by storing solar energy latently.

The MIT Solar Building No. 5* was completed for monitoring purposes on January 27, 1978. Building materials and construction labor were paid for by the MIT Godfrey Cabot Fund for Solar Research. The 866 ft^2 *(80.5 m^2)* building is a single, one-story space that is used as an experimental studio/classroom by the Department of Architecture (Figs. 1 and 2).

Solar heating is accomplished by directing insolation to dark-colored ceiling tiles containing a phase change material for thermal storage and temperature regulation (Fig. 3). Sunlight is placed on the ceiling by exceptionally narrow, upside-down reflectorized Venetian blinds that are fitted between the south-facing glazing. The blinds eliminate glare without sacrificing view. Heat losses through the double, south-facing glazing are reduced to 55% of ordinary double glazing by an indium-tin-oxide (ITO) coating on one side of the two glass sheets. The coating reflects 85% of the room temperature infrared radiation back into the heated space while remaining transparent to visible and solar radiation. The effective normal solar transmission (the sum of the solar transmitted and the absorbed heating component deposited in the building) of the coated glass is 81%. The overall effective solar transmission for the double-glazed system is 69%.

The 1979-80 thermal measurements showed the sun provided 67% of the building's heating requirements while an additional 12% of the load was supplied by internal gains from the lights. During this period the building was used approximately 12 hours a week by up to eight students and public visitors.

BUILDING DESCRIPTION

The flat roof, tan stuccoed building is located at 270 Vassar Street on the MIT Cambridge campus. The site, being aligned with the street, faces southeast. The windows are faced directly south by turning the building within 20° of south and finishing the turn by serrating the southern elevation of the building (Fig. 4). The resulting four window bays contain 180 ft^2 *(16.7 m^2)* of the special double glazing. The two westernmost bays contain outside panes of 0.25-in. *(0.32-cm)* PPG Industries' low iron glass** (91% normal effective solar transmission), and for visual comparison purposes, the two easternmost bays contain standard production double-strength float glass (88% normal effective solar transmission) furnished by PPG Industries. The inside panes are standard double-strength glass coated with ITO on one surface. Additional natural light and view are furnished by two ordinary double-glazed casement windows of 15 ft^2 *(1.4 m^2)* each in the north wall and one double-glazed casement of 15 ft^2 *(1.4 m^2)* in the east wall. The classroom is entered through an unheated north-facing 49 ft^2 *(4.5 m^2)* vestibule (Fig. 5). The 817 ft^2 *(76 m^2)*

---

*Solar Engineers: Timothy E. Johnson, Charles C. Benton, and Stephen Hale.

**Trade names rather than generic terms are used in this article since this is a specification report of a building as built.

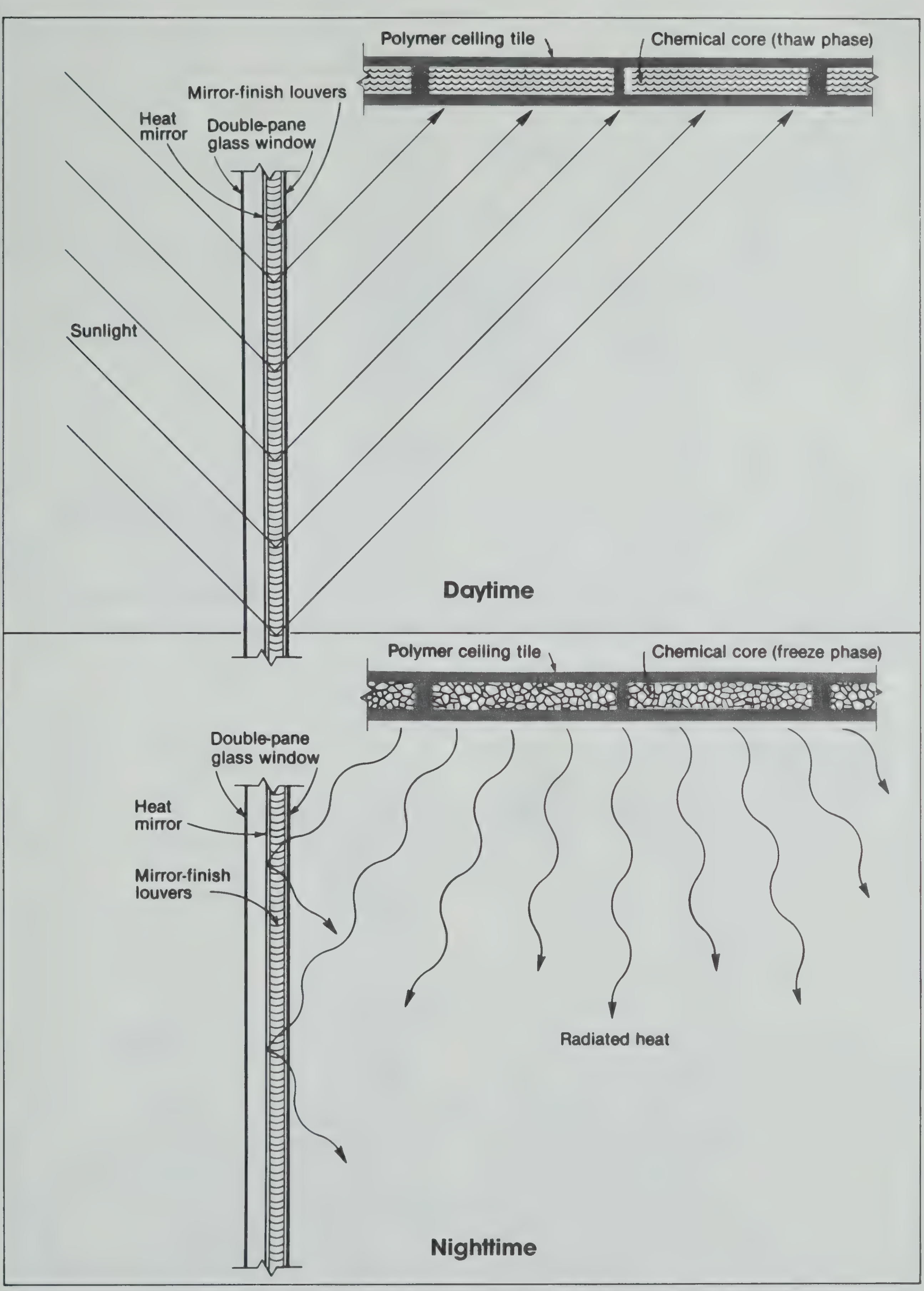

Figure 3: During the day, exceptionally narrow Venetian blinds reflect sunlight onto dark-colored ceiling tiles containing a phase change material. At night, heat is radiated from the tiles into the room.

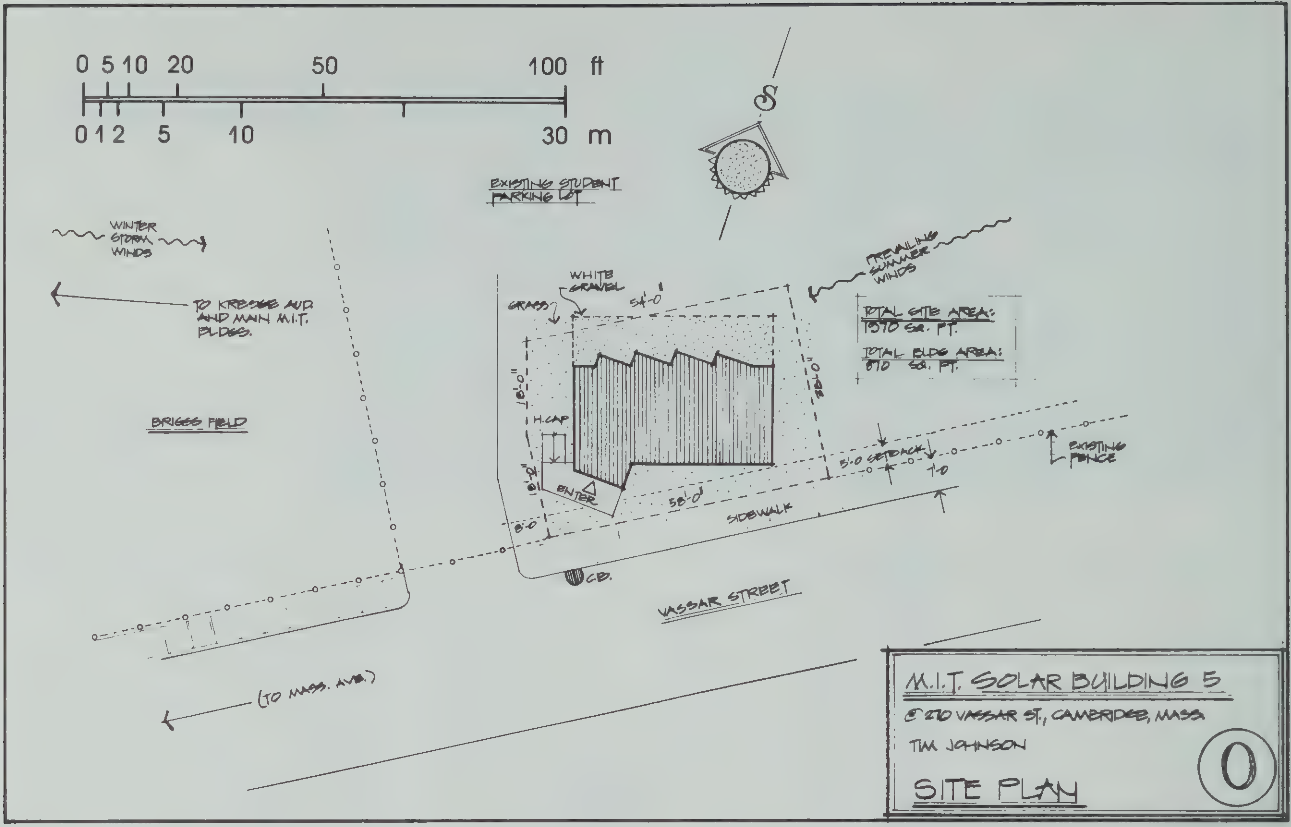

Figure 4: The site plan of the building shows the windows facing directly south while the building itself faces southeast and is aligned with the street.

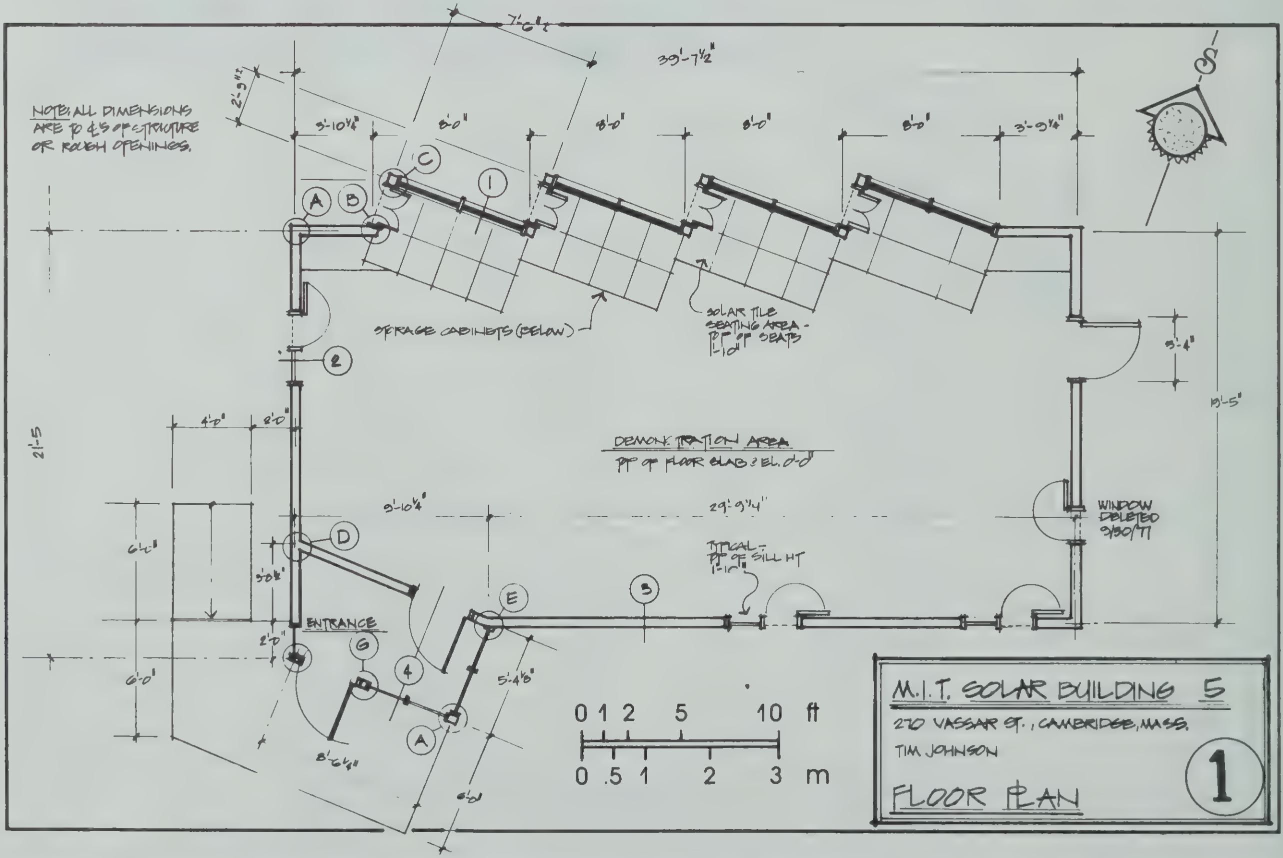

Figure 5: The building is entered through a north-facing vestibule. The settees under the windows provide cabinet space and additional seating, and also act as thermal storage areas.

heated classroom has a 10-ft *(3-m)* ceiling.

Heat is stored latently in the southern half of the tiled 817-ft^2 *(76-m^2)* ceiling and in the 88 ft^2 *(8.2 m^2)* of the thermal storage tiles placed on the southern settees. The four settees provide cabinet space for storage of classroom materials and additional seating area. Heat is also stored sensibly in the .625-in. *(1.6-cm)* drywall and to some degree in the 4-in. *(10-cm)* slab under the carpet and pad. The slab is poured on 2 in. *(5 cm)* of gravel on compacted earth. Edge losses are minimized with 4-in. *(10-cm)* Styrofoam SM perimeter insulation. Rather than skirt the building with 4-ft *(1.2-m)*-deep board insulation, the 4-in. *(10-cm)*-thick insulation goes down only 18 in. *(0.5 m)* to the depth of the perimeter's 18 x 18 in. *(.5 x .5 m)* concrete piers and then extends outward 3 ft *(1 m)* horizontally below grade (Fig. 6). The soil heat conduction paths are just as long as the paths in the conventional full-vertical sections, but excavation costs are minimized by using the 90° turn system. No frost heaving was observed during this heating season.

Because of the Cambridge fire codes, the building was framed with 18-gauge Wheeling steel studding rather than wood. The studding was joined with sheet metal screws so future alterations could be easily accomplished. The thermal bridging in the 2 x 6 in. *(5 x 15 m)* steel studs and 12-in. *(30-cm)* sheet metal ceiling joists was brought under control with exterior board insulation. The exterior walls are made up of .5-in. *(1.3-cm)* exterior gypsum, 1-in. *(2.5-cm)* Styrofoam and a proprietary fiberglass reinforced stucco weather skin called Dryvit. The Dryvit forms a continuous membrane that cuts down infiltration losses. The ceiling joists are covered with steel decking, 2-in. *(5-cm)* of Styrofoam, and a built-up tar and felt roof (Fig. 6). All this exterior insulation makes the steel behave thermally like wood. The bulk of the insulation is accomplished with 6-in. *(15-cm)* fiberglass batt in the walls and 11 in. *(28 cm)* in the ceiling. Vapor barriers are used throughout the building. The walls are double-caulked at the foundation and the soffit to minimize infiltration. Measured nighttime winter thermal losses due to infiltration and conduction are 270 Btu/h °F *(142 W/°C)* or 7.48 Btu/ft^2 °F-DD *(42 Wh/m^2 °C-DD)*.

The measured infiltration rate varied between .33 and .50 air changes per hour as determined by several wintertime experiments using sulphur hexaflouride as a tracer gas. The total measured heat conduction coefficient of 270 Btu/h °F *(142 W/°C)* represents a thermal load that is typical of energy-conserving, single-family, detached housing for the Boston area, even though the building has twice as much glass as most ordinary homes of comparable area. Housing and Urban Development minimum property standards (HUD MPS) state that a single-family, detached residence in the Boston area should exhibit a load less than or equal to 7.1 Btu/ft^2°F-DD *(40 Wh/m^2 °C-DD)* based on an average living area of 1,600 ft^2 *(149 m^2)*. Even though insulation levels are high, the Solar 5 thermal load of 7.48 Btu/ft^2 °F-DD *(42 Wh/m^2 °C-DD)* is slightly higher due to the larger surface-to-volume ratio encountered in a smaller building of the Solar 5 type.

One of the goals of this experiment is to show that multiple-family housing can be solar heated using the three new building materials. In fact, the roof of the MIT Solar 5 building is flat and windowless to demonstrate that another living unit could be placed on top of Solar 5 without affecting the solar heating fraction.

NEW MATERIALS DESCRIPTION

Each of the three new materials demonstrated in the Solar 5 Building emphasizes various thermal-physical properties necessary to accomplish comfortable, direct-gain solar heating.

Selective Transmitter

The southern windows are actually a composite of several materials. The assembly, working from the outside in, is .125-in. *(.32-cm)*-thick float glass (furnished by PPG Industries), a .75-in. *(1.9-cm)* air gap, modified Venetian blinds (fabricated by Rolscreen Co.), and float glass coated with ITO on the side facing the blinds. The overall calculated heat conductance (U-value) for the glazing assembly with the blinds open is 0.32 Btu/ft^2 h °F *(1.82 W/m^2 °C)*.

The major insulating effect is caused by the ITO selective transmitter developed by Airco Temescal Inc., of Berkeley, California. The coating has an emissivity in the thermal radiation region of 15% and a 75% transparency to normal solar radiation when deposited on .125-in. *(.32-cm)*-thick glass. Effective solar transmission increases to 81% when accounting for the absorption heating effect. The coating acts as a selective transmitter of radiation. The atoms in the coating are arranged in such a way that the short-wave radiation (solar energy) can get through, but the returning long-wave radiation (thermal radiation emitted as infrared from the interior building surfaces) cannot pass (Fig. 7). The returning thermal energy is actually reflected into the room by the low-emissivity surface if the coating is placed on the room side of the glass. With the coating facing the air gap as it is in Solar 5, energy cannot leave the surface as radiation because of the low-emissivity surface. This promotes greater thermal comfort because the room side of the glass rises in temperature as it absorbs the thermal radiation. Up to 60% of the heat loss through normal windows is due to radiation (via absorption and re-emission of infrared, IR). The heat mirror stops 85% of this radiation.

The ITO coating is corrosion resistant and may be cleaned manually with ordinary window cleaners. The window cavity is vented to the outside to prevent condensation, so the coating has been exposed to the atmosphere for more than two years. Some fogging has occurred, but only on the inside of the outside pane. No liquid has come in contact

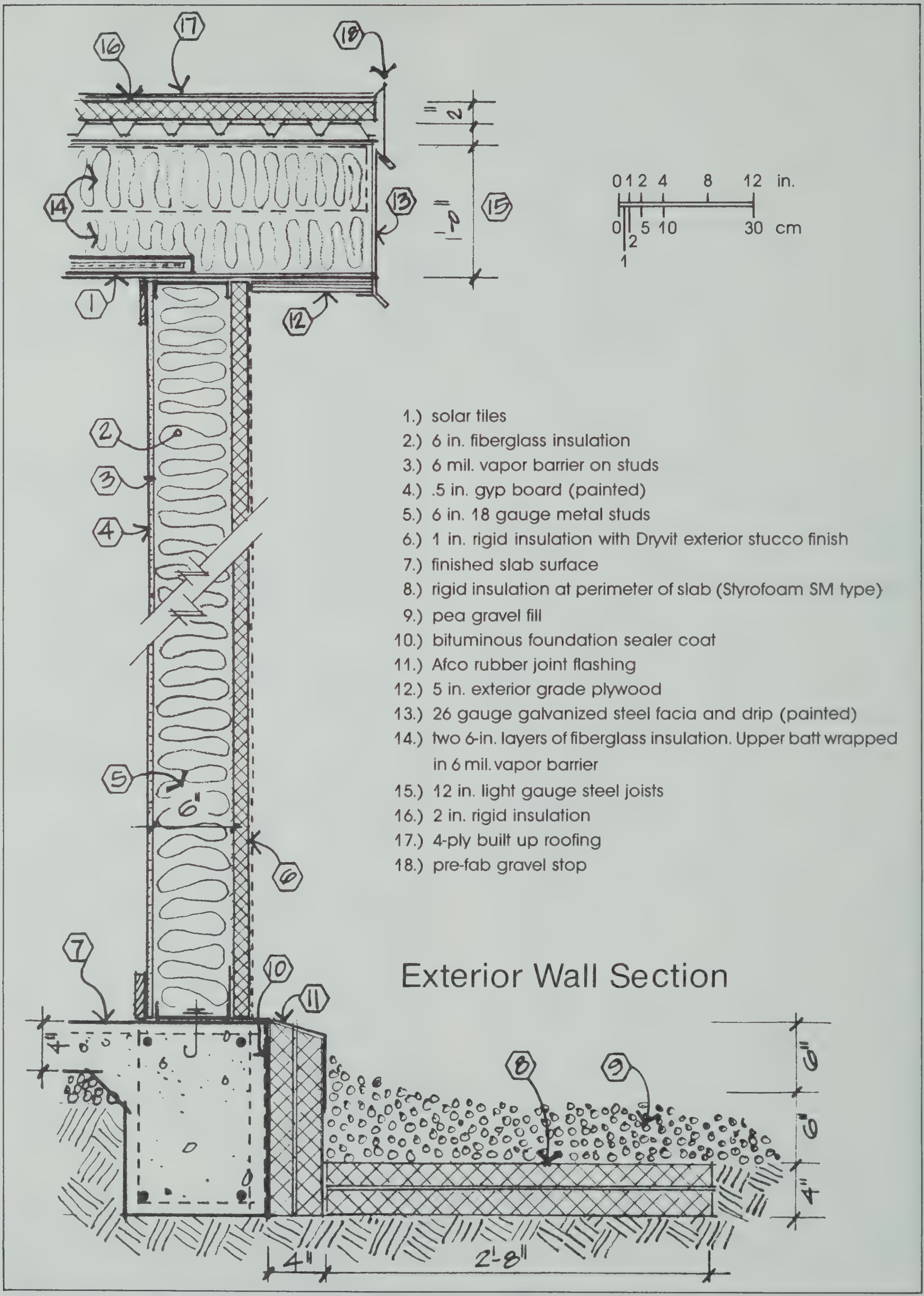

1.) solar tiles
2.) 6 in. fiberglass insulation
3.) 6 mil. vapor barrier on studs
4.) .5 in. gyp board (painted)
5.) 6 in. 18 gauge metal studs
6.) 1 in. rigid insulation with Dryvit exterior stucco finish
7.) finished slab surface
8.) rigid insulation at perimeter of slab (Styrofoam SM type)
9.) pea gravel fill
10.) bituminous foundation sealer coat
11.) Afco rubber joint flashing
12.) 5 in. exterior grade plywood
13.) 26 gauge galvanized steel facia and drip (painted)
14.) two 6-in. layers of fiberglass insulation. Upper batt wrapped in 6 mil. vapor barrier
15.) 12 in. light gauge steel joists
16.) 2 in. rigid insulation
17.) 4-ply built up roofing
18.) pre-fab gravel stop

Exterior Wall Section

Figure 6: A cross section of the roof, a concrete pier, and the foundation shows typical constuction.

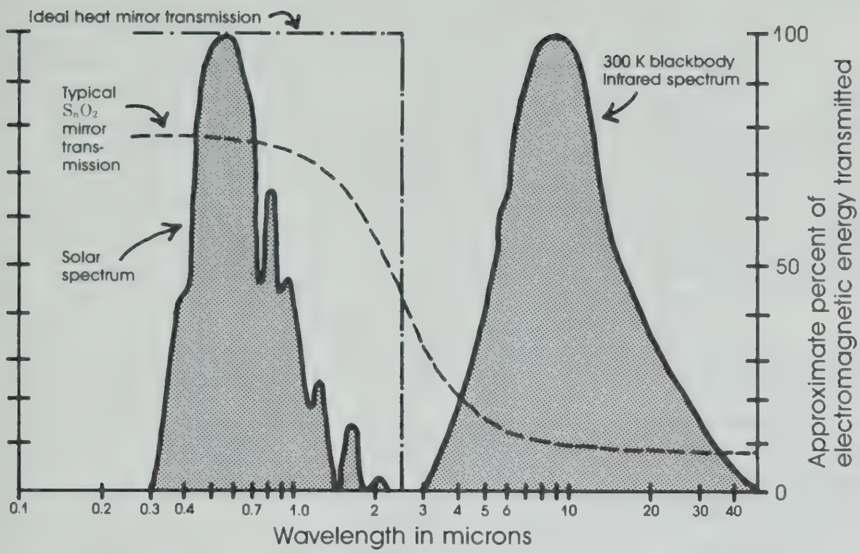

Figure 7: Schematic diagram shows a generalized spectrum of solar radiation (sunlight) with wavelengths of 0.3 to 2 microns and a typical infrared spectrum such as might be generated by heated surfaces near room temperatures. Such an infrared spectrum, roughly symmetrical around a peak wavelength of 10 microns, can be represented by a radiant blackbody at 300 kelvin. The ideal heat mirror transmits all sunlight (shortwave radiation), but blocks infrared frequencies near room temperature. A typical practical heat mirror as shown by the curve may transmit 85% of the sunlight while only transmitting 10% of lower radiation frequencies.

with the ITO coating except during cleaning. No corrosion is evident at the time of this writing.

Light-Directing Louvers

Insolation is directed to the dark blue ceiling tiles by reflecting louvers placed in the southern windows. The movable louvers are designed to minimize interference with views while offering the occupant control over the visual environment. While remaining fixed, the louvers accept a wide range of solar profile angles. This particular design requires only six adjustments during the heating season to keep all reflected solar energy on the ceiling. Large area source glare and glare due to high light intensity ratios at the floor are eliminated by the louvers since sunlight is reflected harmlessly over the occupants' heads. The slats are narrower than normal (.68 vs. 1.0 in. *or 1.73 vs. 2.5 cm*) and give the occupant the impression of a screened view rather than a striped one. The louver spacing is closer than usual to keep sunlight from filtering through to the floor. The louver cross section is a simple arc to facilitate fabrication. Geometric optimization studies[3] show a single arc radius will work throughout the U.S. latitudes, but at least two different slat spacings will be required.

The top surface of the louvers is reflectorized with aluminized Mylar attached by pressure-sensitive adhesive. Rolscreen plans to market the louvers with an integral reflectorized surface to overcome possible delamination problems. Such a louver has recently been placed on the market in the U.S.* and Sweden at costs comparable to ordinary slats. Sunlight nominally leaves the louvers at a 30° angle to the horizontal, but some rays reach a maximum angle of 70°. This causes a higher light intensity near the south edge of the ceiling. The louvers are faced directly south so the solar profile angle variation is minimized. The louver section can readily accept a 5° to 7° variation in solar profile angle without readjustment. This means the louvers need only be adjusted about once every three weeks to compensate for the seasonal movement of the sun, unless visual privacy is required at night. The rotational adjustment is simple; the blinds are rotated by a thumbwheel until sunlight disappears from the floor.

The only problem encountered with the blinds has been the polyester cord ladders that support the blades. Six of the eight ladders have stretched so that the bottom blades are no longer parallel to the top blades. This means some sun rays are beginning to strike people in the eyes. The problem is being investigated by Rolscreen.

Ceiling Thermal Storage Tiles

The polymer concrete ceiling tiles, 2 ft *(0.61 m)* square and only 1.25-in. *(3.2-cm)*-thick, are the storage component of the system. The tile core is filled with a dispersion of 38% sodium sulphate, 43.3% water, 3.4% Cab-O-Sil fumed silica, 2.6% borax, and 7.6% sodium chloride. This .75-in. *(1.9-cm)*-thick core stores a day's heat and then releases the retained heat as needed. Because the core stores heat latently at 73°F *(23°C)*, it maintains nearly a constant room temperature and thus prevents wintertime overheating, which normally leads to wasted heat. At night, as the outside temperature drops, the chemical core sealed within the tile parcels out enough heat to maintain room temperature near its daytime level. The core, therefore, acts as a built-in thermostat to stabilize the temperature in the room. The magnitude of this thermostat effect was readily demonstrated during the last days of construction when the building was complete, except for the ceiling tiles. Before the tiles were installed, the space peaked at 86°F *(30°C)* during sunny February days. After the tiles were installed, the space never exceeded 74°F *(23.4°C)*. Figure 8 shows typical room air and tile core temperatures over a 24-hour period bordered with two sunny days.

The room air temperature is measured at the 5-ft *(1.5-m)* level near the thermostat mounted at the

---

*C.M.I., Andover, Mass.

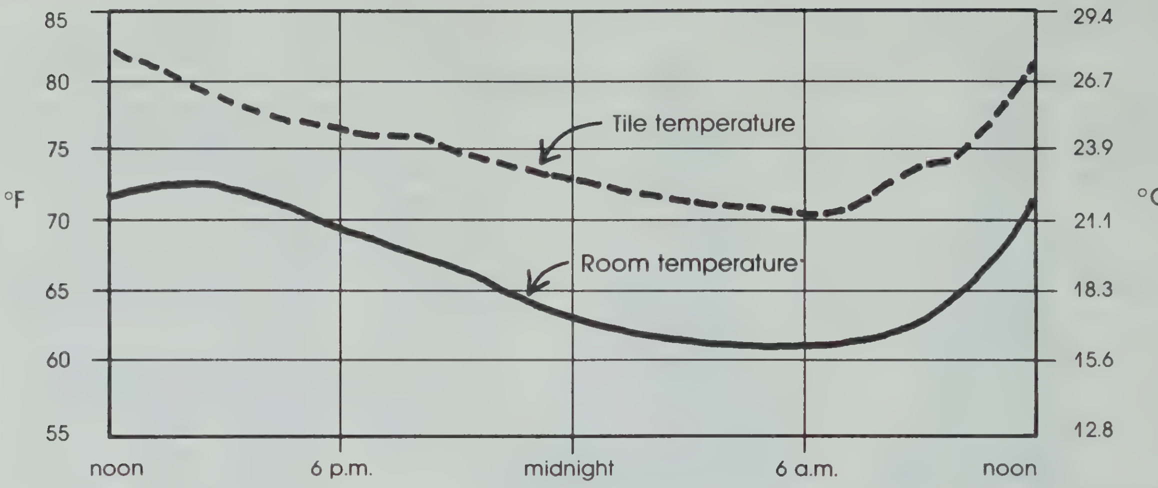

Figure 8: The tile and room temperatures from noon of Feb. 25 to noon of Feb. 26, 1978, are shown here.

southeast corner of the building. The ceiling tile core temperature is measured with a thermistor cast in place at the lower interface between the modified Glauber's salt and the polymer concrete. The ceiling tile is located at the center of the building and 2 ft *(0.61 m)* away from the south windows. The tile temperature profile does not show much of a plateau at the phase change temperature since the growing crystal front offers an increasing resistance to heat flow.

During the day, the solar heat flux is greater than the melting crystal front can accept, so the tile temperature exceeds the melting point of the modified Glauber's salts. Although the tile reaches temperatures in the mid 80s °F *(30s°C)*, this temperature is much lower than temperatures for ordinary masonry products in similar solar exposure situations. During the night, two-thirds of the heat is transferred to the space by radiation, and one-third by convection. Although warm air tends to stratify at the ceiling, convection currents induced by infiltration and incandescent bulbs remove some heat from the ceiling by mass transfer.

The phase change temperature can be adjusted by the amount of sodium chloride added. Obviously, if the temperature is set too high, overheating will occur during the day, and if set too low, underheating will occur at night. The eutectic formed by the salt is less efficient than pure Glauber's salt. The tile stores 200 Btu/ft^2 *(631 Wh/m^2)* over a 10°F *(5.5°C)* swing (most of the heat is released over the interior 5°F, *or 2.8°C*, swing) and weighs 11 lb/ft^2 *(54 kg/m^2)*. Out of the total, the salts contribute 6 lb/ft^2 *(29 kg/m^2)*. Calorimeter tests both by MIT and Brookhaven National Laboratories show the salts release 33 Btu/lb *(21 Wh/kg)* over a 5°F *(2.8°C)* swing. Measurements of pure Glauber's salts thickened with Cab-O-Sil, or Minu-Gel as Dr. Maria Telkes uses, show up to to 50 Btu/lb *(32 Wh/kg)* after several hundred freeze-thaw cycles. The 17 Btu/lb *(11 Wh/kg)* difference is due to the addition of NaCl. Small vials of the MIT dispersion have been stepped through more than 5,000 freeze-thaw cycles without any signs of thermal aging. This is equivalent to over 25 years of operation in a residential environment. The well-known aging problem has been overcome by packaging the salts in two adjacent .375-in. *(.95-cm)* layers that are thin enough to allow crystal growth by diffusion. However, some free solution would still be present unless the Cab-O-Sil were added. Conversely, thicker layers will separate even with the Cab-O-Sil added. Cab-O-Sil was used because it forms a three-dimensional, interlocking matrix that holds the material in suspension. The tiles can only be installed in horizontal positions (floors, ceilings, settees, etc.) since any angular mounting would introduce a hydrostatic head in the salt that would cause separation of the material.

The salts are packaged in a bag formed from 1 mil *(.025 mm)* aluminum foil laminated on both sides with 2 mil polymer composites. The bag is heat sealed with an inner polyethylene divider to form the two .375 in. *(.95 cm)* compartments. The aluminum is used to prevent water permeation over the years. The polyethylene protects the aluminum from corrosion. The chemical core was developed at MIT and produced for the MIT demonstration facility by the Cab-O-Sil Division of Cabot Corporation in their Billerica, Massachusetts, research laboratories. The puncture-proof bag and PCM contents are currently sold by CMI of Andover, Massachusetts, at \$2.10/ft^2 *(\$22.60/m^2)* in large quantities.

The .25-in. *(.62-cm)*-thick polymer concrete tile casing forms a self-supporting, heat-conducting envelope capable of withstanding foot traffic in flooring applications. The tiles were developed at MIT with the assistance of Architectural Research Corporation (ARC) of Livonia, Michigan. ARC currently markets the tiles at \$10/ft^2 *(\$108/m^2)*. The 2 ft x 2 ft x 1.25 in. *(.61 m x .61 m x 3.2 cm)* tiles are placed in the ceiling by suspending them between the flanges of 12-in. *(30-cm)* sheet metal joists mounted on 24-in. *(61-cm)* centers. The tiles can also be mounted in heavy-duty suspended ceiling systems, provided the wire hanger spacing is decreased. At 11 lb/ft^2 *(54 kg/m^2)* the tiles are 20-30% heavier than a plaster ceiling, which means the tiles can only be used as a retrofit in structures built to take the weight.

No tile warping has occurred. Three tiles out of the 257 installed in the ceiling and settees have leaked. The leaks occurred in the top surface of a ceiling tile because excessive air entrainment in the polymer concrete of those particular tiles created an open cell structure. This problem has been corrected by ARC. After one and a half years of operation, one tile was broken open in the frozen state for study. No free solution was observed and no corrosion had occurred in the aluminum foil barrier.

MEASUREMENTS AND EXPERIMENTS

The 1979-80 heating season performance was measured by recording temperature differences between indoors and the ambient air and recording the energy used by the baseboard auxiliary heaters and the lights. The building heat loss rate for an average temperature differential of 20°F *(11.1°C)* was measured experimentally by recording indoor and outdoor temperatures and auxiliary heating use on those nights following two consecutive cloudy days (after all stored solar energy had been exhausted from the building). With this information it is possible to calculate the gross heating load for the building at a measured temperature difference.

SOLAR PARTICIPATION

Table 1 shows the calculated heating loads, along with measured lighting and auxiliary energy use. Internal gains from the occupants were not measured. The energy added by people could not have exceeded 12% of the lighting energy, based on the known attendance figures. Most of this energy was vented to the outside by the accompanying opening and closing of doors (any one occupant did not stay more than two hours). The difference between the building load and the sum of the internal gains and auxiliary gains represents the solar intake. The "% Gross" column represents the percentage of the gross load met by solar. The "% Net" shows the percentage of the normal electric baseboard heater load that was met by the sun (the remaining energy is supplied by the lights). Although the table shows 67% of the net load was met by the sun, at least 70% would be furnished by the sun if the heating season had normal solar exposures. These percentages represent real savings, because even though the building's glass area is twice normal, the glass insulates nearly twice as well as double glazing so losses remain the same. The most revealing figure is the season's auxiliary energy use. The heating total was 2,879 kWh for a 817 ft^2 *(76 m^2)* heated area or 2.16 Btu/ft^2°F-DD. This is as good as many superinsulated homes that depend on double-thick walls and small windows to lower energy consumption. MIT Solar 5 shows the more open direct-gain solar heating approach is equivalent to the defensive superinsulated approach in conserving energy while satisfying our primal ties to the outdoors.

The ITO window system is nearly comparable to R-6 *(1.06 m^2 k/W)* nighttime insulation used with ordinary double glazing. The "% Gross" or "% Net" figure would rise by one percentage point if the nighttime insulation were used rigorously instead of the ITO system. The "% Net" figure would be lowered to 58% if ordinary double glazing were used instead of ITO-coated glass.

EFFECT OF CARPETING

When Solar 5 was first built, the concrete floor slab was left exposed so it would act as a back-up thermal storage element in case the tiles failed. Even though sunlight never reached the floor, the floor absorbed diffuse solar energy and infrared energy transferred from the warm ceiling. Once it was determined the tiles were doing their job, it became time to test the thermal effect of wall-to-wall carpeting. One of the major advantages of the Solar 5 approach to direct-gain solar heating is that the ceiling tiles free up the floor for more prosaic uses.

When the wall-to-wall carpeting was finally installed at the beginning of the 1979-80 heating season, there was concern the space might overheat during sunny winter days now that the concrete floor slab was no longer in radiant contact with the solar illuminated ceiling. Measurements showed that at no time did the indoor air temperature exceed 76°F *(24.5°C)*. Before the carpet was installed, maximum air temperature reached 74°F *(23.3°C)*. Thermistors buried in the drywall, ceiling tiles, and concrete slab showed the reduced participation of the slab was nearly made up by increased par-

**MIT Solar Building No. 5:
1979-80 Heating Season (kWh)**

	Lights	Auxiliary	Load	Solar Used	% Gross	% Net
Sept.	0	0	156*	156	100	100
Oct.	0	0	267*	267	100	100
Nov.	129	0	1082*	953	88	100
Dec.	216	753*	1928*	959	50	56
Jan.	191	907	2167	1069	49	54
Feb.	237	602	1862	1023	55	63
March	236	572	1448	640	44	53
April	177	45	765	543	71	92
May	0	0	162	162	100	100
Total	1186	2879	9827	5762	59	67

*Estimated load assuming ITO glass in place (ITO Heat Mirror installed January 2, 1980).
January and December had approximately 14% more sun than normal; March had 40% less sun than normal. The season degree-days were nearly normal. (1 kWh = 3,413 Btu.)

Table 1: Heating loads, lighting, and auxiliary energy are calculated here.

ticipation of the ceiling tiles and drywall. The participation of the phase change tiles increased by 15% and the gypsum walls picked up 50% in their thermal participation once the rug and pad were installed. The ceiling tiles store six times as much energy as the .625-in. *(1.6-cm)* gypsum walls, while the rug-insulated slab stores approximately 80% of the energy stored in the walls.

SUMMER COOLING

The building is cooled in the summer by massive nocturnal cross ventilation. This is accomplished by opening the four ventilator doors on the south side of the building and three on the north-facing casement windows. Using the SF_6 gas detector, it was determined that with all the windows and ventilator doors open, and with a 5 mph breeze, the quantity of air movement through the building was equal to about 7.5 air changes per hour. This is equal to about 65,000 ft^3/h, or about 1,000 ft^3/min *(472 L/s)*.

This air movement will eventually cool down the internal surfaces to the early morning air temperatures (typically 65°F, *or 18°C*). During the day, the ventilator doors are closed, and the casements are left open a crack for ventilation. The blinds are set so direct sunlight is reflected to the outside. The initially cool building masses then soak up the day's heat. This management procedure resulted in interior peak room air temperatures that ran 8°F *(-13.3°C)* below peak outdoor temperatures. This is not regarded as remarkable performance. Some of the heat added to the room comes from heat absorbed in the low-emissivity glass which radiates into the room. Also, there are no shade trees over the roof, which would be helpful in any situation. Given normal landscaping, it is felt the building would perform acceptably in a Boston climate.

USER REACTION

The building was used by two distinct groups: students and the general public. The only thermal complaints were registered by most of the students on two different cold winter nights. The students felt cold in certain areas of the space when the air temperatures were 61°-62°F *(16.0°-16.7°C)*. Normally the radiantly heated ceiling would compensate for these low temperatures. About half the people felt the space was stuffy (due to the low infiltration rates and relatively small volume).

The natural daylighting was deemed very pleasant during sunny hours. Task lighting was necessary for the students at their drawing boards on most overcast days. The lighting proved to be even and shadowless. Visitors were pleasantly surprised by the view afforded by the narrow louvers and remarked their opinion of Venetian blinds had been altered by the visit. Although glare was greatly reduced, some public visitors complained of the remaining glare. Subsequent questioning showed most of the complaints were due to reflections produced by the cars in the adjoining parking lot.

The dark-colored ceiling received many complaints when viewed during the day—surprising not because of its tone, but because of its color. Most of the complainers did not approve of blue, but would have accepted an equally dark green or terra cotta. A very small percentage of the visitors would not accept any dark ceiling.

The nighttime lighting scheme was a failure; a subject of nearly universal complaint. The room was lit by ten wall washers (a wall fixture that throws light up and down the white wall) and by eight down lights over the south windows, using a total of 2,200 watts. The ceiling absorbed enough light to make the room feel dark (slightly less than 3 fc). One possible solution to this problem is using one or two central ceiling fixtures instead of the wall washers. A central fixture would not interfere with solar collection since only the front half of the ceiling participates.

CONCLUSIONS

All of the materials demonstrated in the MIT Solar Building No. 5 are either on the market or beginning to reach the market. Even the early pricing structures indicate these materials will make passive solar heating using direct-gain principles inexpensive and architecturally pleasing. Overheating and glare need not be a concern when using this approach, which reduces auxiliary energy use to levels associated with superinsulated homes.

REFERENCES

1. Johnson, T.; Hale, Stephen; Benton, Charles C. 1978 (Oct.). "MIT Solar Building No. 5, Initial Performance." Department of Architecture, MIT, Cambridge, Massachusetts.

2. Johnson, T.; Quinlan, Ed. 1979 (Nov.). "MIT Solar Building No. 5, The Second Year's Performance." Department of Architecture, MIT, Cambridge, Massachusetts.

3. Lebens, Ralph. 1979 (Jan.). "Determining the Optimum Design of the Solar Modulator." *Proceedings of the Third National Passive Solar Conference.* Edited by Harry Miller, Michael Riordan, and David Richards. San Jose, California; Jan. 11-13, 1979. Newark, Delaware: American Section of the International Solar Energy Society, Inc. (AS/ISES), University of Delaware; pp. 100-106.

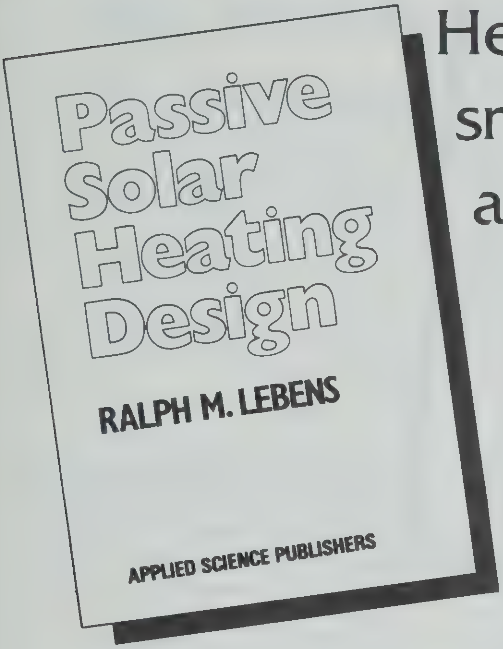

Here's help for small offices and others

Passive Solar Heating Design.
Ralph M. Lebens, John Wiley & Sons, New Jersey, 1980.
234 pp., illus. $54.95.
Published in London by Applied Science Publishers, Ltd.

This is an important and useful text for designers who wish to produce solar-conscious buildings that work and who wish to calculate the expected cost advantages of various solar and heat-conserving measures. It was written by Ralph Lebens and first published in London, but the author, whose graduate degree in architecture is from the Massachusetts Institute of Technology, is very familiar with both U.S. and foreign applications.

Reviewed by Robert O. Smith, founding Board Member of the Passive Systems Division. Robert O. Smith Heating and Solar Engineers at 55 Chester Street, Newton, Massachusetts, provide engineering and teaching services to the design community.

Although in book format, this design manual provides several specific tools:

- A comparative review of passive solar design principles.
- A chapter on design steps with explanations, equations and rules-of-thumb for quantifying the effects of such design elements as mass and aperture. It includes sections on how to calculate cost-benefit ratios and how to monitor thermal performance of the finished building. This chapter is the essence of the book.
- A worked out, step-by-step example of how to predict performance for a passive solar building. The carefully explained input data, would be useful to designers who could not easily find their own values.
- Three fully documented programs for use with the Texas Instruments TI-59 programmable calculator with printer.

The three programs include passive simulation to predict indoor temperatures and the auxiliary heating and cooling required to maintain thermostat settings. The values are produced for only one zone and one twenty-four hour day; the hourly values listed on paper tape are the time beginning at midnight, ambient temperature, solar gain, auxiliary energy required or surplus, cumulative auxiliary energy, and the temperatures at seven selected locations within the building or structural fabric.

They also include a simpler passive design program which calculates the maximum room air temperatures expected in a direct gain zone, but only on a clear day on the equinox dates. This gives maximum temperatures for eight consecutive hours and the number of hours of thermal carry-through resulting from this stored solar heat.

The third, a cost load program, calculates cost-benefit ratios and payback periods for specific proposed changes to a standard or base-case design. Incidental outputs are the balance-point temperature, heating load and heating cost.

The book contains complete listings of its program instructions. Most software vendors sell only protected (copy-proof) programs. The book would be better, though, if these programs were also listed in BASIC for use on microprocessors.

The book introduces the fundamental design principles which are necessary for accuracy in thermal calculations, including heating degree days based upon balance-point temperature; proportioning of solar gain into indoor air, storage masses and back to the outdoors; and quantification of the effects of solar shading, aperture, tilt and azimuth. Both English and metric units are given.

The careful consideration and fairly rigorous quantitative treatment given to these principles, to heat loss and to internal gains enable the reader to obtain more believable cost-benefit estimates for alternative design features than could be obtained from the rules-of-thumb and correlative methods widely available in the passive design literature.

The text does have weaknesses. The core chapter of 97 pages is divided into twenty topics; more sections in a different arrangement would have produced a more convenient designers' manual. Some of the subjects need to be explained more clearly. Instead of one incomplete index, three—to topics, projects and people mentioned—would make the book more helpful.

Even so, this book should be useful. Those who work in very small design offices should find it helpful since the book makes extensive use of a relatively inexpensive programmable calculator. Other books are available which treat the same process, but they do not handle it with the rigor and completeness here.

There are two main competing proprietary calculator programs called PEGFIX/PEGFLOAT and TEANET which are very similar to the design and simulation programs listed in the book. These programs with manuals and prepared magnetic cards cost $75 and $95, respectively. Although they share some additional conveniences not present in Lebens' programs, an estimate of carry-through time is not part of PEGFIX/PEGFLOAT. On the other hand, PEGFIX/PEGFLOAT has other features such as the amount of auxiliary energy required to maintain a thermostat setting; the air exhaust rate needed to maintain a thermostat setting in an overheating space; and temperature and auxiliary heating or cooling energy values for each of twenty-four consecutive hours.

The proprietary programs include convenient input and output worksheets which speed their use. These are not provided with Lebens' programs.

The price of $54.95 may seem somewhat high, but it is considerably lower than the prices charged for most competing proprietary programs. Although parts of this book duplicate methods available elsewhere, there are enough extras that *Passive Solar Heating Design* should find its own niche in the design community. □

A book that too few will use

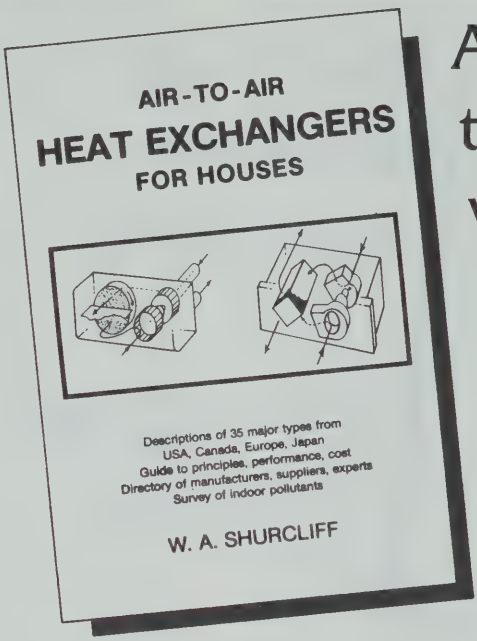
AIR-TO-AIR
HEAT EXCHANGERS
FOR HOUSES

Descriptions of 35 major types from
USA, Canada, Europe, Japan
Guide to principles, performance, cost
Directory of manufacturers, suppliers, experts
Survey of indoor pollutants

W. A. SHURCLIFF

Air-to-Air Heat Exchangers for Houses. William A. Shurcliff. Brick House, Andover, Mass., 1981. 187 pp., $17.95.

Solar enthusiasts of technical or not-so-technical persuasion owe much to William Shurcliff. He has added significantly to the solar literature and is a testament to the notion that someone of emeritus status can remain vibrant and productive. With regard to his recent *Air-to-Air Heat Exchangers for Houses*, however, someone should find him an editor.

Air-to-Air Heat Exchangers for Houses sets out to explore a subject we should examine more closely: the use of these devices to solve the problem of poor indoor air quality resulting from household pollutants or outgassing from certain foundation soils. Air-to-air heat exchangers use blowers and heat exchange surfaces to transfer heat between outgoing and incoming air, bringing fresh, healthy air indoors while minimizing winter heat loss or summer heat gain. They are of particular importance in superinsulated, airtight houses; however, relatively "loose" houses may have unhealthy indoor air if they are built on soils with high levels of radon, or if residents use appliances with noxious combustion products.

Shurcliff's cover describes the book as a "guide to principles, performance, and cost" of heat exchangers and a "directory of manufacturers, suppliers, and experts." Also included is a "survey of indoor air pollutants." As a directory and a survey of pollutants, the book does fairly well. As a guide to principles of heat exchangers, some major reworking is necessary.

Despite the apparent intention of addressing architects, builders, and homeowners, only people with knowledge of thermodynamics and physics at the college level can digest the whole book. At that, the technical presentation is uneven, ranging from the very complicated to the very simplistic, with much of the information scattered. For example, laminar and turbulent air flows are discussed using terms and equations which will lose the nontechnical reader, while the topic of how to calculate convective heat transport is never completed. The hopeful reader is chased to a distant chapter, then directed

Reviewed by Russell G. Derickson, an independent solar consultant in Colorado.

to *Work Heat Transfer* by Chapman (Macmillan), which is a book for engineers.

A better approach would have been to package the facts in a simpler, purely descriptive format aimed primarily at a nontechnical audience, adding appendices to satisfy the needs of the technical reader.

As it stands, this book buries many important and timely bits of information about indoor air pollution, heat exchangers, and energy-efficient housing. For example, one learns on page 10.09 that inflow and outflow rates of exchangers should generally be equal, but this important fact is neither underscored nor included in a chapter summary. In fact, there are no chapter summaries. Likewise, barely noticeable at the bottom of page 11.21 is the statement that no manufacturer provides information on his product's efficiency when latent heat exchange is involved.

On the other hand, the reader is confronted with the "great embarrassment concerning energy" (i.e., the difficulty of determining absolute values) and the "error of calling infrared radiation, 'heat'," neither of which strengthens his grasp of heat exchangers, no matter how interesting it may be. Some day Shurcliff should write a book on scientific tidbits, a sort of "What You Always Wanted to Know About the Paradoxes and Quirks of Science, But Were Afraid to Ask." That is where such information belongs.

Nor can one always find the information even if one looks hard. Like Shurcliff's better edited, identically titled article in the March 1982 issue of *Solar Age*, the book frequently raises questions it makes little or no attempt to answer.

Air-to-air heat exchangers make sense mainly for airtight houses, but the reader is not given information on how to reduce infiltration, or what the risks are. The reader also needs to be told that tight construction requires an unusual amount of attention to detail from builders; if the attention is lacking, the house may not have reduced infiltration and the reader's concern about air quality—or acquisition of an exchanger—may be unwarranted.

Then there is Shurcliff's treatment of indoor air pollution, an issue that has been receiving increasingly urgent attention recently.

> "
> Someday Shurcliff should write a book on scientific tidbits, a sort of 'What You Always Wanted to Know About the Paradoxes and Quirks of Science, But Were Afraid to Ask.'
> "

The International Symposium on Indoor Air Pollution, Health, and Energy Conservation held in Amherst, Massachusetts, in November 1981, pointed to the combustion products of the commonly used gas range as a potential cause of respiratory illness, especially in young children. Stand-alone, unvented kerosene heaters likewise generate harmful by-products. Radon outgassing from the soil beneath a house, which then seeps upward into the living space, is a serious threat to health. The list goes on and on.

Shurcliff assumes a "surge of interest" and knowledge on the part of architects, builders, and homeowners regarding indoor air pollution and heat exchangers. In my experience, such optimism is unwarranted.

The book covers the types of pollutants quite well, especially radon gas, which has deleterious effects that may not appear for 10 to 40 years after exposure. This sort of information needs to be brought to public attention, especially in view of the increasing evidence of high pollutant levels in all modern housing. I am afraid, however, that *Air-to-Air Heat Exchangers for Houses* will not find its way into the average person's hands if it remains in its present form.

Even as an engineer, after reading the book I am left with much confusion and several batches of questions: Why does exchanger efficiency drop dramatically with lower outside temperatures? If, as Shurcliff suggests, blower power is reduced during extreme cold, what are the implications for tight houses in Canada and the northern United States? Must indoor air quality suffer under these circumstances? What is meant by a "tight" house? The term is never quantified, even roughly, in terms of air change rate.

Many times Shurcliff provides only conjecture on such things as why a rotary exchanger may be better than a fixed type or on how to size an exchanger. Are these issues that complicated or intractable? Are there not some useful rules of thumb which could be set forth? Perhaps the technology is not well enough developed for us to use exchangers on a wide-scale basis.

Finally, Shurcliff mentions in his introduction that the presented information may have "serious errors of fact" and that one should not rely on "any specific statement without making independent confirmation." This is a cop-out. I did not discover any serious errors (not to say that there are none), but the book does commit sins of omission.

Air-to-Air Heat Exchangers for Houses, as presently structured, is a book that too few will find useful. This is a shame considering the importance and timeliness of the subject matter. □

A Proposed Review Process

By WILLIAM A. WRIGHT
Design Tools Review Editor

Over the last two years it has become clear that low energy buildings *are* possible, and that passive solar methods are an important part of the designer's bag of tricks. As the lure of low energy design has penetrated more and more of the building design community, a strong hunger for objective information on design tools has become evident.

During the same two year period there has been intense activity in the development of tools which attempt to predict the comfort, performance, and cost produced by passive solar design. Unfortunately, the current channels of dissemination (word of mouth and conferences) are frequently incomplete and as a result, tool developers are at least as frustrated as designers.

This journal intends to help fill the need for objective review by regularly conducting design tool evaluations and by reporting the results for as many tools as often as space and the volunteer process allow. Peer review is the only respected reference source for tools, so the procedure proposed here is based on synthesis of review information from four different, but professional points of view.

METHODS

The proposed review process has been written and published here both to subject the process itself to peer review and to provide a fairly complete background of thinking in this relatively new and occasionally treacherous area. Little has been published in the area of tool review, although the DOE Passive Program did survey designer needs and preferences. The International Energy Agency (IEA) has recently begun a multiyear, multitask program which develops a review process for passive design tools. The IEA passive design tool task is oriented toward selection of tools appropriate to each of the three design phases. In contrast to that effort, the review process described here is intended to regularly publish reviews on a wide range of tools. This article presents an attempt to organize a dispassionate procedure which would reliably report to designers on a regular basis.

While reviews by organizations such as ASHRAE have consisted primarily of algorithm endorsement, it is clear that a review which treats many of the other issues that face designers will be valuable. In the end, a designer wants to contrast the value attending use of a particular tool with the actual investment and operating costs. Criteria which enable a designer to make such judgments include the start-up cost in both labor and cash, as well as operating and maintenance costs. Value is added as the tool becomes more general in application, and as its use causes the least change in current design modes. Further value accrues to tool results which can be used directly in client presentations. And last, but not least, the degree to which the tools are valid has multiple effects on both value and liability or cost.

In addition to the dimension of review which establishes value and cost, the considerable variation of experience and capability among designers causes judgments of value and cost to be relative. This is especially true in passive design, since the field is constantly absorbing those who are new to concepts such as thermal mass, while old hands in passive are moving on to advanced approaches such as selective surface mass walls.

Thus, a second major dimension in a review is the point of view of the reviewer. The developer of the tool, a novice tool user, an experienced user of the tool, and a technical expert are four major points of view which are needed for a complete picture of a tool.

The proposed process would use four questionnaires, each similar to Fig. 1, to extract some of the necessary factual data. Following responses from each of the four review sources, a summary review would be written. Factual data such as cost and intended range of application would be presented in tabular form while more subjective information from the reviewers such as ease of use, quality of documentation, and start-up labor would be summarized in the discussion form of a traditional review.

It is important to note that the proposed process is not intended to replace, or even attempt, validation. The thrust of the reviews will be the practical issues associated with design, and the technical verification attempts being made elsewhere will be drawn on wherever they are known.

POINTS OF VIEW

The following four points of view would be solicited for each review:

- **The Tool Developer**—Whatever a tool's weaknesses and strengths, one wonders what its creator intended. What were meant to be its audience, application, and costs?

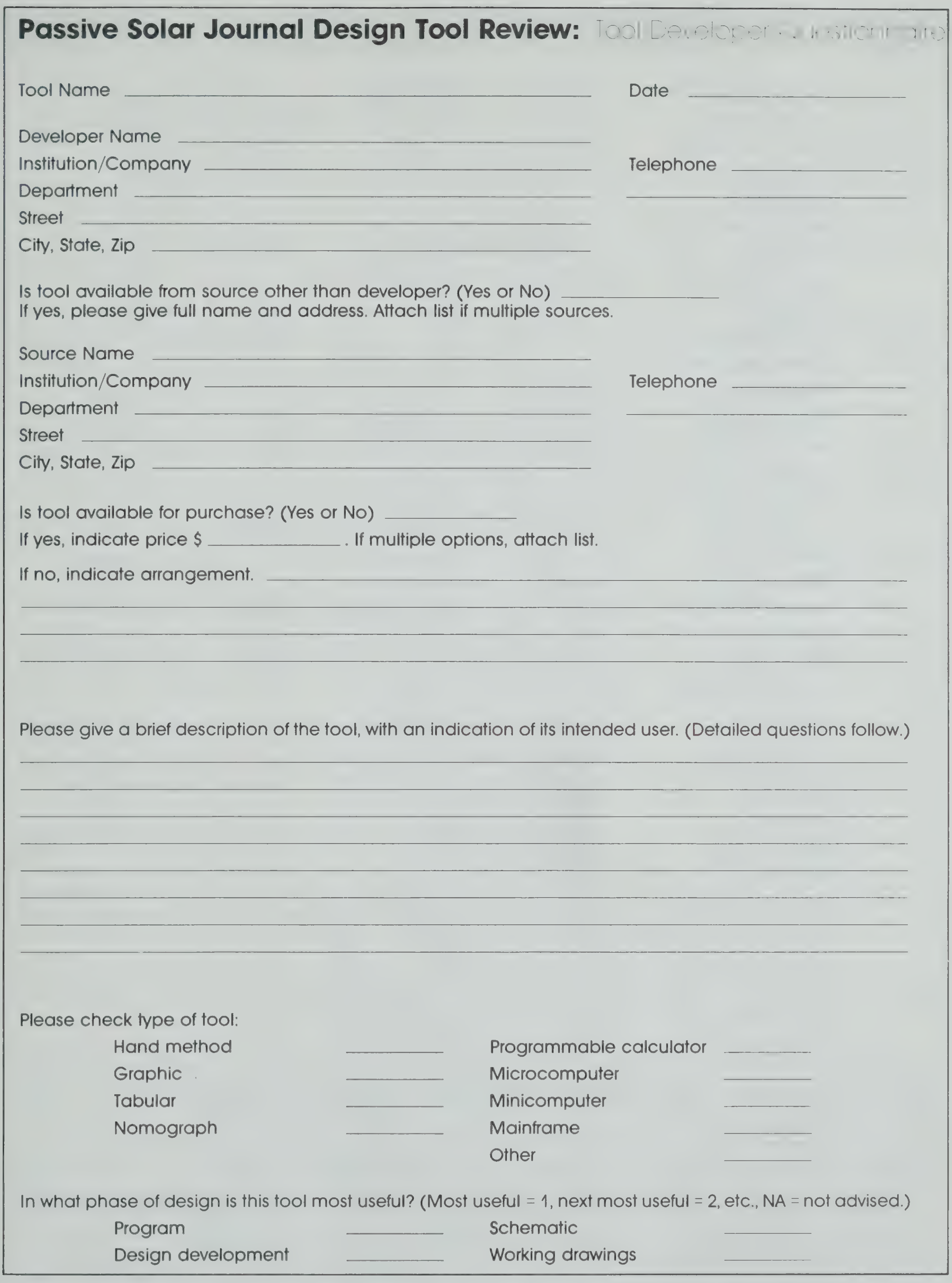

Passive Solar Journal Design Tool Review: Tool Developer Questionnaire

Tool Name ____ Date ____

Developer Name ____
Institution/Company ____ Telephone ____
Department ____ ____
Street ____
City, State, Zip ____

Is tool available from source other than developer? (Yes or No) ____
If yes, please give full name and address. Attach list if multiple sources.

Source Name ____
Institution/Company ____ Telephone ____
Department ____ ____
Street ____
City, State, Zip ____

Is tool available for purchase? (Yes or No) ____
If yes, indicate price $ ____. If multiple options, attach list.

If no, indicate arrangement. ____

Please give a brief description of the tool, with an indication of its intended user. (Detailed questions follow.)

Please check type of tool:

Hand method	____	Programmable calculator	____
Graphic	____	Microcomputer	____
Tabular	____	Minicomputer	____
Nomograph	____	Mainframe	____
		Other	____

In what phase of design is this tool most useful? (Most useful = 1, next most useful = 2, etc., NA = not advised.)

Program	____	Schematic	____
Design development	____	Working drawings	____

Figure 1a: Facts about a particular design tool will be gathered from four points of view using forms similar to this questionnaire for a tool developer. Figure 1b. shows the reverse side of the form.

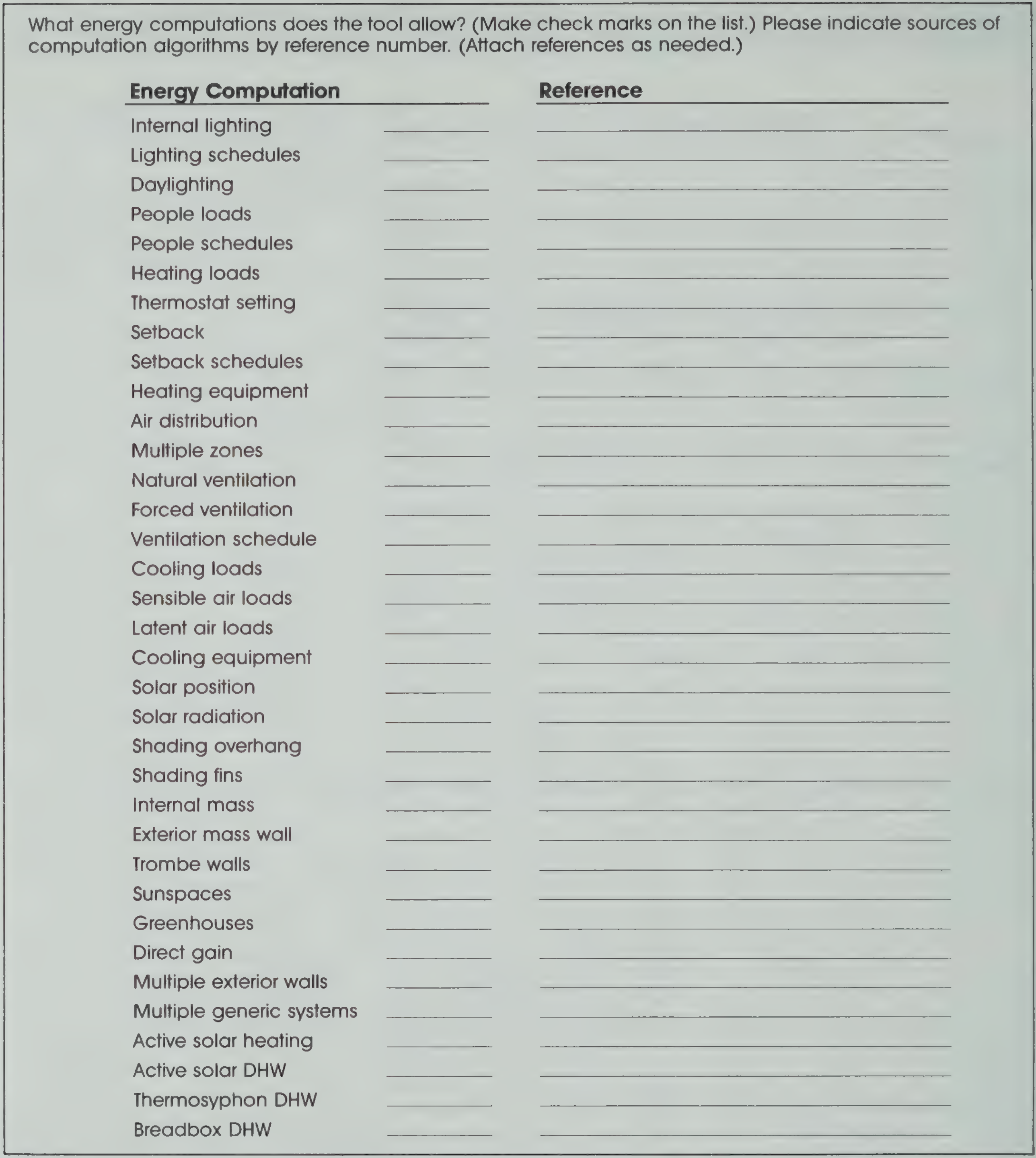

What energy computations does the tool allow? (Make check marks on the list.) Please indicate sources of computation algorithms by reference number. (Attach references as needed.)

Energy Computation		Reference
Internal lighting		
Lighting schedules		
Daylighting		
People loads		
People schedules		
Heating loads		
Thermostat setting		
Setback		
Setback schedules		
Heating equipment		
Air distribution		
Multiple zones		
Natural ventilation		
Forced ventilation		
Ventilation schedule		
Cooling loads		
Sensible air loads		
Latent air loads		
Cooling equipment		
Solar position		
Solar radiation		
Shading overhang		
Shading fins		
Internal mass		
Exterior mass wall		
Trombe walls		
Sunspaces		
Greenhouses		
Direct gain		
Multiple exterior walls		
Multiple generic systems		
Active solar heating		
Active solar DHW		
Thermosyphon DHW		
Breadbox DHW		

Figure 1b: The reverse side of the questionnaire asks the developer to mark applications and reveal his computation sources. Additional types of computation have been eliminated from this figure but appear on the form.

What are future intentions for modifications, support, documentation? What technical sources were used as the basis for the various computations? What limitations does the developer wish to note? Although the majority of the information to be collected is factual, giving the developer an opportunity for input on his intended purpose and future direction will help to make a more informative review.

- **A First Time User**—One simple way to answer questions about first time use is to quiz a first time user. By providing a designer with a copy of the tool and requesting its use on test problems, it will be possible to collect data which other potential new users will find useful. A first time user is not necessarily a novice to passive design; rather, a first time user is simply a designer who has not had the opportunity to use the particular tool under review. As a means of understanding the start-up time and effort involved, this review is crucial.

- **Experienced User**—Each tool has at least a few users who have applied the tool over a number of design problems. Such users are really the only source of information on limitations which may be fairly subtle. For example, a ventilation cooling algorithm may include sensible loads, but not latent loads, or a shading algorithm may work for vertical off-axis shading, but tilted off-axis shading may not be calculated properly. Although finding such is not necessarily easy, their input is needed to develop a feel for the tool's ultimate capability.
- **Technical Reviewer**—In order to determine whether any major questions about computation methods exist, the fourth point of view should be that of a technical expert. This part of the review is perhaps the most difficult since the complexity of the review is at least proportional to the generality of the tool under review. For a simple tool such as a sun angle protractor, the sources are usually clear and easy to verify. When a large computer simulator is involved, however, there may be a sizeable number of traceable sources of computation. In such cases, the review should summarize the *status* of the technical issues and point the reader to the current sources of technical literature for more details.

  Similarly, it is clear that attempts to validate computer tools by comparison to actual field measurements are beyond the scope of *Journal* resources. For that reason, the technical review would report on the degree to which validation is complete, and in which areas the tool may be untested. For example, the reviewer might report that the daylighting calculation is based on untested (or tested) algorithms and more testing is (or is not) required.

REVIEW CRITERIA

In any review process, the subjective opinions of a reviewer are injected, and are, of course, solicited because it is assumed that the reviewer represents an important point of view. As a means of attempting consistency, the review criteria have been broken into five major parts, and then reduced to questionnaires. By placing more or less emphasis on the major criteria for each point of view, the questionnaires have been customized to yield one questionnaire per point of view.

From a designer's point of view, there are a series of pragmatic questions to be answered. Tools should be exactly that—items which allow the designer to carve out the design. Just as a sculptor needs tools ranging in crudeness from heavy mauls to fine files, the passive designer needs to wield tools ranging from rules of thumb to simulators. For any tool to be used, it must ultimately become an extension of the designer's thinking, and not require loving to be used. Thus, practical issues are crucial. How a hammer feels in the hand and how much it costs are at least as important as how well it drives the chisel.

Criteria would include:

- **Initial Investment**—The cash outlay for the tool is the least part of the investment. The dollar value of the learning time invested may be 10 times the purchase price. Ancillary costs for some tools may not be obvious. For example, a microcomputer program which costs $250.00 may also require the purchase of a new language, which may itself cost more than the $250.00. Also, the program may require two days of setup and familiarization. Thus $250.00 may escalate to a true cost of well over $1,000.00

Questions to be answered about first costs would include:

1.) What is the cost of the item?
2.) What additional books, languages or hardware may be needed, and what are their costs?
3.) How much time does a novice require to be able to operate the tool? To become proficient?
4.) How long would an expert require to become able to operate the tool? To become proficient?

- **Operating Costs**—Here again, time and money are the critical concerns. Cash required for the operating costs may be zero, or several hundred dollars per use. A profile angle chart can be copied regularly as it wears out, while a simulator may cost $1,000.00 for a single data point. The amount of time needed to use any tool will vary from the first use to the nth use, and will also vary across the range of user sophistication and prior experience. The peculiarities of a particular tool consistently require spending large amounts of time on its use, that should be noted.

Cost questions to be answered include:

1.) How long does a single use of the tool take? If a single parameter is changed, how is the second use affected? How does the user background influence time per use?
2.) What dollar costs are typical per use? How do these vary with the nature of the design problem?

3.) Are there monthly or other maintenance (i.e., updating) costs? What are they?

- **Ease of Use**—The feel of the hammer handle is dependent not only on the handle, but also on the hand of the user. Designers' backgrounds, orientations, and personal preferences determine how "friendly" a particular tool is to a user. Nonetheless, it is possible to describe some aspects of a tool that will allow a reader to decide whether he or she will be interested.

Typical questions to be answered:

1.) What type of input does it have? Is the input in terms of design parameters, or must external calculations be done?
2.) Is its ouput a single number or a range of values? Does it present results graphically?
3.) What is the appropriate background for a user? Architecture? Engineering?
4.) How transportable is it? Is other equipment required? Does it take long to use? Are the instructions clear?

- **Range of Application**—Current energy design tools cover such a wide range of applications that both their generality and their focal points need to be explained. A program such as BLAST can be used over a wide range of building types, while a graphic direct gain temperature swing method is restricted to single-zone applications. A review needs to specify the tool's range of applications, including limitations it has in any particular application.

Typical application range questions:

1.) In what phases of design does the tool perform well?
2.) Does it handle generic passive systems or is it more general?
3.) Can whole buildings be represented, or is the tool better used for some aspect of a design?
4.) Is it restricted to residential only? Commercial only?
5.) Does it allow investigation of lighting, comfort, annual performance, heating, cooling, etc.?
6.) In what areas should the tool *not* be used?

- **Calculations Methods Base**—Most tools are developed by using an algorithm which traces back to a physical analysis. The variation is extreme. Sun angle and shading angle calculations are based on first principle descriptions of celestial mechanics while annual cooling load methods may have internal components no more trustworthy than a local utility's guess at a daily consumption profile.

Typical technical questions:

1.) Are the methods used available in the literature? If not, are they available for examination anywhere?
2.) Are the methods used appropriate to the applications recommended by the developer? Why?
3.) In what areas should this tool be used with caution? With confidence? Why?
4.) What aspects of the tool have been validated? Are the results of such attempts clear-cut?
5.) To what other similar tools has this tool been compared? What were the results?
6.) Is this tool based on direct physical law? On correlations? On what?

Following the tool developer's commitment, as evidenced by filling in a questionnaire, each of the three other reviewers would complete their review tasks, submitting two copies of the tool, and their evaluation would be summarized by *Journal* editors and staff. The composite review plus the questionnaires would be forwarded to the developer for comments and reply. These would be taken into account in the final draft of the review.

As proposed, the design tool review for this journal is a synthesis of the two review processes now in use for articles and book reviews. Just as authors are apprised of comments by peers, so the developer is informed of comments from the several points of view. Tool developers may choose to explain further where questions were raised or the developer may wish to improve documentation or the tool itself. Past experience has shown that scrutiny tends to cause improvements to be made. As a direct result of a similar process during the early days of programmable calculator passive design software, several developers made major changes in their documentation, and both tool users and developers benefited.

Making sure all four points of view are brought to bear on all of the questions may seen an ungainly task. Certainly use of forms and a clear procedure will help, but no number of forms will make the process easy. On the other hand, if the result is to be of actual use to designers, and if tool developers are to benefit, then the effort is justified easily. Since tool developers vary from nonprofit to commercial ventures, their interests must be respected by a thoughtful process. Similarly, designers deserve a probing and genuinely revealing review. A balancing of the interests of each is the final objective.

CONCLUSION

It may not be possible to provide direct answers to subjective designer questions like "Will the ABC tool help me make more profit, or just add to the overhead?" and "Will the developer be available to answer questions and provide improvement next year?" Nevertheless, it may very well be possible to provide data which helps designers and developers communicate more completely.

Passive Solar Journal

Heating, Cooling, Hybrid Technologies and Strategies for Sustainable Design

BOSTON ARC
LIBRARY
320 NEWBURY ST.
BOSTON, MA 02115

Volume 1, Number 4: Fall 1982

Passive Design Competitions; F. Moore: **Data Acquisition** in Test Modules; M. Mostrel and B. Givoni: **Windscreens** in Radiant Cooling; **Book Reviews** by D. Abrams, D. Andrejko, G. Arnold, B. Hamilton, W. Langdon, W. Morris, W. Shurcliff, and W. Wright; **Annual Index.**

Official Journal of the Passive Systems Division of the American Solar Energy Society,® Inc.

PASJDF 1(4) 193-256(1982)   ISSN: 0277-6456

Passive Solar Journal

Editor-in-Chief:
Jeffrey Cook, Department of Planning, College of Architecture, Arizona State University, Tempe, Arizona (602) 965-6210

Associate Editors:
John Hayes (Book Review Editor), Marlboro College, Marlboro, Vermont (802) 257-4333
William A. Wright (Design Tools Review Editor), Cambridge Energy Corporation, Cambridge, Massachusetts (617) 491-0903
J. Douglas Balcomb, Los Alamos National Laboratory, Los Alamos, New Mexico (505) 667-2619
Michael Holtz, Architect, Boulder, Colorado (303) 440-3436
Fred Nelson, Sunset Magazine, Menlo Park, California (415) 321-3600

Production Editor:
Heidi Osselaer

Editor/Writer:
Peter Brown

Typesetting:
Paradise Valley Typesetting Studio, Phoenix, Arizona

Chief Artist, consulting:
Mark Woodruff, Glendale, Arizona

Director of Publications:
Albert Henderson, ASES, New York, New York (212) 736-8227

Publications Production Manager:
Barbara Bradley, ASES, Newark, Delaware (302) 738-1153

Executive Director, ASES:
G. Lee Salmon, Boulder, Colorado (303) 492-6017

The *Passive Solar Journal* gratefully acknowledges the use of office facilities provided by Arizona State University.

Publisher: The *Passive Solar Journal* is published by the American Solar Energy Society, Inc. (ASES): The United States Section of the International Solar Energy Society, 110 West 34th St., New York 10001: Quarterly: Winter, Spring, Summer, Fall. It is the official journal of the Passive Systems Division of ASES. (Solar Energy Society is a registered trademark.)

ASES assumes no responsibility for the statements and opinions advanced by contributors to the society's publications. Editorial views do not necessarily represent the official position of ASES.

This publication contains accounts of work sponsored by the United States Government. Neither the United States nor the United States Department of Energy, nor the American Solar Energy Society, nor any of their employees, nor any of their contractors, subcontractors, or their employees, makes any warranty, express or implied, or assumes any legal liability or responsibility for the accuracy, completeness, or usefulness of any information, apparatus, product, or process disclosed or represents that is use would not infringe privately owned rights.

Subscription rates: Corporate/Nonmembers, one year, U.S. $162.00, foreign, $194.00. Members of the Passive Systems Division receive the *Passive Solar Journal* as a benefit of membership. Individual member rates are for personal use only, paid with personal funds.

For membership information, write to ASES, 1230 Grandview Ave., Boulder, Colorado 80302.

Business correspondence:

Changes of address should be sent by members and subscribers to ASES offices at 1230 Grandview Ave., Boulder, Colorado 80302. Allow six weeks for the notification to become effective. All communications should include both old and new addresses with zip codes and should be accompanied by a recent mailing label.

Claims for missing issues will not be allowed if received more than 90 days from date of mailing plus the time normally required for postal delivery of the issue and claim. No claims will be allowed because of failure to notify a change of address or because a copy is "missing from files."

Editorial correspondence:

The editorial office of the *Passive Solar Journal* may be contacted through Editor-in-Chief Jeffrey Cook, Dept. of Planning, College of Architecture, Arizona State University, Tempe, Arizona 85287.

Access: The Passive Solar Journal is covered by *Engineering Index* (monthly and annual), *Energy Abstracts* and *Energy Information Abstracts*, and *Solar Index*.

Copyright © American Solar Energy Society, Inc. 1983

It is a condition of publication that manuscripts submitted to this journal have not been published and will not be simultaneously submitted or published elsewhere. By submitting a manuscript, the authors agree that the copyright for their article is transferred to the publisher if and when the article is accepted for publication. However, assignment of copyright is not required from authors who work for organizations which do not permit such assignment. The copyright covers the exclusive rights to reproduce and distribute the article, including reprints, photographic reproductions, microform or any other reproductions of similar nature and translations. No part of this publication may be reproduced, stored in a retrieval system or transmitted in any form or by any means, electronic, electrostatic, magnetic tape, mechanical, photocopying, recording or otherwise, without permission in writing from the copyright holder.

U.S. COPYRIGHT LAW APPLICABLE
TO USERS IN THE USA

The Article Fee Code on this page indicates the copyright owner's consent that, in the U.S.A., copies may be made for personal or internal use provided the stated fee for copying beyond that permitted by Section 107 or 108 of the United States Copyright Law, is paid. The appropriate remittance should be forwarded with a copy of the first page of the article to the Copyright Clearance Center Inc., 21 Congress Street, Salem, MA 01970 U.S.A. If a code does not appear, copies of the article may be made without charge, provided permission is obtained from the publisher. The copyright owner's consent does not extend to copying for general distribution, for promotion, for creating new works or for resale. Specific written permission must be obtained from the publisher for such copying.

Copyright Passive Solar Journal 0277-6456/83 $3.00/0

Passive Solar Journal

The Official Journal of the Passive Systems Division
of the American Solar Energy Society, Inc.®
The United States Section of the International Solar Energy Society

Fall 1982 Volume 1, Number 4

CONTENTS

Perspective

194

The National Passive Solar Design Competitions

The standards set at the First National Passive Solar Design Competition held during the 1980 Amherst conference were continued at the second competition in 1982 at Knoxville. Portfolios of the Albany County Airport Terminal, the Consolidated Edison House, and the Lake House in Central Florida are presented here, with the remainder of the second competition's first-place winners to appear in our next issue.

Testing and Monitoring

219

Data Acquisition in Test Modules

Fuller Moore surveys current practices with data sensors, recording, and processing systems, providing recommendations for testing and monitoring techniques.

Applied Research

229

Windscreens in Radiant Cooling

Marco Mostrel and Baruch Givoni of the Jacob Blaustein Institute for Desert Research discuss the effect of windscreens on radiant cooling systems. The prediction models for radiant cooling are compared to the authors' actual research results at Sede Boqer.

Book Reviews

239

W. Scott Morris, Dennis A. Andrejko, and William A. Shurcliff evaluate Los Alamos National Laboratory's *Passive Solar Design Handbook, Volume Three: Passive Solar Design Analysis.*

George Arnold, Blair Hamilton, Donald Abrams, William A. Wright, and Dennis A. Andrejko review sections of the *Seventh National Passive Solar Conference* from Knoxville.

William K. Langdon considers the *Passive Solar Construction Handbook* by Steven Winter Associates, Inc.

Annual Index

253

Volume 1, 1982, of the *Passive Solar Journal* is indexed.

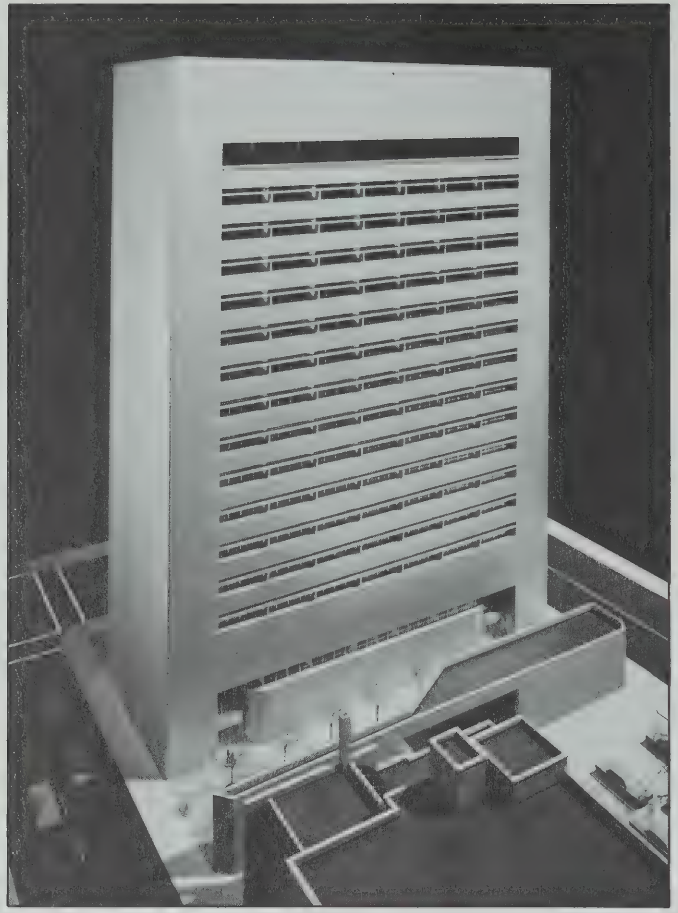

Photo: Photography Unlimited

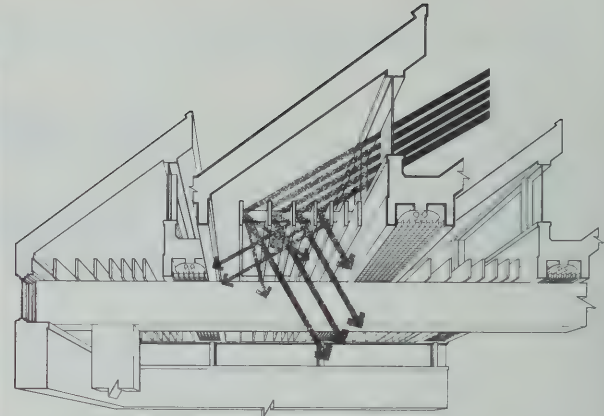

WINTER – Clear Day

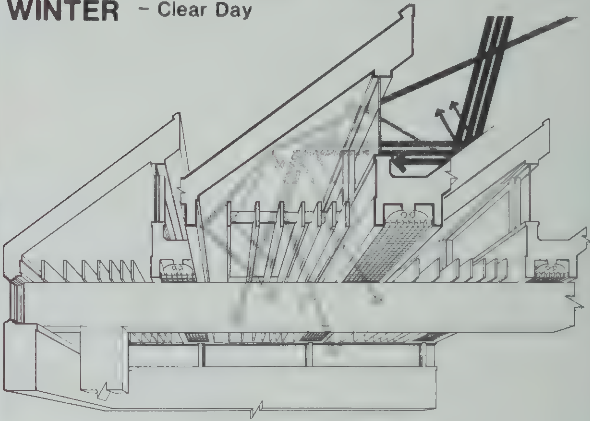

SUMMER – Clear Day

Honored as prototypes for commercial and institutional buildings at the First National Passive Solar Design Competition, both models have now been built. Both the high-rise office of the Farm Credits Bank in Spokane, Washington, and the State Office Building at San Jose, California, integrate daylighting and passive/hybrid cooling techniques. The section drawings illustrate how the Trust Pharmacy design combines daylighting and heating in a sawtooth skylight configuration.

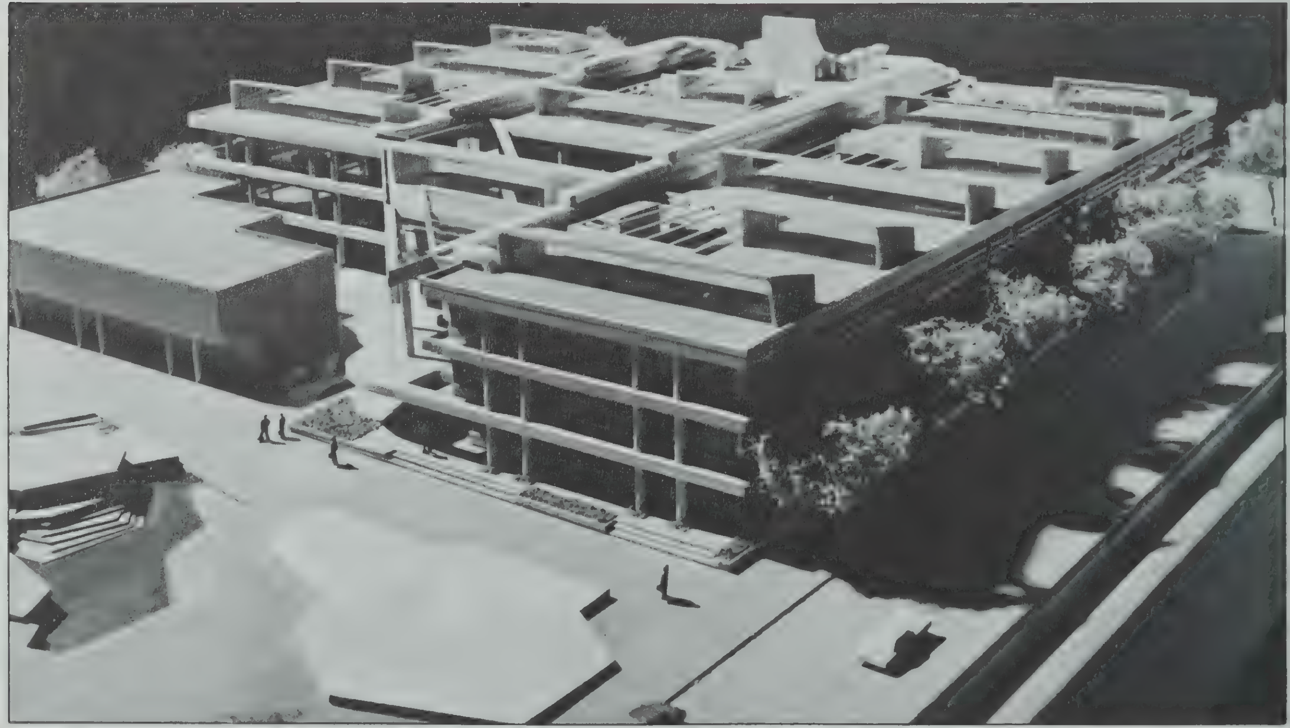

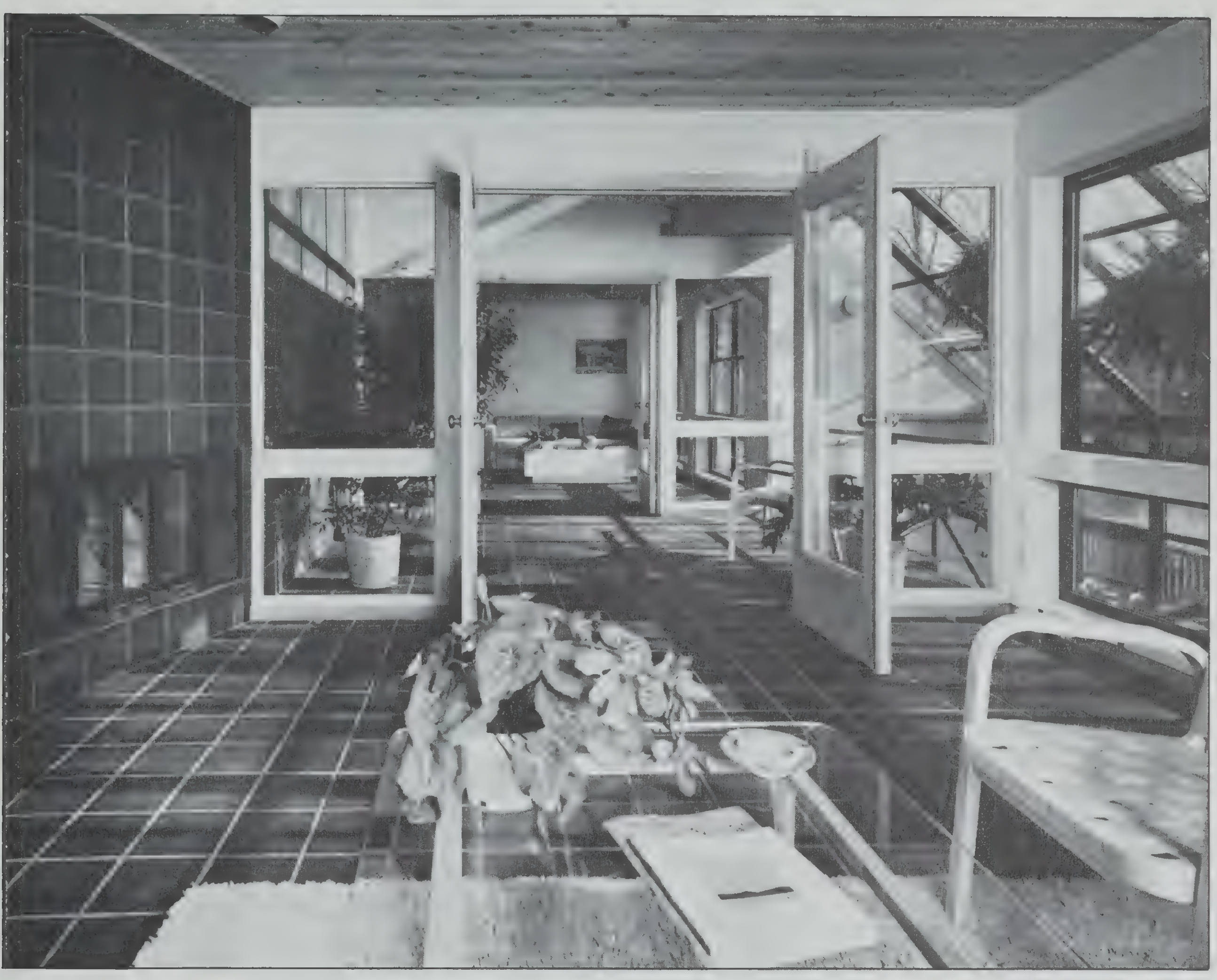

Photo: Norman McGrath

Passive design competitions have been a critically important means of improving the standards of architectural integration of passive thermal techniques. Sunspaces, once known as greenhouses, are no longer only for plants, and passive design approaches popularized in residential design have been increasingly applied to commercial and institutional buildings. The interior of the award-winning New York Consolidated Edison Demonstration House from the 1982 Second National Passive Design Competition illustrates a sunspace outside a living area. Extensive tile on the walls and floor provides distributed thermal mass.

The National Passive Solar Design Competitions

Between 1975 and 1980, a number of statewide as well as national solar building design competitions were held in the United States. Each had its own goals and restrictions. Each aimed at extending the visibility and the quality of the field of solar building design. The first one of major significance was the First Passive Solar Home Awards Competition conducted nationally by the U.S. Department of Housing and Urban Development during the summer of 1978. Over 550 applications for funding new house designs were submitted. Of these, 162 entries were recognized by HUD and provided with additional modest financial assistance for their construction. However, the most potent competition for solar building designs was the First National Passive Solar Design Competition, organized in association with the October 1980 Amherst, Massachusetts, meeting of the Fifth National Passive Solar Conference.

Although labeled "national," since its sponsors have been the U.S. Section of the International Solar Energy Society, the Passive Solar Conferences have always been international in scope, no restrictions ever having been placed on national origin or climatic region. Thus, it was natural for the hosts of the Fifth Conference and the organizers of the

First Passive Design Competition First-Place Award Winners

Designer	Project
Beckman, Blydenburgh and Associates	Simmons Building Davol Square Providence, Rhode Island
Bohlin, Powell, Larkin Cywinski	Shelley Ridge Girl Scout Center Philadelphia, Pennsylvania
Tom DeAngelo Architectural Alliance	Vocational Technical Educational Facility St. Paul, Minnesota
Richard Fernau with Laura Hartman and Jim Axley	Brodhead House La Honda, California
Harrison Fraker with Short and Ford, Architects and the Princeton Energy Group	Princeton Professional Park Princeton, New Jersey
Mike Funderbunk and John Meachem	Sunshelter Design Raleigh, North Carolina
J.E. Fryett	Row Housing Project Kitchener, Ontario
Hugh and Shirley Kirley	Solar Woodbox Amherst, Massachusetts
Edward Mazria and Associates	Trust Pharmacy Grants, New Mexico
Mogavero and Unruh	Windcreek Condominiums Sacramento, California
Robert W. Peters Alienza Arquitectos	Residence of Dr. and Mrs. Michael Ogg Second Village Santa Fe, New Mexico
Peter Pfister Architectural Alliance	Pfister Retrofit Minneapolis, Minnesota
Walter F. Roberts, Jr.	Sundance I Reston, Virginia
Daniel V. Scully Total Environmental Action, Inc. with Ballou-Levy-Fellgraff, Architects	Flat Rock Brook Nature Center Englewood, New Jersey
Sizemore/Floyd	TVA Solar Modular Homes Memphis, Tennessee
SOL-ARC/David Baker	Solar Duplex Berkeley, California
SOL-ARC Architects and Energy Consultants ELS Design Group, Consultants	San Jose California State Office Building San Jose, California
Christopher Theis	Waugh Residence ("The Mossman") Eskridge, Kansas
Walker McGough Folts Lyerla	Farm Credits Bank Spokane Office Building Spokane, Washington
C. Stuart White, Jr. Banwell, White and Arnold, Inc.	Manhattan Loft Conversion New York, New York

building design competition, the New England Solar Energy Association, headed by John Hayes, Dennis Jaehne, and Drew Gillett, not to limit entries to U.S. designers. As a result, competition codirectors Josephine Carothers and Mark Kelly received portfolios from Canadian, European, and Asian solar designers as well.

The rules of the Amherst competition made no attempt to define "passive" or "solar design." The prospectus stated simply that "excellence in the synthesis of architecture and engineering in commercial and residential designs will be judged by a panel of nationally recognized experts." In fact, the judges all had international stature (see box, p. 198). Furthermore, no restriction was placed on building type, and both built and buildable entries,

First Passive Design Competition Award of Merit Winners

Designer	Project
Alfred van Bachmayr	Fountain Valley School Solar Dormitory Colorado Springs, Colorado
Carey Cliff	Residence for Mr. and Mrs. John Black Veedersburg, Indiana
The Colyer/Freeman Group	Visitor Center for the Antelope Valley California Poppy Reserve Lancaster, California
Roger East, Architect	Elliot/Mulready Residence Belmont, California
Charles Eley Associates	Larchmont Passive Solar Homes Sacramento, California
David Finholm and Associates	Sun Up: A Dormitory for Colorado Rocky Mountain School Carbondale, Colorado
Jay M. Johnson	Sun Up Excelsior, Minnesota
Marquis Associates	Department of Justice Sacramento, California
Edward Mazria and Associates	Detroit Edison Passive Solar Demonstration House Detroit, Michigan
Edward Mazria and Associates	Wood Residence Wintergreen, Virginia
William T. Meyer, AIA	Brookside Two Family House Yorktown Heights, New York
Miller/Hull Architects	Hansen Residence Moses Lake, Washington
Miller/Hull Architects	Kimmick Lodge Cle Elum, Washington
Dan Nall of Berkeley Solar Group	Atlantic Community College Mays Landing, New Jersey
Perry Dean Stahl & Rogers, Inc.	Richard Salter Storrs Library Longmeadow, Massachusetts
Guilford Rand	The Energy Roof-II: Residence for Frank and Nina Fry Yuma, Arizona
Jefferson B. Riley	Klugman House Guilford, Connecticut
Runderburk-Meachem Sunshelter Design	Sunshelter Cooling Concept House Raleigh, North Carolina
T. Valle	Nuova Sede Della Societa Alitalia Rome, Italy
William R. Watkins	Melrose Condominium Glendale, California

including retrofit designs, were permitted.

Perhaps the most significant element of the First National Competition was that its sponsors were neither an architectural society, such as the American Institute of Architects, nor an engineering society, such as ASHRAE. Four of its seven judges were nonarchitects. Thus, the 1980 First National provided the most open kind of competition in which the maturity of an emergent solar-design discipline could be tested by an interdisciplinary jury.

Over 350 entry portfolios were submitted by architects and nonarchitect building designers. A technical summary, including common thermal performance data, was required of all entries. In addition, the judges, together with their technical

Both exterior and interior views are required in the comprehensive portfolio judging of National Passive Solar Design Competitions. In the 1980 Amherst competition, a local house called the Solar Woodbox by its owners-builders, the Kirleys, was one of the winners. Shown during its first New England winter and without solar water heater collectors on the south slope of the roof, the house uses both the snow and the white crushed-rock ground covering to add to the solar heat available to the south wall.

advisors, in many cases performed separate calculations to verify the efficacy of thermal design. While each entry was judged ultimately on its own merit, the 20 winners and 20 finalists were especially commended for their synthesis of thermal and architectural design.

Almost every building type—modest shelter to large-scale office complex—from virtually every climate could be found among the Amherst entries. Collectively, they represented a select sample of the state of solar building design at the beginning of the 1980s. According to Jeffrey Cook, author of two forthcoming books on the competition, "The unbuilt designs displayed impressive creativity, but it was the quantity of first-class passive solar buildings already constructed that was most startling."

The Second National Passive Solar Design Competition was held in conjunction with the 1982 conference at Knoxville, Tennessee. Although no such historic backlog of constructed solar buildings existed for the Second National as it did for the First, more than 400 portfolios were entered. As in the

First Passive Design Competition Jurors

J. Douglas Balcomb
Los Alamos National Laboratory
Los Alamos, New Mexico

Peter Calthorpe
Van der Ryn, Calthorpe & Partners
Sausalito, California

William Caudill
Caudill, Rowlett, and Scott
Houston, Texas

Ralph Johnson
National Association of Home Builders Research Foundation
Rockville, Maryland

Douglas Kelbaugh
Kelbaugh & Lee
Princeton, New Jersey

William M.C. Lam
William Lam Associates
Cambridge, Massachusetts

Richard Rush
Progressive Architecture
Stamford, Connecticut

Second Passive Design Competition First-Place Award Winners

Designer	Project
Banwell White & Arnold Hanover, New Hampshire	Society for the Protection of New Hampshire Forests Headquarters Concord, New Hampshire
Alfredo De Vido New York, New York	Consolidated Edison Demonstration House Briarcliff, New York
Einhorn Yaffee Prescott Krouner, P.C. Albany, New York	Albany County Airport Terminal Colonie, New York
Ronald W. Haase Gainesville, Florida	Lake House in Central Florida Micanopy, Florida
William Leddy San Francisco, California	San Francisco Residence and Remodel San Francisco, California
Eric Meng Associates and E. Mark Smith Seattle, Washington	Wildwood Place Townhouses Seattle, Washington
Jorge Y. Ramos and Associates Manila, Philippines with the Architects Collaborative Cambridge, Massachusetts	Government Service Insurance Systems Headquarters Manila, Philippines

A waterwall for thermal storage inside the 1980 award-winning Solar Woodbox also provides a special natural source of soft light across a dark, tiled floor. The weight of cylindrical water columns is supported by a timber frame which also allows an open interior for convective and radiative heat transfer.

1980 competition, entries were solicited in three building categories: single-family residential, multi-family residential, and commercial/institutional/industrial. Once again, built, unbuilt, and retrofit projects were accepted in the three categories.

Entrants were required to submit not only building plans, elevations, renderings, and photographs, but also five pages of data on energy collection and use in a revised format reflecting the maturity of calculation procedure. These data were subjected to computer analysis at Energy Works, Inc., of West Newton, Massachusetts, using the SUNDAY program created by Ecotope, Inc., of Seattle, Washington. Commenting on the high quality of the submittals, the seven-person jury singled out 25 entries for recognition. Seven first-place awards and 18 awards of merit were given (see boxes, p. 199 and p. 200).

Judging the 1982 entries continued to pose some significant problems. While the quality of the design portfolios was high—with only a few screened out for noncompliance with the rules—the jury

Second Passive Design Competition Award of Merit Winners

Designer	Project
Architectural Alliance	Land O Lakes Corporate Offices Arden Hills, Minnesota
Buchanan & Associates Donald Watson, FAIA Architects	New Canaan Nature Center Horticultural Education Building New Canaan, Connecticut
Peter Calthorpe Van der Ryn, Calthorpe and Partners	Wisconsin Street Houses San Francisco, California
Chilless Nielsen Architects P.C.	Chilless Residence Portland, Oregon
Leo A. Daly Company	Lockheed Missiles & Space Company Building 157 Sunnyvale, California
James Joseph Doolan, Architect Don Felts, Engineer	Window Rock Elementary School Addition Window Rock, Arizona
Richard Fernau and Laura Hartman	Maoli House San Rafael, California
Ray D. Greco	Bluestem Meadows Ames, Iowa
Hammel Green & Abrahamson, Inc. Architects-Engineers Dubin-Bloome Associates, P.C. Energy Consultant	H.B. Fuller Company Willow Lake Laboratory Vadnais Heights, Minnesota
Robert E. Hicks, Architect, P.C.	Brooks Residence Holland, Michigan
Kelbaugh & Lee Associates	Sisko House Metuchen, New Jersey
MassDesign Architects & Planners	Independence IV Potter Residence Butler, Maryland
Meierienes Bygningskontor Dag Borgen, Architect	Indre Østfold Meieri Mysen, Near Oslo, Norway
Total Environmental Action, Inc. David Norris and Peter Temple	Botswanna Technology Center Headquarters Gaborone, Botswana
Darleen D. Powers with John S. Crowley	Westland Avenue Renovations Boston, Massachusetts
Walter F. Roberts, Jr.	One University Place Fairfax, Virginia
Jack Travis, Architect	An Arizona Residence for an Architect and Artist Phoenix, Arizona
Niels E. Valentiner & Associates	Utah Projects Office Complex Provo, Utah

had just two days to evaluate hundreds of projects. In addition, the volume of data was difficult to reduce to usable form in the time allotted to the task, since no computer program existed with the necessary capabilities of comparative building analysis, cooling load analysis, and rapid data entry. Finally, according to Competition Director Carothers, the diversity of the jurors' backgrounds—an asset in many ways—at times precluded agreement. "This meant," Carothers said, "that while the award-winning buildings were excellent, many very fine projects went unrecognized."

Based on the positive experiences of the first two competitions, the Passive Systems Division is developing parameters for the Third National planned for 1984. In the following pages and in the next issue, the *Passive Solar Journal* presents the award-winning building designs from the 1982 competition. All photographs, illustrations, and technical matter are drawn from the portfolios submitted by the entrants.

—The Editors

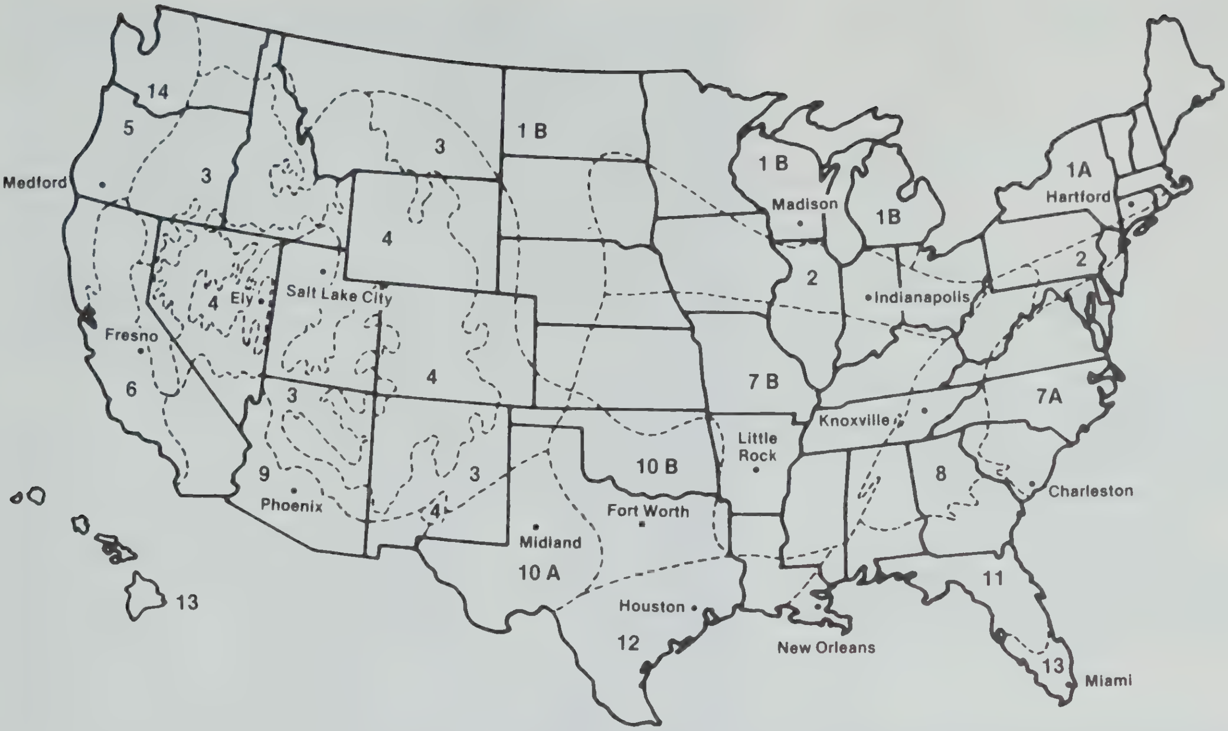

General climatic zones for the calculations of thermal performance were standardized in both the First and Second National Passive Solar Design Competitions. The map above is taken from *Regional Guidelines for Building Passive Energy Conserving Homes*, published by the U.S. Department of Housing and Urban Development. Based on research by the National Climate Center of NOAA and the AIA Research Corporation, 13 characteristic climates were identified with the weather data of reference cities. The addition of an area associated with the weather data of Portland, Oregon, and the subdivision of 3 others bring the number of climate zones to 17.

Climate Zone	Reference
1A	Hartford, Connecticut
1B	Madison, Wisconsin
2	Indianapolis, Indiana
3	Salt Lake City, Utah
4	Ely, Nevada
5	Medford, Oregon
6	Fresno, California
7A	Charleston, South Carolina
7B	Little Rock, Arkansas
8	Knoxville, Tennessee
9	Phoenix, Arizona
10A	Midland, Texas
10B	Fort Worth, Texas
11	New Orleans, Louisiana
12	Houston, Texas
13	Miami, Florida
14	Portland, Oregon

Second Passive Design Competition Jurors

William Glennie
Princeton Energy Group
Princeton, New Jersey

Parambir S. Gujral
Skidmore, Owings & Merrill
Chicago, Illinois

Robert B. Marquis
Marquis Associates
San Francisco, California

Edward Mazria
Mazria, Schiff Associates
Albuquerque, New Mexico

William Morgan
William Morgan Architects
Jacksonville, Florida

Susan Nichols
Communico, Inc.
Santa Fe, New Mexico

Richard Rush
Progressive Architecture
Stamford, Connecticut

Albany County Airport Terminal

Colonie, New York

Second National Passive Design Competition First-Place Award Winner

Photo: Norman McGrath

One of the goals of the designers of the Albany County Airport Terminal was to integrate passive solar features into a visually stimulating architectural design statement.

Photo: Norman McGrath

The skylight arrangement provides 40% of the building's lighting requirements and 20% of its heating needs. A minicomputer is programmed to operate the louvers, opening them on winter days and closing them at night and on warm summer days.

The firm of Einhorn Yaffee Prescott Krouner, P.C., was confronted with the dual task of designing an energy-efficient, heavily used public facility and integrating passive solar features into a visually stimulating architectural design statement. The terminal was built to serve the busy New York capital region and operates 126 hours per week. It is subject to widely varying occupancy coupled with unique infiltration problems created by passenger arrivals and departures.

In an attempt to provide a highly visible example of Albany County's commitment to energy conservation, the building was designed around a strong architectural feature: a 176-ft (*53.6-m*) -long, skylight-topped "solar court." This distinctive element provides 40% of the building's lighting requirements and 20% of its heating needs. The new terminal will use *75% less* energy than the existing adjacent terminal, built in 1960, which is almost identical in size.

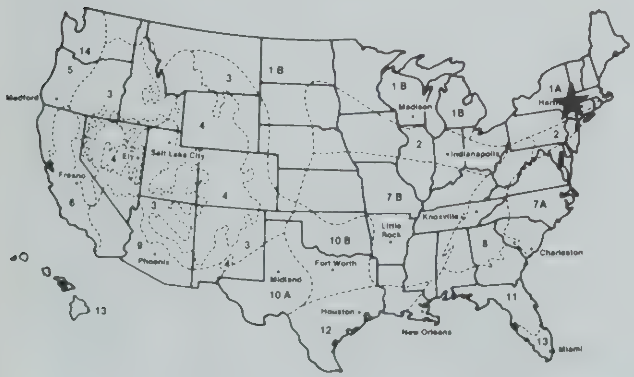

Designed by: Einhorn Yaffee
Prescott Krouner, P.C.
P.O. Box 627
Albany, New York 12201

Consultants: W.S. Fleming Associates, Inc.
Albany, New York
Scott-Healey Associates, Inc.
Albany, New York

Built by: Bunkoff Construction
Albany, New York

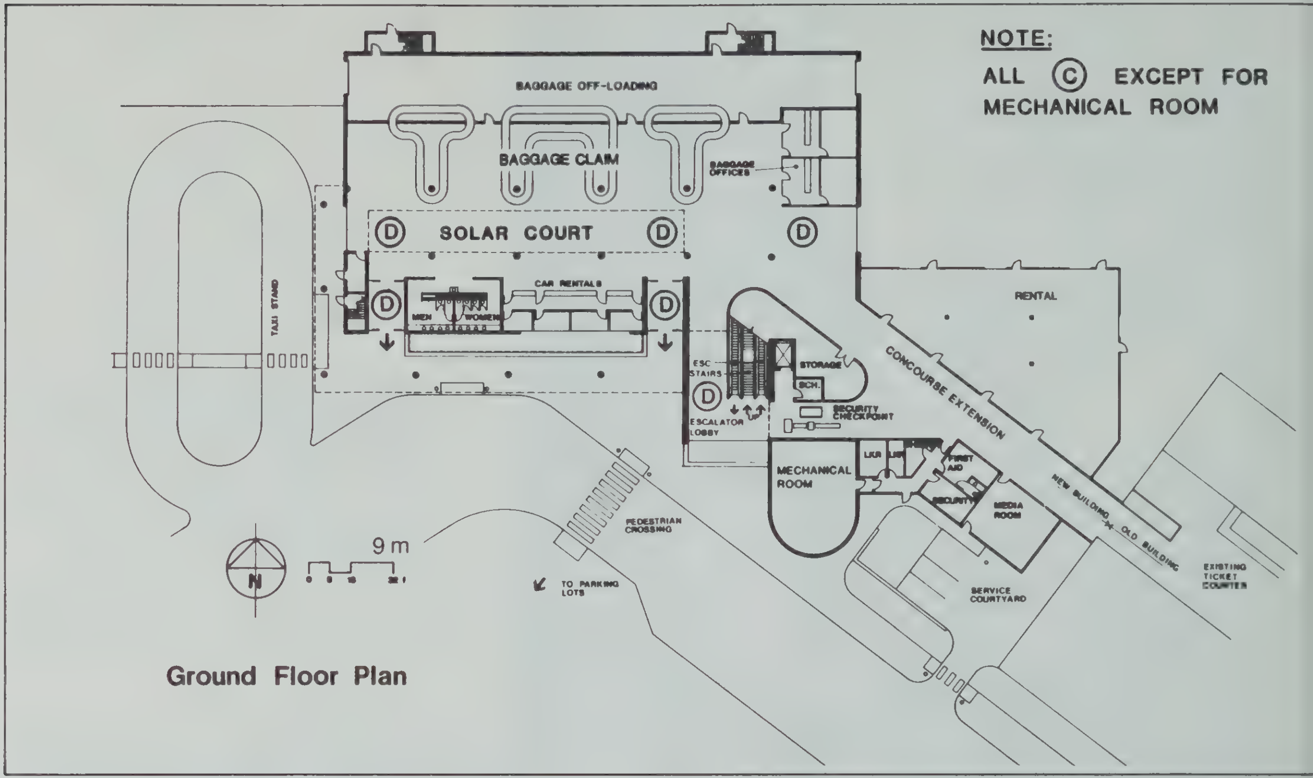

Ground Floor Plan

These energy savings are primarily attributable to a highly efficient building envelope combined with unique hybrid solar features. These systems are integrated into a sophisticated VAV air distribution system which is also linked to high-efficiency boilers with dual fuel burners.

The hybrid solar features include an atrium skylight system with intelligent, operable louvers which maximize the efficiency of energy collection. In this unique application, the louvers have been foam-filled, gasketed for positive sealing, and installed with a continuous, adjustable linkage system. The louvers open to permit full penetration of the sun on winter days and close to reduce heat loss at night. In summer, the blades adjust to prevent unwanted solar heat gain, yet provide indirect light. A minicomputer, programmed with the solar azimuth and angle to the year 2000, continually examines interior and exterior environmental conditions and selects optimal louver position for energy efficiency. The masonry wall supporting the skylight is designed as a thermal mass which, in winter, distributes the solar heat gain to the areas of greatest heat loss.

Design Data	**English**	**Metric**
Heating degree days	7,000° F	3,900° C
Heating auxiliary energy	43,100 Btu/ft^2 yr	136 kWh/m^2 yr
Cooling degree days	400° F	220° C
Cooling auxiliary energy	8,000 Btu/ft^2 yr	25 kWh/m^2 yr
Solar aperture area	4,060 ft^2	377 m^2
Movable insulation area, R-7 (R_{SI}-1.2)	4,060 ft^2	377 m^2
Thermal storage surface area	2,024 ft^2	188 m^2
Total effective thermal storage capacitance	12,760 Btu° F	6.7 kWh/° C
Volume of conditioned air space	678,128 ft^3	19,200 m^3
Total cost	$3,932,00	
Total cost attributable to energy conservation measures	$279,000	
Total annual solar contribution:		
Space heating	155 x 10^6 Btu	45,400 kWh
Space cooling	149.3 x 10^6 Btu	43,700 kWh
Lighting	542.1 x 10^6 Btu	158,800 kWh

The black slate floors also absorb heat from the winter sun through the south-facing windows.

Natural light is augmented by a zoned system of efficient artificial lighting. In keeping with the philosophy of saving energy without sacrificing architectural design, the artificial lighting is task-ambient. Fluorescent lights, designed as functional and aesthetic components of the aluminum-slatted ceiling, produce ambient light of moderate levels to circulation and lounge areas. Ceiling-recessed mercury vapor lamps provide high-intensity light to areas where specific tasks require it—car rental counters, for example. A series of sensors on the building's perimeter measures the amount of available daylight and automatically determines how many lights are needed at a given time. ☐

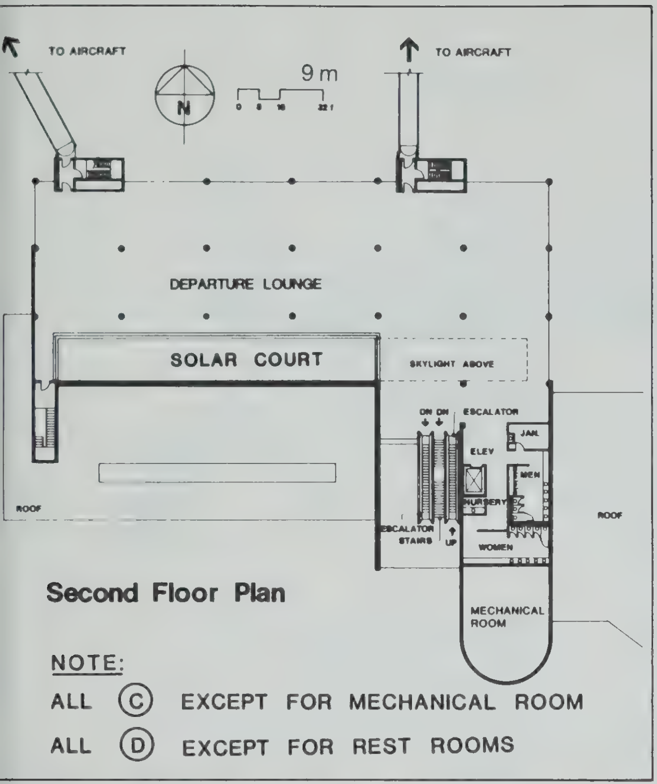

Second Floor Plan

NOTE:

ALL Ⓒ EXCEPT FOR MECHANICAL ROOM

ALL Ⓓ EXCEPT FOR REST ROOMS

Natural lighting from the skylight (below) is augmented by a zoned system of efficient artificial lighting. Fluorescent lights, designed as functional and aesthetic components of the aluminum-slatted ceiling, produce ambient light of moderate levels for the lounge and circulation areas.

Photo: Norman McGrath

Sunny Summer Day

The sun is used to provide light, but is not allowed to penetrate into the building and generate excessive heat.

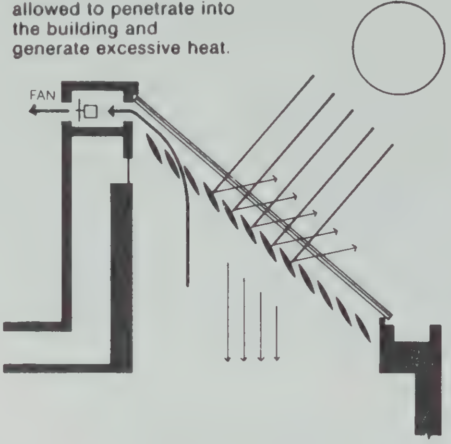

1. **The operable louvers are partially open.**
2. **Direct sunlight is reflected by the louvers.**
3. **Diffuse northern light is provided to the spaces below.**
4. **The area below the skylight serves as a heat banking space. Warm air from the building below will collect beneath the skylight. Exhaust fans will then discharge the warm air from the building.**

Sunny Winter Day

The sun is used to provide heat and light.

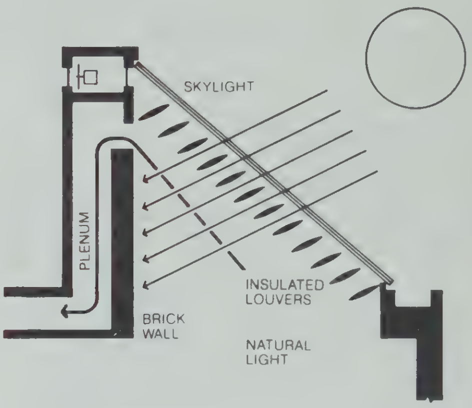

1. **The operable louvers are open to allow sunlight into the building.**
2. **The sunlight warms a brick wall at the back of the skylight.**
3. **Air is drawn through a plenum behind the wall, and is heated during its passage over the warm bricks.**
4. **The heated air is drawn into the building heating system for distribution.**
5. **Natural light is provided to the space below.**

Photo: Norman McGrath

The airport terminal was designed around a skylight-topped solar court. This distinctive element defines the building as a true energy form.

Passive Solar Journal

The Official Journal of the Passive Systems Division
of the American Solar Energy Society.®
The United States Section of the International Solar Energy Society

Volume 1, 1982

American Solar Energy Society, Inc.

New York
Boulder, Colorado

Volume 1 Number 1 Pilot Edition

Editors

Jeffrey Cook
Arizona State University
Tempe, Arizona

Michael J. Holtz
Solar Energy Research Institute
Golden, Colorado

Editorial Advisory/Review Board

Dennis A. Andrejko
SEAgroup
Nevada City, California

Don Elmer
Lawrence Berkeley Laboratory
Berkeley, California

Keith Haggard
Solar Energy Research Institute
Golden, Colorado

Ron Judkoff
Solar Energy Research Institute
Golden, Colorado

Edward Mazria
Edward Mazria & Associates
Albuquerque, New Mexico

Lynn Nelson
The Habitat Center
Pacheco, California

Joseph K.E. Ortega
Solar Energy Research Institute
Golden, Colorado

Executive Director
Lee Salmon
ASES
1230 Grandview Avenue
Boulder, Colorado 80302

Editorial Staff

Rachel Snyder
Managing Editor

Susan Sczepanski
Art Director

Suzanne Gripman
Contributing Editor

Volume 1 Numbers 2, 3, and 4

Editor-in-Chief

Jeffrey Cook
Arizona State University
Tempe, Arizona

Associate Editors

John Hayes
Book Review Editor
Marlboro College
Marlboro, Vermont 05344

William A. Wright
Design Tools Review Editor
Cambridge Energy Corporation
Cambridge, Massachusetts 02138

J. Douglas Balcomb
Los Alamos National Laboratory
Mail Stop K 571
Los Alamos, New Mexico 87545

Michael Holtz
Architectural Energy Corporation
3600 E. Virginia Avenue
Denver, Colorado 80209

Fred Nelson
Sunset Magazine
Willow and Middlefield Roads
Menlo Park, California 94025

Editorial Staff

Cyndi Meagher
Managing Editor

Heidi Osselaer
Production Editor

Peter Brown
Editor/Writer

Copyright © American Solar Energy Society, Inc. 1982

No part of this publication may be reproduced, stored in a retrieval system, or transmitted in any form or by any means, electronic, electrostatic, magnetic tape, mechanical, photocopying, recording, or otherwise, without permission in writing from the copyright holder.

The Article Fee Code on the first page of an article in this journal indicates the copyright owner's consent that, in the U.S.A., copies may be made for personal or internal use provided the stated fee for copying beyond that permitted by Section 107 or 108 or the United States Copyright Law, is paid. The appropriate remittance should be forwarded with a copy of the first page of the article to the Copyright Clearance Center Inc., 21 Congress Street, Salem, MA 01970 U.S.A. If a codes does not appear, copies of the article may be made without charge, provided permission is obtained from the publisher. The copyright owner's consent does not extend to copying for general distribution, for promotion, for creating new works or for resale. Specific written permission must be obtained from the publisher for such copying.

Albert Henderon, Director of Publications
American Solar Energy Society, Inc.
Publications Office:
110 W. 34th Street, New York, New York 10001

Production Office
American Solar Energy Society, Inc.
205B McDowell Hall, University of Delaware
Newark, Delaware 19711

Membership Services
American Solar Energy Society, Inc.
1230 Grandview Avenue, Boulder, Colorado 80302

ISSN 0277-6456

Passive Solar Journal Editorial Office
College of Architecture, Arizona State University
Tempe, Arizona 85287

Cumulative Table of Contents, Volume 1

2	**Editor's Note**	Rachel Snyder
3	**Statements of Intent**	Michael Maybaum Michael J. Holtz Jeffrey Cook
4	**A Comparison of Ground and Above-Ground Climates for Identifying Appropriate Cooling Strategies**	Kenneth Labs Keith Harrington
12	**Transparent and Opaque Louvers for Thermal Control in Passive Solar Buildings**	Joseph K.E. Ortega J. Michael Connolly Carl E. Bingham Mark McDade Michael J. Holtz
21	**New Mexico Solar Greenhouse Study**	W. Scott Morris Claire Reiniger
28	**Natural Convection in Passive Solar Buildings: Experiments, Analysis, and Results**	Ashok Gadgil Fred Bauman Ronald Kammerud
41	**Market Potential Indexing: A New Technique for Analyzing Solar Markets**	Scott A. Noll William M. Robson Marilyn K. Yeamans

TECHNICAL NOTES

52	**Heat Exchangers Effective in Radon Control Condensed from** *Atmospheric Environment*	William W. Nazaroff Mary L. Boegel Craig D. Hollowell Gary D. Roseme
54	**Overview: Procedures for Validating BEAS**	David Wortman Bob O'Doherty Ron Judkoff

UPDATES

56	**Trinity Develops Efficient AC Unit**	E.S. Doderer
57	**SERI to Publish Monitoring Results**	Sharyn Towle
57	**Double-Envelope Evaluation Begun**	Joseph K.E. Ortega
58	**New Prototype of Transwall Tested**	John F. McClelland

BOOK REVIEWS

59	*Passive Solar Design Handbook (Volumes 1 and 2)*	Jeffrey Cook
61		Bill Wright
62		William A. Shurcliff

DESIGN TOOLS

67	**Expanding the SLR Method**	J. Douglas Balcomb Robert W. Jones Robert D. McFarland William O. Wray

RESEARCH METHODS

91	**Passive Solar Test Modules**	Fuller Moore

BUILDING EVALUATION

109	**Non-Instrumented Performance Evaluation of Passive Solar Homes**	Beth Sachs Blair Hamilton Katherine Clough Ron Alward

BASIC RESEARCH

121 **Thermal Impedance in Multi-Pane Windows** Joseph K.E. Ortega

BOOK REVIEWS

128 *Easy to Build Solar Batch Heater, Thermosiphoning Air Panel and Retrotrombe* Alex Wilson

COOLING

131 **Cooling by Longwave Radiation** Baruch Givoni

BUILDING EVALUATION

151 **The Mastin Double-Envelope House** Ralph F. Jones, Gerald Dennehy

MATERIALS

175 **MIT Solar Building No. 5's Third Year Performance** Timothy E. Johnson

BOOK REVIEWS

185 *Passive Solar Heating Design* Robert O. Smith
185 *Air-to-Air Heat Exchangers for Houses* Russell G. Derickson

DESIGN TOOLS

188 **A Proposed Review Process** William A. Wright

PERSPECTIVE

194 **The National Passive Solar Design Competitions** The Editors

202 **Albany County Airport Terminal** Einhorn Yaffee Prescott Krouner, P.C.

208 **Consolidated Edison Demonstration House** Alfredo De Vido

214 **Lake House in Central Florida** Ronald W. Haase

TESTING AND MONITORING

219 **Data Acquisition in Test Modules** Fuller Moore

APPLIED RESEARCH

229 **Windscreens in Radiant Cooling** Marco Mostrel, Baruch Givoni

BOOK REVIEWS

Passive Solar Design Handbook, Volume Three: Passive Solar Design Analysis
239 W. Scott Morris
242 Dennis A. Andrejko
244 William A. Shurcliff

Seventh National Passive Solar Conference
245 Daylighting George Arnold
246 Performance Monitoring Blair Hamilton
247 Cooling Donald W. Abrams
248 Design Tools and Simulations William A. Wright
250 Emerging Architecture Dennis A. Andrejko

251 *Passive Solar Construction Handbook* William K. Langdon

253 **Annual Index, Volume 1, 1982** The Editors

Winter Night

Loss of heat through the skylight is reduced.

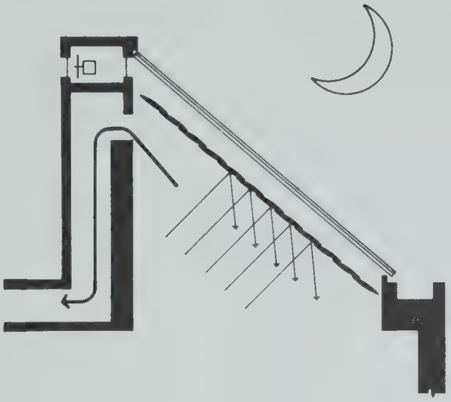

① The operable louvers are closed to provide an insulated "ceiling" below the glass and reduce heat loss through the skylight.

② The louvers are insulated, blocking the flow of heat from the building.

③ The brick wall remains warm for some time after sunset due to its "thermal mass".

④ Air is drawn through a plenum behind the wall, and is heated during its passage over the warm bricks. When the heat stored in the brick wall is used up, air flow through the plenum is stopped.

⑤ The heated air is drawn into the building heating system for distribution.

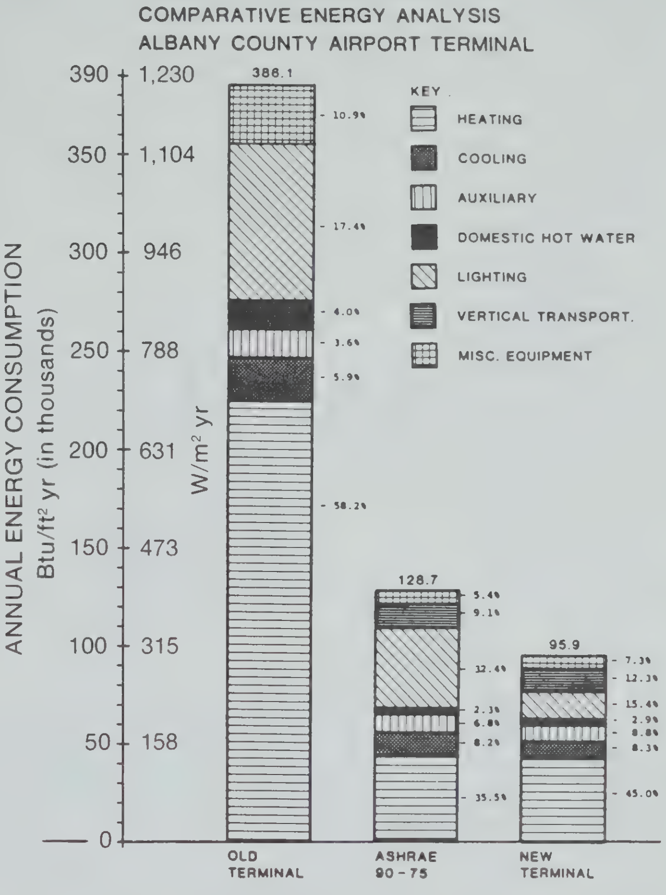

A comparative energy analysis of the old and new terminals of Albany County Airport shows that the old terminal uses 75% more energy than the new terminal.

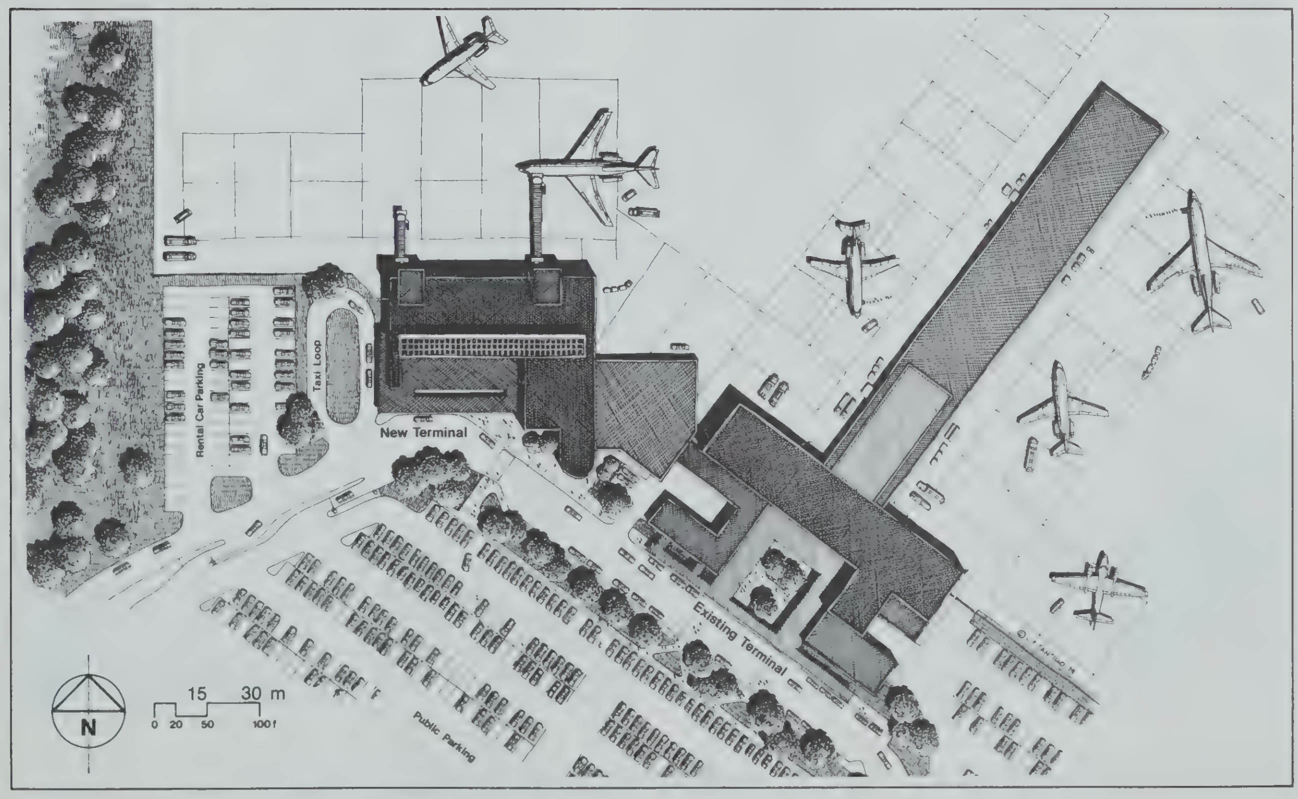

A site plan of the entire airport shows the relationship of the new and the existing terminal.

Consolidated Edison Demonstration House

Briarcliff, New York

Second National Passive Design Competition First-Place Award Winner

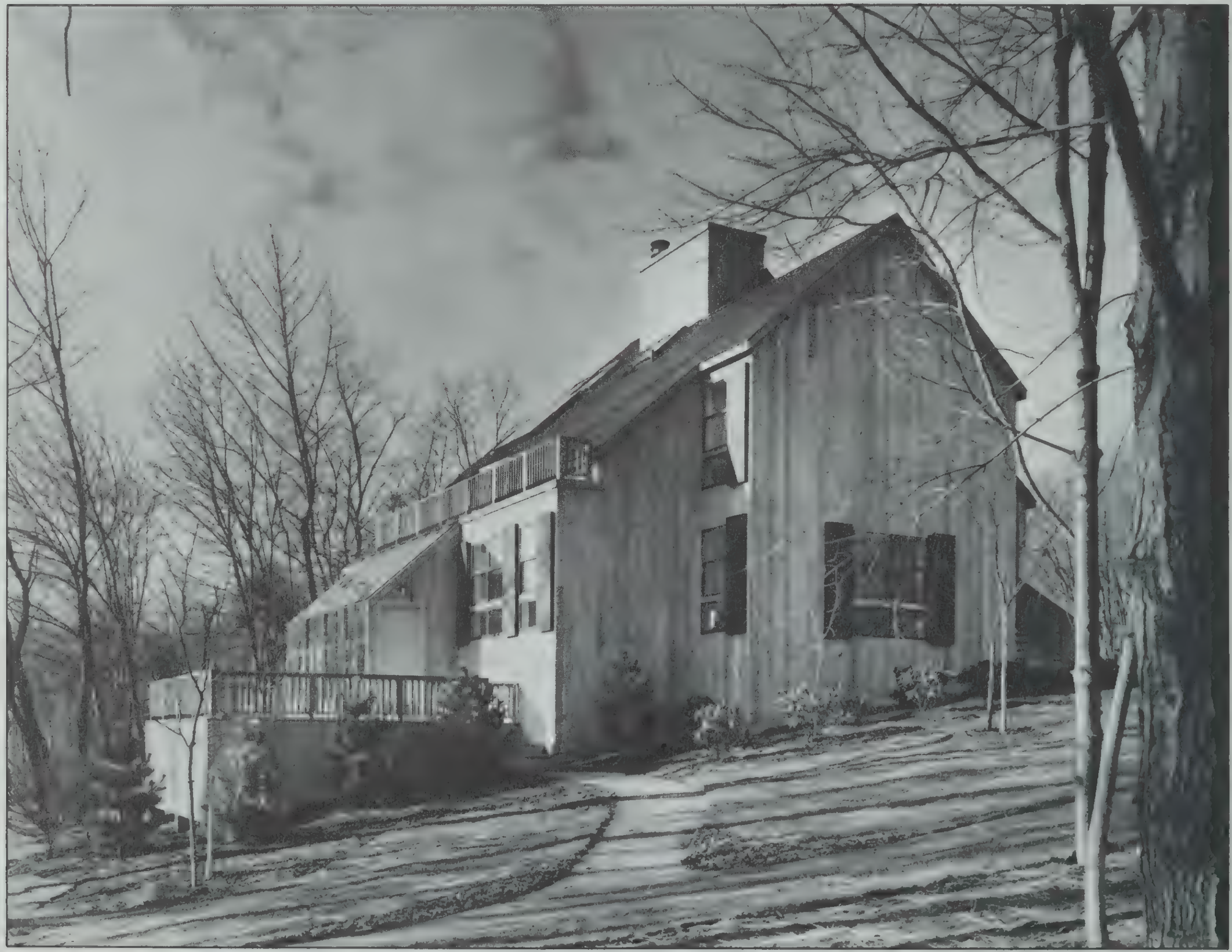

Photo: Norman McGrath

The windows and atrium/greenhouse on this south-facing view of the Consolidated Edison house are double glazed, with an equivalent R-value of 2.0 (R_{SI}-*0.3*). The east-facing window is triple glazed, with an equivalent R-value of 2.4 (R_{SI}-*0.4*).

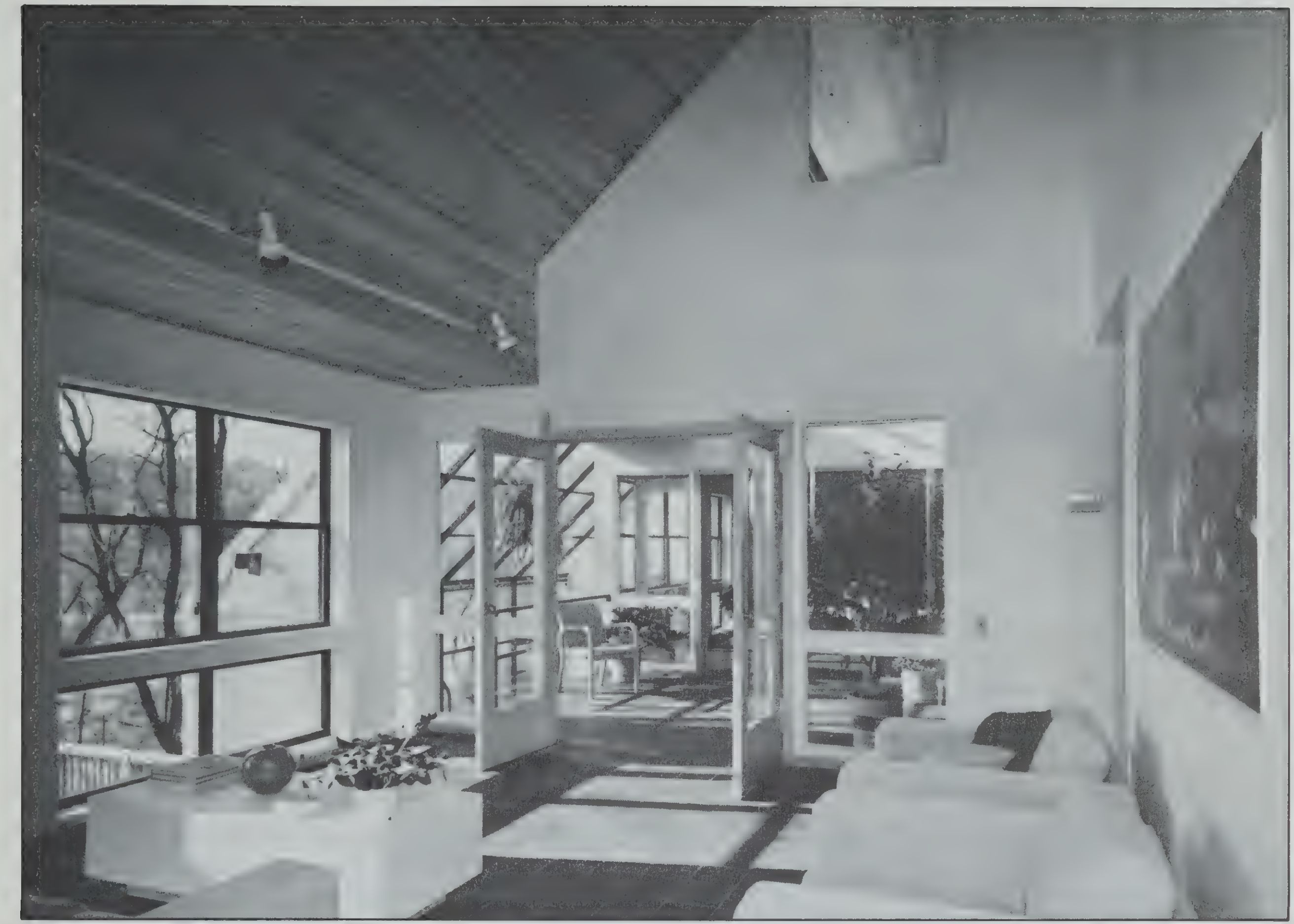

Photo: Norman McGrath

The quarry-tile-covered concrete floors of the living room (foreground) and atrium/greenhouse (background) act as the heat storage elements of the house. The concrete slab beneath is more than 6 in. (*15 cm.*) thick.

Consolidated Edison, an electric and gas utility company, commissioned architect Alfredo De Vido to design a single-family house which would demonstrate energy conservation concepts and solar techniques in a New York climate. Computer analyses before construction indicated that the 2,300 ft^2 (*214 m^2*) house would use only 40% of the energy of a comparable new house, yet the direct-gain, movable insulation, atrium/greenhouse, and other passive solar features added less than 10% to construction costs. The actual thermal performance will be measured after data for several seasons are collected.

The walls have R-27 (R_{SI}-*4.7*) insulation and the ceilings have R-30 (R_{SI}-*5.2*). A continuous 6-mil polyethylene vapor/infiltration barrier covers the insulation on the interior. Windows facing south are double glazed, and those facing east and west are triple glazed. A heat exchanger was installed to introduce fresh air into this tightly constructed house. The heat exchanger performs with a minimal loss of energy.

The entire ground floor of the building is on a 6-in. (*15-cm*) concrete slab covered with quarry tile that acts as the home's thermal mass. The sun's light and heat enter the south-facing, double-glazed windows, as well as the atrium/greenhouse. In this particular passive feature, heat is absorbed by the floor and the north wall of the atrium, both of which are made of concrete and covered with tile. An automatically controlled vent near the top of the atrium's north wall opens to allow excess heat into a duct. A fan forces this solar-heated air into the house's gas-furnace heating system, where it is mixed with the furnace-heated air and circulated throughout the house. To prevent heat loss, the

Designed by:	Alfredo De Vido, Architect 699 Madison Avenue New York, New York 10021
Solar consultants:	Princeton Energy Group Princeton, New Jersey
Built by:	Syracuse Brothers Peekskill, New York

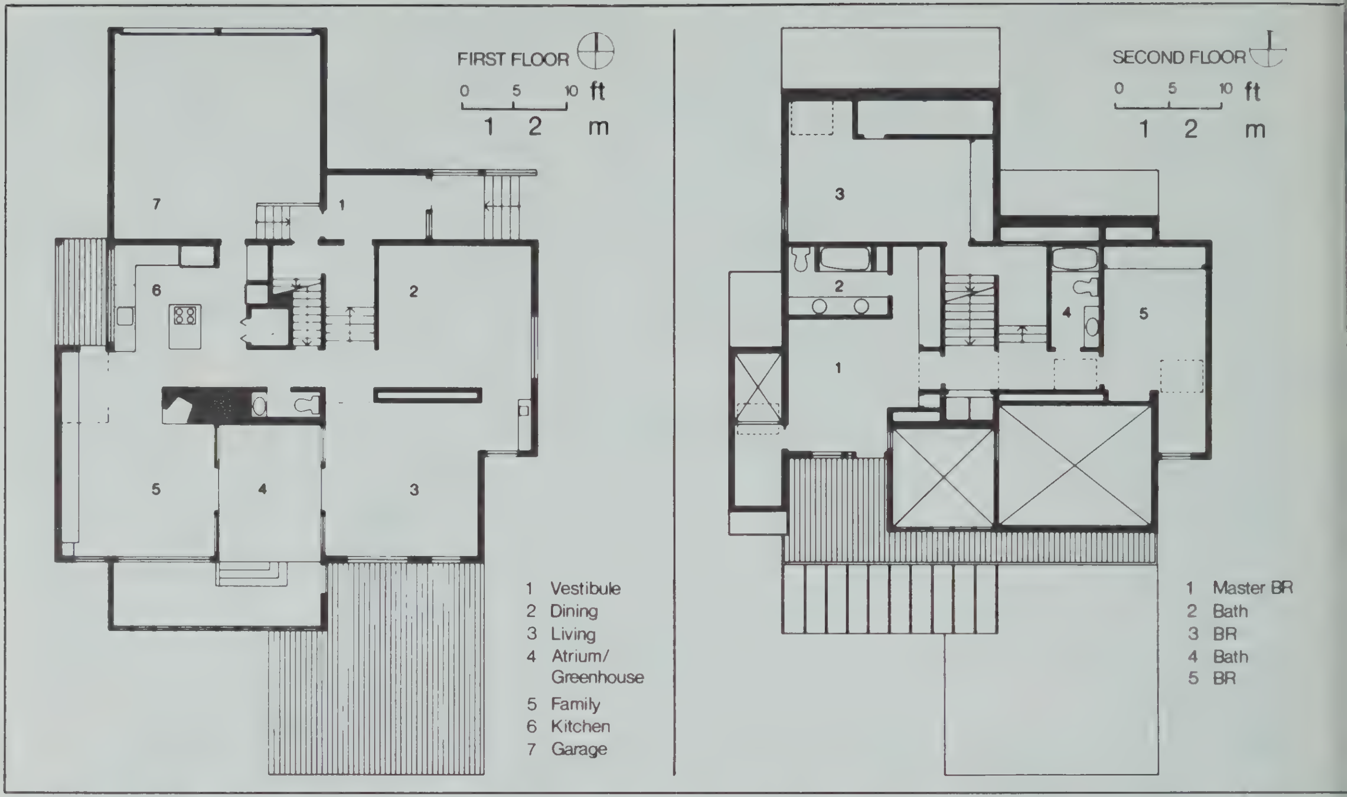

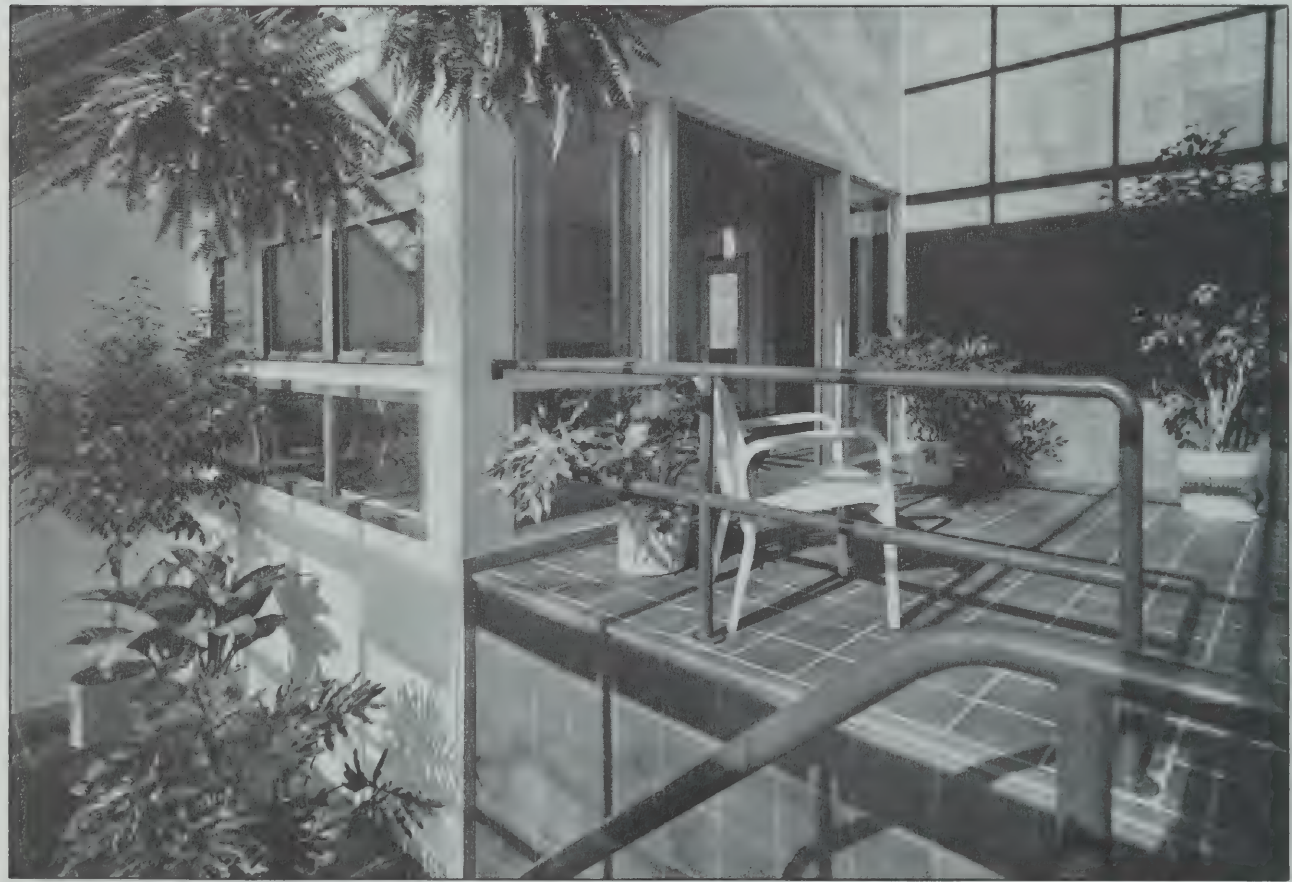

Photo: Norman McGrath

Heat is absorbed by the north wall and the floor of the atrium. The atrium is separated from the family room (to the left) and the living room (to the right) by large windows and glass doors. The doors can be closed to minimize heat loss on winter nights and overcast days. When the atrium is closed off as one of the three heating zones of the building, it still can be heated independently.

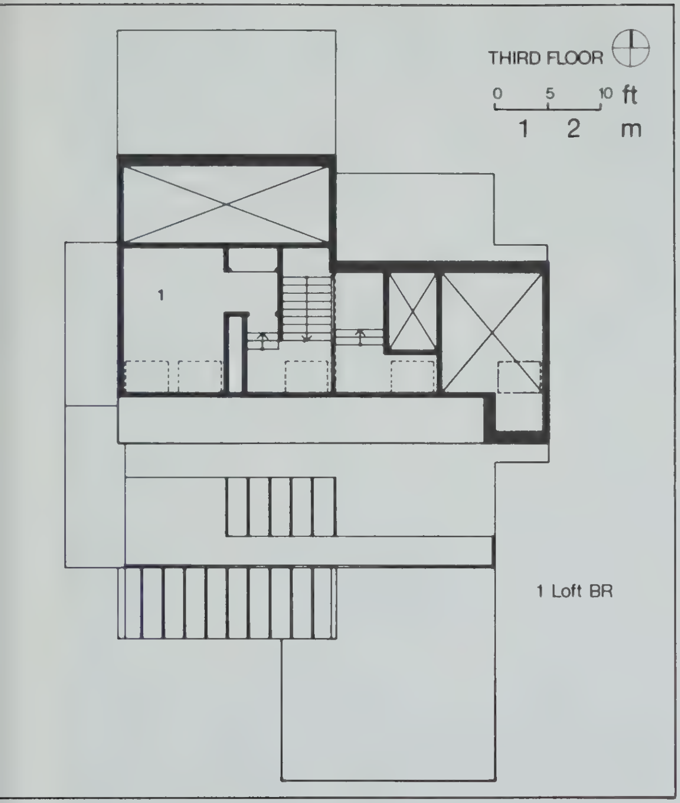

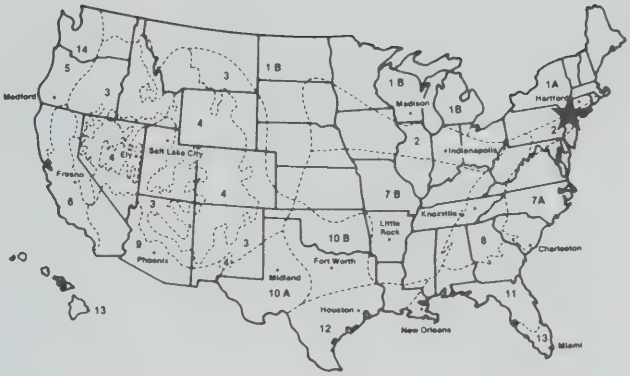

atrium/greenhouse is equipped with roll-down, insulating shades on the outside and is separated from the living and family rooms by large windows and doors on the inside.

The house also demonstrates a functional approach to electric lighting; it uses a combination of general, task, and decorative artificial light. In addition, occupancy sensors were installed to turn lights on automatically when a person enters a space. Thus, lights are turned off automatically in unoccupied rooms, preventing wasted energy. Energy-efficient kitchen appliances are run by gas.

It is suggested that cooling requirements can be cut by at least 50% through the use of movable shading and venting in the summer in such a house design. However, such estimates are difficult to make with much precision, because extensive on-site climate data were not available for design. The mechanical cooling system is a refrigerated two-stage, two-zone design intended to optimize the cooling available through natural means.

The Briarcliff house is only one of several demonstration houses built by Consolidated Edison. Although well instrumented and monitored, the thermal performance of the design may be less important than the exhibition aspects of the program. Since the house is not lived in, it does not have the usual demands for comfort and hot water that would be required by a family in residence. On the other hand, the popularization of solar and conservation ideas as part of an attractive display house may be much more important than any set of performance numbers. ☐

Photo: Norman McGrath

The only window on the north side of the building is over the stairway.

Design Data	English	Metric
Heating degree days	6,000° F	3,333° C
Heating auxiliary energy, gas	27,600 Btu/ft^2 yr	87 kWh/m^2
Cooling degree days	—	—
Cooling auxiliary energy	19.9 Btu/ft^2 yr	0.06 kWh/m^2 yr
Solar aperture area	350 ft^2	32.5 m^2
Movable insulation area, R-7 (*R_{SI}-1.2*)	275 ft^2	25.5 m^2
Thermal storage surface area	1,200 ft^2	111 m^2
Total effective thermal storage capacitance	11,000 Btu/° F	5.8 kWh/° C
Net floor area	2,300 ft^2	214 m^2
Volume of conditioned air space	23,000 ft^3	650 m^3
Total cost (excluding land and site work)	$150,000	
Total cost attributable to energy conservation measures	$12,000	
Total annual solar contribution:		
Space heating	23.4 x 10^6 Btu	6,860 kWh
Service hot water	N/A	

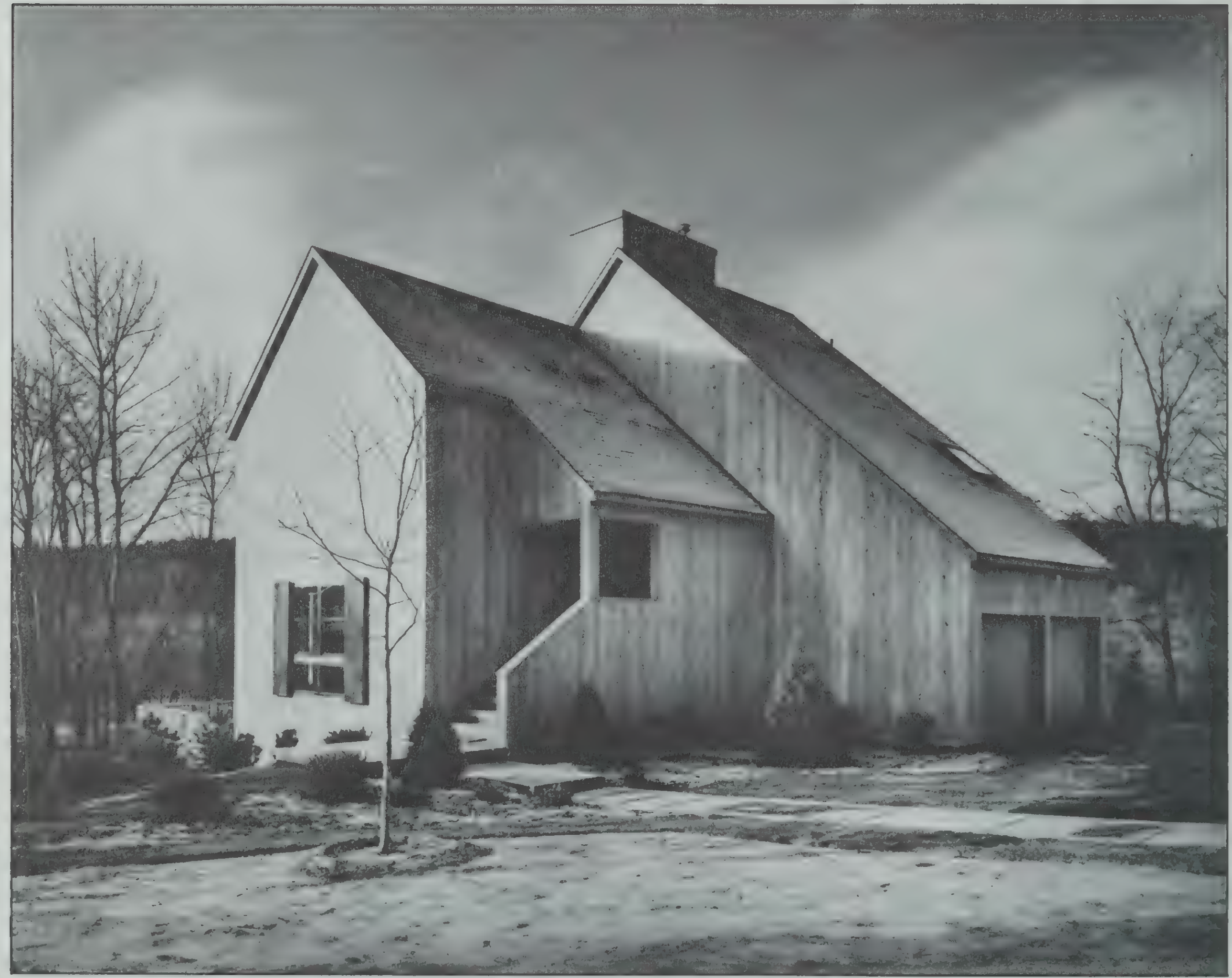

Photo: Norman McGrath

This north view of the house shows the long, sloping roof line. Because of this design, ceiling insulation had to be installed in the spaces between the roof rafters instead of in the ceiling joists. The thickest insulation which fits between the 2 x 12 in. (*5.1 x 30.5 cm*) rafters is R-30 (*R_{SI}-5.2*), about 9 in. (*22.9 cm*) thick. An air space above the insulation was left so that air circulation could carry off any moisture which might penetrate the vapor barrier.

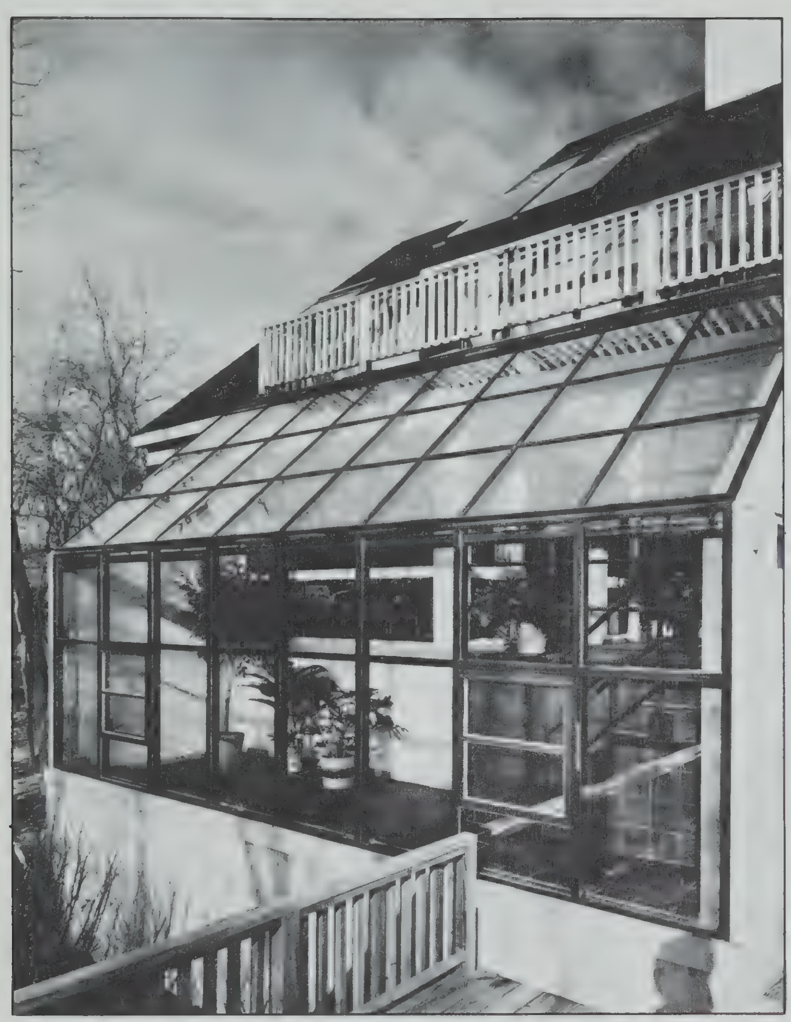

Photo: Norman McGrath

Heat loss from the greenhouse is minimized in winter by glazing and roll-down insulating shades. In summer, two windows may be opened for summer ventilation. This natural circulation is assisted by fans which draw air upward through vents at the top of the greenhouse, the same system used to draw warm air through the house in winter.

Photo: Norman McGrath

Windows in the sloping roof allow light from the south to enter upstairs bedrooms.

Lake House in Central Florida

Micanopy, Florida

Second National Passive Design Competition First-Place Award Winner

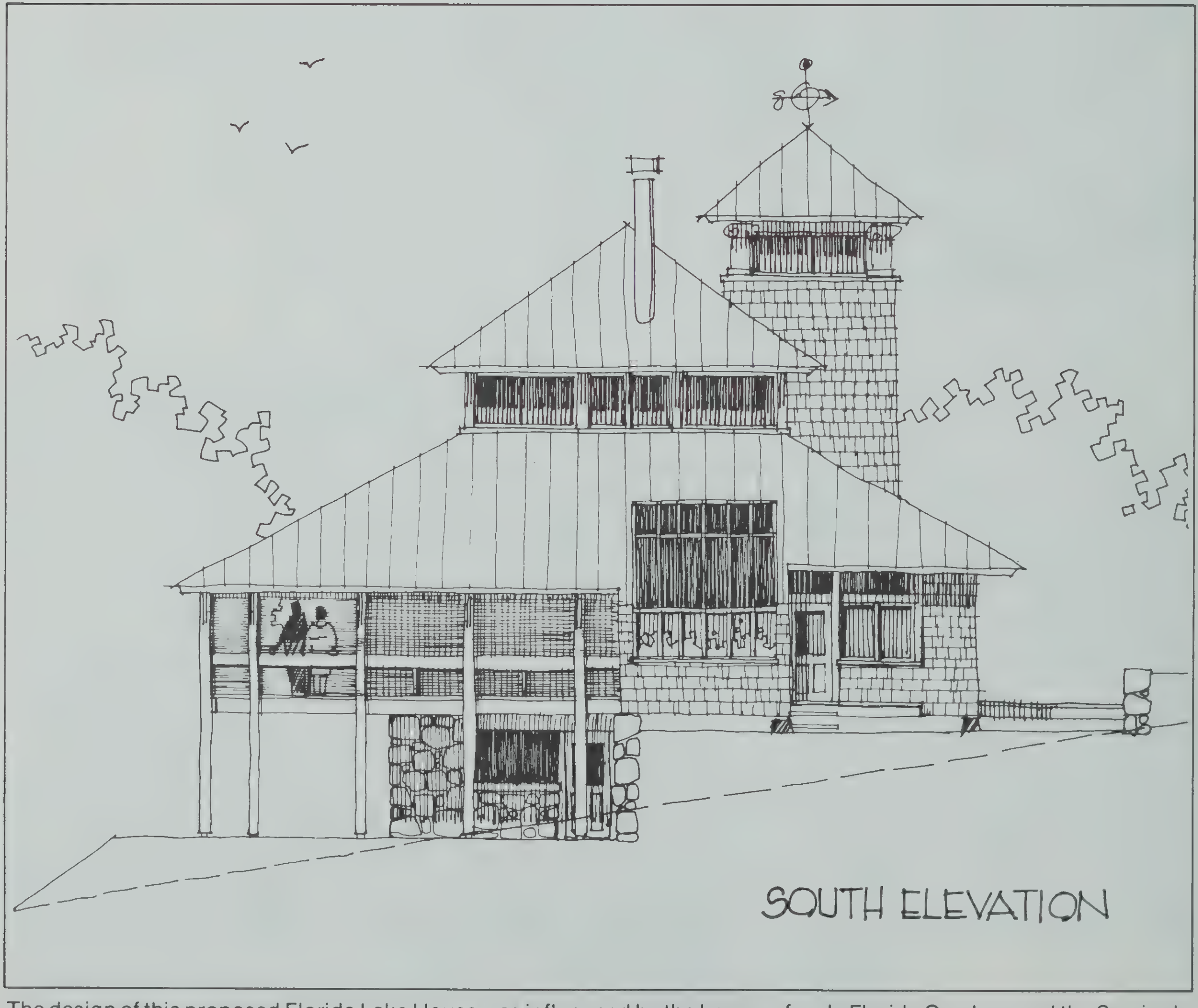

The design of this proposed Florida Lake House was influenced by the homes of early Florida Crackers and the Seminole Indians. It uses porches for shade to minimize solar buildup and induced air movement to minimize humidity and provide an immediate cooling effect. The south elevation of the building is shown above.

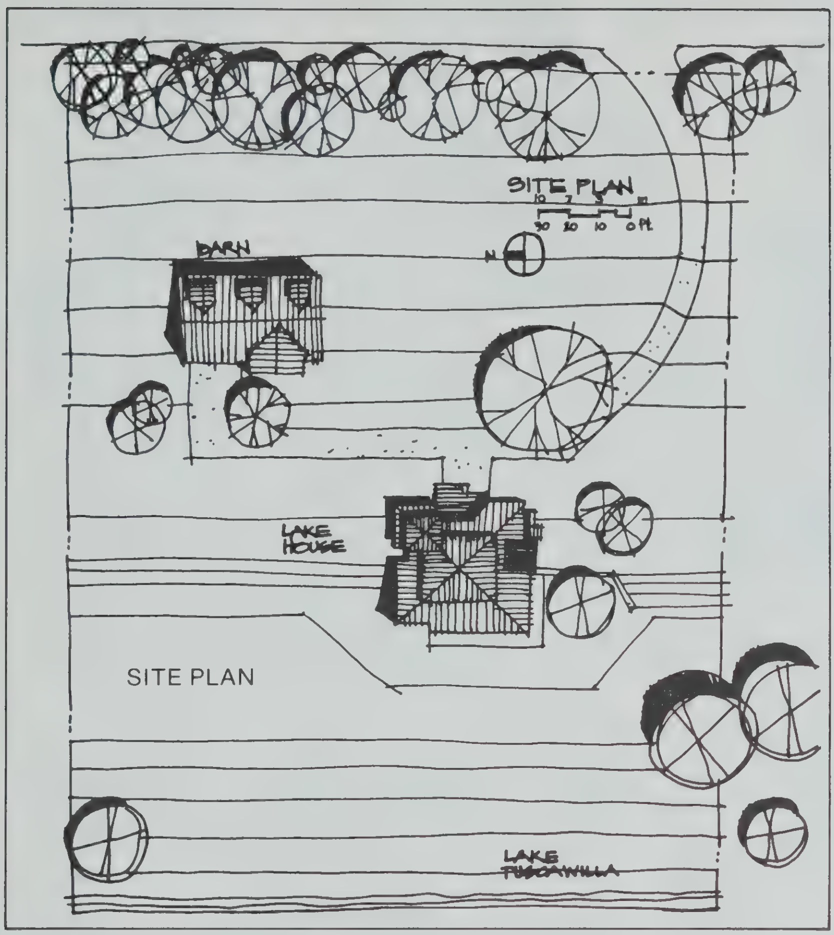

Plans for building the Lake House have been held up because the lake it was to be built near, Lake Tuscawilla, has developed a sinkhole. Since the water is disappearing, this site is no longer attractive. The designer is currently looking for another.

Designed by: Ronald W. Haase, Architect
College of Architecture
University of Florida
Gainesville, Florida 32611

The architect of this house for a family of four relied upon extensive studies of local climate and past experience with other low-energy homes when designing his own residence. He realized that shade to cool the house and air movement to reduce humidity would be the two most important elements in the design of a natural house. For this Florida location on a lake near Gainesville, the cooling load of heat and humidity is twice as much as the winter heating load. Thus, passive cooling was much more important to the design than passive heating.

Since a prevailing breeze cannot be counted on during hot, humid Florida summers, Haase relied on induced air movement through a chimney effect to achieve cooling. This design relies less on orientation and cross ventilation than it does on the gravity flow of cool air up and out the four-story stair tower. Air circulation is augmented by ceiling fans, and shade is provided by extensive screened porches.

The house expands from its basic 1,600 ft² (*149 m²*) of enclosed space by adding porches and a terrace. But in winter, the house retreats to its basic size and to introverted gatherings around the fireside. Additional heating is obtained from a convection greenhouse and wood stoves. With the exception of a thermostatically supervised furnace in the children's rooms, all heat is provided by wood fires. It is estimated that one cord of wood and 80 gal (*303*

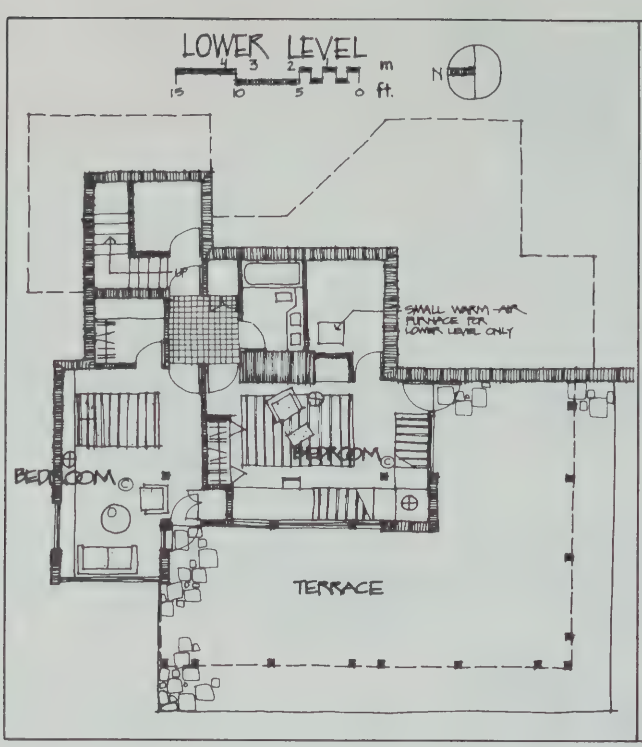

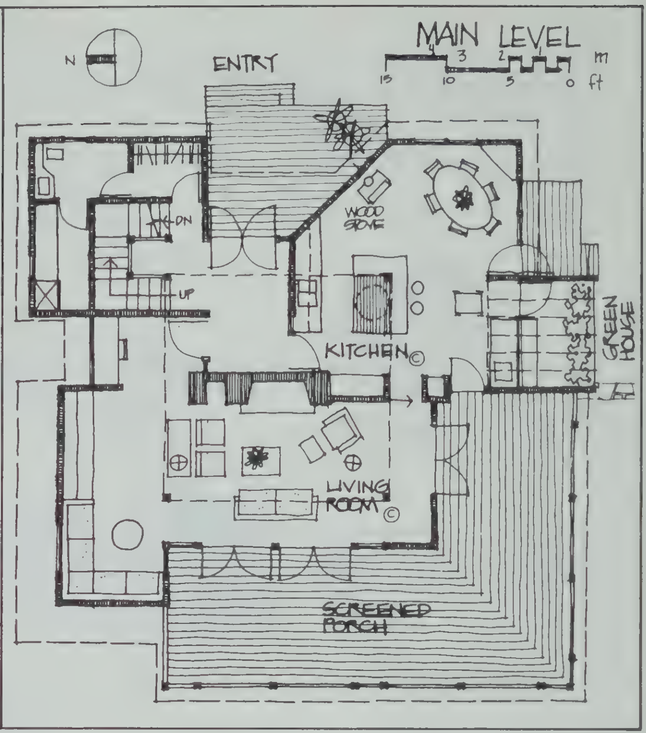

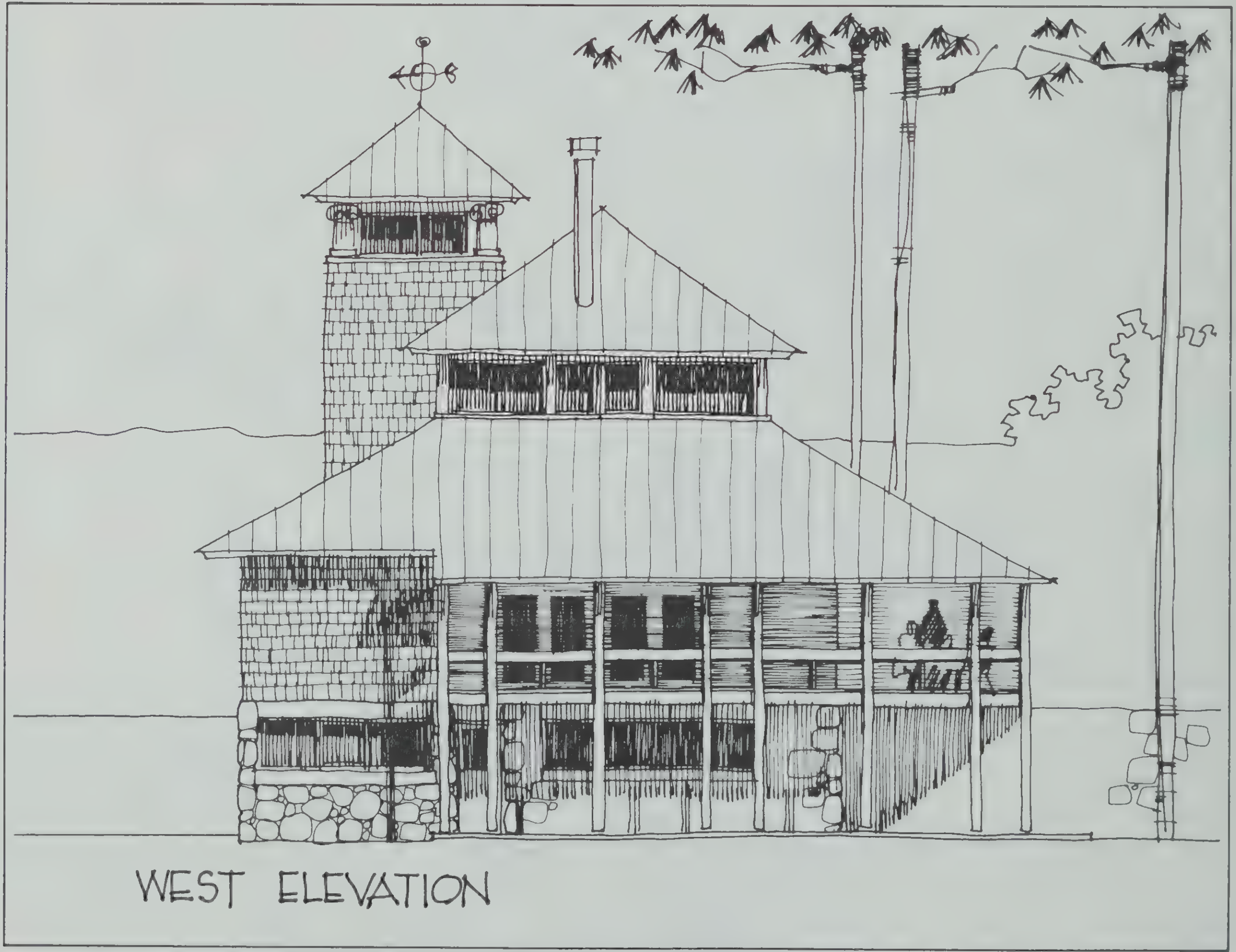

The screened porch extends around this, the west side, and the south side of the house. On warm days, the porch can be used as a dining and living area. Cypress piers will support the structure, and cedar shingle siding is planned for the exterior walls.

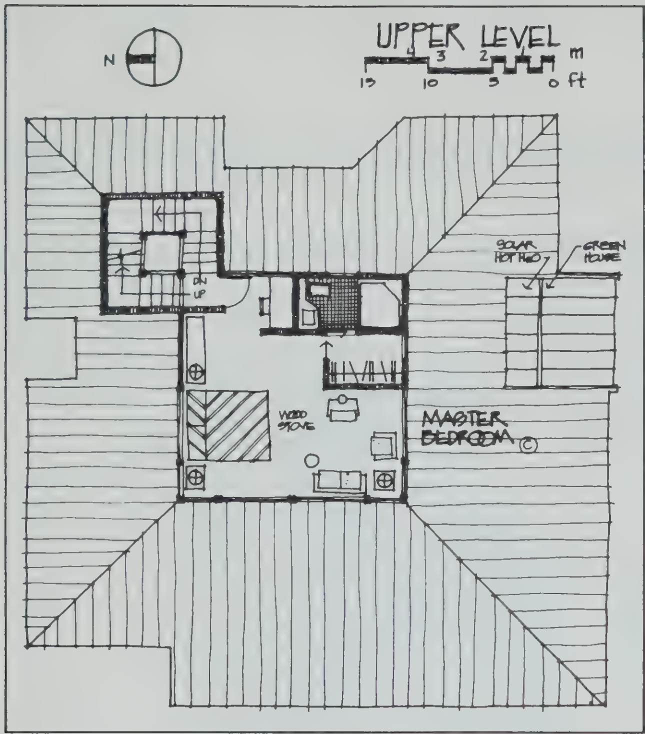

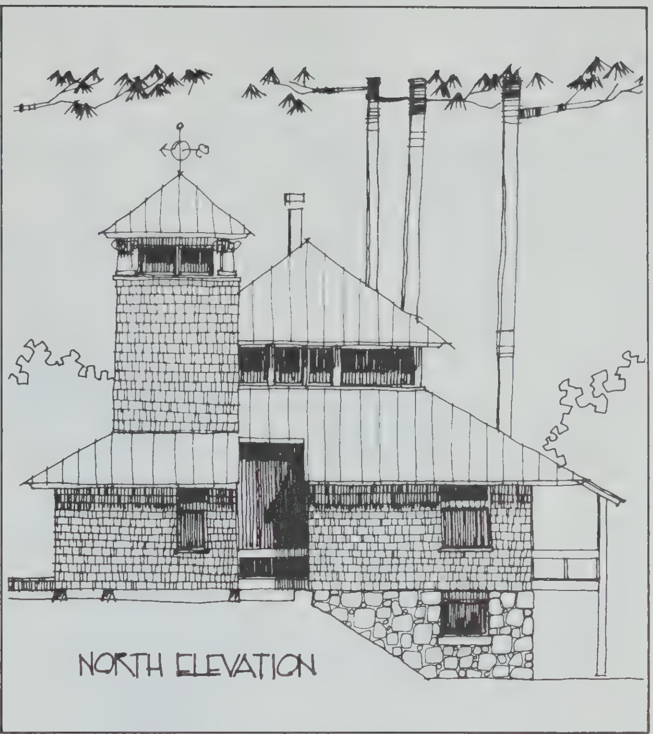

L) of oil, at a total cost of $180, are all that would be required to heat the house in winter.

In designing his own house, the architect has examined many aspects of his life-style. In addition to a passively cooled and heated structure, he has weighed the need for household appliances. Such energy-consuming appliances as a clothes dryer, dishwasher, frost-free refrigerator, and self-cleaning oven have been eliminated. Haase believes that a willingness to participate in one's own environment is a measure of how well a strong relationship with nature is embraced.

The architect was influenced by historic precedent and the life-style and dwellings of the Seminole Indians. This design makes more than a passing reference to the honorable early-Cracker farmhouse described by Marjorie Kinnan Rawlings in *The Yearling*. The fictional site of this personal favorite of the architect is no more than 10 mi (*16 km*) from the proposed building site, and the countryside is scattered with old, sagging, tin roofs and wood clapboard houses raised up on cypress piers. The cedar shingle siding proposed by the designer is an anomaly, however, and probably falls out of his New England background. Normally, shiplap clapboards would be used. More important, the regional character grows out of a bioclimatic design discipline, realized with local materials. □

Design Data	**English**	**Metric**
Heating degree days	1,385° F	769° C
Heating auxiliary energy	31,530 Btu/ft^2 yr	99.4 kWh/m^2 yr
Cooling degree days	2,500° F	1,390° C
Cooling auxiliary energy	0	0
Solar aperture area	70 ft^2	6.5 m^2
Thermal storage area	—	
Total effective thermal capacitance	—	
Net floor area	1,600 ft^2	149 m^2
Volume of conditioned air space	15,217 ft^3	431 m^3
Total cost (excluding land and site work)	$125,000 (est.)	
Total cost attributable to energy conservation measures	$5,800 (est.)	
Total annual solar contribution:		
Space heating	2.1 x 10^6 Btu	615 kWh
Solar hot water	36,100 Btu	10.6 kWh

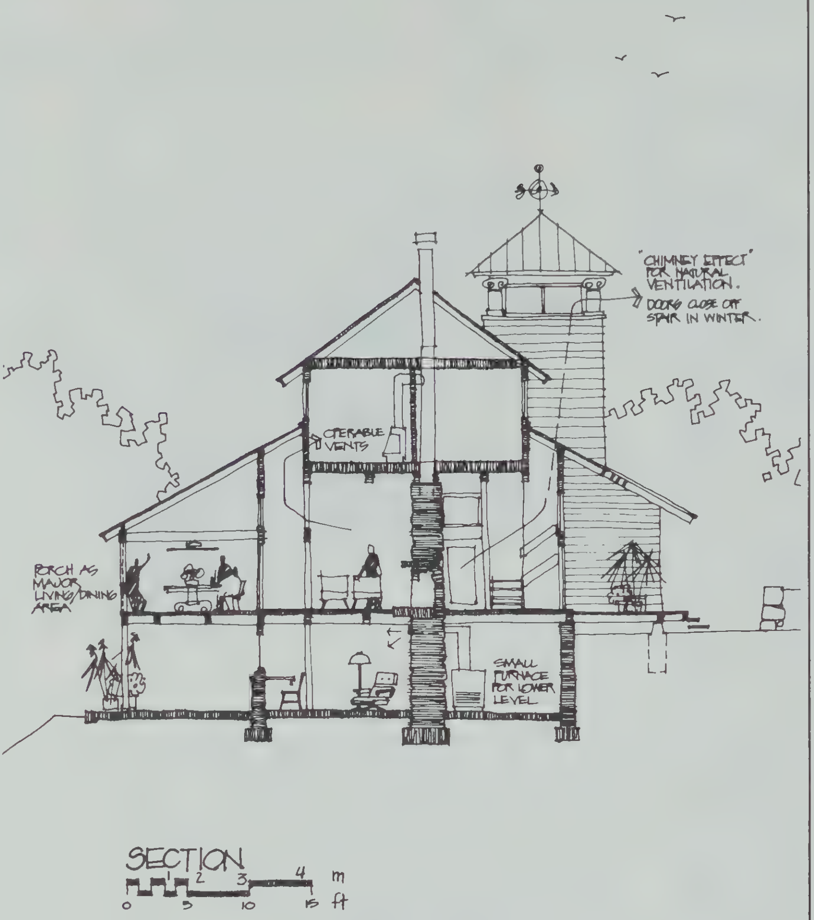
"CHIMNEY EFFECT" FOR NATURAL VENTILATION.
DOORS CLOSE OFF STAIR IN WINTER.
OPERABLE VENTS
PORCH AS MAJOR LIVING/DINING AREA
SMALL FURNACE FOR LOWER LEVEL
SECTION
1 2 3 4 m
0 5 10 15 ft

Because on warm Florida days a natural breeze cannot be counted on for cooling, induced air movement from ceiling fans was introduced by the designer. Cool air flows up and out the four-story stair tower. In the winter, the house is heated almost exclusively by wood stoves and a fireplace.

OPERATIONAL HEATING DIAGRAM

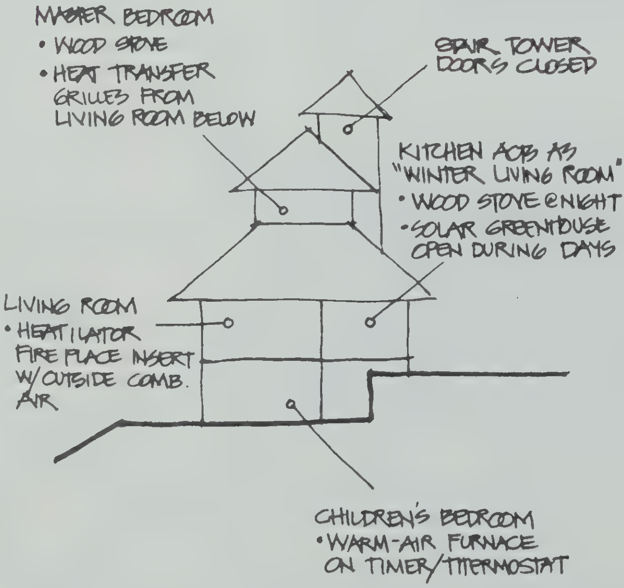
MASTER BEDROOM
• WOOD STOVE
• HEAT TRANSFER GRILLES FROM LIVING ROOM BELOW
STAIR TOWER DOORS CLOSED
KITCHEN ACTS AS "WINTER LIVING ROOM"
• WOOD STOVE @ NIGHT
• SOLAR GREENHOUSE OPEN DURING DAYS
LIVING ROOM
• HEATILATOR FIRE PLACE INSERT W/OUTSIDE COMB. AIR
CHILDREN'S BEDROOM
• WARM-AIR FURNACE ON TIMER/THERMOSTAT

OPERATIONAL COOLING DIAGRAM

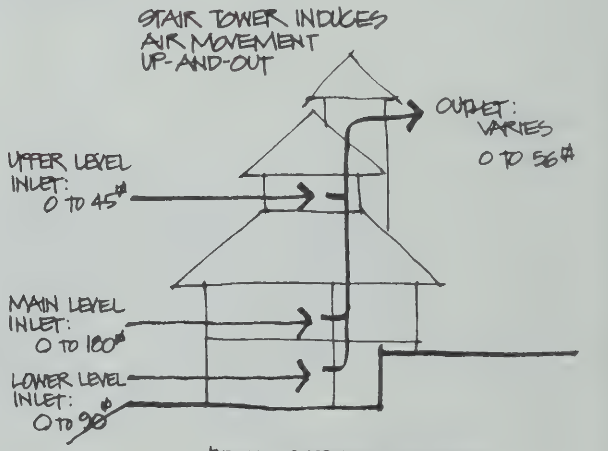
STAIR TOWER INDUCES AIR MOVEMENT UP-AND-OUT
OUTLET: VARIES 0 TO 56#
UPPER LEVEL INLET: 0 TO 45#
MAIN LEVEL INLET: 0 TO 180#
LOWER LEVEL INLET: 0 TO 90#

- BROAD OVERHANGS ELIMINATE DIRECT SOLAR HEAT GAIN
- GREENHOUSE CLOSED-OFF FROM HOUSE AND VENTED
- NO MECHANICAL COOLING SYSTEM
- SEVEN CEILING FANS

DATA ACQUISITION IN TEST MODULES

Current Research Practices with Data Sensors, Recording, and Processing Systems

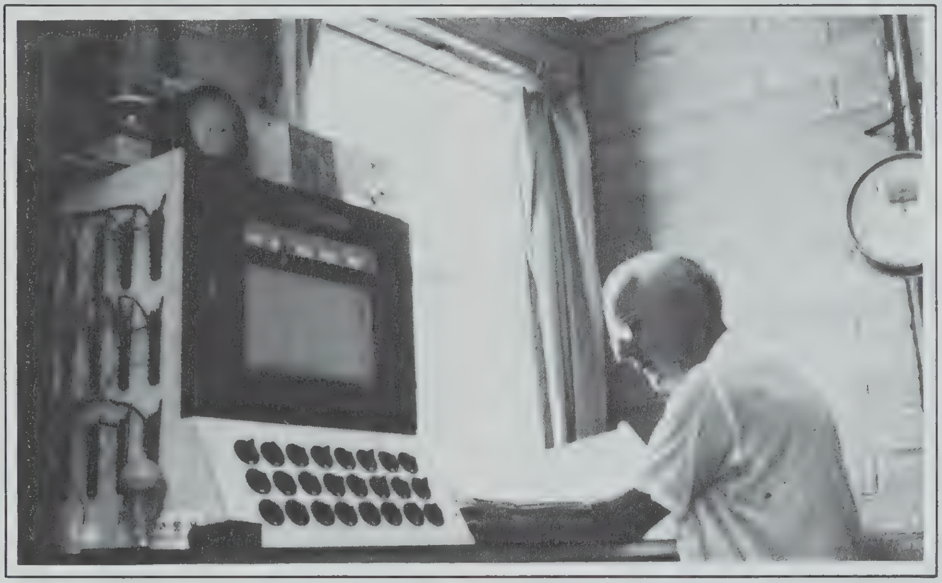

Photo: J. Yellott

Figure 1: Harold Hay logs data in 1968 using a strip chart recorder, a typical acquisition system then.

By FULLER MOORE
Department of Architecture, Miami University, Oxford, Ohio, 45056

ABSTRACT

Various current monitoring techniques and equipment available for test modules are described and evaluated, including measurement devices such as pyranometers, pyrheliometers, thermocouples, platinum resistance temperature detectors, thermistors, and temperature transducers, as well as recording equipment. Recommended methods for measuring temperature conditions, air movement, and power consumption are also explored. Monitoring equipment is discussed in terms of both usability and cost.

INTRODUCTION

The experimental practices of data acquisition in passive solar research are undergoing continuous change. The availability, dependability, and costs of instrumental and recording devices have benefited greatly in the past decade from general improvements and refinements in all scientific fields. Research applications from the semiconductor industry have improved the documentary potentials of tracing energy and environmental research conditions.

In order to monitor relevant ambient and experimental conditions in passive solar test modules, sensors are required to measure at least some of the following conditions: solar radiation, temperature (air, globe, surface, solid, liquid), air move-

---

The author worked on this survey while he was a guest scientist at Los Alamos National Laboratory. The work was performed under the auspices of the Office of Solar Heat Technologies of the U.S. Department of Energy and supported by Miami University.

This is the second in a series of review articles on passive solar research using test modules.

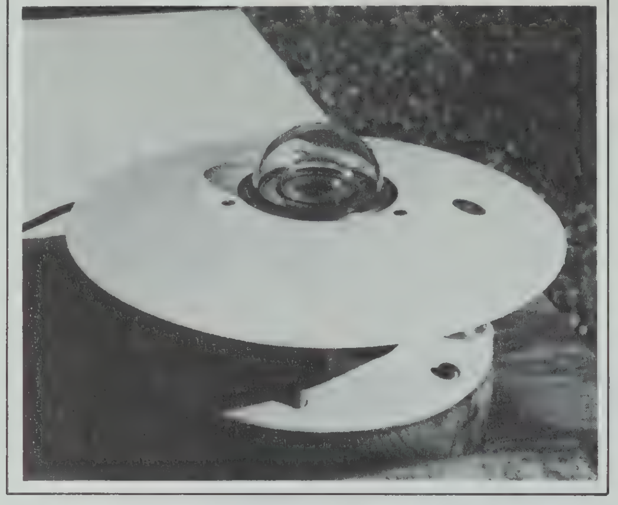

Figure 2: The Eppley PSP is a thermal pyranometer of laboratory quality.

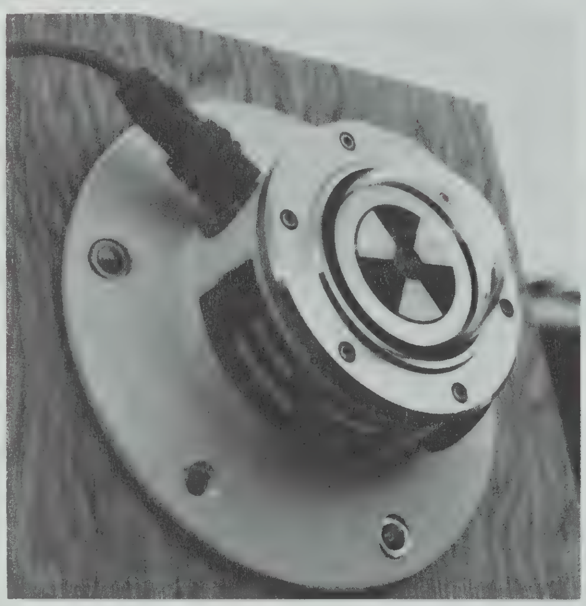

Figure 3: The field quality Eppley 8-48 is one of the most widely used thermal pyranometers.

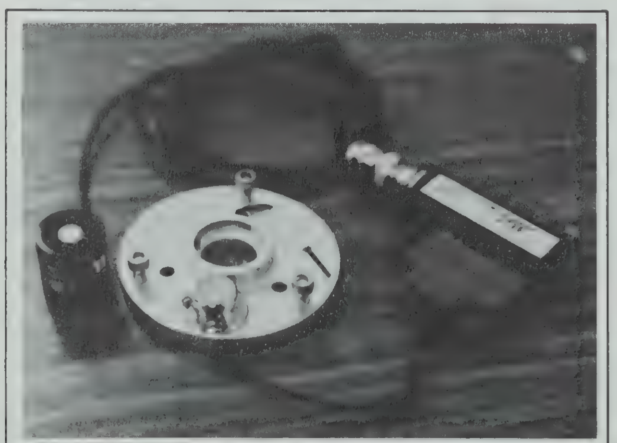

Figure 4: The Lambda Licor 200S photovoltaic pyranometer is often used for test module research because of its low cost.

ment (infiltration rate, wind speed, interior convection), auxiliary power consumption, and events. Much of the scientific success of passive solar research depends on the identification of pertinent parameters and on the selection of appropriate data acquisition systems.

Because of the amount of data involved, an automatic acquisition and recording system is usually employed, called simply the data acquisition system or DAS. (See Fig. 1.) This introduction and preview which characterizes the present recommended status is based primarily on current practices and experiences at the Los Alamos National Laboratory and extensive readings in the field.

SOLAR RADIATION

There are two basic types of solar radiation measuring instruments of interest: the pyranometer and the pyrheliometer.

Pyranometers:

The pyranometer is designed to measure the total radiation on a plane, including both direct radiation from sun and diffuse radiation reflected/refracted by clouds, atmosphere, and ground.

Total radiation on the plane of the collector glazing is of particular interest to test module researchers if these data are to be used later for validation of computer simulations. Total radiation on the horizontal plane is the measurement used for most standard weather data; this fact makes it a desirable measurement for comparing test conditions with standard weather data in other locations.

Pyranometers are of two basic types, thermal and photovoltaic. Thermal pyranometers employ a thermopile (a set of thermocouples connected in series) to measure the temperature of a black (or black and white) surface under a clear dome. The most widely used thermal pyranometers are the Eppley PSP (laboratory quality) and the Eppley 8-48 (field quality). (See Figs. 2 and 3.)

Photovoltaic pyranometers use silicon photovoltaic cells that generate direct electric current in proportion to solar radiation. Although thermal pyranometers continue to be the accepted standard research instrument, some photovoltaic pyranometers such as the Lambda (Licor 200S) are becoming widely used for test module research because of their low cost (approximately 15% of the cost of a comparable thermal instrument) and relative accuracy (±5%). (See Fig. 4.)

One error associated with pyranometer measurements of particular concern to test module researchers is nonhorizontal mounting. Some earlier versions of the Eppley Model 8-48 had errors exceeding 5% when mounted vertically. This was apparently due to internal convection currents. (More recent versions of the 8-48 have been modified to minimize this effect.) Photovoltaic pyranometers are not sensitive to tilt.[1]

Pyrheliometers:

The pyrheliometer is intended for measurement of direct-beam solar radiation only. It resembles a small telescope, and is aimed directly at the sun by a mechanical tracking system. The Eppley NIP is the most commonly used pyrheliometer. (See Fig. 5.)

While direct-beam radiation is of primary concern in concentrating collector research, it is of only minor interest in passive test module research. At Los Alamos National Laboratory, the principal uses of direct-beam data have been for (1) verification of previously proposed procedures for estimating radiation on tilted surfaces, given total horizontal and direct-beam data, and (2) testing the performance of specular horizontal reflectors.

Figure 5: The Eppley NIP is one of the most commonly used pyrheliometers.

TEMPERATURE

While direct-reading thermometers are useful for limited measurement of temperature in certain experiments, sensors with automatically recordable output are generally preferable for monitoring test modules. There are three main categories of thermometers: thermocouples, resistance thermometers, and transducers. In the resistance category, platinum resistance temperature detectors and thermistors are of particular interest.

Temperature Sensors

Thermocouples:

If two wires of dissimilar metals are joined at each end to form a circuit, and these ends are at different temperatures, then a small voltage is developed in the circuit. This voltage can be used to measure the temperature difference between the two junctions; the arrangement is called a thermocouple. In order to use a thermocouple for temperature measurement, it is necessary to maintain one of the junctions at a known reference temperature. In a laboratory, an ice bath is often used. In test module experiments, electronic cold reference junctions are usually used instead.

If the distance between the two junctions is large, it is possible to use less expensive extension wire. It is necessary that this wire be matched to the thermocouple used if calibration is to remain unaffected. The two thermocouples most frequently used for Los Alamos test module measurements are Type K (chromel alumel) and Type T (copper constantan). Because of the modest cost of these types, thermocouple wire is used continuously from the sensor junction to the electronic reference junction, and problems associated with splices and extension wires are eliminated.

Thermocouple wire is available in standard and precision grades. In standard grades, manufacturing variations necessitate the individual calibration of each thermocouple. At Los Alamos, precision grade is used because accuracy of ±.5°F *(.9°C)* can be achieved consistently without calibration.

A twisted junction of the bare, dissimilar wires is sufficient to create a thermocouple. The joint may be soldered to assure permanent contact; it may also be sealed with a plastic coating for use in corrosive environments. Although thermocouples are temperature sensitive (for practical purposes) only at the junction, there is one placement consideration of particular concern in test module experiments. Because the thermocouple wire is more thermally conductive than its surrounding environment, it can influence measurements by conducting heat to or from the sensor location. For that reason, it is recommended that the last 50 diameters of wire length be positioned to be at the same temperature as the measured point. (See Figs. 6 and 7.)

The voltage created by the temperature difference between the two junctions is measured by a voltmeter and converted to temperature difference by a formula or tabular values for the thermocouple type used.

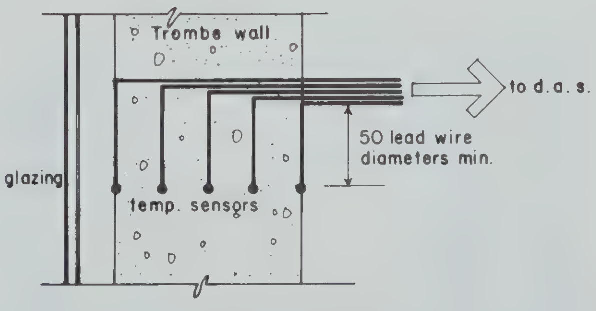

Figure 6: The Trombe wall cross section shows how an isothermal temperature sensor lead wire configuration can be used to reduce conduction errors.

Platinum Resistance Temperature Detectors (RTD):

All metallic conductors exhibit an electrical resistance that changes with temperature. The resistance and changes in resistance are measurable directly with an ohmmeter[2] or indirectly with a voltmeter. The results are converted to temperature by translating equations or tabular values.

While many metals theoretically can be used for RTDs, platinum is the material of choice because of high resistivity, good temperature coefficient, broad temperature range capability, and outstanding resistance stability.

The principal advantages of platinum RTDs over thermocouples are increased accuracy (± 0.2°F) and simpler signal conditioning. The principal disadvantage is higher cost per sensor ($40-100 per RTD vs. $3-10 per thermocouple). Nevertheless, platinum RTDs have been selected by some solar researchers. Craig[3] has reported that entire system costs are comparable (due to cheaper lead wire and no cold reference junction required for platinum RTDs). An ice bath is the traditional reliable thermal reference.

Thermistors:

Thermistors, like RTDs, change resistance with temperature. They consist of a small bead of semiconducting material that has a very high negative temperature coefficient of resistance (which varies inversely as the square of the absolute temperature).[2] The relative increase in resistance per degree temperature rise is much greater in thermistors than RTDs making them more sensitive (although not necessarily more accurate). The midrange coverage of moderate cost thermistors is similar to the temperature ranges in nonfocusing active and passive systems. Installation is greatly simplified (compared with thermocouples) by the use of conventional two-lead extension wire. Calibration stability is considerably affected by overheating. Because the sensor is sensitive to moisture, proper sheathing (i.e., glass sealed) is required for submersion. Thermistors are the most widely used sensor for active solar controls.

Temperature Transducers:

A recent development in temperature sensors is the integrated circuit transducer. Each small sensor is an entire circuit (composed of transistors and laser-trimmed resistors) that modulates a supplied current in proportion to absolute temperature. The transducers are nearly linear over the operating range (-41° to 328°F, *or -40.6° to 164.5°C*), thus simplifying signal conditioning. Their cost is low ($2 each, uncalibrated and unsheathed, to $54 each, calibrated and sheathed, with signal conditioner). They do not require special extension wire. They are not considered as reliable as thermocouples, but this handicap may be offset by advantages for test module applications. Transducers are the standard sensor used in the Aeolean Kinetics PDL data acquisition system (developed for use in the SERI Class B passive solar monitoring program).[4]

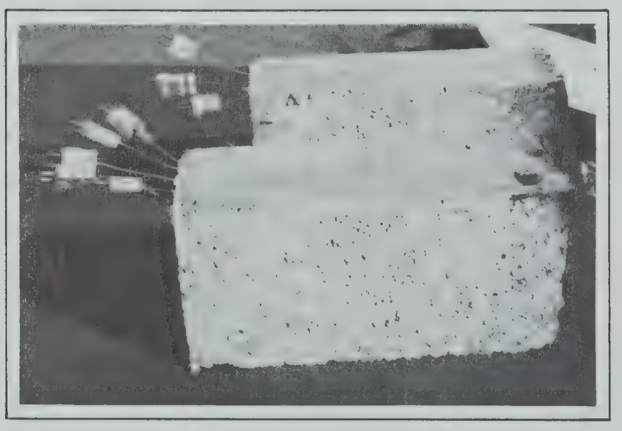

Figure 7: Thermocouples are cast into Trombe wall masonry units.

Measurement of Temperature Conditions

Air Temperature:

When sensors are used to measure air temperature, care must be taken to avoid inaccuracies due to radiation. If the sensor is not exposed to direct sunlight or surrounding surface temperatures substantially different from that of the air, no radiation shielding of the sensor is required. For the measurement of ambient air temperature, a standard U.S. Weather Bureau-type instrument shelter is preferred. (This is a white, wood-louvered box mounted 5 ft above the ground.) (See Fig. 8.)

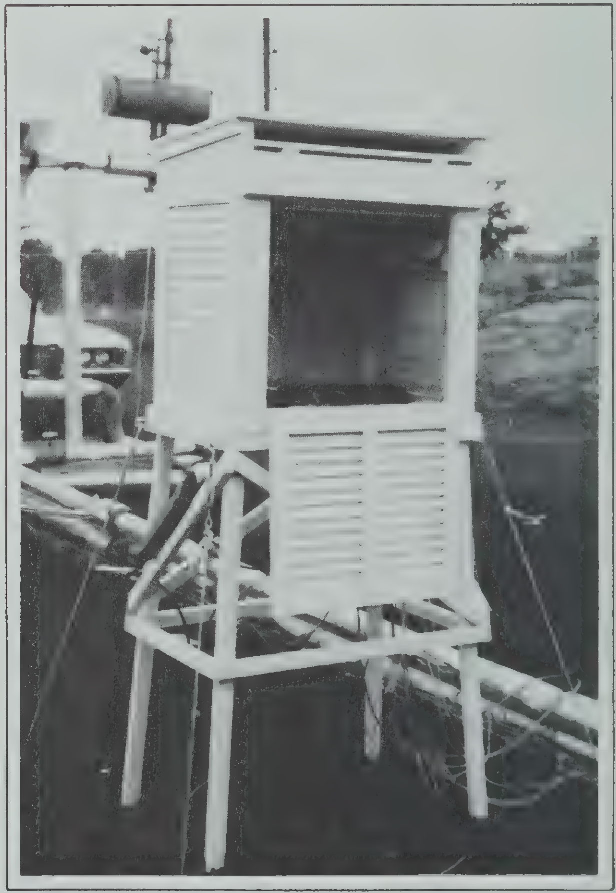

Figure 8: A standard U.S. Weather Bureau instrument shelter contains temperature measuring devices.

For air temperature measurements in the test module, an unaspirated, tubular radiation shield should be used. Wadsworth and Palmiter[5] have proposed a double concentric tube shield for this purpose; a shield of this design is commercially manufactured by Aeolean Kinetics.[6] Such a shield is acceptable for ambient measurements in lieu of an instrument shelter. (See Fig. 9.)

Globe Temperature:

Globe temperature measurements are useful in assessing human thermal comfort in passive solar environments. These measurements combine the effect of air temperature and radiation by enclosing the sensor in the center of a hollow, colored globe. Ideally, the globe should have minimum thermal mass, be thin, highly conductive, and have high surface emissivity inside and out. ASHRAE Standard 55-74 describes such an enclosure, and precision globes (in black or pink color) are commercially available.[7] However, most test module researchers contacted by this author used a black PVC toilet float for a globe enclosure.

Because globe temperature is used to assess human comfort, the recommended sensor location is the center of the occupied space at a 4 ft *(1.3 m)* height.

Surface Temperature:

Because of the substantial contribution of radiation exchange in passive solar structures, surface temperatures are of considerable theoretical interest.

In practice, surface temperatures are difficult to monitor accurately in test modules. The difficulty is associated with the infinitestimal thinness characteristic of a surface. If the sensor is simply applied to the surface, it projects into the air film and is unduly influenced by convective transfer. Moreover, any method of attachment (tape, adhesive, mechanical) affects surrounding temperatures and can introduce an insulation between the sensor and the surface. Covering the sensor with a small piece of insulation reduces the effect of the air film on the sensor, but also reduces the normal heat transfer between the surface and air film at that point.

At Los Alamos, in measuring masonry surface temperatures, a groove is scored in the surface, and the thermocouple is embedded in the groove using a cement similar to the original masonry. Hall[2] has described adding a reflective 3-in.-diameter *(7.5-cm)* hemisphere to reduce the effect of the air film.

If the surface is metallic, the ends of the thermocouple wires may be soldered directly to the surface about 1 in. *(2.5 cm)* apart (rather than joined conventionally into a junction). The temperature measured will be the average of the surface between two wires. The same principle can be used for nonmetallic surfaces by bonding a metallic foil to the surface using a conductive adhesive. Care should be taken to match the surface emissivity to the surrounding area. This method of surface measurement is probably justifiable only for large (i.e., 50°F, *or 28°C*) temperature differences.

The method of surface temperature measurement is dependent on temperature difference, convective velocity, and material conductivity. Ideally, two conditions must be satisfied: (1) the sensor must be brought to the same temperature as the surface, and (2) its presence must not alter the surface temperature (by insulating, conducting heat away, or acting as a radiation shield).

Solid Temperatures:

Similar conditions must be satisfied in measuring the interior temperature of solids. Care must be taken to ensure good contact between the sensor and the material; in masonry materials, the sensor should ideally be cast into the material. When installed after construction, a hole is drilled, the sensor is inserted, and the void filled with a material of similar conductivity. Care should be taken to prevent air gaps.

As described previously, the lead wires should be positioned to stabilize at the same temperature as the sensor. This means that the lead wires should be perpendicular to the direction of heat flow in Trombe walls and floor slabs. This requirement makes installation after construction difficult. If it is not possible to drill into the edge of the wall or slab, a large hole should be drilled into the surface, allowing a length of 50 diameters of the lead wire to be bunched at the sensor location, and the hole filled with a mixture of the wall material.

In Trombe walls, it has been determined at Los Alamos that a rake of five sensors (two surface,

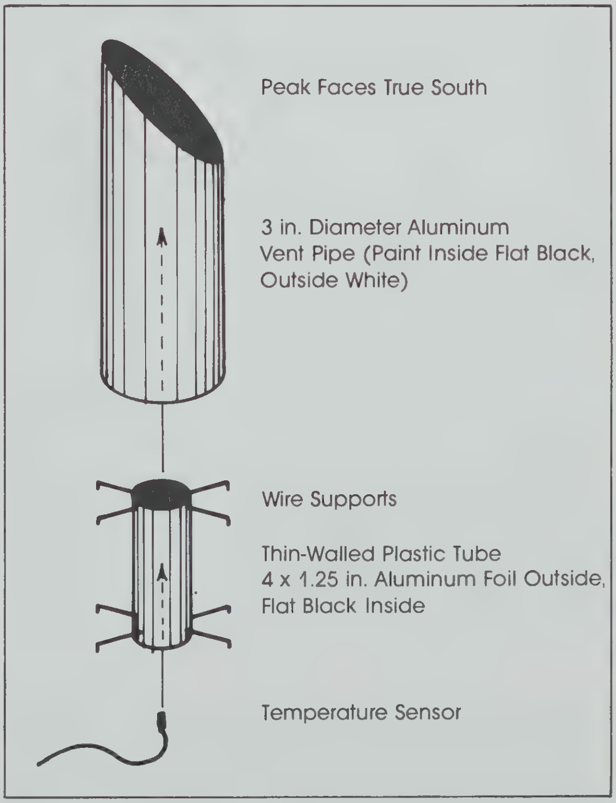
Peak Faces True South
3 in. Diameter Aluminum Vent Pipe (Paint Inside Flat Black, Outside White)
Wire Supports
Thin-Walled Plastic Tube
4 x 1.25 in. Aluminum Foil Outside, Flat Black Inside
Temperature Sensor

Figure 9: A double concentric, unaspirated radiation shield may be used in lieu of an instrument shelter for ambient measurements.

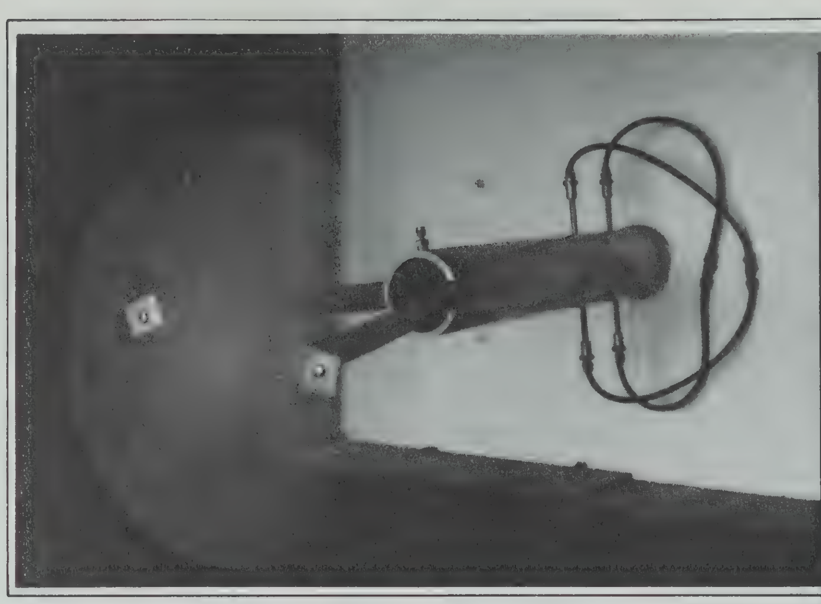

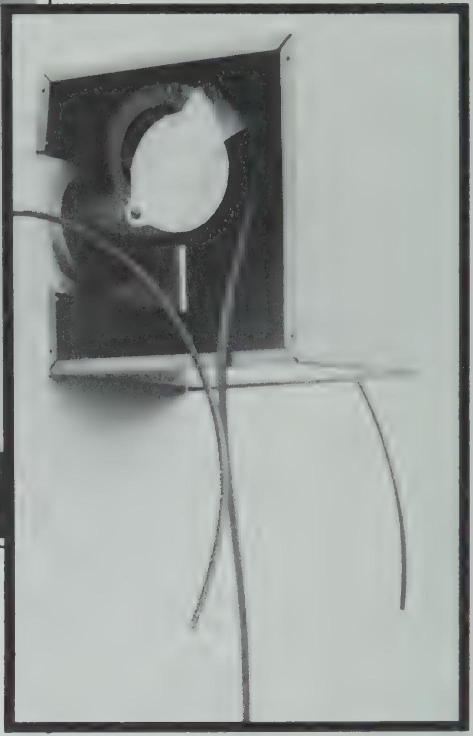

Figure 10 (at right): An exterior-mounted, centrifugal fan blows outside air into a Los Alamos test room to standardize the infiltration rate.

Figure 11 (above): Air from the exterior fan flows into a LANL test room through an ASTM-type calibrated nozzle. Manometer tubes, connected to the internal nozzle, permit measurement of pressure differences.

three interior) is sufficient to describe the horizontal heat flow through the wall. This rake is located at the midheight of the wall; this location approximates the mean of several rakes positioned from the top (where the wall is hottest due to the stack effect) to the bottom. (In reality, the temperature variation is not linear from bottom to top, but instead changes most abruptly in the lowest 25%.)

Liquid Temperatures:

Because of convective mixing and intimate thermal contact between the liquid and the sensor, liquid temperatures (as in waterwalls) are easy to measure. As with solids, care should be taken to keep the first 50 diameters of the sensor lead in isothermal conditions. To prevent sensor junction corrosion, thermocouples may be coated with plastic. Otherwise, thermocouples and RTDs are unaffected by moisture. (Thermistors and integrated circuit temperature transducers require watertight sheathes to prevent erroneous readings due to moisture contamination.)

Because of convective mixing, liquid thermal storage elements are virtually isothermal horizontally, allowing the internal temperature to be measured at one location (center at midheight). As with Trombe walls, there is significant vertical temperature variation, with the greatest change occurring near the bottom.

MEASURING AIR MOVEMENT

Three types of air movement are of direct concern to passive solar researchers: infiltration rate, wind speed, and interior natural convection air movement.

Infiltration Rate:

Wind speed and the stack effect of the inside-outside temperature differential directly affect the rate of air infiltration in buildings and test modules. The air infiltration rate and the temperature difference combine to determine the heat loss or gain of the structure due to infiltration. Because it is impractical to measure air infiltration continuously in test modules, researchers at Los Alamos and other labs eliminate the influence of variable wind speed and stack effect by using a fan to pressurize the module slightly, producing a relatively constant infiltration rate. At Los Alamos, an exterior centrifugal fan blows outside air into the test room through an ASTM-type calibrated nozzle. Two tubes (connected to the front and back of the nozzle) permit periodic measurement of the pressure difference with a manometer. From this measurement, the flow volume can be determined. The volume can be adjusted by a fan damper. (See Figs. 10 and 11.)

The infiltration rate can also be measured by adding tracer gas (SF_6) to the room, sampling the room air at 30-minute intervals thereafter, and analyzing these samples in a remote laboratory using a gas chromatograph. If this method is used alone, the fan adjustments necessary for matching infiltration in several test modules become a trial-and-error procedure. For this reason, the calibrated nozzle is recommended as the primary control measurement, with the tracer gas technique used for validation.

One infiltration consideration is of particular concern to test module researchers. Because the total heat loss due to infiltration is a function of inside-outside temperature difference, a given volume of infiltration from an unusually warm area will disproportionately affect the rate of heat loss. For this reason, particular care should be taken to minimize infiltration from the volume between storage walls and glazing. This will assure that comparable infiltration rates in test modules translate to comparable infiltration heat losses. This precaution is of particular importance if the glazing is reconfigurable and is not caulked.

Wind Speed:

If the infiltration rate is fixed (using the above procedure), the only effect of wind speed on heat loss is to change the effective R-value of the exterior air film. (The ASHRAE-recommended R-value of .17 corresponds to 15 mph *(25 km/h)* wind and is excessive for most conditions.) Continuous monitoring of wind speed allows adjustment of this loss. At Los Alamos, this variation is not considered significant and is ignored.

A cup anemometer is usually employed to measure wind speed. An electrical circuit inside the instrument creates a pulse that is counted. The anemometer is calibrated so that a certain number of pulses represents the passage of one mile or kilometer of wind.

The position of the anemometer is a subject of considerable controversy if the results are to be used to determine building thermal loss. No standard seems to exist; however, the author has used a location 4 ft *(1.3 m)* above the center of the test module. At Los Alamos, the location is the top of an adjacent building at a height of approximately 25 ft *(8.2 m)* above ground.

Interior Air Movement:

Interior natural-convection air movement is very slow and often unrestricted in direction. It is difficult to measure speed directly and impractical to measure direction. Los Alamos has used a precision, low-velocity, hot-wire anemometer for such measurements.[8] Convective movement direction is deduced from temperature readings by suspended thermocouples.

Smoke (cooled to air temperature) can be used as a crude aid to convective flow visualization.

POWER CONSUMPTION

Because passive solar test modules are often fitted with auxiliary electric resistance heat (preferred because of easy measurement due to 100% conversion efficiency) some method of monitoring of electricity consumption is required.

Fixed Rate Heater (On/Off Status Monitored):

If an automatic, digital data acquisition system is used to sample data frequently, the simplest method is to use a fixed rate resistance heater and monitor its on/off status. It is necessary to make a one-time measurement of consumption rate (some researchers have expressed concern that, because resistance varies with temperature, the heating rate is not constant). The status is monitored using a relay in the heater power supply to open and close a low-voltage circuit from the data acquisition system.

Watt-Hour Meter:

The total consumption can be monitored using a watt-hour meter with a pulse initiator to record power consumption via a pulse counter. Meters of this type are expensive ($150 and more) and require a standard utility base.

Current Transducer with Voltage Sensor:

A third alternative is the use of a clip-on Hall effect current transducer to measure amperes and a simple line-voltage sensor to monitor voltage. These values can then be converted to determine power consumption in kW. Both the watt-hour meter and the current transducer are capable of monitoring variable consumption rates and are therefore preferred for monitoring occupied buildings.

Control of Auxiliary Heat:

Both residential and industrial thermostats have been used at Los Alamos to control auxiliary heaters in test rooms. It was determined that neither of these was sufficiently accurate to maintain identical thermostat set temperatures in separate test rooms. Instead, the data acquisition system now controls the heaters using the interior air temperature sensor as the thermostat sensor.

EVENT SENSORS

The two types of event sensors of interest for test cell monitoring are status and counting.

Physical status (i.e., position of night insulation) and electrical status (i.e., operation of auxiliary heat) are typical monitoring requirements. The data acquisition system is used to monitor the open/closed status of a low-voltage circuit (current supplied by the DAS). Simple microswitches (with normally open/normally closed circuitry reconfigurable by changing the lead attachment) are used for physical events. Relays opened/closed by line-voltage current are used for electrical events to open/close the low-voltage circuit. No DAS signal conditioning is required.

Event counting (door openings, anemometer rotation) is a regular monitoring requirement for occupied buildings, but less typical of test modules. Because simple electrical contacts can vibrate after opening or closing (i.e., "bounce"), erroneous readings can occur. Special magnetic microswitches can be used to eliminate bounce, or the circuit can be "debounced" electronically by the DAS. A special signal conditioner is required to hold the accumulated total events between sensor readings.

DATA ACQUISITION SYSTEMS (DAS)

While direct graphic recording of data (i.e., strip-chart recorder) can be used, the large amount of data generated by test module experiments coupled with recent developments in digital sys-

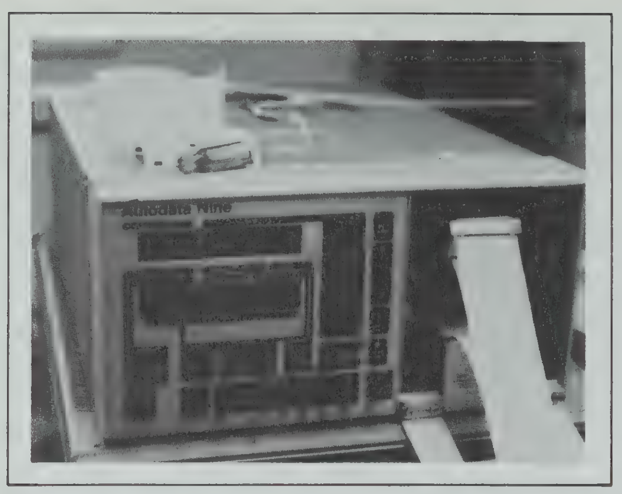

Figure 12: The Accurex Autodata Nine digital data logger was used extensively in the mid-1970s by Los Alamos to monitor passive and active solar buildings.

tem hardware have made digital DAS the preferred choice for this application. Digital systems can be further categorized as data loggers (which simply record raw data, usually on printed paper tape and/or magnetic tape cassette) and those that are programmable and can additionally process and store results. The Accurex Autodata Nine is an example of the former, and was used extensively in the mid-1970s by Los Alamos and others for monitoring passive and active solar buildings. (See Fig. 12.)

As the cost of microcomputers dropped dramatically in the late seventies, they were adapted by many researchers for combined data acquisition, recording, and simultaneous reduction.[9-31]

These systems usually include the following components:

- a cold reference junction (required for thermocouples only);
- a digital voltmeter (for converting analog voltage-sensor signals to digital data for processing);
- a digital clock or controller to control data sampling;
- a programmable microcomputer to control the clock as well as read, process, and store data;
- a data-storage device (printer, cassette, and/or disk drive);
- a display to facilitate programming or temporary display of data (video monitor or LED alphanumeric display).

At Los Alamos, the 14 passive test rooms are monitored using a Hewlett-Packard 9845 desktop computer (performs control functions, data reduction, and recording), with HP 3546 digital voltmeter (for analog-to-digital conversion), three HP 3495A scanners (80 channels each), and an HP 6942 multiprogrammer to control auxiliary heat in cells. (The approximate cost of this hardware was $44,000.) Temperature sensors are Type K precision thermocouples, and solar radiation instrumentation includes Eppley PSP and 8-48 pyranometers, and Eppley NIP pyrheliometer. Data are stored on HP 9-channel cassettes. These data are transferred to floppy and hard disks for further processing on separate HP 9845 and HP 1000 computers. (See Fig. 13.)

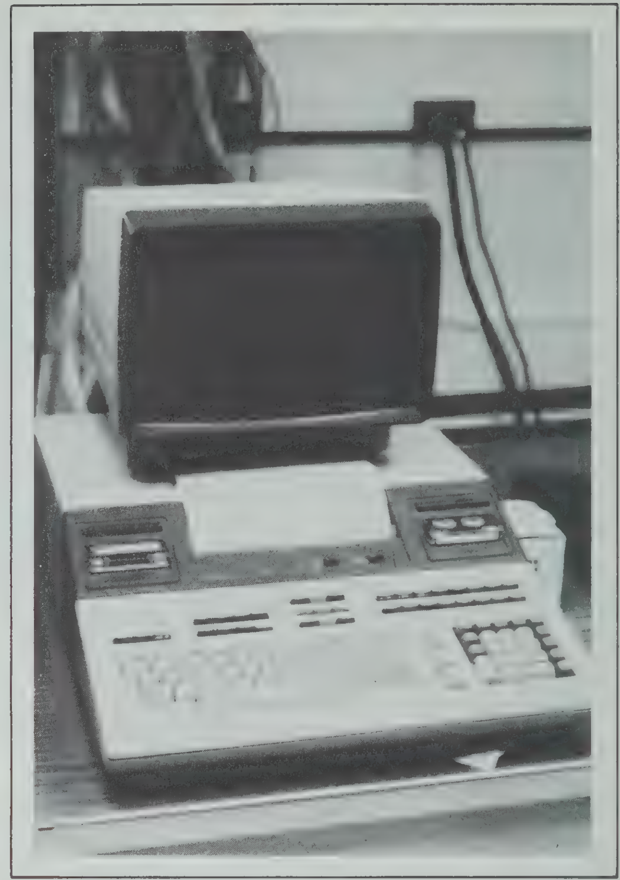

Figure 13: The Hewlett-Packard 9845 computer is used for data acquisition at Los Alamos.

A low-cost programmable DAS was developed for the SERI Class B monitoring program by Aeolean Kinetics.[12,27] The entire system, suitable for test cell monitoring, is approximately $5,500 and consists of 16 analog plus 8 digital channels, including pyranometer, temperature sensors, printer, magnetic tape data recorder, and data reduction software. The system is expandable to a total of 88 channels. (See Fig. 14.)

Los Alamos is currently configuring an alternative, low-cost DAS using an Apple II+ computer (for control and data reduction), a monitor, a 5.5 in. disk drive for data storage, a clock-card control, and an interactive structure 16-channel A/D converter for field monitoring of active systems using thermocouples. System cost excluding pyranometer is approximately $3,000.

CONCLUSIONS

Data acquisition is fundamental to any experimental passive solar test module research program. Measurement techniques for these modules, while similar to other areas of thermal research, have certain unique requirements for range, sensitivity, and

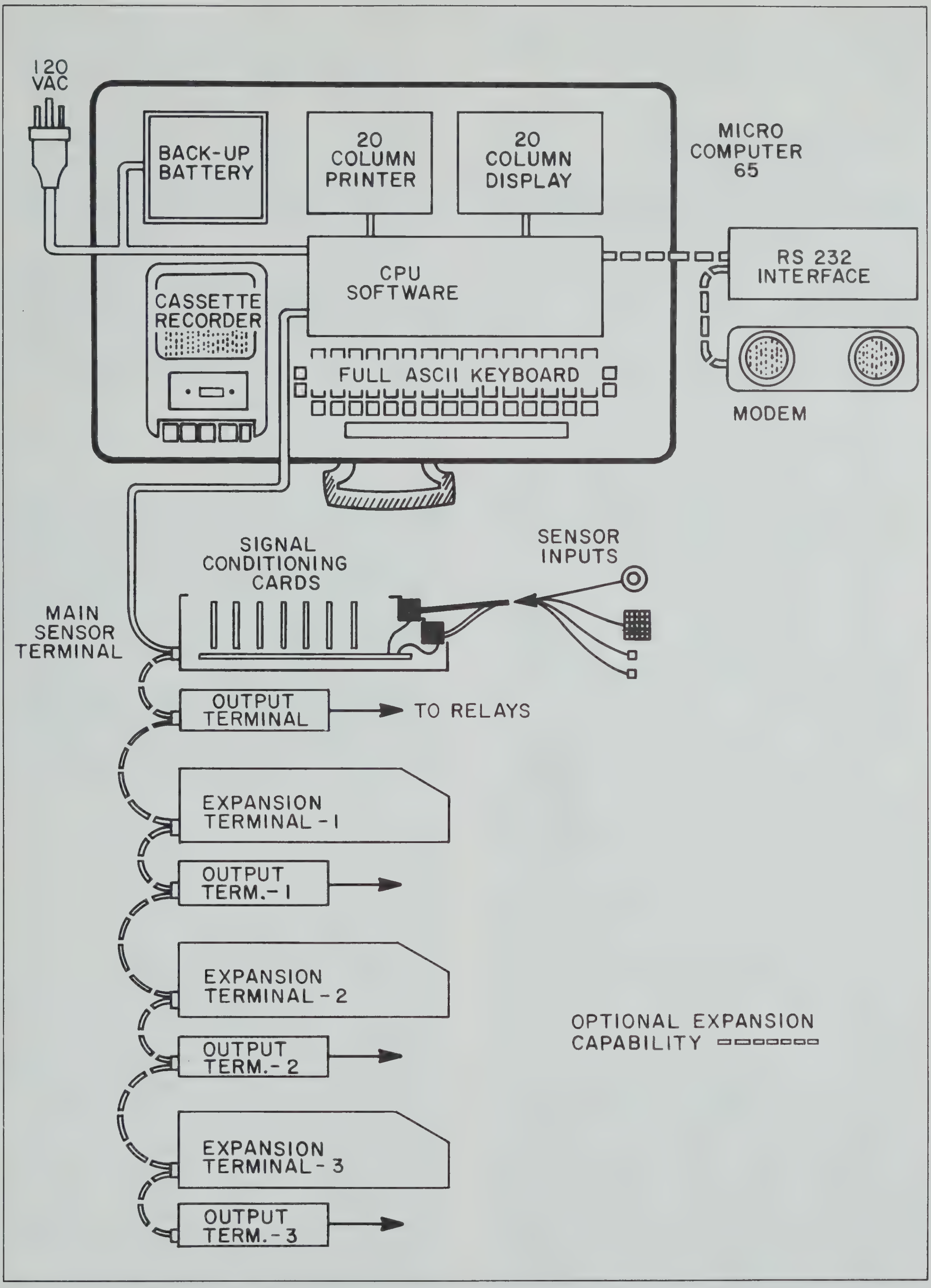

Figure 14: Aeolean Kinetics' PDL-24 monitoring system is suitable for test cell monitoring. This expandable system is available at a cost of about $5,500.

integration. Low-cost microprocessors have greatly enhanced the researcher's capability through interfacing simplicity, automatic data logging onto magnetic media, and on-line data analysis.

ACKNOWLEDGEMENTS

The author wishes to thank LANL Group Q-11 for their enthusiasm and assistance on this project, and particularly Lee Dalton and Stan Moore for their many helpful discussions on DAS, sensors, and measurement strategies.

REFERENCES

1. Bahm, R.J.; Nakos, J.C. 1979 (Nov.). "The Calibration of Solar Radiation Measuring Instrument." Bureau of Engineering Research Report No. BER-1 (79) DOE-684-1. Albuquerque, New Mexico: University of New Mexico.
2. Hall, J.A. 1966. *The Measurement of Temperature*. London: Chapman and Hall, Ltd.
3. Craig, J.I.; Williams, J.R. 1978 (April). "Moderate Cost, Calculator-Based Data Acquisition for Solar HVAC Systems." *Proceedings of the Conference on Performance Monitoring Techniques for Evaluation of Solar Heating and Cooling Systems*; Washington, D.C.: U.S. Department of Energy; April 3-4, 1978; p. 139.
4. Halperin, D.A. 1980 (Oct.). "The PDL-24 Solar Monitoring System." *Proceedings of the Fifth National Passive Solar Conference*. Vol. 5.2. Edited by John Hayes and Rachel Snyder. Amherst, Massachusetts; Oct. 19-26, 1980. Newark, Delaware: American Section of the International Solar Energy Society, Inc. (AS/ISES), University of Delaware; pp. 1114-1118.
5. Wadsworth, B.; Palmiter, L. 1979 (Aug.). "A Radiation Shield for Air Temperature Measurement." *SOLAR 1979 Northwest Conference*; Seattle, Washington; Aug. 10-12, 1979; pp. 176-180.
6. Halperin, D., et al. 1980. *PDL-24 User's Manual*. Providence, Rhode Island: Aeolian Kinetics Corp.
7. Software Corporation, Pawlet, Vermont.
8. *User's Manual*. Franklin Lakes, New Jersey: Disa Electronics. (Type 55D 80/81 Low Velocity Anemometer.)
9. Gioima, J.P.; Clower, C.A. 1981 (Nov.). "Instrumentation of a Passive Test Facility." *Passive Cooling: Proceedings of the International Passive/Hybrid Cooling Conference*. Edited by Arthur Bowen, Eugene Clark, and Kenneth Labs. Miami Beach, Florida; Nov. 6-16, 1981. Newark, Delaware: AS/ISES, University of Delaware; pp. 442-445.
10. Garbini, J.L.; Emery, A.F.; Heerwagen, D.R.; Kippenhan, C.J.; Down, R.J.; Johnson, B.R. 1981 (Sept.). "Design of a Moderate-Cost Microcomputer Data Acquisition System for Experimental Investigations of Thermal Systems." *Proceedings of the Sixth National Passive Solar Conference*. Edited by John Hayes and William Kolar. Portland, Oregon; Sept. 18-20, 1981. Newark, Delaware: AS/ISES, University of Delaware; pp. 195-199.
11. Sash, Roger D.; Hollingsworth, E.; Chen, B. 1979 (Oct.). "Low Cost and Reliable Microprocessor Based Data Acquisition Systems Applied to the Passive Solar Research Experiments at the University of Nebraska." *Proceedings of the Fourth National Passive Solar Conference*. Edited by Gregory Franta. Kansas City, Missouri; Oct. 3-5, 1979. Newark, Delaware: AS/ISES, University of Delaware; pp. 749-752.
12. Fowlkes, C.W. 1981 (Sept.). "Interfacing a $10 Calculator for Data Acquisition." *Proceedings of the Sixth National Passive Solar Conference*. Edited by John Hayes and William Kolar. Portland, Oregon; Sept. 18-20, 1981. Newark, Delaware: AS/ISES, University of Delaware; pp. 168-172.
13. Michels, T. 1978 (March). "A Low Cost Data Acquisition and Data Processing System." *Proceedings of the Second National Passive Solar Conference*. Edited by Don Prowler. Philadelphia, Pennsylvania; March 16-18, 1978. Newark, Delaware: AS/ISES, University of Delaware; pp. 452-456.

References 14-31 are all from the *Proceedings of the Conference on Performance Monitoring Techniques for Evaluation of Solar Heating and Cooling Systems*; Washington, D.C.: U.S. Department of Energy; April 3-4, 1978.

14. Woell, R.L. "Data Acquisition Using a Modular Data Logger." P. 61.
15. Trump, M. "Data Acquisition and Monitoring System for Los Alamos National Security and Resources Study Center." P. 69.
16. Murray, H.S.; Hedstrom, J.C. "On-Line Performance Calculations for the Los Alamos National Security and Resources Study Center." P. 75.
17. Richtmyer, T.E. "The Use of Computer-Controlled Data Acquisition Systems in Determining Solar Heating and Cooling System Performance." P. 95.
18. Potishnak, M.; Winn, C.B.; Lantz, L. "Relationship Between Instrumentation and Validation." P. 129.
19. Wildin, M.W.; Fong, A.; Nakos, J. "Use of an Automated, Centrally-Controlled Data Acquisition System for Monitoring Multiple Remote Sites." P. 149.
20. McClenahan, D. "The Advantages of a Real Time Data Acquisition, Monitoring, and Analysis System for a Restaurant Equipped for Energy Conservation, Heat Reclamation, and Solar Energy." P. 163.
21. Johnson, R. "A Moderate-Cost Data Gathering System." P. 173.
22. Moran, W.; Kouba, G.E. "A Microprocessor Based Solar Monitoring System." P. 183.
23. Kouba, G.E. "A Microprocessor Compatible Temperature Measuring System." P. 191.
24. Taylor, H.E. "A Microprocessor Monitoring System for a Solar Energy Installation." P. 197.
25. Higgins, J.H. "Design of the Data Acquisition System at Solar One." P. 207.
26. Schlag, J.H.; Sheppard, A.P.; Wood, J.M. "Low Cost Microprocessor Based Data Acquisition System." P. 219.
27. Hedstrom, J.C. "Data Acquisition and Processing with a HP 9825 Desk Top Calculator Controlled Instrumentation System in The Los Alamos Solar Mobile/Modular Home." P. 229.
28. Cummings, R.D.; Peck, D.J. "Low Cost Monitoring System." P. 241.
29. Whitehurst, B.M. "Simple, Low Cost Monitoring Methods for Solar Hot Water System." P. 259.
30. Russell, J. "Low-Cost Monitoring of Solar System Performance." P. 269.
31. Evans, R.D.; Greeley, D.; Martin, R. "An Inexpensive Multiplexer Temperature Measuring System for Monitoring and Evaluation of Solar Collectors." P. 327.

Windscreens in Radiant Cooling

By MARCO MOSTREL AND BARUCH GIVONI
The Jacob Blaustein Institute for Desert Research,
Ben-Gurion University of the Negev, Sede Boqer Campus, Israel

ABSTRACT

The effect of transparent polyethylene windscreens on radiant cooling systems is discussed. The effectiveness of single- versus double-covered radiators as well as the thickness and color of the polyethylene are also examined. Environmental considerations such as cloudiness and dew formation are analyzed with respect to windscreen performance.

INTRODUCTION

Windscreens are used in radiant cooling systems to reduce convective heat gain from the ambient air to the radiator. Since they must be infrared (IR) transparent, thin films of polyethylene, usually without ultraviolet (UV) inhibitors, are typically used for such windscreens. This material is commonly available, inexpensive, and about 70% transparent to IR radiation.

The application of polyethylene windscreens adds to the complexity and cost of a radiant cooling system for the following reasons:

- The polyethylene film must be held taut to minimize fluttering from wind. Such fluttering induces convective currents in the stagnant air layer between the radiating surface and the windscreen and thus reduces the insulating value of this air layer. Fluttering also rapidly produces structural fatigue in most films, causing material failure. To prevent this, a lattice can be constructed to support the polyethylene film. Other solutions include mounting the polyethylene in a warped plane and using the film as a tensile skin in air-pressured structures.
- During the day, the polyethylene must be shaded to prevent rapid deteriorization of the material and to avoid frequent replacements.
- The polyethylene film collects dust, thus reducing its transparency, and its regular cleaning is not an easy task.

Therefore, it is of interest to evaluate the real contribution of the windscreen to the performance of nocturnal radiators. In a preliminary study, it was observed that dew usually formed on the polyethylene, nullifying the difference in performance between an exposed radiator and a windscreened one.

The experiments performed between May 1981 and January 1982 and described in the following pages were intended to obtain additional data, with more detailed recording of the environmental conditions than in the preliminary study. This paper reviews the mathematical model used by the research team at Trinity University, San Antonio, Texas, for the prediction of radiator stagnation temperatures. Then, it summarizes the experimental study at the Sede Boqer campus of the Ben-Gurion University of the Negev. Finally, it compares the predicted temperatures of exposed and screened nocturnal radiators with the measured data.

THE MATHEMATICAL MODEL

The literature contains various prediction models for radiant cooling, a discussion of which can be found in Givoni's review paper.[1] All are static models predicting the net outgoing radiation and the radiator stagnation temperature for given meteorological data (that is, dry bulb and wet bulb temperatures, cloudiness, and wind velocity). Only one of the models[2] takes into account the effects of windscreening or dew formation. This paper will investigate how windscreening affects absorbed,

Drawings are by Paul David Glosniak of Arizona State University

emitted, and convective radiation. Dew formation is discussed here only as it pertains to the performance of windscreens. An in-depth discussion of dew formation is reserved for a later paper.

Below is a summary of the empirical formulas used in the model proposed by research teams at Trinity University.[3,4] A sketch of the heat transfer paths taking place is shown in Fig. 1.

The sky emissivity, ϵ_s, is one way of specifying the amount of sky radiation:[3,4]

$$\epsilon_s = 0.787 + 0.0028\, T_{dp}\ (°C). \tag{1}$$

Clark and Allen[3] relate the cloudiness coefficient, C_a, to the cloudiness level (in tenths) by the following formula:

$$C_a = 1 + 0.0224n - 0.0035n^2 + 0.00028n^3. \tag{2}$$

The sky temperature is then defined by Clark and Berdahl[4] in the following equations:

Clear sky temperature:

$$T_{clear\ sky}\ (K) = (\epsilon_s)^{1/4} \cdot T_a\ (K) \tag{3}$$

Cloudy sky temperature:

$$T_{cloudy\ sky}\ (K) = (C_a)^{1/4} \cdot T_{clear\ sky}. \tag{4}$$

Incoming Sky Radiation

The incoming sky radiation is determined by the following equation which uses the Stefan-Boltzmann constant:[4]

$$R_{sky} = \sigma\, T_{sky}^{\ 4}$$

where the Stefan-Boltzmann constant is:

0.488×10^{-8} kcal/m^2 h K^4, in metric units,
0.1714×10^{-8} Btu/ft^2 h R^4, in English units,
0.56697×10^{-8} W/m^2 K^4, in SI units.

Net Outgoing Radiation

The net outgoing radiation is the balance between the part of the incoming radiation absorbed, R_{abs}, by the radiator and the radiation emitted, R_{emit}, by it.

For a radiator, an emissivity, ϵ_r, at the stagnation temperature, T_r, and covered with a windscreening system of transparency, trans, the expressions of R_{abs} and R_{emit} are as follows:

$$R_{abs} = \epsilon_r \cdot \text{trans} \cdot R_{sky} \tag{5}$$

$$R_{emit} = \epsilon_r \cdot \text{trans} \cdot \sigma \cdot T_r^{\ 4}\ . \tag{6}$$

Thus, net outgoing radiation, R_{net}, is:

$$R_{net} = R_{emit} - R_{abs} = \epsilon_r \cdot \text{trans} \cdot \sigma \cdot (T_r^{\ 4} - C_a \cdot T_{clear\ sky}^{\ 4}). \tag{7}$$

Clark and Allen[3] introduce another cloudiness coefficient:

$$C_n = 1 - 0.056n \tag{8}$$

which can be used directly to compute R_{net} as follows:

$$R_{net} = C_n \cdot R_{net/clear\ sky} \tag{9}$$

where

$$R_{net/clear\ sky} = \epsilon_r \cdot \text{trans} \cdot \sigma \cdot (T_r^{\ 4} - T_{clear\ sky}^{\ 4}). \tag{10}$$

By linearization, since $T_r - T_{sky} << T_{sky}$ (in kelvins), one obtains the following approximation for R_{net}, expressed in W/m^2 (SI units):

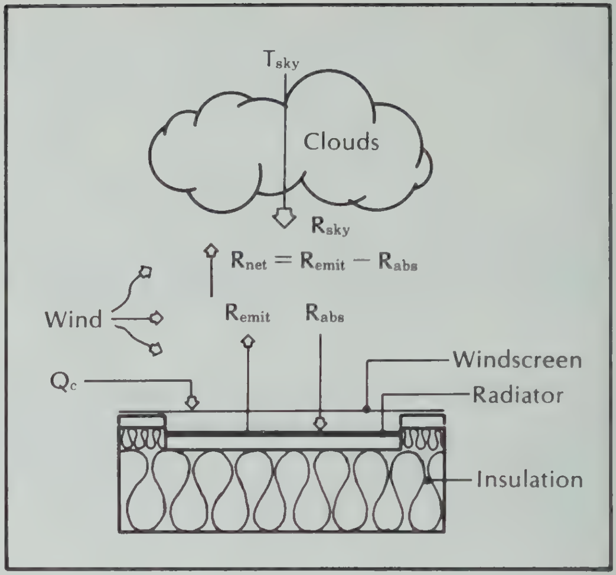

Figure 1: A schematic diagram indicates the heat transfer paths of nocturnal radiant cooling. Mathematical models examine their relationships.

$$R_{net} = C_n \cdot \text{trans} \cdot \epsilon_r \cdot 0.544 \cdot (T_r - T_{sky})\ (°C). \tag{11}$$

Convective Heat Intrusion

As soon as the radiator reaches temperatures below the ambient air temperature, T_a, the wind carries heat into the system by convection. This heat is quantified by the equation:

$$Q_c = h_c\, (T_a - T_r)\ (°C). \tag{12}$$

Various convective heat transfer coefficients can be found in the literature on radiant cooling. The effect of windscreening on reducing the convective heat intrusion can be taken into account in the expression of h_c. A comparison of the various models proposed for h_c of exposed radiators is shown in Fig. 2.

The following formulas for h_c are suggested by various authors and are given in SI unit (W/m^2 K), where the wind speed is given in km/h:

(A) Bainbridge[5]
  $h_c = 5.6 + 1.1v$
  for $v < 18$
(B) Clark and Berdahl[4]
  $h_c = 2.8 + 1.1v$
  for $5 < v < 16$
(C) Duffie and Beckmann[6]
  $h_c = 5.7 + 1.1v$
(D) Hansen and Yellott[7]
  Yellott[8]
  $h_c = 5.7 + 1.2v$
(E) Givoni[9]
  $h_c = 0.6 + 3.5\sqrt{v}$
  for an exposed radiator
  $h_c = 0.5 + 1.2\sqrt{v}$
  for a single-covered radiator
  $h_c = 0.3 + 0.8\sqrt{v}$
  for a double-covered radiator

(F) Givoni[1]

$$h_c = 1.2 + 2.7\ v^{3/4}$$

for an exposed radiator

$$h_c \text{ single-covered} = 0.4 \cdot h_c.$$

Equation (E) is used in the mathematical model that we chose to compare the predicted and measured stagnation temperatures of the radiator.

Stagnation Temperature

By writing the heat equation balance

$$R_{net} = Q_c,$$

one can find an expression for the radiator's stagnation temperature in °C:

$$T_r = \frac{0.544 \cdot C_n \cdot \text{trans} \cdot \epsilon_r \cdot T_{clear\ sky} + h_c \cdot T_a}{0.544 \cdot C_n \cdot \text{trans} \cdot \epsilon_r + h_c}$$

where h_c is in W/m^2 K and $T_{clear\ sky}$ and T_a are in °C.

THE EXPERIMENTAL SETUP

The radiators were made of 450 x 450 mm (*17.7 x 17.7 in.*), thin, painted iron plates. The plates were insulated by 10-cm (*3.9-in.*) -thick slabs of expanded polystyrene on the sides and bottom. An air space of 1 cm (*0.39 in.*) was left between the plate and the bottom insulation. Thermocouples were attached to the top and bottom of the plates. The plates were exposed to the sky.

The windscreens consisted of either one or two layers of polyethylene film, the first stretched taut 3 cm (*1.18 in.*) above the radiating plate and the second (when used) 2 cm (*0.78 in.*) above the first.

Six radiant-cooling test cells were placed on the roof of our laboratory at the Solar Building and Energy Conservation Unit and monitored.

THE DATA ACQUISITION SYSTEM

Temperature measurements were taken with copper-constantan thermocouples. Wind velocity was measured with a three-cup anemometer at the Desert Meteorology Unit located about 50 m (*164 ft*) from the Solar Building. Since the experimental field of the Meteorology Unit is less sheltered than ours, the measurements obtained can only indicate wind conditions.

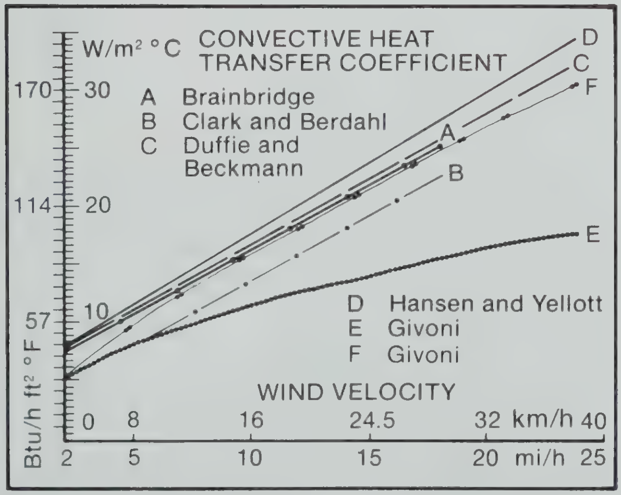

Figure 2: This graph compares the different models proposed for the convective heat transfer coefficient.

Nomenclature

C_a and C_n	= cloud correction factors.
F	= flow rate of radiator.
h_c	= convective coefficient.
Q_c	= convective heat exchange with ambient air.
R_{abs}	= absorbed sky radiation.
R_{emit}	= emitted radiation.
R_{net}	= net radiant heat loss of a radiator.
R_{sky}	= atmospheric incoming radiation.
T	= temperature of radiator.
T_a	= temperature of ambient air.
$T_{clear\ sky}$	= clear sky temperature.
$T_{cloudy\ sky}$	= cloudy sky temperature.
T_{dp}	= ambient dew point temperature.
T_{out}	= air outlet temperature.
trans	= transparency of windscreen.
T_{sky}	= effective sky temperature.
σ	= Stefan-Boltzmann constant, the ratio of the emissive power of a blackbody per unit of area and time to the absolute temperature of the body.
ϵ_s	= variable sky emissivity.

During the preliminary experiments, temperature data were recorded continuously on a Chino chart recorder. The cumulative maximal error of the temperature data, due to thermocouple intrinsic error and reading error, is evaluated at less than 1.5°C (*2.7°F*).

In the next stage, the thermocouples were connected to an Accurex Autodata Ten data logger. All channels were scanned once a minute. Temperature data were recorded by hourly averages, computed by the data logger every hour throughout the night, and then sent automatically into a Superbrain microcomputer with 64K-byte memory (Intertec Data System) through an RS-232C interfacing cable. Storage for the Superbrain was effected on a 162K-byte floppy diskette. In every experiment, the data were processed each half-hour by the FANCY RADCOOL program, written especially for this project by Marco Mostrel. The error of the temperature measurements at this stage of the experiments is evaluated at less than 1°C (*1.8°F*).

THE SEQUENCE OF THE EXPERIMENTS

Miscellaneous Experiments

One-half-mm-, 1-mm-, and 2-mm-thick, white, painted iron plates were tested between May 14 and June 14, 1981. Thermocouples were placed above and below the plates at their centers. For the

0.5-mm (*0.02-in.*) plate, the difference was found to be, at most, 0.5°C (*0.9°F*). For the 2-mm (*0.08-in.*) plate, the difference between the temperatures above and below was found to be, at most, 2°C (*3.6°F*), reflecting the heat capacity effect.

Two 0.5-mm (*0.2-in.*) -thick iron plates were tested between June 15 and 30, 1981, one painted white, the other black. Measurements of the temperature below the plates at their centers were taken at night, beginning two hours after sunset and ending one hour before sunrise. No significant difference in the temperature behavior of the two plates was found, because most commercially available paints have the same IR absorptivity-emissivity (about 90%).

Preliminary Experiments

In July and August 1981, the influence of a windscreen was tested on two, 2-mm (*0.08-in.*) -thick iron plates painted white. One of the plates was covered with a 100-micron, transparent polyethylene film, stretched taut over the wooden frame of the windscreen.

The potential for radiant cooling was assessed over the 60 nights of recorded data for these two summer months; it appeared that the average of the maximal depression between the ambient air temperature and the radiant temperature was 6°C (*10.8°F*) for the exposed radiator and 8.5°C (*15.3°F*) for the windscreened radiator.

The exposed radiator temperature was found to reach, at most, an average of 4°C (*7.2°F*) below the calculated dew point temperature. This average maximal depression was 5.5°C (*9.9°F*) for the windscreened radiator.

Passing clouds were observed only on a few nights. Nevertheless, a simple pattern was deduced from these observations: clouds stop the net outgoing radiation and, thus, reduce a rise in the temperatures of both exposed and windscreened radiators. These results were readily confirmed by the analysis of temperature graphs from further experiments.

The preliminary experiments also showed the effect of increasing humidity during the night and the nocturnal change in cooling pattern as soon as moisture forms on the surface of the radiator, the windscreen, or both. Visual checks of the time when dew formed corroborated our initial assumption that dew caused the observed change in the rate of decrease of the radiator temperature. This decrease appeared to be significantly more important for a windscreened radiator, because dew changes the spectral properties of the polyethylene and transforms it into an opaque film for IR radiation.

Main Experiments

Three sets of tests were performed on 0.5-mm (*0.02-in.*) -thick galvanized iron plates painted with white spray paint. The first set studied the influence of an additional windscreen on the cooling pattern. The second and third dealt with the influence of the type of windscreen used, that is, thickness and color. The FANCY RADCOOL program was used to graph temperature patterns throughout the night and included a sketch of the wind velocity. Hourly average data were processed rather than instantaneous values.

Between September 15 and December 15, 1981, three radiators were monitored: one exposed directly to the sky, the second covered by a film of 100-micron, transparent, polyethylene film, and the third covered by two films of the same polyethylene. Cooling was found to be least efficient for the exposed radiator and most efficient for the single-covered radiator, with the double-covered radiator falling in between. During periods of high humidity, the three radiators reached about the same temperatures, indicating that windscreening would not increase the cooling effect in very humid climates.

During the second and third sets of tests—December 17, 1981 to January 23, 1982—it was first determined that the color of the polyethylene film had no influence on the radiator temperature pattern, presumably because it does not affect the IR transparency of the polyethylene. Three 60-micron polyethylene layers—one transparent, one blue, one white—demonstrated the same performance. Then, three thermocouples were placed at different points below the plates: in the center, in the diagonal corner, and in between these two locations. It was found that the temperature distribution on the plates was uniform except at its ends. Consequently, it appeared that even a single measurement point at the center of the plate could represent it in heat flux analyses.

Later, five radiators were monitored. One was exposed directly to the sun, while a second was single-covered, and a third double-covered, the latter two with 60-micron polyethylene windscreens. Two additional radiators were single- and double-covered with 100-micron polyethylene windscreens. More efficient cooling was realized with the thinner film.

DATA ANALYSIS

Typical Patterns under Different Weather Conditions

Figures 3 through 6 show the temperature patterns of the exposed and the windscreened radiators under different conditions of ambient humidity, cloudiness, and wind velocity. In each of these figures, the following temperatures are shown:

- ambient air, T_a;
- ambient wet bulb, T_{wb};
- computed dew point, T_{dp};
- surface of the exposed radiator;
- surface of the windscreened radiators.

Dry, Clear Nights

The temperatures of the two windscreened radiators (single- and double-covered) on dry, clear nights (see Fig. 3) were significantly lower than those of the exposed one throughout the night. Typical depressions below the ambient air temperature for the exposed radiator were about 4° to 5°C (*7.2° to 9°F*) when the wind was blowing (until 9:00 p.m.) and 6° to 8°C (*10.8° to 14.4°F*) when the wind calmed down (from 9:00 p.m. on). For the covered radiators, the depressions were about 9° to 11°C (*16.2° to 19.8°F*) throughout the night. Such a pattern was observed in only 5% of the entire testing period.

Dry Nights with Passing Clouds

The temperature of the windscreened radiator on dry nights with passing clouds (see Fig. 4) was again significantly lower than that of the exposed one throughout the night. For the exposed radiator, the depression below the ambient air temperature increased as the wind velocity decreased, from about 2°C (*3.6°F*) at the beginning of the night to about 4.5°C (*8.7°F*) at the end of the night, except for two noticeable periods (at around 12:30 a.m. and 2:30 a.m.) when passing clouds covered the sky. At that time, an abrupt elevation of the radiator's temperature was observed. For the windscreened radiator, the depression below the ambient air remained constant at about 6° to 7°C (*10.8° to 12.6°F*) throughout the night, except for the two periods mentioned above, when abrupt elevation of the temperature occurred. Thus, both the exposed and the covered radiators were less

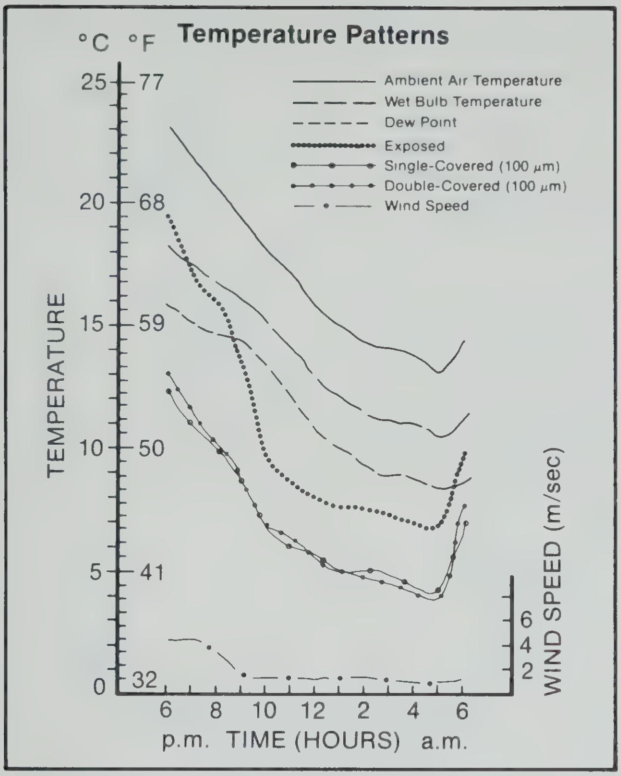

Figure 3: The graph of the night of October 13-14, 1981, compares the temperature patterns of exposed, single-covered, and double-covered radiators on a dry, clear night. The temperatures of the windscreened radiators were lower than the exposed radiator's temperature.

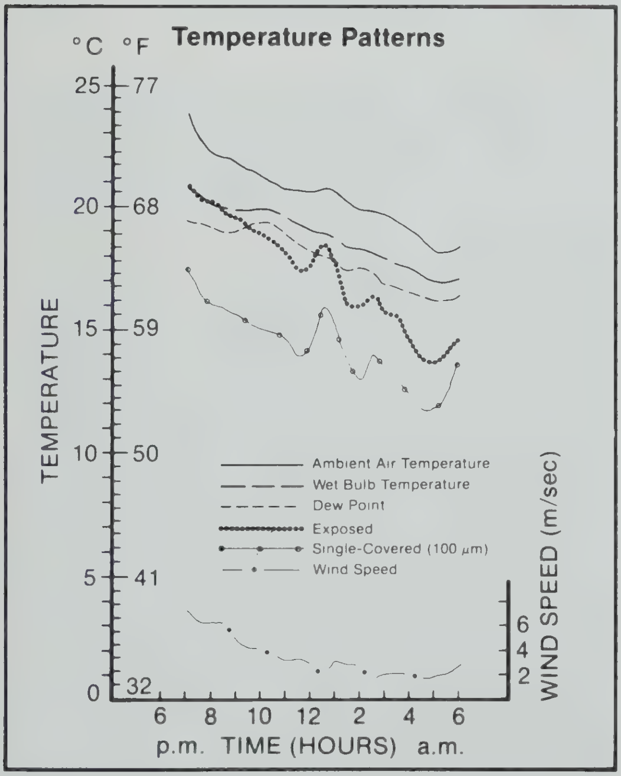

Figure 4: A graph of the dry, cloudy night of August 28-29, 1981, compares the effect of cloudiness on an exposed and a covered radiator. The temperature of the windscreened radiator again was lower than that of the exposed one.

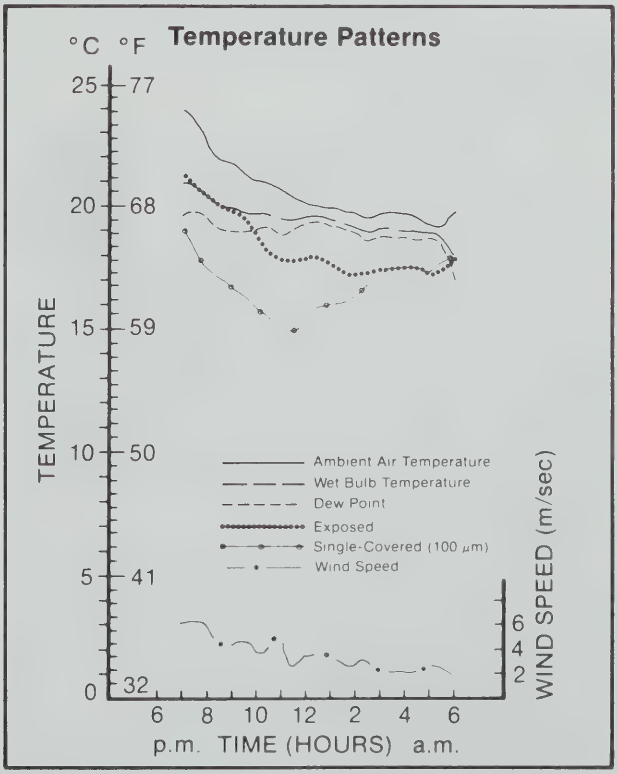

Figure 5: Dew formation does affect the performance of a windscreened radiator. The humid, clear night of August 1-2, 1981, shows that three hours after dew formed on the windscreen the radiator's temperature was the same as the exposed radiator's temperature.

effective on cloudy nights than on clear nights. Such cloudy, but dry, conditions occurred on about 10% of the testing nights.

Humid, Clear Nights

Until about 11:30 p.m., the temperature patterns of both the exposed and the covered radiators on humid, clear nights (see Fig. 5) were approximately parallel to the decrease of the ambient air temperature. At about 11:30 p.m., dew formed on the polyethylene film of the windscreened radiator. The temperature of this radiator then rose sharply, reaching the temperature of the exposed one after a time lag of about three hours. The slight fluctuations in the depression of the exposed radiator temperature below that of the ambient air (at 9:00 p.m., 11:30 p.m., and 2:30 a.m., approximately) are due to variations in the wind velocity.

Humid Nights with Passing Clouds

The pattern for humid nights with passing clouds (see Fig. 6) is similar to that for humid, clear nights. Dew formed around 10:30 p.m., and, after a time lag of one and one-half hours, both the exposed and the covered radiators reached the same temperature. Between 2:30 and 5:00 a.m., large cloud formations caused the radiators' temperatures to rise. The patterns described in this and the preceding paragraph are typical of dew formation and were observed in roughly 85% of the testing period.

DISCUSSION OF THE RESULTS

Dew Formation

The chief element related to the design of the radiant system which negatively affects the radiant cooling of the windscreened radiator is the formation of dew. It was concluded from the observations that dew formation caused the rise in radiator temperature at some stage of the night. A sharp rise in the windscreened radiator's temperature can be observed from the moment when droplets of dew form on the polyethylene. Eventually, the windscreened radiator's temperature reaches that of the exposed radiator after a time lag evaluated to be between one and three hours. A more elaborate attempt to predict the duration of this time lag will be made in the future.

It appears from these observations that windscreening the radiators becomes ineffective in humid weather. The advantages of windscreening are lost when the polyethylene film is covered with dew. Then, the film itself becomes the radiator and behaves nearly like the exposed plate.

Figure 7 shows that dew forms at about the same time on the polyethylene of both the single- and double-screened radiators and that the time lag is about the same in either case.

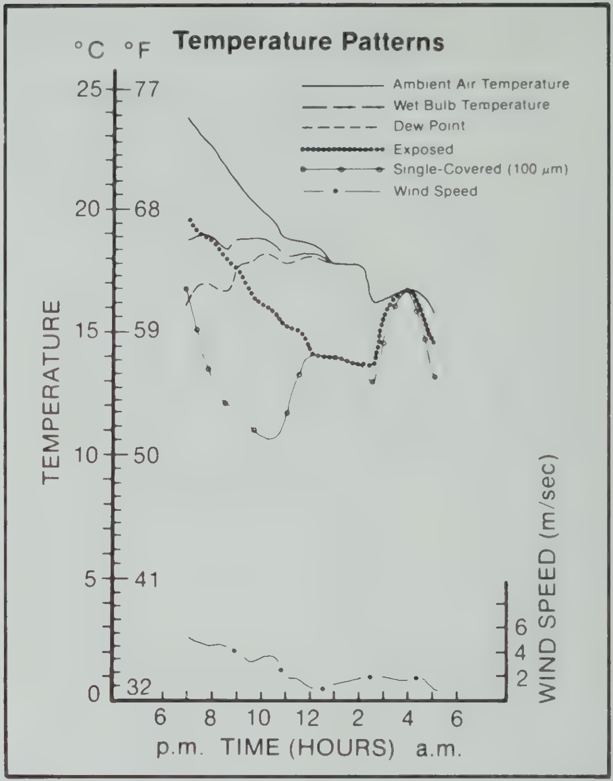

Figure 6: The night of July 12-13, 1981, was humid and cloudy. This graph shows the combined effects of dew formation and cloudiness on an exposed and a covered radiator. After a time lag of one and one-half hours, the temperature of the windscreened radiator reached that of the exposed radiator.

Dew formation depends, of course, on the climatic conditions. To prevent it, the difference between the air and the dew point temperatures should be greater than the drop of the radiator's temperature below that of the ambient air. However, quantitative determination of the combinations of air temperature, humidity, wind speed, and cloud cover when dew starts to form requires more research.

Effect of Windscreening

Windscreening radiators significantly reduces the intrusion of heat by convection. The polyethylene film reduces the wind-driven transfer of heat from the warmer ambient air to the cooler radiator. However, this favorable effect on limiting the convective heat gain of the radiator is counteracted by the reduction of the net outgoing radiation caused by the partial opacity of polyethylene (70% transparency for a single cover, 60% for a double). Evidence of the "wind-stop" effect of windscreening can be seen in the radiator temperature-versus-time graphs. When the wind is blowing and before dew forms, the curve corresponding to the exposed radiator has a slope greater than that of the curve corresponding to the ambient air; however, the curve corresponding to the single- or double-covered radiator has a slope equal to that of the curve corresponding to the ambient air (see Figs. 3, 7, and 8). It is indeed reasonable to infer, as one reviewer pointed out, that because wind speed is strong in the early evening and subsides gradually towards

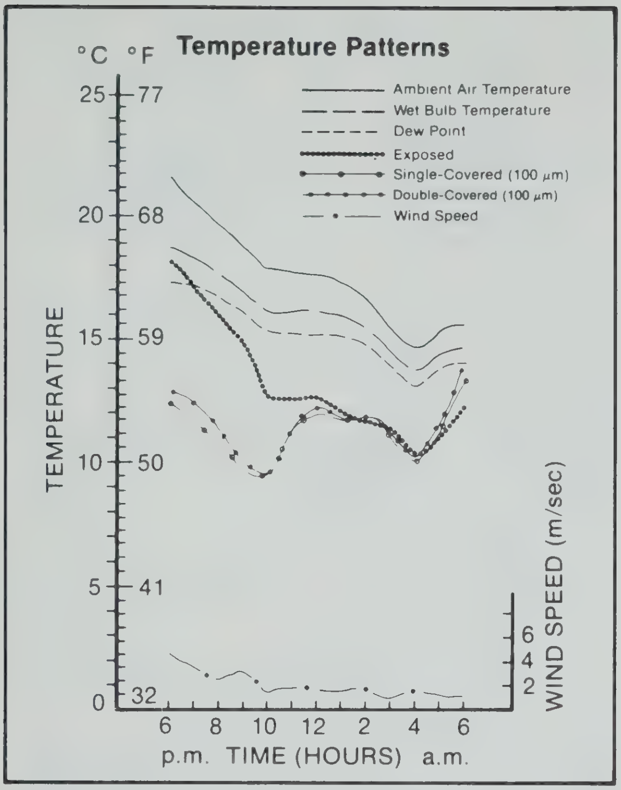

Figure 7: The time lag between dew formation and when the windscreened radiators' and the exposed radiator's temperatures are equal is the same for both single- and double-covered radiators. The night of October 11-12, 1981, also illustrates that dew forms on both of the covered radiators at about the same time.

10 p.m., a change is reflected in the respective temperature patterns of the two radiators.

Single Windscreening Versus Double Windscreening

The effect of the number of windscreens was investigated with polyethylene of different thicknesses: 60 and 100 microns. According to the results obtained for both 60- and 100-micron polyethylene films, a second layer of polyethylene adversely affects the net heat loss (see Fig. 8). Although the second windscreen eliminates wind-driven intrusion of the warmer ambient air and the fluttering of the first windscreen, it apparently also reduces the IR radiation exchange between the sky and the radiator, thus reducing the overall cooling effect. Therefore, maximum net cooling is achieved when a single polyethylene windscreen is used.

Thickness of Polyethylene

In Fig. 8, the influence of the thickness of polyethylene on the effect of windscreening is illustrated. Of the two double-covered radiators, the one covered with 60-micron films was cooled between 1° and 3°C (*1.8° and 5.4°F*) lower than the one covered with 100-micron films; of the two single-covered radiators, the one covered with 60-micron polyethylene was also cooled between 1° and 3°C (*1.8° and 5.4°F*) lower than the one with 100-micron film. Apparently, transparency of polyethylene is a function of its thickness.

Figure 8 also indicates that the thickness of the polyethylene does not affect the time when dew forms (around 7:00 to 8:00 p.m.), but does affect the time lag of the temperature increases.

Effect of Cloudiness

Cloudiness affects the IR radiation exchange between the radiator and the sky by reducing the intensity of the radiation fluxes going each way by the same attenuating factor. The result is a reduction of the net outgoing radiation and a rise in the radiator temperature, whether it is windscreened or not. In Fig. 4, passing clouds occurred between 11:30 p.m. and 4:30 a.m. Greater cloudiness was present between 11:30 p.m. and 2:00 a.m. than between 2:00 a.m. and 4:30 a.m., as demonstrated by the larger rise in temperature of both the windscreened and the exposed radiators during the first period than during the second one. Figure 6 shows that complete overcast between 2:30 and 5:30 a.m. eliminated almost all cooling of both the exposed radiator and the (dew-covered) windscreened one; at 4:00 a.m., the temperatures of both radiators reached that of the ambient air.

Influence of Other Factors

Dust that accumulates on the windscreens reduces the polyethylene transparency. However, the

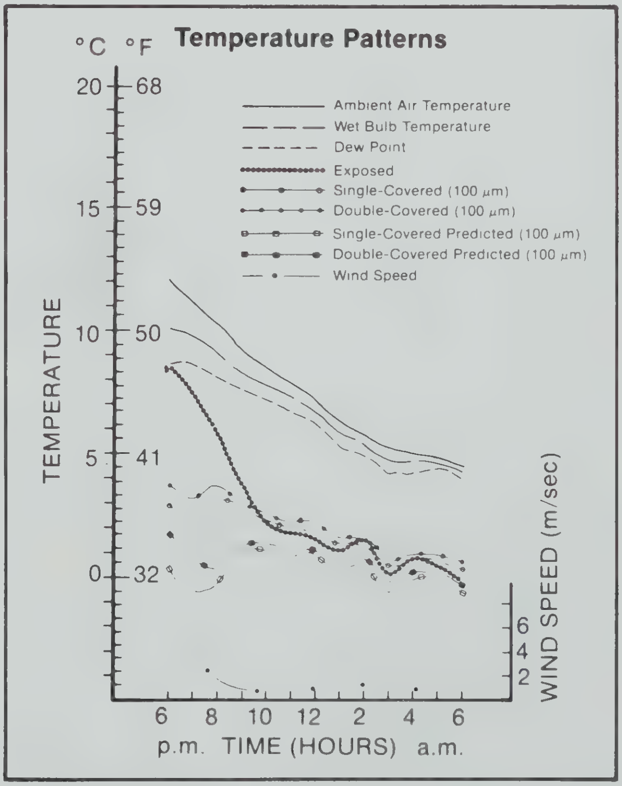

Figure 8: The night of January 11-12, 1982, illustrates that the thickness of the polyethylene windscreens does not affect the time when dew forms, but it does affect the time lag of the temperature increase. The thinner windscreen was more effective than the thicker.

effect of dust was not investigated and will be studied in the continuation of this project. Rain and wind affect, in the long run, the tightness of the windscreen stretching. One way to avoid the rupturing of the polyethylene film and its fluttering in roof-size applications is to stretch the polyethylene over a small-mesh, metal net. Sealing the windscreen onto the support of the radiator—to avoid air infiltration—is also required.

Factors without Apparent Effect

The color of the radiator and the windscreen does not seem to affect any of the cooling patterns described, since most commercially available paints are about 90% black in the infrared range, and the color of polyethylene does not affect its transparency to IR radiation. Thus, the radiating plate and windscreen colors are irrelevant. During the daytime, the color of the radiator would have tremendous effect on its temperature, but it is, of course, covered during these hours.

COMPARISON BETWEEN PREDICTED AND MEASURED DATA

From our data analysis, it appears that dew formation on windscreened radiators affects their temperature patterns in a significant way. In order to interpret this physical phenomenon and to formulate its effect on the radiator's stagnation temperature, the data computed with the mathematical model presented above was compared to our measured data. The sole purpose of this study was to show that dew formation has to be included in the prediction models in order to match experimental results. No validation of the models has been attempted for these reasons:

- wind measurements for the experiments described in this paper were inaccurate;
- no cloudiness measurements were available;
- no measurement of the transparency of the polyethylene films used as windscreens has been done;
- none of the formulas proposed for the convective heat transfer coefficient, h_c, of windscreened radiators has been validated.

The comparison between predicted and measured radiator stagnation temperatures used the following assumptions in the computations:

- a clear sky throughout the night;
- a transparency of 70% for a one-cover windscreening system and of 60% for a two-cover system, since the polyethylene film used was 100-microns thick.

RESULTS OBTAINED

Figures 9 through 12 show the superposition of predicted and measured temperature patterns for an exposed, a single-covered, and a double-covered radiator, using windscreens made of 100-micron-thick, transparent, polyethylene film. Also shown on the temperature-versus-time graphs are:

- measured ambient air temperature, T_a;
- measured wet bulb ambient temperature, T_{wb};
- measured wind speed.

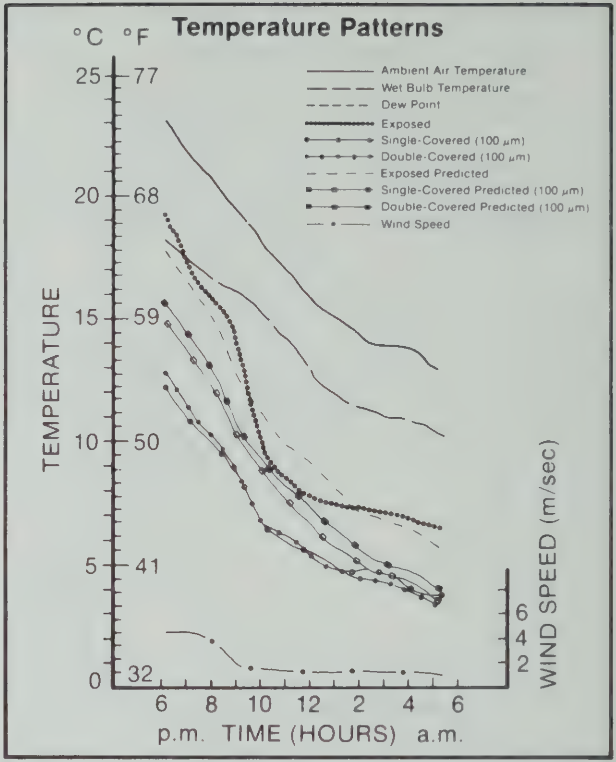

Figure 9: The predicted and the measured temperature patterns for the dry, clear night of October 13-14, 1981, are very similar.

Dry, Clear Nights

For the exposed radiator on dry, clear nights (see Fig. 9), the predicted and the measured temperature patterns are similar, with a maximal discrepancy of 2.7°C (*4.9°F*) between 12:00 and 1:00 a.m. Since the wind speed reached low values after 9:00 p.m., the single- and the double-covered radiators reached about the same temperature throughout the night. Figure 9 shows these results for both the predicted and measured temperature patterns. The predicted data are above the measured data throughout the night. The difference between the predicted and measured data decreases throughout the night, however, from 2° to 3°C (*3.6° to 5.4°F*) at the beginning to 0° to 0.5°C (*0° to 0.9°F*) at the end.

Dry Nights with Passing Clouds

The temperature pattern for an exposed radiator on dry nights with passing clouds (see Fig. 10) is similar to that for dry, clear nights, except for the period after midnight. The maximal discrepancy between predicted and measured data for the exposed radiator is 1.4°C (*2.5°F*) between 12:00 and 1:00 a.m.

No significant difference between the temperature of the single-covered radiator and that of the double-covered occurs throughout the dry, cloudy

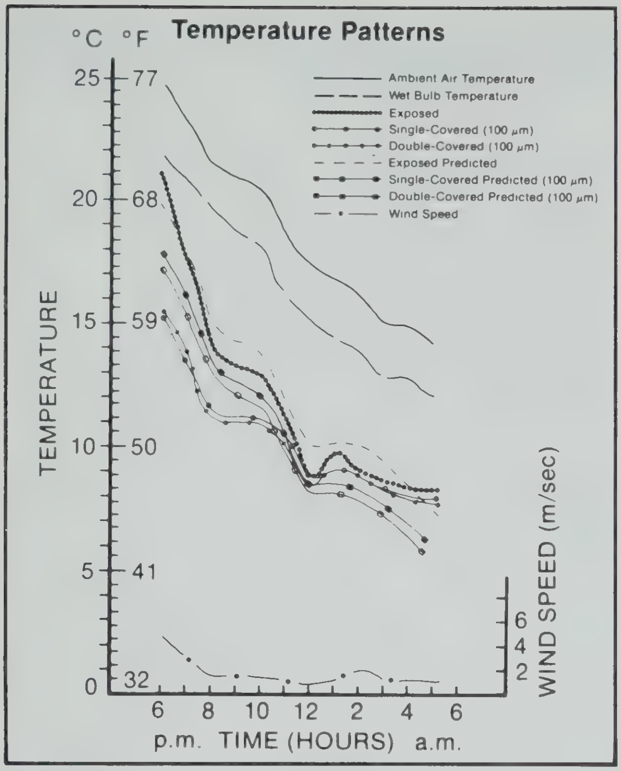

Figure 10: On the dry, cloudy night of October 17-18, 1981, the difference between the predicted and measured temperatures of single- and double-covered radiators was not significant.

night, either in the predicted or the measured pattern. After midnight, a rise in the measured, but not in the predicted, temperature patterns can be seen for all three radiators. This difference is a result of clouds passing by, thereby affecting the IR radiation exchange between the radiators and the sky. For the period ending at midnight, the difference between predicted and measured data decreases from between 1.5° and 2.6°, to 0°C (*2.7° and 4.7° to 0°F*).

Humid, Clear Nights

The nocturnal radiator temperature patterns for humid, clear nights (see Fig. 11) are similar to those for dry, clear nights (see Fig. 9), until dew forms at 10:00 - 11:00 p.m. For the exposed radiator, the predicted and the measured temperature patterns have the same shape, with a maximal discrepancy of about 2.3°C (*4.1°F*). For the single- and the double-covered radiators, the predicted and the measured temperature patterns show little difference because of low wind speed. After dew forms, however, the picture is significantly different from that corresponding to a dry night. For the exposed radiator, the predicted temperature pattern roughly follows the measured one, with a maximal discrepancy of 2.6°C (*4.7°F*). However, for the windscreened radiators, the predicted temperature patterns do not exhibit the sharp rise observed for the measured ones, a rise caused by dew formation.

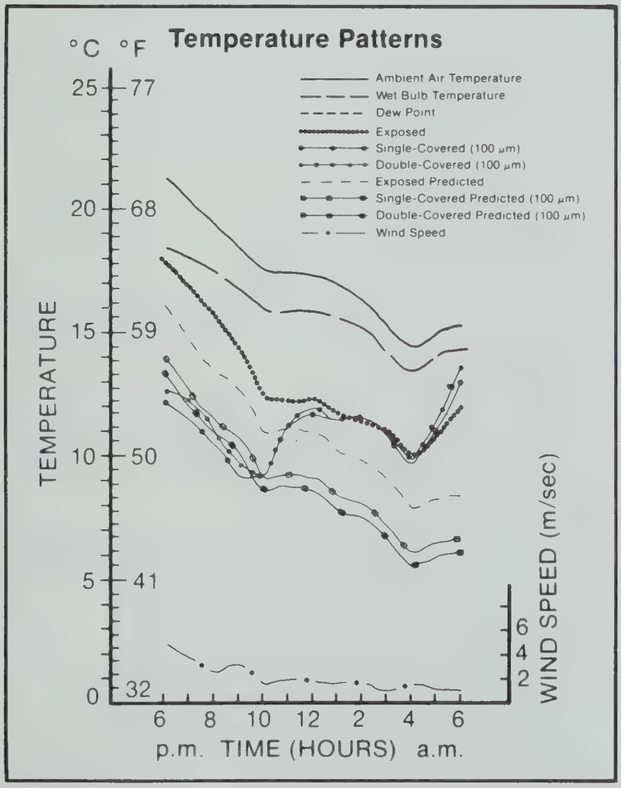

Figure 11: Humid, clear nights, such as the evening of October 11-12, 1981, affect predicted and measured results of windscreened radiators. After dew forms, the measured patterns exhibit a sharp rise not anticipated in the predicted patterns.

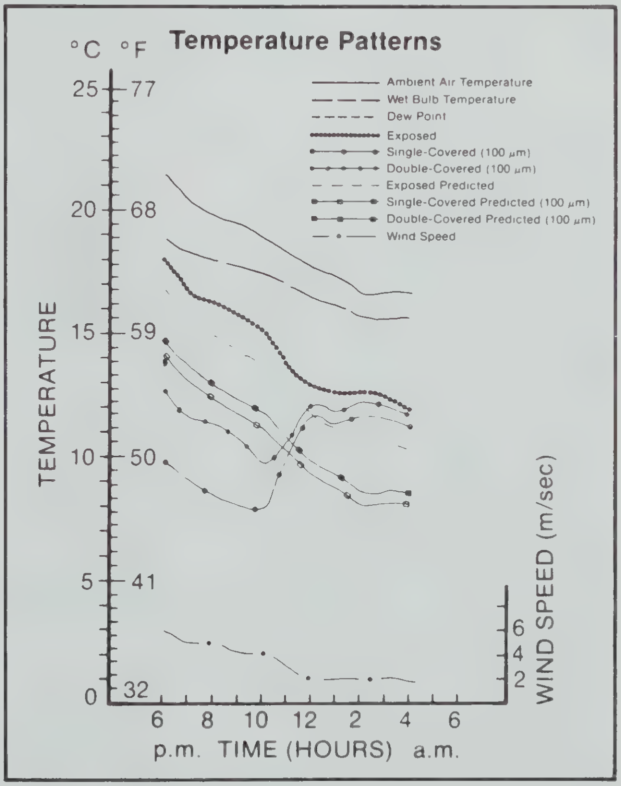

Figure 12: On September 18-19, 1981, a humid, cloudy night, wind speed affected the difference between the double- and single-covered windscreens. The double-covered radiator's predicted temperature was 6°C (*10.8°F*) higher than that of the single-covered's predicted temperature, until around midnight.

Humid Nights with Passing Clouds

The temperature patterns for humid nights with passing clouds (see Fig. 12) are similar to those for humid, clear nights (see Fig. 11). In this case, dew forms between 10:00 and 11:00 p.m. After that time, the predicted temperature patterns for both windscreened radiators do not follow the measured ones, and no sharp temperature increases are observed. The predicted temperature pattern for the exposed radiator roughly follows the measured one, with a discrepancy ranging from 1° to 1.5°C (*1.8° to 2.7°F*).

However, on a humid night with passing clouds, differences in temperature patterns can be noted. Until about midnight, the measured temperature of the double-covered radiator reaches 2° to 3°C (*3.6° to 5.4°F*) above the measured temperature of the covered radiators. The predicted temperature of the double-covered radiator reaches 0.6°C (*1.1°F*) above the predicted temperature of the single-covered radiator, because the wind speed for this period is higher than that for dry, clear nights or for dry nights with passing clouds.

After midnight, this pattern becomes less pronounced, but the influence of passing clouds can be seen. Between 2:00 and 5:00 a.m., the maximal discrepancy between predicted and measured data for the exposed radiator ranges from 1.6° to 2.2°C (*2.9° to 4°F*) and varies from 1° to 1.5°C (*1.8° to 2.7°F*) for the rest of the night. For the windscreened radiators, temperature increases can be seen in the measured temperature pattern, but not in the predicted one.

CONCLUSIONS

Dew Formation

When dew forms on the windscreens of the covered radiators, the radiators' temperatures rise noticeably. Yet, the predicted temperature patterns for humid, clear nights and for humid, cloudy nights did not anticipate such an increase.

Wind-Driven (Convective) Heat Gain

For dry, clear nights and for humid, clear nights, the measured temperature patterns differed from the predicted results only slightly. The exposed radiator had a maximal discrepancy of 3°C (*5.4°F*) and the covered radiators, as long as dew did not form and the wind speed was low, had a maximal discrepancy of 3°C (*5.4°F*). The predicted data were usually above the measured data.

On humid, cloudy nights, for the period preceding the formation of dew, it is seen that, for moderately high wind speeds, the shape of the windscreened radiator temperature pattern is correctly predicted, although the range is not.

Cloudiness

This study demonstrated that the effect of cloudiness on the radiator stagnation temperature is significant. However, no cloudiness measurements were available for the experiments desribed in this paper, and the cloud cover was evaluated visually. Therefore, no quantitative conclusion regarding the cloudiness coefficient used in the mathematical model for the prediction of the radiator stagnation temperature can be made here.

Under stagnation conditions, the temperature of a nocturnal radiating plate can reach more than 10°C (*18°F*) below ambient air, because, at night, the net balance of radiation being transferred to and from the plate is positive. Clear skies, still air, and dry weather increase the net outgoing radiation. Cloudiness reduces the net heat loss, so the effectiveness of radiant cooling is greatly diminished in regions which are cloudy at night.

The intrusion of wind-driven heat can be reduced significantly by covering the radiator system with windscreening of polyethylene film, the best results occurring when the thinnest-possible, single layer of polyethylene is used. However, windscreened radiators provide more cooling than exposed ones only so long as dew does not form on the film. When dew does form, after a short time lag, both exposed and windscreened radiators follow similar temperature patterns. Thus, the dew nullifies the favorable effect of windscreening and becomes the controlling factor in design.

The existing mathematical models for predicting radiator stagnation temperature do not fit the experimental results obtained for windscreened radiators, because they do not address the effect of dew formation. These models must be modified to include the influence of dew on the heat transfer processes, if they are to predict correctly the stagnation temperature of a nocturnal radiator.

REFERENCES

1. Givoni, B. 1982. "Cooling by Longwave Radiation." *Passive Solar Journal.* Vol. 1 (No. 1): pp. 131-150.
2. Blanpied, M. 1979 (Oct.). "A Model of Radiative Cooling Using Infrared Transparent Windscreens." Research Paper. Trinity University, San Antonio, Tex.
3. Clark, E. and Allen, C. 1978. "The Estimation of Atmospheric Radiation for Clear and Cloudy Skies." *Proceedings of the Second National Passive Solar Conference.* 2.2. Edited by Don Prowler. Philadelphia, Penn.; March 16-18, 1978. Newark, Del.: AS/ISES, p. 167.
4. Clark, E. and Berdahl, P. 1981. "Radiative Cooling: Resource and Applications. *Passive Cooling Handbook: Proceedings of the Fifth National Passive Solar Conference.* Edited by Harry Miller. Amherst, Mass.; Oct. 20, 1980. Berkeley, Calif.: Center for Energy Efficient Design, pp. 177-212.
5. Bainbridge, D.A. 1978. "Natural Cooling: Practical Use of Climate Resources for Space Conditioning in California." Report presented at the *Third Annual Solar Cooling Conference.* San Francisco, Calif.
6. Duffie, J. and Beckmann, W. 1974. *Solar Energy Thermal Processes.* New York: Wiley and Sons. Sections 4.8 and 6.1 through 6.5.
7. Hansen, D.G. and Yellott, J.I. 1978. "A Study of Natural Cooling Processes in a Hot, Arid Region." *Proc. of the 2nd National Passive Solar Conf.* 2.2, pp. 653-657.
8. Yellott, J.I. "Passive and Hybrid Cooling Methods." College of Architecture. Arizona State University, Tempe, Ariz.
9. Givoni, B. Personal Communication.

Passive Solar Design Handbook
Volume Three: Passive Solar Design Analysis

Los Alamos National Laboratory. Edited by Robert W. Jones. July 1982.

Is it worth adding a selective surface to a Trombe wall in Medford, Oregon? What is the difference in performance between a vented and an unvented Trombe wall in Charleston, South Carolina? How about sunspaces in Burlington, Vermont: is vertical glazing feasible, or is tilted glazing the only economical approach? What is the penalty for using light-colored thermal mass?

If questions such as these are important to you, the *Passive Solar Design Handbook, Volume Three* should be obtained immediately. Put together by the Solar Group at Los Alamos National Laboratory, this volume greatly expands upon, and in many sections replaces, the material originally presented in the *Passive Solar Design Handbook, Volume Two*, published in January 1980.

Volume Two presented two techniques for analyzing the performance of typical passive solar buildings, the load collector ratio (LCR) method and the solar load ratio (SLR) method. The LCR method, while not as flexible, provides a quick estimate of the annual auxiliary heating needs of any given design using Trombe walls, waterwalls, or direct-gain systems (with or without night insulation). Although limited by certain assumptions about glazing type, amount of thermal mass, and so on, this method is wonderfully simple.

W. Scott Morris is an independent researcher and design consultant based in Santa Fe, New Mexico. He is currently serving his third term on the board of the Passive Systems Division of ASES.

The designer has only to determine the building-load coefficient through standard heat-loss equations and divide by the collector area to obtain the LCR. The LCR tables for 219 cities in the United States and Canada provide another number known as the solar savings fraction (SSF) for direct-gain, Trombe wall, or waterwall systems. The term (1-SSF) is multiplied by the building-load coefficient and the degree days of that location to estimate the building's auxiliary fuel use during a typical winter.

Not only is the LCR method very quick, taking only a few minutes once the heat-loss calculations are done, but the tables provide a means of comparing the performances of different passive solar systems and of visualizing the result of varying the size of the collector area relative to the net heating load of the building.

Available through:
GPO Item 061-000-00598-6 (out of print).
Paper back $12.00.
American Solar Energy Society, Inc.
Volume Three and Supplement.
Hardcover. 668 + 190 pp.
Nonmember: $59.00. Member: $41.00.
Text edition. 668 pp. Paperback.
Nonmember: $25.00. Member $17.50.
Supplement. 190 pp. Paperback.
Nonmember: $20.00. Member $14.00.

The SLR method, on the other hand, requires considerably more work but does allow for changes in orientation and tilt of the glazing, internal heat generation, and variations in the thermostat setpoint. It can also be used for locations not listed in the LCR tables but for which complete weather data are available.

If performed by hand, using the worksheets in *Volume Two*, the full set of SLR calculations for any given design can usually be done in about one hour and result in monthly as well as annual estimates of the SSF and auxiliary fuel use. Because of its greater flexibility and monthly output, the SLR method has been commercially programmed for computers and programmable calculators.

Volume Three retains both the LCR and SLR methods, but expands upon them both. The LCR tables, in particular, have evolved into a veritable ocean of useful data. Whereas *Volume Two* listed only six basic reference designs, *Volume Three* now presents 94, including:

- 15 waterwall designs, including variations in thermal mass, number of glazing, selective surfaces, and night insulation;
- 21 vented Trombe wall designs, including variations in thermal mass, thermal conductivity, number of glazings, selective surfaces, and night insulation;
- 21 unvented Trombe wall designs, allowing for the same variations as in vented Trombe walls;
- 9 direct-gain designs, including variations in thermal mass, mass-to-glazing-area ratio, number of glazings, and night insulation;
- 28 sunspace designs, including two different attached geometries and three semienclosed geometries, and allowing for variations in thermal mass, glazed or insulated end walls, and night insulation.

As in *Volume Two*, these reference designs are given in tables for 219 cities in the United States and Canada, and the SSF is given as a function of the LCR.

At first, the 150-plus pages of LCR tables seem overwhelming. Indeed, there are so many reference designs that they are coded in the tables, making it necessary to flip back constantly to the pages that define each system. While this is a bit of a nuisance, the amount of information, both qualitative and quantitative, in these tables is truly fabulous. One can simply scan the tables for any given location and quickly get a feel for which system will provide the best annual performance and for the effects of changing such things as amount of mass or number of glazings.

For example, if we wished to design a house for Concord, New Hampshire, with a SSF of 30%, a glance at the LCR table would reveal that the best performers are waterwalls and Trombe walls, although both direct gain and sunspaces with night insulation are not far behind, and a mix of systems might prove most attractive. Looking more closely at the data on waterwalls, we notice that a triple-glazed waterwall appears to be relatively ineffective; in fact, by replacing it with an equal area, single-glazed waterwall with night insulation and selective surface (the clear performance winner), the SSF would increase from 30% to almost 60%!

From the same table we might also note that double glazing waterwalls with selective surfaces does not generally improve performance and is actually a detriment if night insulation (R-9) is used. Increasing the mass in waterwalls will increase performance but has little beneficial effect with unvented Trombe walls that do not use selective surfaces or night insulation.

Perhaps the client in Concord is particularly interested in sunspaces. Again, a brief look at the LCR tables shows that without night insulation it would be difficult to obtain substantial solar savings fractions, except perhaps with tilted glazing in semienclosed designs (integrated into the house rather than attached). In attached sunspace designs, glazing the east and west walls will have a detrimental effect but may be acceptable if night insulation is used.

The list of qualitative insights could go on and on just for Concord. To be sure, the quantitative results of the LCR method will not always be as accurate as the SLR method, which in turn will not be as accurate as full-blown computer simulations, but they provide something which may be even more important: initial guidance on any project involving passive solar design. Knowing where to start can save a tremendous amount of time later in the design process.

To add to the usefulness and flexibility of the LCR tables, many sensitivity curves are included for direct-gain and sunspace designs in *Volume Three*. These allow for graphic interpretation of varying different parameters in the reference designs. What happens, for instance, if the mass distribution is substantially different from that assumed in the reference design? Or if the Trombe wall is made of brick rather than concrete? Or if the glazing tilt on the sunspace is different from 90° or 50°? The sensitivity curves cover most important variables in typical systems and are reasonably easy to use. Together with the LCR tables, they offer a very valuable tool, particularly in the schematic design phase, where a few minutes with these tables and curves can be worth days of computer simulations or years in the school of hard knocks. Unfortunately, *Volume Three* does not include sensitivity curves for Trombe walls and waterwalls. This information, however, is covered quite well in *Volume Two*, which should be considered an indispensible companion to *Volume Three*.

A new and very welcome addition to *Volume Three* is the chapter on "Balancing Conservation and Solar" by J. Douglas Balcomb. This addresses the questions asked during the preliminary design phase of every low-energy building: How much energy conservation and how much passive solar? What is the optimum mix? In a very straightforward way, with excellent discussion and good examples, this chapter explains how to answer these questions.

To determine the near optimum mix, the designer first chooses the intended passive system and the approximate SSF he or she hopes to achieve. A "conservation factor" is obtained from the tables and entered in a set of simple equations that provide the optimum R-values for walls, ceilings, floors, basements, perimeters, and even the optimum air-infiltration rates. Since this procedure gives

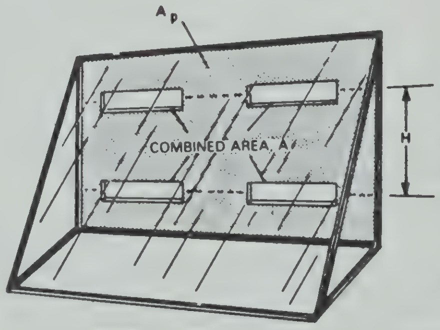

Fig. 4-23. Common wall vents. The projected area, A_p, equals the north common-wall area in the sunspace reference designs. The combined vent area is A. The vent area fraction is A/A_p (0.06 for the reference designs). The vertical distance between the vent centers is H (8 ft for the reference designs).

Volume Three extends the Los Alamos passive calculations methods by increasing the number of base cases, reference designs, and sensitivities of varying parameters. This figure from page 111 identifies the reference design dimensions for thermocirculation vents in a Trombe-like application.

the most economical mix of conservation and solar, it requires typical cost data on both the passive system and conservation features. These cost data have become readily available in recent years, and since there is a very large range of near optimum mixes, the procedure should prove very useful even when exact costs are not known.

Helpful recommendations are provided for choosing the value of SSF, including a map of the United States showing suggested starting-point values. Selecting the system type is also of great importance, but this is left to the reader. It must be realized from the previous discussion that some systems in given locations are clearly superior to others, both in terms of performance and economics. It is highly recommended that the user spend some time with both the LCR tables and cost data before choosing the system type.

Volume Three also includes some modifications to the SLR method of calculating the monthly SSF and auxiliary fuel use, which is of prime importance during the final design stages. A new parameter, the average clearness ratio, is introduced and is included in the weather data tables. This factor apparently improves the accuracy of the calculations which estimate the solar radiation incident on various surfaces, particularly in cloudy climates. New graphs are presented which estimate the amount of solar radiation transmitted through glazings at different orientations and tilts. The procedure, which requires the use of weather data tables, is relatively easy to use and provides site-specific results. In addition, this procedure may well be used by itself during the schematic-design phase to determine the effects of changes in orientation and tilt of the glazing.

The other modification to the SLR method is the addition of tables which provide an estimate of the amount of light actually absorbed in the space (versus the light reflected back out through the glazing). This can have a significant impact on the results and is most important for sunspaces of direct-gain systems which may have light-colored interiors. The tables for these absorption factors, however, are not particularly easy to use and are clearly limited by the initial assumptions of the actual colors of various surfaces behind the glazing. Since the owner of the building may well change surface colors radically, the prediction of solar absorptance is somewhat academic, and these tables will probably be abandoned in favor of simpler sensitivity curves (curves for mass absorption are provided for both direct gain and sunspaces in *Volume Three*).

The monthly SLR method is a powerful and accurate technique for analyzing the performance of typical passive solar buildings. It does take some time when done by hand, however, and is often used in computer and calculator programs. To encourage this development, all SLR correlations, as well as the basic equations used in formulating all tables and graphs, are given in the text and appendices.

Although the inclusion of this information should be very helpful for developing computer software, its presence may lead to confusion. In many places the discussion shifts abruptly from necessary basic information to descriptions of equations and correlations which are of interest only to scientists and programmers. The unwary reader may well become frustrated trying to understand seemingly irrelevant material.

As with *Volume Two*, *Volume Three* makes no attempt to consider the issue of cooling, an important consideration in many parts of the country which may indeed be affected by designs using large amounts of glass for passive gains. Generally, precautions dictated by common sense will prevent these problems, but until further work has been done in this area, the cooling issue must be dealt with by the individual designer.

The most common criticism of *Volume Three* will undoubtedly be that it is an incomplete work. The designer will have to refer to *Volume Two* for some definition or procedure, and this can be time consuming. In many instances, finding a piece of information may require searching through various parts of *Volume Three*, only to be referred finally to *Volume Two*. In other cases, such as using the SLR method, the basic information in *Volume Two* must be modified with the new material in *Volume Three*.

The problem, of course, is that *Volume Three* expands upon but does not replace *Volume Two*. Fortunately, *Volume Three* contains a very thorough 34-page index which covers both volumes.

All in all, *Volume Three* is very well done, and what faults it does have are far outweighed by the tremendous amount of invaluable information presented. Many building designers whose main contact with passive solar designs has been through picture books may be scared off by the sounds of crunching numbers which seem to emanate from this volume. It is, however, written for the intelligent layman and rarely uses more than basic arithmetic (the authors, most of whom are used to having differential equations for breakfast, deserve major credit here).

With both *Volume Two* and *Volume Three*, a typical home designer with only minimal exposure to solar heating should be able to understand and use the LCR method in about five to ten hours and the full SLR approach in an additional five to ten hours. The time spent on understanding the tools presented here should pay for itself on just one project. Some skeptics may still ask, "Is it worth the time and trouble?" I can only answer, "Are birds glad they have wings?"□

The first *Passive Solar Journal* issue (vol. 1, no. 1, January 1982) published comprehensive book reviews of the *Passive Solar Design Handbook, Volume One* and *Two*. The final review concluded with a statement that *Volume Two* "is without parallel and fills . . . a big void. Let us hope that a revised edition, with clearer logic and better writing, will be prepared soon." Slightly over a year later, *Volume Three*, a reiteration, partial refinement, partial replacement, and extension of *Volume Two* has arrived. Is it clearer in its logic and better written?

The answer to this question is yes, no, and sometimes. First, it has a thorough index covering both volumes which makes locating and identifying information vastly easier. This comes as a welcome relief to all users of both works. Second, *Volume Three* provides much more detail, offering the designer greater variety, flexibility, and opportunity in selecting and evaluating passive system options. The number of reference designs and sensitivity curves is incredibly awesome.

Chapter 1 introduces the information presented in *Volume Three*. It contains an excellent section on terminology which concludes with a discussion of solar savings. Solar savings fraction (SSF) is accurately defined and emphasized as being useful only as an intermediate step toward bottom-line energy performance: auxiliary heating requirement.

Dennis A. Andrejko, formerly a principal of SEAgroup, now heads Andrejko and Associates, Energy Conscious Architecture and is an associate professor of architecture at the State University of New York at Buffalo.

As for summer performance, cooling considerations are given only nine lines of discussion in the entire 650-page-plus document. Designers need to know and understand the thermal impact of passive systems on an annual basis. Too often, sacrifices are made in summer performance for increased winter benefit, while the net annual result is an increased thermal liability. Although not necessarily the intent of the authors of *Volume Three*, what is needed is a comprehensive look at all passive technologies. This would include an analysis of thermosiphon, Skytherm, and roof-pond systems as some additional exemplary types. Energy analysis should assess heating, cooling, daylighting, and integrated approaches. Nine lines on cooling in this document is an embarrassing start.

Chapter 2 partially overcomes this deficit by providing a valuable discussion of an important issue of energy-conscious design: "insolation versus insulation." The chapter describes a process which attempts to optimize both the conservation and passive solar strategies of a design project on a regional basis. A step-by-step procedure is outlined, and a sample problem is presented. Architects always appreciate examples to guide them through a complex quantitative process.

Direct gain is described and defined in chapter 3, but, in terms of overall organization, is better placed in *Volume Two*. In this chapter, the concept of sun tempering or low-mass, direct-gain buildings is also discussed. This information is especially beneficial to those people who approach passive design without incorporating large amounts of thermal storage, often the case for mass-market homebuilders.

The graphic cross section illustrated in chapter 3 does an average job depicting the components of a direct-gain building but needs to present more clearly the basic ingredients of a solar system (collection, storage, distribution, and control), especially at this early stage of introducing the direct-gain concept. Interestingly, the building section is reminiscent of an early Santa Fe solar house. The vertical glazing height and subtle earth berm give it away. We all know that earth berms are not inherent features of a direct-gain building. Overall, many more graphics in a consistent, clear, bold format would improve both *Volume Two* and *Three*. They would help explain and visually reinforce the concepts, while making the material less formidable and more digestible.

Chapter 4 discusses sunspaces and provides information not reported previously in *Volume Two*. Like chapter 3, it concentrates on various sensitivities of the reference designs. In the sensitivity graphs, some design parameters are varied while others are held fixed, resulting in a modified solar savings fraction when compared to the reference design. More on this later.

Chapter 5 identifies the solar load ratio (SLR) method. You will *not* find procedures, worksheets, or examples here. Instead, as in many areas of the text, reference is made to *Volume Two* for specifics.

The nearly 500 pages of appendices represent approximately 75 percent of *Volume Three*. Appendix A consists of *Volume Two* errata and allows those of us who were already keen on the many minor errors in the earlier volume to check and see if we have caught them all. Appendix B provides the conservation factors necessary for the equations used in chapter 2, "Balancing Conservation and Solar."

In Appendix C, SLR correlations are given, and the various SSF-versus-monthly solar/degree day (S/DD) graphs are plotted. These graphs essentially replace those in *Volume Two*, since there are now nine for direct gain and twenty-eight new sunspace options. Why are there no plots for new Trombe-wall and waterwall reference designs?

Appendix D, "Weather Data," and Appendix E, "Solar Radiation Approximations," replace Appendix A and much of Appendix C in *Volume Two*. A significant change here is the addition of a new parameter, the average clearness ratio (K_t), which allows for more accurate solar radiation approximations, especially in cloudy climates. Equally important, but not expanded on, are site context and solar geometry, also briefly discussed in *Volume Two*. A more detailed discussion of these factors is necessary in any future volumes.

Replacing a portion of Appendix F in *Volume Two*, *Volume Three*'s Appendix F lists SSFs resulting from various LCRs for each of the 94 reference designs in each of 219 cities in the United States and Canada. This extensive listing is extremely useful and valuable to a designer, especially during the early design stages when quick and accurate assessments are needed. Design decisions can be evaluated for various system types; systems and variations within the same system can also be compared against one another. The tables are neatly organized and easy to read and use although printed in significantly reduced type size.

Appendix G consolidates the sensitivity data for direct gain and sunspaces onto useful graphs. (Trombe-wall and waterwall sensitivities remain in *Volume Two*.) To good effect, the technique of chapters 3 and 4 is applied: one or two design parameters are varied, while the others remain fixed. At every design stage this becomes an important tool for a designer, since it allows a closer look at a specific design and provides a method to estimate approximate differences in performance based on the changes relative to the reference design. Some of the many parameters that are varied include the following:

- For direct gain: thermal storage mass properties, mass surfaces, mass distribution, solar absorption, mass coverings, number of glazings, temperature bounds, overheating, temperature setbacks.
- For sunspaces: thermal storage volume, storage container shapes, sunspace orientations, glazing tilt, sunspace width, number of glazings, glazing thickness, solar absorptance, vent areas, thermostat set points.

For the sensitivies, several cities are chosen to represent a wide geographical and climatic range. Each city has its January heating degree day and average solar radiation value plotted. From this information a designer can select a city which climatically corresponds closely to the building site and use the corresponding sensitivities. This is where the process begins to break down. There are not enough cities, nor are the cities selected representative enough to cover a full range of climatic zones. According to the plotting, climate zones not fully accounted for are areas with (a) high heating degree day and low solar radiation values and (b) mid-range solar intensities (900-1,200 Btu/ft^2 day, *2.8-3.8 kWh/m^2 day*). For example, it would be difficult for a designer in Buffalo or in a colder climate with equally low solar availability to take full and accurate advantage of the sensitivity data. A sensitivity study should allow a designer to continue to fine tune a design during the various design stages. If a climate area is improperly selected, invalid interpretations can be made. If a representative city is not available, then the ability to further assess and improve upon the design is inhibited.

As a whole, *Volume Three* presents a number of opportunities which permit further exploration of passive solar systems. Its substantially new and updated information verifies the notion that passive solar design and analysis methods are continually evolving. A worthy note: Do not be intimidated by the size of *Volume Three* or by the seemingly endless tables and graphs in the appendices. The LCR and SLR methods are no more complex than in *Volume Two*; in fact, their procedures are identical. Only the reference designs and sensitivity data have increased severalfold, making these tools much more versatile.

Without question, the quality and quantity of information presented should prove to be highly valuable and useful. However, because both *Volume Two* and *Volume Three* must be used simultaneously, it is easy to see that *Volume Three* is essentially an extension of *Volume Two*. It is unfortunate that the wealth of information provided is awkwardly contained in two separate volumes. This disorganization yields a cumbersome process which is potentially high in frustration for the user. It will, sadly, dissuade many people from making full use of *Volume Three*. No matter how complete or important information might be, if it is not easily and readily accessible and retrievable, it will not be fully utilized. In its own right, *Volume Two* is still a valuable and useful document. Designers may, for the time being, opt to use it instead of *Volume Three*, that is, until *Volume Two* and *Three* are consolidated into one package. When this happens, the information can then be conveniently used, and designers will begin to realize its fullest potential.

Thus, this review of *Volume Three* can be concluded much like the previously mentioned review of *Volume Two*: let us hope that a revised, consolidated edition with a clearer format and better organization will be prepared soon. □

Obviously, this is a very important book. A product of the prestigious Los Alamos group and successor and companion to the trail-blazing *Volume Two* of 1980, it is compulsory reading for all designers of passive solar houses. Despite some weaknesses, it has great strength.

What is the book really about? The title, *Passive Solar Design Handbook*, is of little help; it is much too broad. What the authors have focused on are several shortcut methods of predicting the auxiliary heat need of relatively straightforward kinds of passively solar heated houses. Mainly they deal with direct-gain and sunspace designs.

Two methods are expounded: an annual method, which is very simple but not especially accurate, and a monthly method, which is more complicated and more accurate. Using either method, the designer first mentally divides the proposed house into a solar part (south part, with big windows) and a nonsolar part (north part with some windows). The designer then specifies the south part's window area in some detail but specifies for the north part just its general heat-loss property.

William A. Shurcliff, a physicist, is professor emeritus at Harvard University.

What does the annual method consist of? Here is a highly simplified summary. The designer specifies, for the proposed house and the proposed locality, the type of passive solar system to be used (direct gain, for example). He or she then (1) chooses a value of heat-loss rate of the nonsolar part of the house, (2) chooses a value of glazing area of the south part, (3) takes the ratio of these two values (load collector ratio, or LCR), (4) finds, by reference to an Appendix F table, the "solar savings fraction" that is pertinent to this ratio and this type of solar system and this locality (all based on Los Alamos experimentation and computer calculations), and (5) performs a simple multiplication—and the answer is in hand: an estimate of the annual auxiliary heat need. The task was simple: the behind-the-scenes complications of climate, sunshine, and so on have all been taken care of by hard work at Los Alamos and the distilled wisdom incorporated in the pertinent 154-page table. Values are presented for 214 locations, and the method can be adapted to any location for which there is weather data.

What about the monthly method? The designer starts off as before—finding the heat-loss rate of the nonsolar part of the house, choosing a value of glazing area of the south part, and determining the load collector ratio. Then, for each month the designer (1) finds, from tables, the amount of solar radiation incident, the amount that actually enters the south part of the house and is absorbed there, and the amount absorbed per degree day, (2) consults graphs and finds, for the given amount absorbed per degree day, the solar savings fraction, and (3) from this, using arithmetic, determines the monthly auxiliary heat need for the particular month. Adding the values for each month, again the answer is revealed: the annual auxiliary heat need.

The book includes a supplementary tour de force: a set of several hundred graphs that show the designer the consequences, in regard to thermal performance, of each main type of design change. For nearly any change possible in building shape, orientation, and so on or in the glazing (area, orientation, number of glazings, and so on), the designer can find, roughly, the thermal consequences. In summary, the designer can obtain *directly* information on hundreds of specific designs and can find *indirectly*, via these sensitivity graphs (about 1,100 curves), information on thousands of slightly varied designs.

All this for nearly any climate and any latitude in the U.S. and Canada! And all this with no need for a computer, no need for hard thought!

Can a book that has such strengths also have serious weaknesses? It can and it does. Notice first that the book does not deal with passive solar design in general, but only with minimizing the wintertime auxiliary heat need. The subject of summertime cooling is ignored; the authors merely suggest that when the design is essentially complete, a suitable number of shades, vents, and controls be added. But, in fact, should not the cooling problem be tackled from the outset as an integral part of the design problem? Is it right to relegate the problem to a choice of add-ons?

Other ignored topics are: room-to-room uniformity of temperature (fans can help but the word "fan" does not appear in the book!), humidity control, glare in sunspaces, adequacy of east, west, and north window areas for view, daylighting, cross ventilation in summer, strategies relating to basements, attics, and vestibules, the threat posed by radon in houses that have large areas of exposed concrete, the nuisance of operating thermal shades twice a day, use of special absorbing or reflecting films on windows, and tax benefits.

The book contains detailed discussions of only two kinds of passive designs: direct-gain and sunspace. If one is interested in Trombe-wall designs or indirect-gain designs, one must consult the (almost inscrutable) preceding volume.

Little mention is made of one of the most promising kinds of direct-gain passive solar houses: the superinsulated house which has proven so successful in Saskatchewan and elsewhere and which uses only about $100 worth of auxiliary heat per winter and keeps cool in summer. The word "superinsuated" does not appear in the book. In fact, not even the word "insulation" is in the index, even though Chapter Two, authored by Balcomb, is a lengthy dissertation on the need for energy conservation first, including a calculation procedure to optimize the balance of south glass with conservation. In general, the authors appear more interested in large solar windows than in the potentialities of very high quality insulation—perhaps because they reside in a state that has a lot of sunlight and little cold weather.

The writing, usually of high quality, is sometimes heavy and awkward. Ponderous and unclear terms are used. Take, for example, "solar load ratio." Might not a solar designer reasonably assume that "solar load" is a load imposed in summer by excessive solar heating? What the authors mean is a ratio of winter month *solar energy input* to *heating load.*

The fact that the book deals mainly with two methods is not stated clearly at the outset. Nowhere are the two methods given unique names, and nowhere are they adequately compared and contrasted. A casual reader might assume that there is just one general method or perhaps as many as six (If asked to name the six, the reader might reply "BLC, SLR, LCR, annual, monthly, and sensitivity.") Only gradually does the actual scope of the book come into focus.

Some key quantities are poorly defined. Some are defined several times and in contradictory ways. The reader never feels sure where to draw the line between "south portion" and "nonsouth portion." I suspect that the authors also are unsure. The reader is uncertain as to what "projected area of south solar aperture" means. Is the area projected onto a vertical south-facing plane or onto a vertical plane that is parallel to the lower edge of the aperture—a southwest-facing aperture, for example? A glossary is included and is helpful, but some of the definitions are inept or wrong. Key symbols are nowhere listed and defined systematically, nor are they included in the glossary or index.

Surprisingly, the book makes virtually no mention of design analysis work done elsewhere in the world. If dozens of architects and engineers in the U.S., Canada, and elsewhere have worked on passive solar calculations, if several groups in universities and in the building industry have helped in the evolution of successful passive systems and have published articles and books on the subject, you would never learn about them here! The authors treat the Los Alamos methods in strict isolation.

Ultimately, two interrelated questions must be raised concerning this book: Are its "short-cut" methods actually so time-consuming and complicated that a designer might do better to bite the bullet and employ a computer program? Will experts view the book's methods as too oversimplified for their purposes, while nonexperts find them too cumbersome and complex?

Despite its drawbacks, the appearance of this book is a big event. It contains enormous improvements over the preceding volume, not the least of which is the first-rate 35-page index to both *Volumes Two* and *Three*. The book is a must for passive solar designers. ☐

Editor's note: Since writing his review, Dr. Shurcliff has continued to study and comment on *Volume Three*. He now proposes to author a "Simplifying Guide" to what he calls "the world's most important book on passive solar heating calculations."

Seventh National Passive Solar Conference, Knoxville. Reviews of sections included in **Progress in Passive Solar Energy Systems**, Vol. 7. Edited by John W. Hayes. Newark, Del.: ASES, 1983. 1,200 pp. illus. refs. indexes. $150.00 list price. $105.00 member.

Daylighting

Passive '82 continued the format introduced last year at the Portland conference, treating daylighting as a separate topic in both conference activities and in the *Proceedings*. This position reflects the increased attention given within ASES to daylighting design as an energy-conserving strategy in commercial buildings.

The majority of the 12 papers included in the daylighting section of the Passive '82 *Proceedings* outlines efforts to develop design and calculation procedures, including mainframe and microcomputer evaluation methods, rules of thumb, graphic methods, and correlation methods for producing daylight availability data. Case studies of current building projects and a discussion of basic design principles are also featured. Surprisingly, one of the papers in this section does not address daylighting issues at all and seems to have been placed here by mistake.

George Arnold, a graduate of the University of Montreal, is an architect currently working as an energy analysis specialist for the Tennessee Valley Authority.

An intriguing look at how the next generation of daylighting design tools could evolve was provided by the papers focusing on mainframe computer analysis procedures. The power of these routines lies in their ability to directly link daylighting performance and total building energy use.

It is clear that computer routines will be valuable in the development of widely accessible, simplified evaluation procedures that can look at both the qualitative and quantitative issues involved with daylighting design. These include energy- and cost-related factors. A careful reading of the papers, however, shows little agreement among authors as to the nature of a sound technical basis for such procedures, bringing the real usefulness of some of their results into question.

In this regard, the set of tools currently under development at Lawrence Berkeley Laboratory stands as an example to the field (see *The DOE-2 and SUPERLIGHT Daylighting Programs* by Stephen Selkowitz, et al.) A great deal of planning has evidently been invested in designing these programs to avoid most of the obvious limitations shared by the current group of procedures and to ensure that their capabilities can be quickly upgraded as more flexible routines are developed.

It is encouraging to note that the factors limiting the applicability of these procedures are under active review, with most of the researchers intending to make suitable revisions as required. We may eventually have a selection of extremely capable research and design procedures at our disposal.

In the meantime, someone interested in using any of these procedures should read the papers in the *Proceedings* carefully to determine whether or not a particular procedure is currently able to provide meaningful results based on his or her specific needs.

Apart from design tools research, the use of an occupant survey to obtain the specific reactions of a daylit building's users to the daylighting design features, as reported in *User Interaction With a Daylighting System* by Walter F. Roberts, Jr., represents a step forward in the validation of current daylighting design practice. The conclusions of this paper help to place the role of calculation methods and design tools in proper perspective and present a set of considerations rarely addressed in the literature on daylit buildings. This paper serves as a useful counterpoint to the other interests addressed in this section. It is unfortunate that a copy of the original survey was not included with the paper.

The individual papers in the daylighting section of the *Proceedings* generally do a good job of reporting on the work they represent, being reasonably well written and candid in matters of detail. As a group, however, they are too few and too narrow in their interests to constitute a comprehensive summary of efforts in the field. This is in the nature of conference proceedings. In addition, they give regrettably little attention to the role of daylighting design within the context of the architectural design process.

When taken with the technical uncertainties mentioned above, this selection of papers would provide little help to a designer trying to select from the options presented the most useful design tools and procedures for his or her situation. This condition is as much an expression of the real state of the art in daylighting design as it is of the interests of the individual authors; the field lacks a comprehensive statement of purpose that identifies an agreed upon set of issues and priorities for both researchers and designers.

At this point in the development of daylighting as a separate concern—almost a specialization—in the design of energy-efficient buildings, a dialogue between the users and developers of design tools would benefit both groups. As ASES takes a more active role in guiding research efforts, it may move to include sections in its *Proceedings* that present statements of the concerns of the field and ultimately its mandate. This information would help to focus the efforts of research groups at a particular point in time, and increase the value of these documents to ASES' constituency as a whole. ☐

Performance Monitoring

Performance evaluation is the critical feedback loop in the continuing development of passive systems. Twenty-seven papers in these *Proceedings* address performance evaluation, and for twenty it is their primary focus. As a whole they represent significant progress in answering the question "How well does it work?"

While general instrumentation and monitoring techniques for passive systems are not addressed, a few excellent papers examine specific instrumentation techniques, including direct measurement of a passive collector's energy balance, indoor air quality measurement, and thermocouple mounting techniques.

In contrast to this limited number of papers on monitoring techniques, one topic is addressed by no less than five papers: the measured performance of thermosyphon systems. This exemplary collection of papers covers everything from short-term, side-by-side tests to annual performance data from thirty-eight similar systems in the field.

In a distinct improvement over previous *Proceedings*, only a handful of the performance papers deal only with short-term, limited data from a single building. While such short-term measurement of a few performance variables can provide valuable feedback to that building's designers, it is seldom very useful to

Blair Hamilton is technical coordinator for the Memphremagog Group of Newport, Vermont.

a wider audience. Gone are the graphs of inside-versus-outside temperature for a few days; in their place are reports of monthly and annual energy balances. Fewer variables are calculated; more are measured.

Three of the papers present detailed, but generalizable levels of performance for specific buildings. Even more significant are the results from several multiple-building programs in systematic performance evaluation of passive systems. Final results from the Class C noninstrumented performance evaluation program are reported for 335 passive solar homes. A utility reports on long-term performance of four passive and four reference homes, and another paper covers seasonal performance of ten various passive homes monitored through the National Solar Data Network. Preliminary results from the national Class B level of performance evaluation leave one eager for more data from more sites. And it appears that this, and more, is coming.

While a great deal of useful information is included in these *Proceedings*, indications are that within the next two years we will see the results of extensive monitoring programs only described in these papers. For significant results on manufactured buildings, commercial buildings, and more than a handful of Class B sites, we will have to wait a little while longer. □

Cooling

The technical papers addressing cooling in the *Proceedings of the Seventh National Passive Solar Conference* span a broad spectrum of quality, usefulness, and subject matter. Like the conference itself, there has been simultaneous movement in two directions: technological sophistication and a nuts-and-bolts, backyard passive approach. Fortunately, the quest for simple passive cooling panaceas has given way to an appreciation of the limitations of thermodynamics and climate. Only in a few geographic areas of the country do purely passive radiative, evaporative, and diurnal cycle cooling systems provide a complete solution to cooling needs. Elsewhere, particularly in the Southeast, climate conditions and latent loads dictate the use of mechanical equipment and auxiliary energy input to meet modern cooling standards.

Donald W. Abrams has his own energy consulting firm in Atlanta. He is currently assisting Georgia Power Company with the investigation of sprayed roof cooling systems and ice-storage systems, as well as writing a book on cooling energy conservation for hot, humid areas.

The majority of the Knoxville cooling papers recognizes the complexity of the problem and presents integrated approaches combining building load reduction, passive systems, and conventional cooling systems or mechanical devices. More than half of the authors provide the reader with useful information taken from actual buildings and experimental systems. Included are hollow-core concrete-slab circulation systems, radiant panels, roof ponds, ice systems, and residential designs.

Fundamental cooling issues receive an additional bit of much-needed attention. Of particular interest is the discussion of summer aperture shading and passive system glazing areas by Siminovitch, Bergeson, and McCulley. Through BLAST simulations, the annual heating and cooling energy consumption resulting from south-facing glazed areas and common shading and insulating devices is demonstrated. However, the authors neglect one important conclusion of their work: the minimal, but commonly overestimated, value of overhangs in blocking summer solar gains. Although design tools are still being developed to calculate overhang geometry to two decimal places, the typical designer still mistakenly assumes that an overhang provides nearly complete summer shading. While improving winter heating performance, many passive solar designs have resulted in summer discomfort and energy consumption disasters.

Radiative cooling systems receive good treatment, ranging from a time-consuming, but effective, site cooling potential evaluation method to a roof-pond design methodology to application simulations. An experimental assessment of radiative cooling potential in Atlanta demonstrates a usable, but not independently adequate, source of cooling. Two useful night sky irradiance models are presented and compared to measured data in another of the series of cooling research publications from Trinity University. A second Trinity paper proposes several interesting low-energy cooling systems and includes an excellent list of references of recent work on a variety of cooling topics.

Several Knoxville papers suffer from a lack of thorough review and editing. Grammatical and typographical errors, gross errors in citing references, and format shortcomings are obvious problems throughout many conference publications. A more thorough technical evaluation, though difficult and certainly more expensive than the present volunteer system, would undoubtedly improve both the quality of the information presented and the clarity of its presentation. The editors of the *Proceedings* express similar concerns in their Foreward. With a rather static resource available for presentation of information and a growing volume of reportable work, selectivity and improved quality are essential to a more effective role for future passive conferences and ASES.

For the individual looking for guidance in cooling-design decisions, a search of the *Proceedings* is bound to result in frustration. The basic issues of heating/cooling balance and cooling load minimization through building design and internal gain control need further attention, not from a research standpoint, but from an information availability and applications standpoint. A compilation and analysis of the extensive work done by Trinity University, the Florida Solar Energy Center, and the now-defunct regional centers would be invaluable to the design and construction community. Designers and building clients continue to call for case studies of successful projects.

Great progress has been made in the past few years, but the results need to be unified and refined. Significant contributions by passive cooling systems will not occur in the near future. While the technology may exist in some cases, much developmental work remains to be done. In the meantime, more conventional alternatives for cooling energy savings are quite viable and need to be presented to the building industry. In many cases, the application of good, fundamental design principles, simple ventilation, and efficient and properly sized conventional mechanical systems can reduce the cooling energy consumption to a level where the savings incentive for further investment is quite small.

Contrary to the optimistic conclusion of one paper, passive and alternative cooling systems are not currently "easily retrofitted." Despite the enthusiasm and obvious need to reduce cooling energy consumption, we must avoid false starts and dead ends which will ultimately slow the overall progress of design and building improvements. □

Design Tools

The 22 papers in the Design Tools and Simulation section of the *Proceedings of the Seventh National Passive Solar Conference* indicate that some progress has been made in developing tools which designers can actually use. Fourteen papers either report on projects which will result ultimately in such tools or present design tools not seen previously. The other eight concentrate, for the most part, on improving mainframe simulators.

Although some steps forward are demonstrated by the presentations, no great strides are evident. For example, even though a number of the papers deal with heating design calculations, most still do not take into account the cooling load impact of passive solar heating techniques. Indeed, the state of the art for design tools is such that a designer still must use a number of different tools to get a complete heating, lighting, cooling, and ventilation picture of a project.

The subjects taken up in the 22 papers are quite diverse, ranging from such design tools as builder guidelines to national climate zone characterizations. While such a broad range of topics is a plus, the inability to focus on a specific audience is not. Any single reader probably would find the section incoherent as a whole.

William A. Wright is associated with the Cambridge Energy Corporation and serves as Design Tools Editor for the Passive Solar Journal.

The overall aim of this collection is to develop simpler methods of manipulating design parameters. In what is almost a model presentation of rules of thumb, David Zimmerman of the Tennessee Valley Authority clearly provides guidelines which allow a regional designer to quickly determine all key design parameters for an attached sunspace (insulation levels; thermal-storage, vent-area, and ventilation-fan sizing; and glazing size, orientation, and slope). Unfortunately, cooling load impact is not considered in depth, a bothersome omission considering the hot, humid climate of the southeastern United States.

In an elegant presentation of sensitivity curves for the evaluation of direct-gain systems in the northwestern United States, Dean Heerwagen and his colleagues at the University of Washington studied the behavior of total annual energy consumption rather than heating energy alone. Reasoning that the base case is not the conventional R-13 insulation, but rather a superinsulated residence, they used a simulator (HOUSE, derived from UWENSOL) to develop annual heating loads for the superinsulated reference case. Surprisingly, the reference heating load was found to be zero. Thus, the result of their work is a series of curves relating annual cooling loads to the load collector ratio (LCR) and to the mass-to-glazing ratio. In general, the authors found that the passive house had higher cooling loads, but that by using extra shading and an economizer cycle, a cooling load of zero could be obtained. They plan to investigate other climates and different passive configurations.

The trend toward simpler approaches is apparent in all three papers on climate issues. Each treats a different aspect of climate effects on design. Brandt Andersson, William Carroll, and Marlo Martin of Lawrence Berkeley Laboratory use four, simple measures of climate—base 65°F (*18.3°C*) heating and cooling degree days, average annual solar availability, and total annual latent-energy hours—to attempt to construct population-weighted climate groups. Although the authors clearly are still feeling their way, in this first progress report they raise interesting points concerning the establishment of similar climate groups based on what is a more complete set of indicators than just temperature and solar data. They divide the U.S. into 5, 11, and 24 similarity zones, depending on the number of climate variables allowed. Their GLOM program appears to be a worthwhile first step toward reducing the weather data base required for the study of significant portions of U.S. population centers.

In a paper dealing with microclimate data, Edward Arens and Lawrence Flynn of the University of California, Berkeley and Davis, report on a computer program intended to simplify the process of producing extremely site-specific weather data from hourly weather tapes which may not be truly descriptive of the design site. Their work is still in an early stage, but since Arens's developed version of ADJUST at the National Bureau of Standards is the basis for it, the investigation should ultimately provide useful data. The program attempts to construct a locally accurate, hourly tape by taking into account local monthly averages for temperature, humidity, solar radiation, and wind. Other site conditions such as altitude, cloud cover, and surface roughness can also be used. Although this work cannot be put to use at present, it may ultimately produce improved, highly localized climate data in situations where the microclimate is sufficiently different to warrant it.

The third paper on climate, by Vivian Loftness of Carnegie-Mellon, has immediate applicability for designers. It describes a series of 15 graphic, climate "exercises" which they can perform for projects under design. The exercises appear to force designers to develop visual images of site conditions. For those who relate best to visuals, these methods seem to be quite useful.

William Wray and colleagues at Los Alamos National Laboratory and the Naval Civil Engineering Laboratory present what appears to be an important simplification of the solar load ratio (SLR) method. While compiling a solar design manual for the Navy, they developed the fast solar load ratio (FSLR) method: a fairly simple relationship between the annual heating load and a single, monthly heating load. By calculating the minimum monthly SLR and using a graph with two fudge factors, the annual heating and auxiliary loads are obtained. Although the authors do not provide an example which details the method, they do present one which shows the form of the calculations, and the FSLR appears much simpler than the monthly SLR approach. Because the FSLR allows for correction of glazing azimuth and internal gains (by using variable degree base data), it is more general than the LCR, hence a potentially useful adjunct to other Los Alamos methods. Unfortunately, the FSLR requires fudge factors which are climate- and passive-system-dependent, and the reader will have to contact Los Alamos to obtain the complete 209 location tables. Also, the calculation of cooling loads is not discussed.

Simulation workers will want to be aware of a new TRNSYS module for sunspaces, a packaged simulator named GERT which can be used to describe social scale energy networks and systems, a report on the performance of Los Alamos test cells for 1980 through 1982, a description of the early stages of the Class A field data collection and data analysis program, a comparison of DOE 2.1 and the solar savings fraction (SSF) method (which shows consistent differences in results), and a finite difference model for steady-state ground losses. The building simulation papers are like their design-tool counterparts in that they present more developments and refinements, but set forth no definitive accomplishments or major breakthroughs in their field.

The single microcomputer program described in this section of the *Proceedings* is a progress report from Brandt Andersson of Orinda, California. His joint effort with Swedish workers on Microcomputer Energy Programs for Architects (MEPA) is intended to result in a designer-oriented program. Comparisons with BLAST simulations caused a number of revisions in MEPA, which now appears near release.

A single paper in this vital area is not representative of work going on in the field right now. It is something of a puzzle that Andersson's is the only paper in microcomputer development in this section of the *Proceedings*.

Two notably simple, useful, and handy tools are presented. John Moore of Salt Lake City extends work he originally performed at Los Alamos and shows an easy way to obtain the maximum possible system productivity from the mysterious "D" factors in the second volume of the DOE *Passive Solar Design Handbook*. Moore explains how a designer can learn, by a quick calculation, the best possible performance a specific system can be expected to produce. In the early stages of design, this could help eliminate uneconomical passive systems. Jeffrey Yago of Barboursville, West Virginia, tabulates vertical wall shadow factors in a form which will be useful for some designers. Although the trigonometric relationships drawn upon are well known and although the tables presented do not cover all possible cases, when the need arises, these tables will be handy.

The papers in the Design Tools and Simulation section discussed here are representative of the considerable work taking place in the development of passive design tools. Nonetheless, the somewhat inconsistent organization of the conference sessions might cause some design-tool advances to be overlooked; both the Cooling and the Daylighting sessions contain papers on design tools specific to those areas. Overall, however, the *Proceedings* provide a clear picture of the diversity of work now underway. ☐

Emerging Architecture (EA)

In Kansas City at the Fourth National Passive Solar Conference in October 1979, Emerging Architecture sessions were first offered. During the preconference programming this topic was almost eliminated: the technical reviewers questioned the sessions' merit and technical contribution. Fortunately, a number of thorough papers were presented in a series of special sessions, and nearly 50, brief, one-paragraph descriptions "sneaked" into the Kansas City *Proceedings*.

Since the Fourth, Emerging Architecture has become one of the most well-received subjects at passive conferences and has gained an equal billing in the conference *Proceedings* with the other published specialized topics.

Dennis A. Andrejko is the author of many publications, including Passive Solar Architecture: Logic and Beauty *(coauthored) and* Solar 4: Architektur und Energie *(coauthored). He received his Bachelor of Architecture degree, cum laude, from Arizona State University and his Master of Architecture degree from MIT.*

In its brief history, just what has emerged in emerging architecture?

The Knoxville Emerging Architecture papers show a wide range of architectural exploration in contrast to the more singular, small-scale approach of earlier years, and they show it in much more detail. This is the strength of passive architectural design as evidenced, in part, by this year's Emerging Architecture contributions. Of many thematic areas of interest, a few are summarized below.

Building types/scale. It is refreshing to see a redirection from the somewhat exclusive study of single-family residences as a "test tube" scale to that of larger, more complex buildings. Of the 16 Emerging Architecture papers in the Knoxville *Proceedings*, nearly one-half deal with issues and concerns other than single-family houses. In addition, many of the papers on single-family residences exemplify a more advanced design awareness than those of earlier years.

Vernacular. The quest for "true regionalism" continues. Although not "emerging" in the strictest sense, R. Peter Wilcox's excellent paper, "Shakertown: Sun-Light and Sun-Order in Kentucky Communitarian Architecture," explores historical precedent: it elaborates on a celebrated and spiritual basis of Shakertown lifestyle, suggesting "possible new meanings for the term 'solar architecture.' " Sam A. Cravotta's paper describes the revitalization of sun porches, a traditional building style, in the Shenandoah Valley of Virginia. Cravotta mentions that the new sun porches incorporate, among other things, "design innovations." Unfortunately, his examples fail to illustrate anything fresh. The paper deals with a good topic but does not provide enough quality and depth for a national conference.

Materials. As new, alternative materials are developed, an increased variety of building solutions and expressions becomes possible. In their paper, "The MIT Crystal Pavilion," Timothy E. Johnson and Brian Hubbell describe one new expression as they report on an all-glass demonstration building annexed to MIT Solar 5. The new materials evaluated are a phase-change storage material and a copper, tin-oxide-coated, Argon-filled double glazing. They conclude that "the building can provide 100% solar heating during most winter periods" and that "north facing apartments could be solar heated." They also suggest that, in urban settings, such special glazing, sometimes known as Heat Mirror, could outperform an opaque north wall. Very interesting! Weren't we once professing that each face of a building should respond appropriately to its particular orientation and that north walls should have little or no glass? One wonders what architectural and thermal freedom new materials might offer.

Systems/techniques. Daylighting hardly raised an eyebrow with the Emerging Architecture papers, although another whole section of the *Proceedings* is devoted to the topic. But the use of photovoltaics for electrical generation was discussed and demonstrated. One paper by Steven J. Strong and another by Richard M. Sibly and Jon F. Rubel are two good beginnings, but more are needed. Fred S. Dubin's paper, "Department of Justice Office Building, Sacramento, California," evaluates a 380,000 ft^2 (*35,300 m^2*) building designed to a building load of 38,000 (380,000 in the text) Btu/ft^2 yr (*120 kWh/m^2/ yr*). This paper does a good job of summarizing the thermal, energy, and economic merits of several design and mechanical (nonpassive) techniques. Curiously, this is the only paper that fails to include any drawings, sketches, or photographs—vital in describing architectural concepts.

Architectural synthesis. The diversification and exploration of various specialized topic areas are important for continued growth, yet so is the required synthesis. An overall weakness of the 1982 Emerging Architecture papers is their inability to evaluate and integrate thermal and nonthermal issues as they relate to the design process and product. Analysis methods used as design tools and systems evaluation techniques warrant more discussion. Equally important are how various thermal/energy decisions affect and are affected by other nonthermal design components: social, behavioral, societal, structural, environmental, psychological, physiological, and visual-consideration, just to name a few. Fortunately, a few papers begin to address some of these issues, but not enough.

Good, commonsense architecture requires properly balanced solutions that solve all design problems in an integrative fashion. Optimal thermal expression and resolution at the expense of occupant comfort and delight result in a design failure, just as a poor energy solution does. Clearly, the design professions have come a long way in a short period, growing out of infancy and into adolescence. Many of the projects described in the Knoxville *Proceedings* illustrate how various design approaches have become not necessarily more complex, but more sophisticated. Still, there is a long way to go before energy issues are appropriately represented on the architectural palette. □

Passive Solar Construction Handbook

Steven Winter Associates, Inc. Herndon, Virginia: National Concrete Masonry Association, 1982. $22.45
GPO Item 061-000-00525-1. 584 pp. Feb. 1981. $18.00.

The preface to the *Passive Solar Construction Handbook* says it is "intended to help provide the building industry with a starting point for developing standard and accepted construction practices for passive residences."

This bulky, loose-page, three-ring binder notebook may be a starting point, but, for the amount of effort expended and bulk of material produced, it is disappointingly little more.

The book is quite impressive in its crisp graphic content, but weak in overall organization and direction. It is terribly redundant, presenting countless permutations of basic masonry and solar collector details. At the same time, the crucial detailing issues one faces in passive solar construction are not discussed. Rather than presenting new information or at least a thorough assessment of existing guidelines, this book presents confusing information, much of which is so incomplete, erroneous, or outdated that the unassisted use of the book by the passive solar novice could produce disastrous results.

A major portion of this volume falls under the heading "construction," which is neatly subdivided into three generic passive system types: "direct gain," "thermal storage wall," and "attached sunspace." Unfortunately, an elaborate system of subheadings designed to accommodate future pages makes the format confusing.

Each section begins with a description of the system type and general guidelines for its use. This is followed by pages featuring graphic cross sections of a wall, floor, or roof assembly on the front and construction notes on the back. The interface of these various assemblies with other structural or building components is displayed in the following subsection entitled "details," again containing pages of graphics with "construction notes," on the back. At the end of each generic section are several case studies of entire house designs.

William K. Langdon is a solar architect and author of Movable Insulation. *He is currently a member of the Passive Division Board and chair of the Details and Specifications Committee for the Architecture and Construction Division.*

The introduction to each main section contains rules of thumb for sizing the area of collector or heat storage mass. These guidelines do not take into account that the selection of a passive solar construction detail is often, in itself, the most important determinant of the required solar collection area. As a result, the tables as presented without further information are inaccurate and inappropriate.

For example, a rule of thumb in the section on thermal storage walls states: "In general, the farther north the building is located, the larger the Thermal Storage Wall system should be." A table is presented then with recommended ratios of Trombe wall to floor area for climates with 5°F variations in average winter temperatures, the colder climates and higher latitudes requiring a larger ratio. The amount of winter solar radiation in a climate is ignored in this table.

Applying this rule of thumb without careful attention to other important determinants of the building's thermal performance, namely, the building's overall heat-loss coefficient and the glazing, selective, surface, or night insulation characteristics of the Trombe wall assembly, will yield disastrous results. Trombe walls generally show a diminishing yield per square foot as one moves north. To compensate for this lower yield by constructing larger Trombe wall areas is a very limited approach which rapidly becomes self-defeating.

Furthermore, as important as selective film might be to the performance of an indirect-gain wall (equivalent in many climates to R-9 night insulation), it is hardly mentioned in the entire volume. In a brief paragraph about selective films, they are proposed as "another possible finish."

The construction portion of this volume is quite disappointing in the amount of real information it contains. The graphic cross sections have very simple notes identifying the material only, and any further information is referenced in the notes on the back of the page, for example, "Concrete (see note 5), Blocking, Subfloor (see note 6) . . . ." The accompanying notes contain information that is either obvious to anyone in the design and construction field or so ambiguous as to be useless. The note, "All footings must bear on undisturbed soil," appears at least 58 times on the back of 58 separate pages. At the same time, essential information regarding the details on these pages is totally missing.

For example, one might be designing a wood-supported, brick-paver floor for heat storage in a direct-gain space. When supporting rigid and brittle materials, such as brick and mortar, with a wood system which is inherently flexible and resilient, potential cracking of the mortar joints is a serious concern. Turning to page 3.1172, one finds a section drawn through a wood-supported, brick- or CMU-paver floor. The construction notes suggest "consideration must be given to the additional weight of the masonry when selecting and sizing the floor joists." "Consideration to the additional weight" is again the recommendation for the subfloor note.

Still wondering about potential cracking, one reads the note on the "setting bed." Three recommendations are offered: setting the pavers in type N mortar, setting them in a dry cement/sand grout that is wetted after the pavers are laid, or laying them without mortar. The graphic detail shows the brick laid in a similar manner to thin set tile which requires a resilient epoxy or latex grout. To lay the floor mortarless will eliminate the joints and any subsequent cracking problems, but to lay the floor as drawn with type N mortar is asking for trouble.

The notes also say, "Care must be taken to maintain continuous thermal contact between units to ensure optimum thermal performance." How can this be ensured when the bricks are laid without mortar? And why should this matter when they are individually charged and discharged from the top?

Insulation is another incomplete area. One finds notes such as: "Insulation levels in floors and walls must meet or exceed the requirements of local building/energy codes," or "Consult insulation manufacturer for recommended installation methods." It would be most unwise to turn to local building codes for insulation specifications in passive solar buildings, given that most codes require minimal levels and do not address installation methods when multiple layers are used.

The last portion of the book contains a section on "Materials" which has several useful charts and tables on the properties of concrete, brick, concrete masonry units, glazing materials, and sealants. A discussion of the criteria for material selection in passive solar systems is included in this section, the type of discussion that could be very useful. However, the discussion gets bogged down in weak writing.

At the end of the materials section, we find a paragraph typical of this entire piece of work: "It must also be noted that little documentation is available regarding the thermal performance of various types of mortar which can be used in brick construction. Therefore, when conducting a thermal performance analysis, it is recommended that a brick installation be considered solid brick without any mortar joints at all. This is equivalent to assuming that mortar will exhibit the same thermal performance characteristics as the brick itself."

Consistently relying on old and incomplete information to tackle passive solar detailing issues, the notebook advises we ignore an obvious flaw in an analysis method. We have no reason to expect that mortar has the same thermal characteristics as brick. It may well be more similar to that of concrete. Disregarding the thermal properties of mortar is probably allowable for most simple analyses, but why recommend this method when its precision is unproven?

Instead of recommending methods with obvious flaws and omissions, this handbook would do better to present simply the current wealth of knowledge on passive solar construction.

The challenge in preparing a construction handbook is sorting through extraneous information and construction experiences to present only the most meaningful and useful information to practitioners in a condensed and accessible format. With understanding and a proper discussion of current construction methods combined with an awareness of the other issues one faces in construction, architects and builders will develop their own methods, standards, and accepted practices. The *Passive Solar Construction Handbook* makes only the smallest start in that direction. ☐

Editor's note: A new revised edition of the *Passive Solar Construction Handbook* is in preparation by Rodale Press for publication in September 1983. The Rodale version will add details of new systems and bring to date material from the first edition. Hardbound, it will be a more compact volume than the original reviewed above.

Editor's note: The definitive edition of William A. Shurcliff's *Air-to-Air Heat-Exchangers for Homes* is the 1982 version, not the 1981 which was reviewed in the *Journal* (vol. 1, no. 3, summer 1982). It is published by Brick House Publishing Co., 34 Essex Street, Andover, Mass. 01810. The price is $12.95.

Annual Index
Volume 1, 1982

Abrams, Donald W., 247-8
Absorbed sky radiation. *See* Radiation
Achenbach, P.R., 4-5
Active solar
  definition of, 59; test modules, 226
Adiabatic floors and ceilings, 29
Adobe construction, 23-4, 101
Aeolean Kinetics, 222, 223, 226, 227
Agricultural buildings, 42-3
Air conditioning, 56, 211
Air movement
  measuring, 219-20, 224-5
Airport terminal, 202-7
Air-to-air heat exchangers, 4-11, 52-3, 56, 186-7
Air-to-Air Heat Exchangers for Houses, 186-7
Albany County Airport Terminal, 202-7
Allen, C., 136, 137, 138, 230-1
Aluminum
  louvers, 14-20, 181, 205; radiators, 144; in salt bags, 182; thermophysical properties of, 14, 17, 19
Alward, Ron, 109-20
Ames Laboratory
  and test modules, oppo. 96, oppo. 97, 98; and transwalls, 58
Analytical verification technique, 55-6
Anderson, Bruce, 59, 61
Andrejko, Dennis A., 242-3, 250-1
Anemometer, 225, 231
Annual method of LCR, 73, 79
Appliances, 73-4, 155, 160, 212, 217
Arid climates, 4-11
Arnold, George, 245-6
ASHRAE, 117, 188
ASTM-type calibrated nozzle, 93, 224
Atmospheric radiation. *See* Radiation
Atria, 28, 204, 208-10, 213
Attic vents, 170
Attributes of marketability, 42-51
Audit data
  on passive solar homes, 111
Auxiliary heating, 24, 69, 79, 110, 183, 185-6, 204, 207, 209, 215-7, 239-41
    electric, 56, 106, 115-6, 155, 156, 168, 219-20, 225; monitoring of, 114-6, 120, 151-73; natural gas, 114-6, 209; oil, 114-6; in test modules, 93, 104, 105, 106-7, 219-20, 225, 226; wood, 106, 114-6, 120, 155, 156, 169

Bainbridge, D.A., 230
Balance point temperatures, 164, 165, 169, 171
Balcomb, J. Douglas, 28-9, 67-90, 105, 173-4, 240
Basements, 153-5
Base temperature
  definition of, 69
Batch heater, 128
Bauman, Fred, 28-40
Beckmann, W., 230-1
Ben-Gurion University of the Negev, 131-50, 229-38
Berdahl, P. 135, 136, 137, 230-1
Berming, 7-8, 9, 242
Bingham, Carl E., 12-20
Blackbody radiators, 132, 135, 145-6
Blanpied, Mark, 139
BLAST, 35-7, 39, 54, 55, 247, 249
Blinds. *See* Louvers
Boegel, Mary L., 52-3
Borax in ceiling tiles, 181
Boundary conditions
  for windows, 121-7
Brookhaven National Laboratory, 151-74, 182
Building codes
  and greenhouses, 21, 27
Building Energy Analysis Simulation Codes (BEAS), 54-6
Building performance index
  in Class C survey, 118-20
Buoyancy-driven convection, 28, 30, 39
Butler, Lee Porter, 153, 167
Cab-O-Sil, 181, 182
Cabot Corporation, 182
Calculators
  and the SLR method, 78-9
Calorimeter tests, 182
Carothers, Josephine, 196, 200
Carpeting
  effect on thermal participation, 183-4
Ceiling tiles, 175-84
Central Difference Scheme (CDS), 30
Chen, B., 94
Chimney effect, 214-8
Circulation. *See* Ventilation
Clark, Eugene
  on cooling, 135, 136, 137, 138, 139, 230-1
Class A monitoring, 57, 110
Class B monitoring, 57, 110, 222, 226, 247
Class C monitoring, 57, 109-20, 247
Clearness ratio (K_T), 69, 72-3, 75-6
Clerestories, 99
Climate
  study of, 4-11; zones, 201
Clouds
  effect on atmospheric radiation, 132, 134, 137-8, 229-38; and the SLR method, 72; effect on thermal performance, 157
Clough, Katherine, 109-20
CMI, 182
Cold energy, 135
Cold plate, 123, 124, 125
Cold-storage mass, 146, 149
Commercial buildings, 42, 74-8, 199, 202-7
Commonwealth Scientific and Industrial Research Organization (CSIRO), 144
"A Comparison of Ground and Above-Ground Climates for Identifying Appropriate Cooling Strategies," 4-11
Computer models, 41-51, 67-90, 110, 121-7, 203, 204, 209, 245-6. *See also* Computer programs; Design tools
Computer programs, 28-40, 62, 91-108, 185-6, 203, 204, 231-8. *See also* Computer models; Design tools
Concrete slab, 168, 179, 183, 209
  sensors in, 223
Condensation. *See* Dew formation
Conduction, 4, 121-7, 179
  through glass, 166, 167-8
Conductive coupling, 28-9
Connolly, J. Michael, 12-20
Conservation
  compared to passive solar options, 79-80
Consolidated Edison Demonstration House, 195, 208-213
Construction sector
  marketability in, 43
Continuous radon monitor, 52-3
CONVEC 2 and 3, 30
Convection, 12, 15, 28-40, 93, 95, 97, 114, 121-7, 132, 133, 134, 138-50, 182, 214-8, 219-20, 223, 224-5
Convective heat transfer, 54, 199, 231, 236
Convective loop, 29, 97, 153-74
Cook, Jeffrey, 59-61, 198
Cooling, 146, 170, 172, 184, 194, 207, 211, 247-8
    in Class C survey, 114, 120; and convection, 28-40, 214-8; design tools for, 54-6; and ground temperatures, 4-11; radiative, 94, 100, 101, 114, 131-50, 229-38; and the SLR method, 59, 61, 80; and test modules, 91, 95, 98
"Cooling by Longwave Radiation," 131-50
Cooling tubes, 155, 156, 170, 172
Copper radiation plate, 93-4
Correlation methods
  for solar systems performance, 67-90
Corrosion, 182
Crawl space
  in the Mastin House, 168, 169, 172
Czapek, E.L., 93

Data acquisition system, 94, 220, 222, 225-6
"Data Acquisition in Test Modules," 219-228
Data loggers, 13, 156, 168, 226, 231
Daylighting, 58, 60, 172, 184, 194, 203-7, 245-6
Decking, 153, 214-8
Degree days (DD)
  definition of, 69
Dennehy, Gerald, 151-73
Department of Energy, 4, 41, 42, 56, 57, 98, 109-10, 116-7, 120, 188
Derickson, Russell G., 186-7
DEROB 4, 54, 55
Desert conditions
  and cooling, 131-50, 229-38
Design competitions, 194-218
Design tools, 54-6, 188-92, 248-50
Detached housing. *See* Single-family housing
De Vido, Alfredo, 209
Dew formation, 136, 140-1
  on radiators, 133, 144, 145, 149, 229, 232-8
Dietz, A.G.H., 93
Direct-beam solar radiation, 221
Direct-convection cooling, 114
Direct gain, 12-20, 28, 29, 58, 175-84
  in Class C survey, 113-4; MPI values for, 47-50; roofs, 113; and the SLR method, 73, 81, 82, 84, 85, 88, 239-43; in test modules, 95, 96, 99
Doderer, E.S., 56
DOE-2, 35, 54, 55, 249

Index

- Doors, 184. *See also* Entryways
- Double-envelope design, 151-74. *See also* Insulation
  - evaluation of, 57; in test modules, 96
- Drywall
  - thermal storage in, 179; thermistors in, 183-4
- Duffie, J., 230-1
- Dust particles
  - effect on atmospheric radiation, 132; on radiators, 133
- Earth berming, 7-8, 9, 242
- Earth coupling, 114
- Einhorn Yaffee Prescott Krouner, P.C., 203
- Earth cooling tubes, 155, 156, 170, 172
- Earth sheltering, 4-11
  - envelope, 98; in test modules, 96
- *Easy to Build Retrotrombe*, 128
- *Easy to Build Solar Batch Heater*, 128
- *Easy to Build Thermosiphoning Air Panel*, 128
- Economics, 41-51
  - of greenhouses, 25-6
- Ecotope, Inc., 199
- Edge-effect corrections
  - in test boxes, 93
- Ekose'a, 167, 172
  - double-envelope design of, 151-74
- Electric resistance heater plate, 33, 34
- Electricity
  - for auxiliary heating, 56, 106, 115-6, 155, 156, 168, 219-20, 225
- Electromagnetic radiation, 131-50
- Emerging architecture, 250-1
- Emissivity
  - of glass, 121-7, 184; of sky, 131-50, 229-38
- Energy Works, Inc., 199
- Entryways, 74-8, 99, 176, 178-9
- Environmental Research Laboratory, 92, oppo. 96, oppo. 97, 97, 98, 100
- Eppley equipment, 220, 221, 226
- ERN technique, 15
- Evaporation, 146
- Evaporative cooling, 7, 114

- FANCY RADCOOL, 231, 232
- Fans
  - for heat distribution, 209-10, 213; for ventilation, 9, 24, 105, 171, 215, 218, 224, 244
- Farallones Institute, 91, oppo. 96, oppo. 97, 101
- Farm Credits Bank, 194
- Fast solar load ratio method (FSLR), 249
- F-chart technique, 67-8
- Fiberglass glazing, 23
- Fiberglass insulation, 153, 154-5, 167, 179
- Fireplaces, 106, 114-6, 155, 156, 169
- First National Passive Solar Design Competition, 194-8
- Fleming Associates, Inc., W.S., 203
- Floors
  - carpeting of, 183-4; slate, 205; of test boxes, 94; for thermal storage, 109, 183, 208-13; tile, 109, 195, 208-13
- Florida Solar Energy Center, oppo. 96, oppo. 97, 101
- Fog, 153
- Formaldehyde levels, 52. *See also* Infiltration
- FORTRAN, 105
- Foundation, 180. *See also* Infiltration
- Free convection
  - in thermal storage walls, 12; in windows, 121-7
- Frey, Don, 57
- Fuel
  - costs of, 21; oil, 114-6
- Furnaces, 106, 204, 207, 209. *See also* Auxiliary heating
- Gadgil, Ashok, 28-40
- Gas conduction and windows, 121-7
- GERT, 249
- Georgia Institute of Technology, 172
- Ghost Ranch, oppo. 96, oppo. 97, 101
- Gillett, Drew, 196
- Givoni, Baruch, 6-7, 131-50, 229-38
- Glare. *See also* Daylighting
  - problems with, 175, 176, 181
- Glass
  - conduction through, 166, 167-8; low-iron, 176, 179
- Glass louvers, 12-20
- Glauber's salt
  - in ceiling tiles, 182
- Glazings. *See also* Superinsulated windows; Windows
    - on roofs, 159, 160, 167-8; in test rooms, 93, 99, 103, 104, 107; and the SLR method, 61, 73, 81, 82-3, 88-9, 239-43; on windows, 23, 55, 58, 76, 79, 99, 172, 175, 176-7, 179, 183, 209
- Globe temperature
  - measurement of, 223
- GLOM, 249
- Gordon, J., 139
- Government incentives, 45
- Graybody radiators, 134, 135
- Green Bay, Wisconsin, 49-50
- Greenhouses, 57, 93, 208-10, 213, 215, 216, 217. *See also* Sunspaces
    - in New Mexico, 21-7; in test modules, 94, 95, 96, 98
- Grimmer, D.P.
  - on test boxes, 93
- Ground heat storage, 171-2
- Ground temperatures, 4-11
- Ground thermal coupling, 168
- Gypsum
  - for exteriors, 179, 184

- Haase, Ronald W., 215, 217
- Habitat Center, 96, oppo. 97
- Hamilton, Blair, 109-20, 246-7
- Hand, J.W.
  - on cooling, 150
- Hansen, D.G., 230-1
- Harrington, Keith, 4-11
- Hay, Harold, 91, 93, oppo. 97, 102, 219
- Hayes, John, 196
- Heating systems, 56, 106, 155, 156, 168
- Heat loss. *See* Infiltration
- Heat mirror, 177, 179, 250
- Heat pumps, 56, 106. *See also* Auxiliary heating
- Heat sink, 146, 147, 148
- Higgs, F.S.
  - on cooling, 140
- Hollingsworth, F.N., 93
- Hollowell, Craig D., 52-3
- Horticulture. *See* Greenhouses
- Holtz, Michael J., 12-20
- Hot plate, 123, 125
- HOUSE, 248
- Household income characteristics, 45
- Housing and Urban Development (HUD)
  - minimum property standards, 179
- Humidity, 52, 56, 172
  - and cooling, 4-11, 132, 133, 145, 149, 214-8, 229-38
- Hybrid systems, 19, 204
- Hyde, J.C., 103-4
- Hygrometers, 155, 156
- Indirect gain
  - and thermal control, 12-20
- Indium-tin-oxide (ITO)
  - window glazing, 176, 179-81, 183
- Industrial buildings, 42-3
- Infiltration, 14, 52-3, 81, 93, 105, 106, 107, 117, 159, 172, 174, 179, 182, 209, 224-5, 236, 244
- Infrared radiation
  - through windows, 179, 183
- Infrared transparent windscreens, 133, 134, 139-49, 229-238
- Insects
  - in greenhouses, 25
- Insolation, 181
  - in the Mastin House, 160, 161, 162, 163, 164
- Instrumentation
  - measurement, 219-28
- Instrument shelter, 222-3
- Insulation, 13, 14, 72, 93, 151-74, 179, 183, 252. *See also* Double envelope; Superinsulation
    - ceiling, 212; for cooling, 146, 230; Fiberglass, 153, 154-5, 167, 179; movable, 23, 93, 98, 109, 209-10; night, 23, 47-50, 81, 82-3, 85, 103, 104, 183, 236, 237; in test modules, 98, 103, 104; in windows, 121-7
- Interior air movement. *See* Convection
- Internal heat, 67-90, 106, 111-3, 133, 160, 183
- International Energy Agency (IEA), 188
- International Symposium on Indoor Air Pollution, Health, and Energy Conservation, 187
- Isolated storage wall, 113
- Isothermal walls, 29
- Isotherms, 34
- Jacob Blaustein Institute for Desert Research, 131-50, 229-38
- Jaehne, Dennis, 196
- Johnson, Timothy E., 175-84
- Jones, Ralph F., 151-73
- Jones, Robert W., 67-70
- Juchau, B., 147-8
- Judkoff, Ron, 54-6
- Kammerud, Ronald, 28-40
- Kelly, Mark, 196
- Kinematic viscosity, 123
- Kruskopf, M.
  - on cooling, 144-5
- Kusada, T., 4-5, 6

- Labs, Kenneth, 4-11
- Lake House in Central Florida, 214-8
- Lake Tahoe house
  - of Tom Smith, 172
- Lambda Licor equipment, 220
- Landro, B., 45
- Landscaping, 184
- Langdon, William K., 251-2

LASL/UNM EASE III Economic Performance Code, 42-6
Lawrence Berkeley Laboratory, 28-40, 52-3, 135, 144
Lebens, Ralph M., 185-6
Lighting, 73-4, 160, 162, 182, 183, 184, 203, 205, 207, 211
Liquid temperatures, 224
Load collector ratio (LCR), 42, 61, 67-90, 239-45
Longwave radiation, 131-50, 179
Los Alamos National Laboratory, 28-9
  and greenhouses, 25-6; on marketing potential, 41-51; the *Passive Solar Design Handbook*, 59-64, 68, 72, 73, 78, 79, 239-45; and the SLR method, 67-90, 91-2, 173-4; and test modules, 91-2, 93, 94, oppo. 96, oppo. 97, 101, 102, 103, 105, 106, 107, 220, 221, 223, 224, 225, 226
Louvers, 12-20, 109, 155, 175-7, 181, 184, 203, 204
McClelland, John F., 58
McCormick, P.G., 145
McDade, Mark, 12-20
McFarland, Robert D., 67-90, 105
Manometer tubes, 224
Market Facts, Inc., 57, 111
"Market Potential Indexing: A New Technique for Analyzing Solar Markets," 41-51
Masonry walls
  for thermal storage, 12, 24, 81, 101, 103, 223
Massachusetts Institute of Technology, 182
  and natural convection, 28; and test modules, 33-5, 92, 93, oppo. 96, oppo. 97
Massive surfaces
  design tool for, 54
Mass-to-glazing ratio
  SLR correlations of, 82-3
"The Mastin Double Envelope House: A Thermal Performance Evaluation," 151-74
Memphremagog Group, 57, 109-20
MEPA, 249
Miami University, 219-28
Microswitches, 225
Miller, C., 144
Min-u-Gel, 182
"MIT Solar Building No. 5: The Third Year Performance," 175-84
MITAS, 14-15
Mitchell, P., 144
Mobile homes, 43
Model Audit for the Presidential Conservation Service, 117
Moisture. *See* Humidity
Monitoring, 109-20
  by SERI, 57; of test modules, 219-28
Moore, Fuller, 91-108, 219-228
Morris, W. Scott, 21-7, 93, 96, oppo. 96, oppo. 97, 239-42
Mostrel, Marco, 229-38
Movable insulation, 23, 93, 98, 109, 209-10
Multiattribute Decision Analysis, 43-44
Mylar
  aluminized louvers, 181
National Association of Home Builders Research Foundation, 116-7
National Bureau of Standards, 52-3
National Center for Appropriate Technology, 92, 93, oppo. 96, oppo. 97
National Passive Solar Design Competitions, 194-218
"Natural Convection in Passive Solar Buildings: Experiments, Analysis, and Results," 28-40
Natural gas
  for auxiliary heat, 114-6, 209
Nazaroff, William W., 52-3
Net reference load
  definition of, 69
Nevada Desert Research Institute, 144
New England Solar Energy Association, 196
New Mexico Solar Energy Association (NMSEA), 21, 22, 23, 26
"New Mexico Solar Greenhouse Study," 21-7
Nocturnal radiation, 7, 131-50, 229-38
Noll, Scott, 25-6, 41-51
"Non-Instrumented Performance Evaluation of Passive Solar Homes in the United States," 109-20
Oak Ridge National Laboratory, 4
Occupants, 79, 109-20, 160, 184, 223. *See also* Internal heat
O'Doherty, Bob, 54-6
Ohmmeter, 222
Oil
  for auxiliary heat, 114-6
Opaque louvers, 12-20
Ortega, Joseph K.E., 12-20, 57, 121-7
Outgasing
  in houses, 186-7
Overheating
  problems with, 175
"Overview: Procedures for Validating BEAS," 54-6
Pacific Gas & Electric, oppo. 96, oppo. 97, 101, 102
PASOLE, 62, 68, 69, 71, 93, 105
Passive solar
  compared to conservation, 79-80; definition of, 59
Passive Solar Construction Handbook, 251-2
Passive Solar Design Handbook, Volumes One and Two, 59-64, 242; *Volume Three*, 68, 72, 73, 78, 79, 239-45
Passive Solar Heating Design, 185-6
"Passive Solar Test Modules: A Definition and Survey of the Canadian and American Experience," 91-108
Passive Solar at Work, 57
PEGFIX/PEGFLOAT, 186
Pennsylvania State University, oppo. 96, oppo. 97, 98
"Performance Analysis of Passively Heated Buildings: Expanding the SLR Method," 67-90
Performance evaluation, 109-20, 151-73, 246-7
Phase change materials (PCM)
  in ceiling tiles, 176, 177, 182, 184
Platinum resistance temperature detectors, 219, 222
Plenum roof
  on test modules, 98
Plywood
  thermophysical properties of, 14
Pollutants. *See also* Radon
  in houses, 186-7
Polybutylene tubes, 147-8
Polyethylene
  film as infiltration barrier, 209; film as windscreen, 139-49, 229-38; glazing for greenhouses, 23; in salt bags, 182
Polynomial curve, 13-14
Polystyrene insulation, 93
Polyurethane insulation, 13, 14
Population growth, 45-6
Porches. *See also* Decking
  in test modules, 100, 101
Primary mass configuration, 114
Princeton Center for Environmental Studies, 159
Princeton Circuit Analysis Program, 96
Princeton Energy Group, 209
Proceedings of the Seventh National Passive Solar Conference, 245-51
Purdue University, oppo. 96, oppo. 97, 98
Pyranometers, 155, 156, 219, 220, 226
Pyrheliometers, 219, 221
Radiation
  nocturnal, 7, 131-50, 229-38
Radiation and free convection shield (RFS), 12, 13, 17, 19-20, 223
Radiative cooling, 94, 100, 101, 114, 131-50, 229-38
Radiative coupling, 28-9
Radiators, 131-50, 229-38
Radium, 52-3, 226,
Radon, 52-3, 186-7
Reconfigurable
  test rooms, 94, 95; walls, 93, 101
Recording equipment, 219
Reference designs, 70-1
Reference loads
  definition of, 69
Regional Solar Energy Centers (RSEC), 41, 44, 57, 110-11
Reiniger, Clair, 21-7
Residential buildings, 42, 43, 44, 109-20, 175-84, 199, 208-18
Residential Energy Consumption Survey, 116-7
Residential Radon Daughter Monitor, 53
Resistance temperature detectors (RTD), 222, 224
Retrofits, 21-7, 41, 43, 93, 96, 128, 155, 182, 197, 199
Retrotrombe, 128
Reviewers, 66, 130
Robson, William M., 41-51
Rock beds
  for cooling, 147; for thermal storage, 24
Rolscreen louvers, 179, 181
Roof ponds. *See* Water ponds
Roofs, 7-8, 146, 179, 180
  glass on, 166, 168; glazings on, 159, 160, 167-8; insulation of, 153-4, 208-9; as radiators, 131-50, 229-38; in test modules, 94-98; for thermal storage, 113
Roseme, Gary D., 52-3
Ruberg, K.
  test room of, 33-5

Index

R-values, 240
  for windows, 121-7

Sachs, Beth, 109-20
Sakkal, F., 144
San Jose, California, 194
Second National Passive Solar Design Competition, 198-218
Selective longwave radiators, 143-6
Self-sufficiency
  movement towards, 21
Selkowitz, S., 122
Sensitivities, 243
Sensors
  lighting, 205, 211; measurement, 219-28
Shading, 114, 144, 210, 213, 214-8
  greenhouses, 24; and the SLR method, 78
Shortwave radiation, 131-50, 179
Shurcliff, William A., 62-4, 186-7
Silica
  in ceiling tiles, 181
Silverstein, S.D., 127
Single-family residences, 43, 44, 109-20, 175-84, 199, 208-18
Skin-dominated buildings, 42
Skylights, 194, 202-207
Skytherm, 60, 61, 91, oppo. 97
Smith, Robert O., 185-6
Smith, Tom
  house in Lake Tahoe, 172
Sod roofs, 7-8
Soil, 4-11, 52-3, 179
Solar court, 203-7
Solar Energy Analysis Laboratory, 92, oppo. 96, oppo. 97, 98
Solar Energy Research Institute, 12-20, 44, 54-6, 57, 92, 93-4, 95, oppo. 96, oppo. 97, 106, 110, 111, 222, 226
Solar heating fraction (SHF), 73, 173, 174
Solaria, 152, 153, 156, 165, 170, 172-3. *See also* Sunspaces
Solar load ratio (SLR) method, 67-90, 173-4, 239-45, 249
Solar Room Company, oppo. 96, oppo. 97, 98
Solar savings fraction (SSF), 46, 61, 62, 63, 103, 173-4, 239-45
Solar Woodbox, 198, 199
Solid temperature, 223-4
SOLMET, 42, 69, 73
Southern Solar Energy Center, 172
Spectral distribution of radiation, 132, 133
State Office Building, 194
Stokes house
  in Canton, Georgia, 172
Strip chart recorder, 219
Styrofoam insulation, 179
Sulfur hexafluoride gas
  infiltration tests with, 159, 179, 184, 224
SUNCAT 2.4, 54
SUNDAY, 199
Sunspaces, 28, 72, 74-8, 96, 99, 113, 161, 174, 195, 208-13. *See also* Greenhouses; Solaria
    and the SLR method, 70-1, 73, 81, 84-5, 87, 173, 239-43
SUNSPOT
  definition of, 69, 71
Superinsulation, 151-74, 186-7
  of windows, 175-84
Surfaces
  characteristics of, 5-6, 107, 223; selective, 81, 133, 134, 139-49, 229-38
Surveys
  market, 41-51; of greenhouses, 21-7

Tax benefits, 21, 27, 45
TEANET, 186
Tedlar radiator, 144
Telkes, Maria, 182
Tennessee Valley Authority, oppo. 96, oppo. 97, 98
Test modules, 13-20, 33-9, 91-108, 172, 219-28
Thermal bridging, 179
Thermal diffusivity, 6
"Thermal Impedance of Multi-Pane Windows," 121-7
Thermal network, 54, 104-5
Thermal storage, 171-2
  in ceiling tiles, 175-84; cooling of, 114, 133; in floor tiles, 109, 208-213; in greenhouses, 21-7; with louvers, 12-20; in masonry, 24, 103, 113; in rock beds, 24; SLR correlations of, 82-3; in test modules, 107; in water tubes, 103
Thermistors, 155, 156, 182, 183-4, 219, 222
Thermocirculation, 81, 93
Thermocouples, 13, 168, 219, 221-2, 223, 224, 226, 231
Thermosiphoning
  air panel, 128; in test modules, 106
Thermostats, 111, 214-5
  and natural convection, 37-8; and the SLR method, 79
Tile
  on ceilings, 175-84; on floors, 109, 195, 208-13
Total Environmental Action, 57, 59-64, 128
Total load coefficient (TLC)
  definition of, 69
"Transparent and Opaque Louvers for Thermal Control in Passive Solar Buildings," 12-20
Transducers
  current, 225; temperature, 221, 222
Transwall, 58
Trickle roofs
  in test modules, 98
Trident Energy Systems, 147-8
Trinity University
  and cooling, 56, 135, 229-32; and test modules, 92, oppo. 96, oppo. 97, 98, 100
TRNSYS, 68, 249
Towle, Sharyn, 57
Trombe walls, 58, 113, 128, 251-2
  and the SLR method, 60, 73, 81-3, 86, 238-40; in test modules, 96, 99, 103, 104, 105, 106, 221, 222, 223-4
Trust Pharmacy, 194
Typical meteorological year (TMY)
  definition of, 69, 71, 72

Ultraviolet inhibitors, 229
University of Alberta, oppo. 96, oppo. 97, 101
University of California, San Diego, 98
University of Colorado at Denver, 121-7
University of Nebraska, 92, 95, 96, oppo. 96, oppo. 97
    thermal-envelope test room at, 172
University of New Mexico, 42
University of Pennsylvania, 93, oppo. 96, oppo. 97
University of Wisconsin, 67-8
Un-utilizability method, 68
Urethane foam insulation, 153
"The Use of Mechanical Ventilation with Heat Recovery for Controlling Radon and Radon-Daughter Concentrations," 52-3

Vapor barrier, 52-3, 179, 209, 212. *See also* Infiltration
Venetian blinds. *See* Louvers
Ventilation, 4-11, 24, 52-3, 81, 93, 105, 114, 148, 184, 209, 213, 214-8, 224
    in a double-envelope house, 155, 165, 167, 170, 171, 172
Voltmeter, 222, 226

Walnut Creek, California, 96, oppo. 97
Water heaters, 157, 160, 207
Water ponds, 60, 98, 99, 134, 146
Water tube
  thermal storage, 103
Waterwalls, 12, 199
  for cooling, 7; and the SLR method, 73, 81, 83, 87, 237, 240; in test modules, 94, 95, 96, oppo. 96, oppo. 97, 99, 105
Watson, Tom
  greenhouses of, 21
Watt-hour meter, 225
Weather Bureau, 222-3
Wellwater temperatures, 5
Wessling Consulting, oppo. 96, oppo. 97
Wilson, Alex, 128
Wind, 153
  and cooling, 138, 214-8, 229-38; speed, 224-5
Windows, 14, 33-4, 172, 209-13
  conduction through, 166, 167-8; glazing on, 23, 55, 58, 76, 79, 99, 172, 175, 176-7, 179, 183; movable insulation of, 109; and natural convection, 35-6, 37; superinsulated, 175-84; thermal impedance of, 121-7; transwall, 58
Windscreens, 133, 134, 139-40, 229-238
"Windscreens in Radiant Cooling," 229-38
Wood
  for auxiliary heat, 106, 114-6, 120, 155, 156, 169, 215-8
Wood-frame construction, 24, 94, 109-20
Wortman, David, 54-6
Wray, William O., 67-90
Wright, William A., 61-2, 188-92, 248-50

Yanda, Bill and Susan
  greenhouses of, 21, 22, 23, 26, 27
Yeamans, Marilyn K., 41-51
Yellott, John, 93, 230-1

Zarmi, Y.
  on cooling, 139
Zoning regulations
  on greenhouses, 21, 27

7547 073

American Solar Energy Society, Inc.

United States Section of the International Solar Energy Society

Executive Committee

Chairman:
Francis de Winter, Altas Corporation, Santa Cruz, California

Vice-Chairman:
Donald W. Aitken, San Jose State University, San Jose, California

Secretary:
Gregory Franta, ENSAR, Inc., Lakewood, Colorado

Treasurer:
Rebecca Vories, Infinite Energy, Denver, Colorado

Members-at-Large:
J. Douglas Balcomb, Los Alamos National Laboratory, Los Alamos, New Mexico
Keith W. Haggard, Consultant, Denver, Colorado

Directors

Sara A. Balcomb, Passive Solar Associates, Santa Fe, New Mexico
William A. Beckman, University of Wisconsin, Madison, Wisconsin
Karl W. Böer, University of Delaware, Newark, Delaware
Anne C. Cicero, Harvard University, Cambridge, Massachusetts
Jeffrey Cook, Arizona State University, Tempe, Arizona
Fred S. Dubin, Dubin-Bloome Associates, New York, New York
Don Halacy, Solar Energy Research Institute, Golden, Colorado
John Hayes, Marlboro College, Marlboro, Vermont
Ralph Johnson, National Associates of Home Builders Research Foundation, Rockville, Maryland
George O. Löf, Colorado State University, Fort Collins, Colorado
Bruce Wilcox, Berkeley Solar Group, Berkeley, California
Susan B. Yanda, Brother Sun, Santa Fe, New Mexico
Ex-Officio member:
Joseph Farber, Solar Research Systems, Costa Mesa, California

Passive Systems Division Board of Directors

Chairman:
Peggy Wrenn, City of Boulder, Boulder, Colorado

Treasurer:
W. Scott Morris, Researcher, Santa Fe, New Mexico

Dennis Andrejko, State University of New York at Buffalo, Buffalo, New York
John Hayes, Marlboro College, Marlboro, Vermont
William Langdon, William K. Langdon, AIA, Asheville, North Carolina
Edward Mazria, Mazria/Schiff & Associates, Inc., Albuquerque, New Mexico
Marietta Millet, University of Washington, Seattle, Washington
Bill Yanda, Brother Sun, Santa Fe, New Mexico

The administrative office of the American Solar Energy Society is located at 1230 Grandview Avenue, Boulder, Colorado 80302 (303) 492-6017.

Passive Solar Journal

Heating, Cooling, Hybrid Technolgies and Strategies for Sustainable Design

Aims & Scope

Passive Solar Journal is the official journal of the Passive Systems Division of the American Solar Energy Society, the United States Section of the International Solar Energy Society. It is directed by an organization that has sponsored major national and international passive conferences and is guided by an international panel of distinguished advisors and peer reviewers.

The purpose is to stimulate and support the flow and exchange of research and professional information. The Passive Solar Journal is intended to become the archival record and the standard international reference for the field, with principal directions and issues documented in illustrated and referenced presentations. Annual indexes will provide detailed information and cross reference access. Full-length position papers, articles, reviews, technical notes, book reviews, and critical exchanges emphasize clarity of expression and originality of contribution through high standards of verbal and graphic communication. The responsive support of these goals by the U.S. Department of Energy through the Chicago Operations Office is gratefully acknowledged.

Among specific subjects covered in the Passive Solar Journal are:

Design Tools & Methods
Testing & Monitoring
Energy Budgets
Construction Details
Control Systems
Industrial Applications
Energy Storage
Photovoltaic Interface
Codes & Standards
Economic Analysis
User Evaluation
Environmental Quality
Simulation
Component Design
Integration & Optimization
Calculator & Computer Methods
Solar Greenhouses
Underground Climate
Building Synthesis
Radiation Resources
Building Climatology
Conservation
Urban Design
Retrofits
Daylighting
Thermosiphons
Historical Examples
Movable & Fixed Insulation
Solar Architecture
Window Systems
Appropriate Technology
Lifestyles & Needs
Comfort
Education
Operation & Performance
Thermal Networks
Selective Surfaces
Phase Change Materials
Instrumentation
Market Development
Community Planning
Intrinsic Energy Content

Submission of Manuscripts

Manuscripts proposed for publication are solicited. They must be original and unpublished, although previously published data will be permitted. Articles and reviews are also initiated by invitation of the editors. All materials and illustrations are subject to peer review and editing.

Although this is the official journal of the Passive Systems Division, ASES, manuscripts are accepted from solar researchers and professionals throughout the world. Authors may or may not be members of ASES.

Manuscripts must be written in English and include illustrations and references. Four copies are required. All must be typed and double spaced on one side of white paper 8½ x 11 in. (22 x 28 cm) with ample margins. All pages should be numbered consecutively with abstract (up to 150 words), text with subtitles, acknowledgements, appendix, references, notes, figure captions and illustrations. Manuscripts should be prepared according to the "Style Manual" of the American Institute of Physics, 335 East 45th Street, New York, 10017. All materials will be published using both units of measure: Imperial (English) and SI. The units of the original research will take precedence (with the equivalents in parentheses). Manuscripts from a dot matrix printer will not be accepted.

Manuscripts should be sent to the Editor, **Passive Solar Journal**, Department of Planning, College of Architecture, Arizona State University, Tempe, Arizona 85287.

Cover: The relationships of nature, buildings and people form the basis for the study and practice of passive/hybrid solar research and design. Photos by Bruce Flynn, Henry Mueller and Sharyn Towle.

42068